



TESIS DOCTORAL

**CONTROL DE MOHOS TOXIGÉNICOS MEDIANTE LA
PROTEÍNA PgAFP. INFLUENCIA EN EL METABOLISMO,
PROTEOMA Y SÍNTESIS DE MICOTOXINAS**

JOSUÉ DELGADO PERÓN

**Departamento de Producción Animal y Ciencia de los Alimentos
IPROCAR (Instituto Universitario de Investigación de Carne y Productos Cárnicos)**

Conformidad de los Directores:

Fdo: Miguel Ángel Asensio Pérez

Fdo: Félix Núñez Breña

2016



UNIVERSIDAD DE EXTREMADURA

**DEPARTAMENTO DE PRODUCCIÓN ANIMAL
Y CIENCIA DE LOS ALIMENTOS**

Campus Universitario
Avenida de la Universidad, s/n
E-10071 – CÁCERES
Teléfonos: +34 (9) 27 25 71 00
Fax: +34 (9) 27 25 71 10

Miguel Ángel Asensio Pérez, Doctor en Veterinaria y Catedrático de Universidad del área de Nutrición y Bromatología en la Facultad de Veterinaria de la Universidad de Extremadura,

INFORMA:

Que la Tesis Doctoral titulada “**Control de mohos toxigénicos mediante la proteína PgAFP. Influencia en el metabolismo, proteoma y síntesis de micotoxinas**”, de la que es autor el Licenciado en Veterinaria D. Josué Delgado Perón, ha sido realizada en el Instituto Universitario de Investigación de Carne y Productos Cárnicos bajo mi dirección y cumple las condiciones exigidas para optar al grado de Doctor.

Cáceres, 18 de diciembre de 2015



**DEPARTAMENTO DE PRODUCCIÓN ANIMAL
Y CIENCIA DE LOS ALIMENTOS**

Campus Universitario
Avenida de la Universidad, s/n
E-10071 – CÁCERES
Teléfonos: +34 (9) 27 25 71 00
Fax: +34 (9) 27 25 71 10

Félix Núñez Breña, Doctor en Veterinaria y Profesor Titular de Universidad del área de Nutrición y Bromatología en la Facultad de Veterinaria de la Universidad de Extremadura,

INFORMA:

Que la Tesis Doctoral titulada "**Control de mohos toxigénicos mediante la proteína PgAFP. Influencia en el metabolismo, proteoma y síntesis de micotoxinas**", de la que es autor el Licenciado en Veterinaria D. Josué Delgado Perón, ha sido realizada en el Instituto Universitario de Investigación de Carne y Productos Cárnicos bajo mi dirección y cumple las condiciones exigidas para optar al grado de Doctor.

Cáceres, 18 de diciembre de 2015

AGRADECIMIENTOS

Quiero dar las gracias a todas las personas y entidades que de alguna forma u otra han contribuido a la realización de esta Tesis Doctoral.

A mis directores, Dr. Miguel A. Asensio y Dr. Félix Núñez, por haber confiado en mí y darme la oportunidad de realizar esta tesis, así como por el asesoramiento y la labor de dirección desempeñada.

I would like to thank to the entire Department of Biology of National University of Maynooth, Ireland. Particularly to Professor Doyle and Dr. Owens for the work performed with me in Ireland, this thesis would have not been possible without them.

También quiero agradecer a todos y cada uno de los profesores de la Unidad de Higiene por sus consejos en momentos de difícil decisión, en especial a María Jesús y a Elena, a pesar de que la última me “regañe” mucho.

A mis compañeros de batalla en el día a día, Alberto, Belén, Mariví, Arantxa y Lourdes, que a pesar de que no todos los días son buenos, saben quitarle hierro al asunto y sacarme una sonrisa. De todos y cada uno de ellos he aprendido algo muy importante.

Especial mención a Ali, por su apoyo y ayuda incondicional, como siempre he dicho la considero un ejemplo a seguir.

A Libri y Alfredo, por tener la paciencia de aguantar mis dejadeces en el laboratorio y ayudarme en todo lo que pueden con una sonrisa en la cara.

Mi agradecimiento a todo el grupo de Tecnología y del SIPA, porque cada vez que he necesitado algo me han ayudado sin dudarlo. Así como a los profesores Fernando Peña, J. Antonio Tapia y J. Ángel Padilla por la disponibilidad de sus equipos.

A diferentes entidades como el MICIN por financiar el proyecto de investigación en el que he trabajado (AGL2010-21623 y AGL2013-45729-P) y por concederme dos ayudas para la realización de esta tesis BES-2011-043422 y EEBB-I-13-06900 así como al Gobierno de Extremadura (GR115108) y FEDER.

A mis compañeros de fatigas desde que empecé la carrera y que desde que un día coincidimos en unas prácticas de Anatomía, nuestros destinos académicos parecen haberse puesto de acuerdo. Irene, Juan y Dani, gracias por tantos buenos ratos, y ánimo que como veis las tesis se empiezan para acabarlas.

A mis amigos del pueblo, en especial a Acti y a Santi, por aguantar mis dolores de cabeza sobre la “dichosa tesis”.

Y, cómo no, a las personas más importantes de mi vida, mi familia. A mis abuelos y a mis padres, por inculcarme los valores y la educación que me han dado y ser un ejemplo para mí. A ellos les debo todo porque sin ellos no sería la persona que soy hoy, espero que puedan sentirse orgullosos de mí a pesar de no ser un “Veterinario al uso”. A mi hermana con la cual he compartido muchos quebraderos de cabeza en relación a esta tesis, que de una manera u otra convertía en chiste, gracias especialmente por el pasado mes de julio en Cáceres. No puedo olvidarme de Mari, gracias por tu comprensión y apoyo incondicional incluso en los momentos más difíciles. Además de por visitarme dos veces en mi estancia en Irlanda, a pesar de que los aviones no son tu medio de transporte preferido, espero poder compensarte todo ese esfuerzo.

A todos, gracias.

A mis padres

Si no conozco una cosa, la investigaré.

Louis Pasteur

ÍNDICE

I.	INTRODUCCION.....	1
I.1.	Población fúngica en derivados cárnicos curado-madurados.....	3
I.2.	Efectos del desarrollo de mohos en derivados cárnicos curado-madurados	5
I.2.1.	Aflatoxinas.....	7
I.2.2.	Ocratoxinas.....	8
I.3.	Métodos de control de mohos en derivados cárnicos curado-madurados	8
I.3.1.	Bacterias acidolácticas	12
I.3.2.	Lactobacilos	13
I.3.3.	Mohos	14
I.3.3.1.	Proteínas antifúngicas de origen microbiano	14
I.3.3.2.	Características de PgAFP producida por <i>Penicillium chrysogenum</i>	15
I.3.3.3.	Efecto de las proteínas antifúngicas sobre mohos sensibles.....	16
I.4.	Proteómica.....	18
I.4.1.	2D-PAGE	19
I.4.2.	Métodos no basados en PAGE.....	18
I.5.	Métodos para evaluar el efecto de proteínas antifúngicas sobre mohos	19
I.6.	Métodos de detección de micotoxinas.....	20
I.7.	Transcriptómica.....	24
I.7.1.	Métodos moleculares para la cuantificación de expresión génica	24
I.7.2.	Cuantificación de la expresión génica.....	25
II.	OBJETIVOS	26
III.	MATERIAL Y MÉTODOS.....	28
III.1.	Diseño experimental.....	29
III.1.1.	Estudio del espectro de inhibición de PgAFP	29
III.1.2.	Estudio de la influencia de PgAFP sobre la síntesis de micotoxinas	29
III.1.3.	Estudio del mecanismo de acción de PgAFP	29
III.2.	Reactivos químicos	29
III.3.	Medios de cultivo	31
III.4.	Microorganismos.....	31
III.5.	Equipos.....	32
III.6.	Software.....	35
III.7.	Páginas webs y herramientas empleadas.....	35
III.8.	Métodos analíticos	36

III.8.1.	Producción de PgAFP	36
III.8.2.	Ensayos de inhibición	36
III.8.3.	Extracción de proteínas del micelio	36
III.8.4.	Análisis con 2D-PAGE	38
III.8.5.	Análisis con proteómica libre de marcaje	39
III.8.6.	Evaluación de la permeabilidad	39
III.8.7.	Morfología de las hifas	39
III.8.8.	Actividad metabólica	39
III.8.9.	Tinción de quitina	39
III.8.10.	Tinción del núcleo	39
III.8.11.	Localización de PgAFP en los mohos tratados	39
III.8.12.	Detección de especies reactivas de oxígeno (ROS)	41
III.8.13.	Naranja de acridina (NA)/bromuro de etidio (BE) doble tinción	41
III.8.14.	Detección de apoptosis o necrosis	41
III.8.15.	Capacidad de unión de PgAFP a quitina regenerada	41
III.8.16.	Combinación Quitinasa y PgAFP	42
III.8.17.	Extracción ADN	42
III.8.18.	Extracción ARN	43
III.8.19.	Desarrollo del micelio y extracción de micotoxinas en medio de cultivo	43
III.8.20.	Ensayos en alimentos	44
III.8.20.1.	Efecto antifúngico de PgAFP en alimentos madurados	44
III.8.20.2.	Efecto antifúngico de la aplicación conjunta de PgAFP, <i>D. hansenii</i> y <i>P. acidilactici</i> en alimentos madurados	45
III.8.20.3.	Extracción de micotoxinas de alimento	45
III.8.20.4.	Detección y cuantificación de micotoxinas	45
IV.	RESULTADOS	47
IV.1.	Espectro de acción de PgAFP frente a mohos toxigénicos y capacidad antifúngica sobre producto crudo-curado madurado	48
IV.2.	Efecto de PgAFP y de su combinación con microorganismos bioprotectores para maximizar su efecto de inhibición sobre el crecimiento de mohos y producción de micotoxinas en alimentos madurados	49
IV.2.1.	Evaluación en producto cárnico crudo-curado	49
IV.2.2.	Evaluación en queso	79
IV.3.	Estudio del mecanismo de acción de PgAFP en mohos	99
IV.4.	Estudio del mecanismo de resistencia frente a PgAFP en mohos	153

IV.5. Efecto del calcio sobre la actividad de PgAFP y el metabolismo en mohos sensibles en medio de cultivo y queso	185
V. DISCUSIÓN	241
V.1. Espectro de actividad antimicrobiana de PgAFP <i>in vitro</i>	243
V.2. Aplicación de PgAFP en alimentos.....	244
V.3. Mecanismo de acción de PgAFP	246
V.4. Mecanismos de resistencia a PgAFP.....	249
V.4.1. Influencia del calcio en la actividad inhibidora de PgAFP	250
VI. CONCLUSIONS.....	255
VII. BIBLIOGRAFÍA.....	259
VIII. ABSTRACT	271

I. INTRODUCCIÓN

I.1. Población fúngica en derivados cárnicos curado-madurados

Existe una gran diversidad de grupos microbianos capaces de desarrollarse y multiplicarse en alimentos, debido a su ubicuidad y a la gran diversidad fisiológica, y tolerancia a condiciones ambientales diversas (McMeekin et al. 1997). Los factores que determinan qué tipo de microorganismo prolifera en los alimentos viene determinado en gran medida por las características físico-químicas del alimento, tales como: pH, actividad de agua (a_w), concentración de NaCl, temperatura de conservación, presencia o ausencia de oxígeno, etc. En líneas generales, las bacterias suelen predominar en alimentos con una a_w elevada, ($>0,90$). Sin embargo, en alimentos con valores de a_w inferiores las bacterias no pueden competir por el sustrato, y son los mohos y levaduras los que constituyen la población mayoritaria (Pitt and Hocking 1997).

La contaminación inicial de los derivados cárnicos curado-madurados proviene de la piel y del contenido intestinal de los animales sacrificados, de ingredientes como la sal (Sonjak et al. 2011), que puede estar contaminada por microorganismos halófilos y esporas de mohos y del ambiente en que se manipulan las piezas, incluyendo el aire, utensilios y paredes de las salas donde se manipulan (Asefa et al. 2011).

Las condiciones ambientales tanto externas (temperatura y humedad relativa) como propias del producto (a_w , pH) durante el procesado de los derivados cárnicos curado-madurados no permiten el desarrollo de la mayoría de los microorganismos que pueden haber llegado a la carne. En las primeras etapas esta población microbiana se controla manteniendo los productos a temperaturas bajas. Sin embargo, las temperaturas que se alcanzan durante el secado y la maduración en piezas cárnicas o durante el estufaje en embutidos (15-30 °C) permitirían un rápido desarrollo microbiano, que es controlado por los restantes factores ecológicos. Uno de los factores más importantes es la pérdida de agua, que junto a la incorporación y difusión de la sal provoca una reducción progresiva de la a_w . Este parámetro disminuye en los jamones desde niveles de aproximadamente 0,96, al final de post-salado, cuando se inicia el ascenso de la temperatura en fases tempranas hasta valores que oscilan entre 0,81 y 0,87 en el producto final (Rodríguez et al. 1994).

Estos cambios en las condiciones ambientales durante el procesado provocan una evolución de la población microbiana que se traduce en cambios de los grupos microbianos mayoritarios (Figura I1). Durante el post-salado predominan los estafilococos, que van disminuyendo paulatinamente a lo largo de todo el procesado, aunque aún se mantienen en el producto final (Rodríguez et al. 1994). Por su parte los lactobacilos mantienen su población en los primeros 80 días aproximadamente, para descender drásticamente una vez las piezas

comienzan la etapa en secadero. La población de mohos y levaduras se mantiene relativamente estable a lo largo del procesado, convirtiéndose en dominantes después de la etapa de secadero (Rodríguez et al. 2001), donde las condiciones ambientales y del producto hacen que estos microorganismos compitan más fácilmente que los demás, principalmente por su mayor tolerancia a bajas a_w . El crecimiento de mohos en carne fresca es muy poco importante en comparación con las bacterias, ya que debido a la alta a_w de este producto las bacterias tienen ventajas competitivas y se desarrollan más rápidamente, aunque en algunos casos en carne fresca pueden desarrollarse mohos de crecimiento rápido, bien adaptados a valores de a_w elevados, encuadrados en el Orden Mucorales, como *Mucor*, *Thamnidium*, *Rhizopus*, etc. (Hawker and Linton 1971). En la superficie de derivados cárnicos curado-madurados, como embutidos y jamones, donde los valores de a_w son menores, es donde cobran mayor importancia, ya que la competencia de los mohos frente a otros microorganismos es mucho más eficiente. Las especies más frecuentes en estos alimentos pertenecen a los géneros *Penicillium*, *Aspergillus* y *Eurotium* (Hernández and Huerta 1993; Núñez et al. 1996a) que llegan a representar más del 98% de los mohos aislados, ya que están más adaptados a las condiciones ecológicas, principalmente de humedad, que se alcanzan. Los mohos incrementan su proporción y su diversidad a medida que avanza el procesado del producto (Núñez et al. 1996a). Por otra parte, se suelen observar diferencias en cuanto a la distribución de los citados géneros a lo largo del procesado. Así, en las fases en las que la a_w aún no se ha reducido excesivamente, y se mantiene la temperatura en valores relativamente bajos (<20 °C), como sucede en las etapas de post-salado del jamón, predominan los mohos del género *Penicillium*. Consecuentemente, este género es el mayoritario durante todo el procesado en la mayor parte de los embutidos y en jamones de maduración corta. Sin embargo, en jamones con maduración prolongada, como el ibérico, a medida que se incrementa la temperatura y disminuye la a_w al final del proceso, los integrantes del género *Aspergillus* y su teleomorfo *Eurotium* se convierten en los mayoritarios (Asensio et al. 2004; Núñez et al. 1996a), lo que sucede cuando se alcanzan en la superficie valores de a_w 0,88-0,79 (Rodríguez et al. 2001).

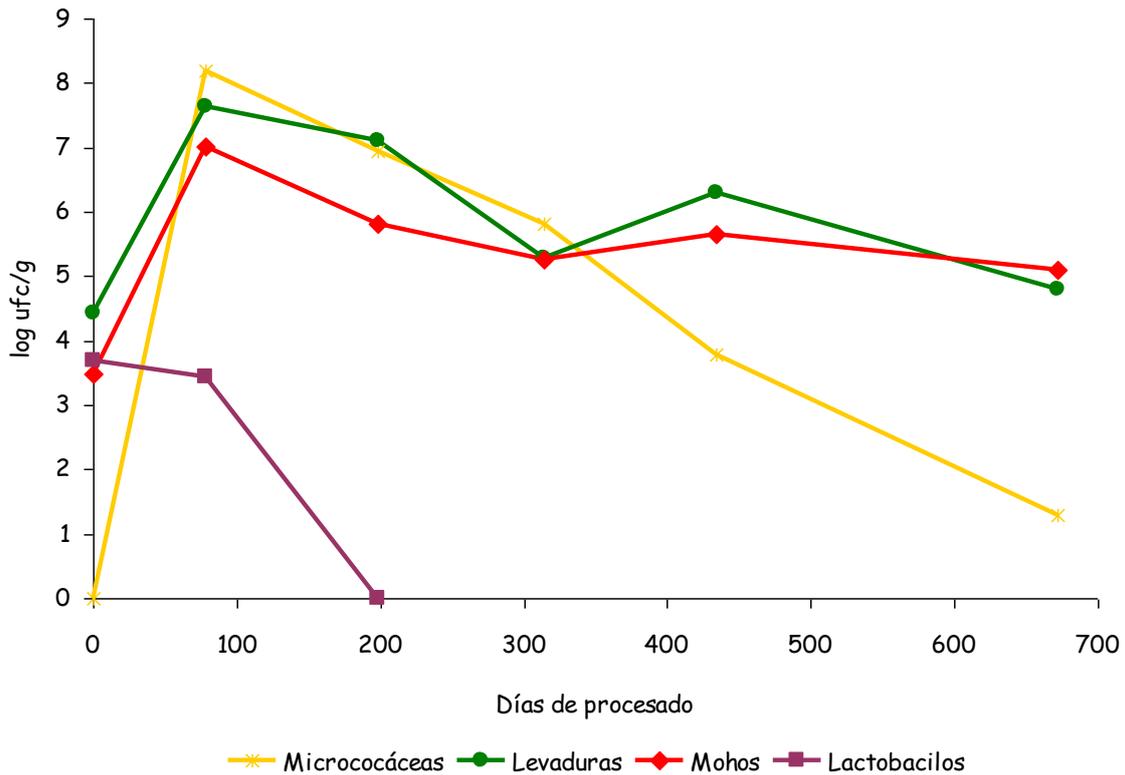


Figura I1. Evolución de la población microbiana en la superficie del jamón (Rodríguez et al. 2001)

I.2. Efectos del desarrollo de mohos en derivados cárnicos curado-madurados

La población fúngica presente en la superficie de los derivados cárnicos curado-madurados durante su maduración puede tener efectos tanto positivos como negativos en relación con la calidad y la seguridad del producto final.

Entre los efectos beneficiosos atribuidos a los mohos durante la maduración de los derivados cárnicos curado-madurados destaca su contribución a los cambios proteolíticos y lipolíticos que se producen durante la maduración (Martín et al. 2002; Martín et al. 2004). Como consecuencia de esta actividad producen un aumento de la concentración de aminoácidos y ácidos grasos libres, precursores de compuestos volátiles deseables en derivados cárnicos curado-madurados (Bruna et al. 2001; Martín et al. 2003). Por otra parte, constituyen una barrera antioxidante por su producción de enzimas como la catalasa (Núñez et al. 1998) sumado a la acción sinérgica del consumo de O_2 y protección frente a la luz, a los que se considera agentes prooxidantes (Boselli et al. 2009; Ferioli et al. 2008). Estas acciones tienen como resultado la formación de una cantidad menor de compuestos volátiles relacionados con la oxidación lipídica y un incremento de compuestos derivados de aminoácidos libres (Martín et al. 2002), asociados de forma positiva a las características sensoriales deseables en los derivados

cárnicos curado-madurados (Ruiz et al. 1999; Martín et al. 2006). En conjunto se relaciona a los mohos con una disminución del enranciamiento, lo que influye positivamente a nivel sensorial (Bruna et al. 2001).

Sin embargo, se han descrito diversos problemas asociados al crecimiento incontrolado de mohos en la superficie del jamón. Por una parte pueden provocar la aparición de defectos o alteraciones sensoriales (Comi et al. 2014; Lozano-Ojalvo et al. 2014; Poma 1998), y por otra parte, lo que es más preocupante desde el punto de vista de la seguridad alimentaria, pueden desarrollarse mohos productores de micotoxinas (Núñez et al. 2000; López-Díaz et al. 2001; Sosa et al. 2002; Núñez et al. 2007; Rodríguez et al. 2012e).

En este sentido, la mayor parte de los mohos aislados de embutidos y jamón curado pertenecientes a los géneros *Penicillium* y *Aspergillus* son potencialmente toxigénicos (Núñez et al. 1996b; López-Díaz et al. 2001), e incluso se ha demostrado la capacidad de producción de micotoxinas de varias especies toxigénicas pertenecientes a estos dos géneros cuando se desarrollan en la superficie de jamón curado (Núñez et al. 2007; Rodríguez et al. 2012e). Debido al peligro potencial que representa la presencia de mohos toxigénicos en alimentos, existe una creciente preocupación por parte de las autoridades sanitarias. Así, en los últimos años se ha producido un incremento paulatino en la normativa legal de la Unión Europea fijándose tanto el contenido máximo de estos contaminantes en una cada vez mayor variedad de alimentos, como métodos de muestreo y de análisis para el control oficial de dicho contenido. Se han establecido límites para aflatoxinas (Ministerio de Sanidad y Consumo 2001; Comisión Europea 2010a), ocratoxina A (OTA) (Ministerio de Sanidad y Consumo 2003; Comisión Europea 2010b), patulina (Ministerio de Sanidad y Consumo 2004; Comisión Europea 2006) y toxinas de *Fusarium* (Comisión Europea 2005; Comisión Europea 2007). Teniendo en cuenta esta evolución legislativa es previsible que se amplíe el número de micotoxinas y de alimentos para los que se establezca un límite máximo en un futuro próximo, entre los que podrían incluirse derivados cárnicos curado-madurados. En este sentido, en algunos países como Italia se ha establecido en 1 ppm el contenido máximo permitido de OTA para carne de cerdo y productos derivados (Ministerio della Sanità 1999).

Por último, la producción de estas toxinas no se limita exclusivamente a productos cárnicos curado-madurados, sino que también se ha demostrado una alta capacidad de producción de estos metabolitos por mohos en otros alimentos de humedad intermedia como quesos son susceptibles de desarrollo de mohos (Lie and Marth 1967; Taniwaki et al. 2001; Crowley et al. 2013)

I.2.1. Aflatoxinas

Las aflatoxinas son metabolitos secundarios producidas por mohos del género *Aspergillus*, siendo las dos principales especies productoras *Aspergillus flavus* y *Aspergillus parasiticus* (Reverberi et al. 2005), aunque también se ha descrito su producción por otros mohos de los géneros *Aspergillus*, *Emericella*, *Penicillium* y *Rhizopus* (Varga et al. 2009; Rodríguez et al. 2012c). Químicamente son policétidos altamente oxigenados (Fig. I2) (Jayashree and Subramanyan 2000), y, debido a sus características químicas, son muy estables frente a tratamientos térmicos y reacciones químicas. Son necesarios tratamientos a temperaturas superiores a 150 °C para reducir la concentración de micotoxinas (Bullerman and Bianchini 2007). Las aflatoxinas más importantes y estudiadas se han clasificado en los tipos: B₁, B₂, G₁ y G₂ según su fluorescencia de color azul o verde en presencia de luz ultravioleta a 365 nm (Liang et al. 1996). Estas micotoxinas se caracterizan por su alto potencial hepatotóxico, inmunosupresor, carcinogénico, teratogénico y mutagénico (Cigić and Prosen 2009), encuadrándose dentro del grupo A según la clasificación de la Agencia Internacional de Investigación sobre el Cáncer (IARC). Las especies productoras están ampliamente distribuidas y tienen capacidad de producir aflatoxinas en un amplio rango de condiciones de temperatura y humedad, así como en diversos sustratos. Entre esta variedad de sustratos, debido a sus características físico-químicas, a las condiciones ambientales y al largo proceso de maduración, se encuentran los derivados cárnicos curado-madurados (Rodríguez et al. 2012e; Bernáldez et al. 2014). Este hecho supone un riesgo para la salud de los consumidores, así como una barrera comercial que podría frenar las exportaciones de estos productos, siendo un factor negativo para la economía de las industrias.

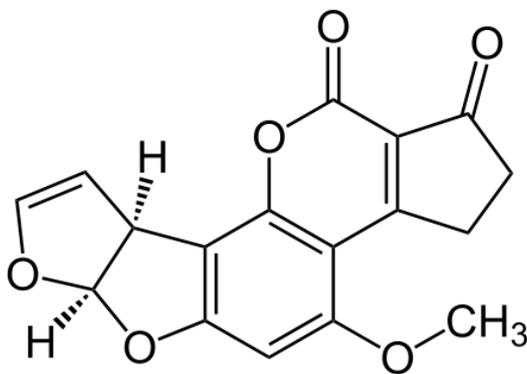


Figura I2. Estructura química de la aflatoxina B₁.

I.2.2. Ocratoxinas

Estas toxinas se constituyen por un pentaquétido cíclico que contienen una porción de dihidroisocumarina clorada ligada a una L-fenilalanina a través de un grupo carboxilo mediante un enlace amida (Fig. 13). *Aspergillus alliaceus*, *Aspergillus auricomus*, *Aspergillus carbonarius*, *Aspergillus glaucus*, *Aspergillus meleus* and *Aspergillus niger*, así como *Penicillium nordicum* y *Penicillium verrucosum*, son productores de OTA (Bezerra da Rocha et al. 2014). La OTA es la más tóxica de las ocratoxinas producidas por mohos, ya que su consumo crónico produce nefropatía intersticial, siendo también teratogénica, hepatotóxica, neurotóxica e inmunotóxica (Soriano del Castillo 2007). Además, está clasificada por la IARC como posible carcinógeno humano de clase 2B.

La OTA es una de las micotoxinas que se encuentran de forma más frecuente en derivados cárnicos curado-madurados, debido a residuos procedentes no solo de la alimentación de los animales, sino también al crecimiento en dichos productos de mohos ocratoxigénicos (Rodríguez et al. 2012d; Bertuzzi et al. 2013). Este peligro ha llevado a autoridades sanitarias de algunos países como Italia a fijar un contenido máximo de residuos en productos cárnicos, como se ha indicado anteriormente.

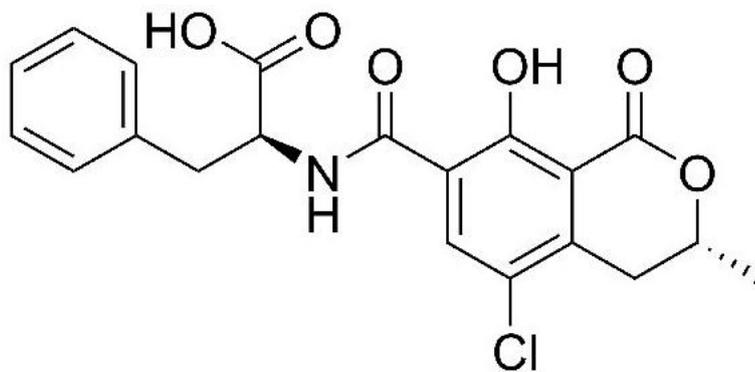


Figura 13. Estructura química de la ocratoxina A.

I.3. Métodos de control de mohos en derivados cárnicos curado-madurados

Debido al peligro que representa la producción de micotoxinas, es necesario establecer estrategias viables para evitar su síntesis durante el procesado de los derivados cárnicos curado-madurados. Existen distintos procedimientos efectivos para controlar este peligro en diferentes alimentos, entre los que se pueden citar métodos físicos (tratamientos térmicos, radiaciones ionizantes o altas presiones) o químicos (atmósferas controladas, ácidos orgánicos, aceites esenciales o peróxido de hidrógeno). Sin embargo, muchos de estos tratamientos no son

aplicables durante el procesado de productos cárnicos curado-madurados ya que impedirían el correcto desarrollo del proceso de maduración. En otros casos, el gran volumen de los secaderos y bodegas que albergan a los productos y el difícil manejo de una gran cantidad de piezas dificultan la aplicación de tratamientos físicos. Para controlar el desarrollo de los mohos se pueden utilizar diversos conservantes químicos. El ácido sórbico y el propiónico limitan la capacidad de los mohos para adaptarse a factores ambientales adversos (Sergeeva et al. 2009), inhibiendo el desarrollo de mohos toxigénicos (Lennox and McElroy 1984), pero no son totalmente eficaces, salvo a valores de pH ácidos o con altas concentraciones de sal (Razavi-Rohani and Griffiths 1999). Además, algunas especies de *Penicillium* o de *Aspergillus* crecen en presencia de altas concentraciones de ácido propiónico o de sorbatos (Bullerman 1984; Mann and Beuchat 2008), e incluso algunos *Penicillium* y *Debaryomyces* decarboxilan el sorbato para producir 1,3 pentadieno de olor a petróleo (Casas et al. 2004). Por ello se ha propuesto la aplicación combinada de distintos compuestos antimicóticos (Mann and Beuchat 2008). Sin embargo, la demanda creciente de alimentos libres de aditivos, y especialmente de conservantes, hace necesario explorar nuevas alternativas para controlar el desarrollo de mohos toxigénicos durante la maduración de los alimentos que evite la utilización de estos conservantes químicos.

Por una parte, se podrían introducir variaciones en las condiciones de maduración que eviten o disminuyan la población fúngica, pero pueden originar problemas tecnológicos en el procesado que impedirían una maduración adecuada y que finalmente radicarían en una merma importante en la calidad sensorial del producto final. Las medidas higiénicas para evitar la contaminación se ven desbordadas en secaderos y bodegas, donde resulta imposible eliminar totalmente la contaminación ambiental. Por tanto, el abanico de posibilidades que la industria puede barajar incluye algunas que resultan poco prácticas y, en muchos casos, imposibles de llevar a cabo. Del mismo modo, es necesario tener en cuenta los requerimientos de fabricantes de otros productos en los cuales no se desea la presencia de moho, como es el caso de algunos embutidos o quesos. Para satisfacer las necesidades del sector en este aspecto, sería necesario ofrecer alternativas que impidan o limiten al máximo el desarrollo de mohos, siendo recomendable que se basen en estrategias que no supongan la adición de aditivos artificiales, de acuerdo a las demandas de los consumidores y además deben descartarse los tratamientos inespecíficos que impidan el desarrollo de la población fúngica deseable en el alimento madurado.

Una de las posibilidades con mejores perspectivas se basa en el empleo de cultivos de cepas no toxigénicas que contribuyan a la maduración del producto donde se inoculan. Para ello,

el uso de la propia microbiota presente de forma habitual durante la maduración de productos presenta grandes ventajas. Por una parte, la adición de estos microorganismos como cultivo protector no supone una ruptura con la microbiota habitual en estos productos, por lo que se reduce al mínimo el riesgo de alteraciones sensoriales derivadas de la adición de estos cultivos protectores. Además, la capacidad de estos microorganismos para implantarse y ejercer su efecto será mejor si se trata de cepas aisladas de productos curados, dada su adecuación a esas condiciones ecológicas particulares. Así desde hace años se han utilizado cultivos iniciadores y, de forma más específica, cultivos protectores para mejorar la seguridad de los alimentos (Holzapfel et al. 1995). Por último, esta estrategia sería adecuada en relación a las demandas de los consumidores con respecto a la minimización del empleo de aditivos artificiales. De los microorganismos presentes en este tipo de productos que pueden interferir con el desarrollo de mohos toxigénicos o con la formación de micotoxinas destacan las bacterias ácido-lácticas (BAL), las levaduras y los mohos productores de proteínas antifúngicas.

I.3.1. Bacterias acidolácticas

Las bacterias acidolácticas (BAL) son habituales en productos crudos curados, especialmente en embutidos y en las primeras etapas de la maduración de jamones. Algunos de estos microorganismos, principalmente de los géneros *Lactococcus* y *Lactobacillus* y, en menor medida, *Pediococcus* y *Leuconostoc*, tienen capacidad de inhibición del crecimiento de mohos toxigénicos y de la producción de micotoxinas (Dalié et al. 2010). La actividad antifúngica de las BAL se ha relacionado principalmente con la producción de compuestos antifúngicos de bajo peso molecular, incluyendo ácidos orgánicos, ácidos grasos, reuterina, peróxido de hidrógeno, compuestos fenólicos, lactonas, dipéptidos cíclicos y compuestos proteicos, que no sólo pueden afectar al desarrollo de mohos sino a la capacidad de producir micotoxinas (Dalié et al. 2010; Crowley et al. 2013; Li et al. 2014; Ryu et al. 2014). Además tampoco puede descartarse el efecto inhibitorio debido a la competencia por el sustrato. De acuerdo con las preferencias de los consumidores, las BAL son buenas candidatas a biocontrol de mohos toxigénicos ya que tienen la consideración americana de GRAS (Generalmente Reconocidas como Seguras) y la europea QPS (Presunción Cualificada de Seguridad), y se les considera que poseen propiedades probióticas saludables. Sin embargo, debido su limitada resistencia a los valores intermedios de actividad de agua los hace inadecuados para productos de larga maduración, en particular cuando no se añade azúcar. Consecuentemente, sería necesario optimizar el momento de inoculación así como posibles reinoculaciones o establecer pequeñas modificaciones en los parámetros de la maduración con el objetivo de maximizar su presencia a lo largo del proceso de maduración.

I.3.2. Lactobacilos

Diferentes levaduras muestran actividad antifúngica o capacidad para disminuir la acumulación de micotoxinas en alimentos (Asensio et al. 2014). En consecuencia, algunas cepas han sido propuestas como cultivos protectores, especialmente en alimentos de origen vegetal con el objetivo de reducir el uso de fungicidas sintéticos para el control de enfermedades de post-cosecha y reducir el crecimiento de mohos, incluyendo algunos toxigénicos (Petersson et al. 1998; Qin et al. 2004; Ponsone et al. 2012; Armando et al. 2013; Spadaro et al. 2013).

En los derivados cárnicos curado-madurados las levaduras predominantes pertenecen a la especie *Debaryomyces hansenii*, llegando a constituir el 99% de los aislados en la fase de bodega de jamones (Núñez et al. 1996b), probablemente debido a ser moderadamente halófila (Breuer and Harms 2006), siendo capaz de desarrollarse con hasta un 15% de NaCl (Asefa et al. 2009). Además, *D. hansenii* es una levadura con importantes aplicaciones biotecnológicas en alimentos debido a sus propiedades metabólicas características (Breuer and Harms 2006). Por lo tanto, su utilización como cultivos protectores podría asegurar su presencia a lo largo de todo el procesado. En los productos cárnicos esta levadura contribuye de manera notable en la textura final gracias a fenómenos de proteólisis (Rodríguez et al. 1998; Martín et al. 2002), así como la generación de compuestos volátiles formados durante la maduración de productos curados (Martín et al. 2003; Martín et al. 2006; Andrade et al. 2009).

En cuanto a su capacidad antifúngica, cepas de *D. hansenii* se han mostrado eficaces para inhibir el crecimiento y la esporulación de mohos de los géneros *Penicillium*, *Aspergillus* y *Eurotium* en diferentes alimentos, por lo que se han propuesto como agentes de control biológico contra mohos en frutas (Chalutz and Wilson 1990; Hernández-Montiel et al. 2010), el yogur y queso (Liu and Tsao 2009). En este sentido, también se ha probado en productos cárnicos la eficacia de cepas de *D. hansenii* autóctonas para reducir el desarrollo y la producción de toxinas de mohos toxigénicos frecuentes en estos productos (Virgili et al. 2012; Andrade et al. 2014; Simoncini et al. 2014; Núñez et al. 2015).

También otras especies de levaduras aisladas de productos cárnicos, como *Candida zeylanoides*, *Candida famata* y *Endomyces fibuliger* son capaces de inhibir el crecimiento de mohos ocratoxinógenos como *A. niger*, *A. ochraceus*, *P. nordicum*, *P. verrucosum*, y en consecuencia la producción de OTA en la superficie de jamón curado (Virgili et al. 2012; Comi and Iacumin 2013). Sin embargo, estas levaduras se encuentran a niveles bajos en los productos cárnicos curado-madurados (Núñez et al. 1996b; Simoncini et al. 2007; Asefa et al. 2009) por lo

que su adaptación a estos alimentos es menor que *D. hansenii* y serían potencialmente menos útiles.

Diferentes mecanismos de acción pueden explicar el efecto antifúngico de estas levaduras, como la competencia por nutrientes y espacio (Druvefors et al. 2005; Coelho et al. 2007), la producción de toxinas killer (Marquina et al. 2001; Hernández et al. 2008), la producción de compuestos volátiles (Masoud et al. 2005), el parasitismo (Wisniewski et al. 1991), la resistencia inducida (El-Ghaouth et al. 1998), y la producción de enzimas hidrolíticas de pared celular (Masih and Paul 2002). En algunas cepas de *D. hansenii* aisladas de productos cárnicos pueden estar implicados varios de estos mecanismos (Andrade et al. 2014; Núñez et al. 2015).

Además, las levaduras pueden disminuir el contenido de micotoxinas por adsorción (Var et al. 2009), su degradación (Patharajan et al. 2011) o por impedir su síntesis mediante el bloqueo de cualquier paso en la ruta biosintética de las micotoxinas. En este sentido, *D. hansenii* es capaz de reducir la concentración de OTA en cultivos mixtos con *A. westerdijkiae* debido a una reducción en la expresión de genes biosintéticos de OTA (Gil-Serna et al. 2011).

I.3.3. Mohos

Algunas cepas de mohos aisladas de productos cárnicos curado-madurados no toxigénicos y con una actividad metabólica adecuada pueden limitar por competición el desarrollo de otros mohos indeseables. No obstante, la evolución de las condiciones ecológicas durante la maduración hace poco probable que una sola cepa seleccionada pueda limitar el crecimiento de todas las especies toxigénicas habituales en todo el rango de temperaturas y de a_w que se alcanzan durante la maduración (Núñez et al. 2000; Sosa et al. 2002). El éxito de esta estrategia sería más probable en el caso de utilizar mohos con capacidad de producir metabolitos, como pueden ser proteínas con actividad antifúngica que pueden inhibir o frenar el desarrollo de determinados mohos toxigénicos, lo que le otorgaría una ventaja competitiva para el control de estos mohos indeseables (Acosta et al. 2009). Para la evaluación de la capacidad antifúngica de estos metabolitos se han diseñado diversas estrategias. Algunas basadas en inhibición en placas de agar (Geisen 2000) y otras en placas microtiter (Broekaert et al. 1990).

I.3.3.1. Proteínas antifúngicas de origen microbiano

En los últimos años se ha producido un incremento importante en la investigación de agentes antifúngicos debido a la aparición de resistencias frente a agentes antimicóticos

empleados habitualmente para el tratamiento de micosis en humanos y en plantas. Entre las distintas opciones, destaca la caracterización de nuevas proteínas con actividad antifúngica (Wang and Ng 2002). Se han purificado y caracterizado proteínas con efecto antifúngico a partir de diferentes organismos tales como plantas (Chu et al. 2003), bacterias (Yang et al. 2002) o mohos (Marx 2004; Acosta et al. 2009). Existe una amplia variabilidad en la composición, estructura secundaria y terciaria de estas proteínas, aunque la mayoría se caracterizan por poseer una carga neta positiva y numerosos residuos de cisteína envueltos en la formación de puentes bisulfuro (Leiter et al. 2005).

Dentro de estos compuestos, se han descubierto varias proteínas antifúngicas producidas por mohos que se caracterizan por ser de naturaleza catiónicas, ricas en cisteína y de bajo peso molecular (Tabla I1).

Tabla I1. Proteínas antifúngicas producidas por mohos

Nombre	Moho productor	pI	Pm (Da)	Referencia
AcAFP	<i>Aspergillus clavatus</i>	-	5773	(Skouri-Gargouri and Gargouri 2008)
AcAMP	<i>Aspergillus clavatus</i>	9.066	5777	(Hajji et al. 2010)
AFP	<i>Aspergillus giganteus</i>	8.8	5800	(Nakaya et al. 1990)
AFP _{NN5353}	<i>Aspergillus giganteus</i>	9.3	-	(Binder et al. 2011)
Anafp	<i>Aspergillus niger</i>	7.14	6583	(Gun Lee et al. 1999)
FPAP	<i>Fusarium polyphilaidicum</i>	6.3	-	(Galgóczy et al. 2013)
NAF	<i>Penicillium nalgiovense</i>	8.93	6300	(Geisen 2000)
NFAP	<i>Neosartorya fischeri</i>	8.93	6625	(Kovács et al. 2011)
PAF	<i>Penicillium chrysogenum</i>	8.93	6250	(Marx et al. 1995)
Pc-Arctin	<i>Penicillium chrysogenum</i>	-	7000	(Chen et al. 2013)
PgAFP	<i>Penicillium chrysogenum</i>	9.22	6494	(Rodríguez-Martín et al. 2010)

I.3.3.2. Características de PgAFP producida por *Penicillium chrysogenum*

La proteína PgAFP es producida por la cepa de *Penicillium chrysogenum* CECT 20922 (previamente nombrada RP42C), aislada de jamón curado (Acosta et al. 2009; Rodríguez-Martín et al. 2010). Esta proteína mostró capacidad de inhibición frente a mohos toxigénicos frecuentes en derivados cárnicos curado-madurados, pertenecientes a los géneros *Penicillium* y *Aspergillus* (Acosta et al. 2009). El peso molecular de la proteína madura es de 6494 Da y su punto isoeléctrico 9.2 (Rodríguez-Martín et al. 2010). Se sintetiza como una pre-pro-proteína de 92

aminoácidos y después de la eliminación de las secuencias N-terminal pre- y pro- (18+16 aminoácidos) la proteína madura se libera en el medio de cultivo (58 aminoácidos). Las prosequencias son de una importancia crucial para impedir el plegamiento adecuado y la actividad biológica completa (Marx et al. 2005) siendo todas éstas, características comunes de las proteínas antifúngicas.

La secuencia que codifica la PgAFP consiste en una región de codificación de 279 pares de bases interrumpido por dos intrones de 63 y 62 pares de bases. La secuencia de aminoácidos deducida de la matriz de la proteína madura muestra un 79% de identidad con Anafp de *Aspergillus niger*, mientras que con PAF muestra un 34% y con AFP un 33% de identidad (Rodríguez-Martín et al. 2010).

P. chrysogenum produce compuestos considerados como seguros (GRAS) según la Food and Drug Administration de EEUU. Este hecho junto a que PgAFP no mostró toxicidad frente a células de mamíferos (Rodríguez 2009) y que es sensible al tratamiento con enzimas como tripsina, pepsina y lisozima (Acosta 2006), permite ser optimistas respecto a su uso en alimentos ya que puede ser degradada en el tracto intestinal.

Aunque se desconoce el mecanismo de acción de PgAFP, debido a las homologías con otras proteínas antifúngicas, se podría presumir que algunos de los mecanismos de acción descritos para estas proteínas podrían explicar la actividad antifúngica de la PgAFP. El conocimiento de dicho mecanismo aportaría una información muy valiosa, tanto para caracterizar mejor a esta proteína, como para establecer condiciones de aplicación de la proteína o del moho productor para obtener la mayor eficacia posible frente a mohos toxigénicos en derivados cárnicos curado-madurados.

1.3.3.3. Efecto de las proteínas antifúngicas sobre mohos sensibles

Los mecanismos de acción de las proteínas que inhiben el desarrollo de los mohos son muy variados. Algunos atraviesan la membrana e interfieren en la síntesis de ADN, ARN o proteínas, inhiben la cadena respiratoria celular (Cociancich et al. 1993) o interaccionan con enzimas ATP-dependientes (Hilpert et al. 2010). En todos ellos la permeabilidad de la membrana parece jugar un papel decisivo en el mecanismo de acción.

Las proteínas antifúngicas de mayor utilidad son las que presentan mecanismos de acción específicos para la cubierta externa de los hongos (Groll et al. 1998), ya que suelen ser poco tóxicas para las células de los mamíferos. En la interacción de la proteína con la membrana juega un papel destacado la carga (Hoover et al. 2003) y el carácter catiónico o hidrofóbico del compuesto (Friedrich et al. 1999). La hidrofobicidad y la estructura en α -hélice se correlacionan

con la toxicidad para las células de mamíferos, mientras que la carga positiva se relaciona con la actividad antimicrobiana (Hong et al. 2001). Se asume que la actividad antifúngica de estas proteínas está relacionada con la capacidad de interactuar con fosfolípidos aniónicos, que forman parte de la membrana de mohos y bacterias, lo que permite la unión de la proteína y su posterior acción (Lacadena et al. 1995). Sin embargo parece poco probable que se trate de una unión inespecífica, ya que la membrana externa de bacterias está principalmente compuesta también por fosfolípidos aniónicos y no se ven afectadas por AFP. En las células de eucariotas superiores al carecer de dichos fosfolípidos o al estar confinados en la cara interna de la membrana plasmática, y no estar en contacto con el medio extracelular se puede descartar este tipo de interacción (Rivas and Andreu 2003; Theis and Stahl 2004).

Del mismo modo, se han descrito diversos efectos de este tipo de proteínas sobre los mohos tratados, tales como reducción del metabolismo celular, cambios drásticos en la morfología de las hifas, incremento en el flujo de K^+ y la formación de especies reactivas de oxígeno (ROS) en el interior de las células (Kaiserer et al. 2003; Marx et al. 2005). Estas sustancias provocan daño celular desencadenando fenómenos apoptóticos y necrosis (Marx et al. 2008; Galgóczy et al. 2013). La reducción del metabolismo celular de las hifas de los mohos sensibles podría considerarse *a priori* como un efecto directo de la capacidad inhibitoria de AFP.

Por otra parte se ha apuntado la posibilidad de que la AFP ejerza algún tipo de señal apoptótica sobre las células tratadas, habiéndose descrito dos tipos de señales que podrían ejercer dicha acción: en el primero está involucrada la proteína heterotrimérica G junto a la transducción de señales y redes de regulación; el segundo se realizaría a través de la alteración de la homeostasis de Ca^{2+} de las células (Hegedus et al. 2011), donde volvería a jugar un papel determinante la membrana celular. También se ha postulado que la actividad de AFP y PAF están relacionadas con la señalización de la ruta metabólica de síntesis de quitina, estando involucrada la cascada de señalización de la proteína Rho1 (Binder et al. 2010; Ouedraogo et al. 2011) que es considerada la principal reguladora de la señalización de la pared celular (Levin 2005).

Algunas cepas presentan resistencia a este tipo de proteínas antifúngicas, relacionada con la capacidad de deponer quitina como protección frente a estas proteínas (Ouedraogo et al. 2011). Esta deposición de quitina colaboraría en el acceso de estas proteínas antifúngicas a receptores específicos relacionados con fosfolípidos de membrana. Además la presencia de cationes en el medio ejerce un efecto protector sobre los mohos sensibles, ya que se ven menos afectados por las proteínas antifúngicas (Thevissen et al. 1999; 1996; Theis et al. 2003; Kaiserer et al. 2003; Galgóczy et al. 2013). Se ha propuesto que los cationes pueden interferir con la AFP bien por inhibición directa de la unión a la membrana o por interacción específica con un posible

receptor en la membrana (Marx 2004). Este hecho limitaría la utilidad de proteínas antifúngicas sobre alimentos ricos en cationes divalentes, como quesos, que contienen altos niveles de calcio (Chekri et al. 2012). Por ello sería interesante conocer cómo actúan los cationes para reducir o anular la actividad de proteínas antifúngicas, para diseñar estrategias que contrarresten el efecto de los cationes divalentes y maximizar el efecto antifúngico de estas proteínas.

El efecto de estas proteínas antifúngicas sobre la señalización de las proteínas G podría influir en la producción de micotoxinas, ya que es requerida para producción de alguna de éstas (Hicks et al. 1997). Además, la inducción de ROS por estos antifúngicos ha sido descrita como desencadenante de estrés oxidativo, que, por otra parte, es un factor importante para la producción de micotoxinas (Reverberi et al. 2005; Kim et al. 2008). El estrés oxidativo provoca cambios en la fisiología de los mohos, induciendo la producción peroxisomas que regulan la β -oxidación de ácidos grasos, afectando ambos a la producción de aflatoxinas (Reverberi et al. 2012). Además, el metabolismo del glutatión es el encargado de contrarrestar la cantidad de ROS en la célula, existiendo una correlación entre la acción de la proteína glutatión S-transferasa y la producción de aflatoxinas (Saxena et al. 1988). Todos estos resultados indican que podría existir un estímulo de la producción de micotoxinas en respuesta a estrés oxidativo provocado por las ROS, que a su vez parecen ser inducidas por este tipo de proteínas antifúngicas. Sin embargo, el efecto inhibitor de las proteínas antifúngicas sobre mohos productores de micotoxinas evitaría el desarrollo de éstos y por consiguiente limitaría su producción, además no puede ser descartada una interacción de estas proteínas antifúngicas con rutas biosintéticas propias de aflatoxinas. Por lo tanto, dado que teóricamente existen fenómenos que pueden parecer contradictorios, es necesario establecer el efecto que las proteínas antifúngicas tienen sobre la producción de micotoxinas en mohos que puedan sobrevivir al tratamiento.

I.4. Proteómica

Para conocer cómo afectan estas proteínas sobre el metabolismo de los mohos frente a los que actúa, se podría emplear el análisis de la expresión génica total. Sin embargo la medición de la expresión de ARNm no suministra valores confiables de los cuales se pudiera deducir la abundancia y la presencia de las proteínas traducidas. Esta falta de precisión se debe principalmente a que el tiempo de vida media de proteínas en el interior de una célula o de un compartimiento celular es variable debido a la acción de proteasas y a la traslocación intra- y extracelular, junto con a la modificación de las proteínas durante su intervención en procesos biológicos. Por tanto, el estudio directo del perfil de proteínas, a través de la Proteómica, puede dar respuesta a estas cuestiones (Castellanos et al. 2004).

La proteómica se define como el estudio y caracterización del proteoma, entendiendo como tal a la totalidad de las proteínas expresadas a partir del genoma bajo unas condiciones y en una fase de desarrollo determinadas. El estudio del proteoma de un organismo puede ofrecer información útil relacionada con su estado fisiológico, relacionándolo con cambios producidos en el organismo por algún factor. El aumento o la disminución relativa de proteínas en un organismo sometido a una determinada variable con respecto a una situación control ofrecen una información valiosa relacionada con los cambios producidos por los factores en estudio sobre el organismo en cuestión. Este análisis basado en la comparación de proteomas se denomina proteómica comparativa, y ha sido empleado, entre otros fines, para conocer cómo afectan diversos compuestos antifúngicos a mohos sensibles (Gautam et al. 2008; Cagas et al. 2011). Para ello es necesario disponer de técnicas que permitan la separación de proteínas, la cuantificación del cambio de magnitud de provocado y finalmente su identificación. Existen varios métodos para llevar a cabo este tipo de análisis pudiendo diferenciarse dos metodologías distintas, dependiendo de si están basados o no en el empleo de electroforesis en geles de poliacrilamida (PAGE).

I.4.1. 2D-PAGE

Esta metodología es adecuada para estudiar el efecto de sustancias antifúngicas sobre mohos, por ello ha sido de elección para este fin en diversos trabajos (Cagas et al. 2011; Carberry et al. 2012). Se basa en conseguir una dispersión de las proteínas que forman el proteoma en un gel en dos dimensiones, en la horizontal las proteínas se distribuyen en base a su punto isoeléctrico (pI) y en la vertical se distribuyen en función de su tamaño. De este modo se consigue una separación óptima de las proteínas, que una vez teñidas, se deben analizar con ayuda de software para obtener las diferencias cuantitativas relativas entre muestras tratadas y muestras control. Para identificar las proteínas es necesario extraerlas del gel, digerirlas y analizarlas, habitualmente por nanocromatografía líquida (nano-LC), para obtener su espectro a través de espectrometría de masas. Finalmente son identificadas comparando el espectro a través de bases de datos disponibles en internet. Esta técnica es robusta y reproducible, siendo una de las mayores ventajas que la caracterizan la capacidad de separar proteínas completas con todas sus modificaciones (Kniemeyer et al. 2011). Sin embargo su sensibilidad reducida es un inconveniente para el estudio de las proteínas de membrana y de aquellas que se encuentran en una cantidad muy pequeña (Rabilloud et al. 2009; Görg et al. 2009). Además, una limitación intrínseca de este método es que trabaja en un rango de pH, generalmente 4-7 (Carberry et al. 2012) o 3-11 (Lessing et al. 2007), que no cubre el proteoma completo, dado que existen proteínas que quedan fuera de este rango.

I.4.2. Métodos no basados en PAGE

Las técnicas basadas en cromatografía líquida acoplada a espectrómetro de masas (LC-MS/MS) permite la cuantificación relativa de proteínas difícilmente separables mediante 2D-PAGE, como proteínas de membrana, proteínas hidrofóbicas o proteínas con pI o peso molecular extremo (Speers and Wu 2007). Los análisis de proteómica basados en MS se realizan tras digestión de los analitos y su posterior fragmentación y el procesamiento de los datos obtenidos mediante programas informáticos. Esta metodología es capaz de identificar de forma habitual entre 1000 y 2000 proteínas en una muestra biológica (Kniemeyer et al. 2011).

Dentro de esta metodología existen dos aproximaciones, los ensayos con marcaje (*labelled*) o sin él (*label-free*). La principal diferencia radica en que en el primero de los casos las proteínas son marcadas, siendo habitual que se analicen conjuntamente por el LC-MS/MS, mientras que las técnicas basadas en label-free, los analitos no se marcan, y son analizados siempre por separado. Esta última técnica ha sido recientemente usada para investigar sobre el proteoma de *Aspergillus fumigatus* (Dolan et al. 2014; Owens et al. 2014) presentando la ventaja de cubrir un mayor número de proteínas identificadas que los métodos que incluyen marcaje (Li et al. 2012). Sin embargo presenta la limitación de que no es capaz de diferenciar entre cambios habituales en las proteínas, tales como isoformas, observándose simplemente una cuantificación total de la proteína, con lo que puede resultar una interpretación errónea con motivo de la no diferenciación entre isoformas habitualmente envueltas en procesos fisiológicos.

Existen diferentes equipos que llevan a cabo este tipo de análisis, como ya se ha citado, suelen estar compuestos en primer lugar por un equipo de LC que permite separar los componentes del analito. A continuación, pueden ir conectados en serie diversos detectores de espectrometría de masas, que van desde baja resolución (trampa de iones) hasta alta alta resolución (q-TOF y Orbitrap) que permiten mejorar la resolución y la precisión del análisis. Los equipos de alta resolución son aquellos que permiten separar partículas con relación m/z muy próximas. Estos espectrómetros pueden ser combinados para formar un equipo híbrido, que junto con otros dispositivos permite una gran resolución y precisión. El conjunto de espectros obtenidos son normalizados previamente al análisis con software específicos, como por ejemplo MaxQuant, una plataforma ampliamente usada para el análisis de estos datos. Por tanto, debido al diferente rango pI analizado, a la presencia de proteínas de membrana e hidrofóbicas así como la diferente sensibilidad de ambos análisis (Rabilloud et al. 2009; Görg et al. 2009), no es esperable una total reproducibilidad de los resultados a través de ambas metodologías. Sin embargo, las limitaciones de un análisis se ven complementadas con el otro. Empleando este

tándem se incrementa considerablemente el número de proteínas analizadas y por tanto se revela un mayor número de aquellas afectadas dentro del proteoma. El análisis del proteoma empleando este tándem incluye además las modificaciones de estas proteínas a nivel estructural que se ven alteradas por la variable en estudio, por ejemplo isoformas.

1.5. Métodos para evaluar el efecto de proteínas antifúngicas sobre mohos

Para el estudio de los fenómenos provocados por proteínas antifúngicas que puedan ser deducidos por los estudios de proteómica, existen diversos métodos, los cuales pueden servir como ensayos confirmatorios. La mayoría se basan en técnicas de visualización utilizando colorantes vitales a través de microscopía fluorescencia. De este modo se ha estudiado la actividad metabólica a través de la tinción FUN®1 (Molecular Probes, Eugene, OR, USA) (Kaiserer et al. 2003), que difunde a través del citoplasma tiñéndolo de verde en todas las células, sin embargo solo en las que mantienen la capacidad metabólica y la membrana íntegra provoca una tinción intravacuolar roja.

La permeabilidad celular ha sido evaluada con SYTOX Green (Molecular Probes) (Kaiserer et al. 2003; Moreno et al. 2006) que tiñe los ácidos nucleicos cuando penetra a través de membranas comprometidas pero no en aquellas intactas. Para determinar la deposición de quitina se ha empleado el calcofluor White o fluorescent brightener 28 (Sigma, St. Louis, MO, USA) (Binder et al. 2010; Galgóczy et al. 2013) que muestra fluorescencia cuando está unido a la quitina, y para estudiar la distribución de los núcleos se ha empleado Hoechst 33258 (Molecular Probes)(Kaiserer et al. 2003) ya que se une al ADN y lo tiñe específicamente. También se ha evaluado la inducción de estas proteínas sobre la formación de ROS a través de 2', 7' dichlorofluorescein diacetate (Sigma-Aldrich, St. Louis, MO, USA)(Kaiserer et al. 2003; Leiter et al. 2005) que se vuelve fluorescente al ser oxidado.

Por último, dado que este tipo de proteínas ha inducido fenómenos apoptóticos en mohos sensibles, se ha evaluado la viabilidad de las hifas empleando el Apoptosis Detection Kit (Sigma-Aldrich) que tiene capacidad para diferenciar entre hifas viables, apoptóticas y necróticas (Leiter et al. 2005; Galgóczy et al. 2013). La anexina V-FITC se une a la fosfatidilserina y la tiñe de verde cuando está traslocada al exterior de la membrana celular, lo que es una señal inequívoca de apoptosis. Las hifas viables no son teñidas, mientras que en células necróticas, tanto la anexina V-FITC como el yoduro de propidio (que penetra en las células la membrana cuya membrana está comprometida), tiñen la célula de color verde y rojo respectivamente. También se ha empleado una tinción conjunta con bromuro de etidio y naranja de acridina para conocer la viabilidad de las células (Baskić et al. 2006; Byczkowska et al. 2012), de modo que el

naranja de acridina penetra todas las células, se une a los ácidos nucleicos y las tiñe de verde, mientras que el bromuro de etidio solo penetra en aquellas cuya integridad de membrana está comprometida, y tras unirse a los ácidos nucleicos produce fluorescencia naranja.

I.6. Métodos de detección de micotoxinas

Existen diversos tipos de métodos analíticos, incluyendo biológicos, inmuno-enzimáticos y cromatográficos, presentando cada uno de ellos diferentes ventajas e inconvenientes. Los métodos biológicos se basan en la exposición de células u organismos vivos frente a muestras que pueden contener micotoxinas. Evaluando la viabilidad de las células u organismos frente a la exposición de muestras problemáticas se puede asociar la presencia de micotoxinas en estas muestras. Uno de los métodos biológicos habitualmente empleado para la detección de tóxicos producidos por mohos se basa en el empleo de microcrustáceos de la especie *Artemia salina* (López-Díaz et al. 2001; Núñez et al. 1996a; Núñez et al. 2007). A pesar de ser un método sencillo, de aportar información sobre la toxicidad y cuyo coste es muy bajo, tiene el inconveniente de que los microcrustáceos no son únicamente sensibles a micotoxinas, por lo que se pueden dar falsos positivos (Harwig and Scott 1971). Además, no tiene la capacidad de identificar que tóxico o tóxicos son los causantes de la muerte. Por tanto, esta metodología es adecuada para trabajar con un gran número de extractos procedentes de mohos, para testar su capacidad de producir toxinas, a modo de cribado previo a otros estudios más sensibles y específicos.

A pesar de que las micotoxinas se caracterizan por carecer de inmunogenicidad, actualmente existe disponibilidad de técnicas inmuno-enzimáticas para prácticamente todas las micotoxinas de interés (Köppen et al. 2010).. Existen variantes de estos métodos, tanto cualitativos como cuantitativos, llegando su sensibilidad a 2,5 µg/kg para el ELISA y a 1 µg/kg para FIA (Zheng et al. 2006). Se caracteriza por ser una reacción rápida, 0,5-2h, en la que un gran número de muestras pueden tener lugar y ser medidas simultáneamente. Sin embargo, presenta la limitación de que se necesita un análisis para cada una de las micotoxinas a determinar, ya que cada anticuerpo es específico para una micotoxina.

Las técnicas cromatográficas son las más sensibles debido a su gran capacidad para separar compuestos y sobre todo a los detectores que se emplean para identificar o cuantificar las micotoxinas. Estas técnicas analíticas se aplican a alimentos y piensos pudiendo ofrecer resultados en horas (Zheng et al. 2006)

La más sencilla de estas técnicas es la thin-layer chromatography (TLC), que se realiza en una placa metálica en la que se asienta la fase estacionaria formada por un gel de sílice a través del cual se separan los componentes del analito arrastrados por una fase móvil, constante en

composición a lo largo del análisis y que asciende por capilaridad. Finalmente, la placa se visualiza con luz ultravioleta que excita a algunas micotoxinas lo que permite revelar su presencia. Este método es rápido, barato y ofrece estimaciones cualitativas o semicuantitativas por inspección visual (Cigić and Prosen 2009), por tanto es capaz de testar un gran número de muestras con un coste muy bajo (Köppen et al. 2010). Sin embargo presenta limitaciones relacionadas con la cuantificación, siendo generalmente empleadas como técnicas cualitativas, además solo algunas micotoxinas son excitables con luz ultravioleta, por lo que para el análisis para aquellas que no presentan esta característica las placas deben tratarse con reactivos que permitan la visualización de las micotoxinas, lo que incrementa el coste económico y operacional del análisis. Debido a estas limitaciones y a la sensibilidad de otros métodos, los métodos de detección basados en TLC no suelen ser empleados en otros análisis que no sean *screenings* (Cigić and Prosen 2009).

La cromatografía de gases (CG) es adecuada para el análisis de compuestos térmicamente estables, de compuestos semipolares y apolares, volátiles y semivolátiles. La mayoría de las micotoxinas son moléculas pequeñas, no volátiles y polares que tienen que ser derivatizadas antes de ser analizadas por este método (Köppen et al. 2010), limitaciones que hacen que no sea la más empleada para analizar estos compuestos.

La metodología más comúnmente empleada para el análisis de un amplio rango de micotoxinas es la cromatografía líquida de alta resolución (HPLC) (Rodríguez et al. 2011; Rodríguez et al. 2012d; Andrade et al. 2014), a la que se le pueden acoplar diversos detectores. El detector ultravioleta es adecuado siempre y cuando la resolución del método cromatográfico sea muy alta, ya que no distingue entre diferentes compuestos que puedan coeluir y pasar por el detector simultáneamente. El detector de fluorescencia ofrece grandes ventajas en cuanto a coste del equipo, sin embargo su principal desventaja es que la mayoría de las micotoxinas tienen que ser derivatizadas para su detección. En general, como se ha citado anteriormente, todos los detectores requieren una buena separación cromatográfica de los compuestos, sin embargo este requisito no es necesario para el detector de masas (MS) ya que éste admite el solapamiento de algunos picos (Cigić and Prosen 2009). Una de las razones principales que han establecido al MS como método de referencia de detección de micotoxinas ha sido el desarrollo de dos tipos de fuentes de ionización: electrospray e ionización química a presión atmosférica (Köppen et al. 2010) que son capaces de ionizar tanto en forma positiva como en negativa, así como alternarse en la misma carrera cromatográfica, lo que radica en la mejor detección posible para todos los analitos. El desarrollo de la espectrometría de masas multietapa (MSⁿ) acoplado a HPLC ha permitido el aumento de la sensibilidad usando el modo *single reaction monitoring*

(SRM) para la determinación e identificación de micotoxinas seleccionadas tanto por sus pérdidas secuenciales características en su espectro como por el escaneo mejorado de iones producto para confirmar el patrón de fraccionamiento (Köppen et al. 2010).

También la electroforesis capilar (CE) también ha sido empleada para la detección de diferentes micotoxinas. La electroforesis capilar en zona (CEZ) se realiza en un capilar que contiene un tampón encargado de transmitir la corriente así como de contener el analito, a este capilar se le aplica una diferencia de potencial que hará desplazarse a través del capilar a los distintos componentes de analito dependiendo de su relación e/z . La electroforesis capilar electromicelar (MECE) contiene en el capilar un compuesto tensoactivo (habitualmente dodecilsulfato de sodio) que forma micelas, que es ideal para compuestos “neutros”. Esta última es la más empleada para el análisis de micotoxinas (Martín et al. 2004; Rodríguez et al. 2011; Rodríguez et al. 2012a; Luque et al. 2013). A ambas se le pueden acoplar los mismos detectores que al GC o al HPLC.

I.7. Transcriptómica.

La transcriptómica se encarga de estudiar y comparar el transcriptoma, o conjunto de ARN mensajero o transcritos presentes en una célula, tejido u organismo en un momento y unas circunstancias específicas. Los cambios provocados por las proteínas antifúngicas sobre los mohos pueden verse reflejados en la expresión génica, ya que es previsible que los antifúngicos influyan sobre ésta, bien por bloqueo de su síntesis en determinados genes como por la inducción en otros.

El estudio de la expresión génica permite conocer la respuesta que un organismo está ofreciendo en un momento determinado frente a cualquier agente. Conocer el valor de la expresión génica de un organismo tratado con respecto al no tratado para una serie de genes determinados ofrece información acerca de cómo el organismo se está viendo afectado por agente en cuestión y de cómo el organismo responde a dicho agente.

I.7.1. Métodos moleculares para la cuantificación de expresión génica

Entre las metodologías que se emplean de forma habitual para la cuantificación de expresión génica destacan los microarrays o chips y la PCR en tiempo real (qPCR). La primera es muy útil para la monitorización de múltiples genes simultáneamente, ofreciendo resultados globales en cuanto a cambios en la expresión abarcando todo el genoma. Sin embargo su principal desventaja es que el genoma a investigar debe haber sido secuenciado previamente. Cuando sólo se desea conocer la variación en la expresión de una serie de genes concretos o el

genoma completo no es conocido, pero sí los genes implicados en alguna ruta de interés, es habitual el uso de la RT-qPCR, en el que como paso previo se convierte el ARNm en ADN complementario (ADNc) mediante la enzima transcriptasa inversa. Este método no sólo permite conocer el desarrollo de la reacción en tiempo real, sino que además permite la cuantificación de la cantidad de ADN diana presente en la muestra. Además este tipo de técnicas presenta mayor sensibilidad y rapidez, y reduce la manipulación de las muestras (Heid et al. 1996)

I.7.2. Cuantificación de la expresión génica

Por lo tanto, mediante la RT-qPCR puede conocerse la cantidad de ARNm diana (tras convertirlo a ADNc) forma de presente en las muestras, y por lo tanto estudiarse la posible alteración de la expresión génica por la acción de proteínas antifúngicas. Para calcular su expresión existen principalmente dos métodos, cuantificación absoluta y cuantificación relativa.

La primera se basa en la cuantificación de las copias de genes diana presentes en el ADNc implicados en alguna ruta metabólica de interés. Mientras que el segundo se basa en la cuantificación de genes diana una vez realizada una normalización, ya sea con la expresión de otros genes que no se ven alterados por el tratamiento aplicado, denominados controles endógenos o con cantidad de ARN. Es muy recomendable que el gen elegido como control endógeno esté correctamente validado para cada experimento, de modo que la expresión génica no se vea afectada por el tratamiento empleado (Livak and Schmittgen 2001). Además son necesarios calibradores internos, que consisten en muestras similares pero que no son sometidas al tratamiento de estudio. De este modo se obtendrá la cuantificación relativa de la expresión génica en relación al calibrador interno.

Para ello existen dos alternativas, denominados método $2^{-\Delta\Delta Ct}$ y método $2^{-\Delta Ct}$, en función de los valores de eficiencia de las curvas estándar obtenidos previamente (Livak and Schmittgen 2001). En el primero las eficiencias de los genes diana y endógeno deben ser similares, no pudiendo ser las diferencias mayores del 10%, (Schmittgen and Livak 2008) y estar comprendidas entre 80 y 110%, lo que se corresponde con unos valores de pendiente de la recta de entre -3.1 y -3.6, además de que su valor de coeficiente de correlación (R^2) debe ser $\geq 0,98$ según ha sido descrito (Suanthie et al. 2009). En este método, como se ha indicado anteriormente se emplea una normalización a través de un gen endógeno. Mientras que el método $2^{-\Delta Ct}$ se emplea cuando las eficiencias de las curvas estándar de ambos genes no son similares. En este caso la normalización se lleva a cabo a través de la cantidad de ARN añadida a la reacción de ADNc (Livak and Schmittgen 2001).

II. OBJETIVOS

II. OBJETIVOS

El presente trabajo se encuadra en la línea de investigación sobre la obtención y caracterización de proteínas antifúngicas producidas por mohos aislados de alimentos, desarrollada por el grupo de Higiene y Seguridad Alimentaria dentro del Instituto Universitario de Investigación de la Carne y Productos Cárnicos de la Universidad de Extremadura. Dado que en los alimentos madurados con humedad intermedia o baja, como quesos y derivados cárnicos se desarrollan mohos que pueden contribuir a las características del producto final, pero que también pueden alterarlo y producir micotoxinas, es necesario disponer de medidas para controlar la población fúngica superficial. Los métodos eficaces para lograr este objetivo resultan poco adecuados para este tipo de alimentos. Una de las estrategias más prometedoras es la utilización de proteínas con efecto antifúngico solas o conjuntamente con microorganismos inhibidores que puedan potenciar mutuamente su actividad antagonista frente a mohos toxigénicos. Además para diseñar adecuadamente su utilización resulta conveniente conocer tanto el mecanismo de acción de estas proteínas antifúngicas, como los posibles mecanismos de resistencia de los mohos toxigénicos.

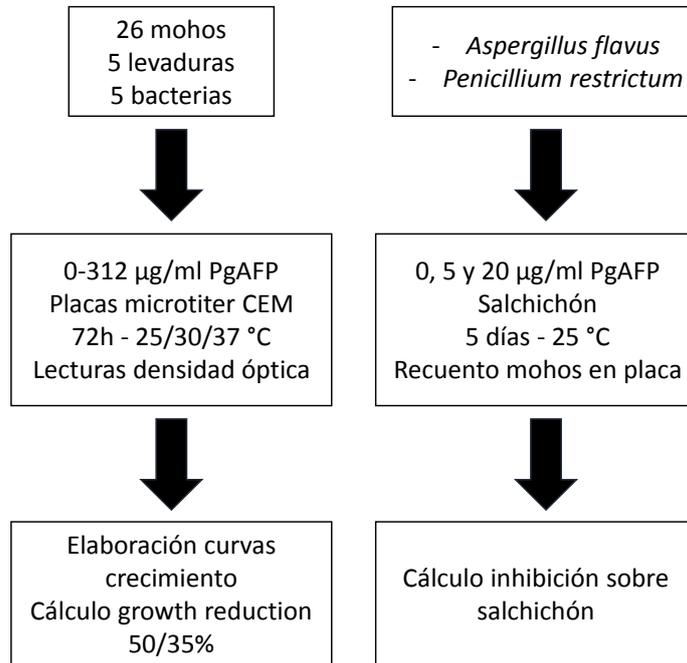
El objetivo fundamental del trabajo ha sido estudiar el efecto antifúngico y el mecanismo de acción de la proteína PgAFP producida por *Penicillium chrysogenum* aislado de jamón curado frente a mohos toxigénicos habituales en alimentos madurados. Para lograr este objetivo se plantearon los siguientes objetivos parciales:

- Establecer el espectro de inhibición de la proteína PgAFP frente a microorganismos habituales en alimentos madurados.
- Evaluar el efecto de PgAFP utilizada sola o en combinación con *Debaryomyces hansenii* o *Pedococcus acidilactici* sobre el crecimiento de mohos y la producción de micotoxinas.
- Estudiar el mecanismo de acción de PgAFP en mohos sensibles utilizando técnicas de proteómica comparativa y ensayos metabólicos y de viabilidad.
- Conocer la respuesta de mohos resistentes frente al tratamiento con PgAFP utilizando técnicas de proteómica comparativa y ensayos metabólicos y de viabilidad.
- Investigar el efecto de la presencia de calcio en el medio sobre la capacidad de inhibición de PgAFP en mohos sensibles utilizando técnicas de proteómica comparativa y ensayos metabólicos y de viabilidad.

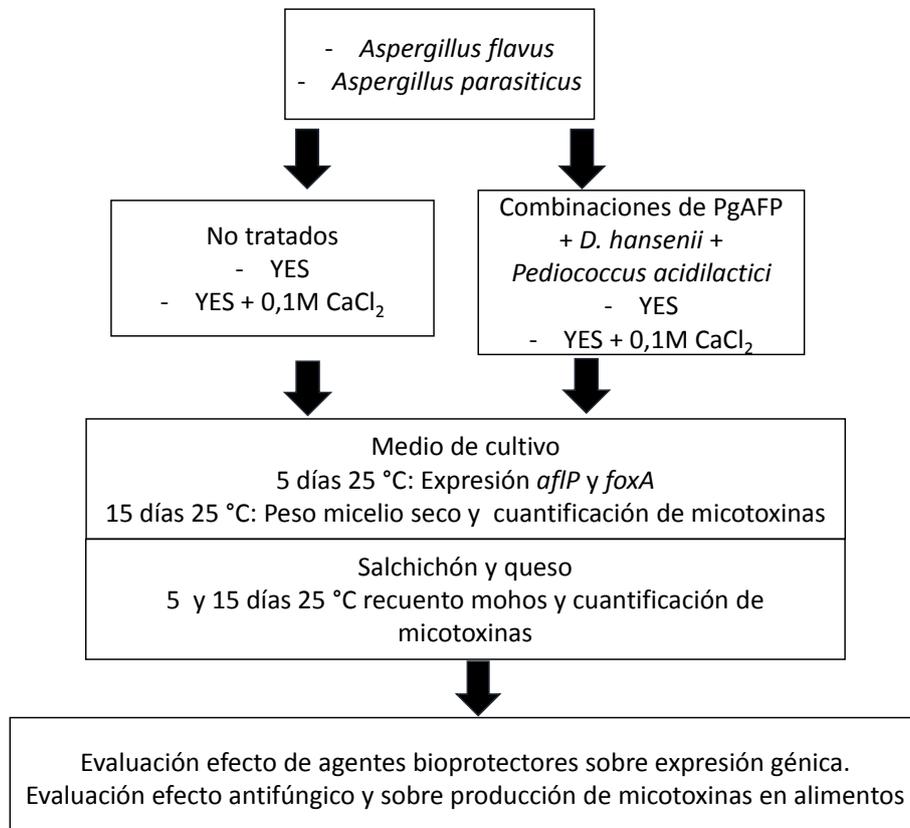
III. MATERIAL Y MÉTODOS

III.1. Diseño experimental

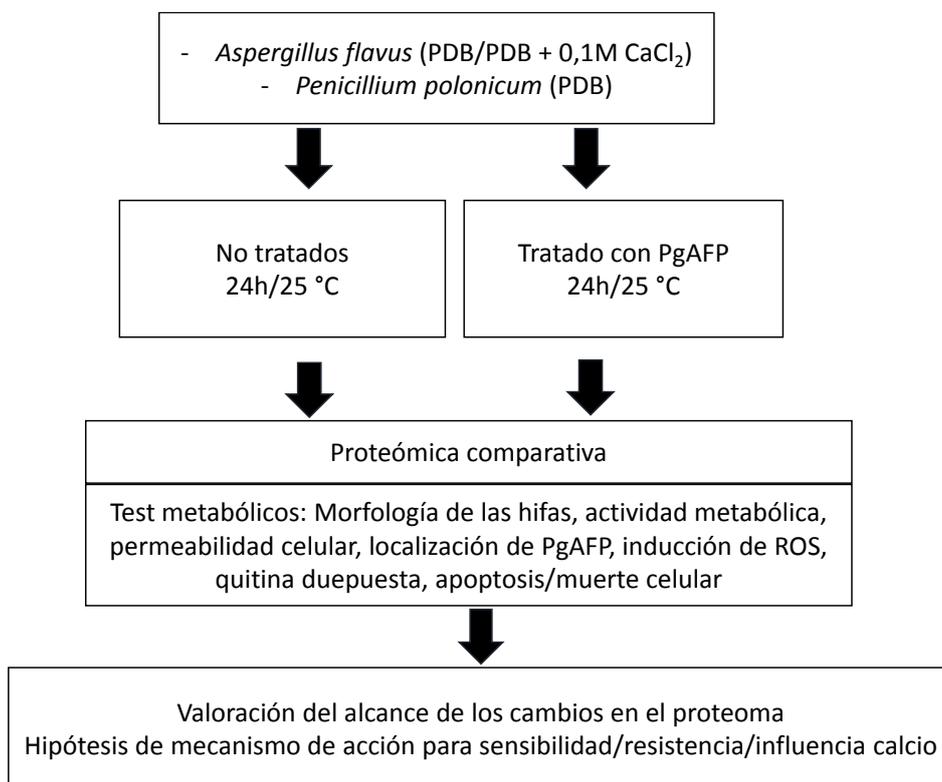
III.1.1. Estudio del espectro de inhibición de PgAFP



III.1.2. Estudio de la influencia de PgAFP sobre la síntesis de micotoxinas



III.1.3. Estudio del mecanismo de acción de PgAFP



III.2. Reactivos químicos

Los productos químicos empleados en el presente trabajo fueron calidad reactivo y suministrados por las firmas comerciales PANREAC (Castellar del Vallès, España), MERCK (Darmstadt, Alemania), Scharlau (Setmenat, España) y SIGMA (St. Louis, EEUU).

Los azúcares empleados fueron suministrados por la firma comercial SIGMA

Los colorantes fluorescentes FUN-1, SYTOX Green y Hoechst 33258 (Molecular Probes, Eugene, EEUU) fueron suministrados por Invitrogen y los colorantes fluorescentes 2', 7' dichlorofluorescein diacetate, apoptosis detection kit y fluorescent brightener 28 por SIGA. El marcaje de la proteína PgAFP con FITC fue realizado por la empresa DareBio S.L. (Elche, España).

Los reactivos SYBR green, ROX y el kit Prime Script™ RT reagent (Perfect Real Time) fueron provistos por Takara Bio Inc. El kit empleado para la extracción de ARN fue RNeasy® Plant Mini kit) (Quiagen, Hilden, Alemania) y el tratamiento con DNase I, RNase-free (Fermentas, St Leon, Alemania)

Los cebadores utilizados en las pruebas de PCR fueron suministrados por la empresa Biomol S.L. (Sevilla, España)

La quitinasa de *Streptomyces griseus* empleada fue adquirida de SIGMA (St. Louis, EEUU).

III.3. Medios de cultivo

Los medios de cultivo elaborados, así como los componentes utilizados procedieron de las casas comerciales OXOID (Unipath, Reino Unido), SCHARLAU (Setmenat, España), CULTIMED y MERCK (Darmstadt, Alemania).

En los diferentes ensayos realizados se utilizaron los siguientes medios:

Caldo extracto de malta (CEM)

Extracto de malta	20 g
Glucosa	20 g
Peptona	20 g
Agua destilada	1000 ml

Se esteriliza a 121°C durante 15 minutos y se ajusta al pH deseado

Caldo patata dextrosa (PDB)

Patata dextrosa	24 g
Agua destilada	1000 ml

Se esteriliza a 121°C durante 15 minutos y se ajusta al pH deseado

Agar patata dextrosa (PDA)

Patata dextrosa	24 g
Agar bacteriológico	20 g
Agua destilada	1000 ml

Se esteriliza a 121°C durante 15 minutos y se ajusta al pH deseado

Caldo yeast extract sucrose (YES)

Extracto de levadura	20 g
Sacarosa	125 g
Agua destilada	1000 ml

Se esteriliza a 121°C durante 15 minutos y se ajusta al pH deseado

III.4. Microorganismos

Se emplearon los siguientes mohos procedentes de la Colección Española de Cultivos Tipo (CECT, Valencia, España), del Centraalbureau voor Schimmelcultures (CBS, Utrecht, Holanda), o de la colección microbiana de Higiene y Seguridad Alimentaria, Universidad de

Extremadura (Cáceres, España): *Penicillium chrysogenum* (RP42C) CECT 20922, *Aspergillus awamori* CBS 101.702, *Aspergillus carbonarius* CECT 20384, *Aspergillus flavus* CECT 2687, *Aspergillus fumigatus* CBS 192.65, *Aspergillus ochraceoroseus* CBS 101.887, *Aspergillus ochraceus* CECT 2092, *Aspergillus oryzae* CECT 2095, *Aspergillus parasiticus* CECT 2682, *Aspergillus tamaris* CBS 109.63, *Aspergillus tubingensis* CECT 20545, *Aspergillus tubingensis* CECT 20932, *Aspergillus versicolor* CECT 2664, *Aspergillus westerdijkiae* CECT 2948, *Penicillium aurantiogriseum* CECT 2918, *P. chrysogenum* Pg222, *Penicillium commune* Pc131, *Penicillium commune* Pc332, *Penicillium echinulatum* Pe321, *Penicillium expansum* CECT 2280, *Penicillium griseofulvum* CECT 2919, *Penicillium nalgiovense* Pj261, *Penicillium nordicum* CBS 110.769, *Penicillium polonicum* Pp51, *Penicillium restrictum* Pr341, *Penicillium solitum* Ps321, *Penicillium verrucosum* AB11C, *Rhizopus oryzae* CBS 607.68 *Aspergillus tubingensis* CECT 20932. La cepa de levadura *Debaryomyces hansenii* 253H procedió de la Colección Española de Cultivos Tipo (CECT, Valencia, España) y la cepa de *Pediococcus acidilactici* (Fargo-35) empleada fue suministrada por la empresa Laboratorios Amerex (Madrid, España)

III.5. Equipos

Los medios de cultivo y otras pesadas rutinarias se realizaron en una balanza KERN (Balingen, Alemania) mod. 440-33 con precisión de 0,01g y las de precisión en una balanza Sartorius (Goettingen, Alemania) mod. LA310S con precisión de 0,1mg.

Las medidas de pH se realizaron en un pH-metro CRISON (Barcelona, España) mod. Basic 20

La esterilización de medios de cultivo, soluciones y material de laboratorio se realizó en un autoclave SELECTA (Barcelona, España) mod. Pesoclave 75.

Para la preparación de medios de cultivo se utilizaron placas calefactoras con agitación SELECTA (Barcelona, España) mod Agimatic N y un baño termostático SELECTA (Barcelona, España) PRECISTERM mod S-140.

Los microorganismos se incubaron en estufas refrigeradas VELP SCIENTIFICA mod. FOC 225 E, en incubadora orbital CERTOMAT™ IS Sartorius (Goettingen, Alemania), las esporas extraídas se conservaron en un congelador THERMO SCIENTIFIC mod. Forma 900 series, a -80 °C.

Las muestras de ADN, PgAFP, algunos reactivos que lo requerían y los extractos clorofórmicos o de acetonitrilo, previamente a su análisis, se almacenaron a -20 °C en un congelador vertical whirlpool modelo 6th sense.

Para la homogeneización de muestra en tubos se utilizó un agita-tubos VELP SCIENTIFICA (Usmate, Italia) mod. Vortex mixer.

Para la agitación de las muestras en la extracción de micotoxinas se empleó un agitador Heidolph (Kelheim, Alemania) mod Unimax 2010.

Las centrifugaciones fueron realizadas en una microcentrífuga refrigerada mod. 5417 C/R de EPPENDORF (Hamburgo, Alemania)

El tratamiento por calor de las muestras se llevó a cabo en un bloque térmico mod. TEMBLOC de SELECTA (Barcelona, España)

Todas las manipulaciones que requerían condiciones de esterilidad, se realizaron en campanas de flujo laminar TELSTAR (Tarrasa, España) mod. AV-30/70.

La filtración de los extractos clorofórmicos se llevó a cabo en una campana de extracción de gases CRUMA (El Prat de Llobregat, España) mod. 1200.

Para la esterilización de la proteína se emplearon filtros con adaptador a jeringa, de acetato de celulosa estériles, tamaño de poro 0,22 μ m (Fisherbrand, Fisher scientific, Waltham, EEUU). Los extractos clorofórmicos se filtraron a través de filtros de 0,45 μ m (Fisherbrand, Fisher scientific, Waltham, EEUU).

El agua destilada se obtuvo utilizando un destilador de USF mod. PURELAB pRO, (Fisher scientific, Waltham, EEUU).

Las placas estériles de 96 pocillos de fondo plano y sus correspondientes tapas empleadas en los diversos ensayos fueron de la marca Deltalab (Rubí, España).

Las cuantificación de fluorescencia en placas multipocillo se realizó en un lector de placas TECAN mod. Infinite M 2000 (Männedorf, Suiza).

Las lecturas de absorbancias de las placas multipocillo para la cuantificación del desarrollo fúngico se llevaron a cabo en un lector de MERCK (Darmstadt, Alemania) mod. MIOS MR 7000.

Las lecturas de absorbancia para la cuantificación proteica se realizaron en espectrofotómetro HitachiU-2000(Tokio, Japón).

El recuento de esporas se realizó en una cámara de Thoma de la marca Brand y un microscopio óptico Nikon SE. (Tokio, Japón)

Para la visualización de hifas con luz visible y sometidas a tinciones con colorantes fluorescentes se empleó un microscopio de fluorescencia Eclipse E200 equipado con una cámara digital DS-Fi2 (Nikon, Tokio, Japón)

La filtración de medios de cultivo y de tampones se realizó con ayuda de una bomba de succión LABOPORT (Trenton, USA) mod. KNF Lab, mediante un dispositivo de filtración de cristal y a través de filtros de membrana de acetato de celulosa de 47 mm de diámetro con poros de 8 μm , 1,2 μm , 0,45 μm y 0,22 μm (Sartorius, Goettingen, Alemania).

Para la evaporación de solventes orgánicos se empleó un rotavapor modelo VV2000 (Heidolph, Kelheim, Alemania)

La separación y purificación de los compuestos de naturaleza proteica con actividad antifúngica se llevó a cabo en un cromatógrafo líquido para la purificación rápida de proteínas (FPLC) mod. ÄKTA_{FPLC} con un colector de fracciones mod. FRAC-950 (Amersham Biosciences, Uppsala, Suecia) . El análisis de los resultados obtenidos se realizó con el programa informático UNICORN versión 4.12. Se utilizaron columnas de sefaroza HiTrapTMSP HP de intercambio catiónico, y columnas de filtración en gel HiLoad 26/60 SuperdexTM 75, (Amersham Biosciences, Uppsala, Suecia).

Para la extracción proteica del micelio, se empleó una sonda de sonicación (Bandelin Sonopuls, Berlin, Alemania), el total de proteínas extraídas fue separado en base al punto isoeléctrico mediante tiras Immobiline Dry strips (IPG strip; Amersham Biosciences, Uppsala, Suecia) de 7 y 13 cm, mediante un sistema de isoelectroenfoque IPGphorTM ambos provistos por GE Healthcare Life sciences (Freiburg, Alemania).

Las electroforesis de proteínas se realizaron en un Mini-PROTEAN System (Bio Rad, Hercules, EEUU) las de una dimensión y en Protean Xi-II Cell (Bio Rad, Hercules, EEUU) las de dos dimensiones.

La evaporación del líquido que contenían las proteínas digeridas previamente a su análisis espectrométrico se realizó en un DNA Speed Vac Concentrator (Thermo Fischer Scientific, Austin, EEUU). Las muestras fueron filtradas a través de filtros de centrifuga de 0,22 μm (Agilent Technologies, Dublín, Irlanda). El análisis espectrométrico se llevó a cabo mediante un Ion Trap LC-Mass Spectrometer 6340 Model (Agilent Technologies, Dublín, Irlanda) usando ionización mediante electrospray. Las muestras fueron cargadas sobre un Zorbax 300 SB C-18 Nano-HPLC Chip (150 mm x 75 μm).

Para los ensayos de proteómica libre de marcaje se realizó un desalado previo al análisis mediante C18 ZipTips[®] (Millipore, Darmstadt, Alemania) para ser analizados mediante un

espectrómetro de masas Q-Exactive acoplado a Dionex RSLCnano (Thermo Scientific, Waltham, EEUU).

Las concentraciones de ADN y ARN fueron medidas con un biofotómetro NanoDrop 2000c (Thermo Scientific, Waltham, EEUU).

El ARN fue transcrito a ADNc en un termociclador Mastercycler epgradient (Eppendorf AG, Hamburgo, Germany).

Las reacciones de q-PCR se llevaron a cabo en un equipo ViiATM 7 Real-Time PCR System (Applied Biosystems, Foster City, EEUU).

El análisis de micotoxinas se realizó mediante cromatografía líquida de alta resolución y detección mediante espectrometría de masas utilizando un uHPLC dionex ultimate 3000 pnp (Thermo Scientific, Waltham, EEUU), acoplado al espectrómetro de masas de tampa iónica Amazon (Bruker Daltonics, Bremen, Alemania). Para la cromatografía se empleó una columna C18 (10cm de longitud, 2,1mm diámetro interno y 2µm de tamaño de partícula) como fase estacionaria.

III.6. Software

Quant/Data analysis de Bruker se empleó para determinar la cantidad de micotoxinas que había en las muestras.

III.7. Páginas webs y herramientas empleadas

Para el estudio proteómico, las manchas seleccionadas de los geles 2D se identificaron utilizando MASCOT MS/MS ion search (http://www.matrixscience.com/cgi/search_form.pl?FORMVER=2&SEARCH=MIS). La búsqueda de proteínas homólogas y ortólogas se realizó en la base de datos del NCBI (National Centre for Biotechnology Information, www.ncbi.nlm.nih.gov/guide/proteins/). Para determinar la ruta metabólica en la que se encontraban involucradas las proteínas identificadas se utilizó el KEGG (Kyoto Encyclopedia of Genes and Genomes, www.genome.jp/kegg/). Para la búsqueda de secuencias genéticas y el diseño de cebadores se utilizó la base de datos del NCBI (<http://www.ncbi.nlm.nih.gov/gene/>) y algunas de sus herramientas como "Pick primers".

El tratamiento estadístico se llevó a cabo mediante el programa IBM SPSS v.22 (www-03.ibm.com/software/products/es/spss-stats-standard)

III.8. Métodos analíticos

III.8.1. Producción de PgAFP

La proteína PgAFP se obtuvo tras cultivar 10^7 esporas de *P. chrysogenum* RP42C en 500 ml de PDB a pH 4,5 durante 15 días a 25°C. Tras a incubación se procedió a separar el micelio y filtrar el medio a través de una membrana con tamaño de poro de 0,22 μm . Un volumen de 450 ml del medio de cultivo filtrado se sometieron a cromatografía líquida rápida de proteínas (FPLC) mediante una columna de intercambio catiónico, y a continuación la fracción que contenía a PgAFP se volvió a someter a cromatografía utilizando una columna de filtración en gel como describe (Acosta et al. 2009). La proteína purificada se esterilizó por filtración utilizando una membrana de 0,22 μm , Fisher scientific, Waltham, EEUU) de diámetro, se determinó su concentración por el método de (Lowry et al. 1951) y se almacenó a -20 °C hasta su uso.

III.8.2. Ensayos de inhibición

Los ensayos de inhibición se realizaron en placas multipocillo, inoculando en cada pocillo 10^5 esporas en 200 μl de PDB. Las placas se incubaron a 25 °C durante 96 h en condiciones estáticas. Para probar la actividad antifúngica en diferentes ensayos se utilizaron concentraciones de la proteína PgAFP entre 1,17 y 312 $\mu\text{g/ml}$. En todos los ensayos se incluyeron controles no tratados con PgAFP de los mohos estudiados. Cada ensayo se realizó por sextuplicado y el desarrollo fúngico se estimó mediante la densidad óptica de los pocillos inoculados medida a 550 nm cada 24 horas.

III.8.3. Extracción de proteínas del micelio

La extracción del total de proteínas del micelio de los mohos se realizó por triplicado inoculando las cepas en 50 ml de PDB en presencia (10 $\mu\text{g/ml}$) o ausencia de PgAFP. Los cultivos se incubaron en agitación (200 rpm) durante 24 horas a 25 °C. El micelio fue recogido, filtrado a través de un dispositivo miracloth (Merck Millipore, Darmstadt, Alemania), lavado con PBS y lisado como se ha descrito previamente (Carberry et al. 2006). El lisado fue centrifugado (10.000 x g; 30 min) para eliminar los restos de micelio y el sobrenadante fue recogido. La concentración total de proteínas fue calculada mediante el método de Bradford, utilizando el Kit proporcionado por Bio-Rad y leyendo a 595 nm: La calidad fue chequeada mediante electroforesis en gel de poliacrilamida (SDS-PAGE) de una dimensión.

Los minigeles de poliacrilamida se elaboraron utilizando los reactivos que se recogen en las tablas II1 y II2.

Tabla II1. Proporción de reactivos utilizados para la elaboración de los geles de poliacrilamida de separación (12% acrilamida).

Número de mini geles	5
1,5 M Tris-HCl, pH 8,3	7 ml
10% Dodecilsulfato sódico (SDS)	280 μ l
30% Acrilamida/0,8% Metilen bis acrilamida	11,3 ml
Agua destilada	9,3 ml
10% Amonio persulfato	100 μ l
TEMED	23 μ l

Tabla II2. Proporción de reactivos utilizados para la elaboración de los geles de poliacrilamida de concentración (4% acrilamida).

Número de mini geles	5
0,5 M Tris-HCl, pH 6,8	4 ml
10% Dodecilsulfato sódico (SDS)	160 μ l
30% Acrilamida/0,8% Metilen bis acrilamida	1,5 ml
Agua destilada	9,6 ml
10% Amonio persulfato	150 μ l
TEMED	15 μ l

En cada pocillo del gel se depositaron 20 μ g de proteínas, se le aplicó un voltaje de 80 V durante la primera hora, posteriormente se subió hasta 120 V y la electroforesis se dio por finalizada una vez que el frente llegó a la parte baja del gel. Una vez finalizada la carrera, el gel se tiñó durante 16 h con una solución compuesta por: 600 ml de agua destilada, 100 ml de ácido acético glacial, 300 ml de metanol y 1 g de comassie® brilliant blue R. Posteriormente, el gel se destiñó con una solución compuesta por 600ml de agua destilada, 100 ml de ácido acético glacial y 300 ml de metanol hasta que las bandas eran visibles sin ruido de fondo, y finalmente se lavó con agua destilada tres veces.

Una vez comprobada la calidad de las proteínas el lisado precipitado con ácido tricloroacético/acetona (Carpentier et al. 2005) para obtener el extracto con el que se llevaron a cabo dos ensayos proteómicos.

III.8.4. Análisis con 2D-PAGE

Un total de 250 µg de proteínas de cada extracto se resuspendieron en 200 µl de isoelectric focusing buffer (9,6 g de urea, 3,04 g de tiourea, 24 mg de Tris-base, 0,8 ml de chaps y 0,2 ml de Triton X-100, llevado a 20 ml de agua destilada) y se cargaron sobre las IPG strips. A continuación se realizó un electroisoelectroforesis y una electroforesis como se ha descrito previamente (Carberry et al. 2006). Los geles resultantes (3 réplicas biológicas y dos réplicas técnicas por tratamiento) fueron teñidas con Azul de Coomassie Coloidal, escaneadas y analizadas usando el software Progenesis™ SameSpot (TotalLab, Newcastle, UK) (O'Keeffe et al. 2013; Collins et al. 2013; Owens et al. 2014). Previamente al análisis comparativo la intensidad de las manchas fue normalizada por el citado software para corregir cualquier variación en la cantidad de proteínas cargada, la tinción/destinción o la adquisición de imágenes. Las manchas que mostraron diferencias significativas en su intensidad ($p < 0,05$, con un cambio cualitativo $\geq 1,5$) fueron recogidas y se realizó una digestión de las proteínas dentro del propio gel como se ha descrito previamente (Shevchenko et al. 2006). Los spots seleccionados fueron desteñidos por adición de 100 mM de amonio bicarbonato:acetonitrilo (1:1 v/v) durante 30 min. Se añadieron 500 µl de acetonitrilo a las muestras para deshidratar las piezas de gel recogidas, una vez deshidratadas el acetonitrilo se retiró y se añadieron 50 µl de tripsina (13 ng/µl). Las muestras fueron incubadas a 4 °C durante 2 h seguidos de una incubación overnight a 37 °C. Las muestras fueron sonicadas durante 10 minutos y el sobrenadante digerido fue transferido a tubos limpios para secarlo completamente con un DNA Speed Vac Concentrator, posteriormente se resuspendió cada muestra en 20 µl de ácido fórmico 0,1%. Las muestras se filtraron a través de filtros para centrífuga 0,22 µm. Las muestras se analizaron con un 6340 Model Ion Trap LC-Mass Spectrometer.. Para ello las muestras se cargaron sobre un Zorbax 300 SB C-18 Nano-HPLC Chip (150 mm x 75 µm) y se sometieron a un flujo de 4 µl/min con 0,1% (v/v) de ácido fórmico. Los péptidos eluidos fueron ionizados mediante electrospray y analizados por espectrometría de masas. El análisis de MSn fue llevado a cabo en los tres iones precursores de cada péptido, seleccionados automáticamente por el espectrómetro de masas. MASCOT MS/MS ion search, la base de datos NCBI (National Centre for Biotechnology Information, www.ncbi.nlm.nih.gov/guide/proteins/) y el KEGG (Kyoto Encyclopedia of Genes and Genomes, www.genome.jp/kegg/) se usaron para identificar las proteínas y su función.

III.8.5. Análisis con proteómica libre de marcaje

Para la cuantificación por proteómica libre de marcaje los lisados precipitados de tres replicas biológicas por tratamiento fueron resuspendidas en urea 8 M. Después de una reducción con dithiothreitol y alquilación mediada por ácido iodoacético (Owens et al. 2014), se añadió tripsina (grado secuenciación) combinada con ProteaseMax. Las muestras digeridas fueron desaladas previamente al análisis con C18 ZipTips® (Millipore, Darmstadt, Germany). De cada muestra digerida se analizó 1 µg a través de un espectrómetro de masas Q-Exactive acoplado a un Dionex RSLCnano (Thermo Scientific, Waltham, MA, USA). La cromatografía líquida se llevó a cabo utilizando un gradiente desde 4 al 35 % B (A: 0,1 % AF, B: 80 % Acetonitrilo, 0,1 % AF) durante más de 2 h, y los datos fueron recogidos usando un método Top15 para MS/MS scans (O’Keeffe et al. 2014; Dolan et al. 2014). La comparativa en la abundancia del proteoma así como el análisis de los datos se llevó a cabo con el software MaxQuant (Version 1.3.0.5; www.maxquant.org/downloads.htm; (Cox and Mann 2008), con Andromeda usado para la búsqueda en la base de datos y Perseus (Version 1.4.1.3) empleado para organizar los datos. Como modificación fija fue establecida la carbamidometilación de cisteínas, mientras que como modificaciones variables fueron fijadas la oxidación de metioninas y acetilación de N-terminales, para la identificación de proteínas mediante los citados softwares. . El máximo péptido/proteína false discovery rates (FDR) fue fijado en el 1 % basado en la comparación con una base de datos reversa. El algoritmo del análisis cuantitativo libre de marcaje fue usado para generar intensidades espectrales normalizadas e inferir la abundancia relativa de proteínas (Luber et al. 2010). Las proteínas fueron mantenidas en el análisis final si eran detectadas en al menos dos réplicas de al menos un tratamiento y las establecidas como contaminantes fueron eliminadas. El análisis cuantitativo fue llevado a cabo usando un t-test para comparar pares de muestras. Debido a la alta sensibilidad y un mayor rango dinámico que el análisis proteómico basado en geles, solo las proteínas con un cambio en cantidad ≥ 2 ($p < 0,05$) fueron incluidas en los resultados cuantitativos (O’Keeffe et al. 2014; Dolan et al. 2014). Los análisis cualitativos fueron llevados a cabo para detectar proteínas que fueron encontradas en al menos dos réplicas de una muestra en particular, pero no detectable en la comparación con el otro tratamiento.

III.8.6. Evaluación de la permeabilidad

Los mohos fueron cultivados a 25 °C durante 24 horas en presencia o ausencia de PgAFP de forma similar a la descrita en el epígrafe Ensayos de inhibición (III.8.2). Después de la incubación se añadió a los pocillos SYTOX Green para alcanzar una concentración final de 0,2 µM. La fluorescencia emitida fue medida en el minuto 10, 30 y 210 tras la adición de este

reactivo. Se empleó una longitud de onda de excitación de 480 nm (slit, 5 nm) y emisión de 530 nm (slit, 10 nm).

III.8.7. Morfología de las hifas

Las cepas fueron cultivadas en tubos que contenían 300 μ l of PDB a 25 °C durante 24 h tanto en presencia y en ausencia de PgAFP. El micelio fue recuperado por centrifugación y observado por microscopía óptica.

III.8.8. Actividad metabólica

Para evaluar la actividad metabólica los mohos se cultivaron, tanto en presencia como en ausencia de PgAFP. Posteriormente el micelio fue lavado con 10 mM HEPES (pH 7,5) antes de teñir con 100 μ l del colorante vital FUN-1 durante 30 min a 25 °C (Kaiserer et al. 2003). Las hifas teñidas fueron examinadas y fotografiadas mediante microscopía de fluorescencia, utilizando una longitud de onda de excitación 482/35 y 562/40 nm.

III.8.9. Tinción de quitina

Las esporas fueron inoculadas en placas de petri que contenían 10 ml PDB e incubados en presencia y ausencia de PgAFP a 25 °C durante 24 h (Harris et al. 1994). El micelio se fijó y tiñó durante 5 minutos con *fluorescent brightener 28* y fue lavado antes de ser visualizada la cantidad de quitina mediante microscopía de fluorescencia con una longitud de onda de excitación de of 387/11 nm.

III.8.10. Tinción del núcleo

Para visualizar la distribución de los núcleos en los mohos tratados y no tratados con PgAFP, los cultivos se tiñeron con 1.6 μ M del colorante Hoechst 33258 durante 30 min a 25 °C (Kaiserer et al. 2003). Este compuesto fluorescente tiñe la doble cadena de ADN, y permite la visualización de los núcleos a través de microscopía de fluorescencia utilizando una longitud de onda de excitación de 387/11 nm.

III.8.11. Localización de PgAFP en los mohos tratados

PgAFP fue marcada con FITC por DareBio S.L. (Elche, Spain). Para ello, 100 μ l de 20 mM FITC (Anaspec, Fremont, CA, USA) en dimetil sulfóxido fueron añadidos a 4 ml de PgAFP (369 μ g/ml). La mezcla se dejó durante 8 h a temperatura ambiente en oscuridad. Posteriormente fueron añadidos 100 μ l de 0,8 M Tris-HCl (pH 8,0) para llegar a una concentración final de 20 mM de Tris-HCl, y fue dializado frente a PBS. Para determinar el lugar de fijación de PgAFP las

cepas fueron cultivadas durante 24 h a 25 °C en presencia de 20 µg/ml de PgAFP marcado con FITC. A las 6 y a las 24 h las hifas fueron lavadas dos veces con PBS y visualizadas por microscopía de fluorescencia 482/35 nm. Como control, se llevó a cabo un ensayo adicional con FITC-PgAFP previamente tratado a 121 °C durante 15 min fue. Además, para comprobar que el marcaje no inactivaba la proteína, se realizó un ensayo de inhibición con 20 µg/ml de PgAFP marcada con FITC.

III.8.12. Detección de especies reactivas de oxígeno (ROS)

La inducción de producción de ROS por parte de PgAFP sobre diferentes cepas fue evaluado usando el 2', 7' diacetato de diclorofluoresceína como describe (Kaiserer et al. 2003) con algunas modificaciones. Los mohos fueron cultivados con 20 µM del citado colorante en presencia y ausencia de PgAFP durante 2 h a 25 °C, para ser observadas posteriormente mediante microscopía de fluorescencia con una longitud de onda de excitación de 482/35 nm.

III.8.13. Naranja de acridina (NA)/bromuro de etidio (BE) doble tinción

Las cepas de mohos cultivadas a 25 °C durante 24 h tanto en presencia y ausencia de PgAFP fueron teñidas con 4 µg/ml de NA/BE, incubadas 30 min a temperatura ambiente y lavadas dos veces con PBS para ser observadas por microscopía de fluorescencia (longitud de onda de excitación: 482/35 y 562/40 nm).

III.8.14. Detección de apoptosis o necrosis

Para distinguir entre células necróticas, apoptóticas tardías, y viables los mohos se cultivaron a 25 °C durante 12 o 24 h tanto en presencia como en ausencia de PgAFP. El ensayo fue llevado a cabo utilizando el kit para la detección de células apoptóticas/necróticas de SIGMA, compuesto por anexina V marcada con isotiocianato de fluoresceína / ioduro de propidio (AnV-FITC/PI). Tras la tinción siguiendo a las instrucciones del fabricante los cultivos se observaron mediante microscopía de fluorescencia utilizando una longitud de onda de excitación de 482/35nm para el FITC y 562/40 nm para el PI.

III.8.15. Capacidad de unión de PgAFP a quitina regenerada

La quitina regenerada fue preparada siguiendo el protocolo descrito por (Souza et al. 2009). Se utilizaron 5 g de quitina pulverizada de conchas de cangrejos a la cual se le añadió 60 ml de HCl concentrado con agitación vigorosa durante una hora y fue filtrada, a continuación se le añadió etanol al 50%. El precipitado fue filtrado y lavado con agua sucesivas veces hasta alcanzar un pH de 7. La quitina coloidal fue almacenada a 4 °C en la oscuridad. El ensayo de

unión de PgAFP a la quitina se llevó a cabo como se ha descrito previamente (Liu et al. 2002). Para ello, 146, 292, y 635 μg de PgAFP se mezclaron con 4mg de quitina y completado hasta 1ml con el buffer de reacción (0,1M Tris/HCl pH 7,4, 150mM NaCl). La mezcla se incubó durante una hora en hielo con agitaciones periódicas cada 15 minutos. Tras la incubación las muestras se centrifugaron y la cantidad de PgAFP contenida en el sobrenadante fue medida por el procedimiento descrito anteriormente (Lowry et al. 1951).

III.8.16. Combinación Quitinasa y PgAFP

Para investigar el papel de la quitina en el mecanismo de defensa de *P. polonicum*, se realizó un ensayo en el que se trató con quitinasa al moho mientras se desarrollaba para debilitar su pared celular y ver como influía este hecho en la resistencia frente a PgAFP. *P. polonicum* se cultivó en placas en cuatro condiciones distintas:

- Control: Medio PDA
- Q: PDA con quitinasa a una concentración final de 0,4 ud/ml.
- P: PDA con PgAFP a una concentración final de 100 $\mu\text{g}/\text{ml}$.
- Q+P: PDA con quitinasa (0,4 ud/ml) y PgAFP (100 $\mu\text{g}/\text{ml}$)

Cada placa fue inoculada por triplicado con 10 μl de una suspensión que contenía 10^4 esporas y el diámetro de los triplicados fue medido cada 24 horas desde la hora 48 a la 144.

III.8.17. Extracción ADN

Para testar la sensibilidad de los cebadores diseñados para la qPCR se extrajo ADN de *A. flavus* y *A. parasiticus*. Se realizó la extracción siguiendo el método previamente descrito por (Rodríguez et al. 2012b), para ello se cultivaron las cepas durante una semana en PDA a 25 °C, se recogió una muestra de 50 mg de micelio en condiciones de esterilidad, se congeló con nitrógeno líquido para facilitar la ruptura del micelio y fue machacado hasta pulverizarlo con ayuda de un mortero y una maza . Se incubaron en 500 μl de buffer CTAB que contenía 5 μl de β -mercaptoetanol y se le añadieron 10 μl de proteinasa K (10 mg/ml) y se incubó durante 1 h a 65 °C. Posteriormente se añadieron 10 μl de ARNasa (10 mg/ml). Entre cada uno de los anteriores tratamientos se aplicaron lavados con cloroformo que se eliminó tras ser separado a través de centrifugación. Se le añadió isopropanol (-20 °C) para precipitar el ADN, se lavó con etanol al 70% y se centrifugó para precipitar el ADN con el fin de retirar el etanol. Finalmente el ADN obtenido se resuspendió en 100 μl de Tris-EDTA buffer pH 8 y se congeló (-20 °C) hasta su posterior empleo.

III.8.18. Extracción ARN

Para evaluar la expresión de algunos genes de interés en presencia de diferentes microorganismos y de PgAFP, se inocularon 10^5 esporas/ml de *A. flavus* o *A. parasiticus* en dos lotes, por una parte 2 ml de YES y por otra 2 ml de YES suplementado con CaCl_2 para obtener una concentración final de 0,1M. Además se inocularon 10^6 células/ml de *D. hansenii* y *P. acidilactici* y $10 \mu\text{l/ml}$ de PgAFP tanto por separado como conjuntamente. Se incubó durante 5 días a 25°C , realizándose cada ensayo por triplicado.

El micelio fue recuperado y lavado con PBS previamente a su congelación con nitrógeno líquido. Fue machacado mientras estaba sumergido en nitrógeno líquido con ayuda de un mortero y maza. El polvo resultante fue resuspendido en $750 \mu\text{l}$ de RLT buffer, proporcionado por el RNeasy® Plant Mini kit, suplementado con $15 \mu\text{l}$ de β -mercaptoetanol y se siguió el protocolo de acuerdo con las instrucciones del fabricante. Para eliminar la contaminación del ADN genómico, las muestras fueron tratadas con DNasa siguiendo las instrucciones del fabricante. La concentración y pureza del ARN se determinó a través de un espectrofotómetro nanodrop.

III.8.19. Desarrollo del micelio y extracción de micotoxinas en medio de cultivo

El efecto de *D. hansenii*, *P. acidilactici* y $10 \mu\text{l/ml}$ de PgAFP frente a *A. flavus* y *A. parasiticus* tanto de forma independiente, como de diferentes combinaciones se estudió en medio YES y en este medio enriquecido con 0,1 M de CaCl_2 , utilizando los siguientes lotes:

- Lote control: inoculación con 10^5 esporas/ml de *A. flavus* o *A. parasiticus*.
- Lote Pg: inoculación con 10^5 esporas/ml de *A. flavus* o *A. parasiticus* y $10 \mu\text{l/ml}$ de PgAFP.
- Lote Dh: inoculación con 10^5 esporas/ml de *A. flavus* o *A. parasiticus* y 10^6 células/ml de *D. hansenii*.
- Lote Pa: inoculación con 10^5 esporas/ml de *A. flavus* o *A. parasiticus* y 10^6 células/ml de *P. acidilactici*.
- Lote Pg+Dh: inoculación con 10^5 esporas/ml de *A. flavus* o *A. parasiticus*, $10 \mu\text{l/ml}$ de PgAFP y 10^6 células/ml de *D. hansenii*.
- Lote Pg+Pa: inoculación con 10^5 esporas/ml de *A. flavus* o *A. parasiticus*, $10 \mu\text{l/ml}$ de PgAFP y 10^6 células/ml de *P. acidilactici*.
- Lote Dh+Pa: inoculación con 10^5 esporas/ml de *A. flavus* o *A. parasiticus*, 10^6 células/ml de *D. hansenii* y 10^6 células/ml de *P. acidilactici*.
- Lote Pg+Dh+Pg: inoculación con 10^5 esporas/ml de *A. flavus* o *A. parasiticus*, $10 \mu\text{l/ml}$ de PgAFP, 10^6 células/ml de *D. hansenii* y 10^6 células/ml de *P. acidilactici*.

Cada muestra contenía 5 ml del citado medio de cultivo y todos los lotes se incubaron durante 15 días a 25 °C. El crecimiento fúngico se evaluó mediante el peso seco del micelio. Para ello se recuperó el micelio con un filtro miracloth, se deshidrató a 100 °C durante 15 min y tras su enfriamiento en un desecador se pesó. La producción de micotoxinas se evaluó tras realizar una extracción clorofórmica. Una vez eliminado el micelio, a cada tubo que contenía el caldo de cultivo donde se habían desarrollado las cepas se añadieron 5 ml de cloroformo. Se incubó durante 1 h en agitación a 100 rpm a temperatura ambiente, posteriormente se separó el cloroformo y se dejó evaporar en una campana de gases durante 72 h en oscuridad. Todos los ensayos se realizaron por triplicado. Las micotoxinas se analizaron como se indica más adelante (apartado III.8.20.4).

III.8.20. Ensayos en alimentos

Para llevar a cabo los ensayos simulando el proceso de maduración de los alimentos (queso y salchichón) se emplearon recipientes de metacrilato que fueron esterilizados previamente a su empleo. Para ello se dejaron 24 horas conteniendo etanol y posteriormente se vaciaron y se dejaron secar 12h bajo luz ultravioleta. Para emular las condiciones ambientales de a maduración, se empleó una solución de KCl sobresaturada que proporciona una humedad relativa del 84% después del equilibrio de vapor. La carga microbiana de los alimentos se redujo mediante inmersión en etanol, que posteriormente se dejó evaporar en la cabina de flujo laminar. A continuación se inocularon los diferentes microorganismos y cantidades de PgAFP dependiendo del experimento a realizar.

III.8.20.1. Efecto antifúngico de PgAFP en alimentos madurados

Una solución de proteína PgAFP (200 µl) se añadió sobre la superficie de salchichón o queso para llegar a una concentración final de 5 y 20 µg/cm². La solución se distribuyó en la superficie y se esperó hasta que el líquido fue absorbido por el alimento. A continuación se procedió a la inoculación de 10⁴ esporas de *A. flavus* o *P. restrictum*. Se preparó un lote control añadiendo un volumen de PBS equivalente al utilizado para incorporar la proteína. Todos los lotes se incubaron durante 5 días a 25 °C. Al final de la incubación se procedió a fotografiar los alimentos y se determinó el recuento de los mohos tras la siembra de diferentes diluciones decimales en placas de PDA, que se incubaron 72 h a 25 °C.

III.8.20.2. Efecto antifúngico de la aplicación conjunta de PgAFP, *D. hansenii* y *P. acidilactici* en alimentos madurados

En este ensayo, realizado en salchichón y queso siguiendo un procedimiento análogo al descrito en el apartado anterior se utilizaron los siguientes lotes:

- Lote control: alimentos inoculados con 10^5 esporas/cm² de *A. flavus* o *A. parasiticus*.
- Lote Pg+Dh: alimentos inoculados con 10^5 esporas/cm² de *A. flavus* o *A. parasiticus*, $10 \mu\text{l/cm}^2$ de PgAFP y 10^6 células/cm² de *D. hansenii*.
- Lote Pg+Dh+Pa: alimentos inoculados con 10^5 esporas/cm² de *A. flavus* o *A. parasiticus*, $10 \mu\text{l/cm}^2$ de PgAFP, 10^6 células/cm² de *D. hansenii* y 10^6 células/cm² de *P. acidilactici*

Los tres lotes se incubaron 15 días a 25 °C y se tomaron muestras a los 5 y 15 días para evaluar el desarrollo de los microorganismos así como la producción de micotoxinas. El desarrollo microbiano se evaluó mediante el recuento en placas de PDA (mohos y levaduras) y MRS (pediococos). Las colonias de mohos y levaduras se diferenciaron de acuerdo con su morfología. La determinación de micotoxinas se realizó como se describe en la siguiente sección. En todos los casos los ensayos se llevaron a cabo por triplicado.

III.8.20.3. Extracción de micotoxinas de alimento

Las micotoxinas producidas sobre el salchichón y queso se extrajeron de acuerdo al método descrito por (Rodríguez et al. 2012d). El alimento troceado se maceró en agitación durante una hora en un matraz opaco con 60 ml de acetonitrilo-agua (9:1, v/v) conteniendo 0,1% de ácido fórmico y además 50 ml de hexano. La fase constituida por acetonitrilo-agua se recuperó, fue filtrada a través de sodio sulfato anhidro. A continuación se le añadieron 50 ml de hexano adicionales y se maceró en agitación durante media hora. La fase compuesta por acetonitrilo-agua fue recuperada nuevamente, filtrada y evaporada por medio de un rotavapor a 40-45 °C. El residuo se resuspendió en 1 ml de cloroformo, filtrado a través de $0,45 \mu\text{m}$ (Fisher scientific, Waltham, EEUU) y evaporado. Se almacenaron a -20 °C hasta su análisis.

III.8.20.4. Detección y cuantificación de micotoxinas

El análisis y caracterización de las micotoxinas se realizó mediante uHPLC-MS, HPLC Thermo Scientific Dionex ultimate 3000 pnmp (Thermo Scientific, Waltham, MA, USA), a mass detector (MS) ion trap model Bruker Amazon S.L., an autosampler (Ultimate 3000), a degasser (3000 Ultimate) (Bruker Daltonics, Bremen, Alemania). La fase estacionaria empleada fue una columna de fase reversa C18 de 10 cm de longitud, 2,1 mm de diámetro y con tamaño de

partícula de 2 µm de diámetro. Mientras que la fase móvil empleada fue tampón 0,1% ácido fórmico-10 mM formiato amónico (solvente A) y acetonitrilo (solvente B), ambos fueron filtrados a vacío con una membrana de 0,22 µm de tamaño de poro previamente a su uso. La separación se realizó con flujo de 200 µl/min mediante un gradiente programado según se describe en la Tabla (II3)

Tabla II3. Gradiente utilizado para la separación mediante uHPLC.

Tiempo (min)	0,00	0,10	4,00	7,00	8,50	8,51	12,00	12,01	15,00
%B	2	40	60	80	80	98	98	2	2

La detección de las micotoxinas se llevó a cabo utilizando una fuente de ionización por electroespray (ESI) en las siguientes condiciones reflejadas en la Tabla II4:

Tabla II4. Condiciones de la fuente de ionización.

Gas de nebulización	N2, 7,3 psi
Gas de secado	N2, 4 l/min, 180°C
Voltaje del capilar	4.500 v
End plate offset	500 v
Modo de trabajo	ESI-MS/MS
Velocidad de scan	32.500 u/s
Rango de m/z	70-2.200

La identificación de las micotoxinas se realizó en base a dos parámetros: tiempo de retención y relación masa/carga de los compuestos detectados. Los resultados de estos parámetros fueron comparados con los obtenidos mediante el análisis de patrones de las diferentes micotoxinas que figuran en la Tabla II5.

Tabla II5. Iones empleados para la detección y cuantificación de aflatoxinas.

Micotoxina	Ión precursor	Ión de cuantificación
Aflatoxina B1	313	285
Aflatoxina G1	329	311

IV. RESULTADOS

IV.1. Espectro de acción de PgAFP frente a mohos toxigénicos y capacidad antifúngica sobre producto crudo-curado madurado

*Growth inhibition and stability of PgAFP from *Penicillium chrysogenum* against fungi common on dry-ripened meat products*



Growth inhibition and stability of PgAFP from *Penicillium chrysogenum* against fungi common on dry-ripened meat products



Josué Delgado, Raquel Acosta, Andrea Rodríguez-Martín, Elena Bermúdez, Félix Núñez, Miguel A. Asensio *

Food Hygiene and Safety, Institute of Meat Products, University of Extremadura, Avenida de la Universidad s/n, 10003 Cáceres, Spain

ARTICLE INFO

Article history:

Received 28 December 2014

Received in revised form 13 March 2015

Accepted 30 March 2015

Available online 3 April 2015

Keywords:

Antifungal protein
Growth inhibition
Aspergilli
Penicillia
Mycotoxin
Dry-ripened foods

ABSTRACT

Dry-ripened foods favor the development of a superficial fungal population that may include toxigenic molds. To combat unwanted molds, an antifungal protein from *Penicillium chrysogenum* (PgAFP) can be useful. The aim of the present work was to study the antimicrobial activity of PgAFP against microorganisms common in dry-ripened foods, and to evaluate its sensitivity to proteolytic enzymes and heat treatments that may be applied to foods, as well as to different pH values. The inhibitory effect of the purified protein on 38 microbial strains grown in culture medium was determined. PgAFP sensitivity to various proteases, heat treatments, and preincubation at different pH values was tested by means of the residual activity on selected reference strains. Inhibitory activity of PgAFP against unwanted molds was tested in a dry-fermented sausage. This protein exhibited potent inhibitory activity against unwanted molds, including the main mycotoxin-producing species of *Aspergillus* and *Penicillium* of concern for dry-ripened foods. PgAFP withstood most proteases, intense heat and a wide range of pH values. PgAFP efficiently reduced counts of *A. flavus* and *P. restrictum* inoculated on a dry-fermented sausage. This protein can be of interest to control hazardous molds in dry-ripened foods.

© 2015 Elsevier B.V. All rights reserved.

1. Introduction

Most dry-ripened foods favor the development of a superficial fungal population that may include toxigenic molds, mainly *Aspergillus* and *Penicillium* spp., and yeasts such as *Debaryomyces* and *Candida* spp. Surface treatments and packaging may help to control unwanted fungi, but they are not adequate to prevent fungal growth during ripening of mold-ripened cheese, ham, or sausage. Research on new antifungal agents has increased during the recent years due to the increase in human fungal infections, mainly involving immunocompromised patients (Fox, 1993). Many proteins and peptides with antifungal activity from plants, bacteria, arthropods, amphibians, or reptiles have been purified and characterized (Dimarcq et al., 1998; Selitrennikoff, 2001; Wang and Ng, 2003). The number of antifungal proteins described from molds so far is rather limited to AFP from *Aspergillus giganteus* (Nakaya et al., 1990; Lacadena et al., 1995), AnaFP from *Aspergillus niger* (Lee et al., 1999), AcAFP from *Aspergillus clavatus* (Skouri-Gargouri and Gargouri, 2008), NFAP from *Neosartorya fischeri* (Kovács et al., 2011), PAF (Marx et al., 1995), PgAFP (Rodríguez-Martín et al., 2010), and Pc-Arctin (Chen et al., 2013) from *Penicillium chrysogenum*. Most of these proteins have some common characteristics, such as small size (5.8–6.6 kDa), high ratio of cysteine residues, and basic character due to the presence of a high content of arginine and lysine residues (Marx, 2004; Skouri-Gargouri et al., 2009; Rodríguez-Martín

et al., 2010). The antifungal proteins from molds show potent activity against filamentous fungi, although differences in sensitivity have been reported (Marx, 2004). Only AnaFP proved to be active against yeasts (Lee et al., 1999) but none has been shown to inhibit the bacteria tested so far (Marx, 2004).

The amino acid sequence of PgAFP showed only 34% identity with PAF, produced by a different strain of *P. chrysogenum* (Rodríguez-Martín et al., 2010). PgAFP is the only antifungal protein isolated from a foodborne mold, as the *P. chrysogenum* strain which produces it (CECT 20922; formerly *P. chrysogenum* RP42C) was isolated from dry-cured ham (Acosta et al., 2009). Given that PgAFP was active against some toxigenic species of both *Penicillium* and *Aspergillus* (Acosta et al., 2009), the potential inhibition of other unwanted organisms of significance for dry-ripened foods, deserves further investigation.

Microbial proteases are responsible for proteolysis on dry-ripened foods. The addition of enzymes of plant or microbial origin, such as pappain or flavourzyme from *Aspergillus oryzae*, has been proposed to accelerate the ripening process of dry-fermented sausages (Fernández et al., 2000). Thus, the antifungal proteins intended for use in foods should be resistant to common proteolytic enzymes. Thus, evaluating the sensitivity of PgAFP to commercial proteases is of interest. The effectiveness of antifungal proteins from molds can also be limited by pH of the food and heat treatments applied.

The efficacy of PgAFP could be affected also by other characteristics of the food, such as water activity, temperature, chemical composition, and microbial population; thus the antifungal activity of PgAFP should be tested on dry-fermented meat products.

* Corresponding author. Tel.: +34 927 257124; fax: +34 927 257110.
E-mail address: masensio@unex.es (M.A. Asensio).

The objective of this work was to study the antimicrobial activity of PgAFP against some of the main microorganisms of significance for dry-ripened foods, to evaluate the sensitivity of the protein to proteolytic enzymes and heat treatments that may be applied to foods, as well as to different pH values. Finally, the inhibitory activity of PgAFP was checked against unwanted molds on dry-fermented sausages.

2. Materials and methods

2.1. Reference organisms

Inhibition tests were carried out against 38 microbial strains from 26 fungal species, five yeasts, and five bacteria. The following strains were obtained from the Spanish Type Culture Collection (CECT, Valencia, Spain), the Centraalbureau voor Schimmelcultures (CBS, Utrecht, The Netherlands), or the microbial collection of Food Hygiene and Safety, University of Extremadura (Cáceres, Spain): *Aspergillus awamori* CBS 101.702, *Aspergillus carbonarius* CECT 20384, *Aspergillus flavus* CECT 2687, *Aspergillus fumigatus* CBS 192.65, *Aspergillus niger* An261, *Aspergillus ochraceo-roseus* CBS 101.887, *Aspergillus ochraceus* CECT 2092, *Aspergillus oryzae* CECT 2095, *Aspergillus parasiticus* CECT 2682, *Aspergillus tamarii* CBS 109.63, *Aspergillus tubingensis* CECT 20545, *Aspergillus versicolor* CECT 2664, *Aspergillus westerdijkiae* CECT 2948, *Penicillium aurantiogriseum* CECT 2918, *P. chrysogenum* CECT 20922 (formerly *P. chrysogenum* RP42C), *P. chrysogenum* Pg222, *Penicillium commune* Pc131, *Penicillium commune* Pc332, *Penicillium echinulatum* Pe321, *Penicillium expansum* CECT 2280, *Penicillium griseofulvum* CECT 2919, *Penicillium nalgiovense* Pj261, *Penicillium nordicum* CBS 110.769, *Penicillium polonicum* Pp51, *Penicillium restrictum* Pr341, *Penicillium solitum* Ps321, *Penicillium verrucosum* AB11C, *Rhizopus oryzae* CBS 607.68; *Candida zeylanoides* CECT 10048, *Debaryomyces hansenii* CECT 10360, *Debaryomyces hansenii* Dh345, *Rhodotorula mucilaginosa* CECT 10359, *Yarrowia lipolytica* CECT 10358; *Brochothrix thermosphacta* PA7B2, *Escherichia coli* CECT 4267, *Listeria monocytogenes* CECT 4032, *Salmonella enterica* subsp. *enterica* CECT 4374, and *Serratia liquefaciens* PA7VRBG.

2.2. Protein purification

The PgAFP producing *P. chrysogenum* CECT 20922 was inoculated into malt extract broth (20 g/L malt extract, 20 g/L glucose, and 1 g/L peptone; MEB), pH 4.5, and incubated up to 21 days at 25 °C without shaking. PgAFP was obtained from the cell free medium by fast protein liquid chromatography with a cationic exchange column HiTrap SP HP (Amersham Biosciences, Uppsala, Sweden), further purified with a HiLoad 26/60 Superdex 75 gel filtration column for FPLC (Amersham Biosciences), and concentrated as previously described (Acosta et al., 2009; Rodríguez-Martín et al., 2010).

Protein concentration in the purified extract was estimated by protein nitrogen determination according to the Johnson method (Johnson, 1941). To calculate the concentration of protein, the nitrogen percentage of 19.17% deduced from the amino acid composition of PgAFP (Rodríguez-Martín et al., 2010) was used.

2.3. Growth inhibition of reference organisms

Quantitative assay for microbial growth inhibition was carried out by a microspectroscopic method (Acosta et al., 2009) adapted from Broekaert et al. (1990). The inhibition test was performed in 96-well microtiter plates, with 100 µL of the purified protein mixed with 100 µL of culture media containing ca. 10⁶ CFU/mL of the reference organism per well. Molds and yeasts were grown in double-strength (82 g/L) MEB, whereas bacteria were cultivated in double-strength (74 g/L) brain heart infusion broth (BHI, Scharlab, Barcelona, Spain). The final concentration of PgAFP in the wells was set from 1.2 to 312.7 µg/mL (0.2 to 48.2 µM). The assay was run in sextuplicate wells, using separate plates for each reference strain. The corresponding

fraction from uninoculated medium, also purified by gel filtration, was used as negative control. Fungal cultures were incubated for up to 120 h at 25 °C and bacterial cultures were incubated for 48 h at 20 °C. Growth was monitored by measuring the optical density variation at 595 nm every 24 h for fungi or 12 h for bacteria. Growth reduction (GR) was defined as the lowest PgAFP concentration that produced prominent growth reduction of 50% (GR50) or 35% (GR35) compared to control plates, according to Espinel-Ingroff et al. (1997).

2.4. Susceptibility to enzymes

The sensitivity of PgAFP to digestion by enzymes was tested using the following commercial enzymes dissolved individually as indicated: pepsin, in 0.3 M KCl, 0.15 M NaCl, pH 2; lysozyme and papain, in 0.3 M PO₄Na₂, 0.15 M NaCl, pH 6.2; ficin, in 0.3 M PO₄Na₂, 0.15 M NaCl, pH 7; flavourzyme, in 0.3 M PO₄Na₂, 0.15 M NaCl, pH 7.5; pronase E and trypsin, in 0.3 M PO₄Na₂, 0.15 M NaCl, pH 7.5. All enzymes were obtained from Sigma Chemical Co. (St. Louis, USA) and used at a final concentration of 500 µg/mL. PgAFP was added at different concentrations (8 to 130 µg/mL, 1.2 to 20 µM) to enzyme preparations, and the mixtures were incubated 12 h at the following optimal temperatures recommended for each enzyme by manufacturer: 25 °C for lysozyme, papain, and trypsin, and 37 °C for the remaining enzymes. Then, the residual antifungal activity against *A. flavus* CECT 2687, *A. niger* An261, *P. griseofulvum* CECT 2919, and *P. restrictum* Pr341 was tested by the microspectroscopic method. Aliquots of the prepared PgAFP concentrations without enzyme treatment were used as positive control. Additional tests with 500 µg/mL of each enzyme and no PgAFP were run to discount interferences with mold growth.

2.5. Stability to heat treatments

The study of the protein stability after heat treatment was carried out according to Okkers et al. (1999). Aliquots of PgAFP protein (300 µg/mL) were exposed to different combinations of temperatures (60, 80, and 100 °C) and times (10, 20, and 30 min) in a dry block heater Termobloc (JP Selecta, Barcelona, Spain), as well as to 121 °C for 15 min in an autoclave cycle. After heat treatment, the samples were cooled on ice and tested for antifungal activity in microtiter plates. The reference strains tested were *Aspergillus niger* An261 and *Penicillium restrictum* Pr341.

2.6. pH stability

PgAFP (300 µg/mL) was retained in microcon centrifugal filter units YM-3 (Millipore) and then dissolved in different buffers at the following values: pH 1, 2 (HCl/KCl); pH 3 (glycine/HCl); pH 4, 5, 6 (citric acid/sodium phosphate); pH 7 (sodium phosphate/NaCl); pH 8 (Tris/HCl); pH 9, 10 (Tris/NaOH); and pH 12 (KCl/NaOH). Samples were incubated at 25 °C for 2 h and the pH adjusted to 4.5 before testing the antifungal activity. Negative controls with no PgAFP added were prepared following the same procedure. The reference strains tested were *Aspergillus niger* An261 and *Penicillium restrictum* Pr341.

2.7. Antifungal activity of PgAFP on dry-fermented sausages

The effect of PgAFP on growth of toxigenic molds was tested using a commercial raw dry-fermented sausage “salchichón” (pH 5.4, 0.95 a_w) shortly after filling into natural casing from beef. The sausage was surface-sterilized by dipping in ethanol and longitudinally cut into ca. 10 cm² over 1 cm thick pieces in a laminar flow cabinet (Bio Flow II, Telstar, Tarrasa, Spain). To simulate the evolution of a_w during industrial sausage processing, the pieces were separately placed in pre-sterilized receptacles with humidity kept constant at 84% after vapor-liquid equilibrium by a saturated potassium chloride solution. A volume of 100 µL of *A. flavus* CECT 2687 or *P. restrictum* Pr341 spore suspensions was

spread onto the casing surface to reach a final concentration of 10^{-4} spores/cm² on each piece. In treated samples, PgAFP was added in 200 µL of phosphate buffer to treated samples at two concentrations (5 and 20 µg/cm²) and was air-dried in the flow cabinet. Control batches received the same volume of phosphate buffer without PgAFP and were inoculated with *A. flavus* or *P. restrictum*. Each treatment was done in three replicates. After inoculation, the samples were incubated at 25 °C for 5 days. The mold load on the sausages was determined from a plating of the whole piece in 90 mL of peptone water by plating decimal dilutions on Potato Dextrose Agar and incubating at 25 °C for 5 days.

2.8. Statistical analysis

Statistical analyses were performed with the IBM SPSS v.19.0. One way analysis of variance (ANOVA) was carried out to determine significant differences within and between groups. Tukey's test was applied to compare mean values.

3. Results

The concentrations of purified PgAFP obtained from *P. chrysogenum* CECT 20922 were 282 and 617 µg/mL at 7- and 14-day incubations in MEB, respectively. Only a limited increase in PgAFP (up to 678 µg/mL) was obtained by extending incubation for one additional week.

3.1. Growth inhibition of reference organisms

All reference organisms tested showed a fair growth in microtiter plates (OD over 1 absorbance unit). The highest concentration of PgAFP tested (312.7 µg/mL) displayed no inhibition against any bacteria (data not shown) or yeast tested, but efficiently retarded growth of most reference molds, including toxigenic, defect-causing, and desirable species. According to sensitivity, two inhibition levels were established (Table 1). In level H, 4.9 µg/mL of PgAFP significantly ($p < 0.001$) reduced over 50% growth of the reference molds, *A. carbonarius*, *A. flavus*, *A. niger*, *A. ochraceus*, *P. chrysogenum*, and *P. restrictum*, as well as the strain Pc332 of *P. commune*. Level L was characterized by a significant ($p < 0.01$) but moderate inhibition, where at least 4.9 µg/mL was necessary to reduce growth 35% for reference strains, such as *A. parasiticus*, *A. versicolor*, *P. expansum*, *P. griseofulvum*, and strain Pc131 of *P. commune*. Due to the slow growth of *P. nordicum* on MEB incubation was extended up to 120 h. At this incubation time a 40% growth reduction of *P. nordicum* was reached with 19.6 µg/mL. However, there was a group of non-sensitive fungi, including *P. polonicum* and *R. oryzae*, in which growth was not significantly ($p > 0.05$) retarded by any PgAFP concentration tested. Inhibition on sensitive molds showed a remarkable dose–effect relationship (Fig. 1). For the highly sensitive reference strains, a noticeable inhibition was observed even at the lowest PgAFP concentration tested (1.2 µg/mL).

3.2. Sensitivity of PgAFP activity to proteases

None of the enzymes tested lead to any statistically significant decrease ($p > 0.05$) on growth of the reference molds when used as a negative control with no antifungal protein. Preincubation of PgAFP with proteases decreased the antifungal activity on the reference molds, but the resulting effect depended not only on the enzyme, but also on both PgAFP concentration and sensitivity level of the reference mold (Fig. 2). Pronase E efficiently eliminated ($p < 0.001$) any inhibitory effect from PgAFP on every selected reference mold, even at the highest PgAFP concentration (130 µg/mL). Flavourzyme and trypsin lowered PgAFP activity, but the effect was less evident, particularly at the highest PgAFP concentration. These two enzymes efficiently eliminated the inhibition on *A. flavus* and *A. niger* by up to 65 µg/mL PgAFP ($p < 0.001$), but not so much at the highest PgAFP concentration ($p < 0.05$). The inhibition

Table 1

In vitro minimal concentrations of PgAFP achieving over 50% (GR₅₀) or 35% growth reduction (GR₃₅) on fungal strains on malt extract broth at 72 h of incubation at 25 °C.

Inhibition level	Fungal strain	GR50 (µg/mL)	GR35 (µg/mL)	
H	<i>A. carbonarius</i> CECT 20384	1.2		
	<i>A. flavus</i> CECT 2687	4.9		
	<i>A. fumigatus</i> CBS 192.65	2.4		
	<i>A. niger</i> An261	4.9		
	<i>A. ochraceus</i> CECT 2092	1.2		
	<i>A. oryzae</i> CECT 2095	2.4		
	<i>A. tamarii</i> CBS 109.63	2.4		
	<i>A. westerdijkiae</i> CECT 2948	2.4		
	<i>P. chrysogenum</i> Pg222	2.4		
	<i>P. commune</i> Pc332	4.9		
	<i>P. nalgiovensis</i> Pj261	2.4		
	<i>P. restrictum</i> Pr341	2.4		
	<i>P. solitum</i> Ps321	4.9		
	L	<i>A. awamori</i> CBS 101.702	19.6	9.8
		<i>A. ochraceoroseus</i> CBS 101.887	312.7	19.6
		<i>A. parasiticus</i> CECT 2682	312.7	39.1
<i>A. tubigenis</i> CECT 20545		19.6	9.8	
<i>A. versicolor</i> CECT 2664		156.4	78.2	
<i>P. aurantiogriseum</i> CECT 2918		>	39.1	
<i>P. commune</i> Pc131		>	78.2	
<i>P. echinulatum</i> Pe321		>	19.6	
<i>P. expansum</i> CECT 2280		9.8	4.9	
<i>P. griseofulvum</i> CECT 2919		>	19.6	
<i>P. nordicum</i> CBS 110.769		312.7	19.6 ^a	
<i>P. verrucosum</i> AB11C		>	9.8	
Non-sensitive		<i>P. chrysogenum</i> CECT 20922	>	—
		<i>P. polonicum</i> Pp51	>	—
	<i>R. oryzae</i> CBS 607.68	>	—	
	<i>C. zeylanoides</i> CECT 10048	>	—	
	<i>D. hansenii</i> CECT 10360	>	—	
	<i>D. hansenii</i> Dh345	>	—	
	<i>R. mucilaginosa</i> CECT 10395	>	—	
	<i>Y. lipolytica</i> CET 10358	>	—	

>: 50% Growth reduction was not reached with 312.7 µg/mL PgAFP.

—: No significant growth reduction was obtained with 312.7 µg/mL PgAFP.

^a Incubation time extended to 120 h.

on the two penicillia strains was occasionally altered by flavourzyme and trypsin ($p < 0.05$). The effect of ficin, pepsin, and papain was less obvious with every reference strain, and decreased at higher PgAFP concentrations.

3.3. Effect of heat-treatments and different pH values

PgAFP showed a remarkable stability at high temperatures, retaining the antifungal activity against *P. restrictum* and *A. niger* even after being heat-treated at 80 °C for 30 min or 100 °C for 15 min (Fig. 3). More intense heating decreased the antifungal activity, reaching an effective ($p < 0.001$) inactivation with the most severe treatments (100 °C for 30 min or autoclave cycle).

Preincubation in buffers at pH values from 1 to 12 had no deleterious effect ($p > 0.05$) on the activity of PgAFP against the reference molds (Fig. 4).

3.4. Antifungal activity of PgAFP on dry-fermented sausages

To test the potential use in foods, the efficiency of PgAFP against unwanted molds was assayed in dry-ripened sausages. The effect on growth of *A. flavus* and *P. restrictum* was evaluated by plating and CFU counting from both PgAFP treated and non-treated sausages. Lower counts were detected in the batches treated with PgAFP (Table 2, Fig. 5) compared to the non-treated control ($p < 0.05$).

4. Discussion

P. chrysogenum CECT 20922 had shown a strong inhibitory activity against *P. echinulatum*, *P. commune*, and *A. niger* due to production of

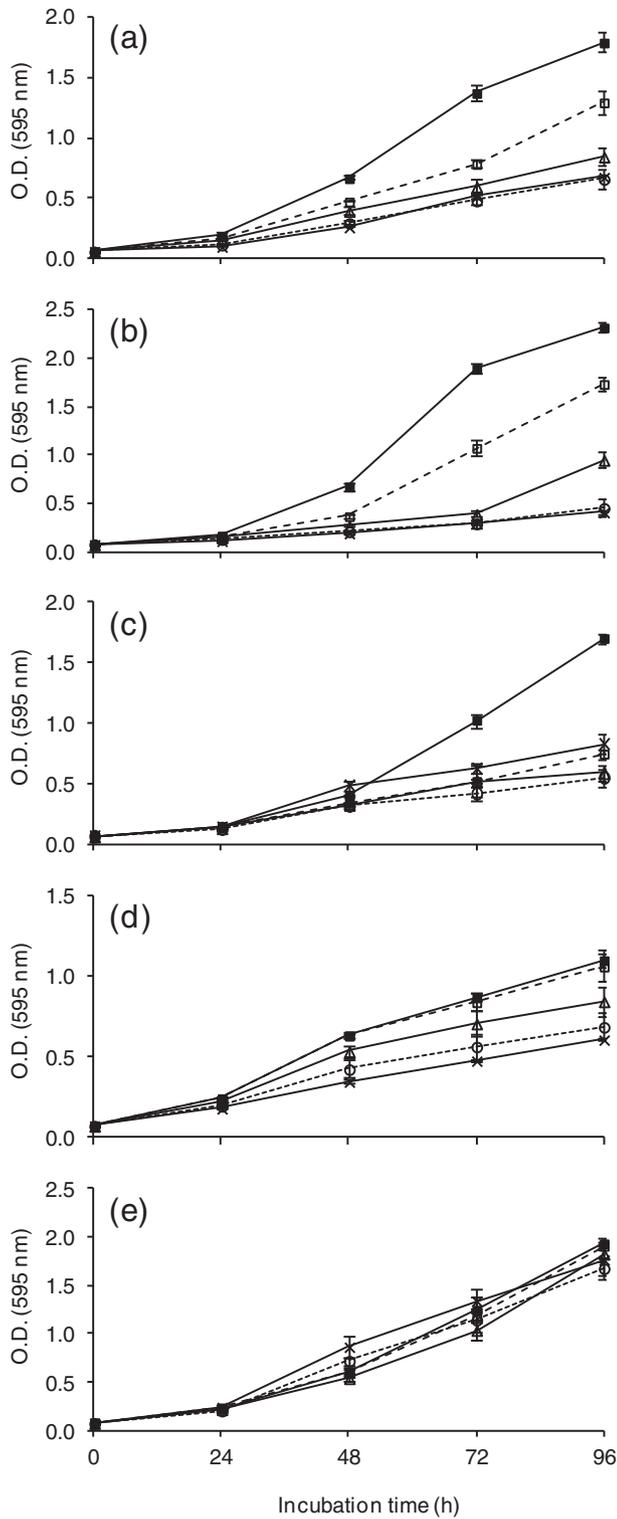


Fig. 1. Effect of PgAFP on growth of selected molds incubated with 0 (■), 1.2 (□), 2.4 (Δ), 18.8 (○), and 37.5 (×) $\mu\text{g}/\text{mL}$ PgAFP. (a) *Aspergillus flavus* CECT 2687; (b) *Aspergillus niger* An261; (c) *Penicillium restrictum* Pr341; (d) *Penicillium griseofulvum* CECT2919; (e) *Penicillium polonicum* Pp51. Values are means with standard deviation of optical density of reference molds.

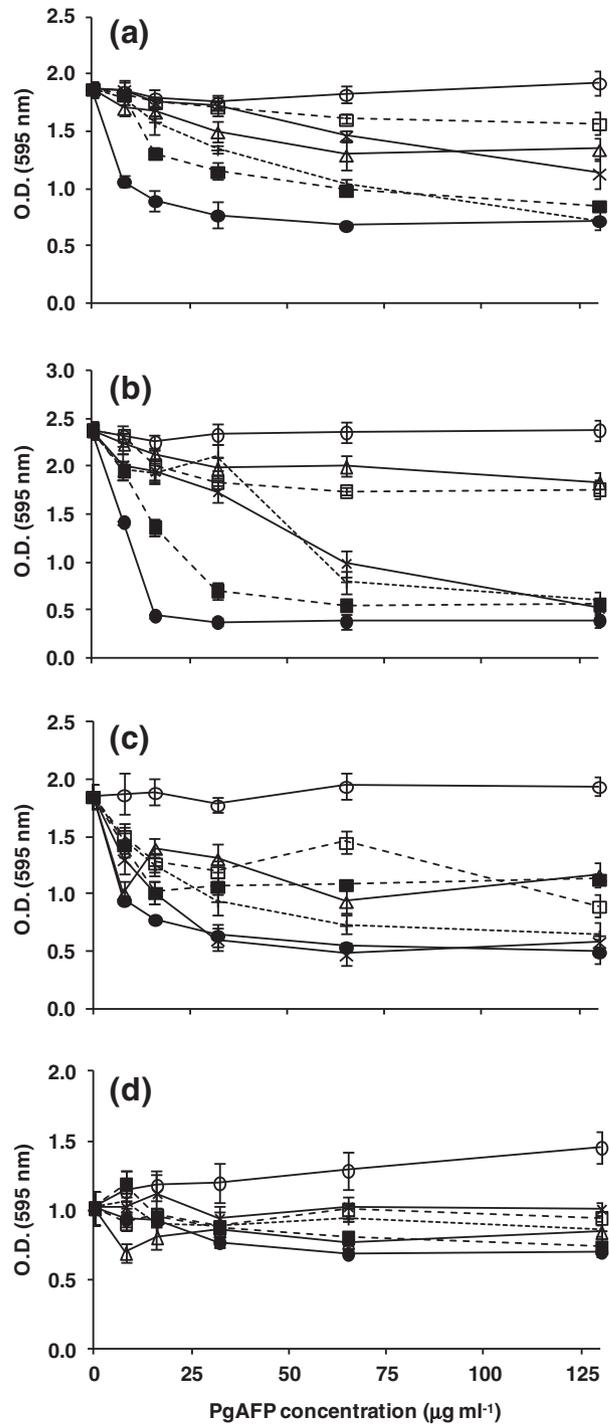


Fig. 2. Effect of proteases on the antifungal activity of different concentrations of PgAFP against selected reference molds. Treatments: (■) pepsin, (×) ficin, (+) papain, (Δ) flavourzyme, (○) pronase E, (□) trypsin, and (●) untreated. (a) *Aspergillus flavus* CECT 2687; (b) *Aspergillus niger* An261; (c) *Penicillium restrictum* Pr341; (d) *Penicillium griseofulvum* CECT2919. Values are means with standard deviation of optical density of reference molds grown for 96 h.

the cationic protein PgAFP (Acosta et al., 2009). The strain CECT 20922 of *P. chrysogenum* has been demonstrated to limit growth of the aflatoxin-producing *A. flavus* and ochratoxigenic molds on dry-cured ham (Bernáldez et al., 2014; Rodríguez et al., 2015). However, no mold growth, including that of protective cultures, is wanted in some

types of dry-ripened sausage. Thus, the use of purified PgAFP could be of interest. To evaluate the activity of the purified protein, its effect on growth of penicillia, aspergilli, yeasts, and bacteria was assessed. No effect on growth of the tested yeasts and bacteria was observed, even at the highest concentration of PgAFP used (312.7 $\mu\text{g}/\text{mL}$). The lack of activity against yeasts and prokaryotes has also been reported for other small, basic antifungal proteins (Marx, 2004). In fact, the only activity reported is limited to Anafp on *Candida albicans*, *Saccharomyces*

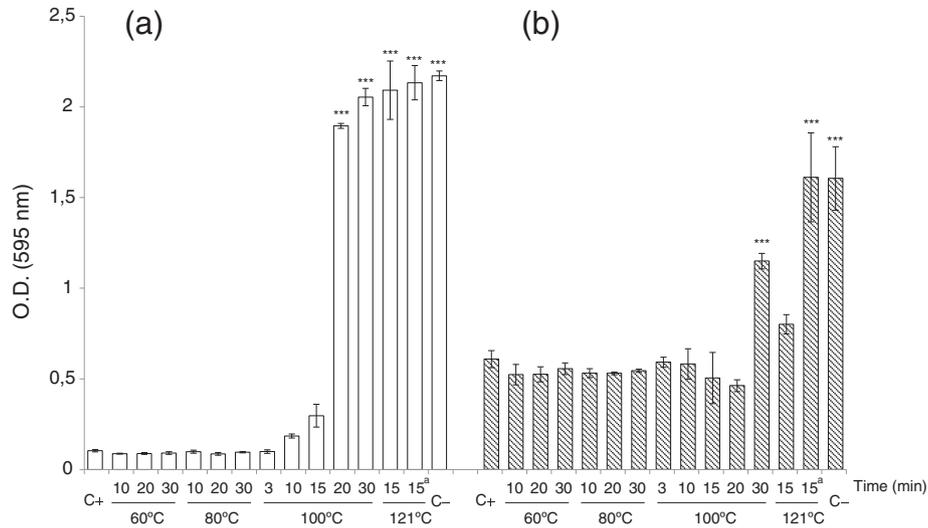


Fig. 3. Antifungal activity of 300 µg/mL heat-treated PgAFP expressed as mean and standard deviation of optical density of reference molds grown for 96 h. (a) *Aspergillus niger* An261; (b) *Penicillium restrictum* Pr341. Asterisks indicate statistically significant differences to growth of the positive control reference mold: *** ($p < 0.001$). C+ : positive control with non-heated PgAFP; C- : negative control without PgAFP. ^a: Autoclave cycle.

cerevisiae, and *Trichosporon beigeli* (Lee et al., 1999). The lack of inhibitory activity on yeasts can be regarded as a positive property. First, because yeasts such as *D. hansenii* contribute to develop the desirable characteristics of dry-ripened meats with no detrimental effects. Second, a limited number of yeasts, including *D. hansenii*, also may combat toxigenic molds (Andrade et al., 2014; Simoncini et al., 2014; Núñez et al., 2015).

PgAFP retarded growth of most molds tested, including the selected aspergilli and most penicillia. Interestingly, the main toxigenic molds tested, such as those producing aflatoxin (*A. flavus* and *A. parasiticus*), ochratoxin A (*A. carbonarius*, *A. ochraceus*, and *P. nordicum*), sterigmatocystin (*A. versicolor*), and patulin (*P. expansum* and *P. griseofulvum*) were in the PgAFP-sensitive group of fungi. The observed effect is fungistatic, not achieving total inhibition of the sensitive mold at the highest concentration tested. Nonetheless, this effect would contribute to reduction of the hazard due to mycotoxins in dry-ripened foods because many secondary metabolites are produced mainly in the idiophase. Despite reports that mycotoxin production may increase in stressed toxigenic fungi, the strong growth inhibition shown in the sausage could be useful to control mycotoxin production, as discussed later. The fact that some molds, such as *P. polonicum* and *R. oryzae*, were not sensitive should not be regarded as a drawback, given that none of them is linked to foodborne mycotoxicosis (Richard, 2007). The minimal inhibitory concentration to reach over 50%

growth reduction was in the range of 1.2–4.9 µg/mL (0.2–0.75 µM) PgAFP for the high sensitive strains (level H), whereas low sensitive strains (level L) required 4.9–78.2 µg/mL (0.75–12 µM) for a 35% growth reduction (Table 1). The inhibition rate for highly sensitive strains can be compared to that of 6 to 25 µM required for complete inhibition of sensitive molds by AFP (Lacadena et al., 1995). Growth inhibition differs greatly not only between species of the same genus, but also within the same species. Accordingly, *P. commune* Pc332 was highly sensitive to PgAFP, with 4.9 µg/mL GR₅₀, whereas *P. commune* Pc131 required 78.2 µg/mL for just a 35% growth reduction. GR₅₀ for *P. chrysogenum* Pg222 was 2.4 µg/mL, but the PgAFP-producing strain *P. chrysogenum* CECT 20922 withstands 312.7 µg/mL, the maximum level tested. Similar differences in sensitivity to antifungal proteins have been reported for AFP, AnaFP, PAF, and AcaFP, showing both sensitive and non-sensitive species in a limited number of strains from genera *Aspergillus*, *Penicillium*, or *Fusarium* (Lee et al., 1999; Kaiserer et al., 2003; Theis et al., 2003; Skouri-Gargouri and Gargouri, 2008).

To study the effect of proteases on the antifungal activity of PgAFP the reference species selected included both sensitivity levels and fungal genera. The enzymes chosen are among the most active proteases that can be added to processed foods or, for flavourzyme and pronase E, have been proposed to enhance flavor development in dry fermented sausages (Fernández et al., 2000). No enzyme tested showed any effect on growth of reference strains (Fig. 2). The activity of the proteases against PgAFP was evidenced by the loss of activity at low PgAFP levels. At higher PgAFP concentrations, the more active proteases decreased the antifungal effect. The less active proteases were less efficient, and the residual amount of antifungal protein seems to be enough to limit growth of the reference molds. This effect was not observed with the low-sensitive *P. griseofulvum*, partially because the short extent

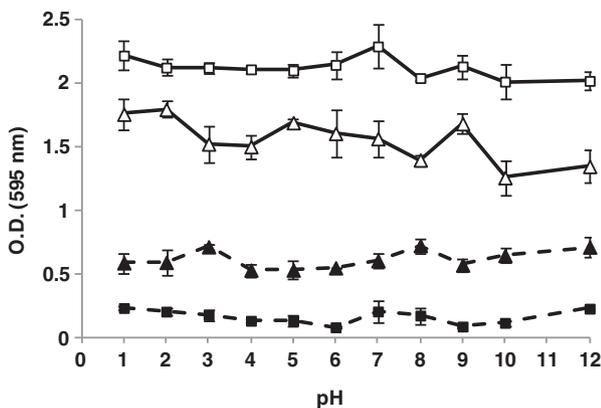


Fig. 4. Antifungal activity of PgAFP after incubation at different pH values, expressed as mean and standard deviation of optical density of reference molds grown for 96 h. *Aspergillus niger* An261 (■) and *Penicillium restrictum* Pr341 (▲) treated with 300 µg/mL PgAFP (closed symbols) or untreated negative controls (open symbols).

Table 2
Effect of PgAFP on growth of *Aspergillus flavus* and *Penicillium restrictum* on a dry-fermented sausage after 5 days at 25 °C. Mold growth is given as mean ± SD.

PgAFP (µg/cm ²)	Fungal species	
	<i>A. flavus</i> CECT 2687 (log CFU/cm ²)	<i>P. restrictum</i> Pr341 (log CFU/cm ²)
0	5.0 ± 0.21	4.7 ± 0.17
5	2.6 ± 0.24 ^a	3.6 ± 0.19 ^a
20	2.1 ± 0.15 ^a	3.1 ± 0.25 ^a

^a Different ($p < 0.05$) from the non-treated control.

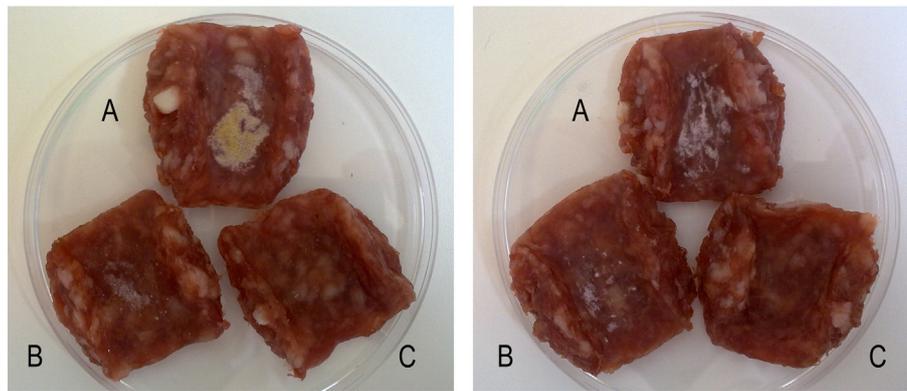


Fig. 5. Effect of 0 (A), 5 (B), and 20 (C) $\mu\text{g}/\text{cm}^2$ PgAFP on growth of *Aspergillus flavus* (left) and *Penicillium restrictum* (right) on dry-fermented sausage after 5 days at 25 °C.

between growth of PgAFP-treated and non-treated samples did not allow detecting the effect due to PgAFP degradation.

Given that PgAFP digestion was run under extreme conditions, for 12 h at favorable temperature and pH values for each enzyme, the observed residual activity reveals a remarkable ability to withstand proteases. Only the mixture of exopeptidases and endopeptidases from *S. griseus* contained in pronase E was able to efficiently inactivate 130 $\mu\text{g}/\text{mL}$ PgAFP. With the latter result, the potential use of PgAFP might be argued, when proteolytic organisms were present. However, highly proteolytic molds from dry-ripened meats, such as *P. chrysogenum* Pg222 and *A. oryzae* CECT 2095 (ATCC 9362) (Trigueros et al., 1995; Benito et al., 2002), were among the highly sensitive molds. The observed protease resistance can be attributed to the compact structure of the small, basic, cysteine-rich antifungal proteins, as it has been proposed for AFP (Lacadena et al., 1995).

Among the main physicochemical factors affecting protein activity in foods are pH and heat treatments. To study the impact of these two factors on PgAFP activity, one sensitive strain from each genus was selected as reference. PgAFP was highly resistant to a wide range of temperature (Fig. 3). Intense heat treatments partially inactivated 300 $\mu\text{g}/\text{mL}$ PgAFP, as can be inferred from the loss of inhibition on the less sensitive *A. niger* and the residual effect on the more sensitive *P. restrictum*. Similarly to its heat stability, PgAFP withstood a broad range of pH values (Fig. 4). These characteristics are similar to those of other antifungal proteins from molds. AFP from *A. giganteus* is stable to protease degradation, high temperature, and a broad pH range due to a specific folding pattern (Lacadena et al., 1995). Similarly, AcAFP from *A. clavatus* is also resistant to 100 °C and is effective in a 5–12 pH range (Skouri-Gargouri et al., 2010). AFP folds into a small and compact β -barrel, stabilized by four disulfide bridges formed by cysteine residues (Campos-Olivas et al., 1995). It has been assumed that AcAFP, Anafp, NAF, and PAF also have a similar tertiary structure, with three or four disulfide bridges formed by the cysteine residues present in these proteins (Marx, 2004; Skouri-Gargouri et al., 2009). PgAFP has characteristics common to these antifungal proteins, including six cysteine residues and a quite high similarity in the amino acid sequence, leading a tertiary structure based on a compact β -barrel (Rodríguez-Martín et al., 2010).

Treatment with the two PgAFP concentrations assayed was effective in reducing growth of *A. flavus* and *P. restrictum* in sausage samples (Table 2, Fig. 5). The counts of *A. flavus* in treated samples were always below 3.5 log CFU/g. This effect can serve to prevent development of hazardous levels at which aflatoxin B1 production has been described on dry-cured hams (Rodríguez et al., 2012). Given the observed fungistatic effect of PgAFP, it is not expected that sufficient inhibition would be maintained throughout the whole ripening time. Thus, the antifungal protein would be most efficient if applied at the time when the product is most susceptible to mold development. Direct application of PgAFP by spraying on the product in the key stages could be useful to delay mold

growth to allow corrective actions to be taken before mycotoxins are produced. The low identity of PgAFP in relation to other antifungal proteins from molds, as well as the differences in site of action and possible targets (Marx, 2004) sustain the combined use of PgAFP with other antifungal proteins to take advantage of complementary effects.

Although the inhibitory activity of some antifungal proteins produced by molds has been reported (Lee et al., 1999; Kaiserer et al., 2003; Theis et al., 2003; Skouri-Gargouri and Gargouri, 2008), this is the first time that the inhibitory effect against toxigenic molds has been proved in foods. Given that *P. chrysogenum* is used to obtain generally recognized as safe (GRAS) compounds and has a long record of industrial use, the potential application of PgAFP in foods should be considered additionally with good manufacturing practice through HACCP procedures for reducing the health hazard due to mycotoxins in dry-fermented sausages. In addition, *P. chrysogenum* CECT 20922 is able to limit growth of aflatoxin and OTA-producing molds and OTA accumulation in dry-cured Iberian ham throughout the processing (Bernáldez et al., 2014; Rodríguez et al., 2015).

In conclusion, PgAFP showed an efficient inhibition of undesired molds, including some of the main toxigenic species for dry-ripened foods, when these fungi were grown in culture medium and in a dry-fermented sausage. Moreover, PgAFP withstands most proteases, intense heat and a wide range of pH values. This protein can be of interest to control unwanted fungi in dry-ripened foods.

Acknowledgments

This work was supported by the Spanish Ministry of Education and Science (AGL2004-06546-ALI, and AGL2010-21623) and FEDER. Raquel Acosta, Andrea Rodríguez-Martín, and Josué Delgado were recipients of FPI grants from the Spanish Ministry of Education and Science. The authors declare no conflicts of interest in this work.

References

- Acosta, R., Rodríguez-Martín, A., Martín, A., Núñez, F., Asensio, M.A., 2009. Selection of antifungal protein-producing molds from dry-cured meat products. *Int. J. Food Microbiol.* 135, 39–46.
- Andrade, M.J., Thorsen, L., Rodríguez, A., Córdoba, J.J., Jespersen, L., 2014. Inhibition of ochratoxigenic moulds by *Debaryomyces hansenii* strains for biopreservation of dry-cured meat products. *Int. J. Food Microbiol.* 170, 70–77.
- Benito, M.J., Rodríguez, M., Núñez, F., Asensio, M.A., Bermúdez, M.E., Córdoba, J.J., 2002. Purification and characterization of an extracellular protease from *Penicillium chrysogenum* Pg222 active against meat proteins. *Appl. Environ. Microbiol.* 68, 3532–3536.
- Bernáldez, V., Rodríguez, A., Martín, A., Lozano, D., Córdoba, J.J., 2014. Development of a multiplex qPCR method for simultaneous quantification in dry-cured ham of an antifungal-peptide *Penicillium chrysogenum* strain used as protective culture and aflatoxin-producing moulds. *Food Control* 36, 257–265.
- Broekaert, W.F., Terras, F.R.G., Cammue, B.P.A., Vanderleyden, J., 1990. An automated quantitative assay for fungal growth-inhibition. *FEMS Microbiol. Lett.* 69, 55–59.

- Campos-Olivas, R., Bruix, M., Santoro, J., Lacadena, L., Martínez del Pozo, A., Gavilanes, J.G., Rico, M., 1995. NMR solution structure of the antifungal protein from *Aspergillus giganteus*: evidence for cysteine pairing isomerism. *Biochemistry* 34, 3009–3021.
- Chen, Z., Ao, J., Yang, W., Jiao, L., Zheng, T., Chen, X., 2013. Purification and characterization of a novel antifungal protein secreted by *Penicillium chrysogenum* from an Arctic sediment. *Appl. Microbiol. Biotechnol.* 97, 10381–10390.
- Dimarcq, J.L., Bulet, P., Hetru, C., Hoffmann, J., 1998. Cysteine-rich antimicrobial peptides in invertebrates. *Biopolymers* 47, 465–477.
- Espinell-Ingroff, A., Bartlett, M., Bowden, R., Chin, N.X., Cooper, C., Fothergill, A., McGinnis, M.R., Menezes, P., Messer, S.A., Nelson, P.W., Odds, F.C., Pasarell, L., Peter, J., Pfaller, M.A., Rex, J.H., Rinaldi, M.G., Shackland, G.S., Walsh, T.J., Weitzman, I., 1997. Multicenter evaluation of proposed standardized procedure for antifungal susceptibility testing of filamentous fungi. *J. Clin. Microbiol.* 35, 139–143.
- Fernández, M., Ordóñez, J.A., Bruna, J.M., Herranz, B., de la Hoz, L., 2000. Accelerated ripening of dry fermented sausages. *Trends Food Sci. Technol.* 11, 201–209.
- Fox, J.L., 1993. Fungal infections rates are increasing. *ASM News* 59, 515–518.
- Johnson, M.J., 1941. Isolation and properties of a pure yeast polypeptidase. *J. Biol. Chem.* 137, 575–586.
- Kaiserer, L., Oberparleiter, C., Weiler-Görz, R., Burgstaller, W., Leiter, E., Marx, F., 2003. Characterization of the *Penicillium chrysogenum* antifungal protein PAF. *Arch. Microbiol.* 180, 204–210.
- Kovács, L., Virágh, M., Takó, M., Papp, T., Vágvölgyi, C., Galgóczy, L., 2011. Isolation and characterization of *Neosartorya fischeri* antifungal protein (NFAP). *Peptides* 32, 1724–1731.
- Lacadena, J., Martínez del Pozo, A., Gasset, M., Patiño, B., Campos-Olivas, R., Vázquez, C., Martínez-Ruiz, A., Mancheño, J.M., Oñaderra, M., Gavilanes, J.G., 1995. Characterization of the antifungal protein secreted by the mold *Aspergillus giganteus*. *Arch. Biochem. Biophys.* 324, 273–281.
- Lee, D.G., Shin, S.Y., Maeng, C., Jin, Z.Z., Kim, K.L., Hahm, K., 1999. Isolation and characterization of a novel antifungal peptide from *Aspergillus niger*. *Biochem. Biophys. Res. Commun.* 263, 646–651.
- Marx, F., 2004. Small, basic antifungal proteins secreted from filamentous ascomycetes: a comparative study regarding expression, structure, function and potential application. *Appl. Microbiol. Biotechnol.* 65, 133–142.
- Marx, F., Haas, H., Reindl, M., Stöffler, G., Lottspeich, F., Redl, B., 1995. Cloning, structural organization and regulation of expression of the *Penicillium chrysogenum paf* gene encoding an abundantly secreted protein with antifungal activity. *Gene* 167, 167–171.
- Nakaya, N., Omata, K., Okahashi, I., Nakamura, Y., Kolkenbrock, H.J., Ulbrich, N., 1990. Amino-acid sequence and disulphide bridges of an antifungal-protein isolated from *Aspergillus giganteus*. *Eur. J. Biochem.* 193, 31–38.
- Núñez, F., Lara, M.S., Peromingo, B., Delgado, J., Sánchez-Montero, L., Andrade, M.J., 2015. Selection and evaluation of *Debaryomyces hansenii* isolates as potential bioprotective agents against toxigenic penicillia in dry-fermented sausages. *Food Microbiol.* 46, 114–120.
- Okkers, D.J., Dicks, L.M.T., Silvester, M., Joubert, J.J., Odendaal, H.J., 1999. Characterization of pentocin TV35b, a bacteriocin-like peptide isolated from *Lactobacillus pentosus* with a fungistatic effect on *Candida albicans*. *J. Appl. Microbiol.* 87, 726–734.
- Richard, J.L., 2007. Some major mycotoxins and their mycotoxicoses—an overview. *Int. J. Food Microbiol.* 119, 3–10.
- Rodríguez, A., Rodríguez, M., Martín, A., Nuñez, F., Córdoba, J.J., 2012. Evaluation of hazard of aflatoxin B1, ochratoxin A and patulin production in dry-cured ham and early detection of producing molds by qPCR. *Food Control* 27, 118–126.
- Rodríguez, A., Bernáldez, V., Rodríguez, M., Andrade, M.J., Núñez, F., Córdoba, J.J., 2015. Effect of selected protective cultures on ochratoxin A accumulation in dry-cured Iberian ham during its ripening process. *LWT- Food Sci. Technol.* 60, 923–928.
- Rodríguez-Martín, A., Acosta, R., Liddell, S., Núñez, F., Benito, M.J., Asensio, M.A., 2010. Characterization of the novel antifungal protein PgAFP and the encoding gene of *Penicillium chrysogenum*. *Peptides* 31, 541–547.
- Selitrennikoff, C.P., 2001. Antifungal proteins. *Appl. Environ. Microbiol.* 67, 2883–2894.
- Simoncini, N., Virgili, R., Spadola, G., Battilani, P., 2014. Autochthonous yeasts as potential biocontrol agents in dry-cured meat products. *Food Control* 46, 160–167.
- Skouri-Gargouri, H., Gargouri, A., 2008. First isolation of a novel thermostable antifungal peptide secreted by *Aspergillus clavatus*. *Peptides* 29, 1871–1877.
- Skouri-Gargouri, H., Ali, M.B., Gargouri, A., 2009. Molecular cloning, structural analysis and modelling of the AcAFP antifungal peptide from *Aspergillus clavatus*. *Peptides* 30, 1798–1804.
- Skouri-Gargouri, H., Jellouli-Chaker, N., Gargouri, A., 2010. Factors affecting production and stability of the AcAFP antifungal peptide secreted by *Aspergillus clavatus*. *Appl. Microbiol. Biotechnol.* 86, 535–543.
- Theis, T., Wedde, M., Meyer, V., Stahl, U., 2003. The antifungal protein from *Aspergillus giganteus* causes membrane permeabilization. *Antimicrob. Agents Chemother.* 47, 588–593.
- Trigueros, G., Garcia, M.L., Casas, C., Ordóñez, J.A., Selgas, M.D., 1995. Proteolytic and lipolytic activities of mold strains isolated from Spanish dry fermented sausages. *Z. Lebensm. Unters. Forsch.* 201, 298–302.
- Wang, H.X., Ng, T.B., 2003. Isolation of cucurmoschin, a novel antifungal peptide abundant in arginine, glutamate and glycine residues from black pumpkin seeds. *Peptides* 24, 969–972.

IV.2. Efecto de PgAFP y de su combinación con microorganismos bioprotectores para maximizar su efecto de inhibición sobre el crecimiento de mohos y producción de micotoxinas en alimentos madurados

IV.2.1. Evaluación en producto cárnico crudo-curado

Effect of PgAFP and protective cultures on Aspergillus parasiticus growth inhibition and aflatoxin production on dry-fermented sausage

1 **Effect of PgAFP and protective cultures on *Aspergillus parasiticus* growth**

2 **inhibition and aflatoxin production on dry-fermented sausage**

3 **Abstract**

4 Toxigenic moulds can grow and produce mycotoxins on intermediate moisture foods. The
5 antifungal protein PgAFP can control this population on dry-cured meat products, but the effect
6 of this protein on mycotoxin production is unknown. Thus, the objective of this work was to
7 study the effect of PgAFP on aflatoxin production through gene expression. In addition, given
8 the limited inhibitory ability of PgAFP, to maximize the inhibitory ability, different combined
9 treatments with PgAFP, *Debaryomyces hansenii* and/or *Pediococcus acidilactici* were studied in
10 culture medium and on dry-fermented sausage against an aflatoxigenic strain of *Aspergillus*
11 *parasiticus*. In culture medium, PgAFP increased aflatoxin production and *P. acidilactici*
12 reduced it dramatically. Relative gene expression of *foxA* involved in peroxisomal β -oxidation
13 and *aflP*, involved in aflatoxin biosynthesis, were studied to reveal the effect of a potential
14 reactive oxygen species (ROS) induced by PgAFP in aflatoxin production. The aflatoxin
15 overproduction by the effect of PgAFP cannot be linked to peroxisomal β -oxidation. The
16 combination of PgAFP and *D. hansenii* provided a successful inhibitory effect on *A. parasiticus*
17 growth as well as aflatoxin production for 15 days on dry-fermented sausage in a wide activity
18 water range. *P. acidilactici* did not enhance the protective effect of the combination of these two
19 agents. Therefore, the combined treatment of PgAFP and *D. hansenii* can provide a protective
20 effect against toxigenic moulds in dry-cured foods.

21

22 Key words: Aflatoxin, antifungal protein, *Aspergillus parasiticus*, dry-fermented sausage.

23 **1. Introduction**

24 The environmental conditions during the ripening of dry-cured meat products favor growth of
25 toxigenic molds (López-Díaz, Santos, García-López, & Otero, 2001; Núñez, Rodríguez,
26 Bermúdez, Córdoba, & Asensio, 1996). These molds can produce mycotoxins, such as
27 aflatoxins, ochratoxin A, and patulin on dry-cured meat products (Rodríguez, Rodríguez,
28 Martín, Delgado, & Córdoba, 2012; Rodríguez, Rodríguez, Martín, Nuñez, & Córdoba, 2012).
29 Aflatoxins, produced mainly by *Aspergillus flavus* and *Aspergillus parasiticus*, have oncogenic,
30 immunosuppressive, and hepatotoxic properties (Bezerra da Rocha, Oliveira Freire, Feitosa
31 Maia, Florindo Guedes, & Rondina, 2014), being classified as group 1 carcinogenic to humans
32 by the International Agency for Research on Cancer. Therefore, it is necessary to carry out
33 strategies to prevent aflatoxigenic molds from growing on dry-cured meat products.

34 Some molds produce proteins that inhibit other molds, whereas the activity against yeasts and
35 prokaryotes is quite limited (Marx, 2004). These antimicrobial proteins may serve to combat
36 unwanted molds in dry-cured meat products. PgAFP from *Penicillium chrysogenum*
37 (Rodríguez-Martín et al., 2010) is one of these antifungal proteins showing multifactorial
38 mechanism of action based on reactive oxygen species (ROS) production, membrane
39 permeability increase, and apoptosis induction (Delgado, Owens, Doyle, Asensio, & Núñez,
40 2015). The antifungal protein PgAFP inhibits some toxigenic molds in culture medium and on
41 dry-fermented sausage, requiring less than 4.9 µg/ml for the highly sensitive molds and from 9.8
42 µg/ml for low sensitive molds, including *A. parasiticus*. However, this effect is rather time-
43 limited, displaying the main effect in the first 96 h of incubation (Delgado, Acosta, et al., 2015).
44 PgAFP can also hamper aflatoxins biosynthesis. *A. flavus* treated with PgAFP for 24 h showed
45 lower relative abundance of key enzymes in aflatoxin biosynthesis pathway, including O-
46 methyltransferase, VERB synthase, and VER1 dehydrogenase (Delgado, Owens, et al., 2015),
47 but the effect on aflatoxin production was not tested. On the other hand, ROS contribute to
48 aflatoxin production (Jayashree & Subramanyan, 2000; Reverberi et al., 2005), which makes it
49 necessary to study the influence of PgAFP on aflatoxin production.

50 The effect of ROS on aflatoxigenic molds is related to redox balance through β-oxidation, and
51 expression of *foxA* gene has been used as a marker for β-oxidation (Reverberi et al., 2012).
52 Thus, studying *foxA* expression could elucidate whether PgAFP treatment increase aflatoxin
53 production by oxidative stress. Similarly, expression of *aflP* gene, coding for O-
54 methyltransferase A, serves to assess the rate of aflatoxin biosynthesis (Lozano-Ojalvo,
55 Rodríguez, Bernáldez, Córdoba, & Rodríguez, 2013).

56 On the other hand, the limited length of inhibition by PgAFP makes it necessary to develop
57 strategies that extend growth inhibition to reduce mycotoxin levels. A plausible alternative can
58 be based on the combined use of PgAFP and microbial strains endowed with antifungal activity.
59 Among the microorganisms usually present on dry cured products, yeasts thrive on dry-cured
60 hams for the whole ripening time, being most of them *Debaryomyces hansenii* in matured hams
61 (Núñez, Rodríguez, Córdoba, Bermúdez, & Asensio, 1996). Some of these strains have shown
62 antifungal capability against toxigenic penicillia cured meat products (Andrade, Thorsen,
63 Rodríguez, Córdoba, & Jespersen, 2014; Núñez et al., 2015). Also lactic acid bacteria have been
64 proved as potent mold inhibitors (Li et al., 2014). *Pediococcus acidilactici* are known producers
65 of antifungal compounds (Effat, Ibrahim, Tawfik, & Sharaf, 2001), some of them being active
66 against *A. parasiticus* (Mandal, Sen, & Mandal, 2013) and assumed to produce bacteriocins
67 (Montiel, Bravo, & Medina, 2013).

68 The aim of this work was to investigate the antifungal capability of PgAFP, *D. hansenii* and
69 *Pediococcus acidilactici* against *A. parasiticus* on culture medium and dry-fermented sausage.
70 To understand how these agents affect mold growth and aflatoxin production, the effect on *foxA*
71 and *aflP* genes expression were studied. This knowledge would allow to get the highest effect
72 from potential biological agents to combat toxigenic molds in dry-cured meat products.

73 2. Material and methods

74 2.1. Strains

75 Two mold strains obtained from Spanish Type Culture Collection (CECT, Valencia, Spain)
76 were used in this study: the PgAFP sensitive aflatoxin-producer *A. parasiticus* CECT 2682 and
77 the PgAFP antifungal protein producer *P. chrysogenum* CECT 20922. In addition, two potential
78 antifungal strains were used: the yeast *D. hansenii* Dh253 from the microbial collection of Food
79 Hygiene and Safety of the University of Extremadura (Cáceres, Spain) and *P. acidilactici* fargo
80 35 supplied by Laboratorios Amerex (Colmenar Viejo, Spain).

81 2.2. PgAFP production and purification

82 *P. chrysogenum* CECT 20922 was grown in potato dextrose broth (PDB) pH 4.5 for 21 days at
83 25 °C. The mycelium was removed and the media was filtered to get cell free media. PgAFP
84 was isolated from 450 ml of the cell-free media through fast protein liquid chromatography
85 (FPLC) with a cationic exchange column HiTrap SP HP (Amersham Biosciences, Uppsala,
86 Sweden), further purified with a HiLoad 26/60 Superdex 75 gel filtration column for FPLC
87 (Amersham Biosciences) as previously described (Acosta, Rodríguez-Martín, Martín, Núñez, &
88 Asensio, 2009). The protein isolated and concentrated was sterilized through filtration (0.22 µm,
89 Thermo Fisher Scientific, Waltham, MA, USA) and its concentration was assessed by the
90 Lowry method (Lowry, Rosebrough, Farr, & Randall, 1951).

91

92 2.3. Growth inhibition in culture media and mycotoxin extraction

93 The effect of PgAFP, *D. hansenii*, and *P. acidilactici* on *A. parasiticus* was evaluated both
94 separately and in all different combinations. For this, 5 ml of yeast extract sucrose broth (YES)
95 were inoculated with 10^5 conidia/ml *A. parasiticus*. To provide a high level of the biological
96 agents, 10^6 cells/ml *D. hansenii* (Dh), 10^6 cells/ml *P. acidilactici* (Pa), and 10 µg/ml PgAFP
97 (Pg) the following 7 different batches were obtained: Pg, Dh, Pa, Pg+Dh, Pg+Pa, Dh+Pa, and
98 Pg+Dh+Pa. Additionally, an untreated batch used as a control. Samples were incubated for 15
99 days at 25 °C to stimulate aflatoxin production (Lozano-Ojalvo et al., 2013). All the assays were
100 carried out in triplicate. After incubation, 5 ml of chloroform were added to each test tube
101 incubated for 1 h shaking at 100 rpm at room temperature in darkness. Then, the chloroform

102 was separated and evaporated to dryness under a gentle stream of N₂. The mycelium was
103 recovered from the aqueous residue by filtering through a miracloth (Calbiochem, Darmstadt,
104 Germany), dried at 100 °C up to constant weight, and weighed.

105 2.4. Growth inhibition on sausages and mycotoxin extraction

106 To test the potential of some combinations of protective cultures, the ripening stage on sausages
107 was simulated using a commercial raw dry-fermented sausage (pH 5.8, aw 0.96) shortly after
108 stuffing in natural casing from beef. The sausage was cut into 7-8 mm thick slices and dipped
109 into ethanol to eliminate outer contamination. The ethanol was left to evaporate in a laminar
110 flow cabinet (Bio Flow II, Telstar, Tarrasa, Spain) prior to placing the slices in pre-sterilized
111 (ethanol and UV-light) receptacles containing a saturated KCl solution to keep relative humidity
112 constant at 84% after vapour-liquid equilibrium. *A. parasiticus* was inoculated (10⁵ conidia/cm²)
113 on both sides of each slice. No antifungal treatment was applied to the untreated batch. Two
114 treated batches were made: Pg+Dh+Pa, with 10 µg/cm² PgAFP, 10⁶ cells/cm² *D. hansenii*, and
115 10⁶ cells/cm² *P. acidilactici*; and Pg+Dh, with 10 µg/cm² PgAFP and 10⁶ cells/cm² *D. hansenii*,
116 similarly to the culture medium. Every batch was carried out in triplicate. All samples received
117 the same volume of liquid by adding sterile phosphate buffer as required, and the liquid excess
118 was left to dry in the laminar flow cabinet. The samples were incubated for 5 and 15 days at 25
119 °C to stimulate aflatoxin production (Lozano-Ojalvo et al., 2013). A_w values were determined in
120 a Novasina Lab Master from Novasina AG (Lachen, Switzerland). *A. parasiticus* and *D.*
121 *hansenii* counts were assessed by plating in PDA and incubated for 72 h at 25 °C, according to
122 the characteristic colony morphology. Lactic acid bacteria counts were evaluated on MRS agar,
123 incubated for 72 h at 30 °C.

124 Mycotoxins produced on sliced sausages were extracted as previously described (Rodríguez,
125 Rodríguez, Martín, Delgado, et al., 2012). Briefly, each sausage slice was macerated under
126 shaking in a dark flask with 60 ml acetonitrile-water (9:1, v/v) containing 0.1% formic acid
127 together with 50 ml hexane. The acetonitrile-water phase was recovered and filtered through
128 sodium sulphate anhydrous. Then, the filtrate was mixed with additional 50 ml of hexane and
129 shaken. The acetonitrile-water phase was filtered again and evaporated in a rotatory evaporator
130 at 40–45 °C. The residue was resuspended in 1 ml chloroform, filtered through a 0.45 µm nylon
131 membrane (MSI, Westboro, MA, USA).

132 2.5. Mycotoxin quantification

133 Extracts from both culture medium and sausages were analysed by ultra high-performance
134 liquid chromatography–mass spectrometry (uHPLC–MS) in an HPLC Thermo Scientific
135 Dionex ultimate 3000 pnmp, a mass detector (MS) model Bruker Amazon S.L., an autosampler
136 (Ultimate 3000), a degasser (3000 Ultimate) and an ion trap (Amazon S.L.). A C18 reverse-

137 phase column of 10 cm length, 2.1 mm inside diameter and 2 μm particle size was used as
138 stationary phase. As mobile phase a 0.1% formic acid-10 mM ammonium formate (solvent A)
139 and acetonitrile (solvent B) was used. The separation was performed with the flow rate set at
140 200 $\mu\text{l}/\text{min}$ and the following gradient: [0 min] 2% B, [0-0.1 min], 40% B, [0.1-4 min] 60%
141 B, [4-7 min] 80% B, [7-8.5 min] 80% B, [8.5-8.51 min] 98% B, [8.51-12 min] 98% B, [12-12.01
142 min] 2% B and [12.01-15 min] 2% B. Precursor ions 313 and 329, and quantitation ions 285
143 and 311 for aflatoxins B₁ and G₁ (AFB₁ and AFG₁), respectively.

144 These parameters were compared to those obtained from commercial mycotoxins (Sigma-
145 Aldrich, Madrid, Spain). The calibration curves for AFB₁ and AFG₁ (1-500 ng) by uHPLC-MS
146 revealed a linear relationship ($r^2 \geq 0.99$) between detector response and amount of AFB₁ and
147 AFG₁ standards. The minimum detectable value or limit of detection (LOD) was estimated from
148 the calibration curve, according to the equation: $\text{LOD} = 3 (s_B^2 + s_i^2 + (i/m)^2 s_m)^{1/2}/m$ (Long &
149 Winefordner, 1983) being “m” the slope of the calibration curve, “I” the intercept term and “s_B”,
150 “s_i” and “s_m” the standard errors of the blank, the intercept term and the slope of the calibration
151 curve, respectively. Assuming a normal distribution of the estimated quantities, α (error of the
152 first type) = β (error of the second type) = 0.05, the quantification limit (LOQ) was 3.04 LOD
153 (Currie, 1999). The LOD obtained in this study were 4 $\mu\text{g}/\text{kg}$ and 1.5 $\mu\text{g}/\text{kg}$, and the LOQ were
154 12 $\mu\text{g}/\text{kg}$ and 4.5 $\mu\text{g}/\text{kg}$ respectively for AFB₁ and AFG₁.

155 2.6. RNA isolation and cDNA synthesis

156 To test the influence of PgAFP, *D. hansenii* and *P. acidilactici* on *A. parasiticus* gene
157 expression, four batches were prepared in YES broth: *A. parasiticus* (10^5 conidia/ml) was co-
158 cultivated in tubes separately with PgAFP (10 $\mu\text{g}/\text{ml}$), *D. hansenii* (10^6 cells/ml) or *P.*
159 *acidilactici* (10^6 cells/ml), and with all of them together. The untreated batch was inoculated
160 solely with *A. parasiticus*. The tubes were incubated at 25°C for 5 days. For RNA extraction,
161 mycelium was -saline buffer (PBS), frozen in
162 liquid nitrogen and ground with a mortar and pestle. Then the powder was resuspended in 750 μl
163 RLT buffer (RNeasy® Plant Mini kit, Qiagen, Hilden, Germany) containing 15 μl β -
164 mercaptoethanol. Samples were processed with the RNeasy® Plant Mini kit according to
165 manufacturer’s instructions. RNA quality and quantity was spectrophotometrically determined
166 using in a NanoDrop 2000c spectrophotometer (Thermo Scientific, Waltham, MA, USA). Then,
167 samples were treated with DNase I, RNase-free (Fermentas, St. Leon-Rot, Germany) following
168 manufacturer’s instructions, and checked for background double stranded DNA by qPCR for β -
169 *tubulin* genes as described below. Finally, cDNA was synthesized using 500 ng RNA according
170 to PrimeScript™ RT Reagent kit protocol (Takara, Otsu, Japan).

171

172 2.7. Real-time PCR analysis of gene expression

173 The expression of genes *aflP* (formerly *omt-1*) for aflatoxin biosynthesis (Yu et al., 2004), *foxA*
174 for β -oxidation (Roze et al., 2010), and *β -tubulin* as housekeeping (Rodríguez, Medina, Córdoba,
175 & Magan, 2014) were assessed to evaluate the effect of the treatments on *A. parasiticus*.
176 Primers to evaluate the *foxA* expression were designed from the gene AFLA_041590
177 (GeneBank accession no. XM_002377580), as previously described (Roze et al., 2010).
178 Similarly, to study *β -tubulin* expression a couple of primers were designed from *A. parasiticus*
179 *β -tubulin* sequence (GeneBank accession no. FR775333.1)

180 To quantify the relative expression of the genes, *foxA* and *β -tubulin* genes expression were
181 assessed by using the SYBR Green qPCR in an Applied Biosystems ViiATM 7 Real-Time PCR
182 System (Applied Biosystems, Foster City, California, USA). To optimize the primer
183 concentration, different concentrations from 800 to 200 nM were tested. The optimized SYBR
184 Green protocol was carried out in a final volume of 25 μ l containing 5 ml of template DNA,
185 12.5 μ l of 2x SYBR® *Premix Ex Taq*TM (Takara, Otsu, Japan), 0.5 μ l of 50x ROXTM Reference
186 Dye (Takara) and 400 nM of each primer. The thermal cycling conditions were the following: a
187 single step of 10 min at 95 °C, 40 cycles of 95 °C for 15 s and 60 °C for 1 min. After the final
188 PCR cycle, a melting curve analysis of the PCR products was carried out by heating from 60 to
189 95 °C and continuous measurement of the fluorescence to verify the PCR product. The *aflP*
190 gene expression was evaluated following the concentrations and conditions previously
191 described (Rodríguez, Rodríguez, Luque, Martín, & Córdoba, 2012). Every qPCR assay
192 described above was carried out by triplicate. Gene expression ratio was calculated using the
193 $2^{-\Delta\Delta CT}$ method (Livak & Schmittgen, 2001). The endogenous control was set as the expression
194 of *β -tubulin* gene and the untreated batch described above was used as calibrator sample. For
195 every primer pair, a standard curve was generated to check the amplification efficiency from
196 ten-fold serial dilution 100 to 0.01 ng/ μ l of DNA from *A. parasiticus*. In addition, the
197 differences in amplification efficiencies between the housekeeping and the target gene were less
198 than 10%, as required to apply the relative quantification method (Schmittgen & Livak, 2008).

199 2.8. Statistical analysis

200 Statistical analyses were performed with the IBM SPSS v.22. Data from mycelia weight,
201 microbial counts, mycotoxin concentration and gene expression were tested for normality
202 (Kolmogorov-Smirnov with Lilliefors correction) and homoscedasticity (Levene's test). Given
203 that these data were non-normally distributed, mean values were compared using nonparametric
204 Kruskal–Wallis test. To compare treatments in pairs, Mann-Whitney U test was applied ($p \leq$
205 0.05). To study the relationship between expression of *aflP* and *foxA* genes, Spearman
206 correlation was applied.

207 3. Results

208 3.1. Growth inhibition and mycotoxin production in YES broth

209 To study the antifungal capability of the three agents, both separately and in the different
210 combinations, eight batches were tested against *A. parasiticus* at 15 days incubation in YES
211 broth. *A. parasiticus* growth was substantial in all treatments tested, with average values ranging
212 from 58 to 142 mg mycelium dry weight per 5 ml YES broth, though heterogeneous within
213 batches. As a result, no statistically significant differences were found in *A. parasiticus* growth
214 between the treatments. All expected mycotoxins were produced in the untreated batches by *A.*
215 *parasiticus*. Aflatoxin production showed differences ($p \leq 0.05$) depending on the treatment
216 applied. AFB₁ and AFG₁ production increased with PgAFP treatment, whereas all treatments
217 containing *P. acidilactici* strongly lowered aflatoxins production. *D. hansenii* inoculation also
218 led to lower AFB₁ production, and when combined with PgAFP seemed to counteract the
219 stimulating effect of PgAFP. AFG₁ was also detected in higher quantity in PgAFP and *D.*
220 *hansenii* co-inoculated than in the untreated batch (Fig. 1).

221 3.2. Growth inhibition and mycotoxin production on sausages

222 The effect of protective cultures on mould development was evaluated in fresh fermented
223 sausages slices simulating the ripening environmental conditions. A_w values reached 0.93 and
224 0.86 at 5 and 15 incubation days, respectively. The microbial load in pre-sterilised slices just
225 before inoculation was 2.3 log cfu/cm² for moulds, 1 log cfu/cm² for lactic acid bacteria, and
226 lower than 1.7 log cfu/cm² for yeasts. Yeasts counts were always over 5 log cfu/cm² in *D.*
227 *hansenii*-inoculated batches, but lower than 2 log cfu/cm² in the untreated batch. Similarly,
228 MRS counts were over 6.8 log cfu/cm² in *P. acidilactici*-inoculated batches, but lower than 4.5
229 log cfu/cm² in all batches not inoculated with *P. acidilactici*. Mould counts from untreated
230 batches both at 5 and 15 days were over 6.5 and 7.4 log cfu/cm² respectively. Pg+Dh or
231 Pg+Dh+Pa treatments dramatically lowered mold counts about 3 log units in *A. parasiticus*
232 batches.

233 On the other hand, mycotoxin production in the sausages was somehow parallel to fungal
234 growth. *A. parasiticus* produced high AFB₁ and AFG₁ levels in untreated sausages, both at 5
235 and 15 incubation days (Table 1). Aflatoxin production by *A. parasiticus* in sausages subjected
236 to any of the two treatments applied showed lower mycotoxin content (than the
237 respective untreated batches both at days 5 and 15.

238 3.3. Gene expression

239 The amplification efficiencies from each primer pair used, calculated from the slopes of the
240 standard curves, revealed that the maximum difference between the amplification efficiency

241 values of the housekeeping and the other two target genes was 5 % for *A. parasiticus* (Table 2),
242 thus the $2^{-\Delta\Delta CT}$ method was applied. Noteworthy, CT values for *aflP* gene from all samples,
243 including untreated batch, were very close to those obtained from the no template controls. On
244 the other hand, the expression of *aflP* gene was repressed in *A. parasiticus* by the sole action of
245 either PgAFP or *P. acidilactici* as well as the combined treatment of Pg+Dh+Pa, at 5 incubation
246 day (Fig. 2).

247 To study the possible effect of ROS induction by PgAFP on *A. parasiticus* the *foxA* gene
248 expression was evaluated at 5 incubation days to make sure that the activity of PgAFP on *A.*
249 *parasiticus* was high. The expression of *foxA* from PgAFP-treated samples did not differ from
250 untreated batch ($p > 0.05$). Only differed the combined treatment of Pg+Dh+Pa differed ($p \leq$
251 0.05) from the untreated batch, leading to a 4-fold over-expression. *aflP* gene expression values
252 did not correlate with *foxA* values ($p > 0.05$).

253 4. Discussion

254 As expected, PgAFP did not show antifungal ability at 15 days on *A. parasiticus* grown on
255 culture medium. The PgAFP concentration used was too low to reach a significant effect, as it
256 was shown previously (Delgado, Acosta, et al., 2015). In addition, none of the two microbial
257 strains, either alone or in any combination used, effectively inhibited mold growth in the culture
258 medium. However, both Pg+Dh and Pg+Dh+Pa combinations showed a remarkable inhibition
259 on *A. parasiticus* counts on the sausages (Table 1). Counts of *A. parasiticus* at day 5 in non-
260 treated sausages were over $6.5 \log \text{cfu/cm}^2$, whereas in the two treated batches, i.e.: PgAFP+Db
261 and PgAFP+Db+Pa, were below $3.5 \log \text{cfu/cm}^2$. Given that $3.5 \log \text{cfu/cm}^2$ has been suggested
262 as the limit to keep minimal risk of AFB₁ accumulation in dry-cured hams (Rodríguez,
263 Rodríguez, Martín, Nuñez, et al., 2012), the two combined treatments applied could be useful to
264 control aflatoxigenic moulds in dry-cured meat products. At 15 days incubation time, period
265 covering most of ripening stage of dry-fermented sausages, mold count in treated batches were
266 still around 0.1% of the fungal load in the untreated sausages.

267 The lack of inhibitory effect of the tested antifungal agents in the culture medium as compared
268 to the efficient inhibition in dry-fermented sausages can be attributed to the differences in
269 substrate availability. The mode of action proposed for yeasts to control molds in culture media
270 is competition for nitrogen compounds, sugars, and vitamins (Liu, Luo, & Long, 2013).
271 However, production of some volatile compounds derived from branched amino acids by *D.*
272 inhibition (Andrade, Córdoba, Casado, Córdoba, &
273 Rodríguez, 2010; Núñez et al., 2015). The culture medium used contains 125 g/l sucrose and 20
274 g/l yeast extract, providing readily available sources of carbon and nitrogen compounds, as well
275 as vitamins, especially those belonging to B complex. Conversely, sausages contain lower

276 amounts of sugars and vitamins, but higher levels of free amino acids throughout the ripening
277 process (Demasi, Wardlaw, Dick, & Acton, 1990; Hierro, de la Hoz, & Ordóñez, 1999).
278 Therefore, the lower amount of sugars and vitamins but higher amino acid content in the
279 sausage can be the key factor for the efficient inhibition of *A. parasiticus* by *D. hansenii* and *P.*
280 *acidilactici*.

281 Applying only PgAFP cannot be supported for dry-cured foods, given that this protein increased
282 aflatoxins production on *A. parasiticus* in YES broth (Fig. 1) and its fungistatic effect was not
283 enough to maintain sufficient inhibition throughout the whole ripening time (Delgado, Acosta,
284 et al., 2015). On the other hand, the same strain of *D. hansenii* used here was barely active at
285 lower (0.84) compared to high (0.94) a_w values when grown on dry-cured ham slices for 15 days
286 (Andrade et al., 2014). Therefore, *D. hansenii* alone is not expected to efficiently inhibit *A.*
287 *parasiticus* in sausages at a_w values around 0.85. Conversely, the combination of PgAFP and *D.*
288 *hansenii* efficiently inhibited *A. parasiticus* growth in the sausage samples (Table 1). This has to
289 be explained by the joint effect of the different mechanisms of action of these two antifungal
290 agents. Thus, the limited effect of PgAFP can be decisive to help other biological agents reach
291 an efficient inhibition of mycotoxigenic molds in dry-cured meats, particularly at low a_w values.
292 Thus, the effect of the combinations Pg+Dh and Pg+Dh+Pa on aflatoxin production was tested
293 on sausage. These two treatments efficiently lowered aflatoxin production for at least 15 days
294 on sausage samples, with no additional effect attributable to *P. acidilactici*. Since yeast extract
295 and glucose enhance production of antifungal metabolites in *P. acidilactici* (Effat, Ibrahim,
296 Tawfik, & Sharaf, 2001), the lack of additional effect due to this bacteria can be explained by
297 the shortage of glucose and readily available nitrogen compounds in sausage samples.

298 However, 10 $\mu\text{g/ml}$ PgAFP increased aflatoxin production by *A. parasiticus* in YES broth (Fig.
299 1), whereas *P. acidilactici* led to lower aflatoxin levels. Therefore, mycotoxin production does
300 not only depend on mould growth. The oxidative status in the fungal cell severely affects
301 mycotoxin production (Schmidt-Heydt, Stoll, Schütz, & Geisen, 2014). Several antifungal
302 proteins from moulds provoke ROS in sensitive strains (Galgóczy et al., 2013; Kaiserer et al.,
303 2003), including PgAFP in *A. flavus* (Delgado, Owens, et al., 2015). ROS production is
304 regarded as a prerequisite for the onset of aflatoxin production (Reverberi et al., 2005; Reverberi
305 et al., 2012). Conversely, several antioxidant substances or enzymes inhibit aflatoxin production
306 (Kim et al., 2008; Reverberi et al., 2005). For all this, the effect of PgAFP and *P. acidilactici* on
307 the oxidative status and the rate of aflatoxin biosynthesis of *A. parasiticus* was studied.

308 The oxidative role of PgAFP could be related to the higher levels of aflatoxins found in *A.*
309 *parasiticus*, as discussed later. Co-inoculation of *A. parasiticus* with *P. acidilactici* led to lower
310 AFB₁ production in YES, irrespectively of the addition of PgAFP, whereas the separate

311 inoculation of *D. hansenii* had no significant effect. Therefore, *P. acidilactici* seems to prevent
312 the increment of mycotoxin production provoked by PgAFP. The mechanism behind the lower
313 aflatoxin biosynthesis is not known. The lower aflatoxin production with lactic acid bacteria has
314 been related to inhibition of aflatoxin biosynthesis by low-molecular-weight inhibitory
315 compounds as well as removing due to aflatoxin binding (Dalié, Deschamps, & Richard-Forget,
316 2010).

317 The PgAFP mechanism of action on sensitive molds seems to be multifactorial, where
318 membrane permeabilization, ROS production or apoptosis induction play a key role (Delgado,
319 Owens, et al., 2015). The effect of ROS on aflatoxin synthesis is related to redox balance
320 through β -oxidation (Reverberi et al., 2012). The expression of genes *foxA* has been used as a
321 marker for peroxisomal β -oxidation (Reverberi et al., 2012). Besides, *aflP* gene has been used to
322 study the effect of environmental factors on aflatoxin production (Lozano-Ojalvo et al., 2013).
323 Thus, *aflP* and *foxA* expression was studied to elucidate the effect of PgAFP on aflatoxin
324 production and the potential role of oxidative stress on such production.

325 *aflP* expression in *A. parasiticus* grown in YES was very low, irrespectively of the treatment
326 applied. PgAFP did not provoke *aflP* overexpression, but it rather repressed *aflP* expression
327 (Fig. 2). Similarly, no statistically significant differences were found for *foxA* gene expression
328 due to PgAFP treatment. These results are consistent with the lower relative abundance of O-
329 methyltransferase, coded by *aflP* gene, and the unaffected level of peroxisomal multifunctional
330 β -oxidation protein, coded by *foxA* gene, found in PgAFP treated *A. flavus* (Delgado, Owens, et
331 al., 2015). In addition, *D. hansenii* did not alter *foxA* and *aflP* expression, supporting that the
332 effect of this yeast reducing antioxidant effect.

333 Therefore, the aflatoxin overproduction observed in PgAFP-treated *A. parasiticus* at 15 days
334 would not be initiated by an increased β -oxidation due to ROS. Given that ROS induction are
335 among the early antifungal effects of PgAFP, no later effect on β -oxidation should be expected
336 to be responsible for the observed aflatoxin production. In addition, the increased *foxA*
337 expression in the combined treatment of Pg+Dh+Pa does not correlate with a higher aflatoxin
338 production at 15 days. These results suggest that the effect of ROS on aflatoxin biosynthesis
339 cannot be explained solely through β -oxidation. In a recent paper (Roze et al., 2015) it is
340 reported that upon exposure to exogenous ROS, secondary ROS are generated in endosomes
341 during aflatoxins biosynthesis. It is suggested that this results in an adaptation of cellular
342 metabolism to promote increased tolerance to H₂O₂ in the next generation of germinating
343 spores. Studying the effect of PgAFP on the secondary ROS will require further studies.

344 On the other hand, *P. acidilactici*, either alone or combined with Pg and Dh, down-regulated
345 *aflP* gene expression in *A. parasiticus* at day 5 (Fig. 2), which is parallel to a lower aflatoxin

378 **5. Bibliography**

- 379 Acosta, R., Rodríguez-Martín, A., Martín, A., Núñez, F., & Asensio, M. A. (2009). Selection of
380 antifungal protein-producing molds from dry-cured meat products. *International Journal of*
381 *Food Microbiology*, 135(1), 39–46. <http://doi.org/10.1016/j.ijfoodmicro.2009.07.020>
- 382 Andrade, M. J., Córdoba, J. J., Casado, E. M., Córdoba, M. G., & Rodríguez, M. (2010). Effect
383 of selected strains of *Debaryomyces hansenii* on the volatile compound production of dry
384 fermented sausage “salchichón.” *Meat Science*, 85(2), 256–264.
385 <http://doi.org/10.1016/j.meatsci.2010.01.009>
- 386 Andrade, M. J., Thorsen, L., Rodríguez, A., Córdoba, J. J., & Jespersen, L. (2014). Inhibition of
387 ochratoxigenic moulds by *Debaryomyces hansenii* strains for biopreservation of dry-cured meat
388 products. *International Journal of Food Microbiology*, 170, 70–77.
389 <http://doi.org/10.1016/j.ijfoodmicro.2013.11.004>
- 390 Bezerra da Rocha, M. E., Oliveira Freire, F. D. C., Feitosa Maia, F. E., Florindo Guedes, M. I.,
391 & Rondina, D. (2014). Mycotoxins and their effects on human and animal health. *Food Control*,
392 36(1), 159–165. <http://doi.org/10.1016/j.foodcont.2013.08.021>
- 393 Chang, I., & Kim, J. (2007). Inhibition of Aflatoxin Production of *Aspergillus flavus* by
394 *Lactobacillus casei*. *Mycobiology*, 35(2), 76–81.
- 395 Currie, L. A. (1999). Nomenclature in evaluation of analytical methods including detection and
396 quantification capabilities. *Analytica Chimica Acta*, 391(2), 105–126.
397 [http://doi.org/10.1016/S0003-2670\(99\)00104-X](http://doi.org/10.1016/S0003-2670(99)00104-X)
- 398 Dalié, D. K. D., Deschamps, A. M., & Richard-Forget, F. (2010). Lactic acid bacteria - Potential
399 for control of mould growth and mycotoxins: A review. *Food Control*, 21(4), 370–380.
400 <http://doi.org/10.1016/j.foodcont.2009.07.011>
- 401 Delgado, J., Acosta, R., Rodríguez-Martín, A., Bermúdez, E., Núñez, F., & Asensio, M. A.
402 (2015). Growth inhibition and stability of PgAFP from *Penicillium chrysogenum* against fungi
403 common on dry-ripened meat products. *International Journal of Food Microbiology*, 205, 23–
404 29. <http://doi.org/10.1016/j.ijfoodmicro.2015.03.029>
- 405 Delgado, J., Owens, R. A., Doyle, S., Asensio, M. A., & Núñez, F. (2015). Impact of the
406 antifungal protein PgAFP from *Penicillium chrysogenum* on the protein profile in *Aspergillus*
407 *flavus*. *Applied Microbiology and Biotechnology*, 99(20), 8701–8715.
408 <http://doi.org/10.1007/s00253-015-6731-x>

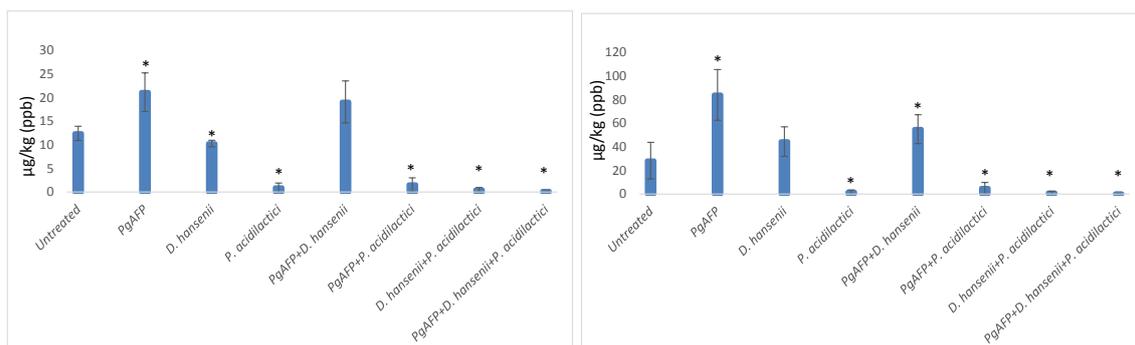
- 409 Demasi, T. W., Wardlaw, F. B., Dick, R. L., & Acton, J. C. (1990). Nonprotein Nitrogen (NPN)
410 and Free amino acid contents of dry, fermented and nonfermented sausages. *Meat Science*,
411 27(1), 1–12. [http://doi.org/10.1016/0309-1740\(90\)90024-Z](http://doi.org/10.1016/0309-1740(90)90024-Z)
- 412 Effat, B. A., Ibrahim, G. A., Tawfik, N. F., & Sharaf, O. M. (2001). Comparison of antifungal
413 activity of metabolites from *Lactobacillus rhamnosus*, *Pediococcus acidilactici* and
414 *Propionibacterium thoenii*. *Egyptian Journal of Dairy Sciences*, 29, 251–262.
- 415 European Commission. (2006). Commission regulation (CE) 1881/2006 of 19 December 2006
416 setting maximum levels for certain contaminants in foodstuffs. *Official Journal of the European*
417 *Union*, 2006(L364), 5–24.
- 418 Galgóczy, L., Kovács, L., Karácsony, Z., Virágh, M., Hamari, Z., & Vágvölgyi, C. (2013).
419 Investigation of the antimicrobial effect of *Neosartorya fischeri* antifungal protein (NFAP) after
420 heterologous expression in *Aspergillus nidulans*. *Microbiology (Reading, England)*, 159(Pt 2),
421 411–419. <http://doi.org/10.1099/mic.0.061119-0>
- 422 Gourama, H., & Bullerman, L. B. (1995). Inhibition of Growth and Aflatoxin Production of
423 *Aspergillus flavus* by *Lactobacillus* Species. *Journal of Food Protection*. 58(11) 1249-1256
- 424 Hierro, E., de la Hoz, L., & Ordóñez, J. A. (1999). contribution of microbial and meat
425 endogenous enzymes to the lipolysis of dry fermented sausages. *Journal of Agricultural and*
426 *Food Chemistry*, 45(8), 2989–2995. <http://doi.org/10.1021/jf970127g>
- 427 Jayashree, T., & Subramanyan, C. (2000). Oxidative stress as a prerequisite for aflatoxin
428 production by *Aspergillus parasiticus*. *Free Radical Biology & Medicine*, 29(10), 981–985.
- 429 Kaiserer, L., Oberparleiter, C., Weiler-Görz, R., Burgstaller, W., Leiter, E., & Marx, F. (2003).
430 Characterization of the *Penicillium chrysogenum* antifungal protein PAF. *Archives of*
431 *Microbiology*, 180(3), 204–210. <http://doi.org/10.1007/s00203-003-0578-8>
- 432 Kim, J. H., Yu, J., Mahoney, N., Chan, K. L., Molyneux, R. J., Varga, J., ... Campbell, B. C.
433 (2008). Elucidation of the functional genomics of antioxidant-based inhibition of aflatoxin
434 biosynthesis. *International Journal of Food Microbiology*, 122(1-2), 49–60.
435 <http://doi.org/10.1016/j.ijfoodmicro.2007.11.058>
- 436 Li, H., Zhang, S., Lu, J., Liu, L., Uluko, H., Pang, X., ... Lv, J. (2014). Antifungal activities and
437 effect of *Lactobacillus casei* AST18 on the mycelia morphology and ultrastructure of
438 *Penicillium chrysogenum*. *Food Control*, 43, 57–64.
439 <http://doi.org/10.1016/j.foodcont.2014.02.045>

- 440 Liu, P., Luo, L., & Long, C. an. (2013). Characterization of competition for nutrients in the
441 biocontrol of *Penicillium italicum* by *Kloeckera apiculata*. *Biological Control*, 67(2), 157–162.
442 <http://doi.org/10.1016/j.biocontrol.2013.07.011>
- 443 Livak, K. J., & Schmittgen, T. D. (2001). Analysis of relative gene expression data using real-
444 time quantitative PCR and the 2(-Delta Delta C(T)) Method. *Methods*, 25(4), 402–408.
445 <http://doi.org/10.1006/meth.2001.1262>
- 446 Long, G. L., & Winefordner, J. D. (1983). Limit of detection, a closer look at the IUPAC
447 definition. *Analytical Chemistry*, 55(7), A712–&. <http://doi.org/10.1021/ac00258a001>
- 448 López-Díaz, T. M., Santos, J. A, García-López, M. L., & Otero, A. (2001). Surface mycoflora
449 of a Spanish fermented meat sausage and toxigenicity of *Penicillium* isolates. *International*
450 *Journal of Food Microbiology*, 68(1-2), 69–74. <http://www.ncbi.nlm.nih.gov/pubmed/11545222>
- 451 Lowry, O. H., Rosebrough, N. J., Farr, L., & Randall, R. J. (1951). Protein measurement with
452 the folin phenol reagent. *The Journal of Biological Chemistry*, 193, 265–275.
- 453 Lozano-Ojalvo, D., Rodríguez, A., Bernáldez, V., Córdoba, J. J., & Rodríguez, M. (2013).
454 Influence of temperature and substrate conditions on the omt-1 gene expression of *Aspergillus*
455 *parasiticus* in relation to its aflatoxin production. *International Journal of Food Microbiology*,
456 166(2), 263–269. <http://doi.org/10.1016/j.ijfoodmicro.2013.07.011>
- 457 Mandal, V., Sen, S. K., & Mandal, N. C. (2013). Production and partial characterisation of an
458 inducer-dependent novel antifungal compound(s) by *Pediococcus acidilactici* LAB 5. *Journal*
459 *of the Science of Food and Agriculture*, 93(10), 2445–2453. <http://doi.org/10.1002/jsfa.6055>
- 460 Marx, F. (2004). Small, basic antifungal proteins secreted from filamentous ascomycetes: a
461 comparative study regarding expression, structure, function and potential application. *Applied*
462 *Microbiology and Biotechnology*, 65(2), 133–142. <http://doi.org/10.1007/s00253-004-1600-z>
- 463 Miller, J. D. (2001). Factors that affect the occurrence of fumonisin. *Environmental Health*
464 *Prospectives*, 109(Supplement 2), 321–324.
- 465 Montiel, R., Bravo, D., & Medina, M. (2013). Commercial biopreservatives combined with salt
466 and sugar to control *Listeria monocytogenes* during smoked salmon processing. *Journal of Food*
467 *Protection*, 76(8), 1463–1465. <http://doi.org/10.4315/0362-028X.JFP-12-560>
- 468 Núñez, F., Lara, M. S., Peromingo, B., Delgado, J., Sanchez-Montero, L., & J. Andrade, M.
469 (2015). Selection and evaluation of *Debaryomyces hansenii* isolates as potential bioprotective
470 agents against toxigenic penicillia in dry-fermented sausages. *Food Microbiology*, 46, 114–120.
471 <http://doi.org/10.1016/j.fm.2014.07.019>

- 472 Núñez, F., Rodríguez, M. M., Bermúdez, M. E., Córdoba, J. J., & Asensio, M. A. (1996).
473 Composition and toxigenic potential of the mould population on dry-cured Iberian ham.
474 *International Journal of Food Microbiology*, 32(1-2), 185–97.
475 <http://www.ncbi.nlm.nih.gov/pubmed/8880338>
- 476 Núñez, F., Rodríguez, M. M., Córdoba, J. J., Bermúdez, M. E., & Asensio, M. A. (1996). Yeast
477 population during ripening of dry-cured Iberian ham. *International Journal of Food*
478 *Microbiology*, 29(27), 271–280. [http://doi.org/10.1016/0168-1605\(95\)00037-2](http://doi.org/10.1016/0168-1605(95)00037-2)
- 479 Payne, G. A., & Hagler Jr., W. M. (1983). Effect of specific amino acids on growth and
480 aflatoxin production by *Aspergillus parasiticus* and *Aspergillus flavus* in defined media. *Applied*
481 *and Environmental Microbiology*, 46(4), 805–812.
482 [http://www.ncbi.nlm.nih.gov/entrez/query.fcgi?cmd=Retrieve&db=PubMed&dopt=Citation&lis](http://www.ncbi.nlm.nih.gov/entrez/query.fcgi?cmd=Retrieve&db=PubMed&dopt=Citation&list_uids=6416168)
483 [t_uids=6416168](http://www.ncbi.nlm.nih.gov/entrez/query.fcgi?cmd=Retrieve&db=PubMed&dopt=Citation&list_uids=6416168)
- 484 Reverberi, M., Fabbri, A. A., Zjalic, S., Ricelli, A., Punelli, F., & Fanelli, C. (2005).
485 Antioxidant enzymes stimulation in *Aspergillus parasiticus* by *Lentinula edodes* inhibits
486 aflatoxin production. *Applied Microbiology and Biotechnology*, 69(2), 207–15.
487 <http://doi.org/10.1007/s00253-005-1979-1>
- 488 Reverberi, M., Punelli, M., Smith, C. a, Zjalic, S., Scarpari, M., Scala, V., ... Fanelli, C. (2012).
489 How peroxisomes affect aflatoxin biosynthesis in *Aspergillus flavus*. *PloS One*, 7(10), e48097.
490 <http://doi.org/10.1371/journal.pone.0048097>
- 491 Rodríguez, A., Medina, Á., Córdoba, J. J., & Magan, N. (2014). The influence of salt (NaCl) on
492 ochratoxin A biosynthetic genes, growth and ochratoxin A production by three strains of
493 *Penicillium nordicum* on a dry-cured ham-based medium. *International Journal of Food*
494 *Microbiology*, 178, 113–119. <http://doi.org/10.1016/j.ijfoodmicro.2014.03.007>
- Rodríguez, A., Rodríguez, M., Luque, M. I., Martín, A., & Córdoba, J. J. (2012). Real
496 PCR assays for detection and quantification of aflatoxin-producing molds in foods. *Food*
497 *Microbiology*, 31(1), 89–99. <http://doi.org/10.1016/j.fm.2012.02.009>
- 498 Rodríguez, A., Rodríguez, M., Martín, A., Delgado, J., & Córdoba, J. J. (2012). Presence of
499 ochratoxin A on the surface of dry-cured Iberian ham after initial fungal growth in the drying
500 stage. *Meat Science*, 92(4), 728–734. <http://doi.org/10.1016/j.meatsci.2012.06.029>
- 501 Rodríguez, A., Rodríguez, M., Martín, A., Nuñez, F., & Córdoba, J. J. (2012). Evaluation of
502 hazard of aflatoxin B1, ochratoxin A and patulin production in dry-cured ham and early
503 detection of producing moulds by qPCR. *Food Control*, 27(1), 118–126.
504 <http://doi.org/10.1016/j.foodcont.2012.03.009>

- 505 Rodríguez-Martín, A., Acosta, R., Liddell, S., Núñez, F., Benito, M. J., & Asensio, M. A.
506 (2010). Characterization of the novel antifungal protein PgAFP and the encoding gene of
507 *Penicillium chrysogenum*. *Peptides*, 31(4), 541–547.
508 <http://doi.org/10.1016/j.peptides.2009.11.002>
- 509 Roze, L., Laivenieks, M., Hong, S.-Y., Wee, J., Wong, S.-S., Vanos, B., ... Linz, J. (2015).
510 Aflatoxin biosynthesis is a novel source of reactive oxygen species—A potential redox signal to
511 initiate resistance to oxidative stress? *Toxins*, 7, 1411–1430.
512 <http://doi.org/10.3390/toxins7051411>
- 513 Roze, L. V, Chanda, A., Laivenieks, M., Beaudry, R. M., Artymovich, K. a, Koptina, A. V, ...
514 Linz, J. E. (2010). Volatile profiling reveals intracellular metabolic changes in *Aspergillus*
515 *parasiticus*: *veA* regulates branched chain amino acid and ethanol metabolism. *BMC*
516 *Biochemistry*, 11, 33. <http://doi.org/10.1186/1471-2091-11-33>
- 517 Schmidt-Heydt, M., Stoll, D., Schütz, P., & Geisen, R. (2014). Oxidative stress induces the
518 biosynthesis of citrinin by *Penicillium verrucosum* at the expense of ochratoxin. *International*
519 *Journal of Food Microbiology*, 192C, 1–6. <http://doi.org/10.1016/j.ijfoodmicro.2014.09.008>
- 520 Schmittgen, T. D., & Livak, K. J. (2008). Analyzing real-time PCR data by the comparative CT
521 method. *Nature Protocols*, 3(6), 1101–1108. <http://dx.doi.org/10.1038/nprot.2008.73>
- 522 Yu, J., Chang, P., Ehrlich, K. C., Cary, J. W., Bhatnagar, D., Cleveland, T. E., ... Bennett, J. W.
523 (2004). Clustered pathway genes in Aflatoxin biosynthesis. *Applied and Environmental*
524 *Microbiology*, 70(3), 1253–1262. <http://doi.org/10.1128/AEM.70.3.1253>
- 525
- 526
- 527
- 528
- 529
- 531
- 532
- 533
- 534

535 **6. Figures and tables**



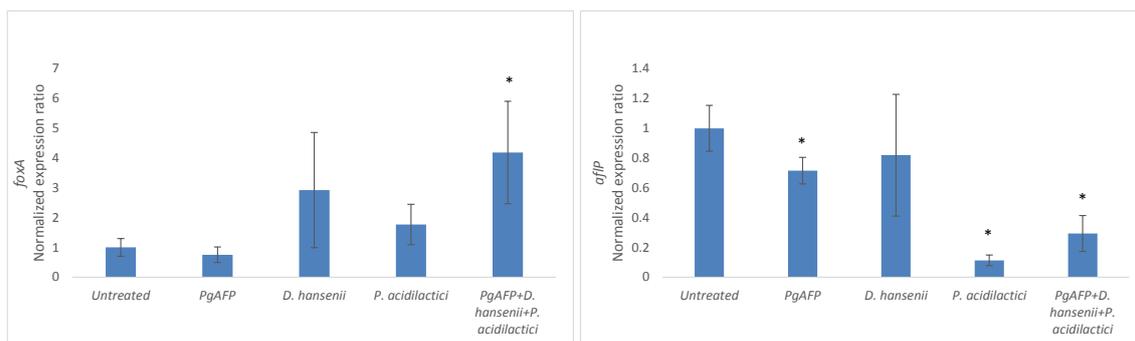
536

537 Figure 1. Effect of different combinations of protective agents in aflatoxin B₁ (left) and G₁
 538 (right) production by *Aspergillus parasiticus* in yeast extract sucrose broth after 15 days. Bars
 539 represent standard deviation. * ($p \leq 0.05$)

540

541

542



543

544 Figure 2. Effect of different antifungal agents on relative gene expression of *foxA* (left) and *aflP*
 545 (right) genes in yeast extract sucrose broth after 5 days. Bars represent standard deviation. * ($p \leq$
 546 0.05)

547

548 Table1. Aflatoxin B₁ (AFB₁) and G₁ (AFG₁) concentrations (µg/kg) and mould counts (log
 549 cfu/cm²) in dry-fermented sausage slices at 5 and 15 incubation days. Data are given as mean ±
 550 SD. * ($p \leq 0.05$)

Day 5			
Mycotoxin	Control	Pg+Dh	Pg+Dh+Pa
AFB ₁	86±8	<LOD	<LOD
AFG ₁	152±9	<LOD	<LOD
Mould counts	6.54±0.22	<3 ^{a*}	<3 ^{a*}
Day 15			
Mycotoxin	Control	Pg+Dh	Pg+Dh+Pa
AFB ₁	115±0,43	<LOD*	<LOD*
AFG ₁	170±31	8.3±4.5*	10±1.3*
Mould counts	7.42±0.09	4.26±0.28 ^a	4.74±0.38 ^a

551

552

553

554

555 Table 2. Nucleotide sequence of primers used for qPCR assay

Primer name	Nucleotide sequences (5'-3')	Efficiencies	Product size	Position	Reference
F-Omt-1	GGCCGCCGCTTTGATCTAGG			^a 1485	(Rodríguez, Rodríguez, Luque, Martín, & Córdoba, 2012)
R-Omt-1	ACCACGACCGCCGCC	104%	123	1593	
F- β -tub	TCTTCATGGTTGGCTTCGCT	101%	98	^b 964	This study
R- β -tub	CTTGGGGTTCGAACATCTGCT			1042	
F- foxA	ACCGCAACCCTCTTCACATT	106%	73	^c 1196	This study
R- foxA	AGACCGTGCAGGATAGGAGT			1268	

556 ^a Positions are in accordance with published sequence of the *aflP* (*omt-1*) gene of *A. flavus*

557 (GeneBank accession no. L25835.1).

558 ^b Positions are in accordance with the published sequences of the β -*tubulin* gene of *A.*559 *parasiticus* (GeneBank accession no. FR775333.1).560 ^c Positions are in accordance with published sequence of the *foxA* gene of *A. flavus* (GeneBank

561 accession no. XM_002377580).

562

IV.2.2. Evaluación en queso

Effect of PgAFP and protective cultures on Aspergillus flavus and Aspergillus parasiticus growth inhibition and aflatoxin production in a calcium-enriched medium and on cheese

1 **Effect of PgAFP and protective cultures on *Aspergillus flavus* and *Aspergillus parasiticus***
2 **growth inhibition and aflatoxin production in a calcium-enriched medium and on cheese**

3

4 Intermediate-moisture foods are adequate substrates for various microorganisms,
5 including lactic acid bacteria (LAB) (Casquete et al., 2012; Papadima and Bloukas, 1999),
6 molds (Núñez et al., 1996) and yeasts (Asefa et al., 2009). These microorganisms play a key
7 role in the development of sensory characteristics of intermediate moisture foods (Andrade et
8 al., 2010; Martín et al., 2006; Urbach, 1995). However, some molds can have a negative impact
9 by altering the sensory characteristics or producing toxic metabolites (Alapont et al., 2014;
10 Filtenborg et al., 1996). Aflatoxins are among the most harmful mycotoxins, displaying
11 oncogenic, immunosuppressive, hepatotoxic, and teratogenic effects (Bezerra da Rocha et al.,
12 2014). Dairy products, including cheese and yoghurt, are susceptible to fungal attack (Crowley
13 et al., 2013) and support the production of high levels of aflatoxins (Lie and Marth, 1967;
14 Taniwaki et al., 2001). To control the mycotoxin risk, it is necessary to establish a Hazard
15 Analysis Critical Control Point (HACCP) plan for intermediate-moisture products (Asefa et al.,
16 2011).

17 Antifungals compounds can be used for this purpose, but chemical fungicides would
18 leave residues, which is against consumers demand (Núñez et al., 2015). Protective cultures and
19 their metabolic products could provide an effective means to control mycotoxins in intermediate
20 moisture foods well accepted by consumers.

21 The antifungal protein PgAFP, produced by *P. chrysogenum* CECT 20922, is within the
22 group of small, basic, and cysteine-rich antifungal proteins (Rodríguez-Martín et al., 2010). This
23 protein inhibits various toxigenic molds and has proved to inhibit *A. flavus* on a dry-fermented
24 sausage (Delgado et al., 2015a). However, the antifungal capability of this kind of proteins is
25 dramatically reduced in presence of divalent cations, such as Ca⁺² (Chen et al., 2013; Galgóczy
26 et al., 2013; Kaiserer et al., 2003). Calcium provokes a strong inhibition on PgAFP antifungal
27 ability, rendering this protein ineffective on cheese (Delgado et al., 2015c). To investigate
28 further strategies to control the mycotoxigenic hazard in cheeses. LAB are commonly used as
29 starter cultures on cheeses, some of them showing strong antifungal activity in dairy products
30 (Cheong et al., 2014; Muhialdin et al., 2011). Yeasts are generally present in aged cheeses,
31 being *Debaryomyces hansenii* the most abundant species isolated (Viljoen and Greyling, 1995;
32 Welthagen and Viljoen, 1998). This yeast has been proposed for biocontrol of *Penicillium* spp.
33 and *Aspergillus* spp. in cheese (Liu and Tsao, 2009). However, the effect of LAB and *D.*
34 *hansenii* is also limited, not being able to efficiently inhibit aflatoxin production in cheese.
35 Therefore, the combined action of the antifungal protein PgAFP with LAB and yeasts to prevent
36 mold development and aflatoxin production deserves to be investigated.

37 PgAFP increased reactive oxygen species (ROS) levels on sensitive strains (Delgado et
38 al., 2015b), but an enhanced response to oxidative stress was obtained when *A. flavus* was
39 grown in 0.1 M CaCl₂, preventing the antifungal activity (Delgado et al., 2015c). ROS and is
40 related with the regulation of β -oxidation and peroxisome proliferation that play a key role in
41 aflatoxin biosynthesis. Thus, the expression of several genes involved in these processes have
42 been used to relate them with aflatoxin production (Reverberi et al., 2012) The gene expression
43 of some of these genes from aflatoxigenic strains treated with PgAFP and/or yeasts and LAB,
44 and grown in cation-rich medium could offer information about the effect of these protective
45 agents on the oxidative status of the mold as well as the aflatoxin biosynthesis.

46 On the other hand, the effect of the antifungal ability of the protective cultures should be
47 evaluated on cheese. Thus, the aim of this work was to investigate the antifungal ability of
48 PgAFP together with *D. hansenii* and/or *Pediococcus acidilactici* in a calcium enriched culture
49 media to study the effect of these two microorganisms on β -oxidation and aflatoxin gene
50 expression. A combined action with microorganisms endowed with other antifungal mechanism
51 of action could alter the successful response of the aflatoxigenic molds to PgAFP. Additionally,
52 the antifungal ability of the combinations and reduction of mycotoxin production on two
53 aflatoxigenic strains were tested on cheese.

54 **Material and methods**

55 **Strains**

56 Three mold strains obtained from Spanish Type Culture Collection (CECT, Valencia,
57 Spain) were used in this study: the PgAFP sensitives aflatoxin-producer *A. parasiticus* CECT
58 2682 and *Aspergillus flavus* CECT 2687, as well as the PgAFP antifungal protein producer *P.*
59 *chrysogenum* CECT 20922. In addition, two potential antifungal strains were used: the yeast *D.*
60 *hansenii* Dh253 from the microbial collection of Food Hygiene and Safety of the University of
61 Extremadura (Cáceres, Spain) and *P. acidilactici* fargo 35 supplied by Laboratorios Amerex
62 (Colmenar Viejo, Spain).

63 **PgAFP production and purification**

64 *P. chrysogenum* CECT 20922 was grown in potato dextrose broth (PDB) pH 4.5 for 21
65 days at 25 °C. The mycelium was removed and the media was filtered to get cell free media.
66 PgAFP was isolated from 450 ml of the cell-free media through fast protein liquid
67 chromatography (FPLC) with a cationic exchange column HiTrap SP HP (Amersham
68 Biosciences, Uppsala, Sweden), further purified with a HiLoad 26/60 Superdex 75 gel filtration
69 column for FPLC (Amersham Biosciences) as previously described (Acosta et al., 2009). The
70 protein isolated and concentrated was sterilized through filtration (0.22 μ m, Thermo Fisher

71 Scientific, Waltham, MA, USA) and its concentration was assessed by the Lowry method
72 (Lowry et al., 1951).

73

74 Growth inhibition in culture media and mycotoxin extraction

75 The effect of PgAFP, *D. hansenii*, and *P. acidilactici* on *A. flavus* and *A. parasiticus* was
76 evaluated both separately and in all different combinations. For this, 5 ml of 0.1 M CaCl₂ Yeast
77 Extract Supplemented broth (YES) were inoculated with 10⁵ conidia/ml *A. flavus* or *A.*
78 *parasiticus*. To provide a high level of the biological agents, 10⁶ cells/ml *D. hansenii* (Dh), 10⁶
79 cells/ml *P. acidilactici* (Pa), and 10 µg/ml PgAFP (Pg) the following 7 different batches were
80 obtained: Pg, Dh, Pa, Pg+Dh, Pg+Pa, Dh+Pa, and Pg+Dh+Pa. Additionally, an untreated batch
81 used as a control. Samples were incubated for 15 days at 25 °C to stimulate aflatoxin production
82 (Lozano-Ojalvo et al., 2013). All the assays were carried out in triplicate. After incubation, 5 ml
83 of chloroform were added to each test tube incubated for 1 h shaking at 100 rpm at room
84 temperature in darkness. Then, the chloroform was separated and evaporated to dryness under a
85 gentle stream of N₂. The mycelium was recovered from the aqueous residue by filtering through
86 a miracloth (Calbiochem, Darmstadt, Germany), dried at 100 °C up to constant weight, and
87 weighed.

88 Growth inhibition on cheese and mycotoxin extraction

89 To test the potential of selected combinations of protective cultures, the environmental
90 conditions for ripening were simulated using a Gouda cheese commercial type (a_w 0.96). The
91 cheese was cut into 5 mm thick slices and dipped into ethanol to eliminate outer contamination.
92 The ethanol was left to evaporate in a laminar flow cabinet (Bio Flow II, Telstar, Tarrasa,
93 Spain) prior to placing the slices in pre-sterilized (ethanol and UV-light) receptacles containing
94 a saturated KCl solution to keep relative humidity constant at 84% after vapour-liquid
95 equilibrium. *A. flavus* or *A. parasiticus* was inoculated (10⁵ conidia/cm²) on both sides of each
96 slice. No antifungal treatment was applied to the untreated batches. Two treated batches were
97 made: Pg+Dh+Pa, with 10 µg/cm² PgAFP, 10⁶ cells/cm² *D. hansenii*, and 10⁶ cells/cm² *P.*
98 *acidilactici*; and Pg+Dh, with 10 µg/cm² PgAFP and 10⁶ cells/cm² *D. hansenii*, to test their
99 ability against *A. flavus* and *A. parasiticus*, similarly to the culture medium. Every batch was
100 carried out in triplicate. All samples received the same volume of liquid by adding sterile
101 phosphate buffer as required, and the liquid excess was left to dry in the laminar flow cabinet.
102 The samples were incubated for 5 and 15 days at 25 °C to stimulate aflatoxin production
103 (Lozano-Ojalvo et al., 2013). A_w values were determined in a Novasina Lab Master from
104 Novasina AG (Lachen, Switzerland). *A. parasiticus* and *D. hansenii* counts were assessed by
105 plating in PDA and incubated for 72 h at 25 °C, according to the characteristic colony

106 morphology. Lactic acid bacteria counts were evaluated on MRS agar, incubated for 72 h at 30
107 °C.

108 Mycotoxins produced on cheese slices were extracted as previously described (Rodríguez
109 et al., 2012b). Briefly, each cheese slice was macerated under shaking in a dark flask with 60 ml
110 acetonitrile-water (9:1, v/v) containing 0.1% formic acid together with 50 ml hexane. The
111 acetonitrile-water phase was recovered and filtered through sodium sulphate anhydrous. Then,
112 the filtrate was mixed with additional 50 ml of hexane and shaken. The acetonitrile-water phase
113 was filtered again and evaporated in a rotatory evaporator at 40–45 °C. The residue was
114 resuspended in 1 ml chloroform, filtered through a 0.45 µm nylon membrane (MSI, Westboro,
115 MA, USA).

116 Mycotoxin quantification

117 Extracts from both culture medium and cheese slices were analysed by ultra high-
118 performance liquid chromatography–mass spectrometry (uHPLC–MS) in an HPLC Thermo
119 Scientific Dionex ultimate 3000 pnmp, a mass detector (MS) model Bruker Amazon S.L., an
120 autosampler (Ultimate 3000), a degasser (3000 Ultimate) and an ion trap (Amazon SL.). A C18
121 reverse-phase column of 10 cm length, 2.1 mm inside diameter and 2 µm particle size was used
122 as stationary phase. As mobile phase a 0.1% formic acid-10 mM ammonium formate (solvent
123 A) and acetonitrile (solvent B) was used. The separation was performed with the flow rate set at
124 200 µl/min and the following gradient: [0 min] 2% B, [0-0.1 min], 40% B, [0.1-4 min] 60%
125 B, [4-7 min] 80% B, [7-8.5 min] 80% B, [8.5-8.51 min] 98% B, [8.51-12 min] 98% B, [12-12.01
126 min] 2% B and [12.01-15 min] 2% B. Precursor ions 313 and 329, and quantitation ions 285
127 and 311 for aflatoxins B₁ and G₁ (AFB₁ and AFG₁), respectively.

128 These parameters were compared to those obtained from commercial mycotoxins (Sigma-
129 Aldrich, Madrid, Spain). The calibration curves for AFB₁ and AFG₁ (1-500 ng) by uHPLC-MS
130 revealed a linear relationship ($r^2 \geq 0.99$) between detector response and amount of AFB₁ and
131 AFG₁ standards. The minimum detectable value or limit of detection (LOD) was estimated from
132 the calibration curve, according to the equation: $LOD = 3 (s_B^2 + s_i^2 + (i/m)^2 s_m)^{1/2}/m$ (Long and
133 Winefordner, 1983) being “m” the slope of the calibration curve, “I” the intercept term and “s_B”,
134 “s_i” and “s_m” the standard errors of the blank, the intercept term and the slope of the calibration
135 curve, respectively. Assuming a normal distribution of the estimated quantities, α (error of the
136 first type) = β (error of the second type) = 0.05, the quantification limit (LOQ) was 3.04 LOD
137 (Currie, 1999). The LOD obtained in this study were 4 µg/kg and 1.5 µg/kg, and the LOQ were
138 12 µg/kg and 4.5 µg/kg respectively for AFB₁ and AFG₁.

139 RNA isolation and cDNA synthesis

140 To test the influence of PgAFP, *D. hansenii* and *P. acidilactici* on *A. flavus* and *A.*
141 *parasiticus* gene expression, four batches were prepared in YES broth: *A. flavus* or *A.*
142 *parasiticus* (10^5 conidia/ml) was co-cultivated in tubes separately with PgAFP (10 µg/ml), *D.*
143 *hansenii* (10^6 cells/ml) or *P. acidilactici* (10^6 cells/ml), and with all of them together. The
144 untreated batch was inoculated solely with *A. parasiticus*. The tubes were incubated at 25°C for
145 5 days. For RNA extraction, mycelium was harvested and washed twice with sterile phosphate-
146 saline buffer (PBS), frozen in liquid nitrogen and ground with a mortar and pestle. Then the
147 powder was resuspended in 750µl RLT buffer (RNeasy® Plant Mini kit, Qiagen, Hilden,
148 Germany) containing 15µl β-mercaptoethanol. Samples were processed with the RNeasy® Plant
149 Mini kit according to manufacturer's instructions. RNA quality and quantity was
150 spectrophotometrically determined using a NanoDrop 2000c spectrophotometer (Thermo
151 Scientific, Waltham, MA, USA). Then, samples were treated with DNase I, RNase-free
152 (Fermentas, St. Leon-Rot, Germany) following manufacturer's instructions, and checked for
153 background double stranded DNA by qPCR for *β-tubulin* genes as described below. Finally,
154 cDNA was synthesized using 500 ng RNA according to PrimeScript™ RT Reagent kit protocol
155 (Takara, Otsu, Japan).

156 Real-time PCR analysis of gene expression

157 The expression of genes *aflP* (formerly *omt-1*) for aflatoxin biosynthesis (Yu et al.,
158 2004), *foxA* for β-oxidation (Roze et al., 2010), and *β-tubulin* as housekeeping (Rodríguez et al.,
159 2014) were assessed to evaluate the effect of the treatments on *A. parasiticus*. Primers to
160 evaluate the *foxA* expression were designed from the gene AFLA_041590 (GeneBank accession
161 no. XM_002377580), as previously described (Roze et al., 2010)(Reverberi et al., 2012).
162 Similarly, to study *β-tubulin* expression a couple of primers were designed from *A. parasiticus*
163 *β-tubulin* sequence (GeneBank accession no. FR775333.1)

164 To quantify the relative expression of the genes, *foxA* and *β-tubulin* genes expression
165 were assessed by using the SYBR Green qPCR in an Applied Biosystems ViiATM 7 Real-Time
166 PCR System (Applied Biosystems, Foster City, California, USA). To optimize the primer
167 concentration, different concentrations from 800 to 200 nM were tested. The optimized SYBR
168 Green protocol was carried out in a final volume of 25 µl containing 5 ml of template DNA,
169 12.5 µl of 2x SYBR® *Premix Ex Taq*™ (Takara, Otsu, Japan), 0.5 µl of 50x ROX™ Reference
170 Dye (Takara) and 400 nM of each primer. The thermal cycling conditions were the following: a
171 single step of 10 min at 95 °C, 40 cycles of 95 °C for 15 s and 60 °C for 1 min. After the final
172 PCR cycle, a melting curve analysis of the PCR products was carried out by heating from 60 to
173 95 °C and continuous measurement of the fluorescence to verify the PCR product. The *aflP*
174 gene expression was evaluated following the concentrations and conditions previously

175 described (Rodríguez et al., 2012a). Every qPCR assay described above was carried out by
176 triplicate. Gene expression ratio was calculated using the $2^{-\Delta\Delta CT}$ method (Livak and Schmittgen,
177 2001). The endogenous control was set as the expression of β -*tubulin* gene and the untreated
178 batch described above was used as calibrator sample. For every primer pair, a standard curve
179 was generated to check the amplification efficiency from ten-fold serial dilution 100 to 0.01
180 ng/ μ l of DNA from *A. flavus* and *A. parasiticus*. In addition, the differences in amplification
181 efficiencies between the housekeeping and the target gene were less than 10%, as required to
182 apply the relative quantification method (Schmittgen and Livak, 2008).

183 Statistical analysis

184 Statistical analyses were performed with the IBM SPSS v.22. Data from mycelia weight,
185 microbial counts, mycotoxin concentration and gene expression were tested for normality
186 (Kolmogorov-Smirnov with Lilliefors correction) and homoscedasticity (Levene's test). Given
187 that these data were non-normally distributed, mean values were compared using nonparametric
188 Kruskal–Wallis test. To compare treatments in pairs, Mann-Whitney U test was applied ($p \leq$
189 0.05).

190

191 Results

192 Growth inhibition and mycotoxin production in calcium-enriched YES

193 *A. flavus* grown for 15 days showed lower mycelium weight ($p \leq 0.05$) in the batches
194 Pg+Dh, Dh+Pa and Pg+Dh+Pa than in non-treated batch (Fig 1). *A. parasiticus* was inhibited by
195 all treatments except for those containing solely PgAFP or *P. acidilactici* (Fig 1). The
196 combination Pg+Dh+Pa achieved the highest inhibition of both *A. flavus* and *A. parasiticus*.

197 *A. flavus* did not produce mycotoxins in Ca-enriched YES, neither in the untreated batch
198 nor in any treatment tested. However, *A. parasiticus* produced AFB₁ and AFG₁ in the untreated
199 batch (Fig 2) and small amounts of AFG₁ in the batch inoculated solely with *D. hansenii*.
200 Therefore, none of the combinations of protective cultures tested increased aflatoxin production
201 in Ca-enriched YES.

202 Growth inhibition and mycotoxin production on cheese slices

203 On cheese slices, the microbial load just before inoculation was about 3 log cfu/cm² for
204 lactic acid bacteria and <2 log cfu/cm² for both molds and yeasts. LAB increased to 6-6.7 log
205 cfu/cm² in Pg+Dh+Pa batch just after inoculation at day 0. At 5 and 15 incubation days, LAB
206 counts were around 3.5 log cfu/cm² for batches not inoculated with *P. acidilactici* (untreated
207 and Pg+Dh), but over 6 log cfu/cm² for Pg+Dh+Pa batches. Similarly, the yeast load was

208 always below 2 log cfu/cm² in the untreated control, but over 5 log cfu/cm² in Pg+Dh and
209 Pg+Dh+Pa batches. A_w values of cheese slices incubated 5 and 15 days were 0.89 and 0.86,
210 respectively. Mold loads at 5 incubation days in untreated Af and Ap batches were around 2 log
211 units higher ($p \leq 0.05$) than in Pg+Dh and Pg+Dh+Pa batches (Table 1). At 15 incubation days,
212 mold counts in untreated controls were over 7 log cfu/cm² for *A. flavus*-inoculated batch, but
213 lower than 5 log cfu/cm² for *A. parasiticus* batch. Significant reductions ($p \leq 0.05$) close to 2-3
214 log cfu/cm² were obtained with Pg+Dh and Pg+Dh+Pa treatments for both molds. A similar
215 level of inhibition was reached with Pg+Dh and Pg+Dh+Pa at both incubation times (Table 1).

216 The only mycotoxin produced at the conditions tested in cheese was AFG₁ in *A.*
217 *parasiticus* untreated batch at 5 and 15 incubation days.

218 Gene expression

219 To study the effect of PgAFP, *D. hansenii*, and *P. acidilactici* on aflatoxin biosynthesis
220 and β -oxidation in *A. parasiticus*, the expression of genes *aflP* for aflatoxin biosynthesis, *foxA*
221 for β -oxidation, and β -*tubulin* as housekeeping were assessed.

222 The maximum differences in amplification efficiency values showed between *aflP* and
223 housekeeping were 6 % for *A. flavus* and 5 % for *A. parasiticus*, thus the $2^{-\Delta\Delta CT}$ method could
224 be applied. The oxidative stress in *A. flavus* and *A. parasiticus*, according to *foxA* gene
225 expression, did not differ ($p > 0.05$) between any of the treatments and the untreated control
226 batches when grown in calcium-rich medium for 5 incubation days. However, *aflP* was
227 overexpressed ($p \leq 0.05$) in Pa treated batches in both molds, whereas it was repressed ($p \leq 0.05$)
228 in Pg batch in *A. parasiticus* (Fig 3).

229 Discussion

230 As it was expected, *A. flavus* or *A. parasiticus* grown in 0.1 M CaCl₂ YES were not
231 inhibited by PgAFP. Thus, it was necessary to explore new alternatives to combat
232 mycotoxigenic moulds in Ca²⁺-rich foods. *A. parasiticus* was inhibited ($p \leq 0.05$) by most
233 treatments tested, whilst *A. flavus* was inhibited only for three of the combinations (Fig. 1). The
234 fact that the highest inhibition was reached by co-inoculation of PgAFP + *D. hansenii* + *P.*
235 *acidilactici* seems to be a consequence of the combined effect of different mechanisms of
236 action. The mechanism of action of PgAFP is based on permeability induction, loss of
237 membrane integrity, and apoptosis induction as a consequence of ROS (Delgado et al., 2015b),
238 whereas the inhibitory effect of *D. hansenii* is attributed to volatile compounds and competition
239 for nutrient and space (Núñez et al., 2015). In addition, *P. acidilactici* produces bacteriocins and
240 organic acids that inhibit mold growth (Cizeikiene et al., 2013; Montiel et al., 2013).

241 On the other hand, aflatoxin production was always inhibited in the batches containing
242 any protective culture, except for AFG₁ in that inoculated only with *D. hansenii* (Fig 1).

243 The ROS induced by antifungal proteins trigger oxidative stress in sensitive molds
244 (Delgado et al., 2015b; Galgóczy et al., 2013; Marx et al., 2008). This stress is a prerequisite for
245 aflatoxin production in *A. parasiticus* (Jayashree and Subramanyan, 2000) and is also involved
246 in peroxisomal β -oxidation of fatty acids, which is linked to aflatoxin biosynthesis (Reverberi et
247 al., 2012). An anti-oxidant status in the fungal cell leads to a depressed aflatoxin production in
248 *A. parasiticus* (Reverberi et al., 2005). *FoxA* gene expression has been used previously to
249 monitor the fatty acids metabolism by β -oxidation in *A. flavus* (Maggio-Hall et al., 2005) and *A.*
250 *parasiticus* (Roze et al., 2010). The expression of this gene was not altered at 5 incubation days
251 in either *A. flavus* or *A. parasiticus* by the effect of PgAFP, *D. hansenii*, *P. acidilactici* or the
252 three applied together (fig 3).. These results imply a mild oxidant effect of PgAFP on both
253 molds grown in Ca-enriched YES, matching the lower aflatoxin production in PgAFP-treated
254 samples (fig 2). These findings are consistent with the low levels of intracellular ROS detected
255 in PgAFP-treated *A. flavus* grown with 0.1 M CaCl₂ PDB. The *aflP* gene was expressed at a
256 higher level in both moulds treated only with *P. acidilactici*, but at a lower level in *A.*
257 *parasiticus* treated only with PgAFP (Fig. 4). However, the mycotoxin levels obtained in these
258 batches were all lower than those in the untreated control batch. Similar inconsistent results
259 between gene expression and aflatoxins production have been obtained for the interaction of
260 *Streptomyces sp.* and *A. flavus* (Verheecke et al., 2015), where reduced aflatoxin concentrations
261 were not accompanied by significantly repressed aflP expression. According to these results, the
262 effect of PgAFP promoting aflatoxin production can be ruled out in calcium enriched media.

263 Given that both mycelial weight and mycotoxin production were inhibited by some
264 treatments in 0.1M CaCl₂ YES, the actual efficacy of the most effective treatments containing
265 PgAFP was tested on cheese slices. Protective cultures require favorable environmental
266 conditions to develop their antifungal properties. The low a_w levels reached during cheese
267 ripening, as low as 0.80 at the outer-most layer of some cheeses, could restrict survival of *P.*
268 *acidilactici* and *D. hansenii*. The a_w values in treated cheese slices decreased to 0.89 and 0.86 at
269 days 5 and 15, respectively (Table 1), which are below the 0.90 minimum a_w level for
270 *Pediococcus* growth in foods (Leistner et al. 1981), but not below the 0.83 minimum value for
271 *D. hansenii* (Troller and Christian, 1978).

272 Both Pg+Dh and Pg+Dh+Pa treatments effectively inhibit *A. flavus* and *A. parasiticus*
273 growth as well as AFG₁ production by *A. parasiticus* on cheese slices for 15 days, thus
274 contributing to obtain a safer food. This effect was stronger than that reported by the sole action
275 of *D. hansenii* on ochratoxigenic *P. nordicum* in dry-cured ham incubated at 0.84 a_w (Andrade

276 et al., 2014). No additional inhibition was observed by the combined use of *P. acidilactici* with
277 PgAFP+Dh, which can be explained by the failure of *P. acidilactici* to correctly implantation or
278 development of this strain can be hypothesized, but the counts of LAB showed the highest LAB
279 load in the batches were *P. acidilactici* was inoculated. This lack of inhibitory activity has to be
280 explained by the differences in the substrate between YES broth and cheese slices, but not to the
281 fact of calcium concentration. In addition, a minor LAB load was noticed in the batch
282 inoculated with *D. hansenii* and PgAFP, this fact can be due to a well substrate competition of
283 *D. hansenii*, as reported previously (Núñez et al., 2015).

284 In non-treated slices, high levels of aflatoxin G1 were detected, being always over 10 ppb
285 in both sampling days. The levels reached in this batch, in particular at 15 incubation days, were
286 well over the limit established from the Spanish legislation that has been set in 10 ppb
287 (Ministerio de Sanidad y Consumo, 1988)

288 In spite of the fact of a lower inhibition on cheese provided by the combination
289 containing *P. acidilactici*, the mycotoxin content of the cheese slices was similar in both
290 experimental batches where no mycotoxin was detected for 15 incubation days. Thus, the
291 presence of *P. acidilactici* does not seem to hinder the antifungal activity of PgAFP and *D.*
292 *hansenii*. However, given that *P. acidilactici* did not enhance the antifungal ability of PgAFP
293 and *D. hansenii*, together with the fact of that *P. acidilactici* provoked overexpression of *aflP*
294 gene in the first stages of the incubation in rich-calcium culture media, the inoculation of this
295 strain should be avoid in cheese as protective culture.

296 The combination of PgAFP and *D. hansenii* could be proposed as the best combination
297 for protective culture, given that no one provoked an overexpression of genes related to
298 mycotoxin production and an enhanced antifungal ability has been proved on cheese.

299 This work studies the effect of a strain of *D. hansenii*, *P. acidilactici* and the antifungal
300 protein PgAFP on aflatoxigenic strains grown in rich-calcium medium. In addition, it offers a
301 complementary strategy to combat toxigenic molds in rich-calcium foods and their mycotoxin
302 production, given the limited effect of PgAFP in these type of foods.

303

304

305

306

307

308

309 Bibliography

- 310 Acosta, R., Rodríguez-Martín, A., Martín, A., Núñez, F., Asensio, M.A., 2009. Selection
311 of antifungal protein-producing molds from dry-cured meat products. *International journal of*
312 *food microbiology* 135, 39–46. doi:10.1016/j.ijfoodmicro.2009.07.020
- 313 Alapont, C., López-Mendoza, M.C., Gil, J. V, Martínez-Culebras, P. V, 2014. Mycobiota
314 and toxigenic *Penicillium* species on two Spanish dry-cured ham manufacturing plants. *Food*
315 *additives & contaminants. Part A, Chemistry, analysis, control, exposure & risk assessment* 31,
316 93–104. doi:10.1080/19440049.2013.849007
- 317 Andrade, M.J., Córdoba, J.J., Casado, E.M., Córdoba, M.G., Rodríguez, M., 2010. Effect
318 of selected strains of *Debaryomyces hansenii* on the volatile compound production of dry
319 fermented sausage “salchichón.” *Meat Science* 85, 256–264. doi:10.1016/j.meatsci.2010.01.009
- 320 Andrade, M.J., Thorsen, L., Rodríguez, A., Córdoba, J.J., Jespersen, L., 2014. Inhibition
321 of ochratoxigenic moulds by *Debaryomyces hansenii* strains for biopreservation of dry-cured
322 meat products. *International Journal of Food Microbiology* 170, 70–77.
323 doi:10.1016/j.ijfoodmicro.2013.11.004
- 324 Asefa, D.T., Kure, C.F., Gjerde, R.O., Langsrud, S., Omer, M.K., Nesbakken, T., Skaar,
325 I., 2011. A HACCP plan for mycotoxigenic hazards associated with dry-cured meat production
326 processes. *Food Control* 22, 831–837. doi:10.1016/j.foodcont.2010.09.014
- 327 Asefa, D.T., Møretrø, T., Gjerde, R.O., Langsrud, S., Kure, C.F., Sidhu, M.S.,
328 Nesbakken, T., Skaar, I., 2009. Yeast diversity and dynamics in the production processes of
329 Norwegian dry-cured meat products. *International Journal of Food Microbiology* 133, 135–140.
330 doi:10.1016/j.ijfoodmicro.2009.05.011
- 331 Bezerra da Rocha, M.E., Oliveira Freire, F.D.C., Feitosa Maia, F.E., Florindo Guedes,
332 M.I., Rondina, D., 2014. Mycotoxins and their effects on human and animal health. *Food*
333 *Control* 36, 159–165. doi:10.1016/j.foodcont.2013.08.021
- 334 Casquete, R., Benito, M.J., Martín, A., Ruiz-Moyano, S., Pérez-Nevado, F., Córdoba,
335 M.G., 2012. Comparison of the effects of a commercial and an autochthonous *Pediococcus*
336 *acidilactici* and *Staphylococcus vitulus* starter culture on the sensory and safety properties of a
337 traditional Iberian dry-fermented sausage “salchichón.” *International Journal of Food Science*
338 *and Technology* 47, 1011–1019. doi:10.1111/j.1365-2621.2011.02935.x
- 339 Chen, Z., Ao, J., Yang, W., Jiao, L., Zheng, T., Chen, X., 2013. Purification and
340 characterization of a novel antifungal protein secreted by *Penicillium chrysogenum* from an

- 341 Arctic sediment. *Applied Microbiology and Biotechnology* 97, 10381–10390.
342 doi:10.1007/s00253-013-4800-6
- 343 Cheong, E.Y.L., Sandhu, A., Jayabalan, J., Kieu Le, T.T., Nhiep, N.T., My Ho, H.T.,
344 Zwielehner, J., Bansal, N., Turner, M.S., 2014. Isolation of lactic acid bacteria with antifungal
345 activity against the common cheese spoilage mould *Penicillium commune* and their potential as
346 biopreservatives in cheese. *Food Control* 46, 91–97. doi:10.1016/j.foodcont.2014.05.011
- 347 Cizeikiene, D., Juodeikiene, G., Paskevicius, A., Bartkiene, E., 2013. Antimicrobial
348 activity of lactic acid bacteria against pathogenic and spoilage microorganism isolated from
349 food and their control in wheat bread. *Food Control* 31, 539–545.
350 doi:10.1016/j.foodcont.2012.12.004
- 351 Crowley, S., Mahony, J., Van Sinderen, D., 2013. Current perspectives on antifungal
352 lactic acid bacteria as natural bio-preservatives. *Trends in Food Science and Technology* 33,
353 93–109. doi:10.1016/j.tifs.2013.07.004
- 354 Currie, L.A., 1999. Nomenclature in evaluation of analytical methods including detection
355 and quantification capabilities. *Analytica Chimica Acta* 391, 105–126. doi:10.1016/S0003-
356 2670(99)00104-X
- 357 Delgado, J., Acosta, R., Rodríguez-Martín, A., Bermúdez, E., Núñez, F., Asensio, M.A.,
358 2015a. Growth inhibition and stability of PgAFP from *Penicillium chrysogenum* against fungi
359 common on dry-ripened meat products. *International Journal of Food Microbiology* 205, 23–29.
360 doi:10.1016/j.ijfoodmicro.2015.03.029
- 361 Delgado, J., Owens, R.A., Doyle, S., Asensio, M.A., Núñez, F., 2015b. Impact of the
362 antifungal protein PgAFP from *Penicillium chrysogenum* on the protein profile in *Aspergillus*
363 *flavus*. *Applied Microbiology and Biotechnology* 99, 8701–8715. doi:10.1007/s00253-015-
364 6731-x
- 365 Delgado, J., Owens, R.A., Doyle, S., Asensio, M.A., Núñez, F., 2015c. Proteome
366 changes explain calcium-mediated ineffectiveness of the antifungal protein PgAFP
367 against *Aspergillus flavus* in cheese. Unpublished
- 368
- 369 Filtenborg, O., Frisvad, J.C., Thrane, U., 1996. Moulds in food spoilage. *International*
370 *Journal of Food Microbiology* 33, 85–102.
- 371 Galgóczy, L., Kovács, L., Karácsony, Z., Virágh, M., Hamari, Z., Vágvölgyi, C., 2013.
372 Investigation of the antimicrobial effect of *Neosartorya fischeri* antifungal protein (NFAP) after

- 373 heterologous expression in *Aspergillus nidulans*. Microbiology (Reading, England) 159, 411–
374 419. doi:10.1099/mic.0.061119-0
- 375 Jayashree, T., Subramanyan, C., 2000. Oxidative stress as a prerequisite for aflatoxin
376 production by *Aspergillus parasiticus*. Free Radical Biology & Medicine 29, 981–985.
- 377 Kaiserer, L., Oberparleiter, C., Weiler-Görz, R., Burgstaller, W., Leiter, E., Marx, F.,
378 2003. Characterization of the *Penicillium chrysogenum* antifungal protein PAF. Archives of
379 microbiology 180, 204–210. doi:10.1007/s00203-003-0578-8
- 380 Leistner, L., Rödel, W., and Krispien, K., 1981 Microbiology of meat and meat products
381 in high- and intermediate-moisture ranges. In L.B. Rockland and G.F. Stewart (Eds.), Water
382 Activity: Influences on Food Quality (pp. 855-916). Academic Press, New York.
- 383 Lie, J.L., Marth, E.H., 1967. Formation of aflatoxin in cheddar cheese by *Aspergillus*
384 *flavus* and *Aspergillus parasiticus*. Journal of dairy science 50, 1708–1710. doi:S0022-
385 0302(67)87698-7 [pii]r10.3168/jds.S0022-0302(67)87698-7 [doi]
- 386 Liu, S.Q., Tsao, M., 2009. Biocontrol of dairy moulds by antagonistic dairy yeast
387 *Debaryomyces hansenii* in yoghurt and cheese at elevated temperatures. Food Control 20, 852–
388 855. doi:10.1016/j.foodcont.2008.10.006
- 389 Livak, K.J., Schmittgen, T.D., 2001. Analysis of relative gene expression data using real-
390 time quantitative PCR and the 2(-Delta Delta C(T)) Method. Methods (San Diego, Calif.) 25,
391 402–8. doi:10.1006/meth.2001.1262
- 392 Long, G.L., Winefordner, J.D., 1983. Limit of detection, a closer look at the IUPAC
393 definition. Analytical Chemistry 55, A712–&. doi:10.1021/ac00258a001
- 394 Lowry, O.H., Rosebrough, N.J., Farr, L., Randall, R.J., 1951. Protein measurement with
395 the folin phenol reagent. The Journal of biological chemistry 193, 265–275.
- 396 Lozano-Ojalvo, D., Rodríguez, A., Bernáldez, V., Córdoba, J.J., Rodríguez, M., 2013.
397 Influence of temperature and substrate conditions on the omt-1 gene expression of *Aspergillus*
398 *parasiticus* in relation to its aflatoxin production. International Journal of Food Microbiology
399 166, 263–269. doi:10.1016/j.ijfoodmicro.2013.07.011
- 400 Maggio-Hall, L.A., Wilson, R.A., Keller, N.P., 2005. Fundamental contribution of beta-
401 oxidation to polyketide mycotoxin production in planta. Molecular plant-microbe interactions :
402 MPMI 18, 783–793. doi:10.1094/MPMI-18-0783

- 403 Martín, A., Córdoba, J.J., Aranda, E., Córdoba, M.G., Asensio, M.A., 2006. Contribution
404 of a selected fungal population to the volatile compounds on dry-cured ham. *International*
405 *Journal of Food Microbiology* 110, 8–18. doi:10.1016/j.ijfoodmicro.2006.01.031
- 406 Marx, F., Binder, U., Leiter, E., Pócsi, I., 2008. The *Penicillium chrysogenum* antifungal
407 protein PAF, a promising tool for the development of new antifungal therapies and fungal cell
408 biology studies. *Cellular and molecular life sciences* 65, 445–454. doi:10.1007/s00018-007-
409 7364-8
- 410 Ministerio de Sanidad y Consumo, 1988. Real Decreto 475/1988, de 13 de mayo, por el
411 que se establecen los límites máximos permitidos de las aflatoxinas B1, B2, G1 y G2 en
412 alimentos para consumo humano. BOE 121, 15329.
- 413 Montiel, R., Bravo, D., Medina, M., 2013. Commercial biopreservatives combined with
414 salt and sugar to control *Listeria monocytogenes* during smoked salmon processing. *Journal of*
415 *food protection* 76, 1463–5. doi:10.4315/0362-028X.JFP-12-560
- 416 Muhialdin, B.J., Hassan, Z., Sadon, S.K., 2011. Antifungal activity of *Lactobacillus*
417 *fermentum*Te007, *Pediococcus pentosaceus* Te010, *Lactobacillus pentosus* G004, and *L.*
418 *paracasi* D5 on Selected Foods. *Journal of Food Science* 76, M493–M499. doi:10.1111/j.1750-
419 3841.2011.02292.x
- 420 Núñez, F., Lara, M.S., Peromingo, B., Delgado, J., Sanchez-Montero, L., J.Andrade, M.,
421 2015. Selection and evaluation of *Debaryomyces hansenii* isolates as potential bioprotective
422 agents against toxigenic penicillia in dry-fermented sausages. *Food microbiology* 46, 114–120.
423 doi:10.1016/j.fm.2014.07.019
- 424 Núñez, F., Rodríguez, M.M., Bermúdez, M.E., Córdoba, J.J., Asensio, M.A., 1996.
425 Composition and toxigenic potential of the mould population on dry-cured Iberian ham.
426 *International journal of food microbiology* 32, 185–97.
- 427 Papadima, S.N., Bloukas, J.G., 1999. Effect of fat level and storage conditions on quality
428 characteristics of traditional Greek sausages. *Meat Science* 51, 103–113. doi:10.1016/S0309-
429 1740(98)00103-X
- 430 Reverberi, M., Fabbri, A.A., Zjalic, S., Ricelli, A., Punelli, F., Fanelli, C., 2005.
431 Antioxidant enzymes stimulation in *Aspergillus parasiticus* by *Lentinula edodes* inhibits
432 aflatoxin production. *Applied microbiology and biotechnology* 69, 207–15.
433 doi:10.1007/s00253-005-1979-1
- 434 Reverberi, M., Punelli, M., Smith, C. a, Zjalic, S., Scarpari, M., Scala, V., Cardinali, G.,
435 Aspite, N., Pinzari, F., Payne, GA, Fabbri, A. a, Fanelli, C., 2012. How peroxisomes affect

- 436 aflatoxin biosynthesis in *Aspergillus flavus*. PloS one 7, e48097.
437 doi:10.1371/journal.pone.0048097
- 438 Rodríguez, A., Medina, Á., Córdoba, J.J., Magan, N., 2014. The influence of salt (NaCl)
439 on ochratoxin A biosynthetic genes, growth and ochratoxin A production by three strains of
440 *Penicillium nordicum* on a dry-cured ham-based medium. International Journal of Food
441 Microbiology 178, 113–119. doi:10.1016/j.ijfoodmicro.2014.03.007
- 442 Rodríguez, A., Rodríguez, M., Luque, M.I., Martín, A., Córdoba, J.J., 2012a. Real-time
443 PCR assays for detection and quantification of aflatoxin-producing molds in foods. Food
444 microbiology 31, 89–99. doi:10.1016/j.fm.2012.02.009
- 445 Rodríguez, A., Rodríguez, M., Martín, A., Delgado, J., Córdoba, J.J., 2012b. Presence of
446 ochratoxin A on the surface of dry-cured Iberian ham after initial fungal growth in the drying
447 stage. Meat Science 92, 728–734. doi:10.1016/j.meatsci.2012.06.029
- 448 Rodríguez-Martín, A., Acosta, R., Liddell, S., Núñez, F., Benito, M.J., Asensio, M.A.,
449 2010. Characterization of the novel antifungal protein PgAFP and the encoding gene of
450 *Penicillium chrysogenum*. Peptides 31, 541–547. doi:10.1016/j.peptides.2009.11.002
- 451 Roze, L. V, Chanda, A., Laivenieks, M., Beaudry, R.M., Artymovich, K. a, Koptina, A.
452 V, Awad, D.W., Valeeva, D., Jones, A.D., Linz, J.E., 2010. Volatile profiling reveals
453 intracellular metabolic changes in *Aspergillus parasiticus*: veA regulates branched chain amino
454 acid and ethanol metabolism. BMC biochemistry 11, 33. doi:10.1186/1471-2091-11-33
- 455 Schmittgen, T.D., Livak, K.J., 2008. Analyzing real-time PCR data by the comparative
456 CT method. Nat. Protocols 3, 1101–1108.
- 457 Taniwaki, M.H., Hocking, A.D., Pitt, J.I., Fleet, G.H., 2001. Growth of fungi and
458 mycotoxin production on cheese under modified atmospheres. International journal of food
459 microbiology 68, 125–33.
- 460 Troller, J. A. and Christian, J.H.B., 1978. Water activity and foods. Academic Press, New
461 York.
- 462 Urbach, G., 1995. Contribution of lactic acid bacteria to flavour compound formation in
463 dairy products. International Dairy Journal 5, 877–903. doi:10.1016/0958-6946(95)00037-2
- 464 Verheecke, C., Liboz, T., Anson, P., Zhu, Y., Mathieu, F., 2015. *Streptomyces*-
465 *Aspergillus flavus* interactions: impact on aflatoxin B accumulation. Food additives &
466 contaminants. Part A, Chemistry, analysis, control, exposure & risk assessment 32, 572–576.
467 doi:10.1080/19440049.2014.1003336

468 Viljoen, B.C., Greyling, T., 1995. Yeasts associated with Cheddar and Gouda making.
469 International Journal of Food Microbiology 28, 79–88. doi:10.1016/0168-1605(94)00114-L

470 Welthagen, J.J., Viljoen, B.C., 1998. Yeast profile in Gouda cheese during processing and
471 ripening. International Journal of Food Microbiology 41, 185–194. doi:10.1016/S0168-
472 1605(98)00042-7

473 Yu, J., Chang, P., Ehrlich, K.C., Cary, J.W., Bhatnagar, D., Cleveland, T.E., Payne, G.A., Linz,
474 J.E., Woloshuk, C.P., Bennett, W., Bennett, J.W., 2004. Clustered pathway genes in Aflatoxin
475 biosynthesis. Applied and environmental microbiology 70, 1253–1262.
476 doi:10.1128/AEM.70.3.1253

477

478

479

480

481

482

483

484

485

486

487

488

489

490

491

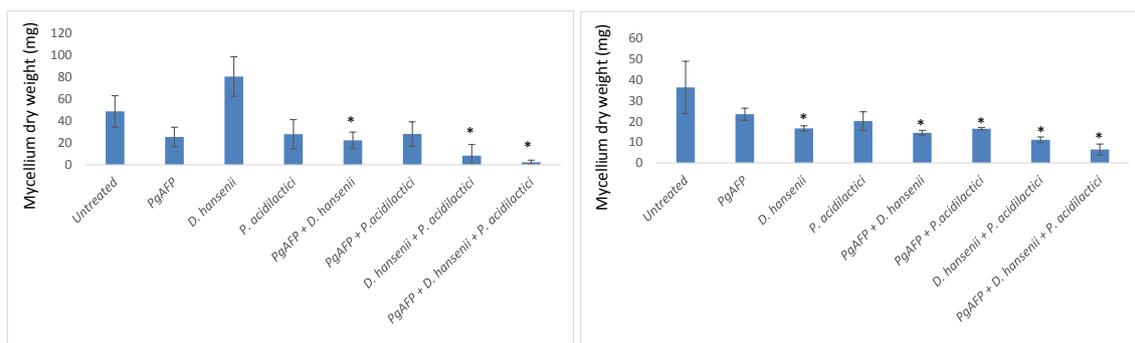
492

493

494

495

496 Figure captions



497

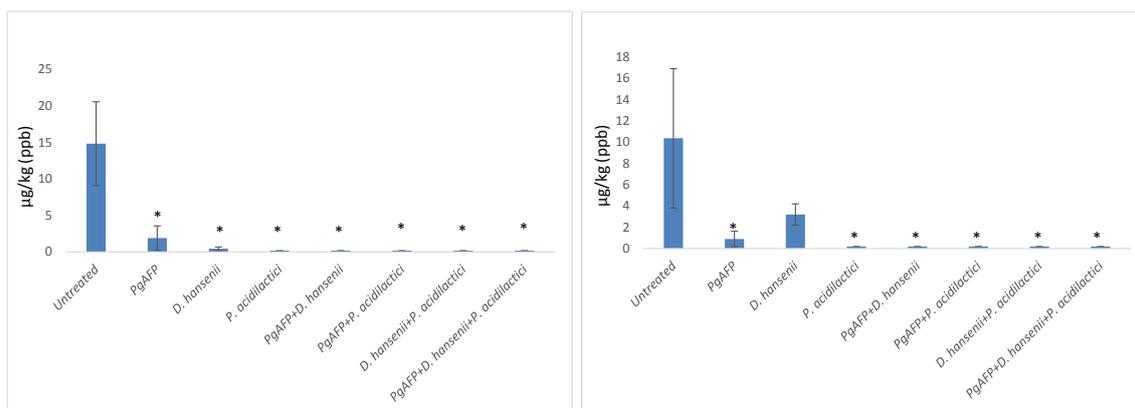
498

499

500

501 Figure 1. Mycelium dry weight of *A. flavus* (left) and *A. parasiticus* (right) cultured for 15 days
 502 in calcium-enriched Yeast Extract Sucrose broth with different combinations of antifungal
 503 agents. Bars represent standard deviation. * Means are significantly different from untreated
 504 batch ($p \leq 0.05$).

505



506

507 Figure 2. Effect of different combinations of protective agents on aflatoxin B₁ (left) and G₁
 508 (right) production by *Aspergillus parasiticus* cultured in calcium-enriched Yeast Extract
 509 Sucrose broth for 15 days. Bars represent standard deviation. * Means are significantly
 510 different from untreated batch ($p \leq 0.05$).

511

512

513

514

515

516

517

518

519

520

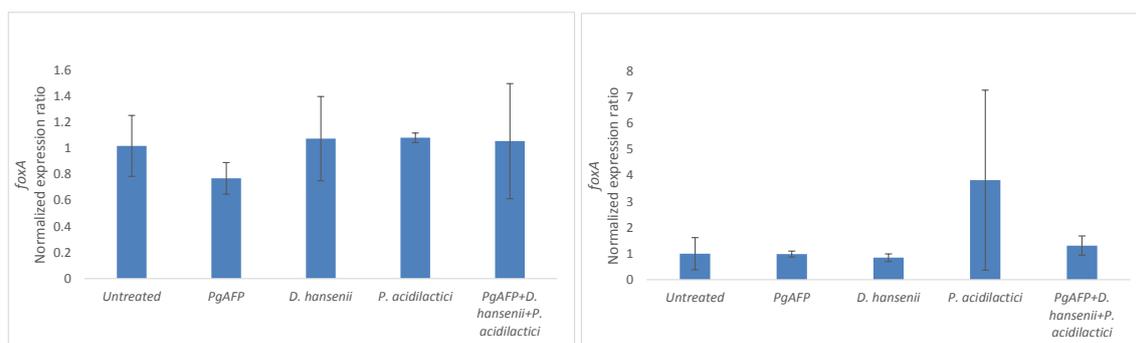
521

522 Table 1. Water activity (a_w), mould counts ($\log \text{cfu/cm}^2$) and aflatoxin G_1 concentration ($\mu\text{g/kg}$)
 523 in cheese slices inoculated with *A. flavus* or *A. parasiticus* at 5 and 15 days of incubation. Data
 524 are given as mean \pm SD.

		Day 5		Day 15	
		<i>A. flavus</i>	<i>A. parasiticus</i>	<i>A. flavus</i>	<i>A. parasiticus</i>
Untreated	a_w	0.89	0.89	0.86	0.86
PgAFP+ <i>D. hansenii</i>		0.89	0.89	0.86	0.86
PgAFP+ <i>D. hansenii</i> + <i>P. acidilactici</i>		0.89	0.89	0.86	0.86
Untreated	Mould counts	3.93 \pm 0.54	4.12 \pm 0.57	7.42 \pm 0.09	4.87 \pm 0.21
PgAFP+ <i>D. hansenii</i>		1.86 \pm 0.85*	2.31 \pm 0.64*	4.26 \pm 0.28*	<2*
PgAFP+ <i>D. hansenii</i> + <i>P. acidilactici</i>		2.63 \pm 0.61*	2.39 \pm 0.75*	4.74 \pm 0.38*	2.99 \pm 0.67*
Untreated	Aflatoxin G_1	<LOD	11 \pm 7	<LOD	29 \pm 24
PgAFP+ <i>D. hansenii</i>		<LOD	<LOD*	<LOD	<LOD*
PgAFP+ <i>D. hansenii</i> + <i>P. acidilactici</i>		<LOD	<LOD*	<LOD	<LOD*

*Means are significantly different from untreated batch ($p \leq 0.05$)

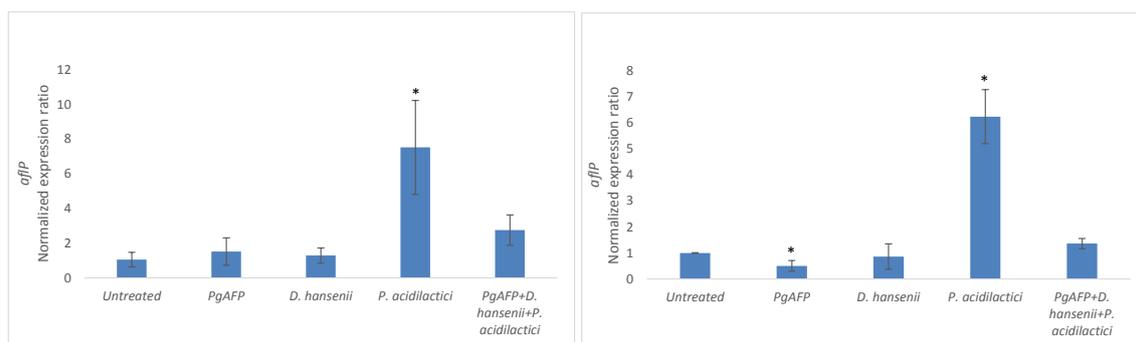
525
526
527
528



529

530 Figure 3. Effect of different antifungal agents on relative gene expression of *foxA* gene in *A.*
 531 *flavus* (left) and *A. parasiticus* (right) after 5 days in calcium-enriched Yeast Extract Sucrose
 532 broth. Bars represent standard deviation.

533



534

535 Figure 4. Effect of different antifungal agents on relative gene expression of *aflP* gene in *A.*
 536 *flavus* (left) and *A. parasiticus* (right) after 5 days in calcium-enriched Yeast Extract Sucrose
 537 broth. Bars represent standard deviation. * Means are significantly different from untreated
 538 batch ($p \leq 0.05$).
 539
 540

541 Table 2. Nucleotide sequence of primers used for qPCR assay.

Primer name	Nucleotide sequences (5'-3')	Efficiencies <i>A. flavus</i> / <i>A. parasiticus</i>	Product size	Position	Reference
F-Omt-1	GGCCGCCGCTTTGATCTAGG	106/104%	123	^a 1485	(Rodríguez, Rodríguez, Luque, Martín, & Córdoba, 2012)
R-Omt-1	ACCACGACCGCCGCC			1593	
F- β -tub	TCTTCATGGTTGGCTTCGCT	101/101%	98	^b 964	This study
R- β -tub	CTTGGGGTTCGAACATCTGCT			1042	
F- foxA	ACCGCAACCCTCTTCACATT	107/106%	73	^c 1196	This study
R- foxA	AGACCGTGCAGGATAGGAGT			1268	

542 ^a Positions are in accordance with published sequence of the *aflP* (*omt-1*) gene of *A. flavus*
543 (GeneBank accession no. L25835.1).

544 ^b Positions are in accordance with the published sequences of the β -*tubulin* gene of *A.*
545 *parasiticus* (GeneBank accession no. FR775333.1).

546 ^c Positions are in accordance with published sequence of the *foxA* gene of *A. flavus* (GeneBank
547 accession no. XM_002377580).

548

IV.3. Estudio del mecanismo de acción de PgAFP en mohos

Impact of the antifungal protein PgAFP from Penicillium chrysogenum on the protein profile in Aspergillus flavus

Impact of the antifungal protein PgAFP from *Penicillium chrysogenum* on the protein profile in *Aspergillus flavus*

Josué Delgado¹ · Rebecca A. Owens² · Sean Doyle² · Miguel A. Asensio¹ · Félix Núñez¹

Received: 25 February 2015 / Revised: 24 May 2015 / Accepted: 27 May 2015 / Published online: 16 June 2015
© Springer-Verlag Berlin Heidelberg 2015

Abstract Antifungal proteins produced by molds are generally small, highly basic, and cysteine-rich. The best known effects of these proteins include morphological changes, metabolic inactivation, and membrane perturbation on sensitive fungi. Reactive oxygen species (ROS) generation leads to apoptosis, with G-protein playing a key role in transduction of cell death signals. The antifungal protein PgAFP from *Penicillium chrysogenum* inhibits growth of some toxigenic molds. Here we analyzed the effect of the antifungal protein PgAFP on the growth of *Aspergillus flavus*. For this, comparative proteomic analysis was used to identify the whole protein profile and protein change in abundance after PgAFP treatment. PgAFP provoked metabolic changes related to reduced energy metabolism, cell wall integrity alteration, and increased stress response due to higher levels of ROS. The observed changes in protein abundance, favoring a higher glutathione concentration as well as the increased abundance in heat shock proteins, do not seem to be enough to avoid necrosis. The decreased chitin deposition observed in PgAFP-treated *A. flavus* is attributed to a lower relative quantity of Rho1. The reduced relative abundance of a β subunit of G-protein seems to be the underlying reason for modulation of apoptosis in PgAFP-treated *A. flavus* hyphae. We propose

Rho1 and G-protein subunit β CpcB to be the main factors in the mode of action of PgAFP in *A. flavus*. Additionally, enzymes essential for the biosynthesis of aflatoxin were no longer detectable in *A. flavus* hyphae at 24 h, following treatment with PgAFP. This presents a promising effect of PgAFP, which may prevent *A. flavus* from producing mycotoxins. However, the impact of PgAFP on actual aflatoxin production requires further study.

Keywords Antifungal compounds · Toxigenic fungi · *Aspergillus flavus* · Apoptosis · Proteomics

Introduction

Antimicrobial proteins are produced by different organisms throughout all kingdoms (Leiter et al. 2005). Some antifungal proteins produced by molds are small, highly basic, and cysteine-rich proteins, such as PAF from *Penicillium chrysogenum* Q176 (Marx et al. 1995), PgAFP from *P. chrysogenum* RP42C (Rodríguez-Martín et al. 2010), Pc-Arctin from *P. chrysogenum* A096 (Chen et al. 2013), AFP from *Aspergillus giganteus* (Nakaya et al. 1990), or NAFP from *Neosartorya fischeri* (Kovács et al. 2011). The expression of these proteins is induced in the presence of other fungi and contributes to an ecological advantage (Marx 2004). Antifungal proteins produced by molds may serve to combat unwanted molds. Toxigenic molds are among the main hazards in intermediate moisture foods, with the aflatoxin producer *Aspergillus flavus* being one of the main concerns. The mechanism of action of antifungal proteins seems to be multifactorial, leading to morphological changes, metabolic inactivation, or membrane perturbation in a dose-dependent manner (Kaiserer et al. 2003). The site of action on sensitive molds does not share the same pattern among antifungal proteins.

Electronic supplementary material The online version of this article (doi:10.1007/s00253-015-6731-x) contains supplementary material, which is available to authorized users.

✉ Miguel A. Asensio
masensio@unex.es

¹ Food Hygiene and Safety, Institute of Meat Products, University of Extremadura, Cáceres, Spain

² Department of Biology, Maynooth University, Maynooth, Co. Kildare, Ireland

PAF penetrates into the cytoplasm (Oberparleiter et al. 2003; Batta et al. 2009); AFP showed co-localization with the nucleus in *Magnaporthe grisea* (Moreno et al. 2006), while it is bound mainly to cell wall in *Aspergillus niger* (Theis et al. 2003, 2005). Membrane permeabilization could be involved in the mechanism of action. Some non-fungal antimicrobial proteins destabilize membranes by pore formation, whereas PAF induces a selective permeability to potassium (Kaiserer et al. 2003; Marx et al. 2008). In addition, PAF and NAFP induce oxidative stress in sensitive fungi, with elevated levels of reactive oxygen species (ROS) being the main effect contributing to apoptosis (Leiter et al. 2005; Galgóczy et al. 2013). It has been proposed that G protein is responsible for the transduction of PAF-initiated apoptotic cell death signals (Leiter et al. 2005). This is achieved through modulation of the intracellular glutathione (GSH) and ROS levels in *Aspergillus nidulans* (Hegedus et al. 2011). Here we used PgAFP, one of these small, basic, and cysteine-rich proteins that inhibits growth of some toxigenic molds (Rodríguez-Martín et al. 2010), to study the effect on the growth of *A. flavus*. Among the possible effects derived from antifungal proteins on *A. flavus*, those related to aflatoxin biosynthesis would be of interest for practical applications. *P. chrysogenum* RP42C isolated from dry-cured ham produces PgAFP and was used here as a source of the antifungal protein.

The mechanism of action of PgAFP on sensitive molds is unknown, and elucidation of this mechanism would allow the evaluation of potential applications for PgAFP. Comparative proteomic analysis constitutes a valuable tool to explore the effect of PgAFP on sensitive molds, which may provide rewarding information to exploit the practical use against toxigenic molds. Comparative proteomic analyses have been used in previous studies to explore the effect of some substances, such as H₂O₂, on molds (Lessing et al. 2007), and to identify resistance to antifungal drugs (Gautam et al. 2008; Cagas et al. 2011). Comparative proteomic 2D-PAGE has the capability to separate proteins in high resolution, even those including post-translational modifications. We used this technique to identify 23 unique proteins, identified from protein spots that showed a significant change in abundance in *A. flavus* in response to PgAFP. However, this technique only reveals a small percentage of the whole proteome depending on the range of pH (Görg et al. 2009), and it is not optimal for the analysis of membrane and hydrophobic proteins (Rabilloud et al. 2009). These features lead to several proteins under-represented on 2D-PAGE. Label-free quantitative proteomics can be used to examine those proteins not analyzable by 2D-PAGE. Therefore, a second proteomic approach, involving label-free proteomics, was used to analyze the proteome quantitatively and qualitatively.

The results of comparative proteomics informed on the mechanisms and systems affected by the antifungal compound in a sensitive mold. Information generated was

subsequently used to select adequate tests to confirm the changes attributed to proteins whose relative abundance is affected. The objective of the present work has been to study the effect of PgAFP on the proteomic profile and the structural and metabolic changes caused in *A. flavus*, a fungus that produces aflatoxins in foods.

Material and methods

Strains

In vitro tests were carried out with the PgAFP producer *P. chrysogenum* strain RP42C (CECT 20922) that resists at least 312.7 µg/ml PgAFP (Delgado et al. 2015), and *A. flavus* (CECT 2687), both from the Spanish Type Culture Collection (CECT). The latter strain produces aflatoxins in dry-cured ham (Bernáldez et al. 2014).

Purification of PgAFP

P. chrysogenum was grown in potato dextrose broth (PDB; Scharlab, Barcelona, Spain) pH 4.5, at 25 °C for 21 days. Mycelium was removed and the culture medium was filtered through a nitrocellulose 0.22-µm pore size (Sartorius, Goettingen, Germany) to obtain cell-free medium. The cell-free medium was applied to an ÄKTA FPLC with a cationic exchange column HiTrap SP HP (Amersham Biosciences, Uppsala, Sweden), equipped with a UV detector at 214 nm. The resulting fraction containing PgAFP was then chromatographed on a HiLoad 26/60 Superdex 75 column for FPLC (Amersham Biosciences, Uppsala, Sweden) as previously described (Acosta et al. 2009) to obtain an extract of the purified protein. The extract containing the purified PgAFP from several batches were pooled in a stock solution. The amount of protein in the stock solution was quantified by the Lowry method (Lowry et al. 1951). For the various assays, the PgAFP stock solution was diluted to the desired active concentration range according to the aim of the test.

Protein extraction

A. flavus CECT 2687 was cultured in triplicate in 50-ml PDB, at 25 °C with shaking at 200 rpm, in either presence (10 µg/ml) or absence of PgAFP for 24 h. Mycelia were harvested, filtered, washed, and lysed as described previously (Carberry et al. 2006). Mycelial lysates were centrifuged (10,000×g; 30 min) to remove cell debris and the subsequent supernatant precipitated with trichloroacetic acid/acetone (Carpentier et al. 2005). From these precipitated lysates, the two following proteomic analysis were carried out. Additionally, to confirm that cultures were in the exponential growth phase, growth in 24- to 48-h cultures was estimated by

mycelium dry weight determination at 100 °C to a constant weight.

Two-dimensional PAGE

For protein separation by 2D-PAGE, resuspended extracts containing 250 µg of protein were loaded onto Immobiline Dry strips (IPG strip; Amersham Biosciences) in the pH range 4–7, followed by electrofocusing, and electrophoresis using the Protean Xi-II Cell (Bio-Rad Laboratories) as described previously (Carberry et al. 2006). Resulting gels (three biological replicates and two technical replicates per treatment) were stained with colloidal Coomassie Blue (Sigma-Aldrich, St. Louis, MO, USA), scanned, and analyzed using Progenesis™ SameSpot software (TotalLab, Newcastle, UK) (O’Keeffe et al. 2013; Collins et al. 2013; Owens et al. 2014). Spot intensities were normalized in Progenesis SameSpot software using the total spot volume normalization method prior to comparative analysis, to correct for any variation in protein loading, staining/destaining, or image acquisition. Protein spots showing differences ($p < 0.05$, fold change ≥ 1.5) were excised and in-gel digested as described previously (Shevchenko et al. 2006). Briefly, selected spots were destained by addition of 100 µl of 100 mM ammonium bicarbonate:acetonitrile (1:1 v/v) for 30 min. Acetonitrile (500 µl) was added to samples to dehydrate the gel pieces, then discarded and replaced with 50 µl of trypsin (13 ng/µl). Samples were incubated at 4 °C for 2 h followed by overnight incubation at 37 °C. Then, samples were sonicated for 10 min, and the digested supernatant was transferred to clean tubes to be completely dried using a DNA Speed Vac Concentrator (Thermo Fischer Scientific, Austin, TX, USA) and resuspended in 0.1 % formic acid (FA; 20 µl). The samples were filtered through 0.22-µm cellulose spin filters (Agilent Technologies, Dublin, Ireland). The samples were analyzed by a 6340 Model Ion Trap LC-Mass Spectrometer (Agilent Technologies, Dublin, Ireland) using electrospray ionization. Samples (3 µl) were loaded onto a Zorbax 300 SB C-18 Nano-HPLC Chip (150 mm × 75 µm) with 0.1 % (v/v) FA at a flow rate of 4 µl/min. The eluted peptides were ionized and analyzed by mass spectrometry. MSⁿ analysis was carried out on the three most abundant peptide precursor ions at each time point, as selected automatically by the mass spectrometer. MASCOT MS/MS ion search, National Centre for Biotechnology Information (NCBI; www.ncbi.nlm.nih.gov/guide/proteins/) database, and Kyoto Encyclopedia of Genes and Genomes (KEGG; www.genome.jp/kegg/) were used for protein identification and function.

Label-free comparative quantitative proteomic analysis

The protein precipitated lysates, from 3 biological replicates per treatment, were resuspended in 8 M urea. After

dithiothreitol reduction and iodoacetic acid-mediated alkylation (Owens et al. 2014), sequencing-grade trypsin combined with ProteaseMax surfactant was added. Digested samples were desalted prior to analysis using C18 ZipTips® (Millipore, Darmstadt, Germany). A quantity (1 µg) was analyzed from each digest, a Q-Exactive mass spectrometer coupled to a Dionex RSLCnano (Thermo Scientific, Waltham, MA, USA). LC gradients ran from 4 to 35 % B (A: 0.1 % FA, B: 80 % acetonitrile, 0.1 % FA) over 2 h, and data was collected using a Top15 method for MS/MS scans (Dolan et al. 2014; O’Keeffe et al. 2014). Comparative proteome abundance and data analysis was performed using MaxQuant software (Version 1.3.0.5; www.maxquant.org/downloads.htm) (Cox and Mann 2008), with Andromeda used for database searching and Perseus (Version 1.4.1.3) used to organize the data. Carbamidomethylation of cysteines was set as a fixed modification, while oxidation of methionines and acetylation of N-terminals were set as variable modifications. The maximum peptide/protein false discovery rates (FDR) were set to 1 % based on comparison to a reverse database. The LFQ algorithm was used to generate normalized spectral intensities and infer relative protein abundance (Luber et al. 2010). Proteins that matched to a contaminant database or the reverse database were removed, and proteins were only retained in final analysis if detected in at least two replicates from at least one treatment. Quantitative analysis was performed using a *t* test to compare pairs of samples. Due to the high sensitivity and larger dynamic range of the gel-free proteomics analyses, only proteins with a fold change ≥ 2 ($p < 0.05$) were included in the quantitative results (Table S1 in the Supplementary Material) (Dolan et al. 2014; O’Keeffe et al. 2014). Qualitative analysis was also performed to detect proteins that were found in at least two replicates of a particular sample but undetectable in the comparison sample (Table S1 in the Supplementary Material).

Effect of PgAFP on *A. flavus* growth

The growth of PgAFP-treated *A. flavus* was evaluated on microtiter plates (DeltaLab, Rubí, Spain), with 200 µl of PDB and 10⁵ conidia per well incubated at 25 °C during 96 h in static conditions. Seven serial 1:2 dilutions of PgAFP (i.e., 75, 37.5, 18.75, 9.38, 4.69, 2.34, and 1.17 µg/ml) and a non-treated control were assayed. Optical density was measured at 550 nm every 24 h in an Infinite M2000 microplate reader (TECAN, Männedorf, Switzerland).

SYTOX Green uptake

A. flavus was grown and treated with the seven PgAFP concentrations from 75 to 1.17 µg/ml described above. Additionally, *P. chrysogenum* was also used as a resistant control. After incubation of test samples for 24 h at 25 °C,

wells were supplemented with 0.2 μM SYTOX Green (Molecular Probes, Eugene, OR, USA). The fluorescence emitted was measured at 10, 30, and 210 min in an Infinite M2000 spectrophotometer (TECAN, Männedorf, Switzerland), with excitation wavelength of 480 nm (slit, 5 nm) and emission wavelength of 530 nm (slit, 10 nm).

Hyphal morphology

A. flavus was grown in tubes containing 300 μl of PDB at 25 °C for 24 h in either presence (20 and 75 $\mu\text{g/ml}$) or absence of PgAFP. Mycelium was collected by centrifugation and observed on a microscope Eclipse E200 equipped with a digital camera DS-Fi2 (Nikon, Tokyo, Japan).

FUN-1 staining

To evaluate the metabolic activity with a viability staining, the mycelium of *A. flavus* in either presence (20 $\mu\text{g/ml}$) or absence of PgAFP was washed with 10 mM HEPES (pH 7.5) before staining with 100 μl FUN-1 (Molecular Probes, Eugene, OR, USA) for 30 min at 25 °C as described previously (Kaiserer et al. 2003). The PgAFP producer strain *P. chrysogenum* was used as a resistant control. Stained hyphae were examined and photographed by fluorescence microscopy (Nikon, Tokyo, Japan).

Chitin staining

Conidia of *A. flavus* were inoculated on 10-ml PDB in a Petri dish containing a cover glass and incubated in presence (20 and 75 $\mu\text{g/ml}$) and absence of PgAFP at 25 °C for 24 h (Harris et al. 1994). Similarly, as a control, *P. chrysogenum* was treated with 75 $\mu\text{g/ml}$ PgAFP. Mycelium was fixed and stained for 5 min with fluorescent brightener 28 (Sigma-Aldrich, St. Louis, MO, USA) and then washed to visualize chitin in a fluorescence microscopy with an excitation wavelength of 387/11 nm.

Nuclei staining

To visualize the distribution of nuclei in PgAFP-treated (20 and 75 $\mu\text{g/ml}$) and non-treated hyphae, double-stranded DNA was fluorescently labeled by incubating with 1.6 μM Hoechst 33258 dye (Molecular Probes, Eugene, OR, USA) for 30 min at 25 °C as described previously (Kaiserer et al. 2003) and visualized through fluorescence microscopy with excitation wavelength of 387/11 nm.

Localization of FITC-labeled PgAFP

PgAFP was labeled by DareBio S.L. (Elche, Spain). For this, 100 μl of 20 mM fluorescein isothiocyanate (FITC; Anaspec,

Fremont, CA, USA) in dimethyl sulfoxide was added to 4 ml of PgAFP (369 $\mu\text{g/ml}$) and left for 8 h at room temperature in the dark. Then, 100 μl of 0.8 M Tris-HCl (pH 8.0) was added, to reach a final Tris-HCl concentration of 20 mM, and dialyzed against phosphate-buffered saline (PBS). The activity of 20 $\mu\text{g/ml}$ of PgAFP labeled with FITC was checked in a growth inhibition assay as described above. Then, *A. flavus* was grown in PDB for 6 and 24 h at 25 °C in presence of 20 $\mu\text{g/ml}$ of PgAFP labeled with FITC. Hyphae were washed twice with PBS and visualized by fluorescence microscopy with excitation wavelength of 482/35 nm. As controls, two additional tests were run: the PgAFP-resistant *P. chrysogenum* grown with PgAFP labeled with FITC and *A. flavus* grown with FITC-PgAFP previously treated at 121 °C for 15 min.

ROS detection

Induction of ROS production by PgAFP was evaluated using 2',7'-dichlorofluorescein diacetate (Sigma-Aldrich, St. Louis, MO, USA) as described previously (Kaiserer et al. 2003) with some modifications. *A. flavus* was grown as described in FUN-1 assay section; hyphae were incubated for 2 h at 25 °C with 20 μM fluorescent dye and observed by fluorescence microscopy with excitation wavelength of 482/35 nm. Additionally, the resistant *P. chrysogenum* was used as negative control.

Acridine orange/ethidium bromide double staining

A. flavus incubated at 25 °C for 24 h in either presence (20 and 75 $\mu\text{g/ml}$) or absence of PgAFP was stained with 4 $\mu\text{g/ml}$ of acridine orange/ethidium bromide (AO/EB; Sigma-Aldrich, St. Louis, MO, USA), incubated 30 min, and washed twice to be observed by fluorescence microscopy (excitation wavelengths, 482/35 and 562/40 nm). *P. chrysogenum* grown with 75 $\mu\text{g/ml}$ PgAFP was also stained as negative control.

Apoptosis induction by PgAFP

Apoptosis Detection Kit (Sigma-Aldrich, St. Louis, MO, USA) composed by annexin V-fluorescein isothiocyanate/propidium iodide (AnV-FITC/PI) was carried out according to manufacturers' instruction to distinguish between necrotic, late apoptotic, and viable cells in cultures of *A. flavus* incubated at 25 °C for 12 and 24 h in either presence (20 $\mu\text{g/ml}$) or absence of PgAFP. Likewise, *P. chrysogenum* was assayed as negative control.

Statistical analysis

Statistical analyses were performed with IBM SPSS v.22 (www-03.ibm.com/software/products/es/spss-stats-standard). Growth inhibition and membrane permeability data were

tested for normality (Kolmogorov–Smirnov with Lilliefors correction) and homoscedasticity (Levene’s test). Given that these data were non-normally distributed, mean values were compared using non-parametric Kruskal–Wallis test. To compare treatments in pairs, Mann–Whitney U test was applied ($p < 0.05$).

Results

Effect of PgAFP on *A. flavus* growth

The study of the inhibitory effect revealed that concentrations of PgAFP from 9.38 $\mu\text{g/ml}$ reduced *A. flavus* growth at 48 h ($p < 0.05$) in static culture, with differences increasing up to the end of the incubation time (Fig. 1). According to optical density reductions, over 50 % growth inhibition was reached with 18.75 $\mu\text{g/ml}$ PgAFP or above, at 96 h. However, no statistically significant difference was found among *A. flavus* inhibition with PgAFP concentrations over 9.38 $\mu\text{g/ml}$. No growth difference was observed at 24-h incubation among samples with the various concentrations assayed. All samples are in the exponential growth phase at 48 h (Fig. 1), revealing that the lag phase was very similar in all conditions tested, even the non-treated samples. Similarly, all cultures were at the exponential growth phase at 96-h incubation time.

Effect on protein profile

A comparative proteomic analysis of *A. flavus* in either presence or absence of PgAFP was carried out to study the metabolic pathways altered by this antifungal protein. A relatively low concentration of PgAFP was used in this assay (10 $\mu\text{g/ml}$) so as to reach a balance between fungistatic effect and sufficient growth in 24 h under continuous shaking. All samples showed a sufficient growth at harvesting time. Both untreated and PgAFP-treated cultures under continuous shaking were in

the exponential growth phase from 24 to 48 h according to mycelium dry weight (data not shown). From gel-based proteomics, only 26 spots showed a fold change ≥ 1.5 between the relative abundance of PgAFP-treated and untreated samples and were identified ($p < 0.05$). However, it appeared that these 26 spots belong to 23 unique proteins. Three spots were isoforms of pyruvate carboxylase, and the putative Hsp70 chaperone HscA was identified from two spots (Table 1), each with different molecular masses and charges possibly due to breakdown and side-chain deamination. In PgAFP-treated samples, the relative abundance was 1.6–3.5-fold higher for 13 spots, whereas 13 were 1.6–3.6-fold lower (Table S2 in the Supplementary Material).

The label-free quantitative analysis led to the identification of 1733 unique proteins (identification by at least 2 peptides per protein), and with each validated protein detected in a minimum of 2/3 biological replicates from at least one treatment group. Of these proteins, 367 were identified whose relative abundance suffered some change, either quantitative ($n = 231$) or qualitative ($n = 136$) (Table S1 in the Supplementary Material), using methods described above. All 23 proteins showing significant changes in 2D gels were also identified by label-free quantitative analysis. From these, six proteins showed a similar fold change in both methods. The remaining 17 reached at least a 1.5-fold change in gel-based analysis but did not reach the twofold change threshold in label-free proteomic analysis. The presence of isoforms could explain these differences. PgAFP-treated samples contained 104 proteins with higher abundance, from 2- to 288-fold ($p < 0.05$), and 67 proteins were exclusively detected following PgAFP exposure. In addition, untreated samples showed 127 proteins in higher abundance, between 2- and 202-fold ($p < 0.05$), and 69 proteins were exclusively detected in these samples. Scatterplot analysis of data from the label-free study revealed strong correlation within the biological replicates from each respective treatment group (Pearson correlation values >0.95), confirming high

Fig. 1 Effect of different concentrations of PgAFP on *A. flavus* growth for 96 h

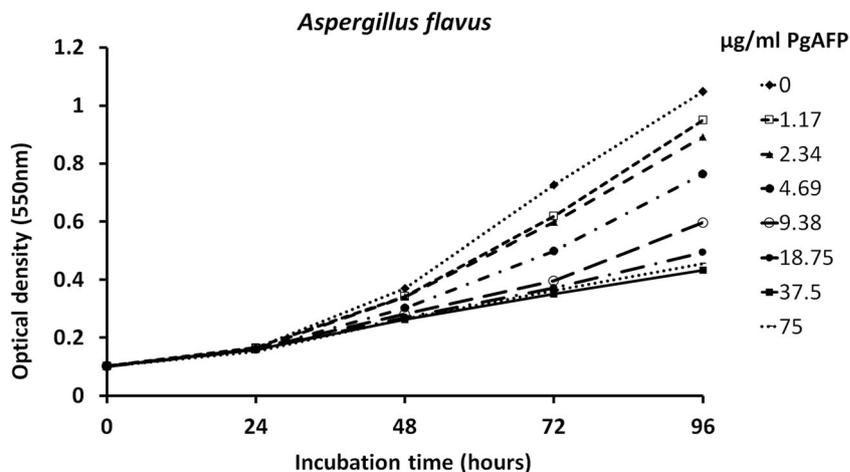


Table 1 Selected proteins whose relative abundance was affected by PgAFP in *A. flavus* reaching over 1.5-fold change in 2D-PAGE or 2.0-fold change in label-free proteomics (LFP) analysis. Data are given according to four groups of metabolic pathways

Proteins involved in pathways	Detection method	Fold change
Energy metabolism related to glycolysis and gluconeogenesis		
Pyruvate decarboxylase	2D-PAGE and LFP	+1.6 and <2
Phosphoglucomutase	2D-PAGE and LFP	+1.6 and <2
Pyruvate carboxylase (three isoforms)	2D-PAGE and LFP	-1.9/-1.7/-1.7, and -2.1
Acetate-CoA ligase	2D-PAGE and LFP	-1.7 and -2.7
Aldose 1-epimerase	LFP	NT ^b
Phosphoenolpyruvate carboxykinase	LFP	-2.67
Aldehyde dehydrogenase	LFP	-2.45
Phosphofructokinase	LFP	-3.34
Acetyl-CoA carboxylase ^a	LFP	-2.34
Malate synthase	LFP	-8.55
Stress response and glutathione metabolism		
Molecular chaperone and allergen Mod-E/Hsp90/Hsp1	2D-PAGE and LFP	+3.3 and <2
Hsp70 chaperone (two isoforms)	2D-PAGE and LFP	+1.7/+1.7 and <2
Chaperonin	LFP	+5.63
Cys-Gly metalloprotease Dug1	2D-PAGE and LFP	+1.7 and <2
Glutathione synthetase	2D-PAGE and LFP	+1.6 and <2
Elongation factor 1 gamma	LFP	NT
Gamma-glutamyltranspeptidase	LFP	-2.63
Glutathione S-transferase ^a	LFP	-2.42
G protein complex beta subunit CpcB	LFP	-2.85
Cell wall integrity, chitin biosynthesis, and permeability		
Actin Act1	2D-PAGE and LFP	-2.2 and -5.16
Septin AspA	2D-PAGE and LFP	-2 and -2.15
Probable beta-glucosidase btgE	LFP	+3.64
Cell wall glucanase	LFP	T ^c
Mannose-1-phosphate guanylyltransferase	LFP	-11.9
Glucosamine-fructose-6-phosphate aminotransferase	LFP	-5.64
Alpha, alpha-trehalose-phosphate synthase subunit putative	LFP	-4.21
Septin	LFP	-3.02
Rho GTPase Rho1	LFP	-2.68
GDP-mannose pyrophosphorylase A	LFP	-2.42
Septin AspB	LFP	-2.06
Aflatoxin biosynthesis		
Acetyl-CoA carboxylase ^a	LFP	-2.34
AflK/vbs/VERB synthase	LFP	NT
AflM/ver-1/dehydrogenase/ketoreductase	LFP	NT
Glutathione S-transferase ^a	LFP	-2.42
O-Methyltransferase, putative	LFP	-30.18

^a Protein involved in more than one pathway

^b NT: Protein only detected in non-treated samples

^c T: Protein only detected in treated samples

reproducibility from the biological replicates (Fig. S1, Table S3 in the Supplementary Material). Among the characterized proteins, the highest increases in PgAFP-treated samples were detected for ribosomal 40S and

60S proteins, as well as other putative proteins such as translation initiation factors, small nuclear ribonucleo-proteins, RNA binding, and splicing proteins, many being uniquely detected in PgAFP-treated samples.

According to KEGG, in addition to ribosomal, spliceosomal, RNA transport, and degradation proteins, hyphae biogenesis proteins also increased upon PgAFP exposure. Interestingly, PgAFP exposure attenuated abundance of proteins related to a number of cellular systems, such as glycolysis and gluconeogenesis, stress response, cell wall integrity, and aflatoxin biosynthesis (Table 1). Two of these proteins play crucial roles in signaling the cell response to external factors, including antifungal compounds in *A. nidulans* (Coca et al. 2000) and in *Saccharomyces cerevisiae* (Fuchs and Mylonakis 2009): the G protein complex β subunit CpcB and Rho-GTPase Rho1, respectively. The aflK/vbs/VERB synthase and AflM/ver-1/dehydrogenase/ketoreductase, both involved in the aflatoxin pathway (Yu et al. 2004) and identified in all control samples, were no longer detectable following PgAFP treatment. Additionally, acetyl-CoA carboxylase, *O*-methyltransferase, and glutathione S-transferase also related to aflatoxin production (Allameh et al. 2002) were found in lower relative amounts in PgAFP-treated samples.

Effect on metabolic activity

To obtain evidences of the metabolic alterations suggested by the comparative proteomics, the metabolic activity was checked with FUN-1 staining. The reduction of metabolic activity was assessed by the yellow-green fluorescence of treated sensitive hyphae, in contrast to the presence of intravacuolar red spots in unaffected controls, as described by Kaiserer et al. (2003). A dramatic difference between PgAFP-treated and untreated *A. flavus* was found. PgAFP-treated samples showed green fluorescence but almost no red intravacuolar fluorescence (Fig. 2), meaning metabolically inactive hyphae. In contrast, untreated *A. flavus* (Fig. 2) and PgAFP-treated *P. chrysogenum* (data not shown) exhibited a high content of red intravacuolar fluorescence due to unaltered metabolic activity.

Morphology

To study morphological changes, septa distribution, nuclei localization, and chitin deposition, in addition to the standard

concentration of 20 $\mu\text{g/ml}$ used in other assays, an additional test was run with 75 $\mu\text{g/ml}$ PgAFP to obtain unambiguous results. Among the different tests used to visualize morphological changes induced by PgAFP, no changes in germination or branching were detected by bright light microscopy. Nuclei localization and distribution by fluorescence microscopy with Hoechst 33258 stain showed no abnormal distribution compared to control samples. Septa distribution, checked with fluorescent brightener 28, showed no differences between PgAFP-treated and untreated samples after 24-h incubation (data not shown). Figure 3 shows the fluorescence intensity of the stained PgAFP-treated and untreated hyphae at an early incubation time (12 h). Both micrographs were taken with the same exposure to compare the chitin present. The fluorescence of PgAFP-treated hyphae appeared to be lower than that of untreated samples (Fig. 3).

Effect on membrane permeability and PgAFP localization

Given that the activity of most studied small, highly basic, and cysteine-rich antifungal proteins from molds has been related to interactions with the outer layer of sensitive molds, the level of cell membrane compromise was tested with the SYTOX Green uptake test. Mean (\pm SD) fluorescence values at 210 min after SYTOX Green addition to *A. flavus* increased up to 23,342 (\pm 2992) arbitrary units as PgAFP concentration increased from 0 to 4.69 $\mu\text{g/ml}$ but progressively decreased down to 11,550 (\pm 2155) arbitrary units from 9.38 to 75 $\mu\text{g/ml}$ (Fig. 4). Nonetheless, the fluorescence in all PgAFP-treated *A. flavus* was at least 27 % ($p < 0.05$) higher than that in the untreated control, except for the lowest PgAFP concentration (1.2 $\mu\text{g/ml}$) at 10 min after SYTOX Green addition. In contrast, the fluorescence after SYTOX Green addition to the PgAFP producer *P. chrysogenum* did not exceed 25 % over that in non-treated samples at any PgAFP concentration assayed (data not shown). To determine the localization of PgAFP, *A. flavus* was treated with FITC-labeled PgAFP. To check whether FITC labeling decreased the antifungal activity of PgAFP, an antifungal assay was run. No differences ($p > 0.05$) were found between cultures treated with labeled

Fig. 2 Metabolic activity of *A. flavus* tested with FUN-1 staining. Non-treated hyphae (left) showed intravacuolar activity as red spots; hyphae treated with 20 $\mu\text{g/ml}$ PgAFP for 24 h (right) showed scarcely red spots

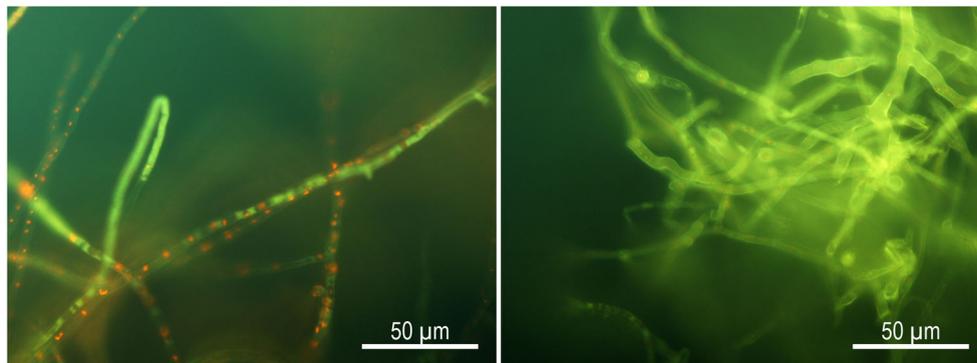
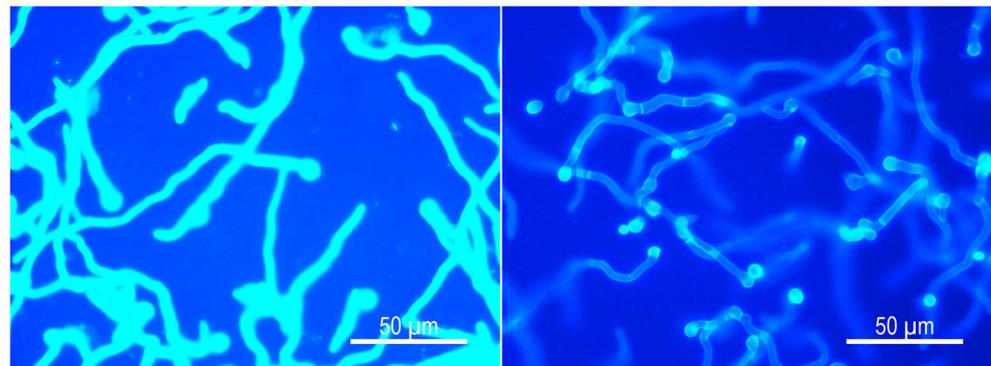


Fig. 3 Chitin distribution on *A. flavus* stained with fluorescent brightener 28. *Left*: non-treated hyphae; *right*: hyphae treated with 75 $\mu\text{g/ml}$ PgAFP for 12 h



and those treated with non-labeled PgAFP (data not shown). Localization of PgAFP by fluorescence microscopy after treatment of *A. flavus* with FITC-labeled PgAFP revealed green fluorescence only at the outer layer at 6-h incubation time but both inside and bound to the outer layer on treated hyphae at 24 h (Fig. 5). In contrast, FITC-labeled PgAFP neither bound nor penetrated in the resistant *P. chrysogenum* (Fig. 5). Additionally, the heat-denatured FITC-PgAFP was not bound to or inside the hyphae (data not shown).

Effect on oxidative status and viability

To discern whether the changes in the proteins related to oxidative stress were provoked by a high ROS level, staining with 2',7'-dichlorofluorescein diacetate was carried out, where a green fluorescence reveals the presence of intracellular ROS as described by Kaiserer et al. (2003). The most intense oxidative activity was observed in PgAFP-treated *A. flavus*, whereas non-treated hyphae only showed a very weak halo (Fig. 6). Given that ROS may induce severe cell damage, the viability of PgAFP-treated *A. flavus* was evaluated with the AO/EB double staining to check for necrosis and also with AnV-FITC/PI staining to detect apoptotic processes. With AO/EB double staining, an additional treatment with

75 $\mu\text{g/ml}$ PgAFP was also tested to obtain unambiguous results. A massive loss in viability was observed at 24 h in hyphae treated with 75 $\mu\text{g/ml}$ (Fig. 7). Untreated hyphae displayed a green color, meaning that they remained viable (Byczkowska et al. 2012). The intense orange staining revealed a high penetration of EB in the PgAFP-treated hyphae through a highly compromised cell membrane. Untreated samples were not stained by AnV-FITC/PI, indicating that they were viable. (Fig. 8a). The orange staining of DNA in PgAFP-treated samples by PI indicated cell membrane damage associated with a necrotic stage (Fig. 7b). The generalized necrosis observed can be due to the fact that an advanced stage of cell death was reached at 24 h in nearly all PgAFP-treated hyphae. AnV-FITC staining was used to detect phosphatidylserine translocation to the external side of the plasma membrane due to apoptosis. However, the green fluorescence observed in PgAFP-treated hyphae at 24 h cannot be attributed to apoptosis, because the compromised cell membrane would allow AnV-FITC to enter and bind phosphatidylserine at the inner layer of plasma membrane. To detect potential apoptotic signals previous to the necrotic stage, an additional AnV-FITC/PI staining was carried out at 12 h. The evaluation of phosphatidylserine translocation at this earlier stage revealed some hyphae showing solely green color due to apoptosis (Fig. 8c). All these ROS and viability assays for PgAFP-treated and untreated *P. chrysogenum* gave very similar results to those obtained for untreated *A. flavus* (data not shown).

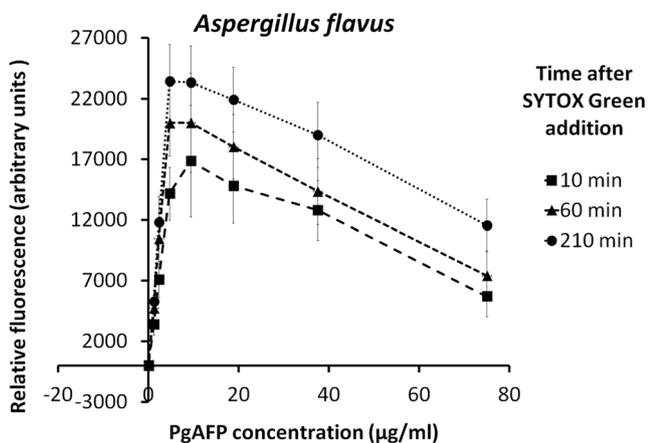
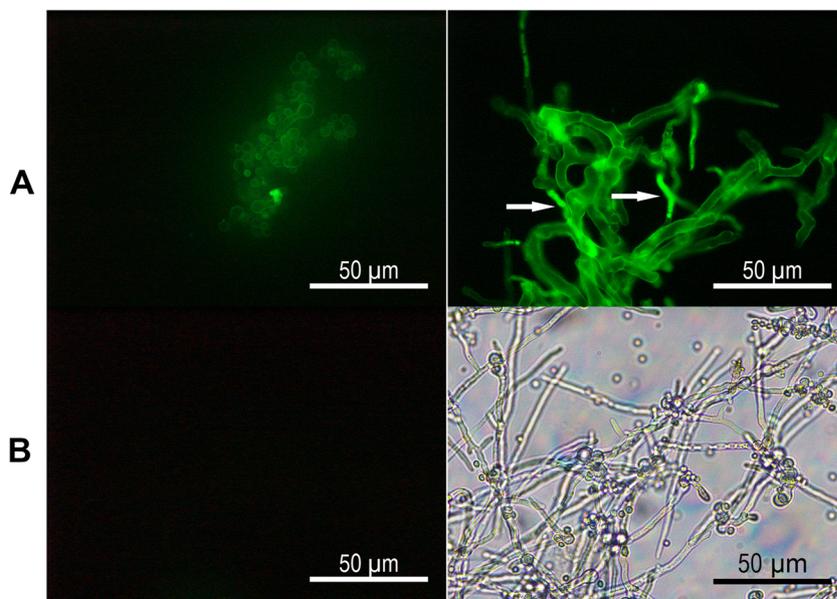


Fig. 4 SYTOX Green uptake with different concentrations of PgAFP on *A. flavus* at 24 h (bars represent standard deviation of the mean)

Discussion

PgAFP reduced *A. flavus* growth following a dose-dependent pattern (Fig. 1). The inhibition rate reached with PgAFP at 37.5 $\mu\text{g/ml}$ was 59 %, calculated from the percent difference in OD_{550} compared to untreated controls. Similar results were obtained with PAF against *A. flavus*, reaching a 69 % growth reduction with 50 $\mu\text{g/ml}$ (Kaiserer et al. 2003) and 50 % growth reduction with 3 μM (18.9 $\mu\text{g/ml}$) (Marx et al. 2008). The first 24 h of incubation did not show any statistical

Fig. 5 PgAFP localization in *A. flavus* and *P. chrysogenum* treated with 20 $\mu\text{g}/\text{ml}$ FITC-labeled PgAFP. **(a)** *A. flavus*. *Left*: At 6-h incubation, PgAFP was found solely bound to the outer layer. *Right*: At 24-h incubation, PgAFP was detected bound to the outer layer and occasionally inside the cell (*arrows*). **(b)** *P. chrysogenum*. *Left*: At 24-h incubation, PgAFP was neither bound nor inside the hyphae. *Right*: Bright field observation of the same preparation showing profuse growth



differences in growth, due to the limited fungal growth at this time point under the conditions assayed. Even the highest PgAFP concentrations tested (75 $\mu\text{g}/\text{ml}$) did not lead to total inhibition of *A. flavus*, which implies only a fungistatic effect.

Using gel-based proteomics, a total of 23 unique proteins, identified from 26 independent spots (Table S2 in the Supplementary Material), were observed to undergo a significant change in abundance in *A. flavus* in response to PgAFP. A concurrent analysis using label-free quantitative mass spectrometry-based proteomics revealed a more in-depth view of the response to PgAFP, with 231 quantitative changes in protein abundance and 136 qualitative differences following treatment. The dynamic range of gel-based proteomics, using colloidal Coomassie Blue stain as a visualization technique, is limited to approximately 1 order of magnitude (Gauci et al. 2011). As a result, the proportion of the proteome available for analysis using gel-based methods is constrained by relative protein abundance. In comparison, label-free proteomics is capable of measuring protein abundances across larger dynamic ranges, with proteins identified across 4 orders of magnitude in this study (Table S1 in the Supplementary Material).

In order to reduce the possibility of inclusion of false positives in this larger data set, a fold change cutoff of 2 was employed. In addition, differing capacities for resolution of proteins with extremes in pI , molecular mass, and hydrophobicity (Owens et al. 2014) can contribute to the lower number of abundance changes detected using gel-based proteomics. Furthermore, the limitations of the label-free proteomic technique with regard to capability to analyze isoforms could explain the different quantification of proteins when isoforms were involved. For example, multiple Hsp70 isoforms have been described in the eukaryotic cytosol (Kabani and Martineau 2008). Although an increase of Hsp70 chaperone (HscA) was detected in gel-based proteomic analysis, no significant change in abundance was detected for Hsp70 chaperone (HscA) by label-free analysis. This may indicate that the abundance difference detected by 2D-PAGE for this protein may be the result of a post-translational event, which altered the ratio of the different isoforms instead of the total HscA protein abundance.

A substantial number of ribosomal proteins were detected with increased abundance in response to PgAFP, in addition to

Fig. 6 ROS induction by PgAFP on *A. flavus* detected by 2',7'-dichlorofluorescein diacetate staining. Non-treated *A. flavus* (*left*) did not show green fluorescence inside of the cells; hyphae treated with 20 $\mu\text{g}/\text{ml}$ PgAFP for 24 h (*right*) showed strong green fluorescence due to intracellular ROS

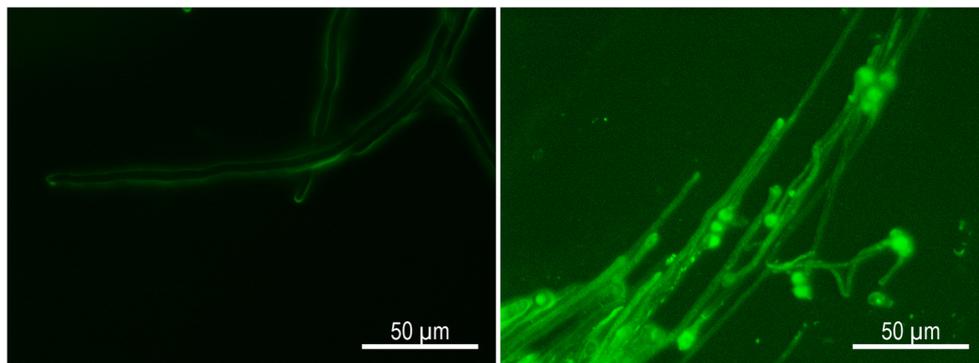
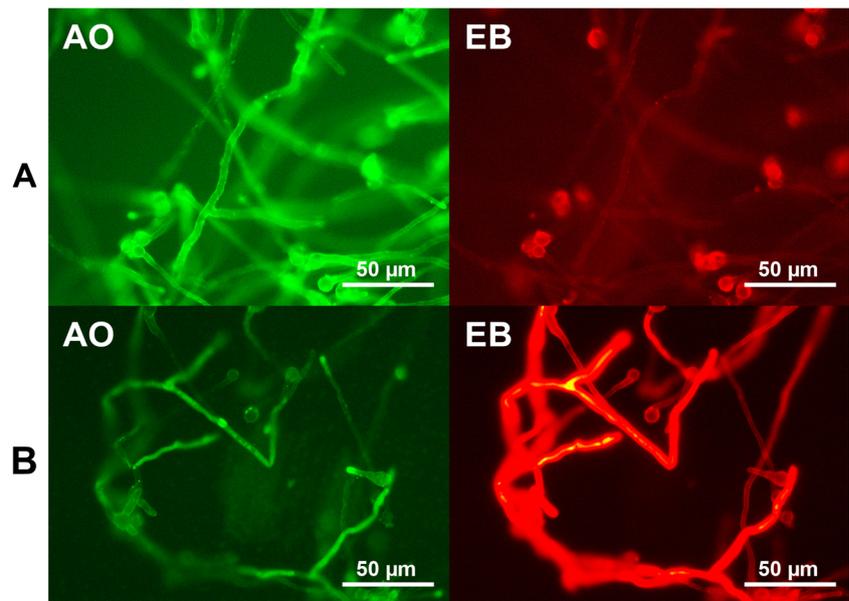


Fig. 7 Effect of PgAFP on hyphae viability evaluated with vital acridine orange (AO)/ ethidium bromide (EB) staining. **a** Non-treated hyphae of *A. flavus* showing an intense green color (AO). **b** Seventy-five microgram per milliliter PgAFP-treated hyphae showing an intense red color (EB) due to compromised cell membrane



proteins involved in RNA transport and degradation, and the spliceosome. Ribogenesis and translation are energy-hungry processes, which are normally associated with germination or cell growth (Lamarre et al. 2008). This observed increase in

the translational machinery, coupled with the decrease in metabolism-associated mechanisms, could lead to depletion of the cell energy reserves and result in the fungistatic effect of PgAFP on *A. flavus*. The main pathways identified with

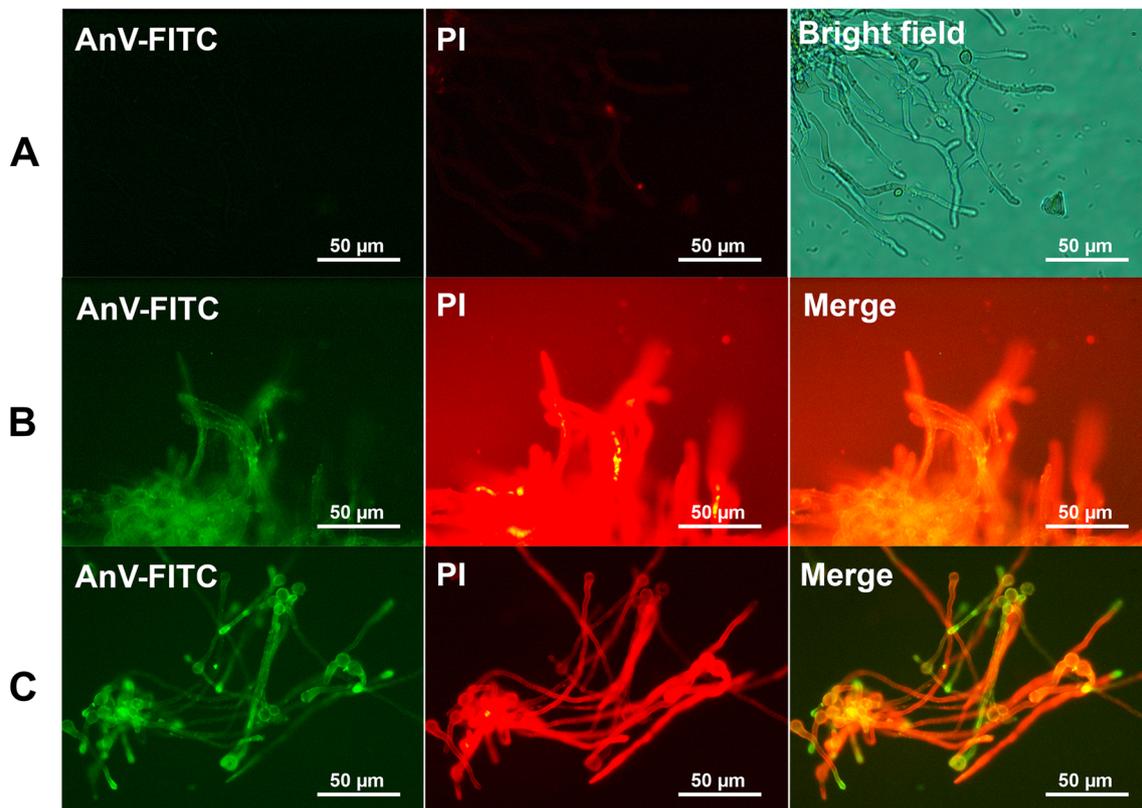


Fig. 8 Effect of PgAFP on *A. flavus* hyphae viability evaluated with apoptosis detection kit. **a** Non-treated hyphae showing no apoptosis or necrosis signal at 24 h. **b** Hyphae treated with 20 $\mu\text{g}/\text{ml}$ PgAFP for 24 h showing an intense red color (PI) due to necrosis that leads to mainly

orange color in the merged picture. **c** Hyphae treated with PgAFP for 12 h revealing apoptotic signals by the green fluorescence (AnV-FITC) that leads to green hyphae in the merged picture

proteins showing changes in relative abundance due to PgAFP are involved in energy metabolism, cell stress response, hyphae biogenesis, and aflatoxin biosynthesis (Table 1). The proteins related to energy metabolism showing a lower abundance in PgAFP-treated samples were pyruvate carboxylase, phosphofructokinase, aldose 1-epimerase, phosphoenolpyruvate carboxykinase, aldehyde dehydrogenase, malate synthase, acetate-CoA ligase, and acetyl-CoA carboxylase. These enzymes play essential roles in glycolysis and gluconeogenesis pathways, and the lower quantity would depress the metabolic activity. This effect is supported by the results obtained from the FUN-1 staining (Fig. 2) where PgAFP-treated samples showed reduced metabolic hyphae activity. A reduced metabolic activity has been also described with FUN-1 staining for PAF in *A. niger* (Kaiserer et al. 2003).

A. flavus is not completely killed, even at the highest PgAFP concentration assayed. This fact suggests that *A. flavus* invests in alternative ways to obtain the necessary energy to grow. This seems to be achieved through anaerobic pathways led by pyruvate decarboxylase, whose relative quantity was higher in PgAFP-treated samples. Pyruvate decarboxylase is involved in alcoholic fermentation under anaerobic stress (Lockington et al. 1997). Thus, the pyruvate presumably accumulated due to the lower pyruvate carboxylase presence with PgAFP would be used as substrate by pyruvate decarboxylase. However, this pathway would not provide enough energy to keep a normal growth rate. The lower abundance of proteins involved in hyphae structure, such as septins and actin, may provoke morphological changes, such as those caused by AFP1 from *Streptomyces tendae* and PAF in sensitive molds (Bormann et al. 1999; Kaiserer et al. 2003). Septin AspA, AspB, and AspC are necessary for normal development and morphogenesis (Lindsey et al. 2010; Hernández-Rodríguez et al. 2012). Actin is necessary for cell wall and membrane extension (Fischer et al. 2008). The lower relative abundance of septins and actins detected in PgAFP-treated *A. flavus* suggests morphological changes, as it has been shown for *Aspergillus* spp. treated with PAF due to actin gene repression (Kaiserer et al. 2003; Binder et al. 2010). Despite the altered quantity of proteins, no morphological change was visualized in hyphae and nuclei distribution in PgAFP-treated *A. flavus*.

Similarly to PgAFP, AFP from *A. giganteus* did not cause morphological changes in sensitive molds (Theis et al. 2003) but binds to regenerated chitin (Liu et al. 2002) and specifically inhibits chitin synthesis, causing cell wall stress and disturbing cell integrity (Hagen et al. 2007). However, AFP1 also binds to chitin but causes severe alteration in cell morphogenesis (Bormann et al. 1999). In fact, proteins participating in chitin pathway were found in lower relative amount in PgAFP-treated *A. flavus*, such as the putative α -trehalose-phosphate synthase subunit α , glucosamine-fructose-6-phosphate aminotransferase, mannose-1-phosphate

guanylyltransferase, and GDP-mannose pyrophosphorylase *A. flavus*. Furthermore, a cell wall glucanase, whose main function involves degrading chitin, was found exclusively in PgAFP-treated samples. These changes in the relative abundance of chitin-related proteins could explain a smaller deposition of chitin on cell wall of *A. flavus* at 12-h incubation time as suggested by the fluorescent brightener 28 staining (Fig. 3). A lower quantity of chitin may be related to the mode and the site of action of PgAFP, as it has been reported for AFP (Hagen et al. 2007). Regarding cell wall glucanase, its detection only in PgAFP-treated samples can be a consequence to counteract PgAFP binding to chitin. PAF exposure resulted in a deregulation of the chitin deposition at hyphal tips (Binder et al. 2010). Therefore, the smaller amount of septins, actin, and chitin, seems not to be enough to provoke morphological changes in hyphae but could affect normal growth and cell wall integrity. In addition, eleven proteins related to cell wall integrity showed lower relative abundance in PgAFP-treated samples (Table 1). Rho1 GTPase is considered the master regulator of cell wall integrity signaling and it is involved in actin organization in *S. cerevisiae* (Levin 2005). *A. nidulans* cells treated with PAF fail to activate MpkA, a target of GTPase RhoA signaling, disrupting basal resistance towards antifungal activity (Binder et al. 2010). In addition, *A. nidulans* lacking RhoA display pronounced hypersensitivity to cell wall-interfering drugs (Guest et al. 2004). GDP-mannose pyrophosphorylase has been described as essential for cell wall integrity, morphogenesis, and viability of *Aspergillus fumigatus* (Jiang et al. 2008), and it also seems to be related to regulation of the selective permeability (Agaphonov et al. 2001).

AFP specifically inhibits *in situ* activity of chitin synthases classes III and V in sensitive fungi, which would disturb cell integrity, but it strongly induced cell wall integrity pathway in *A. niger* as a compensatory response (Hagen et al. 2007). Similarly, reinforcement of chitin synthesis has been described as a distinctive feature of AFP-moderate sensitive and AFP-resistant fungi, whereas it is not realized in AFP-sensitive fungi (Ouedraogo et al. 2011). This elevation of chitin levels has been interpreted as the necessary response to survive an AFP attack. Therefore, it seems that the mode of action of AFP is based on cell wall alterations. However, as it has been mentioned above, PgAFP repressed the cell wall integrity pathway and chitin biosynthesis in treated *A. flavus*. This would increase membrane exposure to PgAFP. Actually, PgAFP increased permeability at all concentrations tested (Fig. 4). Notwithstanding this, the highest SYTOX Green uptake was observed at low PgAFP concentrations (4.69 $\mu\text{g/ml}$). A similar fact has been described for plant defensin Dm-AMP1, whose dose–response curves for SYTOX Green uptake declined at doses above those providing maximum effect (Thevissen et al. 1999). In contrast, the inhibition assay exhibited a dose–response effect of PgAFP in the whole range of

concentrations tested. The lower SYTOX Green uptake at the highest PgAFP concentrations could be related to the apparent dependency of membrane polarization, as it has been shown for various antifungal proteins that depolarize the membrane (Thevissen et al. 1996).

Treatment of *A. flavus* with PgAFP-FITC revealed that PgAFP is bound to outer layer and also is present in the cytoplasm. Other antifungal proteins, such as AFP, bind the outer layer of sensitive fungi and also can be found intracellularly in collapsed and dead cells (Theis 2003, 2005). The antifungal activity of AFP is related to its ability to interact with anionic phospholipids (Lacadena et al. 1998). Such interaction would promote the insertion of the antifungal protein into the plasma membrane of the sensitive fungi (Marx et al. 2008). In contrast, PAF is actively internalized only in sensitive fungi (Oberparleiter et al. 2003; Batta et al. 2009). Thus, it seems that PgAFP induces the aforementioned changes in membrane permeability after binding to the outer layer. Given that the results obtained at 24 h did not allow the confirmation that PgAFP is inside non-compromised cells, PgAFP internalization cannot be ruled out.

Additionally, the above changes in energy metabolism and cell wall integrity are aggravated by cell damage due to ROS generation. Among other negative effects on lipids and nucleic acids, ROS also cause protein aggregation and amyloid formation (Squier 2001), compromising cell viability (Cabiscol et al. 2000). Heat shock proteins were found in higher relative abundance in PgAFP-treated samples. These proteins are involved in stress, preventing aggregation and assisting refolding of misfolded proteins (Bukau and Horwich 1998). The observed higher abundance of heat shock proteins could represent a defense mechanism to neutralize ROS effects on proteins.

Increased abundance of two proteins involved in the glutathione pathway was also found: glutathione synthetase (GS) and Cys-Gly metallodipeptidase Dug1. Glutathione (GSH) has pivotal roles in protection against oxidative stress provoked by exposure of cells to ROS (Penninckx 2002). Therefore, GSH overproduction due to the increased GS could counteract ROS present in the cell, as it has been described for PAF (Leiter et al. 2005). A higher amount of ROS was confirmed by fluorescence staining in PgAFP-treated samples (Fig. 6). In addition, γ -glutamyltranspeptidase (γ GT) was found in lower amount in PgAFP-treated *A. flavus*. This enzyme is involved in glutathione catabolism, releasing the Cys-Gly dipeptide (Kaur et al. 2009). Furthermore, the Cys-Gly metallodipeptidase Dug1 degrades the Cys-Gly dipeptide, recovering glycine and cysteine for GSH synthesis by GS. The higher relative abundance of Cys-Gly metallodipeptidase Dug1 observed in PgAFP-treated *A. flavus* would help counteract high ROS levels. Thus, it seems that *A. flavus* also uses GSH metabolism to counteract PgAFP action due to ROS production. However, as discussed later, G protein subunit β

CpcB may also play an essential role modulating the intracellular levels of glutathione and ROS.

Despite the production of heat shock proteins and GSH to combat ROS, the defense mechanism of *A. flavus* does not seem to be effective against PgAFP. The observed increase of ROS in PgAFP-treated samples could explain *A. flavus* inhibition. These substances can act as primary triggers of apoptosis (Slater et al. 1995). The loss of cell membrane integrity revealed by AO/EB double staining and the annexin V-FITC and PI staining (Figs. 7 and 8) is a necrotic signal derived from the observed apoptotic process, likely triggered by ROS (Hamann et al. 2008). Thus, the *A. flavus* response to counteract ROS seems insufficient to prevent the necrotic process. PAF needs active G protein signaling to inhibit the growth of the sensitive organism (Leiter et al. 2005). A lower relative amount of G protein complex β subunit CpcB was found in PgAFP-treated *A. flavus*, but changes in neither G protein complex α subunit GpaA/FadA nor G protein complex β subunit SfaD were detected. Thus, the relative abundance of the G protein complex β subunit CpcB seems to be the key factor involved in the modulation of apoptotic cell death signals, and the lower amount of this protein could be responsible for the modulating PgAFP toxicity in *A. flavus*.

Until now, the effect of antifungal proteins from molds has been explained by signaling processes via G protein and RhoA (Binder et al. 2010; Ouedraogo et al. 2011). We propose the lower relative abundance of Rho1 and G protein subunit β CpcB to be the main factors in the mode of action of PgAFP. The precise mechanisms responsible for the decrease of these proteins, either by a higher degradation or a decreased biosynthesis, cannot be established at present.

In addition, several proteins involved in the biosynthesis of secondary metabolites were found at lower relative abundance in PgAFP-treated samples. This fact seems to be related to the reduced metabolic hyphae activity revealed with FUN-1 staining (Fig. 2). The suppression of non-essential functions, such as biosynthesis of secondary metabolites, could be explained by the lack of energy due to the described shortage of proteins related to energy metabolism. Among the secondary metabolites produced by *A. flavus*, the hepatocarcinogenic aflatoxins are of utmost interest (Kim et al. 2008). The proteomic analysis did not detect aflK/vbs/VERB synthase and AflM/ver-1/dehydrogenase/ketoreductase following PgAFP treatment, which are essential enzymes in key steps for aflatoxin synthesis in *A. flavus* and *Aspergillus parasiticus* (Yu et al. 2004). Additionally, glutathione S-transferase was found in lower quantities in PgAFP-treated samples. A higher activity of this protein was always associated with increased aflatoxin production in *A. flavus* (Saxena et al. 1988) and *A. parasiticus* (Allameh et al. 2002). These results suggest that aflatoxin production is likely to be delayed in PgAFP-treated *A. flavus*. Despite these results having been obtained in an incubation time of only 24 h, the lack of enzymes essential for aflatoxin

biosynthesis together with the slower hyphae development could delay aflatoxin production in a longer incubation time. On the other hand, oxidative stress has been shown to stimulate aflatoxin biosynthesis in *A. parasiticus* (Jayashree and Subramanyan 2000; Reverberi et al. 2005). Due to the induction of ROS by PgAFP, the impact of this antifungal protein on aflatoxin biosynthesis enzymes and also on aflatoxin production will require additional studies.

In conclusion, the mode of action of PgAFP seems to be multifactorial implying membrane changes, reduced metabolic activity, and intracellular ROS production. The changes in the proteins that favor a higher GSH concentration and the increase in heat shock proteins by *A. flavus* do not seem to be enough to avoid apoptosis. There is also a depression of proteins involved in the biosynthesis of secondary metabolites, including aflatoxin. However, further investigations are required to discern the effect of PgAFP on aflatoxin production prior to the use of this protein to control toxigenic molds.

Acknowledgments This work was supported by the Spanish Ministry of Education and Science, Ministry of Economy and Competitiveness, and FEDER (AGL2010-21623, AGL2013-45729-P). Josué Delgado was a recipient of a FPI grant from the Spanish Ministry of Education and Science (BES-2011-043422 y EEBB-I-13-06900). Rebecca A. Owens was funded by a 3U Partnership Award (<http://www.3UPartnership.ie/>). Mass spectrometry facilities were funded by Science Foundation Ireland (Q-Exactive; 12/RI/2346(3) and PI/11/1188) and the Irish Higher Education Authority (Agilent Ion Trap 6340).

Conflict of interest The authors declare that they have no competing interests.

References

- Acosta R, Rodríguez-Martín A, Martín A, Núñez F, Asensio MA (2009) Selection of antifungal protein-producing molds from dry-cured meat products. *Int J Food Microbiol* 135:39–46. doi:10.1016/j.ijfoodmicro.2009.07.020
- Agaphonov MO, Packeiser AN, Chechenova MB, Choi ES, Ter-Avanesyan MD (2001) Mutation of the homologue of GDP-mannose pyrophosphorylase alters cell wall structure, protein glycosylation and secretion in *Hansenula polymorpha*. *Yeast* 18:391–402. doi:10.1002/yea.678
- Allameh A, Razzaghi Abyane M, Shams M, Rezaee MB, Jaimand K (2002) Effects of neem leaf extract on production of aflatoxins and activities of fatty acid synthetase, isocitrate dehydrogenase and glutathione S-transferase in *Aspergillus parasiticus*. *Mycopathologia* 154:79–84
- Batta G, Barna T, Gáspári Z, Sándor S, Kövér KE, Binder U, Sarg B, Kaiserer L, Chhillar AK, Eigentler A, Leiter E, Hegedüs N, Pócsi I, Lindner H, Marx F (2009) Functional aspects of the solution structure and dynamics of PAF—a highly-stable antifungal protein from *Penicillium chrysogenum*. *FEBS J* 276:2875–2890. doi:10.1111/j.1742-4658.2009.07011.x
- Bernaldez V, Rodríguez A, Martín A, Lozano D, Córdoba JJ (2014) Development of a multiplex qPCR method for simultaneous quantification in dry-cured ham of an antifungal-peptide *Penicillium chrysogenum* strain used as protective culture and aflatoxin-producing moulds. *Food Control* 36:257–265. doi:10.1016/j.foodcont.2013.08.020
- Binder U, Oberparleiter C, Meyer V, Marx F (2010) The antifungal protein PAF interferes with PKC/MPK and cAMP/PKA signalling of *Aspergillus nidulans*. *Mol Microbiol* 75:294–307. doi:10.1111/j.1365-2958.2009.06936.x
- Bormann C, Baier D, Hörr I, Raps C, Ho I (1999) Characterization of a novel, antifungal, chitin-binding protein from *Streptomyces tendae* Tü901 that interferes with growth polarity. *J Bacteriol* 181:7421–7429
- Bukau B, Horwich AL (1998) The Hsp70 and Hsp60 chaperone machines. *Cell* 92:351–366
- Byczkowska A, Kunikowska A, Kaźmierczak A (2012) Determination of ACC-induced cell-programmed death in roots of *Vicia faba* ssp. minor seedlings by acridine orange and ethidium bromide staining. *Protoplasma* 250:121–128. doi:10.1007/s00709-012-0383-9
- Cabiscol E, Piulats E, Echave P, Herrero E, Ros J (2000) Oxidative stress promotes specific protein damage in *Saccharomyces cerevisiae*. *J Biol Chem* 275:27393–27398. doi:10.1074/jbc.M003140200
- Cagas SE, Jain MR, Li H, Perlin DS (2011) Profiling the *Aspergillus fumigatus* proteome in response to caspofungin. *Antimicrob Agents Chemother* 55:146–154. doi:10.1128/AAC.00884-10
- Carberry S, Neville CM, Kavanagh KA, Doyle S (2006) Analysis of major intracellular proteins of *Aspergillus fumigatus* by MALDI mass spectrometry: identification and characterisation of an elongation factor 1B protein with glutathione transferase activity. *Biochem Biophys Res Commun* 341:1096–1104. doi:10.1016/j.bbrc.2006.01.078
- Carpentier SC, Witters E, Laukens K, Deckers P, Swennen R, Panis B (2005) Preparation of protein extracts from recalcitrant plant tissues: an evaluation of different methods for two-dimensional gel electrophoresis analysis. *Proteomics* 5:2497–2507. doi:10.1002/pmic.200401222
- Chen Z, Ao J, Yang W, Jiao L, Zheng T, Chen X (2013) Purification and characterization of a novel antifungal protein secreted by *Penicillium chrysogenum* from an Arctic sediment. *Appl Microbiol Biotechnol* 97:10381–10390. doi:10.1007/s00253-013-4800-6
- Coca MA, Damsz B, Yun DJ, Hasegawa PM, Bressan RA, Narasimhan ML (2000) Heterotrimeric G-proteins of a filamentous fungus regulate cell wall composition and susceptibility to a plant PR-5 protein. *Plant J* 22:61–69
- Collins C, Keane TM, Turner DJ, O’Keeffe G, Fitzpatrick DA, Doyle S (2013) Genomic and proteomic dissection of the ubiquitous plant pathogen, *Armillaria mellea*: toward a new infection model system. *J Proteome Res* 12:2552–2570. doi:10.1021/pr301131t
- Cox J, Mann M (2008) MaxQuant enables high peptide identification rates, individualized p.p.b.-range mass accuracies and proteome-wide protein quantification. *Nat Biotechnol* 26:1367–1372. doi:10.1038/nbt.1511
- Delgado J, Acosta R, Rodríguez-Martín A, Bermúdez E, Núñez F, Asensio MA (2015) Growth inhibition and stability of PgAFP from *Penicillium chrysogenum* against fungi common on dry-ripened meat products. *Int J Food Microbiol* 205:23–29. doi:10.1016/j.ijfoodmicro.2015.03.029
- Dolan SK, Owens RA, O’Keeffe G, Hammel S, Fitzpatrick DA, Jones GW, Doyle S (2014) Regulation of non-ribosomal peptide synthesis: bis-thiomethylation attenuates gliotoxin biosynthesis in *Aspergillus fumigatus*. *Chem Biol* 21:999–1012. doi:10.1016/j.chembiol.2014.07.006
- Fischer R, Zekert N, Takeshita N (2008) Polarized growth in fungi—interplay between the cytoskeleton, positional markers and membrane domains. *Mol Microbiol* 68:813–826. doi:10.1111/j.1365-2958.2008.06193.x
- Fuchs BB, Mylonakis E (2009) Our paths might cross: the role of the fungal cell wall integrity pathway in stress response and cross talk

- with other stress response pathways. *Eukaryot Cell* 8:1616–1625. doi:10.1128/EC.00193-09
- Galgóczy L, Kovács L, Karácsony Z, Virágh M, Hamari Z, Vágvölgyi C (2013) Investigation of the antimicrobial effect of *Neosartorya fischeri* antifungal protein (NFAP) after heterologous expression in *Aspergillus nidulans*. *Microbiology* 159:411–419. doi:10.1099/mic.0.061119-0
- Gauci VJ, Wright EP, Coorsen JR (2011) Quantitative proteomics: assessing the spectrum of in-gel protein detection methods. *J Chem Biol* 4:3–29. doi:10.1007/s12154-010-0043-5
- Gautam P, Shankar J, Madan T, Sirdeshmukh R, Sundaram CS, Gade WN, Basir SF, Sarma PU (2008) Proteomic and transcriptomic analysis of *Aspergillus fumigatus* on exposure to amphotericin B. *Antimicrob Agents Chemother* 52:4220–4227. doi:10.1128/AAC.01431-07
- Görg A, Drews O, Lück C, Weiland F, Weiss W (2009) 2-DE with IPGs. *Electrophoresis* 30(Suppl 1):S122–S132. doi:10.1002/elps.200900051
- Guest GM, Lin X, Momany M (2004) *Aspergillus nidulans* RhoA is involved in polar growth, branching, and cell wall synthesis. *Fungal Genet Biol* 41:13–22. doi:10.1016/j.fgb.2003.08.006
- Hagen S, Marx F, Ram AF, Meyer V (2007) The antifungal protein AFP from *Aspergillus giganteus* inhibits chitin synthesis in sensitive fungi. *Appl Environ Microbiol* 73:2128–2134. doi:10.1128/AEM.02497-06
- Hamann A, Brust D, Osiewacz HD (2008) Apoptosis pathways in fungal growth, development and ageing. *Trends Microbiol* 16:276–283. doi:10.1016/j.tim.2008.03.003
- Harris SD, Morrell JL, Hamer JE (1994) Identification and characterization of *Aspergillus nidulans* mutants defective in cytokinesis. *Genetics* 532:517–532
- Hegedus N, Leiter E, Kovács B, Tomori V, Kwon N-J, Emri T, Marx F, Batta G, Csernoch L, Haas H, Yu J-H, Pócsi I (2011) The small molecular mass antifungal protein of *Penicillium chrysogenum*—a mechanism of action oriented review. *J Basic Microbiol* 51:561–571. doi:10.1002/jobm.201100041
- Hernández-Rodríguez Y, Hastings S, Momany M (2012) The septin AspB in *Aspergillus nidulans* forms bars and filaments and plays roles in growth emergence and conidiation. *Eukaryot Cell* 11:311–323. doi:10.1128/EC.05164-11
- Jayashree T, Subramanian C (2000) Oxidative stress as a prerequisite for aflatoxin production by *Aspergillus parasiticus*. *Free Radic Biol Med* 29:981–985
- Jiang H, Ouyang H, Zhou H, Jin C (2008) GDP-mannose pyrophosphorylase is essential for cell wall integrity, morphogenesis and viability of *Aspergillus fumigatus*. *Microbiology* 154:2730–2739. doi:10.1099/mic.0.2008/019240-0
- Kabani M, Martineau CN (2008) Multiple hsp70 isoforms in the eukaryotic cytosol: mere redundancy or functional specificity? *Curr Genomics* 9:338–348. doi:10.2174/138920208785133280
- Kaiserer L, Oberparleiter C, Weiler-Görz R, Burgstaller W, Leiter E, Marx F (2003) Characterization of the *Penicillium chrysogenum* antifungal protein PAF. *Arch Microbiol* 180:204–210. doi:10.1007/s00203-003-0578-8
- Kaur H, Kumar C, Junot C, Toledano MB, Bachhawat AK (2009) Dug1p is a Cys-Gly peptidase of the γ -glutamyl cycle of *Saccharomyces cerevisiae* and represents a novel family of Cys-Gly peptidases. *J Biol Chem* 284:14493–14502. doi:10.1074/jbc.M808952200
- Kim JH, Yu J, Mahoney N, Chan KL, Molyneux RJ, Varga J, Bhatnagar D, Cleveland TE, Nierman WC, Campbell BC (2008) Elucidation of the functional genomics of antioxidant-based inhibition of aflatoxin biosynthesis. *Int J Food Microbiol* 122:49–60. doi:10.1016/j.ijfoodmicro.2007.11.058
- Kovács L, Virágh M, Takó M, Papp T, Vágvölgyi C, Galgóczy L (2011) Isolation and characterization of *Neosartorya fischeri* antifungal protein (NFAP). *Peptides* 32:1724–1731. doi:10.1016/j.peptides.2011.06.022
- Lacadena J, Martínez del Pozo A, Lacadena V, Martínez-Ruiz A, Mancheño JM, Oñaderra M, Gavilanes JG (1998) The cytotoxic α -sarcin behaves as a cyclizing ribonuclease. *FEBS Lett* 424:46–48. doi:10.1016/S0014-5793(98)00137-9
- Lamarre C, Sokol S, Debeauvais JP, Henry C, Lacroix C, Glaser P, Coppée JY, François JM, Latgé JP (2008) Transcriptomic analysis of the exit from dormancy of *Aspergillus fumigatus* conidia. *BMC Genomics* 9:417. doi:10.1186/1471-2164-9-417
- Leiter É, Szappanos H, Oberparleiter C, Kaiserer L, Csernoch L, Pusztahelyi T, Emri T, Pócsi I, Salvenmoser W, Marx F (2005) Antifungal protein PAF severely affects the integrity of the plasma membrane of *Aspergillus nidulans* and induces an apoptosis-like phenotype. *Antimicrob Agents Chemother* 49:2445–2453. doi:10.1128/AAC.49.6.2445
- Lessing F, Kniemeyer O, Wozniok I, Loeffler J, Kurzai O, Haertl A, Brakhage AA (2007) The *Aspergillus fumigatus* transcriptional regulator AfYap1 represents the major regulator for defense against reactive oxygen intermediates but is dispensable for pathogenicity in an intranasal mouse infection model. *Eukaryot Cell* 6:2290–2302. doi:10.1128/EC.00267-07
- Levin DE (2005) Cell wall integrity signaling in *Saccharomyces cerevisiae*. *Microbiol Mol Biol Rev* 69:262–291. doi:10.1128/MMBR.69.2.262
- Lindsey R, Cowden S, Hernández-Rodríguez Y, Momany M (2010) Septins AspA and AspC are important for normal development and limit the emergence of new growth foci in the multicellular fungus *Aspergillus nidulans*. *Eukaryot Cell* 9:155–163. doi:10.1128/EC.00269-09
- Liu R, Huang H, Yang Q, Liu W-Y (2002) Purification of α -sarcin and an antifungal protein from mold (*Aspergillus giganteus*) by chitin affinity chromatography. *Protein Expr Purif* 25:50–58. doi:10.1006/prep.2001.1608
- Lockington RA, Borlace GN, Kelly JM (1997) Pyruvate decarboxylase and anaerobic survival in *Aspergillus nidulans*. *Gene* 191:61–67
- Lowry OH, Rosebrough NJ, Farr L, Randall RJ (1951) Protein measurement with the folin phenol reagent. *J Biol Chem* 193:265–275
- Luber CA, Cox J, Lauterbach H, Fancke B, Selbach M, Tschopp J, Akira S, Wiegand M, Hochrein H, O’Keeffe M, Mann M (2010) Quantitative proteomics reveals subset-specific viral recognition in dendritic cells. *Immunity* 32:279–289. doi:10.1016/j.immuni.2010.01.013
- Marx F (2004) Small, basic antifungal proteins secreted from filamentous ascomycetes: a comparative study regarding expression, structure, function and potential application. *Appl Microbiol Biotechnol* 65:133–142. doi:10.1007/s00253-004-1600-z
- Marx F, Binder U, Leiter E, Pócsi I (2008) The *Penicillium chrysogenum* antifungal protein PAF, a promising tool for the development of new antifungal therapies and fungal cell biology studies. *Cell Mol Life Sci* 65:445–454. doi:10.1007/s00018-007-7364-8
- Marx F, Haas H, Reindl M, Stöffler G, Lottspeich F, Redl B (1995) Cloning, structural organization and regulation of expression of the *Penicillium chrysogenum paf* gene encoding an abundantly secreted protein with antifungal activity. *Gene* 167:167–171
- Moreno AB, Martínez Del Pozo A, San Segundo B (2006) Biotechnologically relevant enzymes and proteins. Antifungal mechanism of the *Aspergillus giganteus* AFP against the rice blast fungus *Magnaporthe grisea*. *Appl Microbiol Biotechnol* 72:883–895. doi:10.1007/s00253-006-0362-1
- Nakaya K, Omata K, Okahashi I, Nakamura Y, Kilkenbrock H, Ulbrich N (1990) Amino acid sequence and disulfide bridges of an antifungal protein isolated from *Aspergillus giganteus*. *Eur J Biochem* 193:31–38
- O’Keeffe G, Hammel S, Owens RA, Keane TM, Fitzpatrick DA, Jones GW, Doyle S (2014) RNA-seq reveals the pan-transcriptomic

- impact of attenuating the gliotoxin self-protection mechanism in *Aspergillus fumigatus*. BMC Genomics 15:894. doi:10.1186/1471-2164-15-894
- O’Keeffe G, Jöchl C, Kavanagh K, Doyle S (2013) Extensive proteomic remodeling is induced by eukaryotic translation elongation factor 1 β deletion in *Aspergillus fumigatus*. Protein Sci 22:1612–1622. doi:10.1002/pro.2367
- Oberparleiter C, Kaiserer L, Haas H, Ladurner P, Andratsch M, Marx F (2003) Active internalization of the *Penicillium chrysogenum* antifungal protein PAF in sensitive *Aspergilli*. Antimicrob Agents Chemother 47:3598–3601. doi:10.1128/AAC.47.11.3598
- Ouedraogo JP, Hagen S, Spielvogel A, Engelhardt S, Meyer V (2011) Survival strategies of yeast and filamentous fungi against the antifungal protein AFP. J Biol Chem 286:13859–13868. doi:10.1074/jbc.M110.203588
- Owens RA, Hammel S, Sheridan KJ, Jones GW, Doyle S (2014) A proteomic approach to investigating gene cluster expression and secondary metabolite functionality in *Aspergillus fumigatus*. PLoS One 9:e106942. doi: 10.1371/journal.pone.0106942
- Penninckx MJ (2002) An overview on glutathione in *Saccharomyces* versus non-conventional yeasts. FEMS Yeast Res 2:295–305
- Rabilloud T, Vaezzadeh AR, Potier N (2009) Power and limitations of electrophoretic. Mass Spectrom Rev 28:816–843. doi:10.1002/mas
- Reverberi M, Fabbri AA, Zjalic S, Ricelli A, Punelli F, Fanelli C (2005) Antioxidant enzymes stimulation in *Aspergillus parasiticus* by *Lentinula edodes* inhibits aflatoxin production. Appl Microbiol Biotechnol 69:207–215. doi:10.1007/s00253-005-1979-1
- Rodríguez-Martín A, Acosta R, Liddell S, Núñez F, Benito MJ, Asensio MA (2010) Characterization of the novel antifungal protein PgAFP and the encoding gene of *Penicillium chrysogenum*. Peptides 31: 541–547. doi:10.1016/j.peptides.2009.11.002
- Saxena M, Mukerji KG, Raj HG (1988) Positive correlation exists between glutathione S-transferase activity and aflatoxin formation in *Aspergillus flavus*. Biochem J 254:567–570
- Shevchenko A, Tomas H, Havlis J, Olsen JV, Mann M (2006) In-gel digestion for mass spectrometric characterization of proteins and proteomes. Nat Protoc 1:2856–2860. doi:10.1038/nprot.2006.468
- Slater AFG, Stefan C, Nobel I, Van den Dobbelaars DJ, Orrenius S (1995) Signalling mechanisms and oxidative stress in apoptosis. Toxicol Lett 82(83):149–153
- Squier TC (2001) Oxidative stress and protein aggregation during biological aging. Exp Gerontol 36:1539–1550
- Theis T, Wedde M, Meyer V, Stahl U (2003) The antifungal protein from *Aspergillus giganteus* causes membrane permeabilization. Antimicrob Agents Chemother 47:588–593. doi:10.1128/AAC.47.2.588
- Theis T, Marx F, Salvenmoser W, Stahl U, Meyer V (2005) New insights into the target site and mode of action of the antifungal protein of *Aspergillus giganteus*. Res Microbiol 156:47–56. doi:10.1016/j.resmic.2004.08.006
- Thevisen K, Ghazi A, De Samblanx GW, Brownlee C, Osborn RW, Broekaert WF (1996) Fungal membrane responses induced by plant defensins and thionins. J Biol Chem 271: 15018–15025
- Thevisen K, Terras FR, Broekaert WF (1999) Permeabilization of fungal membranes by plant defensins inhibits fungal growth. Appl Environ Microbiol 65:5451–5458
- Yu J, Chang P, Ehrlich KC, Cary JW, Bhatnagar D, Cleveland TE, Payne GA, Linz JE, Woloshuk CP, Bennett W, Bennett JW (2004) Clustered pathway genes in aflatoxin biosynthesis. Appl Environ Microbiol 70:1253–1262. doi:10.1128/AEM.70.3.1253

Journal: **Applied Microbiology and Biotechnology**

Supplementary Information

Impact of the antifungal protein PgAFP from *Pencillium chrysogenum* on the protein profile in *Aspergillus flavus*

Josué Delgado,^a Rebecca A. Owens,^b Sean Doyle,^b Miguel A. Asensio^a and Félix Núñez.^a

^a Food Hygiene and Safety, Institute of Meat Products, University of Extremadura, Cáceres, Spain.

^b Department of Biology, Maynooth University, Maynooth, Co. Kildare, Ireland.

Corresponding author:

Miguel A. Asensio

masensio@unex.es, Tel.: +34 927 257124; Fax: +34 927 257110.

Supplementary Table S1. Data on proteins obtained from label-free proteomics from *A. flavus* treated with 10 µg/ml PgAFP and untreated control.

Table with columns: A. Total data, Log2 LFQ intensity A. flavus Control 1, Log2 LFQ intensity A. flavus Control 2, Log2 LFQ intensity A. flavus Control 3, Log2 LFQ intensity A. flavus Treated 1, Log2 LFQ intensity A. flavus Treated 2, Log2 LFQ intensity A. flavus Treated 3, PEP, Intensity, Peptides, Razor + unique peptides, Unique peptides, Sequence coverage [%], Mol. weight [kDa], Log2 (Mean), Log2 (Mean A. flavus Control), Log2 (Mean A. flavus Treated), Valid values, Valid values A. flavus Control, Valid values A. flavus Treated, Protein IDs, Majority protein IDs, Proteins, Gene ID (ORF), Protein Function. The table lists 556 protein entries with their corresponding data across the columns.

Supplementary Table S1. Data on proteins obtained from label-free proteomics from *A. flavus* treated with 10 µg/ml PgAFP and untreated control.

A. Total data																							
Log2 LFQ intensity <i>A. flavus</i> Control 1	Log2 LFQ intensity <i>A. flavus</i> Control 2	Log2 LFQ intensity <i>A. flavus</i> Control 3	Log2 LFQ intensity <i>A. flavus</i> Treated 1	Log2 LFQ intensity <i>A. flavus</i> Treated 2	Log2 LFQ intensity <i>A. flavus</i> Treated 3	PEP	Intensity	Peptides	Razor + unique peptides	Unique peptides	Sequence coverage [%]	Mol. weight [kDa]	Log2 (Mean)	Log2 (Mean A. <i>flavus</i> Control)	Log2 (Mean A. <i>flavus</i> Treated)	Valid values	Valid values A. <i>flavus</i> Control	Valid values A. <i>flavus</i> Treated	Protein IDs	Majority protein IDs	Proteins	Gene ID (ORF)	Protein Function
29.7322	29.8975	29.6229	29.3302	30.2442	29.9366	0	9003400000	36	36	36	48.7	147.49	29.794	29.7509	29.837	6	3	3	B8NQA1	B8NQA1	1	AFLA_004920	Phosphoribosylformylglycinamide synthase
32.1627	32.5732	32.338	33.2	32.5726	32.8781	0	7773900000	37	37	37	82.7	57.288	32.6207	32.358	32.8835	6	3	3	B8MZQ0	B8MZQ0	1	AFLA_085400	Phosphoglycerate mutase, 2,3-bisphosphoglycerate-independent
33.9045	33.7489	33.9995	34.0502	33.8966	33.5411	0	1.8309E+11	37	37	37	64.6	74.803	33.8568	33.8843	33.8293	6	3	3	B8N4T2	B8N4T2	1	AFLA_017910	Transketolase
29.8283	30.05	29.4194	28.6938	29.9098	29.9054	0	8515300000	38	38	38	50	124.24	29.6345	29.7659	29.503	6	3	3	B8N4R2	B8N4R2	1	AFLA_017710	Isoleucyl-tRNA synthetase ,cytoplasmic
31.4931	30.9698	31.1742	29.8247	30.1413	30.4402	0	17011000000	38	38	38	42.2	131.2	30.6739	31.2124	30.1354	6	3	3	B8N9R6	B8N9R6	1	AFLA_112120	Pyruvate carboxylase
31.4198	31.5297	31.1396	31.2758	30.9437	31.2847	0	26177000000	38	38	38	56.5	116.05	31.2655	31.363	31.1681	6	3	3	B8NCU9	B8NCU9	1	AFLA_041840	Glycine dehydrogenase
33.4995	33.6191	33.2363	33.4024	33.5662	33.975	0	1.4977E+11	38	38	38	44.2	96.549	33.5497	33.4516	33.6478	6	3	3	B8NYQ1	B8NYQ1	1	AFLA_012200	Hsp70 chaperone (HscA), putative
29.6844	29.3089	29.725	29.4625	29.3286	28.9754	0	86101000000	39	39	39	46.3	134.5	29.4141	29.5728	29.2555	6	3	3	B8NZ23	B8NZ23	1	AFLA_025170	A-pheromone processing metalloproteinase Ste23
34.0112	34.0645	33.8435	34.3849	34.4799	34.3065	0	2.1721E+11	39	39	39	65.1	69.704	34.1818	33.9731	34.3905	6	3	3	B8NSB0	B8NSB0	1	AFLA_022380	Molecular chaperone Hsp70
31.5545	31.1482	31.5804	31.3683	31.1436	30.9415	0	30946000000	40	40	40	73.7	57.904	31.2894	31.4277	31.1511	6	3	3	B8NQ22	B8NQ22	1	AFLA_086620	Glucose-6-phosphate 1-dehydrogenase
30.6184	30.6472	30.7379	29.8915	29.7847	30.1399	0	12130000000	40	40	40	47.4	126.92	30.3033	30.6678	29.9387	6	3	3	B8N248	B8N248	1	AFLA_034420	Leucyl-tRNA synthetase
29.0453	29.3963	28.9941	28.0798	28.6054	28.7521	8.99E-181	42043000000	41	40	40	21.5	279.52	28.8122	29.1452	28.4791	6	3	3	B8NSV0	B8NSV0	1	AFLA_108960	Bifunctional pyrimidine biosynthesis protein (PyrABCN), putative
31.1146	31.1361	30.9873	30.4746	30.6031	30.7728	0	24412000000	41	41	41	58.9	114.85	30.8481	31.0793	30.6168	6	3	3	B8NG60	B8NG60	1	AFLA_015230	Poly(A)- RNA transport protein (UbaA), putative
30.253	30.1834	30.4308	30.9096	30.6262	30.2289	0	16046000000	41	41	41	64.3	79.759	30.4387	30.2891	30.5883	6	3	3	B8NGS8	B8NGS8	1	AFLA_137960	Arginyl-tRNA synthetase
31.7007	31.2455	31.8012	31.657	31.7632	31.2767	0	38543000000	41	41	41	55.5	99.049	31.574	31.5825	31.5656	6	3	3	B8NRE7	B8NRE7	1	AFLA_007140	Aminopeptidase, putative
32.2183	32.4268	32.4332	33.3307	32.9836	32.7544	0	74761000000	42	42	42	78.6	62.213	32.6912	32.3594	33.0229	6	3	3	B8NBK0	B8NBK0	1	AFLA_045750	Antigenic mitochondrial protein HSP60, putative
30.3686	30.4978	30.5495	30.8334	30.3644	30.163	0	14777000000	42	42	42	38.9	131.45	30.4628	30.472	30.4536	6	3	3	B8NP45	B8NP45	1	AFLA_128280	M protein repeat protein
30.3679	30.8961	30.4185	29.7857	31.4549	31.4347	0	27929000000	44	44	44	65.2	90.553	30.7263	30.5608	30.8918	6	3	3	B8NQU3	B8NQU3	1	AFLA_002370	Cell division control protein Cdc48
29.5729	29.4736	29.5086	28.403	29.1482	28.9513	0	61572000000	45	45	45	32.1	233.2	29.1763	29.5184	28.8342	6	3	3	B8NSA6	B8NSA6	1	AFLA_022340	Glutamate synthase Glt1, putative
32.381	32.3648	32.4895	33.0522	32.9699	32.6248	0	64800000000	45	45	45	64.7	79.792	32.6471	32.4118	32.8823	6	3	3	B8NL13	B8NL13	1	AFLA_095970	Hsp70 chaperone Hsp88
32.9475	32.907	32.7759	31.8417	32.9248	32.8286	0	92218000000	46	46	46	71.6	85.596	32.7043	32.8768	32.5317	6	3	3	B8N211	B8N211	1	AFLA_034050	Mitochondrial aconitate hydratase, putative
33.0993	32.7139	33.0851	32.9086	32.8598	32.461	0	95074000000	48	48	48	57.8	106.78	32.8546	32.9661	32.7432	6	3	3	B8N9B4	B8N9B4	1	AFLA_110600	Aminopeptidase
33.3726	33.4249	33.5916	33.3654	33.3414	33.1933	0	1.0129E+11	50	50	50	62.8	79.631	33.3815	33.463	33.3	6	3	3	B8NQL4	B8NQL4	1	AFLA_006960	Molecular chaperone and allergen Mod-E/Hsp90/Hsp1
30.388	30.5115	30.7913	29.567	29.8252	30.4088	0	12390000000	52	52	52	45.7	199.56	30.2487	30.5636	29.9337	6	3	3	B8N9R7	B8N9R7	1	AFLA_112130	Clathrin heavy chain
31.0906	31.3736	30.6269	31.0646	31.6436	31.59	0	33235000000	53	53	53	60.1	129.3	31.2316	31.0304	31.4328	6	3	3	B8NB80	B8NB80	1	AFLA_044550	Carbamoyl-phosphate synthase, large subunit
29.1398	29.3639	29.2243	29.9699	29.7067	29.4168	0	90339000000	53	53	53	52.4	167.27	29.4702	29.2427	29.6978	6	3	3	B8N6M9	B8N6M9	1	AFLA_015420	Sulfite reductase, putative
34.4655	34.3765	34.0718	32.9566	33.7757	33.7585	0	1.7991E+11	55	55	55	75.6	87.163	33.9008	34.3046	33.4969	6	3	3	B8NSV1	B8NSV1	1	AFLA_112470	Cobalamin-independent methionine synthase Meth/D
34.492	34.6353	34.1843	33.6423	34.8952	34.6871	0	2.7021E+11	59	59	58	68.2	94.226	34.4227	34.4372	34.4082	6	3	3	B8NGN7	B8NGN7	1	AFLA_136640	Translation elongation factor eEF-2 subunit, putative
32.7015	33.1785	32.2671	32.0643	33.1828	33.3952	0	90854000000	62	62	62	74.4	117.9	32.7982	32.7157	32.8808	6	3	3	B8MX73	B8MX73	1	AFLA_076600	Translation elongation factor eEF-3, putative
32.4156	32.8302	32.4269	32.6239	32.725	32.3689	0	52322000000	80	80	79	56.6	204.29	32.5651	32.5576	32.5726	6	3	3	B8NL81	B8NL81	1	AFLA_089170	Fatty acid synthase alpha subunit FsaA
32.1971	32.0647	32.3483	30.5036	30.943	31.4773	0	31931000000	85	85	85	56	236.61	31.589	32.2034	30.9746	6	3	3	B8NBR1	B8NBR1	1	AFLA_046360	Acetyl-CoA carboxylase, putative
33.075	33.4761	33.0352	33.2332	33.356	32.9881	0	86246000000	99	99	99	66.4	232.14	33.1939	33.1954	33.1924	6	3	3	B8NL80	B8NL80	1	AFLA_089160	Fatty acid synthase beta subunit, putative

Supplementary Table S1. Data on proteins obtained from label-free proteomics from *A. flavus* treated with 10 µg/ml PgAFP and untreated control.

B. Quantitative results

Log2 LFQ intensity <i>A. flavus</i> Control 1	Log2 LFQ intensity <i>A. flavus</i> Control 2	Log2 LFQ intensity <i>A. flavus</i> Control 3	Log2 LFQ intensity <i>A. flavus</i> Treated 1	Log2 LFQ intensity <i>A. flavus</i> Treated 2	Log2 LFQ intensity <i>A. flavus</i> Treated 3	PEP	Intensity	Peptides	Razor + unique peptides	Unique peptides	Sequence coverage [%]	Mol. weight [kDa]	Log2 (Mean)	Log2 (Mean <i>A. flavus</i> Control)	Log2 (Mean <i>A. flavus</i> Treated)	Valid values <i>A. flavus</i> Control	Valid values <i>A. flavus</i> Treated	t-test p value	Log2 (t-test Difference)	Fold Change (Treated v Control)	Protein IDs	Majority protein IDs	Gene Name (ORF)	Protein Function
32,2693	31,7467	32,375	31,1869	31,3549	30,5972		2,91E+10	11	11	11	79	23,229	31,5883	32,1303	31,0463	6	3	0,022695	-1,084	-2,1199056	B8N419	B8N419	1 AFLA_033420	Superoxide dismutase
29,0568	29,0745	29,085	27,7126	27,8937	28,364	5,95E-33	3,37E+09	7	7	7	29,9	24,083	28,5311	29,0721	27,9901	6	3	0,005095	-1,08198	-2,1169394	B8N442	B8N442	1 AFLA_033650	GTP-binding nuclear protein Ran, putative
31,4931	30,9698	31,1742	29,8247	30,1413	30,4402		1,7E+10	38	38	38	42,2	131,2	30,6739	31,2124	30,1354	6	3	0,010012	-1,07698	-2,1096154	B8N9R6	B8N9R6	1 AFLA_112120	Pyruvate carboxylase
30,9782	30,4755	31,003	29,8387	29,6012	29,7963		1,01E+10	23	23	23	58,6	57,696	30,2822	30,8189	29,7454	6	3	0,004544	-1,07349	-2,1045182	B8NUL4	B8NUL4	1 AFLA_100670	ATP sulphurylase
27,7813	27,7267	28,0254	26,9677	26,7112	26,6381	1,24E-75	1,17E+09	7	7	7	18,5	64,711	27,3084	27,8445	26,7724	6	3	0,00139	-1,07211	-2,1025061	B8NA09	B8NA09	1 AFLA_113050	Asparagine synthetase
25,4197	26,2736	25,9741	24,5942	24,8852	25,0204	3,64E-10	5,6E+08	4	4	4	23,4	25,648	25,3612	25,8891	24,8333	6	3	0,01958	-1,05587	-2,0789715	B8MX61	B8MX61	1 AFLA_076480	Glutathione S-transferase, putative
26,3346	26,6938	26,9119	26,0062	24,9284	25,839	3,98E-117	9,58E+08	8	8	8	35,4	33,553	26,119	26,6468	25,5912	6	3	0,048005	-1,05561	-2,0785969	B8NG94	B8NG94	1 AFLA_134340	BAR domain protein
31,5453	30,6777	31,2887	30,1156	30,389	29,8506		3,44E+10	13	13	13	60,6	32,512	30,6445	31,1706	30,1184	6	3	0,024898	-1,05219	-2,0736753	B8NE88	B8NE88	1 AFLA_059970	Short-chain dehydrogenase, putative
28,5363	28,5593	28,6057	27,5927	27,3424	27,6235	3,57E-188	2,51E+09	11	10	10	32,5	59,145	28,0433	28,5671	27,5195	6	3	0,00033	-1,04755	-2,0670166	B8MX20	B8MX20	1 AFLA_076070	Septin AspB
26,761	26,1014	26,5021	25,4209	25,6554	25,1717	5,77E-45	7,95E+08	6	6	6	15,7	66,631	25,9354	26,4548	25,416	6	3	0,0119	-1,03884	-2,054575	B8NLP8	B8NLP8	1 AFLA_092640	Alkaline phosphatase
24,9992	25,025	25,0904	23,567	23,9843	24,4912	5,86E-42	1,3E+09	7	7	7	23,6	27,221	24,5262	25,0382	24,0142	6	3	0,018899	-1,02401	-2,0335634	B8N370	B8N370	1 AFLA_026830	40S ribosomal protein S6
27,6898	27,4631	27,7298	27,0419	26,5399	26,2644	6,19E-73	1,72E+09	10	10	10	21,6	78,809	27,1215	27,6276	26,6154	6	3	0,01394	-1,01217	-2,0169426	B8MY11	B8MY11	1 AFLA_079480	Oligopeptidase family protein

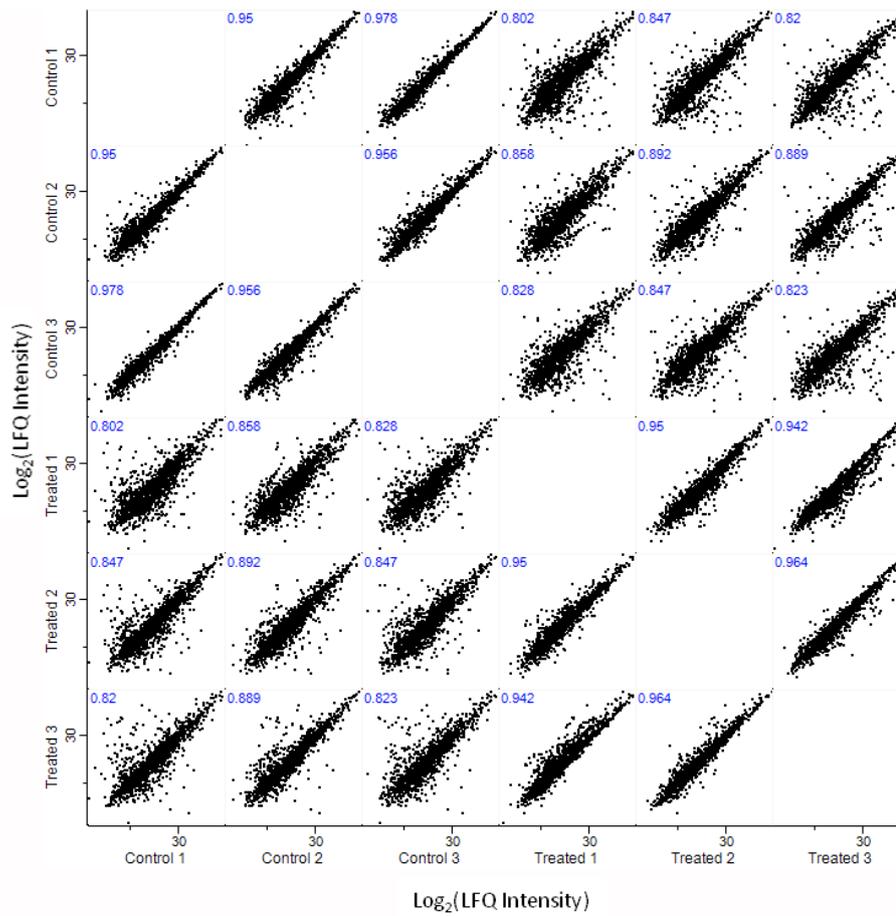
Supplementary Table S2. Data on proteins whose relative abundance was affected by 10 µg/ml PgAFP in *A. flavus* reaching over 1.5 fold change in 2D-PAGE.

Protein name	p-value	Fold Change	% coverage	Unique peptides	Score	tMr (Da)	Protein accession (GI)	Gene
Enolase/allergen Asp F 22	0.00003141	↑3.5	15	4	177	47434	238488036	AFLA_037480
Molecular chaperone and allergen Mod-E/Hsp90/Hsp1	0.000003077	↑3.3	19	10	491	79640	238503321	AFLA_006960
Poly(A)+ RNA transport protein (UbaA), putative	0.001	↑2.3	14	8	340	115238	238488611	AFLA_015230
60S acidic ribosomal protein P0	0.0005509	↑2.2	40	7	382	33420	238486572	AFLA_030140
Translation elongation factor EF-2 subunit, putative	0.0001213	↑1.9	12	8	501	94681	238496883	AFLA_136640
Hsp70 chaperone (HscA), putative	0.004	↑1.7	9	3	178	96833	238508549	AFLA_012200
Hsp70 chaperone (HscA), putative	0.005	↑1.7	19	12	521	96833	238508549	AFLA_012200
Mitochondrial-processing peptidase subunit beta	0.0008611	↑1.7	31	13	866	53195	238488967	AFLA_017010
Cys-Gly metalloprotease dug1	0.002	↑1.7	26	8	395	53164	238506124	AFLA_103940
Glutathione synthetase	0.003	↑1.6	13	3	134	57079	238494330	AFLA_056570
Pyruvate decarboxylase	0.005	↑1.6	65	22	1260	63457	238486858	AFLA_031570
Phosphoglucomutase	0.006	↑1.6	8	4	237	62379	238497666	AFLA_065080
Conserved hypothetical protein	0.003	↑1.5	7	3	148	59673	238489765	AFLA_021000
L-xylulose reductase	0.0001245	↓3.6	16	3	199	31595	238505028	AFLA_098700
Conserved hypothetical protein	0.0002845	↓2.4	5	2	109	59673	238489765	AFLA_021000
Actin Act1	0.000061	↓2.2	39	11	562	41910	238494062	AFLA_055230
Septin AspA, putative	0.0003508	↓2	8	2	118	43393	238499547	AFLA_091880
Short-chain dehydrogenase, putative	0.001	↓2	37	7	322	32620	238495010	AFLA_059970
Metalloprotease MepB	0.005	↓1.9	12	4	167	81812	238482735	AFLA_076890
Pyruvate carboxylase	0.006	↓1.9	3	4	190	131917	238491688	AFLA_112120
Elongation factor 3	0.045	↓1.8	23	16	857	118573	238482677	AFLA_076600
Acetate--CoA ligase	0.006	↓1.7	6	3	98	79217	238485958	AFLA_027070
Aspartyl-tRNA synthetase, cytoplasmic	0.008	↓1.7	17	6	349	62180	238496255	AFLA_133490
Pyruvate carboxylase	0.036	↓1.7	3	3	143	131917	238491688	AFLA_112120
Pyruvate carboxylase	0.032	↓1.7	9	7	313	131917	238491688	AFLA_112120
Autophagic serine protease Alp2	0.021	↓1.6	8	2	104	52539	238505092	AFLA_099020

Supplementary Table S3: Summary of Pearson correlation values for label-free quantitative analysis of *A. flavus* response to PgAFP treatment, as displayed in supplementary Fig. S1.

Pearson Correlation Values	Control¹	Treated²	Control v Treated³
Number of values	3	3	9
Mean	0.9613	0.952	0.8451
Std. Deviation	0.01474	0.01114	0.03076
Std. Error	0.008511	0.006429	0.01025

¹Each biological replicate from the control group, cross-compared. ²Each biological replicate from the PgAFP treated group, cross-compared. ³Each biological replicate from the PgAFP treated group compared to each biological replicate from the control group.



Supplementary Fig. S1: Multi-scatter plot demonstrating correlation between all samples included in LFQ proteomics analyses. Blue values included in each box indicate respective Pearson correlation values.

IV.4. Estudio del mecanismo de resistencia frente a PgAFP en mohos

Increased chitin biosynthesis contributes to the resistance of *Penicillium polonicum* against the antifungal protein PgAFP

Increased chitin biosynthesis contributes to the resistance of *Penicillium polonicum* against the antifungal protein PgAFP

Josué Delgado¹ · Rebecca A. Owens² · Sean Doyle² · Miguel A. Asensio¹ · Félix Núñez¹

Received: 7 July 2015 / Revised: 23 August 2015 / Accepted: 5 September 2015
© Springer-Verlag Berlin Heidelberg 2015

Abstract Antifungal proteins from molds have been proposed as a valuable tool against unwanted molds, but the resistance of some fungi limits their use. Resistance to antimicrobial peptides has been suggested to be due to lack of interaction with the mold or to a successful response. The antifungal protein PgAFP produced by *Penicillium chrysogenum* inhibits the growth of various ascomycetes, but not *Penicillium polonicum*. To study the basis for resistance to this antifungal protein, localization of PgAFP and metabolic, structural, and morphological changes were investigated in *P. polonicum*. PgAFP bound the outer layer of *P. polonicum* but not regenerated chitin, suggesting an interaction with specific molecules. Comparative two-dimensional gel electrophoresis (2D-PAGE) and comparative quantitative proteomics revealed changes in the relative abundance of several proteins from ribosome, spliceosome, metabolic, and biosynthesis of secondary metabolite pathways. The proteome changes and an altered permeability reveal an active reaction of *P. polonicum* to PgAFP. The successful response of the resistant mold seems to be based on the higher abundance of protein Rho GTPase Rho1 that would lead to the increased chitin deposition via cell wall integrity (CWI) signaling pathway. Thus, combined

treatment with chitinases could provide a complementary means to combat resistance to antifungal proteins.

Keywords Antifungal proteins · Proteomics · Resistance · *Penicillium polonicum* · Chitin · Cell wall integrity pathway

Introduction

The antifungal protein PgAFP produced by the strain *Penicillium chrysogenum* CECT 20922 (formerly RP42C) is within a group of small, highly basic and low molecular mass proteins (Rodríguez-Martín et al. 2010). PgAFP inhibits various pathogenic and spoilage ascomycetes of interest in foods, including strains of various *Aspergillus* spp., such as *A. carbonarius*, *A. flavus*, *A. ochraceus*, *A. fumigatus*, and *A. tubingensis*, as well as *Penicillium* spp., such as *P. commune*, *P. restrictum*, *P. nalgiovense*, and *P. chrysogenum* (Delgado et al. 2015a). However, *Penicillium polonicum* and the PgAFP-producer strain of *P. chrysogenum* were not inhibited by PgAFP.

Other antifungal proteins produced by ascomycetes are PAF from *P. chrysogenum* Q176 (Marx et al. 1995), Pc-Arctin from *P. chrysogenum* A096 (Chen et al. 2013), BP from *Penicillium brevicompactum* (Seibold et al. 2011), AFP and AFP_{NN5353} from *Aspergillus giganteus* (Nakaya et al. 1990; Binder et al. 2011), Anaafp from *Aspergillus niger* (Gun Lee et al. 1999), AcAFP and AcAMP from *Aspergillus clavatus* (Skouri-Gargouri and Gargouri 2008; Hajji et al. 2010), FPAP from *Fusarium polyphialidicum* (Galgóczy et al. 2013b), and NFAP from *Neosartorya fischeri* (Kovács et al. 2011). Mechanisms of action of antifungal proteins from molds have been described as multifactorial, where membrane permeabilization, changes in actin distribution, chitin biosynthesis inhibition, destabilization of cell wall,

Electronic supplementary material The online version of this article (doi:10.1007/s00253-015-7020-4) contains supplementary material, which is available to authorized users.

✉ Miguel A. Asensio
masensio@unex.es

¹ Food Hygiene and Safety, Institute of Meat Products, University of Extremadura, Cáceres, Spain

² Department of Biology, Maynooth University, Maynooth, Co., Kildare, Ireland

and oxidative stress lead to apoptosis (Leiter et al. 2005; Moreno et al. 2006; Hagen et al. 2007; Binder et al. 2010; Virágh et al. 2015; Delgado et al. 2015b). AFP binds chitin, inhibits chitin biosynthesis, permeabilizes the cell membrane, and penetrates into the cell and binds nucleic acids (Liu et al. 2002; Moreno et al. 2006; Hagen et al. 2007), and AcAFP also binds chitin altering cell wall (Skouri-Gargouri et al. 2009), whereas PAF, NFAP, and PgAFP lead to apoptosis mediated by G-protein signaling (Binder et al. 2010, 2015; Virágh et al. 2015; Delgado et al. 2015b). Both PAF and NFAP activate the cAMP/protein kinase A pathway via G-protein signaling (Leiter et al. 2005; Virágh et al. 2015) and PgAFP provoked a lower amount G-protein subunit β CpcB (Delgado et al. 2015b).

However, the defensive strategies of resistant molds are poorly described. The lack of electrostatic affinity or receptors in cell surfaces has been suggested as the cause of the resistance to antimicrobial peptides (Yeaman and Yount 2003). PgAFP does not bind to the producer strain *P. chrysogenum* CECT 20922 that withstands at least 312 $\mu\text{g/ml}$ (Delgado et al. 2015a, b). The lack of interaction between antifungal proteins and mold surface results in the absence of major metabolic responses in the resistant fungi. Another successful strategy of resistant fungi to counteract AFP is chitin synthesis stimulation (Ouedraogo et al. 2011). The latter strategy implies interaction with the resistant fungus and active metabolic response to the antifungal protein. Thus, studying the mechanisms involved in the resistance requires in-depth investigation of the metabolic response of resistant fungi to antifungal proteins.

Comparative proteomic analysis is a powerful tool to study metabolic changes at the molecular level (Kim et al. 2007). Two-dimensional gel electrophoresis (2D-PAGE) has the ability to separate complete proteins including those with post-translational modifications, but only a small percentage of the whole proteome is revealed (Görg et al. 2009). On the other hand, comparative quantitative proteomics is able to identify proteins not detectable by 2D-PAGE. These two techniques have been used to complementarily evaluate the effect of PgAFP on the proteins involved in signaling pathways and selecting adequate tests to study the metabolic response in molds (Delgado et al. 2015b). In addition, localization of the antifungal protein in non-sensitive molds can give valuable information on the possible interaction at the surface or inside the cell. Given that antifungal proteins provoke oxidative stress leading to apoptosis in sensitive mold, knowing the extent of these two phenomena in resistant molds would contribute to clarify the defense mechanism.

To study the effect of PgAFP on resistant molds, *P. polonicum* was chosen because it was the only resistant ascomycete known, apart from the PgAFP-producer *P. chrysogenum* CECT 20922 (Delgado et al. 2015a). *A. niger* has been used as sensitive control with various

antifungal proteins (Kaiserer et al. 2003; Hagen et al. 2007; Kovács et al. 2011). *A. tubingenensis* CECT 20932, formerly *A. niger* An261, has been used in the present work as sensitive control because it is the closest species to *A. niger* known to be sensitive to PgAFP (Delgado et al. 2015a).

The aim of this work was to investigate the effect of PgAFP on the proteome profile and selected characteristics to disclose the resistance response of *P. polonicum*. Localization of PgAFP was studied for a better understanding of the interaction with *P. polonicum*. This knowledge would allow designing new strategies to maximize the inhibition effect and spectra of PgAFP in molds.

Material and methods

Strains

In vitro tests were carried out with three molds isolated from dry-cured ham available from the Spanish Type Culture Collection (CECT, Valencia, Spain): *P. chrysogenum* CECT 20922, *P. polonicum* CECT 20933, and *A. tubingenensis* CECT 20932.

Purification of PgAFP

PgAFP was obtained from *P. chrysogenum* CECT 20922 grown in potato dextrose broth (PDB, Scharlab, Barcelona, Spain) pH 4.5, at 25 °C for 21 days, as described previously (Acosta et al. 2009). To get cell-free medium, mycelium was removed by filtering through Miracloth (Calbiochem, Darmstadt, Germany) and the culture medium was filtered through a nitrocellulose 0.22 μm pore size (Sartorius, Goettingen, Germany). Cell-free media were applied to an ÄKTA FPLC with a cationic exchange column HiTrap SP HP (Amersham Biosciences, Uppsala, Sweden) with 20 mM sodium acetate, pH 4.5. Adsorbed proteins were eluted with 20 mM sodium acetate buffer (pH 4.5) containing 1 M NaCl and detected at 214 nm. The fraction containing PgAFP protein was then gel filtered on a HiLoad 26/60 Superdex 75 column for FPLC (Amersham Biosciences, Uppsala, Sweden) using 50 mM sodium phosphate buffer, pH 7 containing 0.15 M NaCl as elution buffer. PgAFP concentration in a pooled stock solution was measured by Lowry method (Lowry et al. 1951), sterilized through 0.22 μm acetate cellulose filters (Fisher Scientific), and stored at -20 °C until use.

Effect of PgAFP on mold growth

As a preliminary test, to confirm the known effect of PgAFP on growth of both sensitive and resistant molds in malt extract broth (Delgado et al. 2015a), *P. polonicum* and *A. tubingenensis*

were grown in PDB treated with PgAFP in the whole range of concentrations used in this work (0 to 75 µg/ml) for 96 h.

Proteomics

To obtain the protein extracts, *P. polonicum* CECT 20933 was cultured in triplicate in 50 ml of PDB, at 25 °C with continuous shaking at 200 rpm in either presence (10 µg/ml) or absence of PgAFP. Mycelia were harvested, filtered, washed, and lysed as previously described (Carberry et al. 2006). Mycelial lysates were centrifuged to remove cell debris and the subsequent supernatant precipitated with TCA/acetone (Carpentier et al. 2005). The following two proteomic analyses were carried out from these precipitated lysates, similar to the procedure described by Delgado et al. (2015b).

Two-dimensional electrophoresis For protein separation by 2D-PAGE, resuspended extracts containing 250 µg of protein were loaded onto Immobiline Dry strips (IPG strip; Amersham Biosciences) in the pH range 4–7, followed by electrofocusing and electrophoresis as described previously (Carberry et al. 2006). Gels obtained from 3 biological replicates and 2 technical replicates per treatment were stained and analyzed using Progenesis™ SameSpot software (TotalLab, Newcastle, UK) as previously described (O’Keeffe et al. 2013; Collins et al. 2013; Owens et al. 2014). Spot intensities were normalized in Progenesis SameSpots software (Delgado et al. 2015b). Protein spots showing differences ($p < 0.05$, fold change ≥ 1.5) were excised, destained, and in-gel trypsin digested (Shevchenko et al. 2007). Then, samples were sonicated and the digested supernatant was dried, resuspended in 0.1 % formic acid, and filtered through 0.22 µm cellulose spin-filters according to Delgado et al. (2015b).

The samples were loaded onto a Zorbax 300 SB C-18 Nano-HPLC Chip and analyzed by a 6340 Model Ion Trap LC-Mass Spectrometer (Agilent Technologies, Dublin, Ireland) using electrospray ionization. The eluted peptides were ionized and analyzed by mass spectrometry. MSⁿ analysis was carried out on the three most abundant peptide precursor ions at each time point, as selected automatically by the mass spectrometer. MASCOT MS/MS Ion search, NCBI (National Centre for Biotechnology Information, www.ncbi.nlm.nih.gov/guide/proteins/) database and KEGG (Kyoto Encyclopedia of Genes and Genome, www.genome.jp/kegg/) were used for protein identification and function, also BLAST® protein was employed to find orthologous proteins.

Label-free proteomics Proteins precipitated from three biological replicates were resuspended in 8 M urea, dithiothreitol reduced and iodoacetic acid alkylated (Collins et al. 2013), and trypsin digested. Digested samples were desalted using C18 ZipTips® (Millipore, Darmstadt, Germany). One microgram from each digest was analyzed via a Thermo Scientific

Q-Exactive mass spectrometer coupled to a Dionex RSLCnano (Thermo Scientific, Waltham, MA, USA). Data was collected using a Top15 method for MS/MS scans (Dolan et al. 2014; O’Keeffe et al. 2014). Comparative proteome abundance and data analysis was performed using MaxQuant software (Version 1.3.0.5; www.maxquant.org/downloads.htm) (Cox and Mann 2008), with Andromeda used for database searching and Perseus (Version 1.4.1.3) used to organize the data, as per Delgado et al. (2015b). Data were searched against a *P. chrysogenum* database from Uniprot (www.uniprot.org; March 2014). In the absence of sequenced *P. polonicum* or any other species from Section *Fasciculata* (Houbraken and Samson 2011), *P. chrysogenum* also from subgenus *Penicillium* was chosen for comparison. Quantitative analysis was performed using a *t* test. Due to the high sensitivity and larger dynamic range of the gel-free proteomics analyses, only proteins with a *p* value < 0.05 and fold change ≥ 2 were included in the quantitative results (Dolan et al. 2014; O’Keeffe et al. 2014). Qualitative analysis was also performed, to detect proteins that were found in at least 2 replicates of a particular sample, but undetectable in the comparison sample. Blast2GO analysis was utilized to further elucidate putative functions of proteins identified with abundance changes (Conesa et al. 2005).

Hyphal morphology

P. polonicum and *A. tubingensis* were grown on tubes containing 300 µl of PDB at 25 °C for 24 h in either the presence (75 µg/ml) or absence of PgAFP. Mycelia were collected by centrifugation and observed on a microscope Eclipse E200 equipped with a digital camera DS-Fi2 (Nikon, Tokyo, Japan).

Metabolic tests

To study the response to PgAFP, various metabolic tests were performed as described previously (Delgado et al. 2015b). For this, the resistant *P. polonicum* (c.a. 5×10^5 conidia per ml) was cultured in PDB at 25 °C for 24 h in static conditions with and without PgAFP. To rule out even potential weak effects, the highest concentration of 75 µg/ml PgAFP was used. Additionally, to study the effect on membrane permeability throughout a wide concentration range of PgAFP (i.e., 75, 37.5, 18.75, 9.38, 4.69, 2.34, 1.17, and 0 µg/ml) were assayed.

To test membrane permeability, cultures in microtiter plates were supplemented with SYTOX Green (Molecular Probes, Eugene, OR, USA) at a final concentration of 0.2 µM. The fluorescence emitted was measured at 10, 30, and 210 min.

Metabolic activity was assessed by FUN-1 staining. Grown mycelia was washed with 10 mM HEPES (pH 7.5) before staining with 100 µl FUN-1 (Molecular Probes, Eugene, OR, USA) for 30 min at 25 °C as described previously (Kaiserer et al. 2003). Stained hyphae were visualized and

photographed by fluorescence microscopy. Induction of reactive oxygen species (ROS) production was evaluated using 20 μM 2', 7' dichlorofluorescein diacetate (Molecular Probes, Eugene, OR, USA) according to Kaiserer et al. (2003) and observed by fluorescence microscopy.

Membrane integrity was assessed by the acridine orange/ethidium bromide (AO/EB) double staining. Hyphae were stained with 4 $\mu\text{g}/\text{ml}$ of AO/EB (Sigma-Aldrich, St. Louis, MO, USA), incubated for 30 min, washed, and observed by fluorescence microscopy.

To distinguish between necrotic, late apoptotic, and viable cells, the Apoptosis Detection Kit (Sigma-Aldrich, St. Louis, MO, USA), composed by Annexin V-fluorescein isothiocyanate/propidium iodide (AnV-FITC/PI), was used according to manufacturer's instructions.

For each of these metabolic tests, the sensitive *A. tubingensis* was used as a positive control to confirm the effect of PgAFP in the various assays.

Chitin staining

Conidia of *P. polonicum* were inoculated on 10 ml PDB in a Petri dish containing a coverglass and incubated in the presence (75 $\mu\text{g}/\text{ml}$) and absence of PgAFP at 25 °C for 24 h. Mycelium was fixed, stained for 5 min with fluorescent brightener 28 (Sigma-Aldrich, St. Louis, MO, USA), and then washed, to visualize chitin (Harris et al. 1994) in a fluorescence microscope with an excitation wavelength of 387/11 nm.

Effect of PgAFP combined with chitinase on *P. polonicum* growth

Four different batches were prepared by pouring the reagents onto 15 ml potato dextrose agar plates made with PDB (Scharlab, Barcelona, Spain) and 20 g/l bacteriological agar (Scharlab, Barcelona) as follows: (a) 2.5 ml of 600 $\mu\text{g}/\text{ml}$ PgAFP in phosphate elution buffer and 0.1 ml PBS, (b) 2.5 ml of phosphate elution buffer and 0.1 ml of ≥ 60 units/ml chitinase from *Streptomyces griseus* (Sigma-Aldrich, St. Louis, MO, USA) in PBS, (c) and 2.5 ml of 600 $\mu\text{g}/\text{ml}$ PgAFP in phosphate elution buffer and 0.1 ml of ≥ 60 units/ml chitinase from *S. griseus* (Sigma-Aldrich, St. Louis, MO, USA) in PBS, and (d) 2.5 ml of phosphate elution buffer and 0.1 ml PBS as control samples. Every plate was surface three-point inoculated with 10 μl of a suspension containing 10^4 conidia and incubated at 25 °C for 168 h. The diameter of the colonies were measured every 24 h. To elucidate whether the combined treatment of PgAFP and chitinase has an additive or synergistic effect, the expected efficacy of this combination was determined by the Abbott formula and the interaction ratio as described by Moreno et al. (2003). Interaction ratios between 0.5 and 1.5 are considered to be additive

interactions, and ratios over 1.5 are considered to be synergistic interactions.

Chitin-binding ability of PgAFP

Regenerated chitin was prepared as previously described (Souza et al. 2009), using chitin powder from crab shells (Sigma-Aldrich, St. Louis, MO, USA) added to concentrated HCl with vigorous stirring, filtered, and precipitated with ethanol 95 %. The precipitate was filtered and washed with water until neutral pH. Chitin-PgAFP binding assay was carried out as described by Liu et al. (2002). Briefly, three different amounts of PgAFP were mixed with 4 mg of regenerated chitin in a 0.5 ml 0.1 M Tris-HCl pH 7.4, 0.15 M NaCl buffer, incubated in ice for 1 h with stirring every 15 min. After incubation, samples were centrifuged and the quantity of protein contained in the supernatant was measured by the method described by Lowry (Lowry et al. 1951).

PgAFP localization

PgAFP was labeled by DareBio S.L. (Elche, Spain) as described previously (Delgado et al. 2015b). For this, 100 μl of 20 mM fluorescein isothiocyanate (FITC; Anaspec, Fremont, CA, USA) in dimethylsulfoxide was added to 4 ml of PgAFP (369 $\mu\text{g}/\text{ml}$) and left for 8 h at room temperature in the dark. Then, 100 μl of 0.8 M Tris-HCl pH 8 were added and dialyzed against PBS.

P. polonicum and *A. tubingensis* were grown in PDB in the presence of 20 $\mu\text{g}/\text{ml}$ PgAFP-FITC for 24 h at 25 °C. Hyphae were washed twice with PBS and visualized by fluorescence microscopy with excitation wavelength of 482/35 nm.

Statistical analysis

Statistical analyses were performed with the IBM SPSS v.22 (www-03.ibm.com/software/products/es/spss-stats-standard). Growth inhibition and membrane permeability data were tested for normality (Kolmogorov–Smirnov with Lilliefors correction) and homoscedasticity (Levene's test). Given that these data were non-normally distributed, mean values were compared using non-parametric Kruskal–Wallis test. To compare treatments in pairs, Mann–Whitney *U* test was applied ($p < 0.05$).

Results

As expected, PgAFP showed no effect ($p > 0.05$) on *P. polonicum* grown in PDB in the whole range of

concentrations tested. *A. tubingensis* growth was affected ($p < 0.05$) from 4.7 $\mu\text{g/ml}$ PgAFP at 48 h (data not shown).

Effect on proteome

2D-PAGE comparative proteomic analysis, in the presence or absence of 10 $\mu\text{g/ml}$ of PgAFP, showed 37 spots with differences ($p < 0.05$) over 1.5-fold change in relative abundance between treated and untreated *P. polonicum*. The abundance in treated samples was higher (1.5–3-fold) in 9 spots and lower (1.5–4.1-fold) in the remaining 27 proteins, including 2 spots from separate isoforms (Table S1 in the Supplementary Material).

Comparative label-free quantitative proteomic analysis showed a total of 918 proteins from *P. polonicum*, 93 of them displayed altered relative abundance ($p < 0.05$) over twofold change with PgAFP treatment (Table S2 in the Supplementary Material). Thirty eight proteins were found in higher amounts (2–12.4-fold) in treated samples, 19 were only detected in treated samples, 25 were obtained in lower amounts (2–663-fold) following treatment, and 11 were only detected in non-treated samples (Table S2 in the Supplementary Material).

Eight of the nine proteins found in higher amounts in treated samples by 2D-PAGE were also detected by label-free proteomic analyses, with six of them showing similar increases in both methods (Tables S1 and S2 in the Supplementary Material). Also 26 of the 27 proteins found in lower relative abundance in treated *P. polonicum* by 2D-PAGE were also detected by label-free proteomics. However, only 16 of them were also detected at a lower relative abundance in the latter.

According to KEGG pathway analysis, most of the 57 proteins from label-free proteomics with higher relative abundance or only detected in treated *P. polonicum* were ribosomal and spliceosomal proteins (39 %), or involved in biosynthesis of secondary metabolites and metabolic pathways (14 %), such as pyruvate decarboxylase, pyrimidine biosynthesis, glycerol kinase, and asparagine synthetase (Table 1). The remaining proteins with higher relative abundance or only detected in treated samples were distributed across various pathways, such as Rho GTPase Rho1 involved in MAPK signaling pathway and, interestingly, glucosamine-6-phosphate *N*-acetyltransferase involved in chitin biosynthesis. Additionally, the antifungal protein PgAFP was detected in each of the triplicate treated sample, but not in any non-treated sample. Most of the proteins found in lower quantity or only detected in non-treated samples were related to biosynthesis of secondary metabolites and metabolic pathways (33 %), including phosphoglucosmutase, and glucose 6-phosphate isomerase related to glycolysis and gluconeogenesis (Table 1). Only

limited changes in stress-related proteins, including glyceraldehyde-3-phosphate dehydrogenase (GAPDH) and heat shock proteins, were found in treated *P. polonicum* (Tables S1 and S2 in the Supplementary Material).

SYTOX green uptake

Upon PgAFP exposure up to 4.7 $\mu\text{g/ml}$, a 7 (± 3.4) % increase (\pm standard error) in fluorescence was observed in *P. polonicum* ($p < 0.05$) at 210 min after SYTOX Green addition (Fig. 1). Fluorescence at intermediate PgAFP concentrations (9.37–18.75 $\mu\text{g/ml}$) did not differ from untreated control ($p > 0.05$), while concentrations higher than 18.75 $\mu\text{g/ml}$ decreased ($p < 0.05$) permeability below the levels of untreated samples, being the fluorescence values up to 21 (± 7.1) % lower at 210 min after SYTOX Green addition. On the other hand, the sensitive *A. tubingensis* showed a high increase of permeability ($p < 0.05$) at all PgAFP concentrations assayed (Fig. 1), reaching with 9.37–18.75 $\mu\text{g/ml}$ over 110 (± 9.8 –15) % fluorescence higher than in the untreated control.

Hyphal morphology and FUN-1 staining

PgAFP exposure provoked no morphological change on either *P. polonicum* or the sensitive *A. tubingensis* (data not shown). To know whether PgAFP affects the metabolic activity, the viability was evaluated with FUN-1 using *A. tubingensis* as sensitive control. The FUN-1 metabolic staining showed red intravacuolar stains in both treated and untreated *P. polonicum* revealing no reduction in the metabolic activity (Fig. 2). Conversely, intravacuolar red stains were not observed in PgAFP-treated *A. tubingensis*, revealing a lower metabolic activity.

Chitin staining

To study the effect of PgAFP on chitin deposition on the resistant mold, the quantity of chitin was estimated by staining with fluorescent brightener 28. The observed fluorescence indicated a higher chitin deposition in the cell wall of treated than in non-treated *P. polonicum* (Fig. 3).

Effect of PgAFP-chitinase combined treatment on *P. polonicum* growth

For the whole incubation time, no statistically significant difference was found among growth of the untreated control and *P. polonicum* treated only with PgAFP (Fig. 4). Chitinase treatment reduced growth compared to control batch. Growth of *P. polonicum* treated with

Table 1 Selected proteins whose relative abundance was affected by PgAFP in *Penicillium polonicum* reaching over 2.0-fold change in label-free proteomics (LFP) analysis or 1.5-fold change in 2D-PAGE. Data are given according to four groups of metabolic pathways

Proteins involved in pathways	Fold change	Detection method
Ribosomal and spliceosomal proteins		
Pc12g05940 40s ribosomal protein s13	T	LFP
Pc13g01870 60s ribosomal protein 116	T	LFP
Pc16g04770 formin binding protein	T	LFP
Pc20g10480 small nuclear ribonucleoprotein	T	LFP
Pc22g08360 pre-mrna branch site protein p14	T	LFP
Pc20g00680 60s ribosomal protein 123	+11.16	LFP
Pc20g13260 ribosomal protein 114	+6.32	LFP
Pc13g02890 60s ribosomal protein 127	+5.32	LFP
Pc13g05540 60s ribosomal protein 118	+4.17	LFP
Pc18g04110 60s ribosomal protein 134	+4.05	LFP
Pc22g02060 60s ribosomal protein 18	+3.88	LFP
Pc21g16520 60s ribosomal protein 14	+3.83	LFP
Pc16g14740 40s ribosomal protein s22	+3.21	LFP
Pc16g09160 60s ribosomal protein 115	+3.14	LFP
Pc22g00880 40s ribosomal protein s18	+2.73	LFP
Pc21g18200 60s ribosomal protein	+2.51	LFP
Pc16g12990 60s ribosomal protein 117	+2.47	LFP
Pc13g07190 60s ribosomal protein 111	+2.32	LFP
Pc13g05920 60s ribosomal protein 17	+2.21	LFP
Pc20g03340 60s ribosomal protein 133	+2.19	LFP
Pc13g06740 60s ribosomal protein 113	+2.06	LFP
Pc20g02900 40s ribosomal protein s4	+2.02	LFP
Biosynthesis of secondary metabolites and metabolic pathway		
Pc21g21940 bifunctional pyrimidine biosynthesis protein	T	LFP
Pc22g06070 glycerol kinase	T	LFP
Pc22g17940 asparagine synthetase	T	LFP
Pc22g23800 glucosamine 6-phosphate N-acetyl transferase ^a	T	LFP
Pc21g15760 glutamyl-tRNA synthetase	+12.44	LFP
Pc20g07710 sulfate adenylyltransferase	+6.9	LFP
Pc22g07020 nitrilase	+3.49	LFP
Pc18g01490 pyruvate decarboxylase	+2.01	LFP
Phosphoglucomutase	-2	2D-PAGE
Pc16g05080 adenosylhomocysteinase	-2	LFP
Pc12g05750 d-xylulose kinase	-2.31	LFP
Pc21g04710 phospho-2-dehydro-3-deoxyheptonate aldolase	-2.52	LFP
Pc22g19440 aspartate aminotransferase	-2.58	LFP
Pc21g03190 glycerate dehydrogenase	-2.66	LFP
Pc22g02810 methylmalonate-semialdehyde dehydrogenase	-3.05	LFP
Pc22g19730 glucose-6-phosphate isomerase	-3.49	LFP
Pc15g01900 putative oligo-glucosidase	-6.9	LFP
Pc15g01880 phosphatidylglycerol specific phospholipase	-633	LFP
Pc13g03600 thiamine biosynthetic bifunctional	NT	LFP
Pc14g00170 phosphatidylglycerol specific	NT	LFP
Pc22g24860 aldehyde dehydrogenase	NT	LFP
CWI pathway		
Pc22g23800 glucosamine-6-phosphate N-acetyl transferase ^a	NT	LFP
Pc14g01930 protein Rho gtpase rho1	+9.04	LFP
Pc21g11950 UDP-N-acetylglucosamine pyrophosphorylase	-2	2D-PAGE
UDP-glucose 4-epimerase	-1.5	2D-PAGE
Gamma-actin act	-1.6	2D-PAGE

T protein only detected in treated samples, NT protein only detected in non-treated samples

^a Protein involved in more than one pathway

combined PgAFP and chitinase was the lowest ($p < 0.05$). The interaction ratios between these

antifungal compounds at 96 and 120 h incubation were 1.93 and 1.70, respectively. Thus, the slower growth in

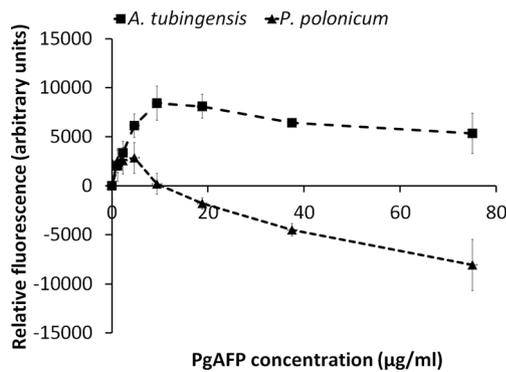


Fig. 1 SYTOX Green uptake with different concentrations of PgAFP on *P. polonicum* and *A. tubingensis* at 24 h (bars represent standard deviation of the mean)

the combined treatment is attributed to a synergistic effect of chitinase and PgAFP.

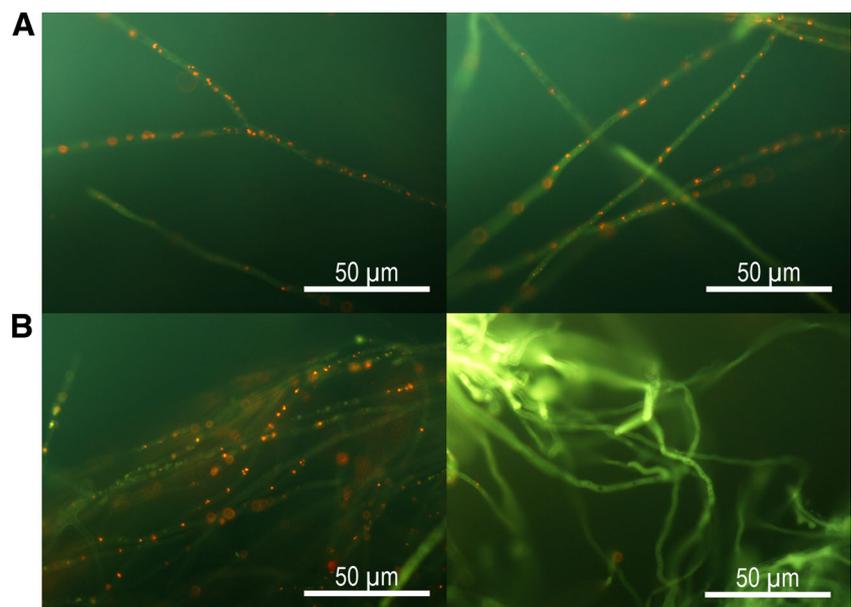
PgAFP localization

PgAFP localization was investigated in *P. polonicum* by incubation with FITC-labeled PgAFP. *P. polonicum* showed green fluorescence only bound to the outer layer (Fig. 5). However, the labeled protein was found both inside the hyphae and bound to the outer layer in *A. tubingensis*, revealing that PgAFP had entered *A. tubingensis*.

Chitin-PgAFP binding assay

Given that PgAFP was located at the outer layer of *P. polonicum*, a chitin-binding assay was performed. When PgAFP was added to a solution of regenerated chitin, over 91 % of the antifungal protein was recovered from the supernatant after incubation, even at the lowest concentration tested

Fig. 2 Metabolic activity of *P. polonicum* (panel A) and *A. tubingensis* (panel B) tested with FUN-1 staining. Non-treated hyphae (left) showed intravacuolar activity as red spots. Hyphae treated with 75 µg/ml PgAFP for 24 h (right) showed intravacuolar activity in *P. polonicum* but very low metabolic activity in *A. tubingensis*



(146 µg/ml). Thus, PgAFP does not specifically bind to regenerated chitin.

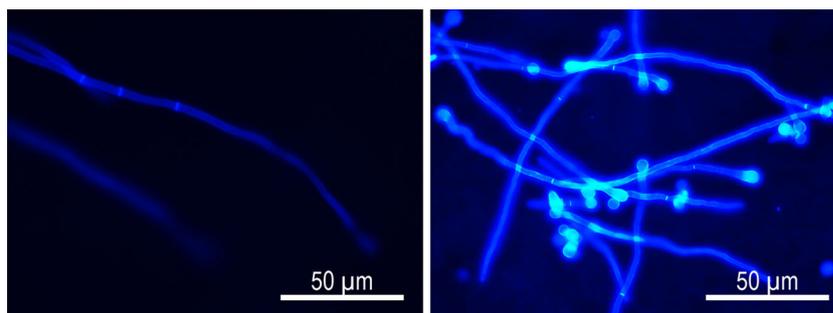
Effect on oxidative status and viability

To test the influence of PgAFP on ROS production, staining with 2', 7' dichlorofluorescein diacetate was used. Both treated and untreated *P. polonicum* showed similar levels of emitted fluorescence (data not shown), revealing that PgAFP does not increase ROS in the resistant *P. polonicum*. The effect of PgAFP on membrane integrity was evaluated by AO/EB double staining. EB was taken only by PgAFP-treated *A. tubingensis*, showing orange hyphae, while non-treated *A. tubingensis* and both treated and non-treated *P. polonicum* only showed green hyphae due to AO uptake (Fig. 6). These results reveal that *P. polonicum* membrane was not compromised by PgAFP, which is the opposite to *A. tubingensis*. The evaluation of apoptosis or necrosis confirmed the above-reported effects on viability. *A. tubingensis* treated hyphae showed orange color as a consequence of AnV-FITC and PI staining, meaning a necrotic stage. Non-treated *A. tubingensis* and both treated and untreated *P. polonicum* were not dyed, showing no sign of apoptosis or necrosis (Fig. 7).

Discussion

Both proteomic methods used in this work revealed differences in the relative abundance of proteins after treatment of *P. polonicum* with PgAFP (Tables S1 and S2 in the Supplementary Material). Discrepancies were detected in the fold change estimated by each method. Such discrepancies can be explained by the fact that 2D-PAGE compares one

Fig. 3 Chitin distribution on *P. polonicum* stained with fluorescent brightener 28. *Left*, non-treated hyphae; *right*, hyphae treated with 75 $\mu\text{g/ml}$ PgAFP for 24 h



isoform of a protein at a time, whereas label-free proteomics combines every isoform together and gives the final total abundance of that protein (Delgado et al. 2015b). Therefore, changes in the relative quantity of each isoform could be detected using 2D-PAGE, while in the label-free proteomics only a measure of total abundance of all isoforms of a given protein is carried out.

Label-free proteomics showed an increased abundance of 22 proteins related to ribosomes and spliceosomes in PgAFP-treated *P. polonicum*, according to KEGG. However, only two ribosomal proteins were found in higher amount by 2D-PAGE analysis. This fact can be explained by the narrow range of pH chosen for 2D-PAGE analysis (Görg et al. 2009). In particular, the analysis carried out is suitable for proteins with pI between 4 and 7, while proteins involved in ribosome structure or function are generally out of this range (Görg et al. 2004). Therefore, the combinatorial deployment of proteomic tools used in this study works complementarily to obtain further information about the effect of PgAFP on the proteome.

The higher relative abundance of proteins from ribosomal and spliceosomal pathways in PgAFP-treated *P. polonicum* could be regarded as a response of the mold to counteract the protein's antifungal activity. A higher relative abundance

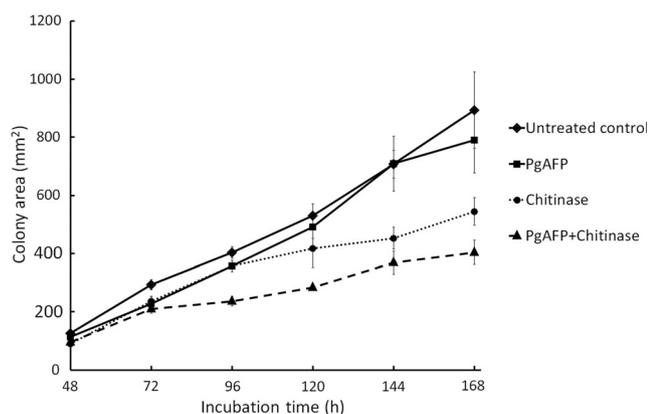


Fig. 4 Effect of PgAFP and chitinase combined treatment on *P. polonicum* growth. Untreated control: added with 2.5 ml of phosphate elution buffer and 100 μl PBS; PgAFP: added with 2.5 ml of 600 $\mu\text{g/ml}$ PgAFP in phosphate elution buffer and 100 μl PBS. Chitinase: added with 2.5 ml of phosphate elution buffer and 100 μl of ≥ 60 units/ml chitinase from *Streptomyces griseus*; PgAFP + Chitinase: added with 2.5 ml of 600 $\mu\text{g/ml}$ PgAFP in phosphate elution buffer and 100 μl PBS

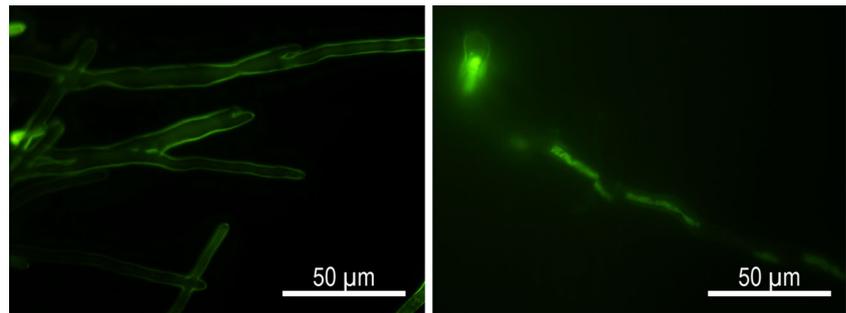
of a substantial number of ribosomal and spliceosomal proteins has also been described in a recent work on the effect of PgAFP on the sensitive *A. flavus* (Delgado et al. 2015b). Twelve of the 22 proteins from this group that increased with PgAFP in *P. polonicum* also increased in *A. flavus*. Thus, the increase in proteins from ribosomal and spliceosomal pathways solely would not explain the resistance mechanism in *P. polonicum*.

The changes observed in the proteins related to metabolic pathways and biosynthesis of secondary metabolites were heterogeneous, with 8 proteins increasing and 12 decreasing in PgAFP-treated *P. polonicum* (Table 1). From these proteins, only pyruvate decarboxylase, aldehyde dehydrogenase, and phosphatidylglycerol-specific phospholipase showed similar changes in PgAFP-treated *A. flavus* (Delgado et al. 2015b). However, these enzymes are scattered among various metabolic routes, including glycolysis gluconeogenesis, purine metabolism, and aminoacyl-tRNA biosynthesis, making it unlikely that any of them explain the ability of *P. polonicum* to withstand PgAFP.

All the above changes in the abundance of the metabolic-related proteins did not entail dramatic changes in the metabolic activity, which in turn is consistent with the resistance of *P. polonicum* to PgAFP. The abundance of intracellular red spots in FUN-1 staining (Fig. 2) revealed that the metabolic activity in *P. polonicum* remained substantially unaffected by PgAFP, whereas it was greatly reduced in the sensitive *A. tubingenensis* used as a control (Fig. 2), as well as in PgAFP-treated *A. flavus* (Delgado et al. 2015b).

Other effects reported for antifungal proteins, including PAF, NFAP, and PgAFP, are increased ROS levels leading to programmed cell death in sensitive molds (Leiter et al. 2005; Galgóczy et al. 2013a; Delgado et al. 2015b). Increased ROS levels have been linked to higher relative abundance of proteins involved in the glutathione pathway and heat shock proteins in PgAFP-treated *A. flavus* (Delgado et al. 2015b). The limited changes in such stress-related proteins in treated *P. polonicum* do not reveal a strong response to oxidative stress. In addition, none of the negative effects related to oxidative stress was observed in PgAFP-treated *P. polonicum*, including increased ROS levels, loss of cell membrane integrity, and necrotic signs.

Fig. 5 PgAFP localization in *P. polonicum* (left) and *A. tubingensis* (right) treated with 20 $\mu\text{g}/\text{ml}$ FITC-labeled PgAFP for 24 h. PgAFP was found solely bound to the outer layer in *P. polonicum* but mainly inside *A. tubingensis*



All the changes in the proteome discussed so far reveal that PgAFP interacts with the non-sensitive *P. polonicum*, but do not seem to explain the successful defense response. As discussed later, proteins from the cell wall integrity (CWI) pathway seem to be involved in the successful defense response.

Membrane permeabilization is a main effect described for other antifungal proteins (Thevissen et al. 1999; Hagen et al. 2007). Increased permeability also contributes to PgAFP inhibition on *A. flavus* (Delgado et al. 2015b). Similarly, the permeability of the sensitive *A. tubingensis* to SYTOX Green increased at all PgAFP concentrations tested (Fig. 1). However, membrane permeabilization in *P. polonicum* exhibited a two-step pattern: first increasing slowly at low PgAFP concentrations, then slowly declining even below the level of untreated controls with the two highest concentrations tested (Fig. 1). A similar two-step pattern in membrane permeabilization was also described for *Neurospora crassa* treated with plant defensins (Thevissen et al. 1999). The lower permeability at the highest concentrations of defensins has been explained by the apparent dependency of permeabilization on membrane polarization. The higher permeability of fungal membranes treated with defensins causes depolarization, which may ultimately decrease membrane permeability (Thevissen et al. 1996, 1999). The decline in *P. polonicum* membrane permeability at high PgAFP concentrations might be partially explained by membrane depolarization. As discussed later, other changes in membrane and cell wall can

contribute to reach permeability levels well below that in untreated controls.

Growth inhibition by AFP, PAF, and PgAFP has been related to the ability to interact with specific molecules or anionic phospholipids in the cell wall and/or plasma membrane (Lacadena et al. 1998; Theis et al. 2003; Marx et al. 2008; Delgado et al. 2015b). Similarly, NFAP might bind to a G-protein-coupled receptor in a sensitive mold (Virágh et al. 2015) and AFP_{NN5353} does not bind to insensitive *Mucor circinelloides* (Binder et al. 2011). Interestingly, PgAFP was located at the outer layer in the resistant *P. polonicum* (Fig. 5). This binding may be due just to adherence to chitin or to specific receptors, but PgAFP did not bind to regenerated chitin in vitro. Given that PgAFP was not internalized by the resistant mold, no internal receptor can be detected. In addition, the proteome changes observed in PgAFP-treated *P. polonicum* can only be due to transduction signals derived from the interaction with outer layer receptors. Therefore, PgAFP may interact with specific molecules in the outer layer of *P. polonicum*, similarly to PAF (Marx et al. 2008; Batta et al. 2009). As a consequence, PgAFP resistance could be related with the ability of *P. polonicum* to produce structural changes that prevent the interaction with the specific receptors or the negatively charged phospholipids.

The fungal cell wall acts as an initial barrier in contact with hostile environments (Latzé 2007). The main components of the cell wall that may act as a barrier against antifungal proteins are polysaccharides, including glucans, glucomannans,

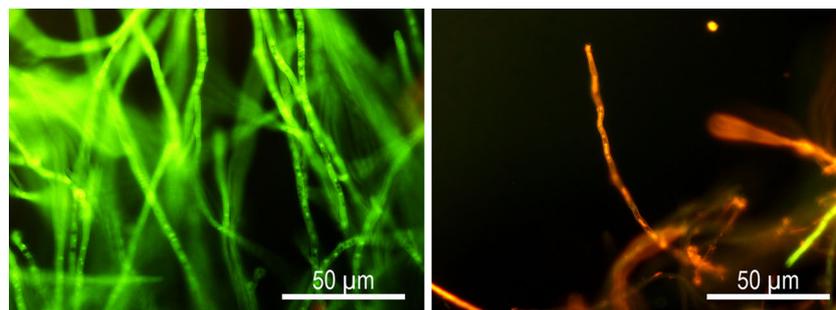
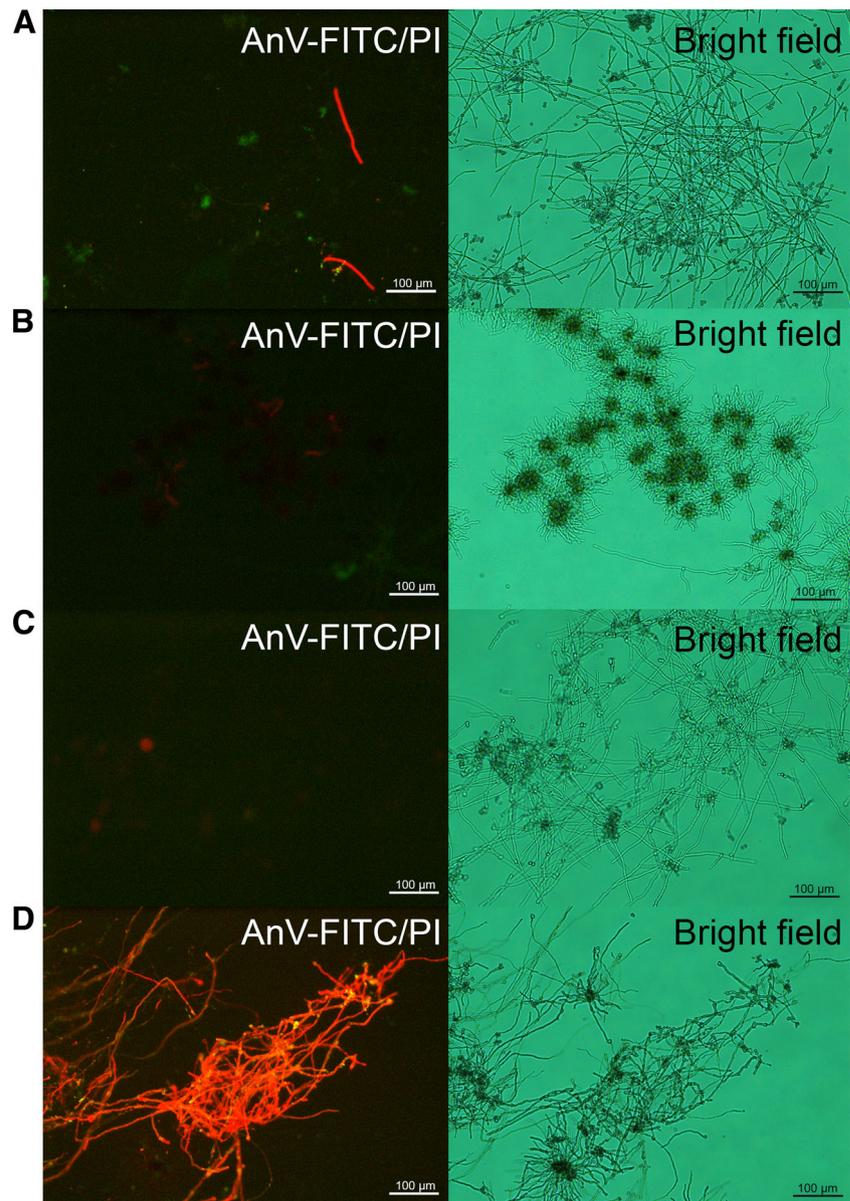


Fig. 6 Effect of 75 $\mu\text{g}/\text{ml}$ PgAFP on membrane integrity of *P. polonicum* (left) and *A. tubingensis* (right) evaluated with vital acridine orange (AO)/ethidium bromide (EB) staining. *P. polonicum* hyphae showed intense

green color due to only AO penetration through non-compromised membrane. *A. tubingensis* hyphae showed intense orange color due to both AO and EB penetration through compromised cell membrane

Fig. 7 Effect of 75 $\mu\text{g/ml}$ PgAFP on *P. polonicum* and *A. tubingensis* hyphae viability evaluated with apoptosis detection kit at 24 h of incubation. **a** Non-treated *P. polonicum*. **b** PgAFP-treated *P. polonicum*. **c** Non-treated *A. tubingensis*. **d** PgAFP-treated *A. tubingensis*. *Left*, annexin V/FITC-propidium iodide (An/FITC-PI) staining. *Right*, the corresponding bright field view. No intense green or orange color due to apoptosis or necrosis was observed in PgAFP-treated *P. polonicum*. Only PgAFP-treated *A. tubingensis* showed intense orange color due to necrosis



and chitin. A lower chitin content in the fungal cell wall has been related to a higher permeability (Mellado et al. 2003; Rementeria et al. 2005), suggesting a barrier role of chitin. The higher amount of chitin observed in the cell wall of *P. polonicum* treated with the highest PgAFP concentration (Fig. 3) can be responsible for the lower permeability observed, being a key factor in the successful response to this antifungal protein. Chitin synthesis is also stimulated by AFP in resistant fungi (Ouedraogo et al. 2011), but not by AFP, PAF, and PgAFP in sensitive molds (Hagen et al. 2007; Binder et al. 2010; Delgado et al. 2015b). In addition, PAF and NFAP provoke delocalized chitin deposition at the hyphal tips (Binder et al. 2010; Virágh et al. 2015). Therefore, the altered chitin deposition can be related to sensitivity to antifungal proteins in contrast to our findings in *P. polonicum*.

To confirm if the increased chitin deposition itself is enough to explain the resistance to PgAFP, a joint treatment of PgAFP and chitinase was applied to *P. polonicum*. The slowest growth obtained with the combined treatment strongly infers that the increased chitin content plays a key role in the resistance of *P. polonicum* to PgAFP. Therefore, we propose that chitin cell wall reinforcement is responsible for the successful response of *P. polonicum*, due to a hampered interaction of PgAFP with specific receptors or the negatively charged phospholipids.

From the proteins involved in chitin biosynthesis, glucosamine-6-phosphate *N*-acetyltransferase was only found in treated *P. polonicum* (Table 1). The gene coding for this protein, as well as the gene encoding an α -1,3-glucan synthase, is upregulated in *A. niger* treated

with sublethal doses of caspofungin (Meyer et al. 2007). Given that an increase of glucan but not chitin synthesis results in an ineffective survival response (Hagen et al. 2007), the increase in glucosamine-6-phosphate *N*-acetyltransferase could be important for *P. polonicum* to counteract PgAFP. The increased chitin content can also be related with CWI signaling activation. The stress signals sensed by the receptor protein Wsc are transmitted to Rho1, which has been considered the master regulator of cell wall integrity signaling pathway in yeasts (Levin 2005). Then, Rho1 binds and activates Pkc (Nonaka et al. 1995; Kamada et al. 1996; Lodder et al. 1999), and the signals channeled through the Mpk signaling lead to activation of genes involved in cell wall synthesis (Igual et al. 1996; Jung and Levin 1999), resulting in an elevated chitin content (Munro et al. 2007). Rho1 and Pkc1 have been suggested as the only proteins of CWI pathway that could be involved in the survival response of AFP-resistant *Saccharomyces cerevisiae*, but its relevance has not been established (Ouedraogo et al. 2011).

In sensitive molds, chitin synthesis is not increased by antifungal proteins, as for *A. nidulans* treated with PAF (Binder et al. 2010) or *A. niger* treated with AFP (Hagen et al. 2007). The resistant *P. polonicum* showed an increased abundance of Rho1 and in chitin synthesis when treated with PgAFP (Table 1 and Fig. 3). Conversely, the sensitive *A. flavus* showed a lower relative abundance of Rho1 and a lower chitin deposition when treated with PgAFP (Delgado et al. 2015b). Therefore, it seems that the efficient response of CWI pathway activation by Rho1 could be a key role in the resistance to PgAFP, in contrast to the basal ineffective compensatory response of this pathway in sensitive molds.

In conclusion, the proteome changes and the altered permeability imply an active reaction of *P. polonicum* to PgAFP, where the increased chitin content can be related with a higher abundance of glucosamine-6-phosphate *N*-acetyltransferase and Rho1. Moreover, the combined treatment with chitinase could provide a complementary means to combat resistance to antifungal proteins.

Acknowledgments This work was supported by the Spanish Ministry of Education and Science, Ministry of Economy and Competitiveness and FEDER (AGL2010-21623, AGL2013-45729-P). Josué Delgado was recipient of a FPI grant from the Spanish Ministry of Education and Science (BES-2011-043422 y EEBB-I-13-06900). Rebecca A. Owens was funded by a 3U Partnership Award (<http://www.3UPartnership.ie/>). Mass spectrometry facilities were funded by Science Foundation Ireland (Q-Exactive; 12/RI/2346(3) & PI/11/1188) and the Irish Higher Education Authority (Agilent Ion Trap 6340).

Compliance with ethical standards

Ethical statement This article does not contain any studies with human participants or animals performed by any of the authors.

Conflict of interest The authors declare that they have no competing interests.

References

- Acosta R, Rodríguez-Martín A, Martín A, Núñez F, Asensio MA (2009) Selection of antifungal protein-producing molds from dry-cured meat products. *Int J Food Microbiol* 135:39–46. doi:10.1016/j.ijfoodmicro.2009.07.020
- Batta G, Barna T, Gáspári Z, Sándor S, Kövér KE, Binder U, Sarg B, Kaiserer L, Chhillar AK, Eigentler A, Leiter E, Hegedüs N, Pócsi I, Lindner H, Marx F (2009) Functional aspects of the solution structure and dynamics of PAF—a highly-stable antifungal protein from *Penicillium chrysogenum*. *FEBS J* 276:2875–2890. doi:10.1111/j.1742-4658.2009.07011.x
- Binder U, Oberparleiter C, Meyer V, Marx F (2010) The antifungal protein PAF interferes with PKC/MPK and cAMP/PKA signalling of *Aspergillus nidulans*. *Mol Microbiol* 75:294–307. doi:10.1111/j.1365-2958.2009.06936.x
- Binder U, Bencina M, Eigentler A, Meyer V, Marx F (2011) The *Aspergillus giganteus* antifungal protein AFPNN5353 activates the cell wall integrity pathway and perturbs calcium homeostasis. *BMC Microbiol* 11:209. doi:10.1186/1471-2180-11-209
- Binder U, Benčina M, Fizil Á, Batta G, Chhillar AK, Marx F (2015) Protein kinase A signaling and calcium ions are major players in PAF mediated toxicity against *Aspergillus niger*. *FEBS Lett* 589:1266–1271. doi:10.1016/j.febslet.2015.03.037
- Carbery S, Neville CM, Kavanagh KA, Doyle S (2006) Analysis of major intracellular proteins of *Aspergillus fumigatus* by MALDI mass spectrometry: identification and characterisation of an elongation factor 1B protein with glutathione transferase activity. *Biochem Biophys Res Commun* 341:1096–1104. doi:10.1016/j.bbrc.2006.01.078
- Carpentier SC, Witters E, Laukens K, Deckers P, Swennen R, Panis B (2005) Preparation of protein extracts from recalcitrant plant tissues: an evaluation of different methods for two-dimensional gel electrophoresis analysis. *Proteomics* 5:2497–2507. doi:10.1002/pmic.200401222
- Chen Z, Ao J, Yang W, Jiao L, Zheng T, Chen X (2013) Purification and characterization of a novel antifungal protein secreted by *Penicillium chrysogenum* from an Arctic sediment. *Appl Microbiol Biotechnol* 97:10381–10390. doi:10.1007/s00253-013-4800-6
- Collins C, Keane TM, Turner DJ, O’Keeffe G, Fitzpatrick DA, Doyle S (2013) Genomic and proteomic dissection of the ubiquitous plant pathogen, *Armillaria mellea*: toward a new infection model system. *J Proteome Res* 12:2552–2570. doi:10.1021/pr301131t
- Conesa A, Götz S, García-Gómez JM, Terol J, Talón M, Robles M (2005) Blast2GO: a universal tool for annotation, visualization and analysis in functional genomics research. *Bioinformatics* 21:3674–3676. doi:10.1093/bioinformatics/bti610
- Cox J, Mann M (2008) MaxQuant enables high peptide identification rates, individualized p.p.b.-range mass accuracies and proteome-wide protein quantification. *Nat Biotechnol* 26:1367–1372. doi:10.1038/nbt.1511
- Delgado J, Acosta R, Rodríguez-Martín A, Bermúdez E, Núñez F, Asensio MA (2015a) Growth inhibition and stability of PgAFP from *Penicillium chrysogenum* against fungi common on dry-ripened

- meat products. *Int J Food Microbiol* 205:23–29. doi:10.1016/j.ijfoodmicro.2015.03.029
- Delgado J, Owens RA, Doyle S, Asensio MA, Núñez F (2015b) Impact of the antifungal protein PgAFP from *Penicillium chrysogenum* on the protein profile in *Aspergillus flavus*. *Appl Microbiol Biotechnol* 99:8701–8715. doi:10.1007/s00253-015-6731-x
- Dolan SK, Owens RA, O’Keeffe G, Hammel S, Fitzpatrick DA, Jones GW, Doyle S (2014) Regulation of nonribosomal peptide synthesis: bis-thiomethylation attenuates gliotoxin biosynthesis in *Aspergillus fumigatus*. *Chem Biol* 21:999–1012. doi:10.1016/j.chembiol.2014.07.006
- Galgóczy L, Kovács L, Karácsony Z, Virágh M, Hamari Z, Vágvölgyi C (2013a) Investigation of the antimicrobial effect of *Neosartorya fischeri* antifungal protein (NFAP) after heterologous expression in *Aspergillus nidulans*. *Microbiology* 159:411–419. doi:10.1099/mic.0.061119-0
- Galgóczy L, Virágh M, Kovács L, Tóth B, Papp T, Vágvölgyi C (2013b) Antifungal peptides homologous to the *Penicillium chrysogenum* antifungal protein (PAF) are widespread among Fusaria. *Peptides* 39:131–137. doi:10.1016/j.peptides.2012.10.016
- Görg A, Weiss W, Dunn MJ (2004) Current two-dimensional electrophoresis technology for proteomics. *Proteomics* 4:3665–3685. doi:10.1002/pmic.200401031
- Görg A, Drews O, Lück C, Weiland F, Weiss W (2009) 2-DE with IPGs. *Electrophoresis* 30(Suppl 1):S122–S132. doi:10.1002/elps.200900051
- Gun Lee D, Shin SY, Maeng CY, Jin ZZ, Kim KL, Hahn KS (1999) Isolation and characterization of a novel antifungal peptide from *Aspergillus niger*. *Biochem Biophys Res Commun* 263:646–651. doi:10.1006/bbrc.1999.1428
- Hagen S, Marx F, Ram AF, Meyer V (2007) The antifungal protein AFP from *Aspergillus giganteus* inhibits chitin synthesis in sensitive fungi. *Appl Environ Microbiol* 73:2128–2134. doi:10.1128/AEM.02497-06
- Hajji M, Jellouli K, Hmidet N, Balti R, Sellami-Kamoun A, Nasri M (2010) A highly thermostable antimicrobial peptide from *Aspergillus clavatus* ES1: biochemical and molecular characterization. *J Ind Microbiol Biotechnol* 37:805–813. doi:10.1007/s10295-010-0725-6
- Harris SD, Morrell JL, Hamer JE (1994) Identification and characterization of *Aspergillus nidulans* mutants defective in cytokinesis. *Genetics* 136:517–532
- Houbraken J, Samson RA (2011) Phylogeny of *Penicillium* and the segregation of *Trichocomaceae* into three families. *Stud Mycol* 70:1–51. doi:10.3114/sim.2011.70.01
- Igual JC, Johnson AL, Johnston LH (1996) Coordinated regulation of gene expression by the cell cycle transcription factor Swi4 and the protein kinase C MAP kinase pathway for yeast cell integrity. *EMBO J* 15:5001–5013
- Jung US, Levin DE (1999) Genome-wide analysis of gene expression regulated by the yeast cell wall integrity signalling pathway. *Mol Microbiol* 34:1049–1057
- Kaiserer L, Oberparleiter C, Weiler-Görz R, Burgstaller W, Leiter E, Marx F (2003) Characterization of the *Penicillium chrysogenum* antifungal protein PAF. *Arch Microbiol* 180:204–210. doi:10.1007/s00203-003-0578-8
- Kamada Y, Qadota H, Python CP, Anraku Y, Ohya Y, Levin DE (1996) Activation of yeast protein kinase C by Rho1 GTPase. *J Biol Chem* 271:9193–9196. doi:10.1074/jbc.271.16.9193
- Kim Y, Nandakumar MP, Marten MR (2007) Proteomics of filamentous fungi. *Trends Biotechnol* 25:395–400. doi:10.1016/j.tibtech.2007.07.008
- Kovács L, Virágh M, Takó M, Papp T, Vágvölgyi C, Galgóczy L (2011) Isolation and characterization of *Neosartorya fischeri* antifungal protein (NFAP). *Peptides* 32:1724–1731. doi:10.1016/j.peptides.2011.06.022
- Lacadena J, del Pozo Martínez A, Lacadena V, Martínez Ruiz A, Mancheño JM, Oñaderra M, Gavilanes JG (1998) The cytotoxin α -sarcin behaves as a cyclizing ribonuclease. *FEBS Lett* 424:46–48. doi:10.1016/S0014-5793(98)00137-9
- Latgé J-P (2007) The cell wall: a carbohydrate armour for the fungal cell. *Mol Microbiol* 66:279–290. doi:10.1111/j.1365-2958.2007.05872.x
- Leiter É, Szappanos H, Oberparleiter C, Kaiserer L, Csernoch L, Pusztahelyi T, Emri T, Pócsi I, Salvenmoser W, Marx F (2005) Antifungal protein PAF severely affects the integrity of the plasma membrane of *Aspergillus nidulans* and induces an apoptosis-like phenotype. *Antimicrob Agents Chemother* 49:2445–2453. doi:10.1128/AAC.49.6.2445
- Levin DE (2005) Cell wall integrity signaling in *Saccharomyces cerevisiae*. *Microbiol Mol Biol Rev* 69:262–291. doi:10.1128/MMBR.69.2.262
- Liu R, Huang H, Yang Q, Liu W-Y (2002) Purification of α -sarcin and an antifungal protein from mold (*Aspergillus giganteus*) by chitin affinity chromatography. *Protein Expr Purif* 25:50–58. doi:10.1006/prep.2001.1608
- Lodder AL, Lee TK, Ballester R (1999) Characterization of the Wsc1 protein, a putative receptor in the stress response of *Saccharomyces cerevisiae*. *Genetics* 152:1487–1499
- Lowry OH, Rosebrough NJ, Farr L, Randall RJ (1951) Protein measurement with the Folin phenol reagent. *J Biol Chem* 193:265–275
- Marx F, Haas H, Reindl M, Stöffler G, Lottspeich F, Redl B (1995) Cloning, structural organization and regulation of expression of the *Penicillium chrysogenum* paf gene encoding an abundantly secreted protein with antifungal activity. *Gene* 167:167–171
- Marx F, Binder U, Leiter E, Pócsi I (2008) The *Penicillium chrysogenum* antifungal protein PAF, a promising tool for the development of new antifungal therapies and fungal cell biology studies. *Cell Mol Life Sci* 65:445–454. doi:10.1007/s00018-007-7364-8
- Mellado E, Dubreucq G, Mol P, Sarfati J, Paris S, Diaquin M, Holden DW, Rodriguez-Tudela JL, Latgé JP (2003) Cell wall biogenesis in a double chitin synthase mutant (*chsG⁻/chsE⁻*) of *Aspergillus fumigatus*. *Fungal Genet Biol* 38:98–109. doi:10.1016/S1087-1845(02)00516-9
- Meyer V, Damveld RA, Arentshorst M, Stahl U, Van Den Hondel C, Ram A (2007) Survival in the presence of antifungals: genome-wide expression profiling of *Aspergillus niger* in response to sublethal concentrations of caspofungin and fenpropimorph. *J Biol Chem* 282:32935–32948. doi:10.1074/jbc.M705856200
- Moreno AB, Del Pozo AM, Borja M, Segundo BS (2003) Activity of the antifungal protein from *Aspergillus giganteus* against *Botrytis cinerea*. *Phytopathology* 93:1344–1353. doi:10.1094/PHYTO.2003.93.11.1344
- Moreno AB, Martínez Del Pozo Á, San Segundo B (2006) Antifungal mechanism of the *Aspergillus giganteus* AFP against the rice blast fungus *Magnaporthe grisea*. *Appl Microbiol Biotechnol* 72:883–895. doi:10.1007/s00253-006-0362-1
- Munro CA, Selvaggin S, De Bruijn I, Walker L, Lenardon MD, Gerssen B, Milne S, Brown AJP, Gow NAR (2007) The PKC, HOG and Ca²⁺ signalling pathways co-ordinately regulate chitin synthesis in *Candida albicans*. *Mol Microbiol* 63:1399–1413. doi:10.1111/j.1365-2958.2007.05588.x
- Nakaya K, Omata K, Okahashi I, Nakamura Y, Kolkenbrock H, Ulbrich N (1990) Amino acid sequence and disulfide bridges of an antifungal protein isolated from *Aspergillus giganteus*. *Eur J Biochem* 193:31–38
- Nonaka H, Tanaka K, Hirano H, Fujiwara T, Kohno H, Umikawa M, Mino A, Takai Y (1995) A downstream target of RHO1 small GTP-binding protein is PKC1, a homolog of protein kinase C, which leads to activation of the MAP kinase cascade in *Saccharomyces cerevisiae*. *EMBO J* 14:5931–5938
- O’Keeffe G, Jöchl C, Kavanagh K, Doyle S (2013) Extensive proteomic remodeling is induced by eukaryotic translation elongation factor

- 1B γ deletion in *Aspergillus fumigatus*. Protein Sci 22:1612–1622. doi:10.1002/pro.2367
- O' Keffe G, Hammel S, Owens RA, Keane TM, Fitzpatrick DA, Jones GW, Doyle S (2014) RNA-seq reveals the pan-transcriptomic impact of attenuating the gliotoxin self-protection mechanism in *Aspergillus fumigatus*. BMC Genomics 25:1–26. doi:10.1186/1471-2164-15-894
- Ouedraogo JP, Hagen S, Spielvogel A, Engelhardt S, Meyer V (2011) Survival strategies of yeast and filamentous fungi against the antifungal protein AFP. J Biol Chem 286:13859–13868. doi:10.1074/jbc.M110.203588
- Owens RA, Hammel S, Sheridan KJ, Jones GW, Doyle S (2014) A proteomic approach to investigating gene cluster expression and secondary metabolite functionality in *Aspergillus fumigatus*. PLoS One 9:e106942
- Rementería A, López-Molina N, Ludwig A, Vivanco AB, Bikandi J, Pontón J, Garaizar J (2005) Genes and molecules involved in *Aspergillus fumigatus* virulence. Rev Iberoam Micol 22:1–23
- Rodríguez-Martín A, Acosta R, Liddell S, Núñez F, Benito MJ, Asensio MA (2010) Characterization of the novel antifungal protein PgAFP and the encoding gene of *Penicillium chrysogenum*. Peptides 31: 541–547. doi:10.1016/j.peptides.2009.11.002
- Seibold M, Wolschann P, Bodevin S, Olsen O (2011) Properties of the bubble protein, a defensin and an abundant component of a fungal exudate. Peptides 32:1989–1995. doi:10.1016/j.peptides.2011.08.022
- Shevchenko A, Tomas H, Havlis J, Olsen JV, Mann M (2007) In-gel digestion for mass spectrometric characterization of proteins and proteomes. Nat Protoc 1:2856–2860. doi:10.1038/nprot.2006.468
- Skouri-Gargouri H, Gargouri A (2008) First isolation of a novel thermostable antifungal peptide secreted by *Aspergillus clavatus*. Peptides 29:1871–1877. doi:10.1016/j.peptides.2008.07.005
- Skouri-Gargouri H, Ali MB, Gargouri A (2009) Molecular cloning, structural analysis and modelling of the antifungal peptide from *Aspergillus clavatus*. Peptides 30:1798–1804. doi:10.1016/j.peptides.2009.06.034
- Souza CP, Burbano-Rosero EM, Almeida BC, Martins GG, Albertini LS, ING R (2009) Culture medium for isolating chitinolytic bacteria from seawater and plankton. World J Microbiol Biotechnol 25:2079–2082. doi:10.1007/s11274-009-0098-z
- Theis T, Wedde M, Meyer V, Stahl U (2003) The antifungal protein from *Aspergillus giganteus* causes membrane permeabilization. Antimicrob Agents Chemother 47:588–593. doi:10.1128/AAC.47.2.588
- Thevissen K, Ghazi A, De Samblanx GW, Brownlee C, Osborn RW, Broekaert WF (1996) Fungal membrane responses induced by plant defensins and thionins. J Biol Chem 271:15018–15025
- Thevissen K, Terras FR, Broekaert WF (1999) Permeabilization of fungal membranes by plant defensins inhibits fungal growth. Appl Environ Microbiol 65:5451–5458
- Virágh M, Marton A, Vizler C, Tóth L, Vágvölgyi C, Marx F, Galgóczy L (2015) Insight into the antifungal mechanism of *Neosartorya fischeri* antifungal protein. Protein Cell 6:518–528. doi:10.1007/s13238-015-0167-z
- Yeaman MR, Yount NY (2003) Mechanisms of antimicrobial peptide action and resistance. Pharmacol Rev 55:27–55. doi:10.1124/pr.55.1.2

Journal: **Applied Microbiology and Biotechnology**

Supplementary Information

Increased chitin biosynthesis contributes to the resistance of *Penicillium polonicum* against the antifungal protein PgAFP.

Josué Delgado,^a Rebecca A. Owens,^b Sean Doyle,^b Miguel A. Asensio^a and Félix Núñez.^a

^a Food Hygiene and Safety, Institute of Meat Products, University of Extremadura, Cáceres, Spain.

^b Department of Biology, Maynooth University, Maynooth, Co. Kildare, Ireland.

Corresponding author:

Miguel A. Asensio

masensio@unex.es, Tel.: +34 927 257124; Fax: +34 927 257110

Supplementary Table S1. Data on proteins whose relative abundance was affected by 10 µg/ml PgAFP in *P. polonicum* reaching over 1.5 fold change in 2D-PAGE.

Protein name	p- value	Fold Change	% coverage	Unique peptides	Score	tMr (Da)	Protein accession (GI)	Gene
Hypothetical protein PDIG_30840	0.049	↑3	22	1	65	13620	255945719	Pc20g11410
40S ribosomal protein S12	0.032	↑3	29	2	138	16471	255942617	Pc18g02330
40S ribosomal protein S0	0.005	↑2.5	17	3	153	32517	255938175	Pc13g14510
Regulatory protein SUAPRGA1	0.007	↑2.1	22	3	241	32655	255944381	Pc20g04080
Hsp90 binding co-chaperone (Sba1), putative	0.011	↑2	14	2	123	23627	255953251	Pc21g03140
Histone H2B	0.040	↑1.8	18	1	78	15075	255945231	Pc20g08600
Peptidyl-prolyl cis-trans isomerase B	0.002	↑1.6	7	1	74	29893	255950084	Pc22g19060
Elongation factor 1-beta	0.001	↑1.5	19	3	173	25049	255936559	Pc13g08810
14-3-3 family protein ArtA, putative	0.041	↑1.5	16	4	204	29365	255942923	Pc18g03940
Translation elongation factor EF-2 subunit, putative	0.00003	↓4.1	20	13	621	94428	255933099	Pc12g12040
Mannitol-1-phosphate dehydrogenase	0.00003	↓3.2	14	5	264	42533	255950424	Pc22g20800
14-3-3 family protein ArtA, putative	0.004	↓2.8	42	6	492	29365	255942923	Pc18g03940
Carbamoyl-phosphate synthase, large subunit	0.006	↓2.3	5	4	215	128738	255950296	Pc22g20150
Pc15g00640	0.00091	↓2.3	22	8	446	52104	255939043	Pc15g00640
Glyceraldehyde-3-phosphate dehydrogenase	0.00051	↓2.2	4	1	137	36200	255955435	Pc21g14560
Succinate dehydrogenase subunit Sdh1, putative	0.004	↓2.1	4	2	93	71782	255944729	Pc20g06030
UDP-N-acetylglucosamine pyrophosphorylase	0.016	↓2	12	4	272	55800	255954947	Pc21g11950
Glutamine synthetase	0.015	↓2	21	6	278	41735	255947166	Pc22g03070
Glucokinase	0.003	↓2	7	3	92	54152	255950958	Pc22g23550
S-adenosylmethionine synthase	0.002	↓1.9	14	3	144	42211	255940042	Pc16g04380
Heat shock protein (Sti1), putative	0.005	↓1.9	18	10	465	62551	255955103	Pc21g12770
Aminopeptidase P, putative	0.005	↓1.9	9	6	241	65494	255949480	Pc22g15910
Acyl-CoA dehydrogenase, putative	0.003	↓1.8	14	6	256	47445	255941758	Pc16g13490
Heat shock protein	0.016	↓1.8	24	10	489	67033	255948526	Pc22g10220
Aconitate hydratase, mitochondrial	0.001	↓1.8	5	3	128	83969	255935445	Pc13g03110
Unnamed protein product	0.004	↓1.7	3	2	89	94428	255933099	Pc12g12040
Adenylylsulfate kinase AAA81521	0.00002	↓1.7	24	3	89	23642	255936451	Pc13g08270
6-phosphogluconate dehydrogenase, decarboxylating	0.003	↓1.6	32	10	606	54273	255932887	Pc12g10940
Formate dehydrogenase	0.008	↓1.6	15	5	269	50347	255931489	Pc12g04310
Sorbitol/xylulose reductase Sou1-like, putative	0.006	↓1.6	43	8	417	28712	255930855	Pc12g00830
Adenosylhomocysteinase	0.00049	↓1.6	31	12	621	49567	255940172	Pc16g05080
Hypothetical protein PDIG_65240	0.004	↓1.6	8	3	82	57162	255942351	Pc18g00980
Phosphoglucomutase PgmA	0.004	↓1.6	22	9	502	60417	255942431	Pc18g01390
Gamma-actin act-Penicillium chrysogenum	0.022	↓1.6	33	8	338	41958	255945763	Pc20g11630
Aldo/keto reductase, putative	0.003	↓1.6	20	4	217	38968	255956203	Pc21g18620
Aminopeptidase, putative	0.035	↓1.6	12	9	476	99407	255948598	Pc22g11170
UDP-glucose 4-epimerase	0.048	↓1.5	17	4	183	40587	255954639	Pc21g10370

Supplementary Table S2. Data on proteins obtained from label-free proteomics from *P. polonium* treated with 10 µg/ml PgAFP and untreated control.

Table with columns: Log2 LFQ intensity P. polonium Control 1, Log2 LFQ intensity P. polonium Control 2, Log2 LFQ intensity P. polonium Control 3, Log2 LFQ intensity P. polonium Treated 1, Log2 LFQ intensity P. polonium Treated 2, Log2 LFQ intensity P. polonium Treated 3, PEP, Intensity, Peptides, Unique peptides, Sequence coverage [%], Mol. weight [kDa], Log2 (Mean P. polonium control), Log2 (Mean P. polonium Treated), Valid values P. polonium Control, Valid values P. polonium Treated, Protein IDs, Majority proteins, Proteins, Gene ID, Protein Name, Gene ontology (GO), and Subcellular location.

Supplementary Table S2. Data on proteins obtained from label-free proteomics from *P. polonicum* treated with 10 µg/ml PgAFP and untreated control.

B. Quantitative and qualitative results

Majority protein IDs	PEP	Peptides	Sequence coverage [%]	Mol. weight [kDa]	*Log2 (Mean PPS2 Control)	*Log2 (Mean PPS2 Treated)	Valid values PPS2 Control	Valid values PPS2 Treated	t-test p value	Fold Change v Control	Gene ID	Protein Name	Gene ontology (GO)	Sequence Description from Blast2GO analysis
B6GZ62	2.22E-07	3	7.3	42.524	25.3708	24.0189	3	3	0.027743	-2.552586764	B6GZ62	Pc12g05320 protein	oxidoreductase activity	dimeric dihydrodiol
B6HH40	1.50E-38	5	11.8	40.068	28.2027	26.8392	3	3	0.028319	-2.573033071	B6HH40	Pc20g01150 protein	damaged DNA binding; nucleotide-excision repair; nucleus; proteasome-mediated ubiquitin-dependent protein catabolic process	uv excision repair protein rad23
B6HW12	1.47E-159	8	26.4	47.768	28.5874	27.2158	3	3	0.011116	-2.587573782	B6HW12	Pc22g19440 protein	biosynthetic process; cellular amino acid metabolic process; pyridoxal phosphate binding; transaminase activity	aspartate aminotransferase
B6GWS6	2.78E-25	5	46.2	17.636	27.0597	25.6593	3	3	0.031413	-2.639601239	B6GWS6	Pc12g07330 protein	hydrolase activity	nudix family protein
B6HKR7	5.31E-79	6	35.5	36.086	27.1322	25.7191	3	3	0.020853	-2.662958601	B6HKR7	Pc21g03190 protein	NAD binding; oxidoreductase activity, acting on the CH-OH group of donors, NAD or NADP as acceptor	glycerate dehydrogenase
B6HC90	4.94E-09	3	28.3	17.316	26.5598	25.0365	3	2	0.009928	-2.874458098	B6HC90	Pc18g01180 protein	acid-amino acid ligase activity	ubiquitin conjugating enzyme
B6HMQ2	1.26E-199	12	42.9	39.983	30.1086	28.4987	3	3	0.01213	-3.052264527	B6HMQ2	Phospho-2-dehydro-3-deoxyheptanate aldolase	3-deoxy-7-phosphoheptulonate synthase activity; aromatic amino acid family biosynthetic process; chorismate biosynthetic process	phospho-2-dehydro-3-deoxyheptanate aldolase
B6HD76	1.91E-199	19	33.7	81.356	29.355	27.6904	3	3	0.042724	-3.170213494	B6HD76	Pc20g01390 protein	metal ion binding; metalloendopeptidase activity; proteolysis	metallopeptidase
B6HAB8	3.46E-19	3	16.9	15.333	28.5976	26.8879	3	2	0.023759	-3.270769291	B6HAB8	Histone H3	DNA binding; nucleosome; nucleosome assembly; nucleus	histone h3
B6GXR4	2.16E-44	5	35.8	15.5	28.1608	26.3742	3	3	0.01502	-3.4500087	B6GXR4	Pc12g15350 protein	hemolysis by symbiont of host erythrocytes	terl_asptn ame: full=terrelysin ame:
B6HQ15	0	20	47.9	61.293	31.8969	30.0928	3	3	0.02264	-3.492281853	B6HQ15	Glucose-6-phosphate isomerase	gluconeogenesis; glucose-6-phosphate isomerase activity; glycolysis	glucose-6-phosphate isomerase
B6HPL2	1.25E-08	3	25.9	14.925	26.8486	24.8836	3	3	0.006321	-3.904154105	B6HPL2	Pc22g01600 protein	catalytic activity	hit domain protein
B6H823	3.18E-08	3	9.4	41.668	24.8361	22.6955	3	3	0.002985	-4.409515051	B6H823	Pc16g08230 protein	oxidoreductase activity	myo-inositol 2-dehydrogenase
B6H9R2	1.14E-29	4	26.5	27.334	26.571	24.3364	3	3	0.012132	-4.706387142	B6H9R2	Pc16g11920 protein	oxidoreductase activity	short-chain dehydrogenase
B6H6C5	1.86E-110	11	23.1	87.152	28.3333	25.5457	3	3	0.000279	-6.904466771	B6H6C5	Pc15g01900 protein	Mo-molybdopterin cofactor biosynthetic process; carbohydrate metabolic process; cation binding; cytosol; molybdopterin synthase activity; molybdopterin synthase complex	oligo- glucosidase
B6HD89	1.25E-128	10	29.1	52.789	29.184	25.8759	3	3	0.042942	-9.905158081	B6HD89	Pc20g06940 protein	aminopeptidase activity; metallopeptidase activity; proteolysis; zinc ion binding	aspartyl aminopeptidase
B6H6C3	1.72E-42	6	12.6	50.552	30.2304	20.9236	3	2	0.000145	-633.3284155	B6H6C3	Pc15g01880 protein	hydrolase activity, acting on ester bonds	phosphatidylglycerol specific phospholipase
B6GXQ9	2.95E-05	2	3.2	94.834	27.1304	ND	2	0	N/A	Detected in Control Only	B6GXQ9	Pc12g11800 protein		Pc12g11800
B6H1X4	8.74E-06	3	7.9	53.985	23.3828	ND	3	0	N/A	Detected in Control Only	B6H1X4	Pc13g03600 protein	hydroxyethylthiazole kinase activity; thiamine biosynthetic process; thiamine-phosphate diphosphorylase activity	thiamine biosynthetic bifunctional
B6H5I7	1.55E-13	5	12.9	46.869	25.8838	ND	3	0	N/A	Detected in Control Only	B6H5I7	Pc14g00170 protein	hydrolase activity, acting on ester bonds	phosphatidylglycerol specific
B6H7B1	2.62E-05	2	15	16.687	24.3641	ND	2	0	N/A	Detected in Control Only	B6H7B1	Pc16g02280 protein		Pc16g02280
B6H8F4	5.47E-22	2	7.9	39.494	24.6663	ND	3	0	N/A	Detected in Control Only	B6H8F4	Pc16g04220 protein		gpi anchored
B6HDJ9	9.25E-26	3	28.9	17.111	25.8328	ND	3	0	N/A	Detected in Control Only	B6HDJ9	Pc20g07290 protein		Pc20g07290
B6HKJ8	0.001074	2	4.1	51.385	23.5264	ND	2	0	N/A	Detected in Control Only	B6HKJ8	Pc21g15970 protein	cytoplasm; pyrophosphatase activity	exopolyposphatase
B6HP26	1.41E-06	2	15.2	15.429	25.6193	ND	3	0	N/A	Detected in Control Only	B6HP26	Pc22g01300 protein	sterol binding	lipid transfer
B6HRA1	0.000113	2	4	52.756	27.3045	ND	2	0	N/A	Detected in Control Only	B6HRA1	Pc22g24860 protein	oxidoreductase activity, acting on the aldehyde or oxo group of donors, NAD or NADP as acceptor	aldehyde dehydrogenase
B6HU84	0.000196	2	5.4	50.931	23.8742	ND	3	0	N/A	Detected in Control Only	B6HU84	Pc22g22470 protein	carbohydrate catabolic process; mannan endo-1,6-alpha-mannosidase activity	glycosyl
B6HUJ8	3.49E-12	2	14.7	23.846	25.8727	ND	3	0	N/A	Detected in Control Only	B6HUJ8	Pc22g14330 protein		ankyrin repeat protein

*ND: Not detected in sample by LC-MS/MS

IV.5. Efecto del calcio sobre la actividad de PgAFP y el metabolismo en mohos sensibles en medio de cultivo y queso

Proteome changes explain calcium-mediated ineffectiveness of the antifungal protein PgAFP against Aspergillus flavus in cheese

1 Proteome changes explain calcium-mediated ineffectiveness of the antifungal protein
2 PgAFP against *Aspergillus flavus* in cheese

3

4 Josué Delgado^a, Rebecca A. Owens^b, Sean Doyle^b, Félix Núñez^a, Miguel A. Asensio^{a*}

5

6 ^a Food Hygiene and Safety, Institute of Meat Products, University of Extremadura,
7 Cáceres, Spain

8 ^b Department of Biology, Maynooth University, Maynooth, Co. Kildare, Ireland

9

10

11 *Corresponding author

12 Miguel A. Asensio

13 Phone: 34-927-257124, Fax: 34-927-257110

14 E-mail address: masensio@unex.es

15

16

17

18

19

20

21

22

23

24

25

26

27

28 Abstract

29 *Aspergillus flavus* ability to produce aflatoxins in dairy products possesses a hazard
30 potential. The antifungal protein PgAFP from *Penicillium chrysogenum* inhibits various
31 foodborne toxigenic fungi, including *Aspergillus flavus*. However, PgAFP was not
32 capable of inhibiting *A. flavus* growth in cheese, which was related to cations content.
33 CaCl₂ prevented *A. flavus* inhibition in potato dextrose broth (PDB), increasing *A. flavus*
34 permeability, but no further increase was obtained with PgAFP addition. PgAFP did not
35 alter metabolic capability, chitin deposition, intracellular ROS levels, and hyphae
36 viability of *A. flavus* grown with CaCl₂. Comparative proteomic analysis revealed
37 changes in protein abundance after PgAFP treatment of *A. flavus* in a calcium-enriched
38 PDB leading to higher amounts of 125 proteins, related to numerous metabolic
39 pathways, including oxidative stress. Additionally, 70 proteins were found in lower
40 abundance, most of them involved in metabolic pathways and biosynthesis of secondary
41 metabolites. These changes would rule out the blockage of potential PgAFP receptors in
42 *A. flavus* by calcium. *A. flavus* resistance to PgAFP in 0.1 M CaCl₂ seems to be
43 mediated by calcineurin, G-protein, and γ -glutamyltranspeptidase that combat oxidative
44 stress and impede apoptosis. These findings could serve to design new strategies to
45 improve PgAFP activity against aflatoxigenic molds in dairy products.

46

47 **Keywords:** antifungal protein; cheese; proteomics; calcium; calcineurin

48

49 1. Introduction

50 Some moulds are able to produce mycotoxins in foods, which causes serious problems
51 throughout the world. *A. flavus* is one of the most concerning moulds, due essentially to
52 aflatoxin production in cereals and nuts. Additionally, *A. flavus* is able to grow and
53 produce aflatoxins and cyclopiazonic acid on intermediate moisture foods, including
54 ripened cheese (Kokkonen et al., 2005; Lie and Marth, 1967; López-Díaz et al., 1996).
55 The strategies to prevent mycotoxin accumulation on ripened foods include taking
56 advantage of antifungal proteins produced by moulds that prevent growth of
57 mycotoxigenic fungi.

58 The antifungal protein PgAFP is produced by *Penicillium chrysogenum* CECT 20922
59 (formerly RP42C), that was isolated from dry-cured ham (Rodríguez-Martín et al.,

60 2010). PgAFP belongs to a group of small, basic and cysteine-rich proteins, which also
61 includes PAF and Pc-Arctin from *P. chrysogenum* (Chen et al., 2013; Marx et al.,
62 1995), AFP and its variant AFP_{NN5353} from *Aspergillus giganteus* (Binder et al., 2011;
63 Nakaya et al., 1990), AcAFP and AcAMP from *Aspergillus clavatus* (Hajji et al., 2010;
64 Skouri-Gargouri and Gargouri, 2008), NFAP from *Neosartorya fischeri* (Kovács et al.,
65 2011), and FPAP from *Fusarium polyphialidicum* (Galgóczy et al., 2013b). PgAFP can
66 efficiently inhibit various toxigenic moulds in culture medium, even *A. flavus* on a
67 ripened meat product, but not *Penicillium polonicum* (Delgado et al., 2015a). *A. flavus*
68 inhibition coincides with increased permeability to SYTOX Green, depressed metabolic
69 capability, compromised cell membrane, apoptosis, and necrosis. The proposed
70 mechanism of action for PgAFP is based on the lower relative abundance of Rho
71 GTPase Rho1 and G protein subunit β CpcB leading to alteration of both cell wall
72 integrity and response to oxidative stress (Delgado et al., 2015b). Conversely, higher
73 levels of Rho GTPase Rho1 are involved in the resistance of *P. polonicum* leading to
74 increased chitin biosynthesis (Delgado et al., 2015c).

75 The presence of cations in the media has been shown to decrease the antifungal
76 capability of these proteins (Galgóczy et al., 2013a; Kaiserer et al., 2003; Theis et al.,
77 2003; Thevissen et al., 1999, 1996). High levels of extracellular divalent or monovalent
78 cations seem to reduce the antifungal protein's capability of provoking permeabilization
79 or altered calcium influx, as has been described for PAF (Binder et al., 2010), AFP
80 (Theis et al., 2003), and NFAP (Galgóczy et al., 2013a). However, the ultimate
81 mechanism responsible for this effect has not been elucidated. High external calcium
82 levels transiently increase cytosolic calcium levels in *A. nidulans* (Nelson et al., 2004).
83 Intracellular Ca^{2+} is a secondary messenger regulating various responses to stress
84 signals in fungi, including antifungal proteins (Binder et al., 2011, 2010). Given that
85 divalent cations are present in several foods, particularly calcium in cheeses, the effect
86 of high levels of this cation on PgAFP antifungal activity against sensitive moulds
87 should be studied.

88 Comparative proteomic analysis has been described as a powerful tool to study the
89 unknown effect of substances on moulds and yeasts. It has been used to study the effect
90 of H_2O_2 on moulds (Lessing et al., 2007) and to identify the mechanism of action of
91 antifungal compounds (Cagas et al., 2011; Delgado et al., 2015b; Gautam et al., 2008).
92 Comparative 2D-PAGE is able to notice changes in protein expression level, isoforms

93 or post-translational modifications (Görg et al., 2004). However, this technique does not
94 reveal the whole proteome, as it depends on the range of pH chosen (Görg et al., 2009),
95 and it is not able to effectively analyse membrane and hydrophobic proteins (Rabilloud
96 et al., 2009; Zhu et al., 2010). Label-free mass spectrometry-based proteomic analysis is
97 able to identify proteins typically underrepresented in 2D-PAGE studies (Owens et al.,
98 2014), providing deeper proteome coverage. Thus, these two techniques seem to
99 provide complementary information to study the PgAFP mechanism of action in
100 moulds.

101 Results obtained from proteomic analysis guides the use of specific assays to elucidate
102 the mechanisms of action. The relative abundance of *A. flavus* proteins can also give
103 information about the differential response of this mould against PgAFP when grown in
104 a calcium-enriched medium.

105 The objective of the present work was to test the inhibitory activity of PgAFP against *A.*
106 *flavus* growth in cheese, and to study the effect of cations, mainly calcium, on PgAFP
107 antifungal potential. The changes induced by high calcium levels, in the proteome
108 profile and in selected metabolic and structural characteristics of *A. flavus* with and
109 without PgAFP were studied.

110 **2. Materials and methods**

111 **2.1 Strains**

112 The PgAFP producer *Penicillium chrysogenum* RP42C (Spanish Type Culture
113 Collection, CECT 20922) and *Aspergillus flavus* CECT 2687 were used to carry out the
114 tests. The latter produced aflatoxin in an intermediate moisture food (Bernáldez et al.,
115 2014)

116 **2.2 PgAFP Purification**

117 *P. chrysogenum* CECT 20922 was grown in potato dextrose broth (PDB, Scharlab,
118 Barcelona, Spain) pH 4.5, at 25 °C for 21 days without shaking. Mycelium was
119 removed, the culture medium was filtered to get cell-free medium and PgAFP was
120 obtained by fast protein liquid chromatography as previously described (Acosta et al.,
121 2009; Rodríguez-Martín et al. 2010). Briefly, the cell-free medium was
122 chromatographed on cationic and gel filtration columns, and the extracts containing
123 purified PgAFP were pooled from several batches. The protein concentration was
124 quantified by the Lowry method (Lowry et al., 1951) and the stock solution was diluted

125 in the elution buffer to the desired active concentration range (1.17-75 µg/mL) for the
126 various assays.

127 **2.3 Proteomics**

128 **2.3.1 Protein extraction.**

129 *A. flavus* CECT 2687 was cultured in triplicates in 50 mL PDB supplemented with 0.1
130 M of CaCl₂, at 25 °C for 24 h with shaking at 200 rpm in either presence (10 µg/mL) or
131 absence of PgAFP, similarly as previously described to compare the effect of the same
132 PgAFP concentration in *A. flavus* with no calcium added (Delgado et al., 2015b).
133 Mycelium was harvested, filtered, washed, and lysed as described by Carberry et al.
134 (2006). The lysed mycelia were centrifuged (10,000g; 30 min), the supernatant was
135 precipitated with trichloroacetic acid/acetone (Carpentier et al., 2005), and analysed by
136 the two following methods as previously described by (Delgado et al., 2015b).

137 **2.3.2 Two-dimensional PAGE.**

138 Resuspended extracts containing 250 µg of protein were loaded onto Immobiline Dry
139 strips (IPG strip; Amersham Biosciences, Uppsala, Sweden) in the pH range 4–7,
140 followed by electrofocusing, and electrophoresis using the ProteanXi-II Cell (Bio-Rad
141 Laboratories) as described by Carberry et al. (2006). Resulting gels (n=5) were stained
142 with colloidal Coomassie Blue (Sigma-Aldrich, St. Louis, MO, USA), scanned,
143 normalized and analysed using ProgenesisTM SameSpot software (TotalLab, Newcastle,
144 UK).

145 Protein spots showing differences ($p \leq 0.05$, fold change ≥ 1.5) were excised, destained,
146 sonicated, dehydrated, and trypsin in-gel digested according to Shevchenko et al.
147 (2006). Then, the digested supernatant was dried using a DNA Speed Vac Concentrator
148 (Thermo Fischer Scientific, Austin, TX, USA), resuspended in 0.1% formic acid (20
149 µL), and filtered through 0.22 µm cellulose spin-filters (Agilent Technologies, Ireland).
150 The samples were analysed by a 6340 Model Ion Trap LC-Mass Spectrometer (Agilent
151 Technologies, Ireland) using electrospray ionisation on a Zorbax 300 SB C-18 Nano-
152 HPLC Chip (150 mm x 75 µm). The eluted peptides were ionized and analysed by mass
153 spectrometry. MSⁿ analysis was carried out on the three most abundant peptide
154 precursor ions at each time point, as selected automatically by the mass spectrometer.
155 MASCOT MS/MS Ion search, NCBI (National Centre for Biotechnology Information)
156 database, FungiFun (Priebe et al., 2011) and KEGG (Kyoto Encyclopedia of Genes and
157 Genome, www.genome.jp/kegg/) were used for protein identification and functional
158 characterisation.

2.3.3 Label-free comparative quantitative proteomic analysis.

159 The protein precipitated lysates were resuspended in 8 M urea, reduced with
160 dithiothreitol and alkylated with iodoacetic acid (Owens et al., 2014). Samples digested
161 with trypsin combined with ProteaseMax surfactant were desalted prior to analysis
162 using C18 ZipTips® (Millipore, Darmstadt, Germany). One µg of every peptide
163 mixture was analysed via a Thermo Scientific Q-Exactive mass spectrometer coupled to
164 a Dionex RSLCnano. LC gradients ran from 4-35% B (A: 0.1% formic acid, B: 80%
165 acetonitrile, 0.1% formic acid) over 2 h, and data was collected using a Top15 method
166 for MS/MS scans (Dolan et al., 2014; O’Keeffe et al., 2014; Owens et al., 2015).
167 Comparative proteome abundance and data analysis was performed using MaxQuant
168 software (Version 1.3.0.5) (Cox and Mann, 2008), with Andromeda used for database
169 searching and Perseus (Version 1.4.1.3) used to organise the data.
170 Carbamidomethylation of cysteines was set as a fixed modification, while oxidation of
171 methionines and acetylation of N-terminals were set as variable modifications. The
172 maximum peptide/protein false discovery rates were set to 1%. The LFQ algorithm was
173 used to generate normalised spectral intensities and infer relative protein abundance
174 (Luber et al., 2010). Proteins that matched to a contaminants database or the reverse
175 database were removed and proteins were only retained in final analysis if detected in at
176 least two replicates from at least one treatment group. Quantitative analysis was
177 performed using a *t*-test to compare pairs of samples, and proteins with significant
178 change in abundance (p value ≤ 0.05 ; fold change ≥ 2) were included in the quantitative
179 results. Qualitative analysis was also performed, to detect proteins that were found in at
180 least 2 replicates of a particular treatment, but undetectable in the comparison sample
181 group.

2.4 Effect of cations on PgAFP activity

184 The growth of PgAFP-treated *A. flavus* was evaluated on microtiter plates (DeltaLab,
185 Rubí, Spain), containing 200 µL of PDB supplemented with 0.1M and 0.01M CaCl₂ and
186 10⁵ conidia per well incubated at 25 °C without shaking. An additional plate containing
187 only PDB was set as a control. Seven different two-fold dilutions of PgAFP, from 75 to
188 1.17 µg/mL, and a non-treated control were assayed. Optical density was measured at
189 550 nm every 24 h during 96 h in a microplate reader (TECAN Infinite M2000,
190 Männendorf, Switzerland). Additionally, to test the effect of the monovalent KCl and
191 the divalent MgCl₂, two different plates were evaluated following the same procedure

192 described in this paragraph, and containing 0.01 and 0.1 M of KCl or MgCl₂. These
193 cation concentrations were chosen as those present in cheeses (Chekri et al., 2012).

194 Given that 0.1 M CaCl₂ was the concentration that abolished PgAFP antifungal ability
195 and this concentration is well within in the cheese composition, the following assays
196 were carried out using this concentration. Additionally, all the following tests were also
197 carried out with *A. flavus* grown in PDB with no calcium added as controls. All the
198 micrographs from the same assay were taken with the same exposure.

199 **2.5 Metabolic tests**

200 To study the effect of CaCl₂ on the metabolism of PgAFP-treated *A. flavus*, the
201 following tests were carried out according to Delgado et al. (2015b). *A. flavus* was
202 cultured in PDB supplemented with 0.1 M CaCl₂ in either presence (75 µg/mL, to
203 maximise the potential effect of this antifungal protein) or absence of PgAFP at 25 °C
204 for 24 h without shaking. Additionally, to test the effect on membrane permeability on a
205 whole range of PgAFP and calcium concentrations, the seven PgAFP two-fold dilutions
206 from 75 to 1.17 µg/mL as well as 0.1 M and 0.01 M CaCl₂ were assayed.

207 To assess membrane permeability, *A. flavus* grown in microtiter plates with different
208 CaCl₂ and PgAFP concentrations were supplemented with 0.2 µM SYTOX Green
209 (Molecular Probes, Eugene, OR, USA). The emitted fluorescence was measured at 10,
210 30, and 210 min.

211 To study the metabolic capability through viability staining, mycelia were washed with
212 10 mM HEPES (pH 7.5) before staining with 100 µL FUN-1 (Molecular Probes) for 30
213 min at 25 °C according to Kaiserer et al. (2003). Stained hyphae were examined and
214 photographed by fluorescence microscopy.

215 Induction of ROS production was evaluated by incubating the grown hyphae with 20
216 µM 2', 7' dichlorofluorescein diacetate (Molecular Probes) for 2 h at 25 °C, and
217 observed by fluorescence microscopy.

218 Membrane integrity was assessed with acridine orange/ethidium bromide (AO/EB)
219 double staining (Sigma-Aldrich). *A. flavus* cultures were stained with 4 µg/mL of
220 AO/EB, incubated 30 min and washed twice with PBS to be observed by fluorescence
221 microscopy.

222 To detect apoptotic events, grown mycelia were stained with Apoptosis Detection Kit
223 (Sigma-Aldrich) composed by Annexin V-fluorescein isothiocyanate/propidium iodide
224 (AnV-FITC/PI), according to manufacturer's instructions.

225

2.6 Chitin staining

Conidia of *A. flavus* were inoculated in 10 mL PDB in a Petri dish containing a coverglass (Harris et al., 1994) and incubated at 25 °C for 24 h in the presence (75 µg/mL) and absence of PgAFP. Mycelia were washed, fixed and stained with fluorescent brightener 28 (Sigma-Aldrich) to visualize chitin in a fluorescence microscopy as previously described (Delgado et al., 2015b). Additional batches with no CaCl₂ added were also run as controls.

2.7 Localization of FITC-labelled PgAFP

PgAFP was labelled by DareBio S.L. (Elche, Spain), as previously described (Delgado et al., 2015b). *A. flavus* was grown in PDB in presence of 20 µg/mL PgAFP-FITC for 24 h at 25 °C. Hyphae were washed twice with PBS and visualized by fluorescence microscopy.

2.8 Effect of PgAFP on *A. flavus* in cheese

One cm thick wedges of commercial Gouda type cheese of 10 cm² were dipped in ethanol and dried in a laminar flow cabinet (Bio Flow II, Telstar, Tarrasa, Spain). The wedges were separately placed in pre-sterilized containers after vapour-liquid equilibrium with a saturated KCl solution, to reach a_w values of 0.84 similar to those at the final stage of cheese ripening. Next, PgAFP was added in 200 µL PBS to treated samples at two concentrations (18 and 35 µg/cm²) and left to dry in a flow cabinet. The non-treated batch received the same volume of PBS but with no PgAFP. Then, a volume of 100 µL of a suspension of *A. flavus* spores was spread onto the upper surface of cheese wedges to reach *c.a.* 10⁵ conidia/cm². The containers were incubated for 96 h and growth of the resulting mycelia was assessed.

2.9 Statistical analysis.

Statistical analyses were performed with IBM SPSS v.22 (www-03.ibm.com/software/products/es/spss-stats-standard). Growth inhibition and membrane permeability data were tested for normality (Kolmogorov–Smirnov with Lilliefors correction) and homoscedasticity (Levene's test). These data were non-normally distributed, then mean values were compared using non-parametric Kruskal–Wallis test. To compare treatments in pairs, Mann–Whitney U test was applied ($p \leq 0.05$).

3. Results

3.1 Antifungal activity of PgAFP on cheese

To study the potential application of PgAFP against *A. flavus* in the dairy industry, the antifungal activity of 18 and 35 $\mu\text{g}/\text{cm}^2$ PgAFP was tested on cheese wedges incubated simulating common ripening conditions. Growth of *A. flavus* on cheese treated with any of the two PgAFP concentrations was exuberant (Fig. 1). Then, PgAFP did not affect *A. flavus* growth in cheese.

3.2 Effect of cations on PgAFP antifungal activity

The effect of calcium, magnesium, and potassium on PgAFP antifungal ability against *A. flavus* was studied in PDB cultures (Fig. 2). The maximum O.D. reached at 96 h in cultures without PgAFP was affected by KCl and CaCl_2 , being lower with KCl ($p \leq 0.05$) but higher with CaCl_2 ($p \leq 0.05$). Control cultures, with no cations added, confirmed that 18.75 $\mu\text{g}/\text{mL}$ PgAFP reduced *A. flavus* growth over 50% at 96 h. With either 0.01M (data not shown) or 0.1 M KCl, PgAFP antifungal activity was essentially unaffected. Similarly, 0.01 M MgCl_2 did not have a deep impact on PgAFP antifungal activity, whereas 0.1 M MgCl_2 lowered PgAFP effect, so that 50% growth inhibition was not reached at 96 h incubation even at the highest PgAFP concentration tested ($p > 0.05$). The strongest effect was obtained with CaCl_2 ; with 0.01 M CaCl_2 , 37.5 $\mu\text{g}/\text{mL}$ PgAFP was required to reach 50% *A. flavus* growth inhibition at 96 h, but with 0.1 M CaCl_2 no growth inhibition was obtained even with 75 $\mu\text{g}/\text{mL}$ PgAFP ($p > 0.05$).

3.3 PgAFP localization and membrane permeability

Given that 0.1 M CaCl_2 abolished PgAFP antifungal activity, and this concentration is well within the range of calcium levels in ripened cheese (Chekri et al., 2012), only CaCl_2 was tested for the remaining assays. To know whether calcium influences PgAFP localization, *A. flavus* grown in PDB supplemented with 0.1 M CaCl_2 was treated with FITC-labelled PgAFP. The FITC-labelled PgAFP was visualized bound to the outer layer of *A. flavus* hyphae, but it was not able to penetrate into the cytoplasm (Fig. 3). The antifungal activity of FITC-labelled PgAFP was checked against *A. flavus* in CaCl_2 -free PDB, showing similar levels to those of non FITC-labelled PgAFP (data not shown).

To assess the influence of CaCl_2 on *A. flavus* permeabilization by PgAFP, the SYTOX Green uptake test was used. With no calcium added, fluorescence values increased as PgAFP concentration increased from 0 to 4.69 $\mu\text{g}/\text{mL}$ ($p \leq 0.05$) and then progressively decreased from 9.38 to 75 $\mu\text{g}/\text{mL}$ (Fig. 4), similarly to previous results (Delgado et al.,

294 2015b). With 0.01 M CaCl₂, a slightly higher PgAFP concentration (18.75 µg/mL) was
295 required to reach the highest fluorescence values reached at 4.69-9.38 µg/mL PgAFP in
296 the control batch without CaCl₂. In addition, the decrease of fluorescence obtained at
297 the highest PgAFP concentrations (37.5-75 µg/mL) with 0.01 M CaCl₂ was even more
298 pronounced than that obtained with 0 or 0.1 M CaCl₂. Therefore, *A. flavus* permeability
299 was strongly increased by either PgAFP or 0.1 M CaCl₂. However, PgAFP at any
300 concentration barely increased *A. flavus* permeability in 0.1 M CaCl₂ PDB (Fig. 4).

301 **3.4 Effect of PgAFP in presence of calcium on protein profile**

302 No differences ($p > 0.05$) in *A. flavus* mycelia weigh were noticed between PgAFP-
303 treated and untreated samples grown in PDB supplemented with 0.1 M CaCl₂. , 2D-
304 PAGE comparative proteomic analysis revealed 19 unique proteins from 24 spots,
305 whose relative abundance was altered in treated samples (Supplementary material Table
306 S1). In the PgAFP-treated batch, the relative abundance was from 1.5 to 1.6 fold higher
307 for 7 proteins including G-protein complex β subunit CpcB, whilst 12 proteins,
308 identified from 17 spots were found between 1.6 and 2.5 fold lower. Among proteins
309 found in reduced quantities, three isoforms of elongation factor 3, and two isoforms
310 each of aminopeptidase putative, glycogen branching enzyme GbeA putative, and
311 aldehyde dehydrogenase AldA putative were identified. The two spots found from the
312 last protein have different molecular masses and charges, possibly due to breakdown
313 and side-chain deamination.

314 The label-free quantitative analysis in PDB supplemented with 0.1 M CaCl₂ revealed a
315 total of 1651 proteins, 195 of them showed altered relative abundance due to PgAFP-
316 treatment (Supplementary material Table S2). A total of 125 proteins were detected in
317 higher amount in PgAFP-treated *A. flavus*. Among them, 90 proteins were found in a
318 higher concentration, from 2 to 53 fold, and 35 proteins were exclusively detected in the
319 treated batch. In addition, 70 proteins were detected in lower amount in PgAFP-treated
320 samples, 32 of them were found in lower abundance, from 2.1 to 703 fold, and the 38
321 remaining were not detected in the treated batch.

322 According to KEGG, 13 out of the 70 proteins found in lower amount following PgAFP
323 treatment were involved in metabolic pathways and biosynthesis of secondary
324 metabolites. In contrast, among the proteins whose abundance was higher in PgAFP-
325 treated *A. flavus*, 23 of them were related with ribosome and 11 with spliceosome. From
326 the proteins of the oxidative stress-related glutathione metabolism, glutathione S
327 transferase GliG-like and γ -glutamyltranspeptidase (γ GT) showed higher relative

328 abundance in PgAFP-treated samples (Supplementary material Table S2). In addition,
329 G-protein complex β subunit CpcB recently described as related to the mechanism of
330 action of antifungal proteins (Delgado et al., 2015b), was also increased in PgAFP
331 treated samples (Supplementary material Table S1).

332 All 19 proteins showing relative abundance altered in 2D-PAGE were found in the
333 label-free proteomic assay, but showing different fold change in both methods.

334 **3.5 Effect on metabolic capability and chitin deposition**

335 The metabolic capability of *A. flavus* grown with 0.1 M of CaCl₂ was not influenced by
336 PgAFP, as shown by FUN-1 staining. Intravacuolar red spots were present in both
337 PgAFP-treated and non-treated batches, revealing a normal metabolic capability (Fig.
338 5).

339 Chitin deposition has been described as a successful response against PgAFP in
340 resistant *P. polonicum* (Delgado et al., 2015c). Staining with fluorescent brightener 28
341 showed that 0.1 M CaCl₂ made no difference to chitin deposition in non PgAFP-treated
342 *A. flavus* (Fig. 6). However, 0.1 M CaCl₂ prevented the decreased chitin deposition
343 provoked by PgAFP, keeping a similar level to that observed in the non PgAFP-treated
344 control. As expected, PgAFP-treated controls with no calcium added displayed
345 alterations (Fig. 5 and 6), but non-treated *A. flavus* remaining unaltered.

346 **3.6 Effect on oxidative status and viability**

347 Given that oxidative stress is commonly induced by antifungal proteins in sensitive
348 species, the influence of calcium on ROS generation in *A. flavus* by PgAFP was
349 explored by 2', 7' dichlorofluorescein diacetate staining. Both PgAFP-treated and non-
350 treated hyphae showed a very weak green halo, indicating a low level of intracellular
351 ROS (data not shown).

352 Hyphae viability and apoptotic or necrotic processes of *A. flavus* grown in 0.1 M CaCl₂
353 PDB were studied with AO/EB double staining and AnV-FITC/PI staining,
354 respectively. The AO/EB double staining showed a predominant green colour both in
355 PgAFP-treated and untreated samples due to AO but not EB staining (Fig. 7). This
356 implies that 0.1 M CaCl₂ made it possible that PgAFP-treated *A. flavus* remained viable.
357 Moreover, both treated and non-treated batches were not stained by AnV-FITC/PI (Fig.
358 8), implying that PgAFP did not induce apoptosis or necrosis in cultures containing 0.1
359 M CaCl₂. As expected, PgAFP-treated controls with no calcium added displayed
360 alterations (Fig. 7 and 8), whilst non-treated *A. flavus* remained unaltered.

361

4. Discussion

The efficacy of just 5 $\mu\text{g}/\text{cm}^2$ PgAFP to reduce *A. flavus* counts was demonstrated on dry-fermented sausage (Delgado et al., 2015a). Such effect would also be useful in ripened cheese, but the high calcium levels might interfere with PgAFP activity. The treatment with PgAFP was not effective in reducing *A. flavus* growth on cheese (Fig. 1). Both dry-fermented sausage and cheese assays were run under identical environmental conditions of 25 °C and keeping constant relative humidity by means of a saturated KCl solution (Delgado et al., 2015a). Environmental factors such as pH or NaCl concentration may affect PgAFP antifungal activity. However this activity appears not to be affected by monovalent cations, and withstands a broad range of pH values (Delgado et al., 2015a). Given that the PgAFP concentrations tested on cheese were up to 7-fold higher than that effective on the sausage, the lack of PgAFP activity has to be related to cheese composition. Other researchers have proved that over 20-100 mM mono- and divalent cations suppress the inhibitory activity of other antifungal proteins in culture media (Galgóczy et al., 2013a; Kaiserer et al., 2003; Theis et al., 2003; Thevissen et al., 1999, 1996). Average calcium, magnesium, and potassium concentrations in cheese are *c.a.* 0.14, 0.013, and 0.03 M, respectively (Chekri et al., 2012). Given that these concentrations are higher than those suppressing the activity of other antifungal proteins, the effect of each of these minerals on PgAFP activity against *A. flavus* was investigated.

The antifungal capability of all concentrations of PgAFP tested against *A. flavus* in PDB was strongly reduced with 0.1 M CaCl_2 or MgCl_2 (Fig. 2), whereas only the effect of low PgAFP concentrations was prevented with 0.01 M concentrations of these divalent cations. For the monovalent potassium salt, 0.01 and 0.1 M only slightly reduced PgAFP antifungal activity. These results support that the lack of activity of PgAFP on *A. flavus* observed in cheese could be explained solely by the calcium content.

Similar results have been reported for AFP, PAF, NFAP, and plant defensins, where the antifungal activity was significantly counteracted in presence of high concentrations of monovalent cations or MgCl_2 (Galgóczy et al., 2013a; Kaiserer et al., 2003; Theis et al., 2003; Thevissen et al., 1999). This loss of antifungal activity has been explained by a saturation of the cellular target of antifungal proteins with cations, making the target site no longer accessible for the antifungal protein (Theis et al., 2003). Small, basic, and cysteine-rich antifungal proteins from moulds have positive net charge, and cations

395 could interfere by competing for putative binding sites at the fungal cell surface
396 (Martín-Urdiroz et al., 2009; Marx, 2004).

397 FITC-labelled PgAFP was located both bound to outer layer and intracellularly in *A.*
398 *flavus* grown in PDB with no CaCl₂ added (Delgado et al., 2015b). However, when *A.*
399 *flavus* was grown in 0.1 M CaCl₂ PDB, FITC-labelled PgAFP was only found at the
400 outer layer but not internalized (Fig. 3), implying that membrane permeability was not
401 compromised. When grown in 0.1 M CaCl₂ PDB, *A. flavus* permeability to SYTOX
402 Green increased to the maximum level provoked by PgAFP with no calcium added (Fig.
403 4), similarly to the pattern obtained in *A. niger* with 1 M CaCl₂ (Gomaa et al., 2013).
404 When *A. flavus* was grown with both PgAFP and 0.1 M CaCl₂, no further increase in
405 permeability was observed. Thus, all the above results support that calcium ions did not
406 prevent PgAFP from binding the outer layer. Moreover, no other detrimental effect was
407 observed in *A. flavus* at any PgAFP concentration through ROS levels and metabolic
408 capability or viability, as evaluated by FUN-1, AO/EB, and AnV-FITC/PI staining.
409 Therefore, calcium might have rendered the putative membrane targets non-accessible
410 to PgAFP. Nonetheless, comparative proteomics disclosed remarkable changes in
411 fungal metabolism triggered by PgAFP when grown in 0.1 M CaCl₂ PDB.

412 A total of 19 and 195 proteins showed altered relative abundances by CaCl₂ according
413 to 2D-PAGE and label-free proteomics, respectively. The discrepancies between the
414 number of proteins obtained by these two methods have been explained as a
415 consequence of 2D-PAGE being able to separate isoforms and post translational
416 modifications but only within a limited pH range, whereby the whole proteome is not
417 represented (Görg et al., 2009, 2004). In contrast, label-free proteomics is not able to
418 separate isoforms and compares the total quantity of the protein, but has a higher
419 coverage with regard to pH and molecular mass range. Hence, the discrepancies
420 observed in relation to the fold change for any given protein seem to be related to the
421 involvement of isoforms or post-translational modifications, as well as the different
422 threshold used by both methods (Delgado et al., 2015b, 2015c).

423 The comparative proteomic assays for *A. flavus* in presence of CaCl₂ revealed a large
424 number of proteins affected by PgAFP exposure. According to KEGG, proteins related
425 with ribosome and spliceosome accounted for the 27% of the proteins with altered
426 relative amount. The relative quantities for most proteins of these two groups were
427 higher in PgAFP-treated samples. Similar results were obtained for ribosomal and
428 spliceosomal proteins when PgAFP was applied to cultures grown in absence of CaCl₂

429 of both *A. flavus* (Delgado et al., 2015b) and the PgAFP-resistant *P. polonicum*
430 (Delgado et al., 2015c). Given that the increase of these two groups of proteins is a
431 common response to PgAFP in both sensitive and resistant moulds, it does not seem to
432 be crucial to discriminate when inhibition is overcome.

433 The mechanism of action of antifungal proteins has been described through different
434 interrelated metabolic pathways, including oxidative stress, cell wall integrity (CWI)
435 pathway, and chitin synthesis (Delgado et al., 2015b; Hagen et al., 2007; Marx et al.,
436 2008). Some proteins involved in these pathways showed higher relative abundance in
437 response to PgAFP in *A. flavus* grown in 0.1 M CaCl₂ PDB, including G-protein
438 complex β subunit CpcB, and proteins of the oxidative stress-related glutathione
439 pathway, namely glutathione S-transferase GliG-like and γ -glutamyltranspeptidase
440 (γ GT). These proteome changes would rule out the blockage of PgAFP receptors in *A.*
441 *flavus* when grown in presence of CaCl₂, suggesting a survival reaction of *A. flavus* to
442 the antifungal protein as discussed below.

443 No significant differences were found in the protein Rho GTPase Rho1 between
444 PgAFP-treated and untreated *A. flavus* grown with 0.1M CaCl₂ (Supplementary material
445 Table S2). Lower Rho1 levels have been identified among the main factors involved in
446 the inhibition of *A. flavus* by PgAFP in PDB with no CaCl₂ added (Delgado et al.,
447 2015b), whereas higher levels of Rho1 play a key role increasing chitin deposition in
448 PgAFP-treated *P. polonicum*, likely activating Pkc/Mpk pathway (Delgado et al.,
449 2015c). The unaltered chitin deposition in PgAFP-treated *A. flavus* grown with CaCl₂
450 (Fig. 6) can be related by the substantially unaffected quantity of Rho1 and any other
451 protein related to the CWI pathway. This relationship has been demonstrated for
452 PgAFP-treated moulds, with a decreased chitin deposition attributed to the lower
453 relative amount of Rho1 in *A. flavus* (Delgado et al., 2015b), and an increased chitin
454 deposition related to a higher relative amount of Rho1 in *P. polonicum* (Delgado et al.,
455 2015c). High calcium levels *per se* did not increase chitin deposition in cultures without
456 PgAFP (Fig. 6) Extracellular calcium can act as a stress signal in moulds that increases
457 the intracellular Ca²⁺ concentration and leads to the activation of calmodulin, which in
458 turn can activate calcineurin (Thewes, 2014). Calcineurin is a heterodimer comprised of
459 subunits A and B. Calcineurin Ca²⁺-binding regulatory subunit CnaB is essential for
460 activation of the calcineurin A (calmodulin-binding catalytic subunit CnaA) that is
461 important in stress adaptation (Juvvadi et al., 2003). Calcineurin regulates the
462 transcription factor CRZ1A, that induces transcription of chitin synthases *chsA* and

463 chsC in filamentous fungi, but can also control chitin synthases themselves (Fortwendel
464 et al., 2010) or interact genetically with the endogenous calcineurin regulators,
465 calcipressins (Soriani et al., 2008) Activation of calmodulin-calcineurin signalling by
466 high cytosolic Ca²⁺ concentration leads to *A. fumigatus* growth in presence of antifungal
467 drugs (Juvvadi et al., 2015) The 0.1 M CaCl₂ level led to the higher relative abundance
468 of CnaB in both PgAFP-treated and untreated *A. flavus* (Supplementary material Table
469 S1) than with no calcium added (Delgado et al., 2015b). Thus, the protective effect of
470 high calcium levels in *A. flavus* can be mediated by increased CnaB.

471 G protein CpcB may also play a central role in vegetative growth and development, as
472 its deficiency severely impaired cellular growth in aspergilli (Kong et al., 2013). The
473 lower quantity of CpcB has been related to apoptosis signalling in PgAFP-treated *A.*
474 *flavus* (Delgado et al., 2015b). In the present work, the higher relative abundance of
475 CpcB subunit was accompanied by neither apoptotic nor necrotic signals in PgAFP-
476 treated *A. flavus* grown in 0.1 M CaCl₂. Therefore, CpcB can be considered a key factor
477 in promoting or arresting apoptotic events by PgAFP, leading to sensitivity or
478 resistance, respectively. The protective mechanism mediated by CpcB in *A. flavus*
479 grown with calcium seems to be based on the modulation of glutathione and ROS
480 levels.

481 From the proteins related with the oxidative stress, the most outstanding change derived
482 from PgAFP treatment in the present study was a higher relative abundance of GST
483 GliG-like and γ GT. The former does not seem to be involved in the resistance of *A.*
484 *flavus* to PgAFP in presence of high calcium levels, since GST GliG-like also increased
485 when the treatment was applied with no calcium added (Delgado et al., 2015b).
486 However, a lower relative amount of γ GT was observed in non-enriched calcium
487 medium, parallel to high ROS levels in *A. flavus* treated with PgAFP. γ GT has been
488 shown to be important in the maintenance of the redox status upon oxidative stress in
489 fungi (Kang et al., 2005; Park et al., 2005, 2004; Springael and Penninckx, 2003) Thus,
490 the higher γ GT relative abundance could be related to the successful response of *A.*
491 *flavus* to PgAFP in the calcium-enriched culture medium. No direct link between
492 increased calcium levels and γ GT induction can be established at present. However, it is
493 plausible that a primary adaptive response mediated by CnaB or CpcB allow the time
494 for *A. flavus* to develop an effective response to oxidative stress, leading to increased
495 γ GT levels. To overcome the protective role of divalent cations against antifungal

496 proteins, PgAFP treatment could be combined with other preservatives showing
497 complementary mechanisms of action. New studies with extended incubation time
498 would also help to assess the effect of PgAFP on mould growth and mycotoxin
499 production in ripened cheese.

500

501 **5. Conclusion**

502 This work gives the basis to rule out the hypothesis that divalent cations block specific
503 receptors for PgAFP. The obtained results demonstrate that *A. flavus* resistance to
504 PgAFP in 0.1 M CaCl₂ is mainly mediated by an increased CnaB, CpcB and γ GT,
505 enhancing the response to oxidative stress and impeding apoptosis. Understanding the
506 mechanism of resistance against PgAFP can be useful to design strategies aiming to
507 prevent growth of mycotoxigenic moulds in foods with high levels of divalent cations.

508

509 **Aknowledgements**

510 This work was supported by the Spanish Ministry of Education and Science, Ministry of
511 Economy and Competitiveness and FEDER (AGL2010-21623, AGL2013-45729-P).
512 Josué Delgado was recipient of FPI grants from the Spanish Ministry of Education and
513 Science (BES-2011-043422 and EEBB-I-13-06900). Rebecca A. Owens was funded by
514 a 3U Partnership Award (<http://www.3UPartnership.ie/>). Mass spectrometry facilities
515 were funded by Science Foundation Ireland (Q-Exactive; 12/RI/2346(3) & PI/11/1188)
516 and the Irish Higher Education Authority (Agilent Ion Trap 6340). The authors declare
517 no conflicts of interest in this work.

518

519 **References**

- 520 Acosta, R., Rodríguez-Martín, A., Martín, A., Núñez, F., Asensio, M.A., 2009.
521 Selection of antifungal protein-producing molds from dry-cured meat products. Int.
522 J. Food Microbiol. 135, 39–46. doi:10.1016/j.ijfoodmicro.2009.07.020
- 523 Binder, U., Bencina, M., Eigentler, A., Meyer, V., Marx, F., 2011. The *Aspergillus*
524 *giganteus* antifungal protein AFPNN5353 activates the cell wall integrity pathway
525 and perturbs calcium homeostasis. BMC Microbiol. 11, 209. doi:10.1186/1471-
526 2180-11-209
- 527 Binder, U., Chu, M., Read, N.D., Marx, F., 2010a. The antifungal activity of the
528 *Penicillium chrysogenum* protein PAF disrupts calcium homeostasis in *Neurospora*
529 *crassa*. Eukaryot. Cell 9, 1374–1382. doi:10.1128/EC.00050-10

- 530 Cagas, S.E., Jain, M.R., Li, H., Perlin, D.S., 2011. Profiling the *Aspergillus fumigatus*
531 proteome in response to caspofungin. *Antimicrob. Agents Chemother.* 55, 146–
532 154. doi:10.1128/AAC.00884-10
- 533 Carberry, S., Neville, C.M., Kavanagh, K.A., Doyle, S., 2006. Analysis of major
534 intracellular proteins of *Aspergillus fumigatus* by MALDI mass spectrometry:
535 identification and characterisation of an elongation factor 1B protein with
536 glutathione transferase activity. *Biochem. Biophys. Res. Commun.* 341, 1096–
537 1104. doi:10.1016/j.bbrc.2006.01.078
- 538 Carpentier, S.C., Witters, E., Laukens, K., Deckers, P., Swennen, R., Panis, B., 2005.
539 Preparation of protein extracts from recalcitrant plant tissues: an evaluation of
540 different methods for two-dimensional gel electrophoresis analysis. *Proteomics* 5,
541 2497–2507. doi:10.1002/pmic.200401222
- 542 Chekri, R., Noël, L., Millour, S., Vastel, C., Kadar, A., Sirot, V., Leblanc, J.C., Guérin,
543 T., 2012. Calcium, magnesium, sodium and potassium levels in foodstuffs from the
544 second French Total Diet Study. *J. Food Compos. Anal.* 25, 97–107.
545 doi:10.1016/j.jfca.2011.10.005
- 546 Chen, Z., Ao, J., Yang, W., Jiao, L., Zheng, T., Chen, X., 2013. Purification and
547 characterization of a novel antifungal protein secreted by *Penicillium chrysogenum*
548 from an Arctic sediment. *Appl. Microbiol. Biotechnol.* 97, 10381–10390.
549 doi:10.1007/s00253-013-4800-6
- 550 Cox, J., Mann, M., 2008. MaxQuant enables high peptide identification rates,
551 individualized p.p.b.-range mass accuracies and proteome-wide protein
552 quantification. *Nat. Biotechnol.* 26, 1367–1372. doi:10.1038/nbt.1511
- 553 Delgado, J., Acosta, R., Rodríguez-Martín, A., Bermúdez, E., Núñez, F., Asensio, M.
554 A., 2015a. Growth inhibition and stability of PgAFP from *Penicillium*
555 *chrysogenum* against fungi common on dry-ripened meat products. *Int. J. Food*
556 *Microbiol.* 205, 23–29. doi:10.1016/j.ijfoodmicro.2015.03.029
- 557 Delgado, J., Owens, R.A., Doyle, S., Asensio, M.A., Núñez, F., 2015b. Impact of the
558 antifungal protein PgAFP from *Penicillium chrysogenum* on the protein profile in
559 *Aspergillus flavus*. *Appl. Microbiol. Biotechnol.* 99, 8701–8715.
560 doi:10.1007/s00253-015-6731-x
- 561 Delgado, J., Owens, R.A., Doyle, S., Asensio, M.A., Núñez, F., 2015c. Increased chitin
562 biosynthesis contributes to the resistance of *Penicillium polonicum* against the
563 antifungal protein PgAFP. *Appl. Microbiol. Biotechnol.* In press. doi:
564 10.1007/s00253-015-7020-4
- 565 Dolan, S.K., Owens, R.A., O’Keeffe, G., Hammel, S., Fitzpatrick, D.A., Jones, G.W.,
566 Doyle, S., 2014. Regulation of nonribosomal peptide synthesis: bis-

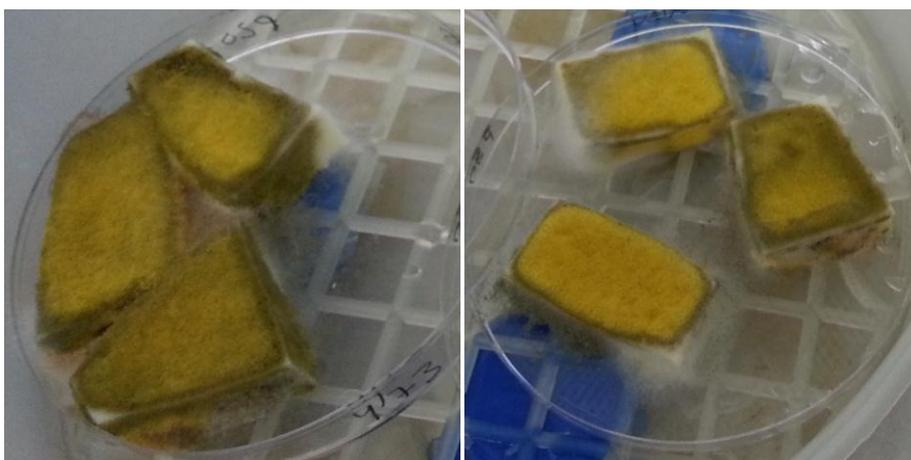
- 567 thiomethylation attenuates gliotoxin biosynthesis in *Aspergillus fumigatus*. Chem.
568 Biol. 21, 999–1012. doi:10.1016/j.chembiol.2014.07.006
- 569 Fortwendel, J.R., Juvvadi, P.R., Perfect, B.Z., Rogg, L.E., Perfect, J.R., Steinbach, W.J.,
570 2010. Transcriptional regulation of chitin synthases by calcineurin controls
571 paradoxical growth of *Aspergillus fumigatus* in response to caspofungin.
572 Antimicrob. Agents Chemother. 54, 1555–1563. doi:10.1128/AAC.00854-09
- 573 Galgóczy, L., Kovács, L., Karácsony, Z., Virágh, M., Hamari, Z., Vágvölgyi, C., 2013a.
574 Investigation of the antimicrobial effect of *Neosartorya fischeri* antifungal protein
575 (NFAP) after heterologous expression in *Aspergillus nidulans*. Microbiology 159,
576 411–419. doi:10.1099/mic.0.061119-0
- 577 Galgóczy, L., Virágh, M., Kovács, L., Tóth, B., Papp, T., Vágvölgyi, C., 2013b.
578 Antifungal peptides homologous to the *Penicillium chrysogenum* antifungal
579 protein (PAF) are widespread among Fusaria. Peptides 39, 131–137.
580 doi:10.1016/j.peptides.2012.10.016
- 581 Gautam, P., Shankar, J., Madan, T., Sirdeshmukh, R., Sundaram, C.S., Gade, W.N.,
582 Basir, S.F., Sarma, P.U., 2008. Proteomic and transcriptomic analysis of
583 *Aspergillus fumigatus* on exposure to amphotericin B. Antimicrob. Agents
584 Chemother. 52, 4220–7. doi:10.1128/AAC.01431-07
- 585 Gomaa, O.M., Selim, N.S., Linz, J.E., 2013. Biochemical and biophysical response to
586 calcium chloride stress in *Aspergillus niger* and its role in malachite green
587 degradation. Cell Biochem. Biophys. 65, 413–423. doi:10.1007/s12013-012-9444-
588 0
- 589 Görg, A., Drews, O., Lück, C., Weiland, F., Weiss, W., 2009. 2-DE with IPGs.
590 Electrophoresis 30 Suppl 1, S122–S132. doi:10.1002/elps.200900051
- 591 Görg, A., Weiss, W., Dunn, M.J., 2004. Current two-dimensional electrophoresis
592 technology for proteomics. Proteomics 4, 3665–85. doi:10.1002/pmic.200401031
- 593 Hagen, S., Marx, F., Ram, A.F., Meyer, V., 2007. The antifungal protein AFP from
594 *Aspergillus giganteus* inhibits chitin synthesis in sensitive fungi. Appl. Environ.
595 Microbiol. 73, 2128–2134. doi:10.1128/AEM.02497-06
- 596 Hajji, M., Jellouli, K., Hmidet, N., Balti, R., Sellami-Kamoun, A., Nasri, M., 2010. A
597 highly thermostable antimicrobial peptide from *Aspergillus clavatus* ES1:
598 Biochemical and molecular characterization. J. Ind. Microbiol. Biotechnol. 37,
599 805–813. doi:10.1007/s10295-010-0725-6
- 600 Harris, S.D., Morrell, J.L., Hamer, J., 1994. Identification and characterization of
601 *Aspergillus nidulans* mutants defective in cytokinesis. Genetics 532, 517–532
- 602 Juvvadi, P.R., Kuroki, Y., Arioka, M., Nakajima, H., Kitamoto, K., 2003. Functional
603 analysis of the calcineurin-encoding gene *cnaA* from *Aspergillus oryzae*: evidence

- 604 for its putative role in stress adaptation. Arch. Microbiol. 179, 416–422.
605 doi:10.1007/s00203-003-0546-3
- 606 Juvvadi, P.R., Muñoz, A., Lamoth, F., Soderblom, E.J., Moseley, M.A., Read, N.D.,
607 Steinbach, W.J., 2015. Calcium-mediated induction of paradoxical growth
608 following caspofungin treatment is associated with calcineurin activation and
609 phosphorylation in *Aspergillus fumigatus*. Antimicrob. Agents Chemother. 59,
610 4946–4955. doi:10.1128/AAC.00263-15
- 611 Kaiserer, L., Oberparleiter, C., Weiler-Görz, R., Burgstaller, W., Leiter, E., Marx, F.,
612 2003. Characterization of the *Penicillium chrysogenum* antifungal protein PAF.
613 Arch. Microbiol. 180, 204–210. doi:10.1007/s00203-003-0578-8
- 614 Kang, H.-J., Kim, B.-C., Park, E.-H., Ahn, K., Lim, C.-J., 2005. The gene encoding
615 gamma-glutamyl transpeptidase II in the fission yeast is regulated by oxidative and
616 metabolic stress. J. Biochem. Mol. Biol. 38, 609–618.
617 doi:10.5483/BMBRep.2005.38.5.609
- 618 Kokkonen, M., Jestoi, M., Rizzo, A., 2005. Determination of selected mycotoxins in
619 mould cheeses with liquid chromatography coupled to tandem with mass
620 spectrometry. Food Addit. Contam. 22, 449–456.
621 doi:10.1080/02652030500089861
- 622 Kong, Q., Wang, L., Liu, Z., Kwon, N.-J., Kim, S.C., Yu, J.-H., 2013. Gβ-like CpcB
623 plays a crucial role for growth and development of *Aspergillus nidulans* and
624 *Aspergillus fumigatus*. PloS ONE 8, e70355. doi:10.1371/journal.pone.0070355
- 625 Kovács, L., Virágh, M., Takó, M., Papp, T., Vágvölgyi, C., Galgóczy, L., 2011.
626 Isolation and characterization of *Neosartorya fischeri* antifungal protein (NFAP).
627 Peptides 32, 1724–1731. doi:10.1016/j.peptides.2011.06.022
- 628 Lessing, F., Kniemeyer, O., Wozniok, I., Loeffler, J., Kurzai, O., Haertl, A., Brakhage,
629 A.A., 2007. The *Aspergillus fumigatus* transcriptional regulator AfYap1 represents
630 the major regulator for defense against reactive oxygen intermediates but is
631 dispensable for pathogenicity in an intranasal mouse infection model. Eukaryot.
632 Cell 6, 2290–2302. doi:10.1128/EC.00267-07
- 633 Lie, J.L., Marth, E.H., 1967. Formation of aflatoxin in cheddar cheese by *Aspergillus*
634 *flavus* and *Aspergillus parasiticus*. J. Dairy Sci. 50, 1708–1710. doi:S0022-
635 0302(67)87698-7 [pii]\r10.3168/jds.S0022-0302(67)87698-7
- 636 López-Díaz, T.M., Román-Blanco, C., García-Arias, M.T., García-Fernández, M.C.,
637 García-López, M.L., 1996. Mycotoxins in two Spanish cheese varieties. Int. J.
638 Food Microbiol. 30, 391–395
- 639 Lowry, O.H., Rosebrough, N.J., Farr, L., Randall, R.J., 1951. Protein measurement with
640 the folin phenol reagent. J. Biol. Chem. 193, 265–275

- 641 Luber, C.A., Cox, J., Lauterbach, H., Fancke, B., Selbach, M., Tschopp, J., Akira, S.,
642 Wiegand, M., Hochrein, H., O’Keeffe, M., Mann, M., 2010. Quantitative
643 proteomics reveals subset-specific viral recognition in dendritic cells. *Immunity*
644 32, 279–289. doi:10.1016/j.immuni.2010.01.013
- 645 Martín-Urdiroz, M., Martínez-Rocha, A.L., Pietro, A. Di, Martínez-del-Pozo, Á.,
646 Roncero, M.I.G., 2009. Differential toxicity of antifungal protein AFP against
647 mutants of *Fusarium oxysporum*. *Int. Microbiol.* 12, 115–121.
648 doi:10.2436/20.1501.01.88
- 649 Marx, F., 2004. Small, basic antifungal proteins secreted from filamentous ascomycetes:
650 a comparative study regarding expression, structure, function and potential
651 application. *Appl. Microbiol. Biotechnol.* 65, 133–142. doi:10.1007/s00253-004-
652 1600-z
- 653 Marx, F., Binder, U., Leiter, E., Pócsi, I., 2008. The *Penicillium chrysogenum*
654 antifungal protein PAF, a promising tool for the development of new antifungal
655 therapies and fungal cell biology studies. *Cell. Mol. Life Sci.* 65, 445–454.
656 doi:10.1007/s00018-007-7364-8
- 657 Marx, F., Haas, H., Reindl, M., Stöffler, G., Lottspeich, F., Redl, B., 1995. Cloning,
658 structural organization and regulation of expression of the *Penicillium*
659 *chrysogenum paf* gene encoding an abundantly secreted protein with antifungal
660 activity. *Gene* 167, 167–171
- 661 Nakaya, K., Omata, K., Okahashi, I., Nakamura, Y., Kolkenbrock, H., Ulbrich, N.,
662 1990. Amino acid sequence and disulfide bridges of an antifungal protein isolated
663 from *Aspergillus giganteus*. *Eur. J. Biochem.* 38, 32–38
- 664 Nelson, G., Kozlova-Zwinderman, O., Collis, A. J., Knight, M.R., Fincham, J.R.S.,
665 Stanger, C.P., Renwick, A., Hessing, J.G.M., Punt, P.J., Van Den Hondel,
666 C.A.M.J.J., Read, N.D., 2004. Calcium measurements in living filamentous fungi
667 expressing codon-optimized aequorin. *Mol. Microbiol.* 52, 1437–1450.
668 doi:10.1111/j.1365-2958.2004.04066.x
- 669 O’Keeffe, G., Hammel, S., Owens, R.A., Keane, T.M., Fitzpatrick, D.A., Jones, G.W.,
670 Doyle, S., 2014. RNA-seq reveals the pan-transcriptomic impact of attenuating the
671 gliotoxin self-protection mechanism in *Aspergillus fumigatus*. *BMC Genomics* 25,
672 1–26. doi:10.1186/1471-2164-15-894
- 673 Owens, R.A., Hammel, S., Sheridan, K.J., Jones, G.W., Doyle, S., 2014. A proteomic
674 approach to investigating gene cluster expression and secondary metabolite
675 functionality in *Aspergillus fumigatus*. *PloS ONE* 9, e106942. doi:
676 10.1371/journal.pone.0106942.g001
- 677 Owens, R.A., O’Keeffe, G., Smith, E.B., Dolan, S.K., Hammel, S., Sheridan, K.J.,
678 Fitzpatrick, D.A., Keane, T.M., Jones, G.W., Doyle, S., 2015. Interplay between

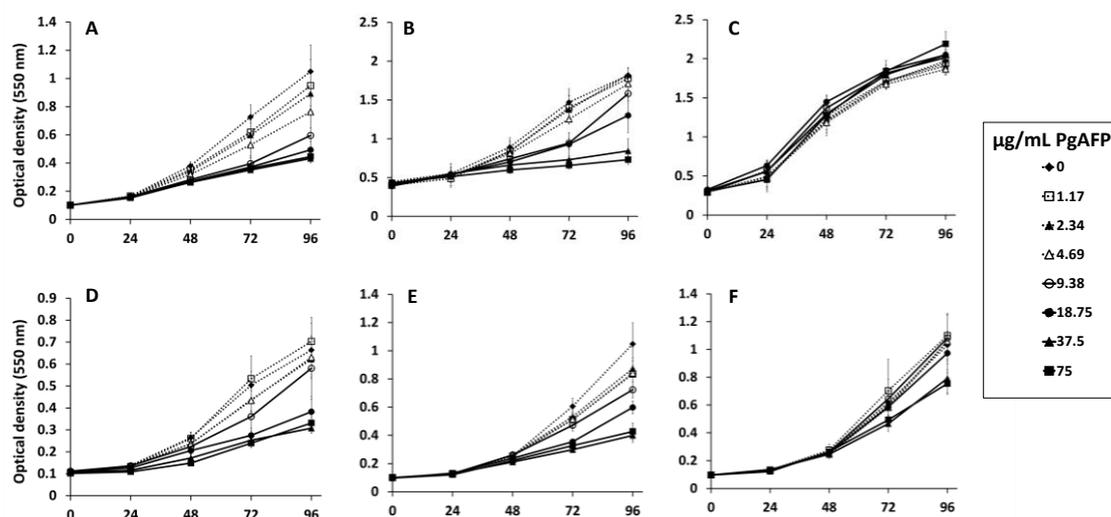
- 679 gliotoxin resistance, secretion, and the methyl/methionine cycle in *Aspergillus*
680 *fumigatus*. Eukaryot. Cell 14, 941–957. doi:10.1128/EC.00055-15
- 681 Park, H.-J., Lim, H.-W., Kim, K., Kim, I.-H., Park, E.-H., Lim, C.-J., 2004.
682 Characterization and regulation of the γ -glutamyl transpeptidase gene from the
683 fission yeast *Schizosaccharomyces pombe*. Can. J. Microbiol. 50, 61–67.
684 doi:10.1139/w03-106
- 685 Park, H.-J., Moon, J.-S., Kim, H.-G., Kim, I.-H., Kim, K., Park, E.-H., Lim, C.-J., 2005.
686 Characterization of a second gene encoding γ -glutamyl transpeptidase from
687 *Schizosaccharomyces pombe*. Can. J. Microbiol. 51, 269–275. doi:10.1139/w04-
688 137
- 689 Priebe, S., Linde, J., Albrecht, D., Guthke, R., Brakhage, A.A., 2011. FungiFun: A web-
690 based application for functional categorization of fungal genes and proteins.
691 Fungal Genet. Biol. 48, 353-358. doi:10.1016/j.fgb.2010.11.001
- 692 Rabilloud, T., Vaezzadeh, A.R., Potier, N., 2009. Power and limitations of
693 electrophoretic. Mass Spectrom. Rev. 28, 816–843. doi:10.1002/mas
- 694 Rodríguez-Martín, A., Acosta, R., Liddell, S., Núñez, F., Benito, M.J., Asensio, M. A.,
695 2010. Characterization of the novel antifungal protein PgAFP and the encoding
696 gene of *Penicillium chrysogenum*. Peptides 31, 541–547.
697 doi:10.1016/j.peptides.2009.11.002
- 698 Shevchenko, A., Tomas, H., Havlis, J., Olsen, J. V., Mann, M., 2006. In-gel digestion
699 for mass spectrometric characterization of proteins and proteomes. Nat. Protoc. 1,
700 2856–2860. doi:10.1038/nprot.2006.468
- 701 Skouri-Gargouri, H., Gargouri, A., 2008. First isolation of a novel thermostable
702 antifungal peptide secreted by *Aspergillus clavatus*. Peptides 29, 1871–1877.
703 doi:10.1016/j.peptides.2008.07.005
- 704 Soriani, F.M., Malavazi, I., Da Silva Ferreira, M.E., Savoldi, M., Von Zeska Kress,
705 M.R., De Souza Goldman, M.H., Loss, O., Bignell, E., Goldman, G.H., 2008.
706 Functional characterization of the *Aspergillus fumigatus* CRZ1 homologue, CrzA.
707 Mol. Microbiol. 67, 1274–1291. doi:10.1111/j.1365-2958.2008.06122.x
- 708 Spitzmüller, Z., Kwon, N.-J., Szilágyi, M., Keserű, J., Tóth, V., Yu, J.-H., Pócsi, I.,
709 Emri, T., 2014. γ -Glutamyl transpeptidase (GgtA) of *Aspergillus nidulans* is not
710 necessary for bulk degradation of glutathione. Arch. Microbiol. 197, 285–297.
711 doi:10.1007/s00203-014-1057-0
- 712 Springael, J.-Y., Penninckx, M.J., 2003. Nitrogen-source regulation of yeast gamma-
713 glutamyl transpeptidase synthesis involves the regulatory network including the
714 GATA zinc-finger factors Gln3, Nil1/Gat1 and Gzf3. Biochem. J. 371, 589–595.
715 doi:10.1042/BJ20021893

- 716 Theis, T., Wedde, M., Meyer, V., Stahl, U., 2003. The antifungal protein from
717 *Aspergillus giganteus* causes membrane permeabilization. Antimicrob. Agents
718 Chemother. 47, 588–593. doi:10.1128/AAC.47.2.588
- 719 Thevissen, K., Ghazi, a, De Samblanx, G.W., Brownlee, C., Osborn, R.W., Broekaert,
720 W.F., 1996. Fungal membrane responses induced by plant defensins and thionins.
721 J. Biol. Chem. 271, 15018–15025
- 722 Thevissen, K., Terras, F.R., Broekaert, W.F., 1999. Permeabilization of fungal
723 membranes by plant defensins inhibits fungal growth. Appl. Environ. Microbiol.
724 65, 5451–5458
- 725 Thewes, S., 2014. Calcineurin-Crz1 signaling in lower eukaryotes. Eukaryot. Cell 13,
726 694–705. doi:10.1128/EC.00038-14
- 727 Zhu, W., Smith, J.W., Huang, C.-M., 2010. Mass spectrometry-based label-free
728 quantitative proteomics. J. Biomed. Biotechnol. 2010, 1-6
729 doi:10.1155/2010/840518
- 730
- 731
- 732
- 733
- 734
- 735
- 736
- 737
- 738
- 739
- 740
- 741
- 742
- 743
- 744
- 745
- 746

747 **Figure captions**

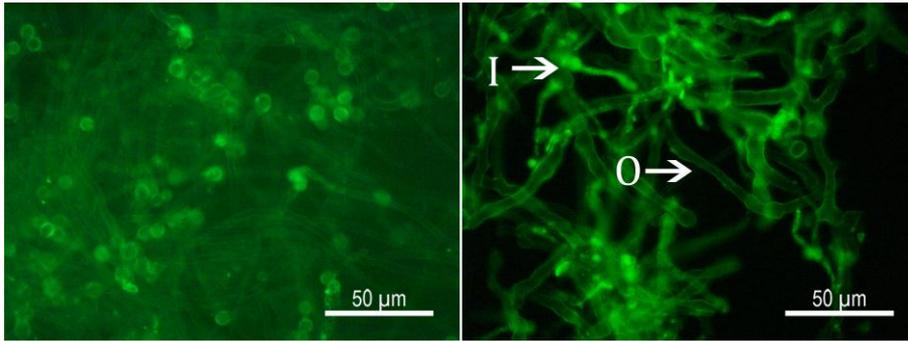
748

749 Figure 1. Exuberant growth of *A. flavus* in cheese wedges treated with 18 $\mu\text{g}/\text{cm}^2$ (left)
 750 and 35 $\mu\text{g}/\text{cm}^2$ PgAFP (right).



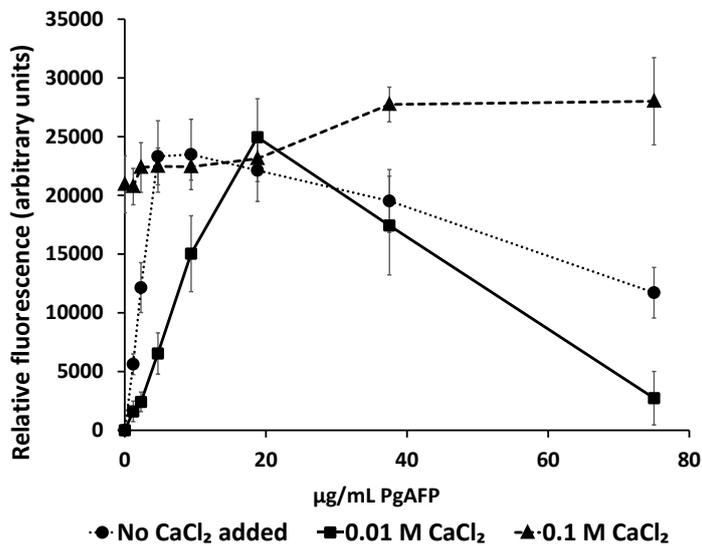
751

752 Figure 2. Effect of selected cations on the antifungal activity of different PgAFP
 753 concentrations against *A. flavus*. Growth development in potato dextrose broth for 96 h
 754 supplemented with (A) no cations, (B) 0.01 M CaCl_2 , (C) 0.1 M CaCl_2 , (D) 0.1 M KCl ,
 755 (E) 0.01 M MgCl_2 and (F) 0.1 M MgCl_2 . Vertical represent standard deviation of the
 756 mean.



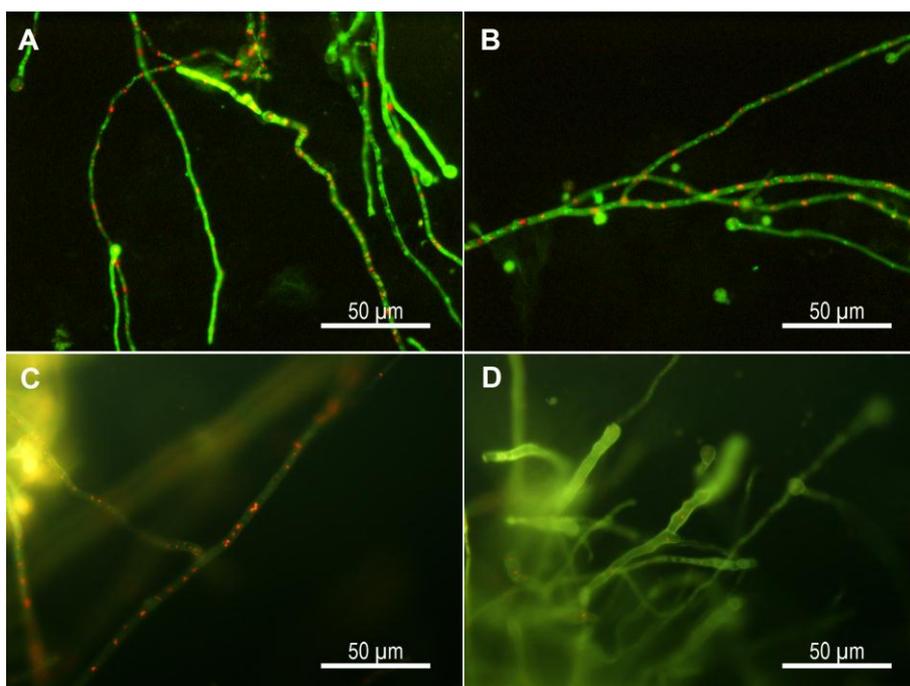
757

758 Figure 3. FITC-labelled PgAFP localization in *A. flavus* grown in presence of 0.1 M
 759 CaCl_2 (left). PgAFP was only visualized bound to the outer layer of *A. flavus* hyphae,
 760 but not in the cytoplasm. FITC-labelled PgAFP localization in *A. flavus* without CaCl_2
 761 (right). PgAFP was visualized both in the cytoplasm (I) and bound to the outer layer (O)
 762 of *A. flavus* hyphae.



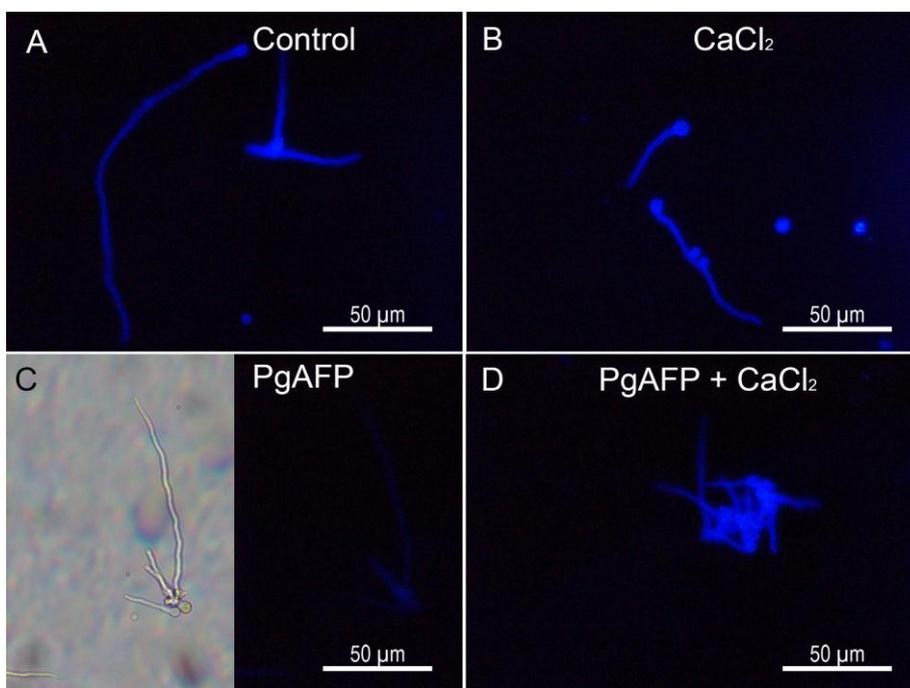
763

764 Figure 4. Effect of two different concentrations of CaCl_2 on membrane permeability of
 765 *A. flavus* treated with PgAFP (0-75 $\mu\text{g/mL}$) at 210 min after SYTOX Green addition.
 766 Vertical represent standard deviation of the mean.



767

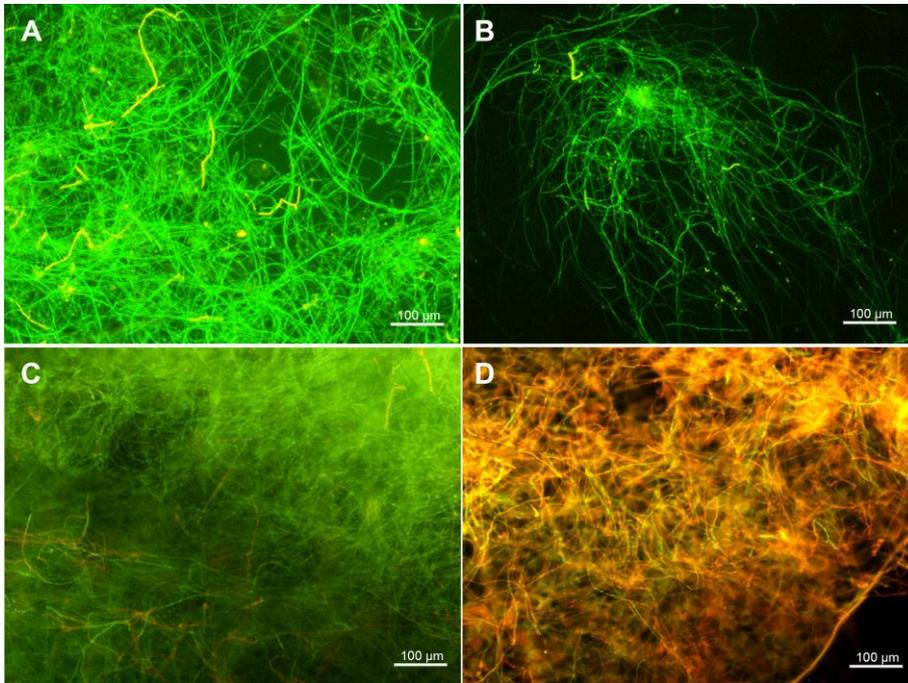
768 Figure 5. Metabolic capability of *A. flavus* grown with 0.1 M CaCl₂ (A and B) or
 769 without calcium (C and D) revealed by FUN-1 staining. Non-treated control (A) and
 770 hyphae treated with 75 µg/mL PgAFP (B) showed intravacuolar red spots, indicating
 771 unaltered metabolic capability with CaCl₂. Vertical represent standard deviation of the
 772 mean). With no calcium added, non-treated control also displayed intravacuolar red
 773 spots (C), whereas *A. flavus* grown with 75 µg/mL PgAFP scarcely showed red spots
 774 (D).



775

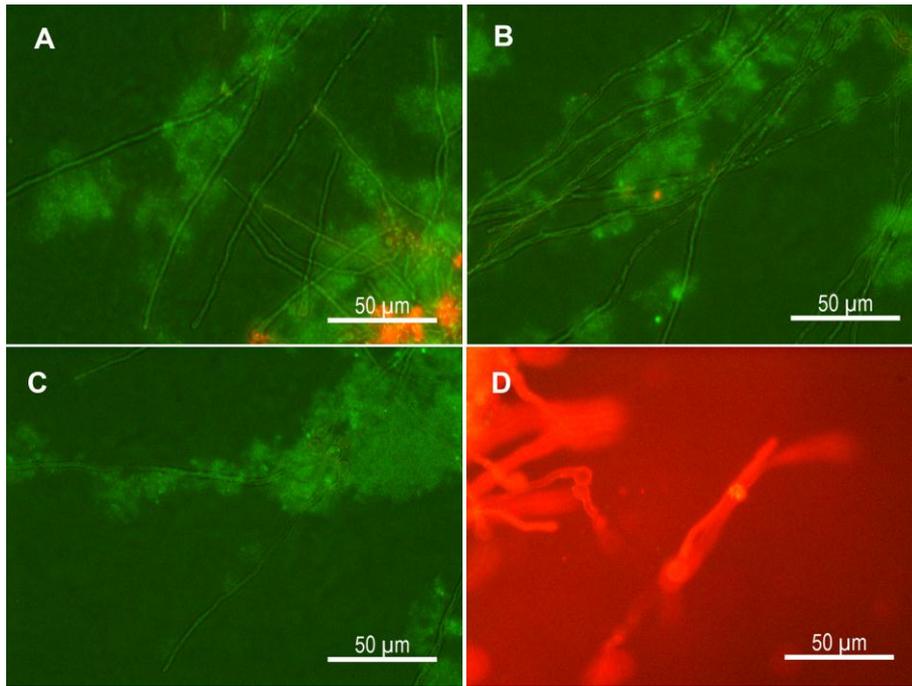
776 Figure 6. Effect of calcium on chitin deposition PgAFP-treated *A. flavus* grown in
 777 potato dextrose broth and stained with fluorescent brightener 28. A: non-PgAFP treated

778 with no CaCl₂ added; B: non-PgAFP treated supplemented with 0.1M CaCl₂; C: PgAFP
779 treated (75 µg/mL) with no CaCl₂ added, bright field (left) and fluorescence observation
780 (right); D: PgAFP treated (75 µg/mL) supplemented with 0.1M CaCl₂. CaCl₂ did not
781 increase chitin deposition *per se* in non-PgAFP treated samples (panels A-B) but
782 prevented lower chitin content in PgAFP-treated samples (panels C-D).



783

784 Figure 7. Effect of PgAFP on hyphae viability revealed by acridine orange/ethidium
785 bromide (AO/EB) double staining of *A. flavus* grown in potato dextrose broth
786 supplemented with 0.1 M CaCl₂ (A and B) and without added CaCl₂ (C and D). Merged
787 pictures of green (AO) and red colour (EB) from samples non-treated (A and C) and
788 treated with 75 µg/mL PgAFP (B) showing scarce orange colour due to the lack of EB
789 penetration, meaning that remained viable. *A. flavus* treated with 75 µg/mL PgAFP
790 grown with no added calcium (D) showed intense orange colour due to compromised
791 membrane.



792

793 Figure 8. Induction of apoptosis or necrosis by PgAFP on *A. flavus* grown in potato
794 dextrose broth supplemented with 0.1 M CaCl₂ (A and B) and with no calcium added (C
795 and D), evaluated with Annexin V-fluorescein isothiocyanate/propidium iodide (AnV-
796 FITC/PI). Merged pictures of green (AnV-FITC) and red colour (PI) from non-treated
797 hyphae (A and C) or treated with 75 µg/mL PgAFP (B) showing no green or red intense
798 fluorescence due to no apoptotic or necrotic event. *A. flavus* grown in PDB with no
799 calcium added and treated with 75 µg/mL PgAFP (D) displayed intense red colour due
800 to AnV-FITC and PI penetration as a consequence of necrotic events.

801

Journal: **Food Microbiology**

Supplementary Information

Proteome changes explain calcium-mediated inefficacy of the antifungal protein PgAFP against *Aspergillus flavus* in cheese.

Josué Delgado^a, Rebecca A. Owens^b, Sean Doyle^b, Félix Núñez^a, and Miguel A. Asensio^a

^a Food Hygiene and Safety, Institute of Meat Products, University of Extremadura, Cáceres, Spain.

^b Department of Biology, Maynooth University, Maynooth, Co. Kildare, Ireland.

Corresponding author:

Miguel A. Asensio

masensio@unex.es, Tel.: +34 927 257124; Fax: +34 927 257110

Supplementary Table S1. Data on proteins whose relative abundance was affected by 10 µg/mL PgAFP in *Aspergillus flavus* grown in 0.1 M CaCl₂ PDB, reaching over 1.5 fold change in 2D-PAGE.

Protein name	p- value	Fold Change	% coverage	Unique peptides	Score	tMr (Da)	Protein accession (GI)	Gene
thiazole biosynthesis enzyme Sti35	5,65E-04	↑1.6	48	9	489	35315	238487974	AFLA_037160
metallopeptidase MepB	0,016	↑1.6	4	2	99	81812	238482735	AFLA_076890
phosphoglucomutase PgmA	0,008	↑1.6	40	14	835	60491	238486686	AFLA_030710
aspartic endopeptidase Pep2	0,002	↑1.6	34	7	448	43394	238486794	AFLA_031250
glyceraldehyde 3-phosphate dehydrogenase GpdA	0,008	↑1.5	53	9	621	36378	238485566	AFLA_025100
G-protein complex beta subunit CpcB	0,008	↑1.5	50	9	543	35395	238504184	AFLA_051980
Coatomer subunit epsilon, putative	0,001	↑1.5	41	7	515	31556	238489197	AFLA_018160
translation elongation factor EF-2 subunit, putative	0,011	↓2.5	20	11	616	94681	238496883	AFLA_136640
glycogen branching enzyme GbeA, putative	0,011	↓2.4	18	9	474	78872	238506945	AFLA_119670
glycogen branching enzyme GbeA, putative	0,002	↓2.1	14	7	326	78872	238506945	AFLA_119670
translation elongation factor eEF-3, putative	0,002	↓1.9	11	7	401	118573	238482677	AFLA_076600
aminopeptidase , putative	0,015	↓1.8	37	22	1270	99216	238503357	AFLA_007140
molecular chaperone and allergen Mod-E/Hsp90/Hsp1	0,001	↓1.8	11	5	203	79640	238503321	AFLA_006960
conserved hypothetical protein	0,002	↓1.8	14	6	315	81507	238499825	AFLA_093270
aminopeptidase, putative	0,009	↓1.7	20	10	581	99216	238503357	AFLA_007140
phosphoglucomutase, putative	0,012	↓1.7	7	3	177	64611	238493075	AFLA_043120
peptidyl-prolyl cis-trans isomerase Cpr7, putative	0,007	↓1.7	29	8	382	41268	238493059	AFLA_043040
UDP-N-acetylglucosamine pyrophosphorylase	0,008	↓1.6	50	17	919	56416	238498918	AFLA_071350
ATP citrate lyase subunit (Acl), putative	0,037	↓1.6	44	12	663	52846	238490538	AFLA_106350
pyruvate dehydrogenase E1 component alpha subunit, putative	0,016	↓1.6	36	11	550	45578	238489957	AFLA_021960
aldehyde dehydrogenase AldA, putative	0,013	↓1.6	11	4	242	54290	238491024	AFLA_108790
aldehyde dehydrogenase AldA, putative	0,008	↓1.6	17	6	335	54290	238491024	AFLA_071350
translation elongation factor eEF-3, putative	0,004	↓1.6	5	3	152	118573	238482677	AFLA_076600
translation elongation factor eEF-3, putative	0,013	↓1.6	15	8	466	118573	238482677	AFLA_076600

Supplementary Table S2. Data on proteins obtained from label-free proteomics from *Aspergillus flavus* grown in presence of 0.1 M CaCl₂ treated with 10 µg/ml PgAFP and untreated control.

A. Total data																										
Lfq intensity	Lfq intensity	Lfq intensity	Lfq intensity	Lfq intensity	Lfq intensity	t-test	Intensity	Peptides	Razor + unique peptides	Unique peptides	Sequence coverage [%]	Mol. weight [kDa]	Mean	Mean	AF_CaCl ₂ PgAFP	Mean	AF_CaCl ₂ Control	Valid values	Valid values	t-test p value	t-test Difference	Protein IDs	Majority protein IDs	Proteins	Gene Names	Protein names
AF_CaCl ₂ PgAFP_1	AF_CaCl ₂ PgAFP_2	AF_CaCl ₂ PgAFP_3	AF_CaCl ₂ Control_1	AF_CaCl ₂ Control_2	AF_CaCl ₂ Control_3	Significant	PEP																			
32,0735	31,5171	31,1105	30,701	30,6453	30,9018	+	0	2,64E+10	18	18	48.3	63,572	31,1597	31,567	30,7524	6	6	3	0,048136	0,184662	B8NPM2	B8NPM2	1	AFLA_000860	Tripeptidyl peptidase A	
24,0678	24,6431	NaN	NaN	24,6052	NaN		2,51E-28	3,35E+08	5	5	14.5	45,487	24,4387	24,3554	24,6052	3	2	1	1	-0,249826	B8NPN7	B8NPN7	1	AFLA_001010	Benzoate 4-monoxygenase cytochrome P450, putative	
24,3051	24,3078	24,8275	24,0966	24,1309	23,5585		4,99E-13	2,26E+08	4	4	9.4	60,765	24,2044	24,4801	23,9287	6	3	3	0,095693	0,551464	B8NPT7	B8NPT7	1	AFLA_001510	Glutathionyl-rRNA(Gln) amidotransferase subunit A, putative	
27,4449	27,0871	25,5714	25,9636	25,6272	25,8664		4,26E-66	5,93E+08	7	7	36.6	38,004	26,2601	26,7011	25,8191	6	3	3	0,204758	0,88206	B8NQM7	B8NQM7	1	AFLA_001710	Aldo-keto reductase, putative	
25,8516	24,5015	NaN	NaN	24,1264	24,229		9,02E-17	1,18E+08	2	2	28.7	17,86	24,6771	25,1766	24,1771	4	2	2	0,278051	0,998899	B8NQP1	B8NQP1	1	AFLA_001850	Uncharacterized protein	
28,0329	28,0245	28,0251	27,8729	27,4412	27,3416	+	3,69E-42	2,16E+09	7	7	24.1	35,104	27,7897	28,0275	27,5519	6	3	3	0,043409	0,475606	B8NQ2	B8NQ2	1	AFLA_001960	Aldehyde dehydrogenase, putative	
29,305	28,6706	28,4263	28,1419	28,4807	28,6314		4,41E-154	4,35E+09	10	10	23.2	63,769	28,6093	28,8006	28,4818	6	3	3	0,270098	0,382648	B8NQR5	B8NQR5	1	AFLA_002090	Extracellular serine carboxypeptidase, putative	
31,213	31,3179	31,6476	31,7722	31,9076	31,5883		0	2,79E+10	44	44	65.2	90,553	31,5744	31,3928	31,7564	6	3	3	0,086156	-0,36322	B8NQ3	B8NQ3	1	AFLA_002370	Cell division control protein Cdc48	
27,631	27,3376	26,8503	27,1315	27,2838	27,3358		9,82E-96	1,73E+09	10	10	44.4	30,601	27,2617	27,273	27,5504	6	3	3	0,928191	0,0226186	B8NQU8	B8NQU8	1	AFLA_002420	Defective in cullin neddylation protein	
26,1672	25,7272	25,5607	25,6725	25,9203	26,0531		1,33E-43	6,18E+08	3	3	45.2	14,756	25,8492	25,8164	25,882	6	3	3	0,771195	-0,065635	B8NQV0	B8NQV0	1	AFLA_002440	Uncharacterized protein	
29,4073	28,44	28,9205	29,3134	28,8754	29,0824		0	4,68E+09	10	10	47.4	37,661	29,0065	28,9226	29,0904	6	3	3	0,513254	-0,167793	B8NQV7	B8NQV7	1	AFLA_002510	Actin monomer binding protein, putative	
NaN	24,4392	27,154	25,9214	24,7349	NaN		1,88E-28	6,22E+08	3	3	29.3	10,128	25,5624	25,7966	25,3282	4	2	2	0,781772	0,064875	B8NPV3	B8NPV3	1	AFLA_002560	60S ribosomal protein L37a	
24,056	29,269	30,6036	30,0802	29,0931	28,5092		3,47E-296	1,1E+10	20	20	56.5	43.9	29,2672	29,3069	29,2755	6	3	3	0,931457	0,079406	B8NPW4	B8NPW4	1	AFLA_002670	Curved DNA-binding protein (42 kDa protein)	
24,256	23,9461	23,9251	23,929	24,1668	24,4084		6,42E-14	1,76E+08	4	4	5.8	78,653	24,1035	24,0389	24,1681	6	3	3	0,496435	-0,129142	B8NPX8	B8NPX8	1	AFLA_002810	tRNA nucleotidyltransferase	
25,45	26,1788	25,3217	25,9767	25,2487	25,0795		1,44E-34	5,42E+08	3	3	33.8	18,242	25,5426	25,8502	25,435	6	3	3	0,604601	0,215167	B8NPY8	B8NPY8	1	AFLA_002910	Uncharacterized protein	
28,8995	28,8123	28,8528	29,0467	28,6346	28,5603		9,32E-245	5,37E+09	12	12	12.5	43,132	28,7994	28,8515	28,7472	6	3	3	0,532517	0,104325	B8NPZ5	B8NPZ5	1	AFLA_002980	N,N-dimethylglycine oxidase	
27,876	27,1573	27,4468	27,5028	27,7038	27,9661		3,17E-103	1,91E+09	6	6	6	48.1	17,749	27,6088	27,4934	27,7242	6	3	3	0,404827	-0,230869	B8NQQ8	B8NQQ8	1	AFLA_003110	Cyanate hydratase (Cyanase) [EC 3.4.2.1.104] (Cyanate hydrolase) (Cyanate lyase)
27,7894	26,9469	25,5887	25,3851	27,0087	27,3322		1,53E-197	2,95E+09	20	20	23.9	145.25	26,6751	26,7575	26,5753	6	3	3	0,831532	0,199713	B8NQQ9	B8NQQ9	1	AFLA_003220	Phospholipase D (PLD), putative	
NaN	NaN	24,9342	25,3021	25,257	24,8017		1,46E-11	3,08E+08	6	6	6	11	76,159	25,0737	24,9342	25,1203	4	1	3	1	-0,186026	B8NQ20	B8NQ20	1	AFLA_003230	Uncharacterized protein
28,8303	28,7327	28,7107	29,069	28,8037	28,7582		1,54E-160	4,59E+09	10	10	30.4	53,426	28,8174	28,7579	28,877	6	3	3	0,31478	-0,119049	B8NQW0	B8NQW0	1	AFLA_003440	Translation initiation factor 4B	
24,7784	24,6044	24,628	25,0364	24,7852	NaN		4,07E-14	2,54E+08	6	6	6	39.2	26,932	24,7665	24,6703	24,9108	5	3	2	0,132256	-0,240543	B8NQW3	B8NQW3	1	AFLA_003470	Oxidoreductase family, NAD-binding Rossmann fold protein
NaN	25,1891	29,344	27,5469	24,4478	NaN		1,47E-72	1E+9	5	5	34.4	14,925	26,632	27,2666	25,9974	4	2	2	0,672783	1,26918	B8NQW4	B8NQW4	1	AFLA_003480	60S ribosomal protein L32	
30,1166	30,0054	29,7777	28,9446	29,5757	29,5781		0	7,45E+09	13	13	71.9	24,841	29,6664	29,9666	29,3661	6	3	3	0,306162	0,600444	B8NQC1	B8NQC1	1	AFLA_003650	Uracil phosphoribosyltransferase	
28,0155	27,6032	26,8272	27,2719	27,5284	27,6195		1,24E-60	1,82E+09	16	16	48.6	55,467	27,4776	27,482	27,4733	6	3	3	0,982061	0,006969	B8NQC6	B8NQC6	1	AFLA_003700	Mitochondrial cytochrome b ₂ , putative	
NaN	NaN	NaN	NaN	23,5699	23,5492		3,31E-26	2,66E+08	4	4	4	17.4	47,811	23,5595	NaN	23,5595	2	0	2	1	NaN	B8NQZ7	B8NQZ7	1	AFLA_003810	Endonuclease/exonuclease/phosphatase family protein
29,8539	29,4853	29,2128	29,546	29,2026	29,7115		6,76E-242	8,19E+09	13	13	68.2	29,218	29,5853	29,5173	29,6533	6	3	3	0,520597	-0,136023	B8NR05	B8NR05	1	AFLA_003890	Proteasome subunit alpha type (EC 3.4.2.5.1)	
27,9617	28,117	27,9017	28,1147	28,1472	28,0886		4,30E-194	2,94E+09	11	11	48.2	39,926	28,0385	27,9602	28,1168	6	3	3	0,165863	-0,156666	B8NR08	B8NR08	1	AFLA_003920	Cysteine synthase (O-acetylserine (Thio)lyase) (CsaE)	
27,224	27,2806	26,9439	27,0498	26,8968	26,9679		2,71E-26	1,4E+09	3	3	5.3	74,929	27,0605	27,1495	26,9715	6	3	3	0,190513	0,178051	B8NR18	B8NR18	1	AFLA_004020	Uncharacterized protein	
26,5554	26,4674	26,5632	26,9564	26,2414	26,3765		4,03E-24	1,09E+09	4	4	66.2	7,7117	26,5267	26,5287	26,5248	6	3	3	0,986797	0,003896	B8NR19	B8NR19	1	AFLA_004030	Uncharacterized protein	
24,9215	25,5144	25,8126	26,0771	25,9349	25,2404		1,73E-86	9,91E+08	15	15	46	59,97	25,5833	25,4162	25,7508	6	3	3	0,414561	-0,334623	B8NR20	B8NR20	1	AFLA_004040	Actin interacting protein 2	
27,8207	27,8237	28,0532	28,2784	27,7921	28,0988		1,37E-101	2,97E+09	4	4	22.6	15,348	27,9201	27,9322	28,0079	6	3	3	0,320069	-0,315693	B8NR25	B8NR25	1	AFLA_004090	Uncharacterized protein	
24,7894	23,8782	23,1912	NaN	NaN	NaN		3,65E-09	1,16E+08	7	7	9	45.489	23,9529	23,9529	NaN	3	0	1	1	NaN	B8NR26	B8NR26	1	AFLA_004100	Transesterase (LovD), putative	
27,7087	28,066	28,3664	28,0188	28,2336	28,4512		7,66E-183	2,3E+09	17	17	16	34.3	77,514	28,1408	28,047	28,2345	6	3	3	0,455919	-0,187527	B8NQC4	B8NQC4	1	AFLA_004550	Vacuolar dynamin-like GTPase YpsA, putative
28,3535	27,6579	27,85	27,2048	28,0342	27,7643		5,18E-236	3,45E+09	23	23	23	43.6	76,132	27,8108	27,9538	27,6678	6	3	3	0,422537	0,286002	B8NQC5	B8NQC5	1	AFLA_004560	Vacuolar ATP synthase catalytic subunit A, putative
25,397	25,1721	25,7024	25,3183	25,3457	24,6603		2,32E-32	1,03E+09	11	11	10	32.8	45,502	25,266	25,4238	25,1081	6	3	3	0,309782	0,153729	B8NQC6	B8NQC6	1	AFLA_004600	Eukaryotic translation initiation factor eIF-4A subunit, putative
30,4934	30,1925	29,8827	29,9779	30,0553	30,213		5,21E-274	1,18E+10	14	14	46.8	39,497	30,1354	30,1895	30,0813	6	3	3	0,598349	0,108242	B8NQ72	B8NQ72	1	AFLA_004630	Farnesyl-phosphatase synthetase	
31,7492	32,1488	31,8322	32,0902	31,6559	31,3933		0	2,23E+10	20	20	69.9	38,243	31,8116	31,9101	31,7131	6	3	3	0,462534	0,196937	B8NQ74	B8NQ74	1	AFLA_004650	Thiamine biosynthesis protein (Nmt1), putative	
27,1048	27,0589	26,9552	27,2195	27,0569	26,9942		1,43E-66	1,39E+09	6	6	37	39.99	27,0649	27,0396	27,0902	6	3	3	0,563367	-0,0505867	B8NQ82	B8NQ82	1	AFLA_004730	Ribokinase	
29,1315	29,0991	29,4057	29,4816	29,5441	29,3631		0	9E+09	36	36	48.7	147.49	29,3375	29,2121	29,463	6	3	3	0,086261	-0,250857	B8NQA1	B8NQA1	1	AFLA_004920	Phosphoribosylformylglycinamide synthase	
NaN	25,496	25,2161	NaN	NaN	NaN		1,19E-26	4,18E+08	4	4	4	30.4	17,901	25,3561	25,3561	NaN										

Supplementary Table S2. Data on proteins obtained from label-free proteomics from *Aspergillus flovus* grown in presence of 0.1 M CaCl₂ treated with 10 μg/ml PgAaP and untreated control.

LFQ intensity AF_CaCl ₂ PgAaP_1	LFQ intensity AF_CaCl ₂ PgAaP_2	LFQ intensity AF_CaCl ₂ PgAaP_3	LFQ intensity AF_CaCl ₂ Control_1	LFQ intensity AF_CaCl ₂ Control_2	LFQ intensity AF_CaCl ₂ Control_3	t-test Significant	PEP	Intensity	Peptides	Razor + unique peptides	Unique peptides	Sequence coverage [%]	Mol. weight [kDa]	Mean	Mean AF_CaCl ₂ PgAaP	Mean AF_CaCl ₂ Control	Valid values	Valid values AF_CaCl ₂ PgAaP	Valid values AF_CaCl ₂ Control	t-test p-value	t-test Difference	Protein IDs	Majority protein IDs	Proteins	Gene Names	Protein names
25.1003	24.7012	24.1308	23.2829	23.5267	24.5395			2,24E+10	1,71E+08	5	5	5	5.8	102.45	24,2136	24,6551	23,7831	6	3	0.145135	0.861034	BBNXL0	BBNXL0	1	AFLA_008290	Kinesin-like protein
26.8243	26.7248	26.4097	26.5098	26.7125	26.7176			9,88E-21	1,16E+09	3	3	3	5.3	17,169	26,6502	26,6529	26,6475	6	3	0.971383	0.0054461	BBNXL1	BBNXL1	1	AFLA_008300	Ubiquitin conjugating enzyme (UbcB), putative
26.271	28.2351	28.1239	28.9199	28.745	28.6706			1,21E-147	3,93E+09	15	15	15	53.5	45,738	28,1616	28,7799	6	3	0.12603	1.23656	BBNXL2	BBNXL2	1	AFLA_008310	Acetyl-CoA acetyltransferase, putative	
25.8273	23.9418	24.6027	24.4603	24.9209	25.8554			6,50E-26	4,25E+08	10	8	8	19.5	77,093	24,9347	24,7906	25,0788	6	3	0.69683	-0.288234	BBNXM6	BBNXM6	1	AFLA_008560	Alpha-1,2-mannosidase, putative subfamily 5
33.1083	32.9815	30.4271	31.982	32.0373	32.267			0	5.19E+10	25	25	24	63.4	58,659	32,1339	32,1723	32,0594	6	3	0.934418	0.0768712	BBNXR9	BBNXR9	1	AFLA_008890	Glutamate decarboxylase (EC 4.1.1.15)
22.588	24.8237	26.2695	28.7058	24.4512	24.3072			8,81E-275	2,53E+09	17	17	17	39.6	64,187	25,1909	24,5604	25,8214	6	3	0.521492	-1.26099	BBNXS1	BBNXS1	1	AFLA_008910	Uncharacterized protein
NaN	NaN	NaN	26.2119	26.2701	26.5487			3,45E-43	8,27E+08	6	6	6	17.5	57,585	26,3436	NaN	26,3436	3	0	1	NaN	BBNXS3	BBNXS3	1	AFLA_008930	Purple acid phosphatase (EC 3.1.3.2)
31.4563	30.9611	30.3612	30.4518	30.8777	30.9745			0	1.71E+10	19	19	19	40	60,878	30,8471	30,9262	30,768	6	3	0.67894	0.158186	BBNXS9	BBNXS9	1	AFLA_008990	Carboxypeptidase Y homolog A (EC 3.4.16.5)
27.1562	27.7956	29.8709	28.1926	28.0242	27.8922			4,64E-103	5,75E+09	10	10	10	53.5	17,943	28,1553	28,2742	28,0363	6	3	0.787134	0.237904	BBNXT0	BBNXT0	1	AFLA_009000	Ribosomal protein S13p/S18e
25.0051	24.7307	24.5684	24.7559	24.4326	24.5595			2,27E-11	2,92E+08	6	6	6	14.5	47,521	24,6754	24,7681	24,5826	6	3	0.306694	0.185435	BBNXT5	BBNXT5	1	AFLA_009050	TPR repeat protein
25.5541	25.0788	24.7048	24.1309	24.9723	24.7866			5,62E-20	4,49E+08	7	7	7	9.3	127,559	24,8713	25,1126	24,263	6	3	0.244807	0.48261	BBNXT9	BBNXT9	1	AFLA_009090	Nuclear serine protease Htra2/Num11, putative
28.5172	28.1975	27.9259	28.2633	28.3694	28.4965			1,34E-59	3,49E+09	8	8	8	73.1	14,415	28,295	28,2135	28,3764	6	3	0.425405	-0.162879	BBNXX3	BBNXX3	1	AFLA_009430	Uncharacterized protein
29.8676	29.4384	29.2236	29.5874	29.8302	29.6018			4,15E-24	9,24E+09	4	4	4	34.2	8,5719	29,5898	29,5065	29,6731	6	3	0.463288	-0.166579	BBNY04	BBNY04	1	AFLA_009740	Uncharacterized protein
26.5066	26.6385	26.4252	26.3014	25.9352	25.9487			9,37E-30	8,07E+08	5	5	5	29.1	34,324	26,2893	26,5168	26,0618	6	3	0.262335	0.454989	BBNY47	BBNY47	1	AFLA_010170	Tropinone reductase, putative
24.1517	23.5019	26.3569	NaN	NaN	NaN			2,41E-16	1,65E+08	5	5	5	12.6	54,048	24,6702	24,6702	NaN	3	0	1	NaN	BBNY90	BBNY90	1	AFLA_010600	Siderophore biosynthesis acetylase Acel, putative
24.7586	23.6293	25.3136	23.7517	NaN	NaN			3,16E-29	3,29E+08	10	10	10	7.5	229,88	24,3633	24,5672	23,7517	4	1	0.815433	0.883992	BBNY92	BBNY92	1	AFLA_010620	Nonribosomal siderophore peptide synthase Sid2
24.6407	25.5185	26.3033	25.827	24.9043	24.761			2,23E-20	5,14E+08	7	7	7	30.9	36,288	25,3258	25,4875	25,1641	6	3	0.609904	0.332385	BBNY47	BBNY47	2	AFLA_010770	Porphobilinogen deaminase Hem3, putative
31.6175	31.218	31.0756	31.3001	31.528	31.661			3,89E-180	2,95E+10	6	6	6	48.4	13,315	31,31	31,3037	31,4964	6	3	0.375953	-0.192663	BBNY1	BBNY1	1	AFLA_010910	Peptidyl-prolyl cis-trans isomerase
28.9811	28.2903	27.8982	28.3312	28.823	29.014			5,42E-216	3,8E+09	10	10	10	57.1	28,833	28,5563	28,3898	28,7227	6	3	0.426283	-0.33288	BBNY3	BBNY3	1	AFLA_010930	Glutathione S-transferase family protein, putative
26.3758	25.5079	26.3682	25.4822	25.9293	25.759			6,27E-83	1,58E+09	8	8	8	42.8	25.3	25,9037	26,0839	25,7235	6	3	0.317818	0.360462	BBNY4	BBNY4	1	AFLA_011240	Uncharacterized protein
NaN	25.275	26.2392	25.833	25.0719	24.904			2,61E-49	7,29E+08	5	5	5	31.8	26,331	25,4646	25,7571	25,2696	5	2	0.413694	0.487511	BBNY8	BBNY8	1	AFLA_011380	Uncharacterized protein
NaN	23.1849	23.552	24.0331	24.1877	24.0115			+ 2.12E-14	3.3E+08	5	5	5	13.2	64,473	23,7938	23,3685	24,0774	5	2	0.019422	-0.708914	BBNY6	BBNY6	1	AFLA_011460	GMC oxidoreductase, putative
27.2886	26.0026	24.9291	31.2714	32.0032	32.0819			+	0.179E+10	15	15	15	45.7	55,696	28,9295	26,0735	31,7855	6	3	0.001434	-5.71204	BBNY6	BBNY6	1	AFLA_011560	Phosphatidylglycerol specific phospholipase, putative
26.1688	25.6611	25.1701	26.1655	26.1926	26.5028			7,88E-105	1,35E+09	10	10	10	36.7	42.97	25,9935	25.7	26,2869	6	3	0.105646	-0.586927	BBNY6	BBNY6	1	AFLA_011660	Uncharacterized protein
25.0172	25.8206	26.7595	27.2321	26.3214	25.8265			1,02E-46	1,82E+09	7	8	8	38.9	42,898	26,1629	25,8658	26,146	6	3	0.412531	-0.594231	BBNY4	BBNY4	1	AFLA_011740	Cystathionine gamma-lyase
30.0856	29.1069	28.5223	28.583	29.3014	29.3014			8,98E-217	5,09E+09	8	7	7	16.8	60,796	29,1698	29,2303	29,1013	6	3	0.807286	0.136971	BBNY2	BBNY2	1	AFLA_012020	Carboxypeptidase S1, putative
NaN	NaN	23.5304	23.8594	23.9646	23.5291			2,31E-33	2,4E+08	4	4	4	10	60,179	23,7209	23,5304	23,7843	4	1	1	-0.25393	BBNY6	BBNY6	1	AFLA_012060	Choline oxidase (CodA), putative
25.4771	24.6085	24.3087	25.1196	25.5816	25.3347			3,90E-07	3,11E+08	4	4	4	11.9	54,189	25,0717	24,7981	25,3453	6	3	0.21821	-0.547191	BBNY7	BBNY7	1	AFLA_012070	Betaine aldehyde dehydrogenase (BadH), putative
26.0145	24.8156	24.4554	NaN	NaN	NaN			2,55E-10	2,38E+08	3	3	3	15.9	39,503	25,0952	25,4151	24,8059	3	2	1	0.95956	BBNY8	BBNY8	1	AFLA_012080	Glucosamine-6-phosphate isomerase (EC 3.5.99.6) (Glucosamine-6-phosphate deaminase)
24.8128	24.9782	24.9845	24.6694	24.966	24.7765			1,27E-134	3,25E+08	7	7	7	6.6	131,39	24,8646	24,9252	24,8533	6	3	0.305769	0.121253	BBNY8	BBNY8	1	AFLA_012110	Cleavage and polyadenylation specificity factor subunit A, putative
24.1325	25.1847	29.5963	30.3477	27.4475	26.9981			0	6.02E+09	18	18	18	67.2	40,005	27,5003	26,8073	28,3934	6	3	0.329672	0.138515	BBNY6	BBNY6	1	AFLA_012160	Acetyl-CoA acetyltransferase, putative
NaN	24.2183	24.7483	24.1631	23.5478	NaN			1,77E-23	3,68E+08	8	7	7	14.7	88,797	26,1694	24,4833	23,8554	4	3	0.262075	0.627869	BBNY7	BBNY7	1	AFLA_012170	US snRNP component SnU14, putative
34.0999	33.9012	33.5563	33.7397	33.7154	33.8729			0	1.5E+11	38	38	38	44.2	96,549	33,8142	33,8525	33,776	6	3	0.66935	0.074669	BBNY1	BBNY1	1	AFLA_012200	Hsp70 chaperone (HscA), putative
NaN	NaN	NaN	24.2323	24.5589	24.6255			2,64E-07	1,78E+08	2	2	2	9.3	18,627	24,4722	NaN	24,4722	3	0	1	NaN	BBNY2	BBNY2	1	AFLA_012220	Cyclin-dependent kinase regulatory subunit, putative
26.2845	26.4895	27.3993	27.0937	27.4519	27.1412			3,32E-115	2,17E+09	7	7	7	48.6	23,448	26,9767	26,7425	27,2289	6	3	0.234316	-0.504465	BBNY3	BBNY3	1	AFLA_012230	Uncharacterized protein
26.3757	26.2584	25.7542	26.9147	26.2359	26.1647			4,56E-16	7,38E+08	4	4	4	28.7	20,109	26,1173	26,1294	26,1051	6	3	0.914985	0.0243327	BBNY7	BBNY7	1	AFLA_012270	Peptidyl-prolyl cis-trans isomerase (EC 5.2.1.8)
NaN	NaN	NaN	23.2952	23.9189	23.3138			2,45E-29	3,74E+08	5	5	5	31	23,258	23,5093	NaN	23,5093	3	0	1	NaN	BBNY5	BBNY5	1	AFLA_013180	Williams-beuren syndrome chromosome region, putative
22.7042	21.4608	NaN	31.4209	31.5292	31.6738			+	0.31E+10	25	25	25	57.4	52,758	27,7578	22,0825	31,5413	5	2	0.000273	-9.45874	BBNY5	BBNY5	1	AFLA_013680	Phosphatidylglycerol specific phospholipase C, putative
NaN	NaN	NaN	22.7949	22.4155	22.3787			7,60E-94	1,73E+09	6	6	6	27.6	32,989	22,5297	NaN	22,5297	3	0	1	NaN	BBNY1	BBNY1	1	AFLA_013740	Acid phosphatase, putative
29.5225	28.9404	28.6591	28.7563	29.1136	29.1869			5,94E-173	4,74E+09	9	9	9	32	54,187	29,0298	29,0407	29,0189	6	3	0.943227	0.0217444	BBNY5	BBNY5	1	AFLA_013980	Peptide lyase (EC 3.4. ...)
29.312																										

Supplementary Table S2. Data on proteins obtained from labelfree proteomics from *Aspergillus flavus* grown in presence of 0.1 M CaCl₂ treated with 10 μg/ml PgAFP and untreated control.

A. Total data				LFQ intensity		LFQ intensity		LFQ intensity		LFQ intensity		LFQ intensity		t-test		Sequence coverage		Mol. weight		Mean		Mean		Valid values		Valid values		t-test p value		t-test		Protein IDs		Majority protein IDs		Proteins		Gene Names		Protein names														
LFQ intensity	LFQ intensity	LFQ intensity	LFQ intensity	LFQ intensity	LFQ intensity	LFQ intensity	LFQ intensity	LFQ intensity	LFQ intensity	t-test	Sequence coverage	Mol. weight	Mean	Mean	Mean	Mean	Valid values	Valid values	t-test p value	t-test	Protein IDs	Majority protein IDs	Proteins	Gene Names	Protein names	LFQ intensity	LFQ intensity	LFQ intensity	LFQ intensity	LFQ intensity	LFQ intensity	t-test	Sequence coverage	Mol. weight	Mean	Mean	Valid values	Valid values	t-test p value	t-test	Protein IDs	Majority protein IDs	Proteins	Gene Names	Protein names									
AF_CaCl ₂	PgAFP_1	AF_CaCl ₂	PgAFP_2	AF_CaCl ₂	PgAFP_3	Control_1	Control_2	Control_3	Control_4	Significant	PEP	Intensity	Peptides	Unique peptides	Sequence coverage	Mol. weight	Mean	Mean	Mean	Mean	Mean	Mean	Valid values	Valid values	t-test p value	t-test	Protein IDs	Majority protein IDs	Proteins	Gene Names	Protein names	LFQ intensity	LFQ intensity	LFQ intensity	LFQ intensity	LFQ intensity	LFQ intensity	t-test	Sequence coverage	Mol. weight	Mean	Mean	Valid values	Valid values	t-test p value	t-test	Protein IDs	Majority protein IDs	Proteins	Gene Names	Protein names			
26.6225	25.3222	28.7883	25.2157	25.594	25.2159						4,48E-22	4,47E+08	5	4	318	27,628	25,6264	25,911	25,3418	6	3	0.22851	0.569181	B8N3W1	B8N3W1	1	AFLA_031950	RAB GTPase Vps21/Ypt51, putative	26.6225	25.3222	28.7883	25.2157	25.594	25.2159	4,48E-22	4,47E+08	5	4	318	27,628	25,6264	25,911	25,3418	6	3	0.22851	0.569181	B8N3W1	B8N3W1	1	AFLA_031950	RAB GTPase Vps21/Ypt51, putative		
25.9504	26.1407	28.8255	28.2836	26.8149	26.9957						6,84E-34	1,63E+09	7	7	403	22,775	27,1685	26,9722	27,3648	6	3	0.724281	-0.392534	B8N3W2	B8N3W2	1	AFLA_031960	40S ribosomal protein S7e	25.9504	26.1407	28.8255	28.2836	26.8149	26.9957	6,84E-34	1,63E+09	7	7	403	22,775	27,1685	26,9722	27,3648	6	3	0.724281	-0.392534	B8N3W2	B8N3W2	1	AFLA_031960	40S ribosomal protein S7e		
27.6261	27.9259	27.8703	28.0214	28.1063	28.0996						+ 6,16E-296	2,89E+09	9	9	762	20,442	27,9416	27,8074	28,0758	6	3	0.049064	-0.268372	B8N3W5	B8N3W5	1	AFLA_031990	Actin-related protein 2/3 complex subunit 5	27.6261	27.9259	27.8703	28.0214	28.1063	28.0996	+ 6,16E-296	2,89E+09	9	9	762	20,442	27,9416	27,8074	28,0758	6	3	0.049064	-0.268372	B8N3W5	B8N3W5	1	AFLA_031990	Actin-related protein 2/3 complex subunit 5		
29.6717	30.1712	30.4267	30.0013	29.9037	29.9478						0.124E+10	53	13	13	45,2	51,026	30,0204	30,0899	29,9509	6	3	0.567844	0.138939	B8N3W9-B	B8N3W9-B	2	AFLA_032030	Hydroxymethylglutaryl-CoA synthase Erg13, putative	29.6717	30.1712	30.4267	30.0013	29.9037	29.9478	0.124E+10	53	13	13	45,2	51,026	30,0204	30,0899	29,9509	6	3	0.567844	0.138939	B8N3W9-B	B8N3W9-B	2	AFLA_032030	Hydroxymethylglutaryl-CoA synthase Erg13, putative		
27.8605	28.0612	27.4339	27.5737	27.5654	27.7762						9,88E-131	2,43E+09	3	3	3	25,6	14,068	27,7058	27,7852	27,6264	6	3	0.471184	0.158749	B8N151	B8N151	1	AFLA_032250	Nuclear transport factor NTF-2, putative	27.8605	28.0612	27.4339	27.5737	27.5654	27.7762	9,88E-131	2,43E+09	3	3	3	25,6	14,068	27,7058	27,7852	27,6264	6	3	0.471184	0.158749	B8N151	B8N151	1	AFLA_032250	Nuclear transport factor NTF-2, putative
24.4953	24.1945	23.8048	24.2519	24.4084	NaN						2,55E-08	1,72E+08	2	2	2	4,3	71,329	24,231	24,1649	24,3302	5	3	0.576467	-0.165271	B8N154	B8N154	1	AFLA_032280	Uncharacterized protein	24.4953	24.1945	23.8048	24.2519	24.4084	NaN	2,55E-08	1,72E+08	2	2	2	4,3	71,329	24,231	24,1649	24,3302	5	3	0.576467	-0.165271	B8N154	B8N154	1	AFLA_032280	Uncharacterized protein
27.9203	27.2017	26.7029	26.9989	27.4383	27.6834						2,21E-71	1,73E+08	8	8	8	43,6	34,316	27,3243	27,275	27,3735	6	3	0.820216	-0.0985406	B8N157	B8N157	1	AFLA_032310	Uncharacterized protein	27.9203	27.2017	26.7029	26.9989	27.4383	27.6834	2,21E-71	1,73E+08	8	8	8	43,6	34,316	27,3243	27,275	27,3735	6	3	0.820216	-0.0985406	B8N157	B8N157	1	AFLA_032310	Uncharacterized protein
24.3122	25.4201	25.1353	25.181	25.3459	25.3663						3,59E-22	6,2E+08	7	7	7	10,1	99,561	25,1268	24,9559	25,2977	6	3	0.3668154	-0.341863	B8N170	B8N170	1	AFLA_032340	Vacuolar protein sorting-associated protein 35	24.3122	25.4201	25.1353	25.181	25.3459	25.3663	3,59E-22	6,2E+08	7	7	7	10,1	99,561	25,1268	24,9559	25,2977	6	3	0.3668154	-0.341863	B8N170	B8N170	1	AFLA_032340	Vacuolar protein sorting-associated protein 35
24.0985	NaN	23.4446	NaN	24.6681	NaN						1,35E-38	6,08E+08	9	9	9	39,6	34,956	24,0704	23,7715	24,6681	3	2	1	-0.895681	B8N172	B8N172	1	AFLA_032460	Pterin-4-alpha-carbinolamine dehydratase, putative	24.0985	NaN	23.4446	NaN	24.6681	NaN	1,35E-38	6,08E+08	9	9	9	39,6	34,956	24,0704	23,7715	24,6681	3	2	1	-0.895681	B8N172	B8N172	1	AFLA_032460	Pterin-4-alpha-carbinolamine dehydratase, putative
28.8771	28.3263	27.9982	28.3752	28.5172	28.7679						4,18E-202	6,32E+09	10	10	10	73,3	24,935	28,477	28,4005	28,5534	6	3	0.615151	-0.152912	B8N173	B8N173	1	AFLA_032470	Phosphoglycolate phosphatase, putative	28.8771	28.3263	27.9982	28.3752	28.5172	28.7679	4,18E-202	6,32E+09	10	10	10	73,3	24,935	28,477	28,4005	28,5534	6	3	0.615151	-0.152912	B8N173	B8N173	1	AFLA_032470	Phosphoglycolate phosphatase, putative
24.5737	25.3946	26.6978	27.2211	25.8998	25.8064						3,31E-34	1,29E+09	8	8	8	20,9	58,992	25,9322	25,5553	26,3091	6	3	0.382378	-0.753794	B8N177	B8N177	1	AFLA_032510	Galactokinase	24.5737	25.3946	26.6978	27.2211	25.8998	25.8064	3,31E-34	1,29E+09	8	8	8	20,9	58,992	25,9322	25,5553	26,3091	6	3	0.382378	-0.753794	B8N177	B8N177	1	AFLA_032510	Galactokinase
25.7136	25.2093	24.5877	24.6759	25.0464	25.9821						5,06E-18	3,63E+08	9	9	9	4,1	266,87	25,2025	25,1702	25,2348	6	3	0.904765	-0.0645994	B8N177	B8N177	1	AFLA_032610	Ccr4-Not transcription complex subunit (NOT1), putative	25.7136	25.2093	24.5877	24.6759	25.0464	25.9821	5,06E-18	3,63E+08	9	9	9	4,1	266,87	25,2025	25,1702	25,2348	6	3	0.904765	-0.0645994	B8N177	B8N177	1	AFLA_032610	Ccr4-Not transcription complex subunit (NOT1), putative
26.4842	26.523	26.4493	24.5883	24.6968	24.2798						+ 1,23E-16	4,5E+08	4	4	4	13,3	35,184	25,5035	26,4855	24,5121	6	3	0.000101	1.96384	B8N178	B8N178	1	AFLA_032620	Acid phosphatase, putative	26.4842	26.523	26.4493	24.5883	24.6968	24.2798	+ 1,23E-16	4,5E+08	4	4	4	13,3	35,184	25,5035	26,4855	24,5121	6	3	0.000101	1.96384	B8N178	B8N178	1	AFLA_032620	Acid phosphatase, putative
27.2029	27.0673	26.8473	27.0646	27.0581	27.1528						6,21E-58	1,56E+09	11	11	11	38,4	37,741	27,0655	27,0392	27,0918	6	3	0.65179	-0.052599	B8N179	B8N179	1	AFLA_032770	Pre-RNA splicing factor Srp2, putative	27.2029	27.0673	26.8473	27.0646	27.0581	27.1528	6,21E-58	1,56E+09	11	11	11	38,4	37,741	27,0655	27,0392	27,0918	6	3	0.65179	-0.052599	B8N179	B8N179	1	AFLA_032770	Pre-RNA splicing factor Srp2, putative
30.0553	29.6923	29.343	29.6892	29.7573	29.8283						6,03E-290	9,23E+09	15	15	15	47,1	45,104	29,7276	29,6969	29,7583	6	3	0.784133	-0.0613798	B8N179	B8N179	1	AFLA_032870	Dihydropyrimidinase domain protein	30.0553	29.6923	29.343	29.6892	29.7573	29.8283	6,03E-290	9,23E+09	15	15	15	47,1	45,104	29,7276	29,6969	29,7583	6	3	0.784133	-0.0613798	B8N179	B8N179	1	AFLA_032870	Dihydropyrimidinase domain protein
27.7601	27.2706	27.0174	27.3881	26.6274	27.8256						9,33E-84	1,93E+09	6	6	6	27,7	50,762	27,4882	27,3494	27,6271	6	3	0.333636	-0.27765	B8N179	B8N179	1	AFLA_032890	Uncharacterized protein	27.7601	27.2706	27.0174	27.3881	26.6274	27.8256	9,33E-84	1,93E+09	6	6	6	27,7	50,762	27,4882	27,3494	27,6271	6	3	0.333636	-0.27765	B8N179	B8N179	1	AFLA_032890	Uncharacterized protein
30.1757	30.1684	30.2138	30.5797	30.6247	30.6783						+ 0.164E+10	20	20	20	75,4	36,716	30,4068	30,186	30,6276	6	3	0.000156	-0.441579	B8N177	B8N177	1	AFLA_033100	Phosphatidylinositol transporter, putative	30.1757	30.1684	30.2138	30.5797	30.6247	30.6783	+ 0.164E+10	20	20	20	75,4	36,716	30,4068	30,186	30,6276	6	3	0.000156	-0.441579	B8N177	B8N177	1	AFLA_033100	Phosphatidylinositol transporter, putative		
26.288	26.2291	25.8768	24.1274	23.8704	24.28						+ 3,99E-28	2,51E+08	7	7	7	16,1	74,805	25,112	26,1313	24,0926	6	3	0.000313	0.20871	B8N329	B8N329	1	AFLA_033220	Amidase family protein	26.288	26.2291	25.8768	24.1274	23.8704	24.28	+ 3,99E-28	2,51E+08	7	7	7	16,1	74,805	25,112	26,1313	24,0926	6	3	0.000313	0.20871	B8N329	B8N329	1	AFLA_033220	Amidase family protein
24.6399	24.5677	NaN	NaN	24.6264	NaN						9,49E-06	1,51E+08	3	3	3	7,7	52,906	24,6113	24,6038	24,6264	3	2	1	-0.0225964	B8N412	B8N412	1	AFLA_033																										

Supplementary Table S2. Data on proteins obtained from label-free proteomics from *Aspergillus flavus* grown in presence of 0.1 M CaCl₂ followed with 10 µg/ml PgAFP and untreated control.

A. Total data

LQF intensity AF_CaCl ₂ PgAFP_1	LQF intensity AF_CaCl ₂ PgAFP_2	LQF intensity AF_CaCl ₂ PgAFP_3	LQF intensity AF_CaCl ₂ Control_1	LQF intensity AF_CaCl ₂ Control_2	LQF intensity AF_CaCl ₂ Control_3	t-test Significant	PEP	Intensity	Peptides	Razor + unique peptides	Unique peptides	Sequence coverage [%]	Mol. weight [kDa]	Mean AF_CaCl ₂ PgAFP	Mean AF_CaCl ₂ Control	Valid values	Valid values AF_CaCl ₂ PgAFP	Valid values AF_CaCl ₂ Control	t-test p value	t-test Difference	Protein IDs	Majority protein IDs	Proteins	Gene Names	Protein names	
27.0001	27.9914	27.915	27.9447	28.0498	27.9886		2,33E-192	2,7E+09	17	17	17	45.4	54.247	27.8483	27.7022	27.9944	6	3	0.313769	-0.292208	B8N2F8	B8N2F8	AFLA_036430	Proteasome regulatory particle subunit (RpnG), putative		
27.4231	27.6453	27.5855	28.0787	27.9659	28.1114		+1.64E-151	2,69E+09	8	8	8	27.5	54.829	27.8016	27.5513	28.052	6	3	0.003277	-0.500666	B8N2F9	B8N2F9	AFLA_036440	Alanine aminotransferase, putative		
NaN	23.2982	24.2621	25.1787	NaN	NaN		6.18E-10	1.6E+08	2	2	2	18.7	23.738	24.301	23.8622	25.1872	3	2	1	-1.31656	B8N2G6	B8N2G6	AFLA_036510	Methionine-R-sulfoxide reductase SeIR, putative		
NaN	24.4029	24.4384	28.0252	28.3331	27.1151		+9.92E-95	1,71E+09	11	11	11	31.6	57.405	26.4629	24.2026	27.2145	5	2	3	0.005506	-3.4038	B8N4G1	B8N4G1	AFLA_036640	PH domain protein	
29.1996	28.9078	28.7983	29.1928	29.2374	29.2067		6.29E-254	6.33E+09	16	16	16	67	36.418	29.0904	28.9686	29.8223	6	3	3	0.113168	-0.243731	B8N4G3	B8N4G3	AFLA_036660	Lactoylglutathione lyase (EC 4.4.1.5) (Glyoxalase I)	
33.5572	33.1554	33.1353	33.0557	33.2528	33.2484		0.104E+11		36	36	36	75.8	54.216	33.2341	33.2826	33.1856	6	3	3	0.558051	0.0970001	B8N4I0	B8N4I0	AFLA_036840	6-phosphogluconate dehydrogenase, decarboxylating (EC 1.1.1.14)	
26.3238	25.8346	25.4439	25.49	25.8246	26.0511		4.11E-22	6,24E+08	3	3	3	18.2	26.494	25.828	25.8674	25.7886	6	3	3	0.807108	0.0788352	B8N4I1	B8N4I1	AFLA_036850	Uncharacterized protein	
25.4565	25.398	25.8965	NaN	25.6164	25.8795		0.000154	5,09E+08	2	2	2	1.3	188.25	25.6494	25.5836	25.748	5	3	2	0.518932	-0.164339	B8N4K1	B8N4K1	AFLA_037050	HEAT repeat protein (DRIM), putative	
NaN	23.5586	23.736	23.4144	23.448	23.581		5.45E-05	1,18E+08	2	2	2	3.3	61.235	23.5476	23.6473	23.4811	5	2	3	0.172488	0.166202	B8N4K2	B8N4K2	AFLA_037060	CwI domain protein	
29.7816	29.4086	29.0082	29.284	29.3834	29.4449		1,75E-189	7,17E+09	10	10	10	52.4	32.871	29.3851	29.3995	29.3708	6	3	3	0.96007	0.0286681	B8N4K7	B8N4K7	AFLA_037110	Proteasome subunit beta type (EC 3.4.25.1)	
30.1848	31.1302	31.216	31.3203	30.6034	30.272		0	1,16E+10	13	13	13	51.7	35.109	30.7878	30.8437	30.7319	6	3	3	0.817065	0.111792	B8N4L2	B8N4L2	AFLA_037160	Thiazole biosynthesis enzyme Sit35	
25.6951	24.9372	24.8324	24.344	25.3998	25.2925		1.96E-22	3.38E+08	5	5	5	10.2	73.648	25.0835	25.1549	25.0121	6	3	3	0.757408	0.142321	B8N4L5	B8N4L5	AFLA_037200	Uncharacterized protein	
25.3698	25.9065	27.3501	27.1834	26.4537	25.885		1.33E-62	1,54E+09	10	10	10	37.9	45.511	26.3747	26.2088	26.5407	6	3	3	0.65401	-0.331903	B8N4L8	B8N4L8	AFLA_037220	Chorismate synthase (EC 4.2.3.5)	
26.6384	25.8913	NaN	25.1075	26.077	26.111		2.41E-17	3,01E+08	6	6	6	28.9	29.94	25.965	26.2648	25.7652	17	2	3	0.397722	0.499672	B8N4M0	B8N4M0	AFLA_037250	Cyanide hydratase/nitrilase, putative	
24.0575	24.4024	24.8802	22.8871	24.1451	24.6103		6.38E-08	1,94E+08	3	3	3	9.8	43.943	24.1638	24.4467	23.8808	6	3	3	0.375009	0.562939	B8N4M5	B8N4M5	AFLA_037300	Methionyl-tRNA formyltransferase family protein, putative	
25.5979	25.8712	25.7718	25.2985	25.1575	25.3141		+2.71E-130	1,25E+09	8	8	8	41.5	21.621	25.5018	25.747	25.2567	6	3	3	0.006473	0.490598	B8N4M7	B8N4M7	AFLA_037320	Rho GTPase Rho1	
25.5634	26.2712	26.5588	25.9226	26.084	26.0181		5.51E-55	7,99E+08	6	6	6	17.8	49.932	26.0697	26.1311	26.0082	6	3	3	0.702484	0.122926	B8N4N0	B8N4N0	AFLA_037350	Casein kinase I, putative	
29.01	28.6667	28.4289	28.7473	28.8807	28.9365		6.14E-146	4,37E+09	12	12	12	47.4	45.809	28.7784	28.7019	28.8548	6	3	3	0.380996	-0.152953	B8N4P0	B8N4P0	AFLA_037450	Probable carboxypeptidase AFLA_037450 [EC 3.4.17.1] (Peptidase M20 domain-containing protein AFLA_037450)	
26.3224	26.8787	26.9781	26.7111	26.6724	26.7561		1.94E-44	1,54E+09	12	12	11	40	46.412	26.7198	26.7264	26.7132	6	3	3	0.951724	0.012357	B8N2H2	B8N2H2	AFLA_037470	Proteasome regulatory particle subunit Rpt4, putative	
30.9885	32.8444	34.4212	34.808	33.6523	33.3054		0.13E+11		19	19	19	54.3	47.406	33.3367	32.7514	33.9219	6	3	3	0.343763	-1.17053	B8N2H3	B8N2H3	AFLA_037480	Enolase/allergen Asp F 22	
26.8497	27.0541	26.8767	27.2048	27.172	27.0233		8,96E-120	1,08E+09	5	5	5	30.6	29.688	27.021	26.9628	27.1151	6	3	3	0.085429	-0.188265	B8N2H4	B8N2H4	AFLA_037490	Eukaryotic translation initiation factor 3 subunit J (eIF3J) (Eukaryotic translation initiation factor 3 30 kDa subunit homolog)	
30.3537	30.3772	30.2035	30.2713	30.2738	30.2732		3,01E-193	1,45E+10	13	12	12	50.2	22.89	30.2921	30.3115	30.2728	6	3	3	0.515986	0.0387724	B8N2H5	B8N2H5	AFLA_037500	14-3-3 protein sigma, gamma, zeta, beta/alpha, putative	
25.5487	NaN	23.6399	NaN	NaN	23.8287		4.32E-23	2,41E+08	6	6	6	8.3	109.14	24.3391	24.5943	23.8287	3	2	1	1	0.765552	B8N2H6	B8N2H6	AFLA_037510	Calcium-transferring ATPase (EC 3.6.3.8)	
28.5466	29.039	29.0736	29.4148	29.3575	29.3729		+2.20E-224	7,2E+09	14	14	14	32.7	76.931	29.1341	28.8664	29.3171	6	3	3	0.044304	-0.495316	B8N2K3	B8N2K3	AFLA_037780	Actin-related protein 2/3 complex subunit 1A, putative	
28.5829	28.2415	27.8324	28.1568	28.2369	28.3733		1.68E-71	3,18E+09	6	6	6	35.4	28.945	28.2373	28.219	28.2557	6	3	3	0.87885	-0.669999	B8N2K9	B8N2K9	AFLA_037840	Proteasome subunit beta type (EC 3.4.25.1)	
29.6964	29.3047	28.8871	29.1185	29.2393	29.4244		3,76E-116	6,48E+09	11	11	11	60.5	28.673	29.3017	29.2961	29.3074	6	3	3	0.966448	-0.0112953	B8N2L0	B8N2L0	AFLA_037850	Proteasome component Prs3, putative	
24.6044	26.3551	27.11	26.3637	27.0501	26.3687		1,04E-168	3,08E+09	16	16	16	49.2	42.261	26.3087	26.0322	26.5992	6	3	3	0.50284	-0.570982	B8N2L6	B8N2L6	AFLA_037910	Isocitrate dehydrogenase [NAD] subunit, mitochondrial (EC 1.1.1.41)	
29.8254	29.5183	29.1752	29.4661	29.5066	29.6048		0.778E+09		13	13	13	57.7	31.719	29.5161	29.5263	29.5249	6	3	3	0.923746	-0.0195885	B8N2L9	B8N2L9	AFLA_037940	Proteasome subunit alpha type (EC 3.4.25.1)	
30.4022	30.071	29.7384	29.7674	30.0778	30.0766		0.129E+10		8	8	8	61.3	21.722	30.1497	27.2943	30.2055	6	3	3	0.624333	0.110694	B8N2M0	B8N2M0	AFLA_037950	6,7-dimethyl-8-ribityllumazine synthase (EC 2.3.1.78)	
23.6363	26.1088	26.9387	25.5692	25.8241	25.6577		0.604E+09		29	29	29	49.4	77.127	25.6225	25.5613	25.6837	6	3	3	0.907984	-0.122416	B8N2M1	B8N2M1	AFLA_037960	Glucosamine-fructose-6-phosphate aminotransferase	
27.4245	26.3567	27.0415	24.5807	24.9304	25.2521		+4.11E-22	4,39E+08	8	8	8	22	54.086	25.931	26.9409	24.9211	6	3	3	0.005349	2.0198	B8N2C4	B8N2C4	AFLA_038390	Sarcosine oxidase, putative	
23.4702	NaN	27.1883	NaN	NaN	NaN		1.45E-49	6,84E+08	9	9	9	20.6	69.301	25.3293	25.3293	NaN	2	2	0	1	NaN	B8NCS8	B8NCS8	AFLA_038530	Extracellular metalloproteinase mep (EC 3.4.24.1) (Elastinolytic metalloproteinase mep) (Fungalsin mep)	
29.398	28.8011	28.6607	27.8362	28.1611	28.3295		+0.784E+09		18	18	18	40.9	65.01	28.5311	28.9533	28.1089	6	3	3	0.034652	0.844376	B8NCH3	B8NCH3	AFLA_038790	Adenosine deaminase family protein	
25.0566	NaN	NaN	23.2502	NaN	23.7905		7,19E-07	1,4E+08	3	3	3	8.3	56.279	24.0325	25.0566	23.5204	1	2	1	1	1.53625	B8NCH7	B8NCH7	AFLA_038840	Uncharacterized protein	
NaN	NaN	NaN	25.5384	26.0352	25.8052		6.39E-08	2,85E+08	2	2	2	5.9	50.604	25.7929	NaN	25.7929	2	0	3	1	NaN	B8NCO0	B8NCO0	AFLA_039370	Acid phosphatase, putative	
25.8532	NaN	24.7597	NaN	24.7036	24.891		4,95E-20	1,71E+08	4	4	4	22.3	26.281	25.0519	25.3065	24.7923	4	2	2	2	0.455551	0.509178	B8N4N3	B8N4N3	AFLA_039410	Cell wall serine-threonine-rich galactomanannoprotein Mp1
27.4748	27.2631	26.6381	26.9729	26.9648	27.1411		6,41E-139	1,6E+09	3	3	3	22.9	37.182	27.0758	27.1253	27.0263	6	3	3	0.720141	0.0990855	B8NCP9	B8NCP9	AFLA_039560	WW domain protein	
26.8105	26.3249	25.8094	23.6535	23.4816	23.8801		+2.19E-35	2,71E+08	5	5	5	15.2	52.932	24.9933	26.315	23.6717	6	3	3	0.001054	2.64323	B8NAC3	B8NAC3	AFLA_039680	Uncharacterized protein	
26.4963	25.9572	26.2933	26.34	26.294	26.5427		3,05E-33	8,16E+08	5	5	5	31.2	26.601	26.3066	26.2209	26.2932	6	3	3	0.379203	-0.171327	B8NAC4	B8NAC4	AFLA_039690	Phosphoglycerate mutase, putative	
25.9183	25.0718	23.953	24.418	24.0786	24.2632		8,15E-18	6,83E+08	5	5	5	24.6	36.352	24.6174	24.981	24.2533	6	3	3	0.276143	0.727757	B8NAC6	B8NAC6	AFLA_039710	Quinone oxidoreductase, putative	
30.058	30.5309	31.1301	31.0686	30.6648	30.4675		0.211E+10		21	21	21	63	45.963	30.6533	30.573	30.7336	6	3	3	0.676164	-0.160616	B8NAG7	B8NAG7	AFLA_040120	Flavohemoprotein	
30.4971	30.2241	29.7106	30.3118	30.4689	30.5562		0.123E+10		20	20	20	52	56.251	30.2948	30.1439	30.4456	6	3	3	0.279462	-0.301708	B8NAJ3	B8NAJ3	AFLA_040380	Mannitol dehydrogenase, putative	
29.9453	29.5184	29.5024	29.0136	29.0914	29.291		+0.128E+10		12	12	12	47.3	50.37	29.3937	29.6554	29.1332	6	3	3	0.035003	0.523361	B8NAJ6	B8NAJ6	AFLA_040430	Tripeptidyl-peptidase (TPPA), putative	
NaN	25.0949	25.4413	24.6792	24.4415	NaN																					

Supplementary Table S2. Data on proteins obtained from label-free proteomics from *Aspergillus flavus* grown in presence of 0.1 M CaCl₂ followed with 10 μg/ml PgAFP and untreated control.

A. Total data

LFQ intensity AF_CaCl ₂ PgAFP 1	LFQ intensity AF_CaCl ₂ PgAFP 2	LFQ intensity AF_CaCl ₂ PgAFP 3	LFQ intensity AF_CaCl ₂ Control 1	LFQ intensity AF_CaCl ₂ Control 2	LFQ intensity AF_CaCl ₂ Control 3	t-test Significant	PEP	Intensity	Peptides	Razor + unique peptides	Unique peptides	Sequence coverage [%]	Mol. weight [kDa]	Mean AF_CaCl ₂ PgAFP	Mean AF_CaCl ₂ Control	Valid values	Valid values AF_CaCl ₂ PgAFP	Valid values AF_CaCl ₂ Control	t-test p value	t-test Difference	Protein IDs	Majority protein IDs	Proteins	Gene Names	Protein names	
25.9905	26.4117	26.678	26.7742	26.6831	26.6645		7,43E-26	1,08E+09	6	6	6	13.7	71.23	26.5347	26.3621	26.7073	6	3	0.161326	-0.35197	B8NB20	B8NB20	1	AFLA_043950	Serine/threonine protein kinase (YPK1), putative	
28.1843	28.2027	28.0174	28.0164	28.1937	28.2387		9,44E-124	2,53E+09	13	13	13	49.6	43.479	28.1422	28.1348	28.1496	6	3	0.877079	-0.0148137	B8NB23	B8NB23	1	AFLA_043980	Manitol-1-phosphate dehydrogenase	
28.963	28.193	27.1472	26.6214	27.8926	28.1444		3,15E-104	3,04E+09	20	20	20	37.6	90.789	27.8281	28.1011	27.5561	6	3	0.483062	0.545599	B8NB25	B8NB25	1	AFLA_044000	COPI vesicle coat beta' subunit, putative	
NaN	24.4035	24.3142	24.7186	23.9135	NaN		2,09E-25	3,44E+08	5	5	5	31.1	26.24	24.3375	24.3589	24.3161	4	2	0.295523	0.042779	B8NB26	B8NB26	1	AFLA_044010	NADH-ubiquinone oxidoreductase 299 kDa subunit, putative	
32.8596	32.5482	32.2355	31.8553	32.3403	32.4192		0	4,26E+10	19	19	19	68.2	34.24	32.3763	32.5478	32.4209	6	3	0.245395	0.342852	B8NB34	B8NB34	1	AFLA_044090	Uricase (EC 1.7.3.3) (Urate oxidase)	
25.8737	26.2932	28.3247	27.2091	26.1649	25.9531		7,71E-44	1,25E+09	5	5	5	39.9	15.923	26.6365	26.8306	26.4424	6	3	0.671815	0.388174	B8NB36	B8NB36	1	AFLA_044110	40S ribosomal protein Rps16, putative	
25.4122	26.1687	29.1969	28.0306	26.2685	26.1138		1,07E-126	1,51E+09	7	7	7	52	15.817	26.8605	26.9166	26.8043	6	3	0.935359	0.112348	B8NB42	B8NB42	1	AFLA_044170	40S ribosomal protein S11	
31.3754	31.3018	31.0993	31.1647	30.9258	31.0317		0	2,34E+10	21	21	21	75.1	44.378	31.1498	31.2588	31.0407	6	3	0.112765	0.218088	B8NB44	B8NB44	1	AFLA_044190	Branched-chain-amino-acid aminotransferase (EC 2.6.1.42)	
26.8544	28.2825	28.1856	27.5691	27.8237	27.7303		5,10E-153	4,49E+09	14	14	14	48.1	54.745	27.7409	27.7741	27.7077	6	3	0.893881	0.0664387	B8NB48	B8NB48	1	AFLA_044230	Eukaryotic translation initiation factor 3 subunit L (eIF3L)	
24.3281	24.1462	24.1743	24.0999	24.1955	24.3117		3,76E-07	2,24E+08	3	3	3	8.6	54.862	24.2093	24.2162	24.2024	6	3	0.87808	0.0138512	B8NB51	B8NB51	1	AFLA_044260	Kynureninase (EC 3.7.1.3) (Biosynthesis of nicotinic acid protein 5) (L-kynurenine hydrolase)	
25.7682	25.5617	25.1388	25.5363	25.3664	25.3794		7,57E-21	5,04E+08	7	7	7	30.6	56.251	25.3951	25.4895	25.3807	6	3	0.396037	0.189844	B8NB55	B8NB55	1	AFLA_044300	SH3 domain protein	
NaN	NaN	24.4895	26.3616	24.664	24.6863		7,39E-46	5,41E+08	6	6	6	23.2	68.968	25.0504	24.4895	25.2373	4	1	0.747761	0.88855	B8NB56	B8NB56	1	AFLA_044310	SH3 domain protein	
29.8108	29.0482	28.8646	28.8556	29.2361	29.2476		3,73E-163	4,73E+09	15	15	15	61.4	36.746	29.1771	29.2412	29.1131	6	3	0.70681	0.128107	B8NB58	B8NB58	2	AFLA_044320	Ketoreductase	
27.1434	27.5683	27.4071	25.1086	25.1061	24.4081		+ 8,72E-38	7,92E+08	10	10	10	29.7	51.166	26.1236	27.3729	24.8743	6	3	0.000694	2.49867	B8NB59	B8NB59	1	AFLA_044340	Uncharacterized protein	
29.5376	29.1187	28.8278	29.1992	29.458	29.3736		1,22E-243	6,84E+09	15	15	13	73.1	34.609	29.2632	29.1614	29.365	6	3	0.411258	-0.20357	B8NB66	B8NB66	1	AFLA_044410	Glycerol dehydrogenase, putative	
27.4721	26.7786	25.5211	26.2421	26.7393	27.0572		1,86E-41	1,02E+09	8	8	8	34.6	29.692	26.6351	26.5906	26.6796	6	3	0.892545	-0.0899702	B8NB70	B8NB70	1	AFLA_044450	Uncharacterized protein	
27.5137	26.6409	25.9234	26.4265	27.1186	26.7136		1,06E-51	8,09E+08	7	7	7	19.6	62.144	26.7228	26.6926	26.4529	6	3	0.910164	-0.0602773	B8NB71	B8NB71	1	AFLA_044460	Phenylacetyl-CoA ligase, putative	
27.6181	27.0357	26.8448	27.1282	27.5615	27.513		7,61E-46	1,59E+09	13	13	13	62.8	39.389	27.2835	27.1662	27.7009	6	3	0.433664	-0.234706	B8NB75	B8NB75	1	AFLA_044500	Yjef domain protein	
31.9513	32.1439	32.1406	31.2945	30.8648	30.7891		+ 7,10E-271	3,38E+10	8	8	8	95.4	11.087	31.5307	32.0786	30.9828	6	3	0.002966	1.09576	B8NB77	B8NB77	1	AFLA_044520	60S acidic ribosomal protein P2/allergen Asp F 8	
29.7982	29.4248	29.991	29.6396	28.8511	29.5695		0	7,23E+09	5	5	5	58.2	17.502	29.5457	29.738	29.3534	6	3	0.271559	0.384623	B8NB78	B8NB78	1	AFLA_044530	40S ribosomal protein S15, putative	
31.8846	31.6609	31.6755	31.8164	31.6978	31.7721		0	3,32E+10	53	53	52	60.1	129.3	31.7512	31.7403	31.7621	6	3	0.799079	-0.021902	B8NB80	B8NB80	1	AFLA_044550	Carbamoyl-phosphate synthase, large subunit	
NaN	25.7627	26.485	26.6206	26.9702	26.4306		1,56E-44	8,62E+08	11	11	11	13.4	108.24	26.4538	26.1239	26.6738	5	2	0.201991	-0.299173	B8NB84	B8NB84	1	AFLA_044590	Nonsense-mediated mRNA decay protein (Nmj5), putative	
32.5814	32.0291	32.5001	32.4429	31.9244	31.8448		0	4,64E+10	35	35	35	58.3	72.467	32.2204	32.3702	32.0707	6	3	0.304603	0.295921	B8NB87	B8NB87	1	AFLA_044620	Mitochondrial Hsp70 chaperone (Esc70), putative	
28.3556	27.5425	26.8298	26.3754	27.5747	27.6728		8,55E-45	1,85E+09	17	17	17	27.9	76.31	27.3911	27.576	27.2063	6	3	0.575048	0.369701	B8NB89	B8NB89	1	AFLA_044640	Fatty acid activator Fa4a, putative	
29.8451	29.6667	29.3256	29.2571	29.4169	29.4873		1,15E-236	9,03E+09	11	11	11	40.4	31.538	29.4998	29.6125	29.3871	6	3	0.248288	0.225375	B8NB96	B8NB96	1	AFLA_044710	Eukaryotic translation initiation factor 3 subunit G (eIF3G) (Eukaryotic translation initiation factor 3 RNA-binding subunit) (Translation initiation factor eIF3 p33 subunit homolog)	
NaN	24.1006	24.5796	24.0271	23.8706	23.9707		3,24E-13	2,46E+08	5	5	5	87.5	24.107	24.1097	24.3401	23.9561	5	2	0.133776	0.383993	B8NB93	B8NB93	1	AFLA_044780	Rbm25 protein, putative	
33.4131	33.3035	33.0756	33.4915	33.4791	33.447		0	1,12E+11	35	35	35	69.4	61.213	33.3683	33.2641	33.4725	6	3	0.106175	-0.208486	B8NB97	B8NB97	1	AFLA_044820	Glucose-6-phosphate isomerase (EC 5.3.1.9)	
27.6992	27.3149	27.2345	27.3973	27.1576	27.3043		4,64E-118	2,05E+09	16	16	16	38.4	26.092	27.3513	27.4162	27.2864	6	3	0.461222	0.12982	B8NB98	B8NB98	1	AFLA_044930	Superoxide dismutase copper chaperone Lys7, putative	
28.747	28.5366	28.5918	29.0093	28.9741	28.9617		+ 2,71E-154	4,46E+09	14	14	14	55.1	48.429	28.8034	28.6251	28.9817	6	3	0.005257	-0.355659	B8NB97	B8NB97	2	AFLA_045020	Aspartate aminotransferase (EC 2.6.1.1)	
27.3363	27.2338	27.2159	27.4221	27.3339	27.4706		+ 9,39E-73	1,63E+09	7	7	7	32	33.561	27.3192	27.2517	27.3872	6	3	0.047966	-0.135578	B8NB82	B8NB82	1	AFLA_045170	Alpha/beta hydrolase, putative	
NaN	NaN	NaN	24.7185	25.3773	25.6684		5,14E-10	4,09E+08	5	5	5	11.3	74.691	25.2547	NaN	25.2547	3	3	1	NaN	B8NBFO	B8NBFO	1	AFLA_045250	Biotin apto-protein ligase, putative	
28.9038	29.6203	29.3583	29.6684	29.5674	29.5698		4,26E-298	8,16E+09	30	30	30	24.3	147.279	29.4641	29.2942	29.6411	6	3	0.183727	-0.339908	B8NB78	B8NB78	1	AFLA_045320	Eukaryotic translation initiation factor subunit eIF4F, putative	
27.0945	26.6613	26.2374	25.5855	25.8555	26.1812		6,38E-41	6,81E+08	6	6	6	2	17.5	27.2	26.2709	26.6644	25.8774	6	3	0.959328	0.786975	B8NB13	B8NB13	1	AFLA_045580	GNAT family acetyltransferase, putative
32.8396	32.7102	32.4377	32.6305	32.5776	32.6842		0	7,48E+10	42	42	42	78.6	62.213	32.6466	32.6625	32.6308	6	3	0.808286	0.0317256	B8NBK0	B8NBK0	1	AFLA_045750	Antigenic mitochondrial protein Hsp50, putative	
25.1799	27.3961	29.2773	27.6885	25.3579	25.4396		3,36E-95	1,87E+09	6	6	6	57.5	11.353	26.7232	27.2844	26.162	6	3	0.470273	1.12244	B8NBK4	B8NBK4	1	AFLA_045790	60S ribosomal protein L30, putative	
25.4875	25.3918	25.2229	25.5799	26.0917	25.3743		1,45E-21	5,2E+08	6	6	6	11.9	70.047	25.5247	25.3674	25.6822	6	3	0.378663	-0.314573	B8NBK5	B8NBK5	1	AFLA_045800	M protein, serotype 2.1, putative	
NaN	NaN	26.64	26.8071	26.628	26.6094		6,87E-30	9,53E+08	3	3	3	23.4	22.048	26.6711	26.64	26.6815	4	1	0.041448	-0.08966	B8NBK6	B8NBK6	1	AFLA_045810	Coatamer subunit zeta, putative	
27.0813	26.2273	26.4931	26.5916	26.4308	26.9013		1,62E-17	8,44E+08	4	4	4	42.2	12.542	26.6209	26.6006	26.6612	6	3	0.894452	-0.040645	B8NBLO	B8NBLO	1	AFLA_045850	Uncharacterized protein	
NaN	23.7788	23.8826	24.9376	23.6777	23.5139		1,02E-09	1,82E+08	3	3	3	12.2	30.065	23.9581	23.8307	23.4043	5	2	0.739378	-0.212354	B8NBLL1	B8NBLL1	1	AFLA_045860	NADH-ubiquinone dehydrogenase 24 kDa subunit, putative	
23.0887	22.8387	22.9976	23.1469	23.5524	NaN		4,80E-09	1,43E+08	4	4	4	6.5	78.912	23.1249	22.975	23.0436	5	3	0.2126207	-0.374603	B8NBLS5	B8NBLS5	1	AFLA_045900	Phenylalanine ammonia-lyase (EC 4.3.1.24)	
28.0478	27.3002	26.1512	26.8734	28.1803	28.2532		1,07E-75	2,15E+09	14	14	14	20.6	91.951	27.4677	27.1664	27.769	6	3	0.444289	-0.602608	B8NBML2	B8NBML2	1	AFLA_045970	Vacuolar transporter chaperone (Vtca), putative	
32.9401	32.5188	33.711	31.0613	31.0406	31.1508		0	5,77E+10	27	27	27	52.7	80.383	32.0704	33.0566	31.0843	6	3	0.040914	1.9724	B8NBML3	B8NBML3	1	AFLA_045980	Proteasome activator complex 1 subunit 1 (Pac1)	
28.669	28.381	28.0109	27.4156	28.1561	28.0555		2,15E-73	2,78E+09	11	11	11	28.9	46.84	28.1147	28.3536	28.8757	6	3	0.186459	0.477905	B8NBML6	B8NBML6	1	AFLA_046010	Eukaryotic translation initiation factor	

Supplementary Table S2. Data on proteins obtained from label-free proteomics from *Aspergillus flavus* grown in presence of 0.1 M CaCl₂ treated with 10 µg/ml PgAFP and untreated control.

LFQ intensity AF_CaCl ₂ PgAFP_1		LFQ intensity AF_CaCl ₂ PgAFP_2		LFQ intensity AF_CaCl ₂ PgAFP_3		LFQ intensity AF_CaCl ₂ Control_1		LFQ intensity AF_CaCl ₂ Control_2		LFQ intensity AF_CaCl ₂ Control_3		t-test Significant	PEP	Intensity	Peptides	Razor + unique peptides	Unique peptides	Sequence coverage [%]	Mol. weight [kDa]	Mean	Mean AF_CaCl ₂ PgAFP	Mean AF_CaCl ₂ Control	Valid values	Valid values AF_CaCl ₂ PgAFP	Valid values AF_CaCl ₂ Control	t-test p value	t-test Difference	Protein IDs	Majority protein IDs	Proteins	Gene Names	Protein names
27.5903	28.9126	26.6158	25.6323	24.9213	24.8968				2,41E-95	1.51E+09	15	15	15	15	14	14	14	61.5	34.409	29.5711	29.4561	29.6861	6	3	3	0.022541	-2.55609	BBN9S7	BBN9S7	1	AFLA_048200	Pseudouridylyl synthase family protein
NaN	26.5634	26.925	26.7894	26.1466	25.9641				2,60E-32	8.77E+08	8	8	8	8	8	8	37.7	37.895	26.4777	26.7442	26.3	5	2	3	0.294045	0.444182	BBN9S6	BBN9S6	1	AFLA_048290	Homoserine kinase	
29.171	29.7219	29.6922	29.9328	29.6707	29.4452				0	9.27E+09	28	28	28	28	28	28	45.9	80.408	29.6056	29.5284	29.6829	6	3	3	0.53452	-0.154554	BBN9S4	BBN9S4	1	AFLA_048370	Glycyl-tRNA synthetase	
26.8729	27.2418	24.8583	27.3538	27.4928	27.5797				6,42E-34	1.31E+09	10	10	10	10	10	10	42.1	30.2	26.8999	26.2444	27.4754	6	3	3	0.196553	-1.15108	BBN9S8	BBN9S8	1	AFLA_048410	BAR adaptor protein RV5161, putative	
29.6736	29.5443	29.2154	29.4294	29.2529	29.4008				0	8.84E+09	9	9	9	9	9	9	51.8	26.568	29.4194	29.4778	29.3611	6	3	3	0.471449	0.116723	BBN9S5	BBN9S5	1	AFLA_048490	Eukaryotic translation initiation factor 6 (eIF-6)	
29.1215	28.6674	28.6345	29.1776	28.8861	28.8784				3,33E-51	4.68E+09	8	8	8	8	8	8	21.4	47.095	28.8943	28.8078	28.9807	6	3	3	0.404014	-0.17288	BBN9S8	BBN9S8	1	AFLA_048510	UV excision repair protein (RadW), putative	
29.2948	29.3361	29.224	29.4681	29.3419	29.403				0	7.49E+09	12	12	12	12	12	12	68.9	18.464	29.3446	29.2849	29.4043	6	3	3	0.071456	-0.119408	BBN9S0	BBN9S0	1	AFLA_048530	E3 ubiquitin ligase complex SCF subunit sconC (Sulfur controller C) (Sulfur metabolite repression control protein C)	
29.3173	29.2112	29.8398	30.0977	29.6541	29.3065				5,72E-291	9.38E+09	14	14	14	14	14	14	61.5	34.409	29.5711	29.4561	29.6861	6	3	3	0.48639	-0.230007	BBN9S8	BBN9S8	1	AFLA_048610	Succinyl-CoA synthetase alpha subunit, putative	
NaN	NaN	NaN	24.0118	24.412	NaN				5,62E-08	1.58E+08	4	4	4	4	4	4	9.4	65.051	24.2124	NaN	24.2124	2	0	2	1	NaN	BBN9S9	BBN9S9	1	AFLA_048620	Histone acetyltransferase, putative	
27.1801	30.809	32.0154	31.831	30.3601	30.0584				0	2.84E+10	19	19	19	19	19	19	78	37.057	30.3823	30.0015	30.7632	6	3	3	0.648866	-0.761674	BBN9H6	BBN9H6	1	AFLA_048690	Alcohol dehydrogenase 1 (EC 1.1.1.1) (Alcohol dehydrogenase I)	
NaN	27.8748	29.4044	28.3256	23.4665	NaN				1,04E-107	9.79E+08	6	6	6	6	6	6	40.6	27.435	26.0178	26.1396	25.8961	4	2	2	0.957726	0.203516	BBN9H6	BBN9H6	1	AFLA_048810	60S ribosomal protein L8, putative	
31.382	31.1808	31.0543	31.4777	31.6623	31.8063				+	0.32E+10	18	18	18	18	18	18	71.7	38.503	31.4289	31.2091	31.6498	6	3	3	0.020762	-0.439738	BBN9H9	BBN9H9	1	AFLA_048840	Adenosine kinase, putative	
27.7822	27.5107	27.9572	27.0257	27.3652	27.381				+	1.41E-43	2.15E+09	12	12	12	12	12	42.5	42.671	27.5038	27.75	27.2575	6	3	3	0.047401	0.492545	BBN9I7	BBN9I7	1	AFLA_049020	AcyI-CoA dehydrogenase family protein	
25.809	26.4659	26.5919	26.9722	26.3391	26.2128				+	1.25E-81	1.97E+09	9	9	9	9	9	43	42.286	26.3993	26.289	26.5097	6	3	3	0.505399	-0.220746	BBN9K3	BBN9K3	1	AFLA_049080	Biotin synthase, putative	
26.7679	26.7089	26.4928	26.5802	26.8663	26.8353				1,34E-32	1.12E+09	12	12	12	12	12	23.2	87.809	26.7086	26.6565	26.7606	6	3	3	0.446168	-0.104083	BBN9K4	BBN9K4	1	AFLA_049090	Onanonoxy-7-omega-8-eneinoitelymoneda		
27.8928	29.5706	29.3097	30.3378	30.4319	30.2497				0	1.06E+10	19	19	19	19	19	19	49.9	51.655	29.6321	28.9244	30.3398	6	3	3	0.053996	-1.41541	BBN9M4	BBN9M4	1	AFLA_049290	Citrate synthase	
25.7983	25.7054	25.7905	25.7177	25.8913	25.9088				9,01E-14	3.62E+08	8	8	8	8	8	8	9	123.55	25.802	25.7647	25.8937	6	3	3	0.333732	-0.075255	BBN9M5	BBN9M5	1	AFLA_049300	mRNA-nucleus export ATPase (Eif1), putative	
25.6451	25.7319	25.4565	25.8924	25.6748	25.7469				8,18E-37	7.11E+08	10	10	10	10	10	10	26	36.237	25.6912	25.6111	25.7714	6	3	3	0.196356	-0.160213	BBN9M9	BBN9M9	1	AFLA_049340	Aldo/keto reductase, putative	
27.8706	27.5955	27.4406	27.7539	27.7328	27.6057				3,21E-69	1.91E+09	6	6	6	6	6	6	30.8	29.823	27.6665	27.6355	27.6975	6	3	3	0.667932	-0.0619348	BBN9N2	BBN9N2	1	AFLA_049370	Short-chain dehydrogenase/reductase family protein, putative	
NaN	24.805	25.2592	24.5689	25.9675	25.2757				4,18E-66	1.06E+09	11	11	11	11	11	11	24.9	61.075	25.1753	25.0321	25.2707	5	2	2	0.692708	-0.238959	BBN9N4	BBN9N4	1	AFLA_049390	Malate synthase (EC 2.3.3.9)	
29.6979	29.4553	29.1971	29.7431	29.8666	29.8132				1,72E-125	7.33E+09	13	13	13	13	13	13	57.8	27.708	29.6289	29.4501	29.6706	6	3	3	0.074331	-0.35751	BBN9P1	BBN9P1	1	AFLA_049920	Dienelactone hydrolase family protein	
29.2279	28.3674	28.6777	28.32	28.6063	28.7086				1,28E-123	3.7E+09	7	7	7	7	7	7	28.7	31.509	28.6533	28.7577	28.549	6	3	3	0.490944	0.208736	BBN9P2	BBN9P2	1	AFLA_049930	Uncharacterized protein	
24.0546	24.3576	28.1999	23.4009	NaN	23.5744				4,05E-19	9.96E+08	6	6	6	6	6	6	28.2	22.986	24.7175	25.5734	24.877	5	3	2	0.319903	2.04972	BBN9P9	BBN9P9	1	AFLA_050000	Ribosomal protein L16a	
26.7664	26.6271	26.3393	26.4077	26.6351	26.772				2,65E-14	1.02E+09	4	4	4	4	4	4	8.9	82.71	26.5913	26.5776	26.6049	6	3	3	0.876172	-0.0273229	BBN9S4	BBN9S4	1	AFLA_050050	AP-1 adaptor complex subunit gamma, putative	
25.0563	24.7144	23.8257	NaN	NaN	24.7874				1,14E-10	2.76E+08	4	4	4	4	4	4	7.8	85.794	24.5959	24.5321	24.7874	4	3	1	1	-0.255218	BBN9S9	BBN9S9	1	AFLA_050100	LMBR1 domain protein	
27.9869	27.7649	28.202	28.9051	28.7235	28.6762				+	4.41E-36	2.65E+09	6	6	6	6	6	57.8	10.968	28.3764	27.9846	28.2683	6	3	3	0.00556	-0.783689	BBN9S1	BBN9S1	1	AFLA_050120	Glutaredoxin Grx1, putative	
23.7744	24.9905	25.15	26.1952	26.6511	26.2122				+	1.16E-33	4.71E+08	6	6	6	6	6	20.2	45.89	25.4456	24.6383	26.7599	6	3	3	0.020965	-1.61451	BBN9S2	BBN9S2	1	AFLA_050130	Uncharacterized protein	
31.2931	31.1475	30.9098	30.9873	30.9647	31.0324				0	2.64E+10	22	22	22	22	22	22	44.8	57.15	31.0468	31.0989	30.9948	6	3	3	0.357265	-0.104126	BBN9S6	BBN9S6	1	AFLA_050270	Conserved lysine-rich protein, putative	
26.4474	26.096	26.1216	26.2063	26.4483	26.4106				4,58E-53	9.48E+08	4	4	4	4	4	4	40.5	13.392	26.384	26.2217	26.3551	6	3	3	0.183729	-0.133406	BBN9S6	BBN9S6	1	AFLA_050370	Prefolitin subunit 1, putative	
24.8965	24.026	23.41	23.6958	24.445	24.345				1,10E-07	1.65E+08	4	4	4	4	4	4	27.4	24.518	24.1364	24.1108	24.162	6	3	3	0.922105	0.051113	BBN9C7	BBN9C7	1	AFLA_050480	ESCRT-II complex component (Vps25), putative	
25.1757	25.1437	24.7907	24.951	24.9604	25.0637				3,54E-12	4.05E+08	4	4	4	4	4	4	13.6	36.963	25.0042	25.0167	24.9711	6	3	3	0.874001	0.0249742	BBN9Q8	BBN9Q8	1	AFLA_050490	tRNA (guanine-N7)-methyltransferase [EC 2.1.1.33] (Transfer RNA methyltransferase 8) (tRNA (guanine(45)-N7)-methyltransferase) (tRNA(m7G46)-methyltransferase)	
27.7535	26.9587	28.4107	27.969	28.1034	27.6845				1,33E-125	2.94E+09	19	19	19	19	19	19	53.4	59.597	27.8133	27.7076	27.919	6	3	3	0.654363	-0.211336	BBN9R9	BBN9R9	1	AFLA_050600	Betaine-aldehyde dehydrogenase, putative	
27.1688	26.1288	28.8564	30.3821	30.5189	30.7118				+	5.34E-125	1.05E+10	5	5	5	5	5	15.1	49.097	28.2945	26.0514	30.5376	6	3	3	0.020668	-4.86227	BBN9R5	BBN9R5	1	AFLA_050610	Aldo-ketoglutarate phosphatase PHOa	
27.7528	23.0281	28.6145	28.6889	23.303	23.5596				6,19E-50	1.03E+09	8	8	8	8	8	8	51.4	16.551	24.9911	24.7985	25.1838	6	3	3	0.889046	-0.385368	BBN9R4	BBN9R4	2	AFLA_050650	40S ribosomal protein S19	
25.274	27.7565	27.9777	26.3483	27.1808	NaN				7,38E-225	2.99E+09	6	6	6	6	6	6	22.1	33.843	26.9075	27.0027	26.7445	5	3	2	0.850598	-0.283399	BBN9R8	BBN9R8	1	AFLA_050690	Mitochondrial ADP-ATP carrier protein (Ant), putative	
29.9498	29.5015	29.8348	29.2593	28.8323	28.6187				+	3.11E-105	9.85E+09	9	9	9	9	9	54.7	16.238	29.3327	29.762	28.9035	6	3	3	0.020641	0.88554	BBN9T9	BBN9T9	1	AFLA_050800	40S ribosomal protein S12	
27.3634	27.4669	27.3234	27.4506	27.3422	27.4691				1,18E-47	1.54E+09	6	6	6	6	6	6	31.2	40.221	27.4026	27.3846	27.2406	6	3	3	0.56949	-0.030572	BBN9U2	BBN9U2	1	AFLA_050830	Uridine nucleosidase Urh1, putative	
26.873	26.5326	26.7078	26.6132	26.6584	26.408				4,93E-58	1.54E+09	14	14	14	14	14	14	24.7	67.381	26.6322	26.7045	26.5599	6	3	3	0.131278	-0.146418	BBN9V1	BBN9V1	1	AFLA_050930	Protein phosphatase 2a 65kd regulatory subunit	
24.6785	27.005	27.2259	26.4801	27.1977	26.3134				2,00E-45	1.51E+09	9	9	9	9	9	9	21.5	67.607	26.4834	26.3031	26.637	6	3</									

Supplementary Table S2. Data on proteins obtained from label-free proteomics from *Aspergillus flovus* grown in presence of 0.1 M CaCl₂ treated with 10 μg/ml PgAFP and untreated control.

A. Total data

LQF intensity AF_CaCl ₂ PgAFP_1	LQF intensity AF_CaCl ₂ PgAFP_2	LQF intensity AF_CaCl ₂ PgAFP_3	LQF intensity AF_CaCl ₂ Control_1	LQF intensity AF_CaCl ₂ Control_2	LQF intensity AF_CaCl ₂ Control_3	t-test Significant	PEP	Intensity	Peptides	Razor + unique peptides	Unique peptides	Sequence coverage [%]	Mol. weight [kDa]	Mean	Mean AF_CaCl ₂ PgAFP	Mean AF_CaCl ₂ Control	Valid values	Valid values AF_CaCl ₂ PgAFP	Valid values AF_CaCl ₂ Control	t-test p value	t-test Difference	Protein IDs	Majority protein IDs	Proteins	Gene Names	Protein names
27.2017	26.2063	25.7228	25.2324	25.9883	26.2289		6.65E+06	5.64E+08	8	8	8	32	35.307	26.1452	26.377	25.9135	6	3	3	0.390833	0.463444	B8NS2	B8NS2	1	AFLA_054340	Isoflavone reductase family protein
28.961	28.3792	28.4702	28.5071	28.4807	28.5846		8.14E+102	4.24E+09	16	16	16	50.8	44.623	28.5638	28.6035	28.2841	6	3	3	0.687474	0.0795384	B8NS3	B8NS3	1	AFLA_054350	Actin-binding protein Fragin, putative
24.861	26.1242	25.7298	23.3385	23.3838	23.1413		7.97E-19	2.88E+08	4	4	4	13	55.58	24.4298	25.5717	23.2799	6	3	3	0.030877	2.28382	B8NC26	B8NC26	1	AFLA_054670	Tryptophanyl-tRNA synthetase, putative
28.6813	28.4468	28.0162	28.1358	28.2366	28.3312		6.97E-126	3.6E+09	15	15	15	67.4	34.641	28.308	28.3814	28.2345	6	3	3	0.509012	0.146852	B8NC27	B8NC27	1	AFLA_054680	Purine nucleoside phosphorylase (EC 2.4.2.1) (inosine-guanosine phosphorylase)
30.8711	30.4805	30.0211	32.354	31.5761	31.4654		3.03E+10		20	18	18	81	34.679	31.4599	31.1205	31.7985	6	3	3	0.27557	-0.677956	B8ND04	B8ND04	1	AFLA_054750	Malate dehydrogenase, NAD-dependent
27.9634	27.4756	27.8533	27.5184	27.7199	27.9976		1.02E-143	3.49E+09	15	15	15	35.3	63.847	27.7547	27.7641	27.7453	6	3	3	0.930649	0.0187289	B8ND10	B8ND10	1	AFLA_054810	Transcriptional repressor TupA/RocA, putative
28.3905	28.8924	28.5003	28.5856	28.8567	28.9128		1.91E-166	3.69E+09	15	15	15	43.7	45.218	28.6897	28.5944	28.785	6	3	3	0.355885	-0.190633	B8ND13	B8ND13	1	AFLA_054840	Glycogen synthase kinase (Skp1), putative
24.0321	23.5884	23.9396	23.7194	23.761	23.7486		1.08E-06	2.07E+08	4	4	4	8.8	61.463	23.7982	23.8534	23.743	6	3	3	0.46171	0.110365	B8ND16	B8ND16	1	AFLA_054870	6-phosphofructo-2-kinase, putative
26.9404	26.4631	26.1183	26.3314	26.2152	26.1423		4.27E-38	7.98E+08	5	5	5	25.1	30.817	26.3685	26.5073	26.2297	6	3	3	0.319886	0.277604	B8ND19	B8ND19	1	AFLA_054900	ABC transporter, putative
27.7408	27.5509	27.502	27.1452	27.6597	27.6583		1.20E-31	1.86E+09	8	8	8	35.3	39.971	27.5427	27.5979	27.4873	6	3	3	0.58478	0.110399	B8ND22	B8ND22	1	AFLA_054930	DUF410 domain protein
24.8801	25.4536	26.0648	26.7104	25.6302	25.3094		7.01E-88	1.28E+09	13	13	13	15.7	133.24	25.4662	25.4662	25.8833	6	3	3	0.486378	-0.41717	B8ND30	B8ND30	1	AFLA_055010	Homocitroninase, mitochondrial [EC 4.2.1.36] (homocitroninase hydratase)
31.5192	31.0407	30.5129	32.3898	32.2883	32.3916			4.87E+10	22	22	22	72.3	40.145	31.6904	31.0243	32.3566	6	3	3	0.010392	1.333232	B8ND35	B8ND35	1	AFLA_055060	NAD-dependent formate dehydrogenase AdhA/Fdh
29.6508	29.2474	28.9932	29.2154	29.2895	29.4432		1.91E-358	6.46E+09	12	12	12	69.5	38.518	29.3066	29.2971	29.316	6	3	3	0.930295	-0.0188904	B8ND48	B8ND48	1	AFLA_055190	Proteasome subunit alpha type (EC 3.4.25.1)
27.8136	27.5782	27.2442	27.4637	27.5196	27.6836		7.24E-75	2.17E+09	8	8	8	51.4	23.558	27.5505	27.5453	27.5557	6	3	3	0.956403	-0.010348	B8ND51	B8ND51	1	AFLA_055220	Hsp70 nucleotide exchange factor (Fes1), putative
28.9381	29.594	29.9338	29.7396	29.2853	29.1522		0.156E+10		19	19	19	68.8	41.639	29.4405	29.4886	29.3924	6	3	3	0.792352	0.0962626	B8ND52.C	B8ND52	2	AFLA_055230	Actin Act1
29.3436	29.2542	28.8832	28.793	29.2604	29.2835		0.674E+09		18	18	18	33	86.584	29.128	29.1437	29.1123	6	3	3	0.895462	0.0313867	B8ND53	B8ND53	1	AFLA_055240	Bifunctional purine biosynthetic protein Ade1, putative
24.2763	24.1626	24.1504	23.8257	24.122	23.6545		1.94E-13	1.95E+08	6	6	6	9.3	91.575	24.0323	24.1971	23.8764	6	3	3	0.08172	0.1338718	B8ND54	B8ND54	1	AFLA_055250	Mitochondrial mRNA processing protein PET127, putative
33.4008	33.2901	33.0995	33.3355	33.2545	33.3577		0.109E+11		31	31	31	68.8	46.388	33.2596	33.2034	33.3192	6	3	3	0.39126	-0.112509	B8NDQ4	B8NDQ4	1	AFLA_055450	Translation elongation factor eEF-1 subunit gamma, putative
26.6098	26.814	26.2816	24.2622	24.2739	24.0779		6.08E-44	5.42E+08	7	7	7	32.2	34.813	25.3866	26.5685	24.2047	6	3	3	0.000147	2.36378	B8NDQ5	B8NDQ5	1	AFLA_055460	37S ribosomal protein S9
27.0132	26.5859	26.2647	26.9319	26.4811	26.2105		5.67E-05	8.07E+08	5	5	5	38.5	23.231	26.5812	26.6213	26.5412	6	3	3	0.804075	0.0800743	B8NDQ7	B8NDQ7	1	AFLA_055480	Calcineurin Ca2+-binding regulatory subunit CnaB
25.4771	25.4369	25.7907	26.3522	26.1089	26.0557		1.35E-37	5.02E+08	7	7	7	27.4	52.827	25.8702	25.5682	26.1723	6	3	3	0.013865	-0.604063	B8NDQ9	B8NDQ9	1	AFLA_055500	SET domain protein
27.5759	26.8811	27.0526	27.1801	27.1748	27.3113		1.26E-60	1.61E+09	8	8	8	51.7	20.917	27.196	27.1699	27.2221	6	3	3	0.819059	-0.0521927	B8NDR9	B8NDR9	1	AFLA_055600	ARD/ARD family protein, putative
NaN	27.2454	26.7823	NaN	NaN	NaN		0.00016	3.57E+08	2	2	2	10	38.792	27.0138	27.0138	NaN	2	2	0	1	NaN	B8NDS7	B8NDS7	1	AFLA_055680	Esterase, putative
27.2372	27.553	27.893	28.0877	28.1059	28.1373		3.80E-86	2.52E+09	17	17	17	25.3	108.39	27.8357	27.5611	28.1103	6	3	3	0.044476	-0.549245	B8NDS9	B8NDS9	1	AFLA_055800	Chromosome segregation protein Cse1, putative
27.9442	27.6418	27.3309	27.9867	28.0084	27.9287		1.26E-49	2.4E+09	13	13	13	49.9	51.881	27.8068	27.639	27.9746	6	3	3	0.133516	-0.335594	B8NDV6	B8NDV6	1	AFLA_055970	Fad NAD binding oxidoreductase, putative
27.9671	27.6087	27.2446	27.657	27.3245	27.3305		3.49E-129	2.18E+09	18	18	18	33.3	92.748	27.5187	27.6002	27.4733	6	3	3	0.356087	0.16285	B8NDV7	B8NDV7	1	AFLA_055980	Mannosyl-oligosaccharide glucosidase, putative
28.7961	28.4803	28.2935	28.7684	29.0912	28.9774		5.12E-241	5.97E+09	30	30	30	57	83.859	28.7345	28.5233	28.9452	6	3	3	0.072742	-0.42234	B8NDX6	B8NDX6	1	AFLA_056170	Catalase (EC 1.11.1.6)
27.6021	27.5674	29.9751	27.3876	26.7032			5.24E-186	2.23E+09	7	7	7	43	17.028	27.7018	28.3815	27.2027	6	3	3	0.173208	1.35953	B8NDY4	B8NDY4	1	AFLA_056250	Ribosomal protein L14
31.0878	31.4448	31.2496	31.1021	30.9588	30.8336		0	2.72E+10	11	11	11	80.7	21.804	31.0629	31.2274	30.8985	6	3	3	0.062339	3.28912	B8NDG5	B8NDG5	1	AFLA_056260	Nascent polypeptide-associated complex (NAC) subunit, putative
29.1911	29.5284	30.5999	31.1599	30.9681	30.5768		0	1.84E+10	29	29	29	58.9	61.708	30.3374	29.7731	30.3016	6	3	3	0.069426	-1.12845	B8NDJ74	B8NDJ74	1	AFLA_056350	2-methylcitrate dehydratase, putative
23.395	25.997	24.5929	26.6012	26.2815	28.3116		2.84E-46	8.82E+08	6	6	6	32.4	21.789	25.2564	24.2833	26.5416	6	3	3	0.318957	-0.550955	B8NDG3	B8NDG3	1	AFLA_056440	Uncharacterized protein
28.7571	28.5104	28.2848	28.3864	28.4174	28.4779		1.93E-109	3.75E+09	14	14	14	45.5	56.772	28.4723	28.5174	28.4272	6	3	3	0.551849	0.0901998	B8NDG6	B8NDG6	1	AFLA_056570	Glutathione synthetase (GSH-S) [EC 6.3.2.3]
31.8968	31.6432	31.5406	31.7457	31.8809			0.306E+10		28	28	28	69.1	57.221	31.7655	31.6996	31.8774	6	3	3	0.280488	-0.142864	B8NDG6	B8NDG6	1	AFLA_056670	4-aminobutrate transaminase GatA
26.5083	26.6274	26.9146	27.1907	26.8596	28.8663		1.24E-39	1.43E+09	13	13	13	39.7	55.765	26.8278	26.8834	26.9722	6	3	3	0.150612	-0.28877	B8NDA8	B8NDA8	1	AFLA_056690	Serine/threonine protein phosphatase (EC 3.1.3.16)
28.0235	27.8022	27.32	27.7446	27.8178	28.0844		1.91E-73	2.29E+09	11	11	11	32.4	53.407	27.7987	27.7152	27.8822	6	3	3	0.511332	-0.167002	B8NDA9	B8NDA9	1	AFLA_056700	DUF89 domain protein
30.6535	30.0335	29.4357	29.308	29.5504	29.7403		0.922E+09		13	13	13	30.8	67.479	29.7869	30.0409	29.5329	6	3	3	0.245024	0.508022	B8NDD0	B8NDD0	1	AFLA_056810	Carboxyltransferase S1, putative
27.0987	27.278	25.6412	24.7721	26.4953	26.7874		1.10E-86	7.34E+08	8	8	8	15.4	81.967	26.3454	26.2676	26.0183	6	3	3	0.466968	0.65435	B8NDC1	B8NDC1	1	AFLA_056820	Garyoxyperanyl pyrophosphate synthase, putative
24.4299	NaN	NaN	NaN	24.2963	24.4601		4.57E-06	941440000	4	4	4	5.7	70.292	24.3954	24.4299	24.2482	3	1	2	1	0.0516729	B8NDC8	B8NDC8	1	AFLA_056890	Uncharacterized protein
29.9071	29.1182	28.7208	29.113	29.2999	29.3231		1.06E-196	5.15E+09	12	12	12	55.3	37.563	29.247	29.2487	29.3764	6	3	3	0.992926	0.0033474	B8NDF3	B8NDF3	1	AFLA_057140	Nucleoside-diphosphate-sugar epimerase, putative
31.1232	30.9472	30.6597	30.2343	30.5978	30.6763		0.155E+10		12	12	12	47.7	38.719	30.7064	30.91	30.5028	6	3	3	0.100992	0.407221	B8NDZ3	B8NDZ3	1	AFLA_057240	RNP domain protein
25.9246	26.078	25.9829	25.4713	26.5285	25.9842		6.34E-45	1.01E+09	11	11	11	33.5	51.609	25.9949	25.9952	25.9947	6	3	3	0.99883	0.0004813	B8NE05	B8NE05	1	AFLA_057360	Proteasome regulatory particle subunit Rpt2, putative
26.116	26.162	26.0047	26.257	26.4929	26.5884		5.03E-20	7.05E+08	6	6	6	49.6	27.18	26.2701	26.0942	26.4661	6	3	3	0.032024	-0.351863	B8NE06	B8NE06	1	AFLA_057370	Ubiquitin conjugating enzyme (UbcA), putative
26.8264	27.5739	28.297	28.4192	28.025	27.7848		1.05E-102	2.23E+09	13	13	13	26.3	69.005	27.8211	27.5658	27.0763	6	3	3	0.332092	-0.510575	B8NE08	B8NE08	1</		

Supplementary Table S2. Data on proteins obtained from label-free proteomics from *Aspergillus flovus* grown in presence of 0.1 M CaCl₂ treated with 10 µg/ml PgAFP and untreated control.

LFQ intensity AF_CaCl ₂ PgAFP_1	LFQ intensity AF_CaCl ₂ PgAFP_2	LFQ intensity AF_CaCl ₂ PgAFP_3	LFQ intensity AF_CaCl ₂ Control_1	LFQ intensity AF_CaCl ₂ Control_2	LFQ intensity AF_CaCl ₂ Control_3	t-test Significant	PEP	Intensity	Peptides	Razor + unique peptides	Unique peptides	Sequence coverage [%]	Mol. weight [kDa]	Mean	Mean AF_CaCl ₂ PgAFP	Mean AF_CaCl ₂ Control	Valid values	Valid values AF_CaCl ₂ PgAFP	Valid values AF_CaCl ₂ Control	t-test p value	t-test Difference	Protein IDs	Majority protein IDs	Proteins	Gene Names	Protein names	
29.1882	28.8006	28.3818	28.4134	28.57	28.4307		1,55E-178	4,16E+09	7	7	7	47.9	15.65	26,9308	28,7902	28,4714	6	3	3	0,251548	0,318787	B8NEG5	B8NEG5	1	AFLA_061630	SSDNA binding protein, putative	
30.8466	30.509	30.3193	30.401	30.4394	30.5134		0	1,55E+10	23	23	23	59	72,825	30,5048	30,5583	30,4513	6	3	3	0,534628	0,107005	B8NEI6	B8NEI6	1	AFLA_061840	Probable Xaa-Pro aminopeptidase P (AMPP) (Aminopeptidase P) (EC 3.4.11.9) (Aminoacylproline aminopeptidase) (Prolidase)	
30.8418	30.808	30.5214	30.9081	30.7509	30.5742		0	2,24E+10	20	20	20	84.2	32,984	30,734	30,7237	30,7444	6	3	3	0,890012	-0,206394	B8NEJ0	B8NEJ0	1	AFLA_061880	Pyridoxine biosynthesis protein	
25.0181	24.6835	25.139	24.9937	24.5774	24.5336		1,13E-11	2,24E+08	5	5	5	16.1	48,922	24,8242	24,9469	24,7016	6	3	3	0,287568	0,245296	B8NEJ3	B8NEJ3	1	AFLA_061910	Arginine biosynthesis bifunctional protein ArgI, mitochondrial [Cleaved into: Arginine biosynthesis bifunctional protein ArgI alpha chain; Arginine biosynthesis bifunctional protein ArgI beta chain] [Includes: Glutamate N-acetyltransferase (GAT) (EC 2.3.1.35) (Ornithine acetyltransferase) (OATase) (Ornithine transacetylase); Amino-acid acetyltransferase (EC 2.3.1.1) (N-acetylglutamate synthase) (AGS)]	
NaN	24.0378	23.4446	NaN	22.2967	NaN		1,15E-26	2,81E+08	4	4	4	10.5	52,195	23,2597	23,7412	22,2967	3	2	1	1	1,4444	B8NEJ4	B8NEJ4	1	AFLA_061920	Protein transport protein SecE1 alpha subunit, putative	
NaN	24.8047	24.5262	24.877	24.7417	NaN		1,64E-11	3,29E+08	3	3	3	14.3	39,539	24,7374	24,6654	24,8094	4	2	2	0,450988	-0,143934	B8NEJ7	B8NEJ7	1	AFLA_061950	Autophagy-related protein 3	
23.5572	27.4163	27.1994	29.6554	27.8424	27.3953		0	2,55E+09	10	10	10	41.4	38,305	27,1443	26,0576	28,2311	6	3	3	0,206215	-2,17345	B8NEK6	B8NEK6	1	AFLA_062040	Stress protein DDR48, putative	
27.7248	26.939	26.5429	26.7638	26.9655	27.2505		8,91E-22	1,17E+09	5	5	5	44.9	23,102	26,9510	26,91	26,9933	6	3	3	0,753849	-0,0823416	B8NEL1	B8NEL1	1	AFLA_062090	MutI/indix family protein	
30.6713	30.181	30.059	30.243	30.3153	30.3522		0	1,29E+10	13	13	13	54.3	28,717	30,3036	30,3038	30,3035	6	3	3	0,998651	0,0003414	B8NEL2	B8NEL2	1	AFLA_062100	HAD superfamily hydrolase, putative	
25.0299	24.9489	24.4517	24.6981	24.739	24.7273		2,99E-10	2,91E+08	4	4	4	8.4	74,268	24,7658	24,8101	24,7215	6	3	3	0,650114	0,088771	B8NEL5	B8NEL5	1	AFLA_062130	Alpha-actinin, sarcomeric (F-actin cross linking protein)	
27.391	27.2011	26.9929	24.86	25.25	25.5167		2,77E-48	9,55E+08	5	5	5	21.7	36,186	26,119	27,0617	25,1763	6	3	3	0,000548	1,88654	B8NEL6	B8NEL6	1	AFLA_062140	RNA binding protein, putative	
28.34	28.1946	27.9834	27.9005	28.034	28.2244		1,02E-105	3,64E+09	14	14	14	23.4	84,821	28,1128	28,1727	28,053	6	3	3	0,440305	0,119673	B8NEL8	B8NEL8	1	AFLA_062160	Polyubiquitin binding protein (Doa1/Ufd3), putative	
22.8681	23.3738	24.8578	24.4216	24.0261	23.928		3,96E-10	1,73E+08	3	3	3	24	28,621	23,9126	23,9999	24,1252	6	3	3	0,277759	-0,425326	B8NEL9	B8NEL9	1	AFLA_062170	Ai-BP family protein	
26.6341	26.4183	26.1295	24.9647	25.2437	NaN		1,65E-58	6,32E+08	4	4	4	64.1	11,564	25,8781	26,3939	25,1042	5	3	2	0,009335	1,28971	B8NEM0	B8NEM0	1	AFLA_062180	37S ribosomal protein S16	
25.1622	24.8487	24.7576	24.4917	NaN	24.6976		1,21E-07	2,5E+08	3	3	3	4.6	64,422	24,8623	25,0408	24,5947	5	3	2	0,255363	0,446155	B8NEM1	B8NEM1	1	AFLA_062190	RNA binding protein	
27.4766	27.6662	27.39	25.2561	25.3826	24.6681		7,93E-57	1,24E+09	10	10	10	35.8	44,771	26,3066	27,5109	25,1022	6	3	3	0,000509	2,4087	B8NEM2	B8NEM2	1	AFLA_062200	Uncharacterized protein	
24.1108	23.8632	23.7915	NaN	NaN	23.7676		4,54E-08	2,07E+08	4	4	4	9	70,661	23,8833	23,9218	23,9218	4	3	1	1	0,154252	0,142899	B8NEN9	B8NEN9	1	AFLA_062370	Mitochondrial outer membrane translocase receptor (TOM70), putative
28.956	28.4693	28.5767	28.7744	28.8167	28.768		5,38E-152	4,5E+09	17	17	17	44.1	49,068	28,7268	28,6673	28,7864	6	3	3	0,467454	-0,119034	B8NEP1	B8NEP1	1	AFLA_062390	Tryptophanyl-tRNA synthetase	
NaN	NaN	NaN	NaN	NaN	NaN		7,84E-34	1,07E+09	9	9	9	20	74,118	27,5351	NaN	27,5351	3	0	3	1	NaN	B8NEP7	B8NEP7	1	AFLA_062450	Sphingomyelin phosphodiesterase	
25.7533	25.5403	25.3161	25.3305	25.5452	25.7044		3,42E-47	5,04E+08	7	7	7	15.7	72,065	25,5316	25,5366	25,5267	6	3	3	0,9355474	0,0098807	B8NEQ3	B8NEQ3	1	AFLA_062510	Myosin heavy chain, embryonic smooth muscle isoform, putative	
NaN	NaN	NaN	NaN	NaN	NaN		1,14E-11	4,08E+08	2	2	2	12	26,52	25,4264	NaN	25,4264	3	0	3	1	NaN	B8NF00	B8NF00	1	AFLA_062640	Uncharacterized protein	
26.8323	26.3541	25.6783	25.0126	24.8458	26.0729		1,65E-20	5,56E+08	6	6	6	21	38,576	25,7994	26,2883	25,3104	6	3	3	0,127468	0,977809	B8NFE6	B8NFE6	1	AFLA_062800	Aldo-keto reductase, putative	
24.1829	23.8556	26.5081	23.5729	23.8771	24.0062		8,90E-27	3,54E+08	6	6	6	24.4	51,673	24,3338	24,8489	23,8187	6	3	3	0,289679	1,03016	B8NFE9	B8NFE9	2	AFLA_062830	Monooxygenase, putative	
25.0149	24.7177	24.1019	24.9614	25.4838	25.103		1,16E-17	3,77E+08	6	6	6	30.4	24,559	24,8971	24,6115	25,1827	6	3	3	0,139971	-0,571211	B8NFI8	B8NFI8	1	AFLA_063320	Uncharacterized protein	
26.4551	24.7685	24.8497	24.9624	24.5729	24.6058		8,25E-26	2,24E+08	3	3	3	19	35,133	25,0504	25,3578	25,5893	5	3	2	0,357831	0,768408	B8NFI9	B8NFI9	1	AFLA_063660	Polysaccharide deacetylase family protein	
28.7051	28.8547	29.0673	28.4059	28.3175	28.0149		1,19E-91	4,69E+09	10	10	10	45.9	34,033	28,6312	27,919	28,9451	6	3	3	0,057741	1,07489	B8NFI5	B8NFI5	1	AFLA_064530	Uncharacterized protein	
25.8966	25.6782	26.5028	23.2843	24.6635	24.4795		1,65E-12	4,8E+08	9	9	9	5	29	38,345	25,0842	26,0259	24,1424	6	3	3	0,019371	1,88343	B8NFI8	B8NFI8	1	AFLA_064530	Glutathione S-transferase GIG-like, putative
29.5954	29.4879	29.4998	29.7309	29.6048	29.7182		+	0,89E+09	28	28	28	60.5	62,245	29,6062	29,5277	29,6847	6	3	3	0,040481	-0,156956	B8NFI7	B8NFI7	1	AFLA_065080	Phosphoglucosyltransferase, putative	
24.9033	24.775	26.4225	27.6445	28.1555	28.0507		7,36E-77	2,36E+09	10	10	10	37.6	45,706	26,6578	26,3669	27,9486	6	3	3	0,009424	2,58163	B8NFI9	B8NFI9	1	AFLA_065230	Glycerophosphoryl diester phosphodiesterase family protein	
24.6989	25.0008	25.19	25.1271	25.2505	25.3663		3,11E-263	1,76E+09	7	7	7	29.1	46,178	25,1552	24,9602	25,3501	6	3	3	0,111615	-0,389903	B8NFI1	B8NFI1	1	AFLA_065540	Peptide hydrolase (EC 3.4...)	
27.7191	27.5115	27.3289	26.9889	27.0623	27.236		1,50E-145	1,77E+09	13	13	13	45.4	44,316	27,3078	27,5198	27,0957	6	3	3	0,034367	0,424077	B8NIC4	B8NIC4	1	AFLA_065570	O-methyltransferase family protein	
28.4343	27.9191	28.1241	26.9104	27.7718	28.0803		8,57E-107	2,56E+09	16	16	16	51.5	50,833	27,8733	28,1592	27,5785	6	3	3	0,207636	0,571672	B8NIE0	B8NIE0	1	AFLA_065730	Guanine deaminase, putative	
27.3843	24.4821	24.9229	23.3499	23.8364	23.8966		2,33E-22	3,26E+08	3	3	3	8.5	45,369	24,6457	25,5964	23,695	6	3	3	0,107461	1,90146	B8NIE1	B8NIE1	1	AFLA_065740	7-dehydrocholesterol reductase, putative	
27.1035	25.6147	25.8383	25.7097	26.1185	26.325		6,37E-36	7,04E+08	9	9	9	30.2	47,815	26,1183	26,1855	26,0511	6	3	3	0,800385	0,134423	B8NIE6	B8NIE6	1	AFLA_065920	Uncharacterized protein	
30.4635	29.8047	29.7286	29.4342	29.8615	30,1187		0	1,27E+10	7	7	7	91.2	15,091	29,9019	29,9989	29,8048	6	3	3	0,561592	0,194123	B8NI98	B8NI98	1	AFLA_065940	Glyoxalase family protein	
28.6244	28.699	28.4089	28.8796	28.4211	28.5436		2,55E-141	3,99E+09	14	14	14	47.1	45,979	28,5961	28,5774	28,6148	6	3	3	0,829231	-0,037365	B8NIA6	B8NIA6	1	AFLA_066020	12-oxophylidione reductase, putative	
28.4295	28.4701	28.6026	28.523	28.5048	28.4647		1,27E-175	4,54E+09	11	11	11	61.8	37,136	28,4991	28,5007	28,4975	6	3	3	0,956294	0,002088	B8NIB4	B8NIB4	1	AFLA_066100	Uncharacterized protein	
29.832	29.8204	29.6229	29.7352	29.545	29.4989		3,18E-292	9,13E+09	19	19	19	52.9	42,938	29,6757	29,7584	29,593	6	3	3	0,17068	0,16538	B8NID1	B8NID1	1	AFLA_066270	RNA-binding L domain protein	
24.1066	23.8038	NaN	23.5907	24.785	NaN		1,01E-08	2,86E+08	2	2	2	6.6	40,824	24,0715	23,9552	24,1879	4	2	2	0,74201	-0,232645	B8NIF9	B8NIF9	1	AFLA_066550	Alcohol dehydrogenase, putative	
25.2242	25.2109	24.47																									

Supplementary Table S2. Data on proteins obtained from label-free proteomics from *Aspergillus flavus* grown in presence of 0.1 M CaCl₂ treated with 10 μg/ml PgAFP and untreated control.

A. Total data

LFQ intensity AF_CaCl ₂ PgAFP_1	LFQ intensity AF_CaCl ₂ PgAFP_2	LFQ intensity AF_CaCl ₂ PgAFP_3	LFQ intensity AF_CaCl ₂ Control_2	LFQ intensity AF_CaCl ₂ Control_3	t-test Significant	PEP	Intensity	Peptides	Razor + unique peptides	Unique peptides	Sequence coverage [%]	Mol. weight [kDa]	Mean AF_CaCl ₂ PgAFP	Mean AF_CaCl ₂ Control	Valid values AF_CaCl ₂ PgAFP	Valid values AF_CaCl ₂ Control	t-test p value	t-test Difference	Protein IDs	Majority protein IDs	Proteins	Gene Names	Protein names	
25.7233	25.2318	25.2808	25.0502	25.669	25.7442	2,26E+11	7,03E+08	8	8	17	68,069	25,499	25,419	25,478	6	3	0.792474	0.0578711	BBNR1	BBNR3	1	AFLA_069410	RNase L inhibitor of the ABC superfamily, putative	
26.154	24.7076	24.6158	26.3338	26.6088	27,1175	+ 1,04E-26	5,55E+08	11	11	39.7	34,644	29,929	25,191	26,687	6	3	0.049561	-1,52756	BBNR6	BBNR6	1	AFLA_069440	Pyridoxal reductase (AKR8), putative	
24.9241	24.7836	NaN	NaN	25.1648	24,7562	4,12E-06	2,13E+08	2	2	6	56,002	24,9072	24,8538	24,9605	4	2	0.670544	-0.106634	BBNIS7	BBNIS7	1	AFLA_069550	Pre-mRNA splicing factor (Prp31), putative	
33.0887	32.6617	32.6401	32.7171	33.2099	33,13	0	1,08E+11	31	31	61.1	48,931	32,9079	32,7968	33,019	6	3	0.352425	-0.222167	BBNIT4	BBNIT4	1	AFLA_069590	Adenylylthiomycetinase (EC 3.3.1.1)	
27.1593	27.0339	25.5066	28.2344	28.4499	28,5881	+ 6,92E-14	2,68E+09	3	3	38.6	13,55	27,4954	26,5666	28,4214	6	3	0.026471	-1,85752	BBNIT4	BBNIT4	1	AFLA_069620	Uncharacterized protein	
28.7004	28.3815	28.1902	28.7225	28.7587	28,8615	3,56E-140	4,25E+09	8	8	39.8	30,254	28,6025	28,424	28,7009	6	3	0.082072	-0.356875	BBNIT8	BBNIT8	1	AFLA_069660	TiM-barrel enzyme family protein	
27.921	27.454	26.989	26.6933	27.4289	26,8816	9,02E-40	1,36E+09	6	6	20.2	36,753	27,228	27,4547	28,3713	6	3	0.026247	0.453445	BBNIU5	BBNIU5	1	AFLA_069730	HMG box protein, putative	
28.2827	28.4852	28.5336	28.6582	28.352	28,1037	1,04E-85	3,53E+09	14	14	40	40,919	28,4026	28,4338	28,3713	6	3	0.742931	0.0625006	BBNIU9	BBNIU9	1	AFLA_069770	Eukaryotic translation initiation factor 3 subunit H (eIF3h)	
24.6278	24.4428	24.1214	24.3513	NaN	NaN	3,10E-05	1,89E+08	2	2	9.8	33,689	24,336	24,3973	24,2439	5	3	0.512571	0.153399	BBNIV0	BBNIV0	1	AFLA_069780	Kynurenine formamidase (KFA) (KFAE) (EC 3.5.1.9) (Arilformylamidase) (N-formylkynurenine formamidase)	
26.0926	26.222	25.8124	25.5124	25.4498	25,1866	+ 1,38E-39	5,49E+08	5	5	30.5	34,445	25,7126	26,0423	25,3829	6	3	0.013628	0.659444	BBNIV1	BBNIV1	1	AFLA_069790	Casein kinase 2 beta' regulatory subunit Ckb2, putative	
33.6165	33.2789	32.9814	33.0112	32.8952	33,0442	0	9,52E+10	28	28	84.2	33,487	33,1379	33,2923	32,9835	6	3	0.177561	0.308764	BBNIV7	BBNIV7	2	AFLA_069850	Glycerol dehydrogenase Gcyl, putative	
31.4246	31.1501	30.9246	30.9049	30.9654	31,0778	0	2,36E+10	28	28	70.6	45,579	31,0762	31,1698	30,9827	6	3	0.296632	0.187079	BBNIV4	BBNIV4	1	AFLA_069920	Ogg-like ATPase 1	
29.8319	29.6174	29.3247	29.4793	29.6099	29,6947	2,89E-290	8,05E+09	13	13	13	50.044	29,593	29,5913	29,5946	6	3	0.984483	0.0033067	BBNIV7	BBNIV7	1	AFLA_069950	Hsc70 co-chaperone (SGT), putative	
27.2066	26.6529	26.417	26.0794	26.7579	26,2197	1,19E-34	8,95E+08	2	2	38.5	8,7148	26,5556	26,7588	26,3523	6	3	0.062884	0.406511	BBNIX3	BBNIX3	1	AFLA_070010	Uncharacterized protein	
25.4611	25.7812	25.3416	26.0678	25.5828	25,4291	4,04E-08	4,72E+08	2	2	8	28,278	25,6106	25,5279	25,6932	6	3	0.517261	-0.165252	BBNIX1	BBNIX1	1	AFLA_070090	Uncharacterized protein	
26.3596	27.7923	28.3062	28.0778	28.2774	27,9744	6,40E-183	2,95E+09	26	26	34.9	120,48	27,798	27,486	28,1099	6	3	0.349373	-0.623837	BBNIV2	BBNIV2	1	AFLA_070100	Importin beta-4 subunit, putative	
26.8904	26.7987	27.3986	26.8322	26.7749	27,0556	5,92E-32	9,91E+08	7	7	10.5	106,25	26,9584	27,0292	26,8776	6	3	0.528034	-0.508618	BBNIV9	BBNIV9	1	AFLA_070170	Lysoosomal alpha-glucosidase, putative	
26.1495	25.8511	25.7515	26.2311	25.976	26,1526	5,90E-39	7,34E+08	4	4	12.7	51,384	26,0186	25,9174	26,1199	6	3	0.225306	-0.202518	BBNK20	BBNK20	1	AFLA_070690	Cystathionine gamma-synthase	
32.2118	32.24	32.01	32.5251	32.7075	32,6564	+	6,46E+10	28	28	67.1	56,313	32,3935	32,1572	32,6297	6	3	0.006727	-0.472418	BBNK50	BBNK50	1	AFLA_070990	UTP-glucose-1-phosphate uridylyltransferase Ugp1, putative	
28.6157	28.2571	27.6857	27.8243	27.7071	28,0367	1,71E-181	2,9E+09	19	19	19.8	166,52	28,0211	28,1861	27,856	6	3	0.314867	-0.30099	BBNK51	BBNK51	1	AFLA_071000	Membrane bound C2 domain protein (Vp115), putative	
31.0897	30.8215	30.5468	30.8029	31.0105	31,0584	0	2,09E+10	28	28	52.5	64,085	30,8913	30,9193	30,9634	6	3	0.451484	0.149318	BBNK52	BBNK52	1	AFLA_071010	Heat shock protein (Stt1), putative	
27.4605	27.1512	27.0996	27.1907	27.1009	27,3198	7,15E-30	1,76E+09	9	9	32.1	55,01	27,2205	27,2371	27,2038	6	3	0.809488	0.0331699	BBNK55	BBNK55	1	AFLA_071040	Nicotinate phosphoribosyltransferase (EC 6.3.4.2)	
24.8813	24.9771	NaN	25.0893	24.9778	25,1124	2,50E-16	3,52E+08	6	6	13.7	55,939	25,0076	24,9929	25,0598	5	2	0.135706	-0.130649	BBNJ01	BBNJ01	1	AFLA_071180	Indoleamine 2,3-dioxygenase family protein	
25.8769	25.7681	25.6855	25.6302	26.2921	26,284	9,33E-25	6,21E+08	3	3	18.4	21,535	25,9228	25,7768	26,0688	6	3	0.266377	-0.291957	BBNJ02	BBNJ02	1	AFLA_071190	Vacuolar ATP synthase subunit G, putative	
24.6153	25.2839	25.5642	27.2808	27.3517	27,3517	+ 1,59E-28	8,89E+08	11	11	22.9	72,599	26,2766	25,1545	27,3988	6	3	0.001582	-2,24434	BBNJ06	BBNJ06	1	AFLA_071230	Aif-like mitochondrial oxidoreductase (Nfrl), putative	
24.8057	24.8212	NaN	NaN	NaN	24,3853	5,86E-09	2,32E+08	4	4	4	11.3	53,513	24,6707	24,8134	24,3853	3	2	1	0.428148	BBNJ17	BBNJ17	1	AFLA_071340	Cyclophilin-type peptidyl-prolyl-cis-trans isomerase, putative
32.1453	31.9435	32.1332	32.5755	32.5687	32,6037	+	4,96E+10	30	30	79.1	56,165	32,3283	32,074	32,5826	6	3	0.001546	-0.508618	BBNJ18	BBNJ18	1	AFLA_071350	UDP-N-acetylglucosamine pyrophosphorylase	
23.8882	24.1056	24.4025	23.126	22.7711	23,425	+ 2,24E-34	3,02E+08	11	11	4	26.1	24,268	23,5697	23,0321	6	3	0.038274	0.924714	BBNJ19	BBNJ19	1	AFLA_071360	Zn ²⁺ knuckle nucleic acid binding protein, putative	
31.1459	30.6648	30.3666	30.237	30.3516	30,484	0	1,42E+10	11	11	33.7	45,881	30,525	30,7258	30,3704	6	3	0.181465	0.401527	BBNJ22	BBNJ22	1	AFLA_071390	mRNA binding post-transcriptional regulator (Cxs1), putative	
24.5775	24.8426	NaN	NaN	24,7966	24,7966	7,40E-11	2,13E+08	5	5	5	20	33,098	26,6079	24,7636	6	2	1	0.466693	BBNJ26	BBNJ26	1	AFLA_071430	USP-RNAP complex subunit, putative	
NaN	NaN	NaN	23.9876	NaN	23,4329	1,30E-10	1,28E+08	4	4	4	21.3	38,879	23,2103	NaN	2	0	1	NaN	BBNJ29	BBNJ29	1	AFLA_071460	Uncharacterized protein	
26.181	27.0768	27.6927	27.7005	27.383	26,9295	2,45E-44	2,37E+09	7	7	7	52.6	23,223	27,1602	26,8827	6	3	0.510471	-0.355035	BBNJ30	BBNJ30	1	AFLA_071470	Adenine phosphoribosyltransferase 1	
30.6304	29.9164	29.9871	30.1153	30.1732	30,1308	3,25E-165	1,07E+10	6	6	59.4	17,394	30,1589	30,178	30,1398	6	3	0.874847	0.0382366	BBNJ33	BBNJ33	1	AFLA_071500	Translation initiation inhibitor, putative	
26.2154	23.8022	NaN	NaN	NaN	24,0213	1,42E-13	1,48E+08	3	3	18.1	31,57	24,6797	25,0088	24,0213	3	2	1	0.987512	BBMV58	BBMV58	1	AFLA_072750	Pyroline-5-carboxylate reductase, putative	
30.1366	29.607	29.0978	27.7892	29.3899	29,3718	0	4,48E+09	19	19	19	44.8	65,751	29,232	29,6138	28,8503	6	3	0.278528	0.786533	BBMV70	BBMV70	1	AFLA_072770	Pyroline-5-carboxylate dehydrogenase, putative
26.4273	27.5057	28.2464	28.7217	28.5034	28,3397	2,65E-122	2,67E+09	10	9	39.8	39,492	27,9573	27,3931	28,3582	6	3	0.104692	-1.12843	BBMV72	BBMV72	1	AFLA_073290	Phospho-2-dehydro-3-deoxyheptonate aldolase (EC 2.5.1.54) (3-deoxy-D-arabino-heptulosonate 7-phosphate synthase) (DAHP synthase) (Phospho-2-keto-3-deoxyheptonate aldolase)	
29.8676	29.52	29.6738	28.1225	28.6653	28,6684	+ 6,77E-158	4,75E+09	20	19	19	44.4	78,235	29,0863	29,6872	28,4854	6	3	0.004414	1.20175	BBMV28	BBMV28	1	AFLA_073450	Amine oxidase
24.4609	26.9345	26.6968	25.5034	26.3444	25,5749	5,37E-161	1,52E+09	12	12	12	34.9	58,819	25,9175	26,0307	25,8042	6	3	0.798809	0.226508	BBMV29	BBMV29	2	AFLA_073460	Cyclopropane-fatty acyl-phospholipid synthase, putative
31.5395	31.6005	31.4816	31.6685	31.6811	31,7231	0	3,46E+10	13	13	70.8	18,83	31,6157	31,5405	31,6909	6	3	0.016869	-0.150349	BBMW01	BBMW01	1	AFLA_073480	Tropomyosin, putative	
27.1608	26.5751	25.7816	25.7143	26.6927	26,6144	1,73E-31	8,1E+08	10	10	15.9	98,082	26,4232	26,5058	26,3405	6	3	0.761196	0.16535	BBMW10	BBMW10	1	AFLA_073570	RhoGAP and Fes/KitP4 domain protein	
25.9694	24.705	24.4722	25.3402	25.6921	24,944	2,18E-19	3,4E+08	7	6	20.6	58,784	25,0047	24,7579	25,2516	6	3	0.110217	-0.493562	BBMW12	BBMW12	1	AFLA_073590	UBX domain protein (Ubx5), putative	
26.991	27.2145	27.4383	25.596	25.8747	25,5202	+ 7,62E-21	1,64E+09	8	8	8	22.4	55,064</												

Supplementary Table S2. Data on proteins obtained from label-free proteomics from *Aspergillus flovis* grown in presence of 0.1 M CaCl₂ treated with 10 µg/ml PgAFP and untreated control.

A. Total data																											
LQF intensity AF_CaCl ₂ PgAFP_1	LQF intensity AF_CaCl ₂ PgAFP_2	LQF intensity AF_CaCl ₂ PgAFP_3	LQF intensity AF_CaCl ₂ Control_1	LQF intensity AF_CaCl ₂ Control_2	LQF intensity AF_CaCl ₂ Control_3	t-test Significant	PEP	Intensity	Peptides	Razor + unique peptides	Unique peptides	Sequence coverage [%]	Mol. weight [kDa]	Mean	Mean AF_CaCl ₂ PgAFP	Mean AF_CaCl ₂ Control	Valid values	Valid values AF_CaCl ₂ PgAFP	Valid values AF_CaCl ₂ Control	t-test p value	t-test Difference	Protein IDs	Majority protein IDs	Proteins	Gene Names	Protein names	
28.4284	28.3363	27.982	28.198	28.029	28.1176		4,08E-246	3.14E+09	17	17	17	50.1	46.285	28.2008	28.2489	28.1528	6	3	3	0.584936	0.0961482	B8MXB5	B8MXB5	1	AFLA_077020	DNA damage-inducible v-SNARE binding protein Dd1, putative	
24.8922	25.0013	24.8516	25.009	24.5304	24.6351		6,09E-06	3.83E+08	3	3	3	25.7	25.879	24.7899	24.915	24.6678	6	3	3	0.270543	0.250221	B8MXD7	B8MXD7	1	AFLA_077240	Uncharacterized protein	
28.0893	27.5951	27.4665	25.8266	26.3498	26.2066		+ 1.36E-60	1.45E+09	14	14	14	27.7	78.204	26.9223	27.717	26.1267	6	3	3	0.002945	1.58932	B8MXD8	B8MXD8	1	AFLA_077250	Acyl-coenzyme A oxidase	
29.4927	28.9216	28.5272	28.6742	28.8578	28.921		3,96E-159	2.97E+09	18	18	17	61.9	45.256	28.8991	28.8805	28.8996	6	3	3	0.064362	0.162795	B8MXE0	B8MXE0	2	AFLA_077270	NADH-dependent flavin oxidoreductase, putative	
23.9076	23.8574	22.5438	25.3155	25.8902	26.013		+ 4.64E-25	2.52E+08	6	6	6	17.8	59.924	24.5879	23.4363	25.7377	6	3	3	0.009673	-2.30329	B8MXH8	B8MXH8	1	AFLA_077850	Phenylalanine ammonia-lyase (EC 4.3.1.24)	
27.6069	26.6356	27.1858	26.7532	27.3027	27.9484		2,78E-163	1.72E+09	13	13	13	39.7	48.158	27.2388	27.1428	27.3347	6	3	3	0.688691	-0.19196	B8MXJ9	B8MXJ9	1	AFLA_077860	Uncharacterized protein	
26.141	25.7214	25.1776	25.3779	25.9295	26.3162		7,20E-09	3.42E+08	3	3	3	15.2	37.687	25.7772	25.68	25.8745	6	3	3	0.643827	-0.194568	B8MXL2	B8MXL2	1	AFLA_077990	Zinc-binding oxidoreductase ToxD, putative	
26.0516	NaN	22.9708	NaN	22.8439	22.7887		8,55E-06	1,04E+08	2	2	2	17.1	23.787	23.6638	24.5112	22.8163	4	2	2	0.683979	1.69494	B8MXL7	B8MXL7	1	AFLA_078040	(S)-2-haloacid dehalogenase IVA, putative	
23.5901	23.515	23.486	23.8735	23.269	23.4454		1,76E-24	2.39E+08	3	3	3	8	61.824	23.5298	23.5304	23.5293	6	3	3	0.995646	0.0010573	B8MPX5	B8MPX5	1	AFLA_078320	Probable beta-glucosidase btgE (EC 3.2.1.21) (Beta-D-glucoside glucylhydrolase btgE) (Cellobiase btgE) (gentiobiose btgE)	
24.6625	27.5931	28.0294	27.8613	28.143	27.6925		1,33E-252	3.93E+09	17	17	17	55.2	58.058	27.3303	26.7616	27.8989	6	3	3	0.345848	-1.13736	B8MQY1	B8MQY1	1	AFLA_078380	Acetyl-coA hydrolase Ach1, putative	
25.6043	25.6138	25.2217	25.7081	25.7772	25.8872		3,44E-15	4.37E+08	5	5	5	4.7	178.78	25.6021	25.4799	25.7242	6	3	3	0.195501	-0.244252	B8MQY2	B8MQY2	1	AFLA_078390	Transcription factor (Sin3), putative	
27.5595	27.3284	26.8862	26.7717	27.1408	27.2744		1,38E-47	1.7E+09	9	9	9	22.9	54.547	27.1268	27.1914	27.0623	6	3	3	0.690513	0.129084	B8MQY3	B8MQY3	1	AFLA_078400	Protein phosphatase PP2A regulatory subunit B	
27.2773	28.5195	28.285	29.1538	29.444	29.2296		+ 3,92E-148	5.5E+09	18	18	18	33.6	67.874	28.6432	28.0106	29.2758	6	3	3	0.035884	-1.26518	B8MQY5	B8MQY5	1	AFLA_078420	Fumarate reductase Osm1, putative	
25.7592	25.8926	25.474	25.492	25.9428	26.0593		1,06E-26	6.16E+08	8	8	8	27.2	45.433	25.77	25.7086	25.8314	6	3	3	0.594504	-0.122751	B8MQX8	B8MQX8	1	AFLA_078450	COP3 signalosome subunit CsdD	
28.9072	28.5428	26.7093	27.6926	28.3543	28.5984		2,80E-169	2.58E+09	17	17	17	43.6	54.228	28.1341	28.0531	28.2151	6	3	3	0.835672	-0.162007	B8MQX1	B8MQX1	1	AFLA_078480	Cysteine protease, putative	
NaN	NaN	NaN	25.4028	25.778	NaN		7,40E-07	1.55E+08	3	3	3	22.3	22.23	25.5904	NaN	25.5904	2	0	2	0	0	NaN	B8MXS2	B8MXS2	1	AFLA_078590	Extracellular matrix protein, putative
27.2826	27.383	27.5105	27.6699	27.3566	27.563		3,65E-107	2.03E+09	10	10	10	48.5	37.292	27.4609	27.392	27.5298	6	3	3	0.290336	-0.137757	B8MXS7	B8MXS7	1	AFLA_078640	Methylenetetrahydrofolate dehydrogenase	
29.163	31.1656	31.4891	31.4141	31.1269	31.2086		0	2,92E+10	25	25	25	51.3	59.938	30.9529	30.6059	31.2999	6	3	3	0.395598	-0.693964	B8MXS8	B8MXS8	1	AFLA_078650	ATP synthase subunit alpha	
24.8323	25.0932	25.0932	25.5296	25.1667	25.2196		1,31E-12	3.21E+08	3	3	3	23.6	21.459	25.1683	24.9628	25.3053	5	2	2	0.146063	-0.342529	B8MXT0	B8MXT0	1	AFLA_078670	RNA polymerase II subunit 7	
26.2349	25.9499	26.0988	26.767	26.2182	26.5825		2,12E-21	8.49E+08	5	5	5	13.9	56.668	26.2985	26.0745	26.5226	6	3	3	0.069423	-0.448042	B8MXT1	B8MXT1	1	AFLA_078680	Uncharacterized protein	
26.856	27.1506	27.006	26.6402	27.3962	26.9469		1,70E-32	1.71E+09	6	6	6	13.5	73.106	26.9993	27.0042	26.9964	6	3	3	0.968742	0.0098152	B8MXT5	B8MXT5	1	AFLA_078720	Peroxisomal targeting receptor pep5, putative	
26.5382	25.9663	25.66	25.9294	26.1915	26.3529		6,61E-26	7.06E+08	12	12	12	24.7	64.064	26.1064	26.0548	26.1579	6	3	3	0.736154	-0.103118	B8MXT7	B8MXT7	1	AFLA_078740	2-hydroxyphytanoyl-CoA lyase, putative	
24.7904	NaN	23.0477	NaN	NaN	NaN		1,08E-06	1.03E+08	2	2	2	2	68.226	23.9191	23.9191	NaN	2	2	0	1	0	NaN	B8MXU4	B8MXU4	1	AFLA_078810	Oxidoreductin
30.1624	29.59	29.242	29.908	29.3534	29.449		0	9,25E+09	22	22	22	47.7	67.541	29.4816	29.6656	29.2977	6	3	3	0.271105	0.367861	B8MXV3	B8MXV3	1	AFLA_078900	Beta-hexosaminidase (EC 3.2.1.5.2)	
28.4499	28.7299	28.352	27.9074	27.9597	27.7471		+ 3,16E-135	3.14E+09	12	12	12	45.2	39.263	28.191	28.5106	27.8714	6	3	3	0.007951	0.639219	B8MXV7	B8MXV7	1	AFLA_079140	Casein kinase, putative	
27.9148	28.3372	29.1739	29.2865	29.2491	29.1925		4,36E-152	5.91E+09	23	23	23	29.3	119.42	28.859	28.4755	29.2427	6	3	3	0.107398	-0.767426	B8MXV8	B8MXV8	1	AFLA_079150	Valyl-tRNA synthetase	
23.2484	23.4539	23.0619	NaN	NaN	NaN		2,05E-09	1.54E+08	4	4	4	10.9	37.363	23.2547	23.2547	NaN	3	3	0	1	0	NaN	B8MXV9	B8MXV9	1	AFLA_079160	Ribosome biogenesis protein, putative
25.9255	26.5566	26.2075	26.1516	26.5855	26.1363		7,08E-96	1.5E+09	25	25	25	27.2	137.48	26.2605	26.2299	26.2911	6	3	3	0.806849	-0.0612513	B8MY03	B8MY03	1	AFLA_079400	NRPS-like enzyme, putative	
26.6738	26.7292	27.4185	27.4991	27.3888	27.2575		1,35E-38	1.43E+09	6	6	6	53.1	26.272	27.1612	26.9405	27.2818	6	3	3	0.1517	-0.441263	B8MY08	B8MY08	1	AFLA_079450	Endoglycosylase hydrolase, putative	
27.1897	26.7652	26.2986	26.308	26.8218	26.6583		5,53E-31	9.45E+08	12	12	12	7.1	249.12	26.7796	26.7512	26.5996	6	3	3	0.530838	0.155149	B8MY10	B8MY10	1	AFLA_079470	Pre-mRNA splicing helicase, putative	
26.9259	27.3454	26.3949	27.298	27.4476	27.5304		6,19E-73	1.72E+09	10	10	10	21.6	78.809	27.157	26.8887	27.4253	6	3	3	0.131118	-0.536605	B8MY11	B8MY11	1	AFLA_079480	Oligopeptidase family protein	
26.8818	25.4058	24.6017	24.2669	24.8408	25.9211		9,55E-22	6.33E+08	6	6	6	8.7	93.504	25.3197	25.6298	25.0096	6	3	3	0.494115	0.620179	B8MY21	B8MY21	1	AFLA_079580	Vesicular fusion ATPase, putative	
27.8179	27.4347	27.4406	27.6099	27.741	27.7956		6,12E-64	2.39E+09	17	17	17	46.6	61.121	27.6399	27.5644	27.7155	6	3	3	0.335736	-0.151094	B8MY33	B8MY33	1	AFLA_079700	Protein arginine methyltransferase Rmtb	
27.5837	26.9206	26.5392	26.7556	27.1863	26.9966		1,17E-14	1.51E+09	8	8	8	17.6	71.422	26.997	27.0145	26.9795	6	3	3	0.205501	0.0350208	B8MY40	B8MY40	1	AFLA_079770	Endothelin-converting enzyme	
30.7568	30.84	30.705	29.4784	28.8326	28.8116		+ 2,21E-42	8.56E+09	6	6	6	46	14.147	29.9041	30.7673	29.0709	6	3	3	0.001483	1.72639	B8MY51	B8MY51	1	AFLA_079880	60S ribosomal protein L22, putative	
25.4483	25.7684	25.8855	24.8764	25.1837	25.1986		+ 5,41E-18	5.47E+08	6	6	6	25.8	33.516	25.3892	25.7007	25.0466	6	3	3	0.019624	0.623128	B8MY53	B8MY53	1	AFLA_079900	Recombinant hotspot-binding protein (Transtin), putative	
29.8697	29.9146	30.1226	30.2839	30.1882	30.2118		+ 6,66E-64	1.1E+10	9	9	9	34	28.156	30.0985	29.969	30.228	6	3	3	0.035585	-0.259019	B8MY54	B8MY54	1	AFLA_079910	Glutathione peroxidase	
NaN	26.7061	27.7025	27.458	26.6026	26.0634		2,76E-196	1.91E+09	8	8	8	40.1	32.288	26.9065	27.2043	26.708	5	2	2	0.496015	0.456326	B8MY65	B8MY65	1	AFLA_080020	ATP synthase subunit gamma	
25.2246	NaN	NaN	23.531	24.5906	NaN		6,99E-09	1.15E+08	4	4	4	5.2	100.79	24.4488	25.2246	24.0608	3	1	2	1	1	1,6382	B8MY66	B8MY66	1	AFLA_080030	Topoisomerase I
26.9821	28.2673	29.2138	29.1097	28.3689	29.152		0	7,02E+08	22	22	22	48	85.571	28.3095	28.1544	28.4646	6	3	3	0.694482	-0.310199	B8MY76	B8MY76	1	AFLA_080130	Protein transport protein Sec23, putative	
30.4844	30.5277	30.4712	29.2864	28.74	28.8897		+ 1,23E-47	8.01E+09	5	5	5	35.8	17.937	29.7332	30.4944	28.972	6	3	3	0.000747	1.52339	B8MY77	B8MY77	1	AFLA_080140	60S ribosomal protein L12	
25.4934	25.8493	27.4139	27.9832	26.6363	26.2287		4,16E-102	1.87E+09	2	2	2	6.7	17.669	26.6008	26.2522	26.9434	6	3	3	0.428975	-0.697208	B8MY87	B8MY87	1	AFLA_080240	ATP synthase delta chain, mitochondrial, putative	
28.6715	28.4696	28.3939	28.8497	28.9325	28.9992		+ 1,88E-133	3.89E+09	7	7	7	38	25.59	28.7194	28.5117	28.9271	6	3	3	0.011286	-0.415482	B8MY92	B8MY92	1	AFLA_080290	DUTPase (Dut), putative	
NaN	24.0368	24.1546	24.1558	23.914	23.9314		1,04E-29	2.36E+08	4	4	4	21.8	37.787														

Supplemental Table S2. Data on proteins obtained from labelfree proteomics of *Aspergillus flavus* grown in presence of 0.1 M CaCl₂ treated with 10 µg/ml PgAFP and untreated control.

LFQ intensity AF_CaCl ₂ PgAFP_1	LFQ intensity AF_CaCl ₂ PgAFP_2	LFQ intensity AF_CaCl ₂ PgAFP_3	LFQ intensity AF_CaCl ₂ Control_1	LFQ intensity AF_CaCl ₂ Control_2	LFQ intensity AF_CaCl ₂ Control_3	t-test Significant	PEP	Intensity	Peptides	Razor + unique peptides	Unique peptides	Sequence coverage [%]	Mol. weight [kDa]	Mean	Mean AF_CaCl ₂ PgAFP	Mean AF_CaCl ₂ Control	Valid values	Valid values AF_CaCl ₂ PgAFP	Valid values AF_CaCl ₂ Control	t-test p value	t-test Difference	Protein IDs	Majority protein IDs	Proteins	Gene Names	Protein names
29.4708	28.9656	28.6111	29.1361	29.5119	29.7716		1,44E-123	7,04E+09	5	5	5	59.6	11.926	29.2445	29.0158	29.4732	6	3	3	0.214515	-0.457326	BBM223	BBM223	1	AFLA_083120	Thioredoxin
28.0034	27.5749	27.5823	27.2791	27.2735	27.3511	+	9.41E-32	1,61E+09	6	6	6	25	44.6	29.7507	27.7022	27.3012	6	3	3	0.043504	0.419008	BBM247	BBM247	1	AFLA_083360	Extracellular cell wall glucanase Crf1/allergen Asp F9
30.7682	30.2976	30.0123	30.1919	30.4176	30.4996		1.4E+10	18	18	18	18	51.1	60.985	30.3645	30.3593	30.3697	6	3	3	0.967424	-0.103772	BBM248	BBM248	1	AFLA_083370	Glutathione oxidoreductase Glr1, putative
22.4239	22.0115	21.7122	29.7705	30.0022	30.2119	+	8.35E+09	17	17	17	18	48.1	69.417	26.022	22.0492	22.9949	6	3	3	5.17E-06	-7.94565	BBM253	BBM253	1	AFLA_083420	Non-hemolytic phospholipase C, putative
26.3916	26.1463	26.1091	25.9854	26.2985	26.3622		9.00E-22	7.88E+08	18	18	18	26.4	35.022	26.2155	26.2157	26.2155	6	3	3	0.998293	0.0003332	BBM255	BBM255	1	AFLA_083440	Ubiquitin carboxyl-terminal hydrolase (EC 3.4.19.12)
24.391	24.4136	29.3914	28.8623	26.3664	27.0186		6.29E-48	2.59E+09	3	3	3	36.8	7.6649	26.7389	26.0653	27.4124	6	3	3	0.501218	-1.3471	BBM258	BBM258	1	AFLA_083470	Ribosomal protein S28e
25.0774	25.1879	24.6269	25.0894	25.3892	25.3672		5.01E-15	3.32E+08	4	4	4	7.7	82.41	25.123	24.9641	25.2819	6	3	3	0.181582	-0.317878	BBM259	BBM259	1	AFLA_083480	Importin beta-2 subunit, putative
24.1446	24.8654	25.409	25.4328	25.4096	24.9372		3.47E-85	5.3E+08	7	7	7	17	57.211	25.0331	24.8063	25.2599	6	3	3	0.320408	-0.453552	BBM266	BBM266	1	AFLA_083550	Coatomer subunit delta, putative
29.1012	28.7719	27.6148	28.8604	28.0199	28.3196		0.215E+09	6	6	6	6	24.3	46.201	28.1146	28.496	27.9333	6	3	3	0.294891	0.762663	BBM270	BBM270	1	AFLA_083590	Fatty acid hydroxylase, putative
25.1881	25.7921	24.7573	23.9946	24.1597	24.4006	+	5.21E-13	3.71E+08	5	5	5	10.9	64.216	24.7154	25.2458	24.185	6	3	3	0.030215	1.06081	BBM271	BBM271	1	AFLA_083600	RNA splicing factor (Psd-1), putative
26.3366	27.2353	28.1911	27.3772	27.1279	27.0278		3.57E-58	1.58E+09	6	6	6	36.9	14.737	27.216	27.2543	27.1777	6	3	3	0.895013	0.076621	BBM285	BBM285	1	AFLA_083740	40S ribosomal protein S22
27.5885	28.2465	28.1018	27.9942	28.7041	28.3366		2.67E-132	4.28E+09	22	22	22	33.3	96.049	28.1953	27.9789	28.4117	6	3	3	0.213577	-0.432725	BBM286	BBM286	1	AFLA_083750	Importin beta-1 subunit
28.8699	28.5657	28.0048	28.8145	28.8319	28.8339		1.18E-176	4.76E+09	9	9	9	51.2	37.506	28.6534	28.4801	28.8268	6	3	3	0.24219	-0.34664	BBM290	BBM290	1	AFLA_083890	Oxidoreductase, zinc-binding dehydrogenase family, putative
28.5072	28.7225	28.7025	28.3072	29.246	29.329		1.79E-128	5.05E+09	18	18	18	51.2	46.282	28.8024	28.6441	28.9607	6	3	3	0.397808	-0.316619	BBM293	BBM293	1	AFLA_083920	Adenylosuccinate synthetase (AMPSase) (EC 6.3.4.4) (IMP-aspartate ligase)
24.851	26.4526	26.8219	26.5546	26.3374	26.2391		2.75E-25	5.95E+08	4	4	4	17.4	23.974	26.2094	26.0418	26.3771	6	3	3	0.612978	-0.335255	BBM297	BBM297	1	AFLA_084160	DUF1014 domain protein
25.8526	26.5986	26.314	25.9841	26.5597	26.2519		1.14E-12	4.31E+08	4	4	4	19.3	41.007	26.2601	26.2551	26.2652	6	3	3	0.972218	-0.101407	BBM304	BBM304	1	AFLA_084230	Homoserine acetyltransferase family protein
25.1023	24.7236	25.0037	NaN	25.1386	24.9752		3.03E-19	2.97E+08	5	5	5	12	68.153	24.9887	24.9432	25.0569	5	3	3	0.255228	-0.113673	BBM305	BBM305	1	AFLA_084240	Poly(A) polymerase Pap
NaN	25.4063	25.9211	23.9452	24.8438	NaN		1.05E-26	6.69E+08	5	5	5	18.9	32.749	25.0291	25.6637	24.3945	4	2	2	0.133848	1.26917	BBM328	BBM328	2	AFLA_084330	Mitochondrial phosphate carrier protein (Mcr1), putative
24.7133	24.1777	23.5656	23.9927	24.3933	24.3555		2.21E-11	2.47E+08	5	5	5	19.9	36.327	24.1997	24.1522	24.2472	6	3	3	0.802417	-0.094891	BBM324	BBM324	1	AFLA_084440	Autophagy protein Atg27, putative
28.8236	28.1928	27.8944	28.6198	28.9469	28.9291		1.72E-91	3.22E+09	16	16	16	47.7	42.38	28.5678	28.3036	28.832	6	3	3	0.146481	-0.528348	BBM325	BBM325	1	AFLA_084450	Uncharacterized protein
28.5982	28.4506	28.2331	28.4384	28.5154	28.6233		2.74E-157	3.62E+09	22	22	22	32.9	102.84	28.4765	28.4273	28.5257	6	3	3	0.454181	-0.098409	BBM326	BBM326	1	AFLA_084460	Heat shock protein Hsp98/Hsp104/C1pA, putative
28.0919	27.9023	27.6632	27.7494	27.7184	27.7189		4.11E-98	3.15E+09	22	22	22	30.5	107.67	27.8178	27.8858	27.7499	6	3	3	0.339416	-0.135909	BBM329	BBM329	1	AFLA_084590	Hsp70 family chaperone Hsc1/Orp150, putative
24.3423	25.8558	28.4269	25.1624	24.8968	25.3934		1.26E-57	2.02E+09	10	10	10	46.3	23.866	25.6796	26.2084	25.1508	6	3	3	0.428238	-0.105755	BBM328	BBM328	1	AFLA_084620	40S ribosomal protein S5, putative
28.1569	27.6819	27.3946	27.7808	28.1512	28.125		1.12E-78	3.03E+09	11	11	11	80.5	26.482	27.8817	27.7445	28.019	6	3	3	0.376338	-0.274551	BBM325	BBM325	1	AFLA_084650	Palmitoyltransferase with autoacylation activity Pf4, putative
30.082	30.1713	30.0358	30.3518	30.1661	30.2498		0.131E+10	30	30	30	30	57.5	71.114	30.1761	30.0963	30.2559	6	3	3	0.075313	-0.195885	BBM326	BBM326	1	AFLA_084660	2-Isopropylmalate synthase
26.2059	26.0593	25.4943	25.6688	26.0275	25.956		1.00E-16	6.27E+08	6	6	6	16.7	55.816	25.9012	25.9198	25.8841	6	3	3	0.890354	0.0356941	BBM325	BBM325	1	AFLA_084750	Probable Xaa-Pro aminopeptidase AFLA_084750 (EC 3.4.11.9) (Aminoacylproline aminopeptidase) (Prolidase)
29.4186	29.0884	28.5534	29.3303	29.4254	29.4151		2.25E-152	5.89E+09	13	13	13	44.4	47.607	29.2052	29.0201	29.3902	6	3	3	0.218644	-0.370113	BBM322	BBM322	1	AFLA_084820	Acyl-CoA dehydrogenase, putative
25.0071	24.6966	24.0641	24.202	24.2425	25.4514		1.81E-10	2.57E+08	3	3	3	9.2	52.445	24.7243	24.5892	24.8593	6	3	3	0.585704	-0.270064	BBM324	BBM324	1	AFLA_084840	Uncharacterized protein
23.1648	23.3272	NaN	NaN	23.0346	23.2928		3.35E-05	7.680E+08	2	2	2	6.2	49.373	23.2049	23.246	23.1638	4	2	2	0.643939	0.022086	BBM324	BBM324	1	AFLA_085020	Exosome complex exonuclease Rrp6, putative
25.7202	25.4998	25.813	NaN	24.1901	24.1029	+	4.78E-07	1.77E+08	2	2	2	8.1	37.627	25.0622	25.6733	24.1465	6	3	3	0.091271	1.22779	BBM322	BBM322	1	AFLA_085040	Class II aldolase/aldolase domain protein
25.8671	25.8152	25.4267	25.7999	25.6162	25.8147		7.06E-23	1.08E+08	3	3	3	27	13.408	25.7233	25.703	25.7436	6	3	3	0.80357	-0.0406354	BBM324	BBM324	1	AFLA_085040	Uncharacterized protein
25.7149	24.9757	26.3913	26.1402	25.8149	25.5351		9.79E-74	1.08E+09	12	12	12	18.4	110.699	25.762	25.694	25.8031	6	3	3	0.774781	-0.136999	BBM323	BBM323	1	AFLA_085130	Sec23/Sec24 family protein
NaN	22.9565	23.6506	NaN	NaN	NaN		6.07E-27	2.91E+08	3	3	3	7.6	58.844	23.3036	23.3036	NaN	2	0	1	NaN	BBM327	BBM327	1	AFLA_085270	T-complex protein 1, zeta subunit, putative	
NaN	NaN	24.9674	25.4293	25.4627	25.3503		8.10E-30	4.07E+08	4	4	4	19.3	38.204	25.3024	24.9674	25.4141	4	1	1	-0.446657	BBM325	BBM325	1	AFLA_085350	AMMECR1 family protein	
26.4714	26.4001	26.3657	26.4921	26.4427	26.6839		2.65E-24	1.06E+09	4	4	4	38.3	13.319	26.476	26.4124	26.5396	6	3	3	0.18671	-0.127155	BBM329	BBM329	1	AFLA_085390	Profilin subunit 6, putative
31.9553	32.8641	32.9116	33.351	32.7465	32.8288		0.777E+10	37	37	37	82.7	57.288	32.7762	32.7772	32.9754	6	3	3	0.335413	-0.398451	BBM300	BBM300	1	AFLA_085400	Phosphoglycerate mutase, 2,3-bisphosphoglycerate-independent	
28.7465	30.0527	30.1719	28.867	30.1492	29.6201		0.139E+10	25	25	25	24	67.51	51.863	29.6012	29.657	29.5454	6	3	3	0.858896	-0.11629	BBM302	BBM302	1	AFLA_085420	Serine hydroxymethyltransferase (EC 2.1.1.2)
25.8498	26.8043	27.4878	27.1294	27.1266	26.9498		3.55E-115	1.98E+09	6	6	6	33.1	28.051	26.8913	26.714	27.0666	6	3	3	0.49994	-0.354631	BBM305	BBM305	1	AFLA_085450	Eukaryotic translation initiation factor 3 subunit K (eIF3) (eIF-3 p25)
26.7326	26.2569	25.5051	24.9025	25.7006	26.0576		2.20E-30	5.46E+08	3	3	3	40	14.692	25.8709	26.1648	25.5769	6	3	3	0.303349	-0.58797	BBM324	BBM324	1	AFLA_085540	Uncharacterized protein
25.4771	24.8841	24.5678	24.8955	25.2706	26.0167		9.65E-25	4.59E+08	5	5	5	33.8	29.098	25.1822	24.9763	25.388	6	3	3	0.387332	-0.411676	BBM320	BBM320	1	AFLA_085600	Uncharacterized protein
28.577	27.9974	27.6477	27.8939	28.212	28.3385		6.25E-87	2.97E+09	11	11	11	86.3	16.691	28.1111	28.074	28.1481	6	3	3	0.817959	-0.0741081	BBM320	BBM320	1	AFLA_085700	Arsenate reductase (Arc2), putative
27.5243	27.5938	27.2722	27.4985	27.2418	27.5108		4.36E-32	1.96E+09	7	7	7	21.8	44.288	27.4402	27.4635	27.4147	6	3	3	0.741407	-0.046435	BBM324	BBM324	1	AFLA_085840	Tubulin-specific chaperone c, putative
NaN	NaN</																									

Supplementary Table S2. Data on proteins obtained from label-free proteomics from *Aspergillus flosus* grown in presence of 0.1 M CaCl₂ treated with 10 µg/ml PgAFP and untreated control.

LFQ intensity AF_CaCl ₂ PgAFP_1	LFQ intensity AF_CaCl ₂ PgAFP_2	LFQ intensity AF_CaCl ₂ PgAFP_3	LFQ intensity AF_CaCl ₂ Control_1	LFQ intensity AF_CaCl ₂ Control_2	LFQ intensity AF_CaCl ₂ Control_3	t-test Significant	PEP	Intensity	Peptides	Razor + unique peptides	Unique peptides	Sequence coverage [%]	Mol. weight [kDa]	Mean	Mean AF_CaCl ₂ PgAFP	Mean AF_CaCl ₂ Control	Valid values	Valid values AF_CaCl ₂ PgAFP	Valid values AF_CaCl ₂ Control	t-test p value	t-test Difference	Protein IDs	Majority protein IDs	Proteins	Gene Names	Protein names		
30.2399	29.6593	29.0674	29.5532	29.7502	29.873			9,37E-133	5,67E+09	12	12	44	33.63	29,6905	29,6555	29,7255	6	3	3	0,851888	-0,069247	B8NOC1	B8NOC1	1	AFLA_087620	NmrA family transcriptional regulator, putative		
NaN	25,1752	25,0662	24,9762	25,2696	24,3428			2,10E-38	7,85E+08	8	8	5	22,8	53,831	24,966	25,1207	24,8629	5	2	3	0,520609	0,257843	B8NOC2	B8NOC2	1	AFLA_087630	Alpha,alpha-trehalose-phosphate synthase (UDP-forming) (EC 2.4.1.15) (Trehalose-6-phosphate synthase)	
23,9952	23,7594	23,1997	23,939	23,704	23,6729			1,21E-14	1,35E+08	2	2	2	7,82	26,372	27,7117	23,6514	24,772	6	3	3	0,655341	-0,120555	B8NOC4	B8NOC4	1	AFLA_087650	Chromatin assembly factor 1 subunit B, putative	
27,468	27,3944	26,5979	26,4552	26,343	26,4452			1,47E-39	1,35E+09	5	5	5	29,4	18,491	27,2427	28,0234	26,4762	6	3	3	0,035148	1,5614	B8NOD5	B8NOD5	1	AFLA_087760	40S ribosomal protein S11	
26,0322	26,5258	26,4764	27,1012	27,7581	26,6811			4,50E-96	1,53E+09	11	11	11	44,1	39,208	26,7625	26,3448	27,1801	6	3	3	0,075732	-0,835254	B8MW92	B8MW92	1	AFLA_087820	Cell wall integrity signaling protein Lsp1/Plt1, putative	
30,6311	30,8276	31,5586	32,4185	32,0477	31,8304				3,89E+10	31	31	31	66,9	58,086	31,5523	31,0058	32,0988	6	3	3	0,029671	-1,09306	B8MWA0	B8MWA0	1	AFLA_087900	Pyruvate kinase (EC 2.7.1.40)	
25,1643	25,1467	24,8488	24,4076	24,3229	24,5095			1,10E-13	3,06E+08	6	6	6	18,5	51,882	24,8154	25,0533	24,4586	5	3	2	0,022778	0,594677	B8MWA2	B8MWA2	1	AFLA_087920	F-box domain protein	
30,2977	30,1364	30,1183	30,2069	30,3729	30,4331			1,39E-168	1,08E+10	19	19	19	48,1	41,263	30,2609	30,1841	30,3376	6	3	3	0,157747	-0,153493	B8MWA5	B8MWA5	1	AFLA_087950	isocitrate dehydrogenase Ly5B	
26,1613	26,3705	26,1261	NaN	23,9114	23,2131			1,84E-16	4,33E+08	6	6	6	54,7	18,499	25,1725	26,2193	23,6022	5	2	2	0,003368	2,17077	B8MWA9	B8MWA9	1	AFLA_087990	40S ribosomal protein S8	
27,0386	26,7351	26,4216	26,6319	26,6779	26,6222			1,30E-24	1,23E+09	7	7	7	22,8	44,789	26,6878	26,7318	26,6499	6	3	3	0,649511	0,087862	B8MWB2	B8MWB2	1	AFLA_088020	Methionine aminopeptidase 1 [MAP 1] (MetAP 1) (EC 3.4.11.18) (Peptidase M 1)	
24,2014	24,1386	23,8664	23,9232	23,8283	24,0662			3,14E-06	1,97E+08	2	2	2	10,4	45,208	24,0024	24,0655	23,9393	6	3	3	0,363849	0,116221	B8MWB8	B8MWB8	1	AFLA_088080	Aspartate aminotransferase, putative	
27,8932	27,811	27,3422	26,4256	25,7199	25,4279			9,71E-45	1,58E+09	7	7	7	50	33,52	26,62	27,7155	25,5265	6	3	3	0,000843	2,19103	B8MWC5	B8MWC5	1	AFLA_088150	Fe superoxide dismutase, putative	
29,0729	29,7671	29,9057	29,8486	29,2818	29,2818				8,67E+09	13	13	13	52,8	37,175	29,5735	29,5819	29,5651	6	3	3	0,958665	0,016831	B8MW06	B8MW06	1	AFLA_088260	Eukaryotic translation initiation factor 3 subunit F (eIF3)	
29,0611	29,3206	29,2588	29,1409	29,0393	29,2342			5,77E-154	6,21E+09	14	14	14	53,2	33,913	29,1758	29,2135	29,1381	6	3	3	0,477858	0,075388	B8MW02	B8MW02	1	AFLA_088320	Protein phosphatase 2C, putative	
27,4014	27,644	29,9933	28,0281	27,4525	27,4127			1,94E-51	3,49E+09	10	10	10	62,5	21,887	27,9786	28,3261	27,6311	6	3	3	0,449812	0,695023	B8MW07	B8MW07	1	AFLA_088370	60S ribosomal protein L9, putative	
28,9978	29,26	29,0831	29,7572	29,1062	28,9119			1,18E-284	6,6E+09	11	11	11	61	20,02	29,186	29,1137	29,2584	6	3	3	0,616496	-0,144761	B8MW07	B8MW07	1	AFLA_088570	Uncharacterized protein	
28,899	28,5334	28,0644	27,9971	28,6454	28,5925			9,79E-133	3,79E+09	13	13	13	49,9	39,699	28,4253	28,4989	28,3517	6	3	3	0,651189	0,147263	B8MW09	B8MW09	1	AFLA_088590	Nuclear pore complex protein (NupA), putative	
29,8914	29,7155	29,4385	29,7521	29,6815	29,7649				0,96E+09	16	16	16	70	41,427	29,7073	29,6818	29,7328	6	3	3	0,723158	-0,051073	B8MWH2	B8MWH2	1	AFLA_088620	UPF0160 domain protein MYG1, putative	
NaN	NaN	NaN	24,1458	24,3954	24,7165			3,11E-10	1,68E+08	4	4	4	23,1	23,68	23,972	24,0718	23,9388	4	1	3	1	0,132984	B8MWH6	B8MWH6	1	AFLA_088660	DUF431 domain protein	
26,0889	25,8688	25,5064	25,9439	25,9517	26,0954			1,35E-14	6,58E+08	2	2	2	40,5	8,3184	25,9092	25,8214	25,9097	6	3	3	0,376755	-0,175641	B8MWS2	B8MWS2	1	AFLA_088720	Iron/copper transporter Atx1, putative	
24,422	24,9915	26,079	25,1129	24,803	24,5156			2,36E-93	7,75E+08	5	5	5	37,7	19,685	24,9907	25,1709	24,8107	6	3	3	0,519484	0,360401	B8MWS6	B8MWS6	1	AFLA_088760	Septin	
28,356	28,9148	28,6832	29,1736	28,7869	28,749			2,42E-101	4,6E+09	11	11	11	55,2	25,898	28,7772	28,6513	28,9031	6	3	3	0,299323	-0,25184	B8MWS7	B8MWS7	1	AFLA_088770	Guanylate kinase	
NaN	24,9103	24,8695	25,037	25,5085	25,5192			2,29E-30	5,71E+08	9	9	9	11,2	123,33	25,1689	24,8899	25,3549	5	2	3	0,108987	-0,465009	B8MWT5	B8MWT5	1	AFLA_088850	Exportin KapK	
24,0109	23,4908	NaN	NaN	NaN	NaN			2,14E-05	74033000	2	2	2	4,1	77,122	23,7509	23,7509	NaN	2	2	0	1	NaN	B8MWT6	B8MWT6	1	AFLA_088860	Acetyltransferase, putative	
24,3617	23,7449	23,9969	24,2052	24,2615	24,458			8,61E-07	1,55E+08	2	2	2	12,6	32,787	24,1714	24,0345	24,3082	6	3	3	0,232568	-0,273477	B8NL76	B8NL76	1	AFLA_089120	Inositol monophosphatase, putative	
31,7115	33,0503	33,132	33,0918	33,5996	32,0942				8,62E+10	99	99	99	66,4	232,14	32,2649	32,6312	31,8995	6	3	3	0,305327	0,732683	B8NL80	B8NL80	1	AFLA_089160	Fatty acid synthase beta subunit, putative	
30,7605	32,559	32,5073	30,2343	31,3023	30,5528				5,23E+10	80	80	80	79,9	56,6	204,29	31,3012	31,9423	30,6661	6	3	3	0,12186	1,28215	B8NL81	B8NL81	1	AFLA_089170	Fatty acid synthase alpha subunit FaaA
32,1611	31,8426	31,4439	31,4016	31,6742	31,6776				0,68E+10	14	14	14	54,8	40,702	31,6927	31,8009	31,5845	6	3	3	0,372181	0,216394	B8NL85	B8NL85	1	AFLA_089210	Pyruvate dehydrogenase E1 beta subunit PdbA, putative	
26,891	26,4208	25,9317	26,092	26,3487	26,6043			1,43E-29	7,74E+08	6	6	6	13,9	70,111	26,3814	26,4145	26,3483	6	3	3	0,843304	0,065977	B8NL86	B8NL86	1	AFLA_089220	Ser/Thr protein phosphatase family	
29,989	29,6577	29,1927	29,6449	29,631	29,7376			2,65E-298	8,44E+09	20	20	19	47,7	62,28	29,266	26,6088	27,6378	6	3	3	0,330541	-0,023362	B8NK38	B8NK32	2	AFLA_089560	Pyruvate decarboxylase, putative	
28,5165	28,0726	27,4743	27,76	29,0038	28,2431			3,11E-31	2,19E+09	6	6	6	42,1	14,649	28,0117	28,0211	28,0023	6	3	3	0,95768	0,0187804	B8NK5	B8NK5	1	AFLA_089590	Uncharacterized protein	
28,8956	28,8834	29,1448	29,3376	29,1096	28,9979			7,65E-129	5,78E+09	15	15	15	44,1	42,417	29,0615	28,9746	29,1484	6	3	3	0,256349	-0,173775	B8NK1	B8NK1	1	AFLA_089750	Tyrosine-tRNA ligase (EC 6.1.1.1) (Tyrosyl-tRNA synthetase)	
27,265	27,0609	27,0108	27,1907	27,1802	27,1225			3,13E-30	1,67E+09	6	6	6	48,1	17,269	27,1383	27,1122	27,1644	6	3	3	0,525353	0,052035	B8NK0	B8NK0	1	AFLA_089940	Thioredoxin, putative	
25,103	25,1707	24,7669	24,8109	24,2204	24,984			2,91E-19	3,49E+08	5	5	5	13,8	73,101	24,849	25,0135	24,6022	5	3	2	0,299323	0,411297	B8NL1	B8NL1	1	AFLA_090380	Chromatin remodeling complex subunit (Arg9), putative	
25,9221	25,5111	26,569	24,6678	25,0753	25,1869			2,77E-21	3,64E+09	7	7	7	9,8	117,64	25,4887	26,0008	24,9767	6	3	3	0,041561	1,02407	B8NL2	B8NL2	1	AFLA_090490	Alpha,alpha-trehalose glycohydrolase Trea/Ata1	
28,6053	28,0431	28,0829	27,1183	27,1388	27,2818			7,73E-105	1,64E+09	16	16	14	27,5	89,135	27,7117	28,2438	27,1962	6	3	3	0,004829	1,06414	B8NL2	B8NL2	1	AFLA_090590	Alpha-1,2-mannosidase, putative subfamily	
32,0197	31,3201	31,4275	31,1325	31,5576	31,7522				0,356E+10	25	25	25	47,3	79,838	31,5349	31,5891	31,4806	6	3	3	0,722451	0,108342	B8NLE2	B8NLE2	1	AFLA_090690	Mycelial catalase Cat1	
27,0785	26,9036	26,6819	26,9933	27,0686	27,075			8,52E-29	1,01E+09	6	6	6	43,9	19,124	26,9668	26,888	27,0456	6	3	3	0,251459	-0,157653	B8NLE9	B8NLE9	1	AFLA_090760	Ankyrin repeat protein	
32,8277	33,2961	33,2156	33,551	32,8139	32,8677				0,108E+11																			

Supplementary Table S2. Data on proteins obtained from label-free proteomics from *Aspergillus flovus* grown in presence of 0.1 M CaCl₂ treated with 10 µg/ml PgAFP and untreated control.

LFQ intensity AF_CaCl ₂ PgAFP_1	LFQ intensity AF_CaCl ₂ PgAFP_2	LFQ intensity AF_CaCl ₂ PgAFP_3	LFQ intensity AF_CaCl ₂ Control_1	LFQ intensity AF_CaCl ₂ Control_2	LFQ intensity AF_CaCl ₂ Control_3	t-test Significant	PEP	Intensity	Peptides	Razor + unique peptides	Unique peptides	Sequence coverage [%]	Mol. weight [kDa]	Mean	Mean AF_CaCl ₂ PgAFP	Mean AF_CaCl ₂ Control	Valid values	Valid values AF_CaCl ₂ PgAFP	Valid values AF_CaCl ₂ Control	t-test p value	t-test p value	Protein IDs	Majority protein IDs	Proteins	Gene Names	Protein names	
23.5404	23.4114	23.0328	23.281	23.213	23.3778			2.98E+10	1,42E+08	3	3	11	40,817	23,261	23,3282	23,324	6	3	3	0.980282	0.0042623	BBNL1R	BBNL1R	1	AFLA_092770	TOR signaling pathway regulator (TapA), putative	
23.0113	23.6072	23.1815	23.575	23.5998	23.1447			5,15E+05	1,01E+08	2	2	3,1	97,076	23,3466	23,2666	23,4265	6	3	3	0.519213	-0,15983	BBNL9R	BBNL9R	1	AFLA_092850	WD repeat protein	
26.2623	29,0689	29,3925	29,3462	29,4226	28,9829			0,701E+09		12	12	52,4	42,101	28,7459	28,2413	29,2506	6	3	3	0.37124	-1,00931	BBNL54	BBNL54	1	AFLA_092900	Oxidative stress protein Svf1, putative	
24.6762	24,7173	24,1414	NaN	NaN	24,3346			9,82E+20	3,02E+08	5	5	6,4	105,72	24,4674	24,5116	24,3846	4	3	1	1	0,17707	BBNL58	BBNL58	1	AFLA_092940	DNA repair and transcription protein (Xab2), putative	
24.1057	24,033	24,2326	22,5802	NaN	NaN			6,24E+09	92011000	2	2	9,5	36,615	23,7379	24,1237	22,5802	4	3	1	1	1,54349	BBNK2P	BBNK2P	1	AFLA_092960	Small nuclear ribonucleoprotein, putative	
28.8386	25,9649	25,9249	24,8671	26,5313	26,9394			3,99E+49	9,58E+08	10	10	68,7	22,593	26,511	26,9095	26,1126	6	3	3	0.527922	0,796857	BBNKR2	BBNKR2	1	AFLA_093160	Rab small monomeric GTPase Rab7, putative	
29.7429	29,7253	29,7791	30,3799	29,9096	29,8063			0	1,03E+10	22	22	22	62,4	53,168	29,8905	29,7491	30,0319	6	3	3	0.185782	-0,282801	BBNKR8	BBNKR8	1	AFLA_093220	Ran-specific GTPase-activating protein 1, putative
26.8039	27,6209	27,963	27,1583	27,2563	27,4419			1,22E+14	1,6E+09	7	7	28	41,309	27,374	27,4626	27,2855	6	3	3	0.64289	0,177113	BBNKS2	BBNKS2	1	AFLA_093260	Oxidoreductase, 2OG-Fe(II) oxygenase family, putative	
27.3391	27,2393	26,8782	26,9477	27,2364	27,1874			3,54E+30	1,41E+09	7	7	30,3	30,343	27,138	27,1522	27,1238	6	3	3	0.872899	0,0283464	BBNKS3	BBNKS3	1	AFLA_093270	Uncharacterized protein	
30.4107	30,0197	29,6405	29,9106	29,8531	29,9546			1,52E+218	1,3E+10	19	19	59	49,59	29,916	29,9649	30,0236	29,9061	6	3	3	0.627907	0,117556	BBNKS4	BBNKS4	1	AFLA_093280	Disulfide isomerase (TigA), putative
NaN	NaN	23,8085	23,5326	NaN	22,5926			2,35E+10	1,21E+08	4	4	4	12,3	25,3112	23,8085	23,0626	6	3	1	2	1	0,745943	BBNKS5	BBNKS5	1	AFLA_093320	Pseudouridine synthase
25.1848	25,484	25,6405	25,6764	25,5953	26,4073			9,43E+32	4,89E+08	5	5	5	30,5	20,676	25,548	25,4364	25,8597	6	3	3	0.103141	-0,423239	BBNK7O	BBNK7O	1	AFLA_093340	Uncharacterized protein
25.8655	26,1263	26,0748	26,7698	26,4142	26,4416			1,07E+29	9,34E+08	9	9	9	29,9	49,501	26,282	26,0222	26,5418	6	3	3	0.020305	-0,519636	BBNKT3	BBNKT3	1	AFLA_093370	Ribonucleotide reductase small subunit RnrA, putative
25.2914	24,799	24,2758	24,4992	NaN	NaN			4,56E+10	2,49E+08	3	3	12,5	49,653	24,7163	24,7887	24,4992	4	3	1	1	1	0,289555	BBNKU4	BBNKU4	1	AFLA_093480	Aminomethyl transferase, putative
29.3255	28,7516	28,757	27,8323	28,641	28,6724			0,431E+09		12	12	55,4	36,305	28,6633	28,9447	27,3819	6	3	3	0.16771	0,562791	BBNKJ8	BBNKJ8	1	AFLA_093520	2-amino-3-carboxymuconate-6-semialdehyde decarboxylase, putative	
28.6237	28,1403	28,4972	27,2556	27,847	27,855			6,27E+102	2,31E+09	12	12	12	45,3	39,245	28,0365	28,4204	27,6525	6	3	3	0.035327	0,767886	BBNKJ9	BBNKJ9	1	AFLA_093530	Oxidoreductase, 2OG-Fe(II) oxygenase family
25.615	24,2822	NaN	24,1046	24,6439	24,7656			2,20E+06	1,3E+08	2	2	8,9	31,827	24,6823	24,9486	24,5047	5	2	3	0.487058	0,443887	BBNKV0	BBNKV0	1	AFLA_093540	Short chain dehydrogenase/reductase family	
26.7506	26,4147	26,0567	26,0508	26,016	25,9711			1,05E+65	8,47E+08	3	3	39,9	10,908	26,21	26,4073	26,1262	6	3	3	0.121949	0,394709	BBNKW0	BBNKW0	1	AFLA_093640	Use nuclear ribonucleoprotein (Lsm3), putative	
24.8829	24,2082	24,1416	24,2064	25,2601	25,1391			9,77E+12	1,96E+08	6	6	12,3	63,286	24,6397	24,4109	24,8686	6	3	3	0.325299	-0,457666	BBNKX5	BBNKX5	1	AFLA_093790	Dihydroxyacetone kinase (DakA), putative	
26.1371	26,6486	26,1072	24,4544	24,6195	24,1401			3,80E+25	5,2E+08	3	3	3	42,6	13,025	26,2976	24,4046	6	3	3	0.001093	1,89297	BBNKX6	BBNKX6	1	AFLA_093800	Small nuclear ribonucleoprotein SmD2, putative	
23.8286	24,5147	24,7801	25,3378	25,0379	25,0176			1,62E+14	3,17E+08	3	3	31,7	13,373	24,7528	24,3744	25,1311	6	3	3	0.066246	-0,756652	BBNKX8	BBNKX8	1	AFLA_093820	sDNA binding protein Ssb3, putative	
27.727	27,3336	27,3739	27,5417	27,5855	27,5808			2,03E+50	1,92E+09	10	10	3	52	28,36	27,5237	27,4782	27,5393	6	3	3	0.508567	-0,091388	BBNLTS	BBNLTS	1	AFLA_093910	Hydroxyacylglutathione hydrolase, putative
26.3248	26,5591	25,5442	24,7399	25,0755	25,8537			3,30E+21	5,29E+08	9	9	9	21,7	48,134	25,3495	26,1427	24,5664	6	3	3	0.029112	1,58634	BBNLTS	BBNLTS	1	AFLA_093940	Mitochondrial large ribosomal subunit Yml35, putative
28.3128	28,2453	28,0929	27,6927	27,6622	27,5712			1,17E+139	2,49E+09	10	10	34,8	55,183	27,9295	28,217	27,6421	6	3	3	0.001524	0,574922	BBNLU0	BBNLU0	1	AFLA_093960	Mitochondrial 3-hydroxyisobutyryl-CoA hydrolase, putative	
27.7779	27,6808	27,2725	27,954	27,8832	27,9935			4,02E+125	2,3E+09	11	11	41,1	42,069	27,7603	27,5771	27,9435	6	3	3	0.081427	-0,366463	BBNLU8	BBNLU8	1	AFLA_094040	CRAI/TRIO domain protein	
24.2307	24,0283	23,4636	23,7866	24,2243	24,1324			0,000276	1,49E+08	2	2	7,2	28,588	23,9776	23,9075	20,4788	6	3	3	0.625125	-0,140258	BBNLW3	BBNLW3	1	AFLA_094190	Uncharacterized protein	
27.5603	27,0715	26,8675	27,2018	27,4691	27,4063			5,51E+215	1,59E+09	10	10	54,1	30,536	27,2628	27,1665	27,3591	6	3	3	0.432296	-0,192623	BBNLW5	BBNLW5	1	AFLA_094210	Chorismate mutase	
30.4457	28,4763	27,988	27,5805	28,7137	28,9121			0,282E+09		9	9	51,5	42,308	28,6861	28,97	28,021	6	3	3	0.544261	0,567907	BBNLW2	BBNLW2	1	AFLA_094280	Agmatinase, putative	
31.8547	31,404	30,2954	30,2868	30,4948	30,746			0,57E+10		19	19	63,9	42,313	30,8436	31,178	30,5192	6	3	3	0.242457	0,668828	BBNLY9	BBNLY9	1	AFLA_094450	Aspartic protease pep1 [EC 3.4.23.18] (Aspergillopepsin A) (Aspergillopepsin I)	
NaN	NaN	26,4143	27,135	27,3503	26,3686			2,11E+58	1,71E+09	10	10	24,7	60,647	26,7415	26,7746	26,7095	5	2	3	0.517239	0,0551567	BBNLZ3	BBNLZ3	1	AFLA_094800	Protein phosphatase 2C, putative	
29.3085	29,0043	28,6221	29,2132	29,2725	29,2725			2,92E+134	6,78E+09	6	6	7	48,5	18,026	28,1373	28,6429	29,2958	6	3	3	0.126233	0,334817	BBNM30	BBNM30	1	AFLA_094560	Putidolyl-protyl diester isomerase (EC 5.2.2.1.8)
33.7774	33,6839	33,3538	33,7174	33,6445	33,7081			0	1,38E+11	17	17	6	17	82,2	33,6476	33,6602	33,6902	6	3	3	0.549694	0,0851145	BBNM07	BBNM07	1	AFLA_094620	Triosephosphate isomerase (EC 5.3.1.1)
27.1212	27,2078	27,0494	25,5732	25,825	25,6162			1,36E+176	1,47E+09	6	6	6	40,9	27,781	26,3988	27,1261	25,7164	6	3	3	0.86E-05	1,45467	BBNM09	BBNM09	1	AFLA_094650	60S acidic ribosomal protein P0, putative
27.336	26,8733	26,575	26,5797	26,6046	27,0142			1,11E+57	1,29E+09	5	5	5	20,7	49,462	26,8305	26,9281	26,7329	6	3	3	0.498185	0,195248	BBNM13	BBNM13	1	AFLA_094690	Cell cycle control protein (Cwf8), putative
NaN	NaN	NaN	25,1091	25,1069	24,5207			2,82E+08	1,92E+08	5	5	22,6	27,235	24,9123	NaN	24,9123	3	0	3	1	NaN	BBNM17	BBNM17	1	AFLA_094730	Exosome complex subunit Csl4, putative	
NaN	NaN	26,214	25,686	25,4968	NaN			5,45E+36	5,44E+08	8	8	8	19	62,607	25,7989	26,214	25,5914	3	1	2	1	0,622573	BBNM53	BBNM53	1	AFLA_094850	Glucose-methanol-choline (Gmc) oxidoreductase, putative
28.9102	28,3073	28,8038	29,1156	28,6519	28,6342			1,33E+111	3,21E+09	8	8	35,2	25,832	28,7372	28,6738	28,8005	6	3	3	0.630308	-0,126758	BBNM55	BBNM55	1	AFLA_095570	RNA annealing protein Yra1, putative	
30.7447	30,553	30,3879	30,6603	30,5461	30,7481			5,67E+117	1,74E+10	9	9	9	43,6	27,256	30,6067	30,5619	30,6515	6	3	3	0.491714	-0,0896304	BBNM7C	BBNM7C	1	AFLA_095590	Hsp90 binding co-chaperone (Sba1), putative
26.2995	25,6819	25,3058	24,6624	24,7967	24,93			9,21E+13	3,52E+08	7	7	7	24,1	38,345	25,2794	25,7624	24,9616	6	3	3	0.032205	0,96012	BBNM01	BBNM01	1	AFLA_095630	FAD dependent oxidoreductase superfamily
25.8601	25,462	25,2658	25,066	25,167	25,672			1,65E+15	4,7E+08	4	4	4	21,7	33,761	25,4155	25,5293	25,3017	6	3	3	0.424717	0,227615	BBNL00	BBNL00	1	AFLA_095840	Fe-S cluster assembly protein dre2 (Anamorsin homolog)
31.6764	32,2872	32,2126	32,5307	32,2914	32,301			0,66E+10		45	45	64,7	79,792	32,2166	32,0587	32,3744	6	3	3	0.20317	-0,315655	BBNL13	BBNL13	1	AFLA_095970	Hsp70 chaperone Hsp88	
NaN	NaN	24,377	NaN	25,8596	25,9604			0,692E+09		9	9	69,4	12,309	25,3108	24,377	25,622	4	1	3	1	-1,24508	BBNL17	BBNL17	1	AFLA_096010	Uncharacterized protein	
NaN	NaN	23,7729	24,1405	22,8744	23,911			4,25E+56	3,19E+08	5	5	5	11,6	80,695	23,6763	23,9567	23,4893	5	2	3	0.355095	0,467392	BBNL54	BBNL54	1	AFLA_097260	Dynamid family GTPase, putative
26.3683	25,8727	NaN	25,4552	26,0991	26,2596			6,08E+24	6,67E+08	5	5	24,3	39,966	26,011	26												

Supplementary Table S2. Data on proteins obtained from label-free proteomics from *Aspergillus flovus* grown in presence of 0.1 M CaCl₂ treated with 10 μg/ml PgAFP and untreated control.

LQF intensity AF_CaCl ₂ PgAFP_1	LQF intensity AF_CaCl ₂ PgAFP_2	LQF intensity AF_CaCl ₂ PgAFP_3	LQF intensity AF_CaCl ₂ Control_1	LQF intensity AF_CaCl ₂ Control_2	LQF intensity AF_CaCl ₂ Control_3	t-test Significant	PEP	Intensity	Peptides	Razor + unique peptides	Unique peptides	Sequence coverage [%]	Mol. weight [kDa]	Mean AF_CaCl ₂ PgAFP	Mean AF_CaCl ₂ Control	Valid values	Valid values AF_CaCl ₂ PgAFP	Valid values AF_CaCl ₂ Control	t-test p value	t-test Difference	Protein IDs	Majority protein IDs	Proteins	Gene Names	Protein names	
27.4075	26.5853	25.7555	25.3642	26.3415	26.7372		1,77E-91	1,45E+09	12	12	12	34.6	57,591	26,3652	26,1476	6	3	3	0.526255	0.435143	BBNT50	BBNT50	1	AFLA_100010	T-complex protein 1 subunit delta	
29.7651	29.9713	29.8813	25.1314	24.9765	24.5285	+	6.55E+09		11	11	11	21.3	55,822	27,3757	29,8726	6	3	3	1.25E+05	4.99378	BBNT52	BBNT52	1	AFLA_100030	Nucleolin protein Nsr1, putative	
29.8745	29.6651	29.8351	29.7407	29.6533	29.7054		3,86E-298	7,93E+09	16	16	16	50.8	46,086	29,656	29,6788	6	3	3	0.587973	-0.0289148	BBNT55	BBNT55	1	AFLA_100060	Ran GTPase activating protein 1 (RNA1 protein)	
25.6716	24.8397	NaN	24.4864	NaN	24.9577		4,41E-11	2,93E+08	4	4	4	13.8	33,554	24,9889	25,2566	4	2	2	0.380519	0.533558	BBNT57	BBNT57	1	AFLA_100080	Transcription elongation factor 5-II	
26.8846	26.8277	27.1267	25.2786	26.5756	26.2823		8,64E-271	2,49E+09	16	16	16	25.6	99,812	26,4959	26,9463	6	3	3	0.089215	0.900841	BBNT70	BBNT70	2	AFLA_100110	Plasma membrane H+-ATPase Pma1	
23.8794	NaN	23.6396	23.984	24.1033	24.0098		2,55E-06	1,49E+08	3	3	3	14.8	37,59	23,9232	23,7955	5	2	2	0.073507	-0.072825	BBNT73	BBNT73	1	AFLA_100140	Metallo-beta-lactamase superfamily protein	
24.3995	24.5706	24.1068	24.2683	24.4267	24.3335		0.00031	2,55E+08	2	2	2	10	38,17	24,3509	24,359	24,3428	6	3	3	0.91551	0.016154	BBNT76	BBNT76	1	AFLA_100170	Complex I intermediate associated protein (Cia30), putative
28.5882	28.3006	28.1649	28.6335	28.5887	28.5962		8,67E-193	3,43E+09	15	15	15	62.3	34,153	28,4787	28,3513	28,6062	6	3	3	0.112215	-0.254878	BBNT77	BBNT77	1	AFLA_100180	Phosphoribosyl-aminimidazole-succinocarboxamide synthase
23.1196	23.1786	23.2721	25.7325	24.4701	24.5863		+1,27E-13	2,12E+08	5	5	5	15.3	66,502	24,0599	23,1901	24,9296	6	3	3	0.012721	-1,73956	BBNTU3	BBNTU3	1	AFLA_100240	Glucose dehydrogenase, putative
29.6592	29.6069	29.0936	30.2753	30.1115	30.1009		+0	1,03E+10	16	16	16	51.2	54,684	29,8085	29,4532	30,1637	6	3	3	0.019764	-0.710486	BBNTU4	BBNTU4	1	AFLA_100250	Catalase [EC 1.11.1.6]
NaN	28.1206	29.2927	29.5932	28.7796	28.1711		6,98E-102	5,96E+09	2	2	2	34.9	7,1109	28,811	28,7566	28,8473	5	2	2	0.306724	-0.0906525	BBNU0	BBNU0	1	AFLA_100630	Uncharacterized protein
30.7566	30.2616	29.099	29.7612	29.8518	30.0839		0	1,34E+10	6	6	6	22.1	54,876	29,9688	30,0387	29,8989	6	3	3	0.793995	0.139804	BBNU2	BBNU2	1	AFLA_100650	Serine carboxypeptidase (Cpd5), putative
28.846	28.3734	28.8448	28.4169	28.7416	28.1558		0	1,01E+10	23	23	23	58.6	57,696	28,5631	28,6881	28,4281	6	3	3	0.34046	0.24999	BBNU4	BBNU4	1	AFLA_100670	ATP sulphurylase
28.0835	27.9808	27.8602	27.6958	27.7127	27.8312		1,11E-130	2,7E+09	13	13	13	33.3	57.52	27,8774	27,9748	27,799	6	3	3	0.065059	-0.194952	BBNUM6	BBNUM6	1	AFLA_100790	Proteasome regulatory particle subunit (RpN6), putative
27.2399	26.8334	26.9653	26.8677	26.9127	26.8923		5,45E-34	1,4E+09	9	9	9	58.9	30.67	26,9519	27,0129	26,8909	6	3	3	0.368492	0.121965	BBNUM7	BBNUM7	1	AFLA_100800	Dihydrofolate reductase
NaN	NaN	NaN	24.9468	24.8329	24.2013		1,04E-20	4,42E+08	3	3	3	27	26,851	24,6603	NaN	24,6603	3	0	1	NaN	BBNUM1	BBNUM1	1	AFLA_100840	Pyridoxamine phosphate oxidase, putative	
29.1483	29.2058	29.0518	29.1471	29.0268	29.1167		9,81E-273	5,89E+09	12	12	12	50.4	39,182	29,1161	29,1353	29,0969	6	3	3	0.541457	0.0384343	BBNUP8	BBNUP8	2	AFLA_101010	Aspartate-semialdehyde dehydrogenase
26.4142	25.8031	28.5262	26.6828	25.8268	26.0658		4,79E-40	1,22E+09	8	8	8	30.3	29,222	26,5532	26,9145	26,1918	6	3	3	0.496967	0.7227	BBNUP9	BBNUP9	1	AFLA_101020	40S ribosomal protein S4
26.5326	26.1319	25.6851	25.7041	26.1677	26.6769		5,76E-10	6,47E+08	3	3	3	25.4	16,755	26,1497	26,1165	26,1829	6	3	3	0.867191	-0.0664183	BBNUQ4	BBNUQ4	1	AFLA_101070	Sorting nexin Snx3, putative
26.2245	25.5672	24.9172	24.8906	25.0744	25.3545		4,48E-10	4,11E+08	3	3	3	15.2	40,121	25,3381	25,5696	25,1065	6	3	3	0.312166	0.463135	BBNUQ7	BBNUQ7	1	AFLA_101100	RRM domain protein
26.0333	26.3263	29.3204	24.9988	23.6411	24.2396		1,16E-110	1,01E+09	6	6	6	43.7	18,044	25,7599	27,2267	24,2931	6	3	3	0.05904	2,9353	BBNUR2	BBNUR2	1	AFLA_101150	60S ribosomal protein L21, putative
24.4268	25.4288	27.7558	24.878	24.6196	24.6519		8,77E-122	1,24E+09	8	8	8	32.1	22,173	25,2935	25,8705	24,7165	6	3	3	0.308286	1,15396	BBNUR3	BBNUR3	1	AFLA_101160	40S ribosomal protein S9
NaN	24.6794	24.8811	24.7342	24.7133	24.9657		9,01E-09	3,5E+08	3	3	3	17.8	32,364	24,7947	24,7802	24,8004	5	2	2	0.862973	-0.0241642	BBNUR5	BBNUR5	1	AFLA_101190	Uncharacterized protein
24.816	25.4521	24.7953	24.2388	24.8552	24.3424		1,90E-16	2,59E+08	5	5	5	12.6	58,533	24,7469	25,0211	24,4724	6	3	3	0.13081	0.548477	BBNTV0	BBNTV0	1	AFLA_101210	Septin
31.0839	30.3486	30.067	29.1636	29.5708	29.7497	+	0	7,72E+09	14	14	14	34	66,878	29,9973	30,4998	29,4947	6	3	3	0.045103	1,00511	BBNTV3	BBNTV3	1	AFLA_101240	Vacuolar carboxypeptidase Cps1, putative
27.4878	27.9073	27.8744	28.0823	28.2747	27.935		4,91E-48	2,7E+09	9	9	9	33.2	45,072	27,9269	27,7565	28,9773	6	3	3	0.110491	-0.340803	BBNTV8	BBNTV8	1	AFLA_101290	FAD binding domain protein
29.6944	28.7581	28.1947	29.2503	29.9106	29.9464		0	1,14E+10	24	24	24	54.6	70,783	29,2924	28,8824	24,3024	6	3	3	0.171201	-0.820031	BBNUO7	BBNUO7	1	AFLA_101780	NADH-cytochrome B5 reductase, putative
24.1839	24.4152	22.1021	23.855	24.5521	24.6501		9,00E-181	1,53E+09	7	7	7	31	38,786	23,9537	23,5671	24,7043	6	3	3	0.375142	-0.7323	BBNU27	BBNU27	1	AFLA_101980	Tartrate dehydrogenase, putative
25.5785	25.5915	24.3975	25.8655	26.5577	26.5576		2,75E-20	5,19E+08	7	7	7	22	47,628	25,7577	25,1891	26,2863	6	3	3	0.068013	-1,13713	BBNU30	BBNU30	1	AFLA_102010	Class V chitinase, putative
26.0587	26.3541	26.0918	26.4948	27.3311	27.4324		2,07E-31	1,11E+09	11	11	11	28.8	68,621	26,7271	26,8682	27,0861	6	3	3	0.101781	-0.717894	BBNU30	BBNU30	1	AFLA_102340	Oligo-1,5-glucosidase
27.9282	27.9447	27.044	27.1859	27.5649	27.7845		5,76E-112	1,73E+09	13	13	13	36.2	63,638	27,4704	27,7229	29,5113	6	3	3	0.808773	0.0827764	BBNUU5	BBNUU5	1	AFLA_102390	Uncharacterized protein
26.5327	26.3195	26.0096	25.6905	26.9343	26.2716		3,10E-45	8,3E+08	7	7	7	17.2	72,541	26,1264	26,2873	25,9655	6	3	3	0.228398	0.318122	BBNUZ1	BBNUZ1	1	AFLA_102850	Rho GTPase activator (Rgd1), putative
NaN	24.0621	26.1543	26.9519	25.0827	24.6013		2,34E-56	9,04E+08	4	4	4	40.7	13,011	25,3075	25,1082	25,5453	5	2	2	0.741889	-0.437121	BBNUZ4	BBNUZ4	1	AFLA_102880	Translational initiation factor SUI1, putative
27.7953	27.8751	27.8406	28.3568	28.0889	28.1956	+	2,02E-95	2,22E+09	5	5	5	44.1	15,474	28,0254	27,837	28,2138	6	3	3	0.099751	-0.376769	BBNV07	BBNV07	1	AFLA_103010	dsDNA-binding protein PDCDS, putative
25.5386	NaN	24.2552	NaN	24.8377	24.97		4,39E-07	2,17E+08	3	3	3	7.2	59,719	24,9004	24,8869	24,9038	6	2	2	0.952379	-0.0069532	BBNV09	BBNV09	1	AFLA_103030	Pre-mRNA splicing factor, putative
30.3972	30.0284	29.7014	29.3137	29.8662	29.9658		5,24E-278	1,01E+10	34	34	34	44.1	127,63	29,8788	30,0423	29,7152	6	3	3	0.315856	-0.327099	BBNV28	BBNV28	1	AFLA_103220	Cytoskeleton assembly control protein Sla2, putative
NaN	23.8758	24.4995	24.3528	NaN	NaN		1,31E-17	2,11E+08	6	6	6	11.9	69,182	24,2427	24,1877	24,3528	3	2	1	1	-0.165137	BBNV31	BBNV31	1	AFLA_103250	Proteasome regulatory particle subunit (RpNc), putative
27.8753	27.8229	NaN	27.2172	28.0678	27.5739		1,46E-18	1,69E+09	3	3	3	15.1	18,155	27,7114	27,8491	27,6196	5	2	2	0.523891	0.229441	BBNV35	BBNV35	1	AFLA_103290	Histone H1
28.8832	28.8876	28.4205	28.4665	28.7293	28.7163		9,84E-65	3,99E+09	3	3	3	10.5	58,197	28,6839	28,7305	28,6394	6	3	3	0.6267	0.0931034	BBNV39	BBNV39	1	AFLA_103330	Glutaryl-CoA dehydrogenase, putative
29.201	29.1605	28.8364	28.6245	28.6666	28.8946		0	5,94E+09	16	16	16	37.1	74,988	28,8973	2											

Supplementary Table S2. Data on proteins obtained from label-free proteomics from *Aspergillus flavus* grown in presence of 0.1 M CaCl₂ treated with 10 µg/ml PgAFP and untreated control.

LFQ intensity AF_CaCl ₂ PgAFP_1	LFQ intensity AF_CaCl ₂ PgAFP_2	LFQ intensity AF_CaCl ₂ PgAFP_3	LFQ intensity AF_CaCl ₂ Control_1	LFQ intensity AF_CaCl ₂ Control_2	LFQ intensity AF_CaCl ₂ Control_3	t-test Significant	PEP	Intensity	Peptides	Razor + unique peptides	Unique peptides	Sequence coverage [%]	Mol. weight [kDa]	Mean	Mean AF_CaCl ₂ PgAFP	Mean AF_CaCl ₂ Control	Valid values	Valid values AF_CaCl ₂ PgAFP	Valid values AF_CaCl ₂ Control	t-test p value	t-test Difference	Protein IDs	Majority protein IDs	Proteins	Gene Names	Protein names			
26.274	26.182	25.971	25.972	25.803	26.039		8,28E-14	7,81E+08	5	5	5	15.8	56,376	26,0081	26,1218	25,8945	6	3	3	0.114763	0.227301	B8N8E2	B8N8E2	1	1	1	AF_L107360	Pre-m-RNA splicing factor, putative	
26.859	28.5918	27.9289	28.2286	28.3803	28.2884		1,23E-94	3,3E+09	9	9	9	26.9	45,682	28,3795	28,4599	28,2991	6	3	3	0.596522	0.160792	B8N8E4	B8N8E4	1	1	1	AF_L107380	PWWP domain protein	
26.127	24.9243	20.8687	26.4911	25.3076	24.8231		1,68E-57	4,86E+08	6	6	6	4.7	172.52	25,4222	25,3038	25,4062	6	3	3	0.731835	-0.236831	B8N8F0	B8N8F0	1	1	1	AF_L107440	Cytoskeleton assembly control protein Sla1, putative	
NaN	NaN	NaN	NaN	23.1509	23.2382		9,47E-07	556,11000	2	2	2	10.6	33,212	23,1945	23,1945	2	0	2	1	NaN	B8N8F1	B8N8F1	1	1	1	AF_L107450	Pirin, putative		
NaN	23.3384	23.9758	NaN	NaN	NaN		3,74E-08	1,7E+08	4	4	4	15.6	41,918	23,6571	23,6571	NaN	2	2	0	1	NaN	B8N8G5	B8N8G5	1	1	1	AF_L107590	3-methyl-2-oxobutanoate dehydrogenase, putative	
24.4592	NaN	25.3271	NaN	24.1185	24.2998		4,77E-13	4,77E+08	6	6	6	10.8	85,746	24,5511	24,8931	24,2092	4	2	2	0.268282	0.683983	B8N8I6	B8N8I6	1	1	1	AF_L107800	Exo-beta-1,3-glucanase, putative	
31.3867	31.0641	30.8687	30.2682	30.3513	30.7671		3,46E-217	2,2E+10	4	4	4	48.8	13,13	30,7844	31,1065	30,4622	6	3	3	0.040581	0.644332	B8N8I7	B8N8I7	1	1	1	AF_L107810	Heterogeneous nuclear ribonucleoprotein G, putative	
25.2559	25,7218	25,6985	25,8544	26,155	26,2429		1,17E-32	1,22E+09	8	8	8	17.6	64,958	25,8214	25,5587	26,0841	6	3	3	0.051997	-0.525368	B8N8J0	B8N8J0	1	1	1	AF_L107840	AMP dependent CoA ligase, putative	
29.157	30.6337	31.1528	31.4335	30.8136	30.5071		0	2,63E+10	21	21	21	57.1	46,804	30,6163	30,3145	30,9181	6	3	3	0.102627	-0.603546	B8N8L6	B8N8L6	1	1	1	AF_L108100	Argininosuccinate synthase	
29.4936	29,3376	29,047	28,7221	28,7954	28,9274		6,60E-298	6,78E+09	9	9	9	65.3	26,615	29,0539	29,2927	28,815	6	3	3	0.029441	0.477738	B8N8N3	B8N8N3	1	1	1	AF_L108270	Formyltetrahydrofolate deformylase, putative	
25.6011	25,0476	24,4188	24,9674	25,0899	24,9743		1,33E-10	3,14E+08	4	4	4	11.9	60,716	25,0165	25,0225	25,0106	6	3	3	0.973936	0.0119476	B8N8P1	B8N8P1	1	1	1	AF_L108350	Alpha/beta hydrolase, putative	
NaN	NaN	NaN	NaN	25.3324	24.9761		9,07E-77	2,12E+08	4	4	4	11.4	75.17	25,1543	NaN	25,1543	2	0	2	1	NaN	B8N8P3	B8N8P3	1	1	1	AF_L108370	Tyrosinase, putative	
27.827	27,0718	26,5908	26,9325	27,2586	27,3668		2,09E-89	1,1E+09	9	9	9	37.6	44,286	27,1746	27,1632	27,186	6	3	3	0.955438	-0.0227566	B8N8P6	B8N8P6	1	1	1	AF_L108410	Dipeptidase [EC 3.4.13.19]	
NaN	24.6491	24.0375	24.9699	NaN	24.951		7,22E-12	2,69E+08	3	3	3	16.2	24,284	24,6519	24,3423	24,9605	4	2	2	0.181149	-0.617185	B8N8P7	B8N8P7	1	1	1	AF_L108420	NUDX domain protein	
24.8348	25,0625	24,7836	NaN	24,5571	NaN		1,70E-11	2,92E+08	5	5	5	15.8	43.37	24,8095	24,8936	24,5571	4	3	1	1	1	3,86489	B8N8Q0	B8N8Q0	1	1	1	AF_L108450	Serine/threonine-protein phosphatase [EC 3.1.3.16]
25.4934	24,0637	NaN	NaN	23,6436	23,5532		2,53E-09	8,8692000	3	3	3	7.3	44,699	24,1885	24,7786	23,5984	4	2	2	0.241187	0.1130189	B8N8Q9	B8N8Q9	1	1	1	AF_L108540	NADH oxidase, putative	
26.5992	26,4257	26,1638	25,8081	26,6232	26,9638		1,00E-19	1,28E+09	6	6	6	23.7	46,238	26,4306	26,3962	26,465	6	3	3	0.859835	-0.068802	B8N8S4	B8N8S4	1	1	1	AF_L108690	Uncharacterized protein	
29.1311	28,4463	27,6211	28,4511	29,2122	29,4178		4,77E-44	3,53E+09	4	4	4	59.8	11,573	28,7289	28,3995	29,0584	6	3	3	0.625848	-0.658889	B8N8S9	B8N8S9	1	1	1	AF_L108740	Uncharacterized protein	
31.7663	31,1153	30,6546	31,1758	31,4372	31,6705		0	4,35E+10	28	28	28	74.8	53,981	31,3033	31,1787	31,4278	6	3	3	0.519028	-0.249092	B8N8T4	B8N8T4	1	1	1	AF_L108790	Aldehyde dehydrogenase AldA, putative	
24.681	24,4606	26,224	24,1837	24,1363	24,1363		2,91E-07	2,19E+08	3	3	3	10.4	51,844	24,7371	25,1218	24,16	5	3	2	0.271929	0.961846	B8N8U1	B8N8U1	1	1	1	AF_L108860	1,3-beta-glucanosyltransferase [EC 2.4.1.-]	
25.1399	23,9849	NaN	NaN	23,5727	23,8766		1,22E-10	3,23E+08	5	5	5	35.4	18,668	24,0358	24,5624	23,6848	5	2	2	0.145063	-0.275118	B8N8U3	B8N8U3	1	1	1	AF_L108880	Mitochondrial import receptor subunit (Tom20), putative	
25.5507	25,7206	NaN	27,7446	27,9553	28,0361		9,14E-136	1,9E+09	13	13	13	45.8	51,072	27,0015	25,6356	27,9142	2	0	2	0.000395	8.76335	B8N8U9	B8N8U9	1	1	1	AF_L108950	Histidine acid phosphatase, putative	
28.9674	27,8194	27,855	26,9918	27,6431	27,6815		8,99E-181	4,2E+09	41	40	40	21.5	27,952	27,8264	28,2139	27,4388	6	3	3	0.15171	0.775109	B8N8V0	B8N8V0	1	1	1	AF_L108960	Bi/bifunctional pyrimidine biosynthesis protein (PyrABC1), putative	
27.5284	27,2313	27,4641	27,5264	27,7589	27,6726		5,94E-127	2,76E+09	11	11	11	50.6	35,179	27,5303	27,4079	27,6526	6	3	3	0.906682	-0.244708	B8N8X0	B8N8X0	1	1	1	AF_L109160	isopenicillin-diphosphate delta-isomerase	
26.2706	26,5718	25,9198	26,4577	26,6371	26,6461		3,92E-13	8,42E+08	5	5	5	23.2	28,801	26,4172	26,254	26,5803	6	3	3	0.174967	-0.326258	B8N8X3	B8N8X3	1	1	1	AF_L109190	Possible replication factor-a protein	
28.3266	27,7794	27,1414	27,7963	27,9173	28,005		1,19E-113	1,88E+09	11	11	11	37.2	39,317	27,8277	27,7491	27,9602	6	3	3	0.674934	-0.157064	B8N8Y6	B8N8Y6	1	1	1	AF_L109320	3-hydroxyisobutyrate dehydrogenase	
27.1255	26,0599	25,6039	24,7884	25,6728	25,3736		1,02E-64	1,03E+09	13	13	13	75.6	36,636	25,7707	26,2631	25,2783	6	3	3	0.131329	0.984849	B8N8Y9	B8N8Y9	1	1	1	AF_L109350	NADPH-cytochrome P450 reductase [EC 1.6.2.4]	
30.0422	29,6007	29,3016	29,5598	29,5024	29,615		0	7E+09	13	11	11	54.5	24,59	29,6036	29,6482	29,5591	6	3	3	0.703222	0.0890624	B8N9A0	B8N9A0	1	1	1	AF_L109860	Translation elongation factor eEF-1B gamma subunit, putative	
26.3981	26,2467	26,2989	26,5909	26,4696	26,5266		2,13E-17	8,8E+08	6	6	6	30.8	38,033	26,4218	26,3146	26,529	6	3	3	0.019247	-0.214437	B8N9A7	B8N9A7	1	1	1	AF_L109930	D-lactate dehydrogenase, putative	
23.8482	26,1151	25,589	NaN	NaN	NaN		5,58E-12	5,79E+000	5	5	5	19.3	41,531	24,7186	24,7186	NaN	2	2	0	1	NaN	B8N950	B8N950	1	1	1	AF_L109960	Uncharacterized protein	
27.2463	26,3479	25,7925	26,4383	27,1325	27,1558		4,26E-08	8,59E+08	6	6	6	25.3	27,489	26,5305	26,5313	6	3	3	0.77667	-0.20135	B8N951	B8N951	1	1	1	AF_L109990	SMAN1 protein like, putative		
28.4048	27,7417	27,9405	27,0921	27,517	27,6322		2,09E-90	2,01E+09	12	12	12	30.6	96,874	27,7213	28,0288	27,4138	6	3	3	0.074106	0.615036	B8N970	B8N970	1	1	1	AF_L110160	Probable dipeptidyl peptidase 4 [EC 3.4.14.5] (Dipeptidyl peptidase IV) (DppIV) (DppIV)	
26.0694	26,0514	26,7135	26,9402	27,3992	27,1502		1,71E-107	2,64E+09	24	24	24	48	69,276	26,7206	26,2781	27,1632	6	3	3	0.025551	-0.885099	B8N980	B8N980	1	1	1	AF_L110160	Flavin-binding protein oxoxygenase-like protein	
29.5629	29,8464	30,0474	30,2572	30,1484	30,1504		0	1,24E+10	22	22	22	68.4	50,261	30,0021	29,8189	30,1853	6	3	3	0.046396	-0.366435	B8N997	B8N997	2	2	2	AF_L110430	L-ornithine aminotransferase Car2, putative	
25.428	26,146	26,517	26,2763	26,8464	26,4596		3,77E-11	1,58E+09	14	14	14	33.1	67.5	26,2789	26,0303	26,5274	6	3	3	0.264976	-0.497084	B8N9A0	B8N9A0	1	1	1	AF_L110460	mRNA splicing protein (Pip39), putative	
25.9946	26,1703	25,9359	24,6189	23,2005	NaN		4,82E-24	4,43E+08	4	4	4	19.2	33,102	25,3841	26,0336	24,4097	5	3	2	0.002899	1.62391	B8N9A8	B8N9A8	1	1	1	AF_L110540	Uncharacterized protein	
33.4804	33,0954	32,7149	33,0522	33,225	33,3511		0	9,51E+10	48	48	48	57.8	106,78	33,1533	33,0969	33,2098	6	3	3	0.659127	-0.112907	B8N9A8	B8N9A8	1	1	1	AF_L110600	Aminopeptidase	
29.6682	29,2738	28,8321	29,0729	29,0752	29,2939		8,64E-267	6,44E+09	16	16	16	70.1	35,782	29,2027	29,258	29,1474	6												

Supplementary Table S2. Data on proteins obtained from label-free proteomics from *Aspergillus flavus* grown in presence of 0.1 M CaCl₂ treated with 10 µg/ml PgAFP and untreated control.

LQF intensity AF_CaCl ₂ PgAFP_1		LQF intensity AF_CaCl ₂ PgAFP_2		LQF intensity AF_CaCl ₂ Control_1		LQF intensity AF_CaCl ₂ Control_2		LQF intensity AF_CaCl ₂ Control_3		t-test Significant	PEP	Intensity	Peptides	Razor + unique peptides	Unique peptides	Sequence coverage [%]	Mol. weight [kDa]	Mean	AF_CaCl ₂ PgAFP	AF_CaCl ₂ Control	Valid values	Valid values AF_CaCl ₂ PgAFP	Valid values AF_CaCl ₂ Control	t-test p value	t-test Difference	Protein IDs	Majority protein IDs	Proteins	Gene Names	Protein names
24.9965	25.2946	24.9387	Na	Na	Na	Na	Na	Na	Na		2,92E-57	2,03E+08	8	6	6	8	34.1	30.478	25,0766	25,0766	Na	Na	0	1	Na	B8N9W4	B8N9W4	AFLA_112600	37S ribosomal protein S25, mitochondrial	
26.8763	26.4935	26.0478	26.1206	26.4775	26.5644	8,50E-26	9,82E+08	6	6	6	11	11	11	11	11	11	43.1	64.29	26.43	26.425	26.3875	6	3	0.772751	-0.088043	B8N9W7	B8N9W7	AFLA_112630	KH domain protein	
26.5836	27.5869	28.0201	28.0318	27.7075	27.318	1,91E-70	2,02E+09	11	11	11	49.17	49.17	49.17	35.221	27.5413	27.3969	27.6875	6	3	0.57426	-0.28886	B8N9W8	B8N9W8	AFLA_112640	Mitochondrial acetylactate synthase small subunit, putative					
29.0362	28.7629	28.3694	28.6502	28.8252	28.9282	1,46E-239	4,78E+09	12	12	12	47.8	40.452	28.7629	28.7228	28.8012	6	3	0.727775	-0.073609	B8N9X0	B8N9X0	AFLA_112660	Ornithine carbonyltransferase							
30.7046	30.4457	30.2753	30.6641	30.5957	30.716	0	1.67E+10	23	23	23	80.9	43.129	30.5669	30.4752	30.6586	6	3	0.22299	-0.183386	B8N9X6	B8N9X6	AFLA_112720	Diphosphomevalonate decarboxylase							
26.2702	25.3832	Na	Na	Na	25.5156	1.69E-13	2.34E+08	2	2	2	8.1	30.666	25.6881	25.8267	25.5495	4	2	0.596733	0.277205	B8N9X8	B8N9X8	AFLA_112740	SNARE domain protein							
23.3258	Na	Na	24.5429	24.4141	25.0399	1,05E-09	2,33E+08	4	4	4	12.8	51.872	24.3368	23.9443	24.6051	5	2	0.297836	-0.670722	B8N9Y3	B8N9Y3	AFLA_112790	Acyl-CoA thioester hydrolase, putative							
Na	21.8936	25.0861	26.0478	22.9643	22.5009	1,19E-11	1,32E+08	4	4	4	17.8	27.534	23.6986	23.4899	23.8377	5	2	0.863991	-0.347844	B8N9Z5	B8N9Z5	AFLA_112910	Uncharacterized protein							
26.9945	26.8059	26.6524	27.1739	27.0258	26.9503	4,41E-62	1,4E+09	10	10	10	39.5	34.894	26.9338	26.8176	27.05	6	3	0.12199	-0.232387	B8NA03	B8NA03	AFLA_112990	UBX domain protein, putative							
28.1751	27.2124	26.8065	26.2596	27.2401	27.4225	1,78E-28	1,44E+09	5	5	5	22.5	30.771	27.186	27.398	26.9741	6	3	0.478765	0.423977	B8NA04	B8NA04	AFLA_113000	Integral ER membrane protein Scs2, putative							
27.7207	28.2641	28.3872	28.2471	27.8763	27.9056	6,50E-122	3,86E+09	12	12	12	43.4	48.527	28.0568	28.124	28.0097	6	3	0.654557	0.114311	B8NA06	B8NA06	AFLA_113020	Methionine aminopeptidase 2-1 (MAP2-1) (MetAP 2-1) (EC 3.4.11.18) (Peptidase M)							
Na	24.0893	24.5601	Na	24.5776	24.1345	6,55E-25	5E+08	4	4	4	14.5	37.064	24.3379	24.3247	24.351	4	2	0.943061	-0.0263491	B8NA08	B8NA08	AFLA_113040	Outer mitochondrial membrane protein porin							
23.1852	24.8663	25.4849	24.2593	24.9196	25.0648	1,24E-75	1,17E+09	7	7	7	18.5	64.711	24.63	24.5121	24.7479	6	3	0.763	-0.235792	B8NA09	B8NA09	AFLA_113050	Asparagine synthetase Asn2, putative							
28.451	27.9236	27.3997	28.2045	28.47	28.5038	9,81E-60	2,7E+09	14	14	14	31.4	56.094	28.1588	27.9248	28.3928	6	3	0.214967	-0.468019	B8NA12	B8NA12	AFLA_113080	Coenzyme A synthetase, putative							
28.3902	27.8226	27.3431	28.1594	28.2779	28.3016	2,06E-16	2,94E+09	3	3	3	20.5	17.792	28.0491	27.852	28.2463	6	3	0.266765	-0.394232	B8NA13	B8NA13	AFLA_113090	Uncharacterized protein							
23.1857	22.5171	22.8478	Na	Na	28.2855	Na	2,68E-16	1,34E+08	4	4	4	11.2	46.831	22.8514	22.8502	22.855	4	3	1	-1	-0.004783	B8NA14	B8NA14	AFLA_113100	N-glycosyl-transferase					
31.9868	31.5682	31.1011	31.501	31.6268	31.7643	0	3.07E+10	12	12	12	33.9	41.463	31.5914	31.552	31.6307	6	3	0.782827	-0.078666	B8NA16	B8NA16	AFLA_113120	GPI-anchored cell wall organization protein Ecm33							
Na	23.8223	23.9259	28.8306	24.9193	24.2199	5,83E-05	1,92E+08	3	3	3	28.9	16.778	24.5436	23.8741	23.971	5	2	0.161455	-1.11587	B8NA21	B8NA21	AFLA_113170	Iron-sulfur cofactor synthesis protein (Isu1), putative							
Na	24.8352	25.3555	24.9782	23.2823	22.9658	9,96E-100	1,27E+09	16	16	16	30.3	95.646	24.2834	25.0954	23.7421	5	2	0.201324	1.35324	B8NA29	B8NA29	AFLA_113250	Ribonucleoside-diphosphate reductase (EC 1.17.4.1)							
35.1754	34.929	34.5838	34.6488	34.7049	34.8044	0	2.9E+11	28	28	28	81.7	49.333	34.8077	34.8961	34.7194	6	3	0.375838	0.176715	B8NA36	B8NA36	AFLA_113320	Glutamate dehydrogenase							
24.8045	24.375	Na	Na	Na	Na	7,79E-15	1,95E+08	5	5	5	7.7	81.936	24.5898	24.5898	Na	2	2	0	1	Na	B8NA76	B8NA76	AFLA_113720	Ribosome biogenesis (Nop4), putative						
26.8362	26.2017	25.9558	26.1619	26.4033	26.4925	3,17E-21	1,02E+09	6	6	6	56.2	13.708	26.3419	26.3312	26.3526	6	3	0.942895	-0.0213642	B8NA77	B8NA77	AFLA_113730	Progesterone binding protein, putative							
25.4463	25.6438	25.5175	24.7562	25.0039	24.802	+	1,43E-35	7,77E+08	4	4	4	17.5	39.67	25.195	25.5359	24.8541	6	3	0.002038	0.6818	B8NA82	B8NA82	AFLA_113780	Casein kinase II subunit beta (CKII beta)						
28.5669	28.7012	28.7975	28.8998	28.6853	28.5828	4,05E-300	3,47E+08	14	14	14	51.9	45.268	28.7056	28.6885	28.7261	6	3	0.781337	-0.034105	B8NA84	B8NA84	AFLA_113800	Branched-chain-amino-acid aminotransferase (EC 2.6.1.42)							
29.5724	29.1379	28.6532	29.1953	29.277	29.3936	0	6.53E+09	17	17	17	52.9	39.319	29.2049	29.1212	29.2886	6	3	0.570974	-0.16743	B8NA87	B8NA87	AFLA_113830	Dipeptidyl peptidase, putative							
25.4934	26.9445	27.3426	27.1868	26.9278	26.5676	4,57E-144	3,08E+09	11	11	11	45.6	34.16	26.7472	26.5935	26.9009	6	3	0.629874	-0.307472	B8NA93	B8NA93	AFLA_113890	Nuclear pore complex subunit (SEC13), putative							
Na	23.26	22.9379	22.9698	Na	23.0749	1,39E-08	1,13E+08	4	4	4	9.2	83.008	23.0606	23.0989	23.0223	4	2	0.695406	0.076106	B8NA96	B8NA96	AFLA_113920	Translation initiation regulator (Gcn20), putative							
Na	Na	Na	24.4964	24.4219	Na	1,41E-24	3,39E+08	8	8	8	11.7	97.024	24.4592	Na	24.4923	2	0	2	1	Na	B8NAA2	B8NAA2	AFLA_113980	Cyclin dependent kinase inhibitor Phc01, putative						
28.2482	28.0213	28.0706	27.9233	28.0441	28.1771	2,01E-92	2,61E+09	13	13	13	51.8	49.825	28.0808	28.1134	28.0482	6	3	0.552217	0.0651957	B8NAA9	B8NAA9	AFLA_114050	Phosphoethanolamine							
27.6522	27.1887	26.9857	27.2311	27.1566	27.308	2,71E-34	1,44E+09	3	3	3	32.1	15.135	27.2537	27.2755	27.2349	6	3	0.389759	0.0435823	B8NAT2	B8NAT2	AFLA_114440	L-PSF endoribonuclease family protein Brt1, putative							
Na	Na	Na	27.7379	Na	26.6547	8,11E-07	1,28E+08	3	3	3	18.6	35.878	27.2362	Na	27.3962	2	0	2	1	Na	B8NAT7	B8NAT7	AFLA_114490	Histidyl phosphatase						
27.2515	27.4169	27.5856	24.8322	26.5341	25.9757	+	5,04E-41	1,17E+08	8	8	8	21.4	61.89	26.5988	27.418	25.7787	6	3	0.032711	1.63836	B8NAY3	B8NAY3	AFLA_114750	Glutathyl-RNA(Gin) amidotransferase subunit A, putative						
26.7695	26.9001	27.0965	27.0509	27.0963	26.9785	1,92E-58	1,34E+09	8	8	8	36.7	43.147	26.982	26.922	27.0419	6	3	0.301111	-0.119855	B8NAY1	B8NAY1	AFLA_114820	Leucine aminopeptidase 1 (EC 3.4.11.-) (Leucyl aminopeptidase 1) (LAP1)							
25.259	25.2019	25.1251	25.1171	25.3029	25.0908	4,44E-12	4,29E+08	5	5	5	18.2	50.034	25.1828	25.1953	25.1703	6	3	0.761616	0.0250765	B8NAY7	B8NAY7	AFLA_114890	Queuine RNA-ribosyltransferase (EC 2.4.2.29)							
Na	23.7848	Na	23.5844	23.69	Na	6,95E-09	1,61E+08	3	3	3	9.9	37.175	23.6864	23.7848	23.6372	3	1	2	1	0.145777	B8NAY8	B8NAY8	AFLA_114900	Thymidylate synthase						
Na	Na	25.2325	24.2473	23.9945	Na	2,33E-07	9,12E+08	5	5	5	5.1	158.06	24.4914	25.2325	24.1209	3	1	2	1	1.11166	B8NAY7	B8NAY7	AFLA_114990	DEAD helicase superfamily protein (Aqaurius), putative						
30.4012	30.9258	31.5159	27.7354	26.4745	26.7871	+	0.29E+09	15	15	15	47.3	25.677	28.9733	30.9476	26.999	6	3	0.001363	3.94864	B8NAY9	B8NAY9	AFLA_115110	60S ribosomal protein L13							
28.7274	29.0087	29.5851	29.7783	29.9497	29.3543	0	1.1E+10	21	21	21	54.8	53.189	29.3081	29.0701	29.5991	6	3	0.329597	-0.402026	B8NZ05	B8NZ05	AFLA_115170	Succinyl-CoA ligase subunit beta (EC 6.2.1.-)							
26.0215	27.508	28.1645	28.0416	27.684	27.1441	7,42E-149	3,9E+09	11	11	11	74.2	22.939	27.4273	27.2313	27.6032	6	3	0.598106	-0.201291	B8NZ08	B8NZ08	AFLA_115200	Xanthine-guanine phosphoribosyltransferase Xpt1, putative							
27.0006	25.7875	26.0523	25.853	25.5204	26.6896	2,93E-58	8,67E+08	10	10	10	32.1	43.417	25.9839	26.2801	25.6877	6	3	0.194515	0.59245	B8NZ22	B8NZ22	AFLA_115340	Proteasome regulatory particle subunit Rpt6, putative							
29.1468	28.833	28.4502	28.6582	28.6016	28.8526	1,17E-105	4,52E+09	12	12	12	49.0	55.471	28.7526	28.81	28.6951	6	3	0.167335	0.114842	B8NZ30	B8NZ30	AFLA_115420	Ran exchange factor Prp20/Pim1, putative							
28.7562	28.4687	29.2016	29.3492	28.9151	28.8554	0	7.29E+09	11	11	11	80.1	16.359	28.9244	28.8088	28.0399	6	3	0.430772	-0.231064	B8NXA7	B8NXA7	AFLA_115930	Uncharacterized protein							
24.7666	25.2187	24.8516	24.4483	24.9989	25.1575	3,05E-16	4,28E+08	2	2	2	8	41.753	24.9069	24.9457	24.8696	6	3	0.777173	0.0774409	B8NV1	B8NV1	AFLA_116780	Homocysteine S-methyltransferase, putative							
28.348	28.1034	27.5894	27.5866	27.5259	27.7031	3,20E-165	2,11E+09	12	12	12	52	30.155	27.8094	28.0136	26.6032	6	3	0.14981	0.408397	B8NVM0	B8NVM0	AFLA_117070	Keich repeat protein							
25.5776	25.4587	25.6285	25.4707	25.4538	25.3751	5,15E-10	4,74E+08	5	5	5	29.1	23.51	25.4941	25.555	25.4752	6	3	0.105011	0.121745	B8NVN9	B8NVN9	AFLA_117260	N-acetyltransferase, GNAT family, putative							
23.7553	Na	28.4655	Na	Na	Na																									

Supplementary Table S2. Data on proteins obtained from label-free proteomics from *Aspergillus flavus* grown in presence of 0.1 M CaCl₂ treated with 10 µg/ml PgAFP and untreated control.

LFQ intensity AF_CaCl ₂ PgAFP_1	LFQ intensity AF_CaCl ₂ PgAFP_2	LFQ intensity AF_CaCl ₂ PgAFP_3	LFQ intensity AF_CaCl ₂ Control_1	LFQ intensity AF_CaCl ₂ Control_2	LFQ intensity AF_CaCl ₂ Control_3	t-test Significant	PEP	Intensity	Peptides	Razor + unique peptides	Unique peptides	Sequence coverage [%]	Mol. weight [kDa]	Mean	Mean AF_CaCl ₂ PgAFP_3	Mean AF_CaCl ₂ Control	Valid values	Valid values AF_CaCl ₂ PgAFP	Valid values AF_CaCl ₂ Control	t-test p value	t-test Difference	Protein IDs	Majority protein IDs	Proteins	Gene Names	Protein names
27.3577	26.6759	26.0462	26.7907	27.4483	27.3189		7,28E-225	5,66E+09	7	7	7	20.6	45,559	26,936	26,693	27,186	6	3	3	0.31461	-0,4928787	BBNW79	BBNW79	1	AFLA_121260	Aspartic-type endopeptidase, putative
26.1533	24,6347	24,691	24,2854	24,1438	24,3869		1,85E-06	2,6E+08	3	3	3	10.2	31,025	24,7609	25,197	24,362	6	3	3	0.184915	0,797766	BBNWV7	BBNWV7	1	AFLA_121440	Fumarylacetoacetate hydrolase, putative
23.6358	Na	Na	22,959	Na	Na		5,25E-06	76535000	2	2	2	5.4	51,017	23,2974	23,294	Na	2	2	0	1	Na	BBNX26, BBNX26, BBNX26	2	AFLA_122130	Mannan endo-1,6-alpha-mannosidase CW1, putative	
24.1106	Na	Na	25,0047	Na	Na		1,99E-09	1,62E+08	3	3	3	4.9	83,122	24,5576	24,5576	24,362	2	2	0	1	Na	BBNX31	BBNX31	1	AFLA_122180	Uncharacterized protein
24.8067	24,6661	24,4605	24,8057	25,475	25,5106		1,02E-158	9,04E+08	10	10	10	24.7	65,47	24,9541	24,6444	24,2637	6	3	3	0.068659	-0,619323	BBNX52	BBNX52	1	AFLA_122400	Glucoamylase (EC 3.2.1.3) (1,4-alpha-D-glucan glucosylase) (Glucan 1,4-alpha-glucosidase)
26.8359	26,2061	Na	24,2495	23,5217	23,7787		1,65E-25	5,04E+08	8	8	8	16.2	63,696	24,9184	26,521	23,8499	5	2	3	0.005131	2,67109	BBNX59	BBNX59	1	AFLA_122470	CobW domain protein
25.5786	25,6045	25,3675	25,5417	25,8452	25,7321		8,32E-38	4,71E+08	4	4	4	39.7	21,287	25,6116	25,5169	25,7064	6	3	3	0.177945	-0,189497	BBNX71	BBNX71	1	AFLA_122590	Translation machinery-associated protein 22
25.8826	24,7669	24,7788	24,8022	25,0366	25,3632		3,16E-18	2,78E+08	4	4	4	38.9	21,849	25,105	25,1428	25,0673	6	3	3	0.861018	0,0754286	BBNX75	BBNX75	1	AFLA_122630	Cytidine deaminase, putative
28.3525	28,5352	28,1793	28,6338	28,4633	28,6343		2,53E-142	3,84E+09	15	15	15	45.4	56,078	28,4664	28,3556	28,5771	6	3	3	0.132406	-0,221495	BBNX84	BBNX84	1	AFLA_122720	Actin binding protein, putative
25.3948	24,7556	24,8642	22,855	23,669	23,1142		2,68E-05	1,55E+08	2	2	2	3.9	65,705	20,584	25,0049	23,112	6	3	3	0.001551	1,89284	BBNX82	BBNX82	1	AFLA_123160	Lactase, putative
26.4784	26,3935	26,148	25,6622	26,7777	25,7443		7,51E-88	1,49E+09	8	8	8	35.5	23,667	26,1006	26,344	25,8612	6	3	3	0.063504	0,478764	BBNX82	BBNX82	1	AFLA_124380	Uncharacterized protein
29.3796	28,6452	28,5507	24,08	Na	24,1384		5,88E-146	1,28E+09	9	9	9	24	74,712	26,9568	28,8585	24,1042	5	3	2	0.000783	4,75425	BBNMK6	BBNMK6	1	AFLA_124420	Amine oxidase, putative
24.6696	24,2241	24,2347	24,4133	24,8066	24,7768		2,76E-32	4,72E+08	4	4	4	25.8	33,215	24,5252	24,3849	24,6656	6	3	3	0.234147	-0,280616	BBNMM0	BBNMM0	1	AFLA_124560	Uncharacterized protein
Na	Na	Na	Na	Na	25,9783		5,20E-32	4,36E+08	5	5	5	31.5	34,069	26,0075	Na	26,0075	2	0	2	1	Na	BBNM48	BBNM48	2	AFLA_124820	Uncharacterized protein
Na	Na	26,8129	28,3775	26,7566	25,7482	26,7665		0,456E+09	8	8	8	52.5	16,407	26,8923	27,5952	26,4238	5	2	3	0.20603	1,17139	BBNMV3	BBNMV3	1	AFLA_125890	40S ribosomal protein S17, putative
Na	Na	Na	24,1066	25,0915	25,0173	Na		2,30E-22	5,94E+08	9	9	33.2	32,784	24,7385	24,1066	25,0544	3	1	2	1	Na	BBNM6	BBNM6	1	AFLA_126390	Oxidoreductase 2-nitroparaoxybenzoyl-CoA oxidase family, putative
26.7842	26,278	25,9903	26,8788	26,9828	26,569		2,36E-90	1,43E+09	8	8	8	38.1	32,663	26,5805	26,3508	26,8102	6	3	3	0.155913	-0,459361	BBNMQ3	BBNMQ3	1	AFLA_126660	Ankyrin repeat protein
26.3356	26,5719	25,8809	26,3214	26,5567	26,5062		1,07E-83	1,31E+09	6	6	6	50.3	19,467	26,3621	26,2628	26,4614	6	3	3	0.407794	-0,198659	BBNMQ4	BBNMQ4	1	AFLA_126670	Uncharacterized protein
25.9268	24,6118	25,314	25,4499	25,8856	25,6587		1,29E-73	8,11E+08	9	9	9	19.9	59,701	25,4745	25,2842	26,6647	6	3	3	0.395541	-0,380517	BBNMQ5	BBNMQ5	1	AFLA_126680	WD repeat-containing protein, putative
26.3042	26,013	25,3187	25,7572	26,3528	25,9932		7,58E-55	1,21E+09	5	5	5	23.5	33,303	25,9565	25,8786	26,0344	6	3	3	0.670323	-0,155807	BBNMQ6	BBNMQ6	1	AFLA_126690	Uncharacterized protein
25.08	24,6787	26,2837	27,4691	25,4898	25,4474		9,55E-36	1,21E+09	6	6	6	48.3	18,988	25,7415	25,3475	26,1354	6	3	3	0.392597	-0,787934	BBNMR6	BBNMR6	1	AFLA_126790	Threonine synthase Thr4, putative
24.856	25,0297	24,4364	24,7395	25,182	24,9772		6,17E-42	7,65E+08	12	12	12	27.6	74,726	24,8701	24,774	24,9662	6	3	3	0.427052	-0,1922	BBNMS3	BBNMS3	1	AFLA_126860	Cell wall cysteine-rich protein
27.8503	27,4645	27,2134	27,4616	27,4417	27,587		6,32E-24	2,21E+09	3	3	3	35.2	11,497	27,5031	27,5094	27,4968	6	3	3	0.950468	0,0126082	BBNMS5	BBNMS5	1	AFLA_126880	Peptidyl-prolyl cis-trans isomerase
23.276	24	25,3599	24,9002	24,4187	24,8051		2,15E-58	5,39E+08	5	5	5	32.5	21,151	24,4519	24,1957	24,7068	6	3	3	0.468585	-0,152241	BBNMV8	BBNMV8	1	AFLA_127210	Pathogenesis associated protein Cap20, putative
28.1488	29,5291	30,38	27,485	26,6826	26,7169		2,17E-105	5,04E+09	8	8	8	47.4	15,612	28,1571	29,3526	26,9615	6	3	3	0.026987	2,39116	BBNMV9	BBNMV9	1	AFLA_127220	60S ribosomal protein L27
25.5382	26,5351	26,7225	26,382	26,2027	26,7169		5,63E-19	1,3E+09	5	5	5	14.7	42,33	26,4918	26,2819	26,7017	6	3	3	0.65812	-0,419794	BBNBS5	BBNBS5	1	AFLA_127260	Cop9 signalosome complex subunit, putative
24.5615	23,7928	23,4176	23,09	23,5498	23,7757		0,000010	1,02E+08	2	2	2	3.8	49,076	23,6979	23,924	23,4718	6	3	3	0.31344	0,452188	BBNCC0	BBNCC0	1	AFLA_127310	CAIB/BAIF family enzyme
27.3286	27,3577	27,139	27,4774	27,3321	27,3446		4,96E-60	1,88E+09	5	5	5	35.2	25,024	27,3299	27,2751	27,3847	6	3	3	0.256469	-0,109858	BBNCC1	BBNCC1	1	AFLA_127320	Riboflavin synthase, alpha subunit
27.0701	28,0084	29,2748	29,4736	28,59	27,9896		6,98E-171	4,72E+09	16	16	16	42.4	58,657	28,4011	28,1178	28,6844	6	3	3	0.502924	-0,566637	BBNCC4	BBNCC4	1	AFLA_127350	N-acetylglucosamine-phosphate mutase
27.3016	27,4966	27,6713	27,7185	27,677	27,5652		9,02E-62	3,22E+09	12	12	12	48.5	38,926	27,5705	27,4899	27,6512	6	3	3	0.236403	-0,161386	BBNCC5	BBNCC5	1	AFLA_127370	Histone H4 arginine methyltransferase RmtA
25.013	24,2791	25,2197	24,8621	25,0854	25,3901		1,12E-21	4,06E+08	6	6	6	19.3	53,465	24,307	24,8961	24,6553	6	3	3	0.666534	0,021985	BBNCC8	BBNCC8	1	AFLA_127390	Proteasome regulatory particle subunit Rpt5, putative
Na	23,8342	23,2648	Na	24,1101	24,4549		1,06E-07	1,11E+08	2	2	2	2.3	122,38	23,916	23,8495	24,2825	4	3	2	0.158543	0,732967	BBND9	BBND9	1	AFLA_127500	Cytochrome P450, putative
Na	Na	Na	Na	Na	27,6342		3,18E-09	8,43E+08	3	3	3	14.1	31,401	27,5852	Na	27,5852	2	0	2	1	Na	BBNNE2	BBNNE2	1	AFLA_127530	BCAS2 family protein
26.1584	26,2865	26,178	24,0663	24,0835	Na		3,27E-28	3,86E+08	5	5	5	17.8	52,303	25,3545	26,2076	24,0749	5	3	2	1.16E-05	2,13272	BBNNE9	BBNNE9	1	AFLA_127600	40S ribosomal protein S2, putative
25.8202	25,2511	25,2158	26,0074	25,4183	25,4266		5,49E-19	4,84E+08	8	8	8	16.5	69,73	25,5232	25,429	25,6174	6	3	3	0.532857	-0,188407	BBNNE9	BBNNE9	1	AFLA_127700	VHS domain protein
25.3022	25,6068	25,6687	25,2563	25,5582	25,3121		7,82E-30	5,58E+08	5	5	5	14.7	55,437	25,4507	25,5259	25,3755	6	3	3	0.362359	0,150392	BBNG1	BBNG1	1	AFLA_127720	CBS domain protein
27.5207	26,6648	Na	25,9951	26,9492	26,9238		2,41E-28	9,91E+08	4	4	4	14.5	44,199	26,8107	27,0928	26,6227	5	2	3	0.429221	0,470072	BBNG3	BBNG3	1	AFLA_127740	Metacaspase CasA
23.8058	24,2053	24,6083	23,8555	24,048	23,9491		1,93E-43	8,3E+08	9	9	9	21.8	61,088	24,0787	24,2065	26,9509	6	3	3	0.343778	0,255599	BBNG4	BBNG4	1	AFLA_127750	T-complex protein 1, eta subunit, putative
Na	23,5398	28,0684	26,6398	Na	Na		1,05E-09	4,67E+08	3	3	3	24.5	16,505	26,0826	25,8041	26,3938	3	2	1	1	-0,835684	BBNG6	BBNG6	1	AFLA_127800	40S ribosomal protein S26
25.3942	26,41	26,8307	27,063	27,479	26,9438		4,14E-58	1,3E+09	20	20	20	25.5	121,58	26,8668	26,2117	27,1619	6	3	3	0.105662	-0,950281	BBNH1	BBNH1	1	AFLA_1	

Supplementary Table S2. Data on proteins obtained from label-free proteomics from *Aspergillus flovus* grown in presence of 0.1 M CaCl₂ treated with 10 µg/ml PgAFP and untreated control.

LFQ intensity AF_CaCl ₂ PgAFP_1	LFQ intensity AF_CaCl ₂ PgAFP_2	LFQ intensity AF_CaCl ₂ PgAFP_3	LFQ intensity AF_CaCl ₂ Control_1	LFQ intensity AF_CaCl ₂ Control_2	LFQ intensity AF_CaCl ₂ Control_3	t-test Significant	PEP	Intensity	Peptides	Razor + unique peptides	Unique peptides	Sequence coverage [%]	Mol. weight [kDa]	Mean	Mean AF_CaCl ₂ PgAFP	Mean AF_CaCl ₂ Control	Valid values	Valid values AF_CaCl ₂ PgAFP	Valid values AF_CaCl ₂ Control	t-test p value	t-test Difference	Protein IDs	Majority protein IDs	Proteins	Gene Names	Chromatin names	
26.91	26.7023	26.4182	26.6909	26.9519	27.0071		1,14E-45	1.41E+09	9	9	26	57	53.615	26.7801	26.6768	26.8833	6	3	3	0.29791	-0.206489	BBNPF6	BBNPF4	1	AFLA_130260	Chromatin remodeling and histone acetyltransferase complexes subunit	
32.2872	31.9449	31.471	31.6405	31.7157	31.8341		0	4.99E+10	28	28	28	62.5	56.397	31.8156	31.901	31.7301	6	3	3	0.520397	0.170941	BBNPF9	BBNPF9	1	AFLA_130310	Protein disulfide-isomerase (EC 5.3.4.1)	
25.7783	26.2814	26.4021	26.1147	26.6583	26.55		9.95E-33	9.01E+08	5	5	5	26.3	26.124	26.2975	26.1539	26.441	6	3	3	0.320158	-0.287039	BBNPF7	BBNPF7	1	AFLA_130390	Glutamine amidotransferase:cytase	
26.57	26.1909	25.6824	25.6469	25.6844	26.0824		9.95E-11	6.7E+08	3	3	3	9.9	42.125	25.9762	26.1478	25.8046	6	3	3	0.305696	0.343192	BBNPF6	BBNPF6	1	AFLA_130480	Replication protein A 70 kDa DNA-binding subunit	
25.3501	25.151	NaN	24.7553	25.5957	25.3815		1.50E-50	1.08E+09	10	10	10	25.1	73.215	25.2467	25.2505	25.2441	5	2	3	0.98589	0.064084	BBNPF7	BBNPF7	1	AFLA_130490	Ubiquitin carboxyl-terminal hydrolase (EC 3.4.19.12)	
26.2923	26.5734	26.5652	24.6066	24.8468	NaN		6.27E-88	5.95E+08	7	7	7	45.3	27.389	25.7765	26.4763	24.7267	5	3	2	0.001321	1.74962	BBNFL4	BBNFL4	1	AFLA_131050	Uncharacterized protein	
NaN	22.9375	22.624	NaN	22.277	NaN		0.00013	88960000	2	2	2	2	5.5	47.754	22.6128	22.7807	22.277	3	2	1	1	0.503738	BBNFL5	BBNFL5	1	AFLA_131060	14-alpha sterol demethylase Cyp51B
28.0342	27.7724	27.25	27.6905	27.7309	27.8604		1.53E-139	2.15E+09	17	17	17	14.4	160.35	27.723	27.6855	27.7606	6	3	3	0.766631	0.0750167	BBNFM7	BBNFM7	1	AFLA_131280	Actin cortical patch assembly protein Pan1, putative	
28.8124	29.3844	29.5525	29.2977	29.0265	28.9572		0	6.79E+09	10	10	10	33.7	50.769	29.1718	29.2498	29.0938	6	3	3	0.561959	0.155959	BBNFOY	BBNFOY	1	AFLA_131410	Eukaryotic translation initiation factor 3 subunit M (eIF3m)	
29.3405	29.1631	28.9811	29.2834	29.1077	29.3053		8.26E-124	5.43E+09	9	9	9	48.4	23.642	29.2125	29.1616	29.2635	6	3	3	0.400661	-0.101883	BBNFY1	BBNFY1	1	AFLA_131420	Uridylate kinase (UK) [EC 2.7.4.14] (ATP:UMP phosphotransferase) (Deoxycytidylate kinase) (Uridine monophosphate kinase)	
30.9681	30.85	30.5577	30.4349	30.602	30.669		0	1.66E+10	25	25	25	25.5	64.887	30.6803	30.7919	30.5686	6	3	3	0.18697	0.223321	BBNFY6	BBNFY6	1	AFLA_131470	Eukaryotic translation initiation factor 3 subunit D (eIF3d)	
27.8282	28.3502	28.2592	28.4897	28.0893	28.2083		2.81E-140	2.85E+09	18	18	18	40.2	72.33	28.2041	28.1459	28.2624	6	3	3	0.593394	-0.11655	BBNG06	BBNG06	1	AFLA_131670	Oxidoreductase, putative	
23.9386	24.1878	23.6001	23.546	23.247	23.1442		1.16E-10	3.28E+08	3	3	3	11.2	47.213	23.6106	23.9089	23.3124	6	3	3	0.045989	0.59643	BBNG30	BBNG30	1	AFLA_131910	Uncharacterized protein	
26.6988	26.3677	26.235	26.5657	26.4013	26.5715		3.85E-30	9.76E+08	9	9	9	54.3	28.925	26.4734	26.4339	26.5138	6	3	3	0.623593	-0.0789789	BBNG46	BBNG46	1	AFLA_132070	Uncharacterized protein	
27.0341	27.1637	26.5167	24.9593	26.1149	25.0284		5.42E-31	8.97E+08	9	9	9	58.6	28.548	26.1362	26.9048	25.3676	6	3	3	0.022109	1.53727	BBNG47	BBNG47	1	AFLA_132080	Small nuclear ribonucleoprotein U2, A	
26.9707	26.8937	26.6267	27.0774	27.0002	26.9743		2.49E-66	1.54E+09	9	9	9	42	37.926	26.9239	26.8304	27.0173	6	3	3	0.160602	-0.186975	BBNG53	BBNG53	1	AFLA_132140	Pantoate-beta-alanine ligase	
27.0615	26.4929	26.6246	26.3955	26.84	26.9184		2.63E-50	9.06E+08	13	11	11	34.9	54.821	26.7162	26.7263	26.7076	6	3	3	0.937835	0.020412	BBNG57	BBNG57	1	AFLA_132180	Aldehyde dehydrogenase ALDH	
26.4452	26.3823	25.7371	25.7499	25.8343	26.0267		1.01E-18	7.28E+08	4	4	4	15.7	36.36	26.0293	26.1882	25.8703	6	3	3	0.257015	0.317889	BBNG67	BBNG67	1	AFLA_132280	Thiamin pyrophosphokinase-related protein	
28.6185	28.2905	28.1627	28.5262	28.4839	28.4904		1.57E-68	3.61E+09	7	7	7	62.7	16.274	28.4287	28.3572	28.5002	6	3	3	0.353624	-0.142951	BBNH12	BBNH12	1	AFLA_132360	Gliaf factor natrium factor, putative	
27.9567	27.7653	27.6342	27.9201	28.0002	27.9735		5.68E-140	2.19E+09	9	9	9	55.7	36.758	27.875	27.7854	27.9646	6	3	3	0.136994	-0.179225	BBNH13	BBNH13	1	AFLA_132370	Molybdopterine binding domain protein	
29.2511	29.1733	29.2094	29.5111	29.2293	29.3786		9.65E-188	6.24E+09	11	11	11	10	35	33.833	29.2921	29.2113	29.3733	6	3	3	0.127988	-0.161762	BBNH15	BBNH15	1	AFLA_132390	Oxidoreductase, short chain dehydrogenase/reductase family
31.3042	30.9727	30.7508	30.7831	30.6371	30.7958		0	2.07E+10	6	6	6	65.5	12.024	30.8739	31.0092	30.7337	6	3	3	0.183889	0.270582	BBNH30	BBNH30	1	AFLA_132540	Thioredoxin	
29.9241	29.5076	29.4449	30.3042	30.1561	30.1796		3.65E-201	1.1E+10	10	10	10	64	22.19	29.9194	29.6255	30.1833	6	3	3	0.020155	-0.587762	BBNH38	BBNH38	1	AFLA_132620	Rho-gdp dissociation inhibitor	
NaN	24.9371	25.3131	25.9565	25.2117	25.0619		3.28E-13	3.77E+08	5	5	5	15.7	52.026	25.2961	25.1251	25.41	5	2	3	0.511448	-0.284988	BBNH39	BBNH39	1	AFLA_132630	APSES transcription factor, putative	
26.1106	25.8688	25.5877	25.3405	25.7635	25.6784		4.16E-27	5.58E+08	4	4	4	11.3	58.551	25.7249	25.8557	25.9462	5	2	3	0.258672	0.261517	BBNH40	BBNH40	1	AFLA_132640	mRNA cleavage and polyadenylation factor CLP1	
28.2907	28.0612	27.9553	28.052	28.1371	28.2666		1.14E-70	2.52E+09	11	11	11	49.4	35.675	28.1271	28.1024	28.1519	6	3	3	0.69423	0.0494703	BBNH43	BBNH43	1	AFLA_132670	Quinone oxidoreductase, putative	
25.1929	25.0399	NaN	24.3449	25.3307	26.6756		0.000131	4.61E+08	2	2	2	2.9	94.875	25.1168	25.1164	25.1571	5	2	3	0.939908	0.0006568	BBNH48	BBNH48	1	AFLA_132720	MYB DNA binding protein (Tb1), putative	
28.1427	27.0036	25.9984	29.9081	25.0248	25.2307		9.31E-35	5.54E+08	9	9	9	25.1	58.984	25.8877	27.0482	24.7272	6	3	3	0.035616	2.32103	BBNH51	BBNH51	1	AFLA_132750	Uncharacterized protein	
27.3932	27.774	27.5665	25.4835	25.2721	24.8319		1.14E-47	1.29E+09	14	14	14	41.6	46.429	26.3869	27.5779	25.1958	6	3	3	0.000422	2.3821	BBNH55	BBNH55	1	AFLA_132790	37S ribosomal protein S5	
26.9459	25.8944	NaN	NaN	24.9609	NaN		9.23E-17	3.34E+08	5	5	5	14.3	52.708	25.6302	25.9648	32.3609	6	2	3	1	1	0.00931	BBNH56	BBNH56	1	AFLA_132800	RNAiMS1/50 methyltransferase
27.6497	28.5263	28.9082	28.9663	28.8762	28.8535		9.88E-287	5.44E+09	17	17	17	61.4	47.205	28.63	28.3614	28.8986	6	3	3	0.224352	-0.537233	BBNH60	BBNH60	1	AFLA_132840	Arp2/3 complex subunit (Arp3), putative	
26.6013	26.7349	26.6602	26.7505	26.2551	26.2482		5.83E-57	1.2E+09	12	12	12	22.1	94.631	26.5417	26.6655	26.4179	6	3	3	0.220664	0.247553	BBNH66	BBNH66	1	AFLA_132900	Protein methyltransferase Rmc1	
24.6072	24.9451	25.0787	NaN	NaN	NaN		1.38E-12	1.94E+08	5	5	5	8	87.029	24.877	24.877	NaN	3	0	1	1	1	NaN	BBNH67	BBNH67	1	AFLA_132910	Pre-mRNA splicing factor RNA helicase (Prp43), putative
25.5321	25.1216	NaN	25.1515	25.0012	25.151		1.44E-16	4.62E+08	2	2	2	15.8	23.454	25.1915	25.3268	25.1012	5	2	3	0.267465	0.2256909	BBNH69	BBNH69	1	AFLA_132930	Secretory pathway protein Ssp120, putative	
24.7696	24.5169	24.2895	24.0439	24.402	24.4852		6.12E-12	2.26E+08	8	8	8	4.8	233.83	24.1178	24.5253	24.3104	6	3	3	0.295556	0.214954	BBNH76	BBNH76	1	AFLA_133000	Pre-mRNA splicing factor (Prp8), putative	
NaN	24.662	25.7913	27.4071	23.9408	NaN		4.88E-58	9.47E+08	2	2	2	17	20.117	25.3515	25.029	25.674	4	2	2	0.765826	-0.644972	BBNH79	BBNH79	1	AFLA_133030	Cytochrome c subunit Vb, putative	
26.7819	25.6843	NaN	25.5733	25.7734	25.8647		2.60E-26	5.89E+08	6	5	5	15.3	34.294	25.9355	26.2331	25.7371	5	2	3	0.326469	0.495972	BBNH86	BBNH86	1	AFLA_133100	Aldehyde reductase, putative	
30.1087	30.0109	29.7583	29.7294	29.7648	29.8821		0	1E+10	15	15	15	63	38.309	29.8757	29.9593	29.7921	6	3	3	0.167653	0.167217	BBNF00	BBNF00	1	AFLA_133290	KH domain RNA-binding protein	
29.1548	29.3356	29.9761	30.3734	29.9598	29.2777		0	8.71E+09	24	24	24	51.7	62.104	29.6189	29.4888	29.7949	6	3	3	0.560106	-0.260139	BBNF50	BBNF50	1	AFLA_133490	Aspartyl-tRNA synthetase Dps1,	

Supplementary Table S2. Data on proteins obtained from label-free proteomics from *Aspergillus flavus* grown in presence of 0.1 M CaCl₂ treated with 10 µg/ml PgAFP and untreated control.

A. Total data																											
LQF intensity AF_CaCl ₂ PgAFP_1	LQF intensity AF_CaCl ₂ PgAFP_2	LQF intensity AF_CaCl ₂ PgAFP_3	LQF intensity AF_CaCl ₂ Control_1	LQF intensity AF_CaCl ₂ Control_2	LQF intensity AF_CaCl ₂ Control_3	t-test Significant	PEP	Intensity	Peptides	Razor + unique peptides	Unique peptides	Sequence coverage [%]	Mol. weight [kDa]	Mean	Mean AF_CaCl ₂ PgAFP	Mean AF_CaCl ₂ Control	Valid values	Valid values AF_CaCl ₂ PgAFP	Valid values AF_CaCl ₂ Control	t-test p value	t-test Difference	Protein IDs	Majority protein IDs	Proteins	Gene Names	Protein names	
25,6284	26,3329	25,7872	24,6025	24,3853	24,2224	+	3,09E-08	5,13E+08	3	3	3	29.3	10,958	25,1598	25,9162	24,4034	6	3	3	0,003242	1,51276	B8NGG5	B8NGG5	1	AFLA_135920	Cytochrome c oxidase polypeptide vib	
24,4638	24,2991	24,207	25,4169	25,3645	24,7353	+	1,91E-10	2,77E+08	3	3	3	24.5	17,865	24,7478	24,3233	25,1722	6	3	3	0,021448	-0,848916	B8NGG8	B8NGG8	1	AFLA_135950	Nudix/MutT family protein	
25,084	25,4094	25,6609	25,8333	25,8358	25,8418			2,33E-28	4,43E+08	4	4	4	19.4	32,89	25,6109	25,3848	25,837	6	3	3	0,053686	-0,452181	B8NGH4	B8NGH4	1	AFLA_136010	Pyrimidine 5'-nucleotidase, putative
25,2236	25,1242	24,953	25,05	24,8133	24,6892			5,54E-21	2,77E+08	4	4	4	11.2	49,272	24,9755	25,1003	24,8508	6	3	3	0,132019	0,249445	B8NGI3	B8NGI3	1	AFLA_136100	GATA transcription factor (AreB), putative
25,0513	24,1358	24,5419	24,1539	24,4618	24,6004			3,80E-13	2,2E+08	3	3	3	6.4	57,774	24,4909	24,5763	24,4054	6	3	3	0,594412	0,170946	B8NGK6	B8NGK6	1	AFLA_136330	Exoenzymes regulatory protein aepA, putative
23,1724	23,8179	24,5234	24,7694	23,9748	23,7419			3,67E-20	1,87E+08	5	5	5	13	52,197	24	23,8379	24,162	6	3	3	0,55132	-0,324149	B8NGK7	B8NGK7	1	AFLA_136340	Aminotransferase family protein (LoIT), putative
26,689	26,7512	26,3499	26,8023	26,6688	26,7054			3,63E-27	1,13E+09	9	9	9	6.5	160,85	26,6611	26,5967	26,7255	6	3	3	0,380805	-0,128805	B8NGK9	B8NGK9	1	AFLA_136360	GYF domain protein
29,3131	29,3292	29,5011	29,4774	29,6353	29,6011			0	7,8E+09	24	24	21	51	77,75	29,4762	29,3811	29,5713	6	3	3	0,068825	-0,190144	B8NGL5;B8NGL6	B8NGL5	2	AFLA_136420	Bifunctional tryptophan synthase TRP8
25,1109	26,6838	27,1063	26,2864	26,7392	26,1462			1,12E-84	1,79E+09	14	14	14	41.9	56,675	26,3455	26,3003	26,3906	6	3	3	0,89345	-0,0902964	B8NGL6	B8NGL6	1	AFLA_136430	V-type ATPase, B subunit, putative
24,2724	23,9539	23,894	NaN	NaN	24,2325			0,000195	1,74E+08	2	2	2	8	37,374	24,0882	24,0401	24,2325	4	3	1	1	-0,192373	B8NGM2	B8NGM2	1	AFLA_136490	NAD dependent epimerase/dehydratase, putative
29,8961	29,7663	29,0698	29,6098	29,6009	29,680			3,71E-57	8,67E+09	8	8	8	47.3	12,139	29,6156	29,5781	29,6532	6	3	3	0,785309	-0,0751502	B8NGN0	B8NGN0	1	AFLA_136570	Cytochrome c
NaN	NaN	NaN	25,1359	26,244	NaN			8,48E-12	4,81E+08	5	5	5	14.1	58,327	25,7789	NaN	25,7789	2	0	2	1						
36,9191	27,8869	28,4759	28,881	28,4381	28,2088			3,62E-164	2,68E+09	11	11	11	44.9	28,09	28,135	27,764	28,5059	6	3	3	0,208664	-0,741966	B8NGN3	B8NGN3	1	AFLA_136600	Phenylalanine tRNA synthetase alpha subunit (PodG), putative
34,6175	34,5527	34,5236	34,727	34,552	34,5872			0	2,7E+11	59	59	58	68.2	94,226	34,5933	34,5646	34,622	6	3	3	0,394287	-0,057443	B8NGN7	B8NGN7	1	AFLA_136640	Translation elongation factor EF-2 subunit, putative
29,4524	29,6669	29,86	29,4907	29,4165	29,0557			3,93E-245	7,4E+09	15	15	15	70.4	34,384	29,4904	29,6598	29,321	6	3	3	0,130675	0,338819	B8NGP4	B8NGP4	1	AFLA_136710	Uncharacterized protein
NaN	NaN	NaN	NaN	24,2863	23,8987			5,20E-14	1,91E+08	6	6	6	17.3	58,227	24,0925	NaN	24,0925	2	0	2	1						
28,7642	28,9348	28,6839	28,1415	28,3232	28,2072			2,49E-175	3,96E+09	14	14	14	52.7	58,402	28,5091	28,7943	28,224	6	3	3	0,003319	0,0573058	B8NH9	B8NH9	1	AFLA_136790	Aromatic aminotransferase Aro8, putative
24,6472	24,1572	23,7888	NaN	24,4426	24,5254			5,58E-06	1,37E+08	2	2	2	16.6	18,162	24,3122	24,1977	24,484	5	3	2	0,44006	-0,286274	B8NHK6	B8NHK6	1	AFLA_137000	Ubiquitin conjugating enzyme, putative
26,7208	25,723	26,1737	26,2577	25,8604	26,7016			4,44E-50	9,47E+08	7	7	7	22.2	32,652	26,2395	26,2058	26,2732	6	3	3	0,866907	-0,0673726	B8NHP7	B8NHP7	1	AFLA_137410	SAP domain protein, putative
26,9461	27,0686	25,4553	27,9557	28,2755	27,7531			1,85E-83	1,12E+09	6	6	6	70.1	18,158	27,2424	26,49	27,9948	6	3	3	0,049587	-1,50474	B8NH50	B8NH50	1	AFLA_137640	Uncharacterized protein
24,6354	25,2275	25,3472	26,0954	26,4485	26,1633			4,30E-126	1,22E+09	10	10	10	24.8	49,624	25,6529	25,07	26,2358	6	3	3	0,008944	-1,16573	B8NGR8	B8NGR8	1	AFLA_137860	Uncharacterized protein
29,785	29,9056	29,7944	29,9905	29,8062	29,9482			0	1,16E+10	28	28	28	69.9	59,793	29,8717	29,8283	29,915	6	3	3	0,270671	-0,0866547	B8NGS7	B8NGS7	1	AFLA_137950	GMP synthase
30,6778	30,5124	30,1722	30,4541	30,4547	30,5457			0	1,6E+10	41	41	41	64.3	79,759	30,4695	30,4542	30,4848	6	3	3	0,849782	-0,0306842	B8NGS8	B8NGS8	1	AFLA_137960	Arginyl-tRNA synthetase
25,8782	25,5421	25,2543	NaN	25,7585	NaN			8,75E-36	7,85E+08	5	5	5	25.3	31,925	26,6083	25,5582	25,7585	4	3	1	1	-0,200334	B8NGT0	B8NGT0	1	AFLA_137980	NADH-cytochrome b5 reductase (EC 1.6.2.2)
25,8154	26,2022	26,4444	26,2241	26,3825	26,1927			1,77E-32	7,77E+08	8	8	8	52.9	26,124	26,2102	26,154	26,2664	6	3	3	0,590349	-0,112406	B8NGT1	B8NGT1	1	AFLA_137990	Uncharacterized protein
28,013	27,5555	26,0788	26,4923	26,6824	27,1067			9,76E-30	2,33E+09	4	4	4	14.1	70,487	26,9881	27,2158	26,7605	6	3	3	0,497745	0,455273	B8NGY8	B8NGY8	1	AFLA_138570	Protease S8 tripeptidyl peptidase 1, putative
NaN	NaN	NaN	23,7701	NaN	24,0625			1,58E-05	68467000	2	2	2	19.4	12,311	23,9163	NaN	23,9163	2	0	2	1						
26,4562	26,1392	26,1391	26,0914	26,2201	26,2375			1,26E-14	6,77E+08	5	5	5	31.4	30,934	26,2139	26,2448	26,183	6	3	3	0,620293	-0,0618051	B8NHV6	B8NHV6	1	AFLA_139020	Uncharacterized protein
27,4819	27,1004	27,5034	26,7919	27,7564	27,8306			0	1,07E+10	14	14	14	40.9	50,794	27,4108	27,3619	27,4596	6	3	3	0,799023	0,0977434	B8NI10	B8NI10	1	AFLA_139470	Beta-cyclopirozate dehydrogenase (EC 1.2.1.99.1) (Beta-Cyclopirozate oxidocyclase) (FAD-dependent oxidoreductase cpsA)
NaN	25,375	26,2025	NaN	25,6191	25,7765			1,29E-303	6,15E+09	11	11	11	35	49,232	25,7433	25,7887	25,6978	4	2	2	0,849133	0,0909014	B8NI11	B8NI11	1	AFLA_139480	Dimethylallyl tryptophan synthase, putative
24,8269	25,07	24,9229	NaN	24,3244	NaN			5,56E-13	1,99E+08	4	4	4	10.5	48,761	24,786	24,9399	24,3244	4	3	1	1	0,615558	H9CNZ7	H9CNZ7	1	AFLA_m0250	Ribosomal protein S5

Supplementary Table S2. Data on proteins obtained from label-free proteomics from *Aspergillus flavus* grown in presence of 0.1 M CaCl₂ treated with 10 µg/ml PgAFP and untreated control.

B. Quantitative and qualitative results

LFQ intensity AF_CaCl ₂ PgAFP_1	LFQ intensity AF_CaCl ₂ PgAFP_2	LFQ intensity AF_CaCl ₂ PgAFP_3	LFQ intensity Control_1	LFQ intensity AF_CaCl ₂ Control_2	LFQ intensity AF_CaCl ₂ Control_3	t-test Significant	PEP	Intensity	Peptides	Razor + unique peptides	Unique peptides	Sequence coverage [%]	Mol. weight [kDa]	Mean AF_CaCl ₂ PgAFP	Mean AF_CaCl ₂ Control	Valid values	Valid values AF_CaCl ₂ PgAFP	Valid values AF_CaCl ₂ Control	t-test p value	Log2(-test Difference)	Fold Change	Protein IDs	Majority protein IDs	Proteins	Gene Names	Protein names	
31.0839	30.3486	30.067	29.1636	29.5708	29.7497	+	0	7,72E+09	14	14	14	34	66,878	29,9973	30,4998	29,4947	6	3	0	0.020912	1,00511	2.007096525	B8NTV3	B8NTV3	1	AFLA_101240	Vacuolar carboxypeptidase Cps1, putative
26.9594	26.6196	26.126	25.6693	25.2932	25.6965	+	3,61E-110	7,07E+08	7	7	7	23,6	47,87	26,0607	26,5683	25,563	6	3	0	0.020912	1,01249	2.021309161	B8N1N1	B8N1N1	1	AFLA_068180	Ethanolamine kinase, putative
25.9221	25.5111	26.569	24.6678	25.0753	25.6589	+	2,77E-21	3,64E+08	7	7	7	9,8	117,64	25,4887	26,0008	24,9767	6	3	0	0.041561	1,02407	2.033648017	B8NLC2	B8NLC2	1	AFLA_090490	Alpha-thalassaemia glycolucholodryase TreA/Ath1
25.1881	25.7921	24.7573	23.9946	24.1597	24.4006	+	5,21E-13	3,71E+08	5	5	5	10,9	64,216	24,7154	25,2458	24,185	6	3	0	0.030215	1,06081	2.086102434	B8MZ71	B8MZ71	1	AFLA_083600	RNA splicing factor (Pad-1), putative
28.6053	28.0431	28.0829	27.1183	27.1388	27.2818	+	7,73E-105	1,64E+09	16	16	14	27,5	89,135	27,7117	28,2438	27,1796	6	3	0	0.004829	1,06414	2.090923095	B8NLD2	B8NLD2	1	AFLA_090590	Alpha-1,2-mannosidase, putative subfamily
28.0544	27.5733	27.1719	26.1577	26.6132	26.8018	+	1,23E-74	9,43E+08	7	7	7	17,8	62,965	27,062	27,5998	26,5242	6	3	0	0.027938	1,07561	2.107613024	B8MW63	B8MW63	1	AFLA_074100	Gamma-glutamyltranspeptidase
31.9513	32.1439	32.1406	31.2945	30.8648	30.7891	+	7,10E-271	3,38E+10	8	8	8	95,4	11,087	31,5307	32,0786	30,9828	6	3	0	0.002966	1,09576	2.137256409	B8NB77	B8NB77	1	AFLA_044520	60S acidic ribosomal protein P2/allergen Asp F 8
25.8096	25.5235	25.3227	24.1945	24.9445	24.1804	+	1,12E-19	3,75E+08	3	3	3	31,4	13,537	24,9959	25,5519	24,4398	6	3	0	0.018382	1,11212	2.161630596	B8NGE7	B8NGE7	1	AFLA_134870	U6 snRNP-associated Sm-like protein LSM4, putative
26.0032	25.8031	25.2907	24.5498	24.5185	24.6825	+	3,05E-10	4,05E+08	3	3	3	34,7	11,23	25,1413	25,699	24,5836	6	3	0	0.006908	1,11544	2.166610774	B8NSV8	B8NSV8	1	AFLA_015720	Small nuclear ribonucleoprotein (LSM2), putative
30.941	30.3806	30.6761	28.9999	29.7498	29.8324	+	0	1,03E+10	13	13	13	72,4	27,369	30,0967	30,6659	29,5274	6	3	0	0.021419	1,13856	2.201611636	B8NZ26	B8NZ26	1	AFLA_034200	2-heptaprenyl-1,4-naphthoquinone methyltransferase, putative
27.518	27.342	26.8867	25.9822	26.2654	26.0739	+	2,67E-30	1,25E+09	4	4	4	39,8	10,067	26,6798	27,2489	26,1072	6	3	0	0.005161	1,1447	2.206408023	B8N8N8	B8N8N8	1	AFLA_015510	Small nuclear ribonucleoprotein F (snRNP-F) (Sm protein F)
29.8676	29.52	29.6739	28.1225	28.6653	28.6684	+	6,77E-158	4,75E+09	20	19	19	44,4	78,235	29,6653	29,6972	28,4854	6	3	0	0.004414	1,20175	2.300185116	B8MVB8	B8MVB8	1	AFLA_073450	Aminase oxidase
29.7975	29.112	29.1525	27.7735	28.2348	28.4026	+	4,67E-251	3,59E+09	11	11	11	34,8	45,235	28,7451	29,3532	28,1369	6	3	0	0.013823	1,21625	2.323420047	B8NA56	B8NA56	1	AFLA_043010	Fornine oxidase
31.7271	31.0988	31.0474	29.8645	30.0048	30.2584	+	0	1,41E+10	20	20	20	58,4	49,457	30,6668	31,2911	30,0426	6	3	0	0.007213	1,24853	2.375992035	B8NAS7	B8NAS7	1	AFLA_043020	Fructosylamine: oxygen oxidoreductase
27.6051	27.6491	27.4452	26.2362	26.5995	26.1732	+	6,59E-94	1,41E+09	3	3	3	45,5	13,43	26,9414	27,5665	26,1631	6	3	0	0.000633	1,25018	2.378710995	B8N488	B8N488	1	AFLA_035010	Small nuclear ribonucleoprotein SmD1, putative
26.6341	26.4183	26.1295	24.9647	25.2437	24.9401	+	1,05E-58	6,32E+08	4	4	4	64,1	11,564	25,8781	26,3939	25,1042	6	3	0	0.009335	1,28971	2.444789072	B8NEM0	B8NEM0	1	AFLA_062180	37S ribosomal protein S16
31.2696	30.7442	30.2784	29.358	29.3959	29.6638	+	0	1,12E+10	18	18	18	25,2	105,17	30,1083	30,7641	29,4256	6	3	0	0.01268	1,31152	2.482029048	B8NEE0	B8NEE0	1	AFLA_060490	Pyridine nucleotide disulphide oxidoreductase family protein
26.3849	26.3853	25.0997	24.5244	24.5491	24.7901	+	1,68E-25	3,29E+08	3	3	3	9	48,41	25,2639	25,9366	24,5912	6	3	0	0.042965	1,34544	2.541076833	B8N429	B8N429	1	AFLA_033520	Ubiquitin-like protein DskB, putative
28.8337	29.55	29.0813	27.5959	27.8819	27.9697	+	1,54E-195	4,51E+09	21	21	20	34	71,973	28,476	29,155	27,797	6	3	0	0.005387	1,35797	2.563242547	B8NS92	B8NS92	1	AFLA_112180	ATP dependent RNA helicase (Dbp1), putative
NaN	25.8932	26.5679	25.3502	24.7942	24.4564	+	7,41E-82	7,1E+08	11	10	10	31,9	50,409	25,412	26,2305	24,8663	5	2	0	0.047686	1,36421	2.574353193	B8N6T0	B8N6T0	1	AFLA_016830	Tubulin subunit TubB
33.6746	33.4854	33.317	32.2475	31.9621	32.1464	+	0	1,02E+11	12	11	11	73,9	17,009	32,8055	33,4924	32,1187	6	3	0	0.000493	1,37371	2.591360982	B8NQF0	B8NQF0	1	AFLA_006300	Nucleoside diphosphate kinase (EC 2.7.4.6)
27.1112	27.2078	27.0494	25.5732	25.825	25.6162	+	1,36E-176	1,47E+09	6	6	6	40,9	27,781	26,3988	27,1261	25,6714	6	3	0	0.006505	1,44571	2.74093858	B8NM09	B8NM09	1	AFLA_094650	60S acidic ribosomal protein P0, putative
29.1856	28.6991	28.565	27.6118	27.9598	27.4143	+	1,67E-68	2,7E+09	8	8	8	30,4	32,116	28,0869	28,8166	27,3573	6	3	0	0.003998	1,45931	2.749768186	B8N7K8	B8N7K8	1	AFLA_104510	Methyltransferase family protein
31.8229	32.0133	31.9106	30.7668	30.238	30.3273	+	0	2,4E+10	10	10	10	48,9	33,441	31,1798	31,9156	30,444	6	3	0	0.001035	1,47159	2.773273689	B8N1E9	B8N1E9	1	AFLA_030140	60S ribosomal protein P0
26.9801	27.2405	26.6433	25.3008	25.7883	25.3957	+	6,11E-47	1,49E+09	7	7	7	46	21,415	26,1605	26,9547	25,4783	6	3	0	0.002482	1,4764	2.782535319	B8N1B1	B8N1B1	1	AFLA_029760	Small monomeric GTPase SarA, putative
25.6284	26.3329	25.7872	24.6025	24.3853	24.2224	+	3,09E-08	5,13E+08	3	3	3	29,3	10,958	25,1598	25,9162	24,4034	6	3	0	0.003242	1,51276	2.853554268	B8NGG5	B8NGG5	1	AFLA_135920	Cytochrome c oxidase polypeptide subunit
28.3924	28.0101	27.4117	26.0774	26.6422	26.5513	+	6,47E-11	1,52E+09	3	3	3	16,3	11,278	27,1809	27,9381	26,4237	6	3	0	0.010635	1,5144	2.856799923	B8NS34	B8NS34	1	AFLA_052650	Uncharacterized protein
30.4844	30.5277	30.4712	29.2864	29.74	28.8977	+	1,23E-47	8,01E+08	5	5	5	35,8	17,937	29,7332	30,4944	28,972	6	3	0	0.000747	1,52239	2.872665476	B8MY77	B8MY77	1	AFLA_080140	60S ribosomal protein L12
25.7025	25.4898	25.813	24.599	24.1901	24.1029	+	4,78E-07	1,77E+08	2	2	2	81	37,827	25,0632	25,6743	24,1465	6	3	0	0.001271	1,52779	2.883437997	B8MZL2	B8MZL2	1	AFLA_085020	Class II aldolase/alducin domain protein
27.0341	27.1637	26.5167	24.9593	26.1149	25.0284	+	5,42E-31	8,97E+08	9	9	9	58,6	28,548	26,1362	26,9048	25,3676	6	3	0	0.022109	1,53727	2.902447557	B8NG47	B8NG47	1	AFLA_132080	Small nuclear ribonucleoprotein U2, A
27.358	27.0344	27.5985	26.1587	26.3663	25.8664	+	6,65E-107	1,17E+09	12	12	12	37,9	44,308	25,8571	26,4303	26,0828	6	3	0	0.001702	1,54649	2.921055965	B8NB27	B8NB27	1	AFLA_052280	Uncharacterized protein
26.991	27.2145	27.4383	25.598	25.8747	25.5202	+	7,62E-21	1,64E+09	8	8	8	24	55,064	26,4391	27,2146	25,6636	6	3	0	0.000769	1,55096	2.930120508	B8MW24	B8MW24	1	AFLA_073710	Mitochondrial ribosomal protein DAP3, putative
27.68	27.3944	28.9959	26.5979	26.343	26.4552	+	1,47E-39	1,33E+09	5	5	5	29,4	18,491	27,2427	28,0324	26,4642	6	3	0	0.035148	1,5614	2.951401103	B8ND05	B8ND05	1	AFLA_087760	40S ribosomal protein S11
28.3727	27.9599	27.1425	26.2009	26.4615	26.0194	+	3,73E-15	1,53E+09	4	4	4	36,2	12,867	27,0425	27,8248	26,2603	6	3	0	0.015161	1,56453	2.957811268	B8N0U1	B8N0U1	1	AFLA_026260	Small nuclear ribonucleoprotein SmD3, putative
26.3248	26.5591	25.5442	24.7399	25.0755	25.3989	+	3,30E-21	5,29E+08	9	9	9	21,7	48,134	25,3495	26,1427	24,5564	6	3	0	0.029112	1,56869	3.002865797	B8NL78	B8NL78	1	AFLA_093940	Mitochondrial large ribosomal subunit YmL35, putative
28.0893	27.5951	27.4665	25.8266	26.3498	26.2066	+	1,36E-60	1,45E+09	14	14	14	71,7	28,204	26,9223	27,717	26,1277	6	3	0	0.002945	1,58932	3.009074863	B8MXD8	B8MXD8	1	AFLA_077250	Acyl-coenzyme A oxidase
25.9946	26.1703	25.9359	24.6189	24.2005	24.001	+	4,82E-24	4,43E+08	4	4	4	19,2	33,102	25,3841	26,												

Supplementary Table S2. Data on proteins obtained from label-free proteomics from *Aspergillus flavus* grown in presence of 0.1 M CaCl₂ treated with 10 µg/ml PgAFP and untreated control.

B. Quantitative and qualitative results

LFQ intensity AF_CaCl ₂ PgAFP_1	LFQ intensity AF_CaCl ₂ PgAFP_2	LFQ intensity AF_CaCl ₂ PgAFP_3	LFQ intensity AF_CaCl ₂ Control_1	LFQ intensity AF_CaCl ₂ Control_2	LFQ intensity AF_CaCl ₂ Control_3	t-test Significant	PEP	Intensity	Peptides	Razor + unique peptides	Unique peptides	Sequence coverage [%]	Mol. weight [kDa]	Mean	Mean AF_CaCl ₂ PgAFP	Mean AF_CaCl ₂ Control	Valid values	Valid values AF_CaCl ₂ PgAFP	Valid values AF_CaCl ₂ Control	t-test p value	Log2(-t-test Difference)	Fold Change	Protein IDs	Majority protein	Proteins	Gene Names	Protein names
30.6685	31.0742	30.9058	28.5294	27.0226	27.0226	+	6,41E-114	1,53E+10	8	8	8	37	16,959	29,1631	30,8828	27,4434	6	3	0,003564	3,43939	10,8482468	B8NSF1	B8NSF1	1	AFLA_048140	60S ribosomal protein L23	
29.2772	29.8472	30.2209	26.9979	25.9408	26,0707	+	4,91E-22	4,39E+09	5	5	5	39	19,978	28,0591	29,7818	26,3365	6	3	0,001372	3,44532	10,89292879	B8N9U3	B8N9U3	1	AFLA_112390	60S ribosomal protein L36	
31.5775	32.1415	32.8978	29.1156	27.988	28,5129	+	0	2,31E+10	24	24	24	71	40,245	30,3722	32,2056	28,5388	6	3	0,001834	3,6668	12,70038213	B8NR98	B8NR98	1	AFLA_005730	60S ribosomal protein L4, putative	
30.4012	30.9258	31.5159	27.7354	26,4745	26,7871	+	0	9,39E+09	15	15	15	47,3	25,677	28,9733	30,9476	26,999	6	3	0,001363	3,94864	15,44041902	B8NV29	B8NV29	1	AFLA_115110	60S ribosomal protein L13	
29.8977	30.5897	30.6484	26.9519	25,7414	26,2005	+	5,21E-111	7,09E+09	7	7	7	22,4	33,628	28,3536	30,4093	26,298	6	3	0,00056	4,11131	17,28333833	B8NM33	B8NM33	1	AFLA_029267	Ribosomal protein L15	
27.4661	27.9398	29.1133	24.337	23,8529	23,8823	+	1,50E-36	1,43E+09	7	7	7	33,1	14,625	26,0986	28,1731	24,0241	6	3	0,00128	4,14898	17,74056436	B8NV8	B8NV8	1	AFLA_069180	60S ribosomal protein L35	
30.9771	31.3758	31.0232	27.5222	26,553	26,7988	+	0	1,46E+10	16	16	16	46,6	29,318	29,0387	31,1254	26,952	6	3	0,000202	4,17335	18,04278327	B8NZ04	B8NZ04	1	AFLA_033980	Cytosolic large ribosomal subunit protein L7A	
29.6524	30.1015	30.4015	25.8646	24,8516	25,4759	+	2,13E-67	5,19E+09	6	6	6	37,5	20,782	27,246	30,0518	25,3974	6	3	0,000222	4,65445	25,1842524	B8NC19	B8NC19	1	AFLA_047440	60S ribosomal protein L18	
29.3796	28.6452	28.5507	24.08	NaN	24,1284	+	5,88E-146	1,28E+09	9	9	9	24	74,712	26,9568	28,8585	24,1042	5	3	2,000783	4,75426	26,98825887	B8NMK6	B8NMK6	1	AFLA_124420	Amine oxidase, putative	
29.7651	29.9713	29.8813	25.1314	24,9765	24,5285	+	0	6,55E+09	11	11	11	21,3	55,822	27,3757	29,8726	24,8788	6	3	1,25E-05	4,99378	31,86233297	B8NSZ2	B8NSZ2	1	AFLA_100030	Nucleolin protein Nsr1, putative	
30.2294	29.1182	30.6719	NaN	24,7705	24,9859	+	1,13E-103	2,83E+09	10	10	10	39,9	39,669	27,8952	30,0065	24,7282	5	3	2,003514	5,2783	38,80847937	B8MYC9	B8MYC9	1	AFLA_080660	L-asparaginase	
29.3324	27.7737	29.8293	22.8134	NaN	23,6589	+	7,76E-209	1,68E+09	12	12	12	34,4	68,812	26,8955	29,9768	23,2362	3	3	2,0006839	5,74084	53,46934131	B8NO78	B8NO78	2	AFLA_024300	Amidase, putative	
24.7894	23.8782	23.1912	NaN	NaN	NaN	+	3,65E-09	1,16E+08	4	4	4	30,4	9,7	45,489	23,9539	NaN	3	3	0	1	NaN	B8NR26	B8NR26	1	AFLA_004100	Transferrase (LuoD), putative	
NaN	25.496	25.2161	NaN	NaN	NaN	+	1,19E-26	4,18E+08	4	4	4	34,4	9,7	17,901	25,3561	25,3561	NaN	2	2	0	1	NaN	B8NQ4A	B8NQ4A	1	AFLA_004950	Cytochrome oxidase subunit Va, putative
23.9111	22.9263	NaN	NaN	NaN	NaN	+	3,40E-05	36316000	2	2	2	6,25	62,125	23,4187	23,4187	NaN	2	2	0	1	NaN	B8NR85	B8NR85	1	AFLA_005600	SNARE domain protein	
25.2682	24.0655	23.1112	NaN	NaN	NaN	+	1,61E-09	1,65E+09	5	5	5	13,5	65,179	24,215	24,215	NaN	3	3	0	1	NaN	B8NR95	B8NR95	1	AFLA_005700	Aromatic amino acid aminotransferase, putative	
24.1517	23.5019	26.3569	NaN	NaN	NaN	+	2,41E-16	1,65E+08	5	5	5	12,6	54,048	24,6702	24,6702	NaN	3	3	0	1	NaN	B8NY90	B8NY90	1	AFLA_010600	Siderophore biosynthesis acetylase ACP, putative	
NaN	24.6347	24.0037	NaN	NaN	NaN	+	2,93E-10	1,49E+08	2	2	2	4,2	87,247	24,3192	24,3192	NaN	2	2	0	1	NaN	B8NS24	B8NS24	1	AFLA_015780	Small oligopeptide transporter, OCP family	
23.3543	NaN	23.2887	NaN	NaN	NaN	+	1,06E-06	83990000	3	3	3	4	95,857	23,3215	23,3215	NaN	2	2	0	1	NaN	B8NSA2	B8NSA2	1	AFLA_022300	Chromosome segregation protein (SepB), putative	
NaN	23.7726	24.1818	NaN	NaN	NaN	+	1,58E-12	2,3E+08	4	4	4	19,8	40,882	23,9772	23,9772	NaN	2	2	0	1	NaN	B8NOP2	B8NOP2	1	AFLA_024850	Deoxyhypusine synthase, putative	
NaN	24.59	24.9343	NaN	NaN	NaN	+	1,37E-08	1,63E+08	4	4	4	26,6	26,433	24,7622	24,7622	NaN	2	2	0	1	NaN	B8N3G8	B8N3G8	1	AFLA_028710	Short chain type dehydrogenase, putative	
25.5719	24.6714	NaN	NaN	NaN	NaN	+	9,65E-08	1,15E+08	4	4	4	19,8	46,735	25,1216	25,1216	NaN	2	2	0	1	NaN	B8N3Q7	B8N3Q7	1	AFLA_031410	Ribonuclease T2 family, putative	
23.4636	23.8317	NaN	NaN	NaN	NaN	+	1,01E-21	4,58E+08	3	3	3	26,3	15,049	23,6477	23,6477	NaN	2	2	0	1	NaN	B8N418	B8N418	1	AFLA_033410	Uncharacterized protein	
25.0694	23.5346	NaN	NaN	NaN	NaN	+	8,84E-07	47980000	2	2	2	12	98,961	24,302	24,302	NaN	2	2	0	1	NaN	B8NB8Y	B8NB8Y	1	AFLA_047130	Uncharacterized protein	
27.6971	27.1201	26.7562	NaN	NaN	NaN	+	4,28E-09	9,42E+08	2	2	2	17,6	19,894	27,1911	27,1911	NaN	3	3	0	1	NaN	B8NS36	B8NS36	1	AFLA_052670	RNA recognition motif (Rim) domain containing protein, putative	
NaN	27.2454	26.7823	NaN	NaN	NaN	+	0,00016	3,57E+08	2	2	2	10,3	38,792	27,0138	27,0138	NaN	2	2	0	1	NaN	B8ND57	B8ND57	1	AFLA_055680	Esterase, putative	
NaN	24.5913	24.8918	NaN	NaN	NaN	+	1,56E-08	2,67E+08	2	2	2	20,7	16,051	24,7416	24,7416	NaN	2	2	0	1	NaN	B8NEW9	B8NEW9	1	AFLA_058330	Mitochondrial intermembrane space translocase subunit Tim9, putative	
NaN	25.2471	24.7419	NaN	NaN	NaN	+	6,80E-09	2,65E+08	2	2	2	17,4	21,01	24,9945	24,9945	NaN	2	2	0	1	NaN	B8NEE9	B8NEE9	1	AFLA_060580	NEDD8 conjugating enzyme (UbcL), putative	
23.6373	23.9637	23.7981	NaN	NaN	NaN	+	8,49E-21	2,93E+08	5	5	5	15,6	53,058	23,7997	23,7997	NaN	3	3	0	1	NaN	B8NFA6	B8NFA6	1	AFLA_061500	Squalene monoxygenase Erg1	
NaN	25.8149	26.7776	NaN	NaN	NaN	+	0,000171	2,15E+08	2	2	2	11,5	25,038	26,2962	26,2962	NaN	2	2	0	1	NaN	B8MFX3	B8MFX3	1	AFLA_076200	HAD superfamily hydrolase, putative	
24.7929	NaN	23.0277	NaN	NaN	NaN	+	1,08E-08	1,93E+08	2	2	2	4,1	68,216	23,9191	23,9191	NaN	2	2	0	1	NaN	B8MK34	B8MK34	1	AFLA_078810	Oxidoreductase	
23.2484	23.4539	23.0619	NaN	NaN	NaN	+	2,05E-09	1,54E+08	4	4	4	10,9	37,363	23,2547	23,2547	NaN	3	3	0	1	NaN	B8MKX9	B8MKX9	1	AFLA_079160	Ribosome biogenesis protein, putative	
NaN	23.9565	23.6506	NaN	NaN	NaN	+	6,07E-27	2,91E+08	3	3	3	7,6	58,844	23,3036	23,3036	NaN	2	2	0	1	NaN	B8MZN7	B8MZN7	1	AFLA_085270	T-complex protein 1, zeta subunit, putative	
24.0109	23.4908	NaN	NaN	NaN	NaN	+	2,14E-05	74023000	2	2	2	4,1	77,122	23,7509	23,7509	NaN	2	2	0	1	NaN	B8MWT6	B8MWT6	1	AFLA_088660	Acetyltransferase, putative	
NaN	24.5129	24.5236	NaN	NaN	NaN	+	1,74E-14	2,91E+08	5	5	5	9,5	80,72	24,5183	24,5183	NaN	2	2	0	1	NaN	B8NKL5	B8NKL5	1	AFLA_091810	Uncharacterized protein	
NaN	23.3384	23.9758	NaN	NaN	NaN	+	3,74E-08	1,7E+08	4	4	4	15,6	41,918	23,6571	23,6571	NaN	2	2	0	1	NaN	B8N8G5	B8N8G5	1	AFLA_107590	3-methyl-2-oxobutanate dehydrogenase, putative	
23.8482	NaN	25.589	NaN	NaN	NaN	+	5,58E-12	57945000	5	5	5	19,3	41,531	24,7186	24,7186	NaN	2	2	0	1	NaN	B8N950	B8N950	1	AFLA_109960	Uncharacterized protein	
24.9905	25.2946	24.9387	NaN	NaN	NaN	+	2,92E-57	2,03E+08	8	8	8	34,1	30,478	25,0766	25,0766	NaN	3	3	0	1	NaN	B8N9W4	B8N9W4	1	AFLA_112600	37S ribosomal protein S25, mitochondrial	
24.8045	24.375	NaN	NaN	NaN	NaN	+	7,79E-15	1,95E+08	5	5	5	7,7	81,936	24,5898	24,5898	NaN	2	2	0	1	NaN	B8NA76	B8NA76	1	AFLA_113720	Ribosome biogenesis (Nop4), putative	
23.7553	NaN	28.4655	NaN	NaN	NaN	+	3,78E-64	9,46E+08	5	5	5	29,1	20,206	26,1104	26,1104	NaN	2	2	0	1	NaN	B8NQV0	B8NQV0	1	AFLA_113730	Uncharacterized protein	
24.175	NaN	25.0388	NaN	NaN	NaN	+	5,12E-69	8,92E+08	3	3	3	22,5	30,301	24,6069	24,6069	NaN	2	2	0	1	NaN	B8NWE1	B8NWE1	1	AFLA_119780	Neutral protease 2 homolog AFLA_119780 (EC 3.4.24.39) (Deuterolysin AFLA_119780)	
23.6358	NaN	22.959	NaN	NaN	NaN	+	5,25E-06	76535000	2	2	2	5,4	51,017	23,2974	23,2974	NaN	2	2	0	1	NaN	B8NX26					

Supplementary Table S2. Data on proteins obtained from label-free proteomics from *Aspergillus flavus* grown in presence of 0.1 M CaCl₂ treated with 10 µg/ml PgAFP and untreated control.

B. Quantitative and qualitative results

LQF intensity AF_CaCl ₂ PgAFP_1	LQF intensity AF_CaCl ₂ PgAFP_2	LQF intensity AF_CaCl ₂ PgAFP_3	LQF intensity AF_CaCl ₂ Control_1	LQF intensity AF_CaCl ₂ Control_2	LQF intensity AF_CaCl ₂ Control_3	t-test Significant	PEP	Intensity	Peptides	Razor + unique peptides	Unique peptides	Sequence coverage [%]	Mol. weight [kDa]	Mean	Mean AF_CaCl ₂ PgAFP	Mean AF_CaCl ₂ Control	Valid values	Valid values AF_CaCl ₂ PgAFP	Valid values AF_CaCl ₂ Control	t-test p value	Log2[-(test Difference)]	Fold Change	Protein IDs	Majority protein IDs	Proteins	Gene Names	Protein names
27,3946	27,3644	27,4069	28,7295	28,5466	28,2777	+	3,70E-274	2,53E+09	13	13	13	37.1	55,616	27,9533	27,3886	28,518	6	3	3	0,001019	-1,12931	-2,187540914	B8NS30	B8NS30	1	AFLA_052610	Succinyl-CoA:3-ketoacid-coenzyme A transferase (EC 2.8.3.5)
30,6311	30,8276	31,5586	32,4185	32,0477	31,8304	+	0	3,89E+10	31	31	31	66.9	58,086	31,5523	31,0058	32,0988	6	3	3	0,029671	-1,09306	-2,13326028	B8MWA0	B8MWA0	1	AFLA_087900	Pyruvate kinase (EC 2.7.1.40)
NaN	NaN	NaN	NaN	23,5699	23,5492		3,31E-26	2,66E+08	4	4	4	17.4	47,811	23,5595	NaN	23,5595	2	0	2	1	NaN	Detected in control only	B8NQZ7	B8NQZ7	1	AFLA_003810	Endonuclease/exonuclease/phosphatase family protein
NaN	NaN	NaN	26,2119	26,2701	26,5487		3,45E-43	8,27E+08	6	6	6	17.5	57,585	26,3436	NaN	26,3436	3	0	3	1	NaN	Detected in control only	B8NXS3	B8NXS3	1	AFLA_008930	Cyclin acid phosphatase (EC 3.1.3.2)
NaN	NaN	NaN	24,2323	24,5589	24,6255		2,64E-07	1,78E+07	2	2	2	9.3	18,627	24,4722	NaN	24,4722	3	0	3	1	NaN	Detected in control only	B8NYQ2	B8NYQ2	1	AFLA_012220	Cyclin-dependent kinases regulatory subunit, putative
NaN	NaN	NaN	23,2952	23,9189	23,3138		2,45E-29	3,74E+08	5	5	5	31	23,258	23,5093	NaN	23,5093	3	0	3	1	NaN	Detected in control only	B8NSH5	B8NSH5	1	AFLA_013180	Williams-beuren syndrome chromosome region, putative
NaN	NaN	NaN	22,7949	22,4155	22,3787		7,60E-94	1,73E+09	6	6	6	27.6	32,989	22,5297	NaN	22,5297	3	0	3	1	NaN	Detected in control only	B8NSN1	B8NSN1	1	AFLA_013740	Acid phosphatase, putative
NaN	NaN	NaN	26,6009	27,3877	NaN		2,72E-12	5,37E+08	3	3	3	16.9	15,333	26,9943	NaN	26,9943	2	0	2	1	NaN	Detected in control only	B8NAQ2	B8NAQ2	1	AFLA_017610	Histone H3
NaN	NaN	NaN	24,1966	24,3803	NaN		2,12E-12	1,52E+08	4	4	4	5.3	90,123	24,2885	NaN	24,2885	2	0	2	1	NaN	Detected in control only	B8NSB4	B8NSB4	1	AFLA_022420	Microtubule binding protein HOOK3, putative
NaN	NaN	NaN	NaN	24,5609	24,3599		6,37E-06	2,14E+08	3	3	3	20.4	21,449	24,4604	NaN	24,4604	2	0	2	1	NaN	Detected in control only	B8NK7	B8NK7	1	AFLA_030720	RNA exonuclease Rex2, putative
NaN	NaN	NaN	NaN	24,4917	24,301		1,56E-16	2,42E+08	5	5	5	7.1	108,52	24,3964	NaN	24,3964	2	0	2	1	NaN	Detected in control only	B8NS56	B8NS56	1	AFLA_031600	SNARE-dependent exocytosis protein (Sro7), putative
NaN	NaN	NaN	25,5384	26,0352	25,8052		6,39E-08	2,85E+08	2	2	2	5.9	50,604	25,7929	NaN	25,7929	3	0	3	1	NaN	Detected in control only	B8NCND	B8NCND	1	AFLA_039370	Acid phosphatase, putative
NaN	NaN	NaN	NaN	24,1963	23,4775		6,84E-16	1,79E+08	4	4	4	8.8	75,098	23,8369	NaN	23,8369	2	0	2	1	NaN	Detected in control only	B8NB18	B8NB18	1	AFLA_043930	MFS phosphatase transporter, putative
NaN	NaN	NaN	24,7185	25,3773	25,6684		5,14E-10	4,09E+08	5	5	5	11	74,691	25,2547	NaN	25,2547	3	0	3	1	NaN	Detected in control only	B8NBF0	B8NBF0	1	AFLA_045250	Biotin ago-protein ligase, putative
NaN	NaN	NaN	24,0118	24,413	NaN		5,62E-08	1,58E+08	4	4	4	9.4	65,081	24,2124	NaN	24,2124	2	0	2	1	NaN	Detected in control only	B8NSJ9	B8NSJ9	1	AFLA_048620	Histone acetyltransferase, putative
NaN	NaN	NaN	27,5088	27,4891	27,6653		1,06E-42	1,57E+09	4	4	4	32.2	19,57	27,5544	NaN	27,5544	3	0	3	1	NaN	Detected in control only	B8NDN7	B8NDN7	1	AFLA_059760	Uncharacterized protein
NaN	NaN	NaN	27,2497	27,6974	27,6582		7,84E-34	1,07E+09	9	9	9	20	74,118	27,5351	NaN	27,5351	3	0	3	1	NaN	Detected in control only	B8NEP7	B8NEP7	1	AFLA_062450	Sphingomyelin phosphodiesterase
NaN	NaN	NaN	25,3229	25,2405	25,716		1,14E-11	4,08E+08	2	2	2	12	26,52	25,4264	NaN	25,4264	3	0	3	1	NaN	Detected in control only	B8NFD0	B8NFD0	1	AFLA_062640	Uncharacterized protein
NaN	NaN	NaN	26,6398	26,5628	26,7352		4,15E-67	1,19E+09	5	5	5	22.3	39,792	26,6459	NaN	26,6459	3	0	3	1	NaN	Detected in control only	B8NIU9	B8NIU9	1	AFLA_069090	GPI anchored protein, putative
NaN	NaN	NaN	23,9876	NaN	22,4329		1,30E-10	1,28E+08	4	4	4	21.3	28,879	23,2103	NaN	23,2103	2	0	2	1	NaN	Detected in control only	B8NI29	B8NI29	1	AFLA_071460	Uncharacterized protein
NaN	NaN	NaN	25,4028	25,778	NaN		7,40E-07	1,55E+08	3	3	3	22.3	22,33	25,5904	NaN	25,5904	2	0	2	1	NaN	Detected in control only	B8MXS2	B8MXS2	1	AFLA_078590	Extracellular matrix protein, putative
NaN	NaN	NaN	26,123	27,431	27,535		1,35E-58	8,57E+08	6	6	6	21.6	50,64	27,0297	NaN	27,0297	3	0	3	1	NaN	Detected in control only	B8MZU5	B8MZU5	1	AFLA_085850	Uncharacterized protein
NaN	NaN	NaN	25,1091	25,1069	24,5207		2,82E-08	1,92E+08	5	5	5	22.6	27,235	24,9123	NaN	24,9123	3	0	3	1	NaN	Detected in control only	B8NM17	B8NM17	1	AFLA_094730	Exosome complex subunit Csl4, putative
NaN	NaN	NaN	24,3513	25,0113	24,9895		8,71E-16	1,67E+08	3	3	3	12.8	40,381	24,784	NaN	24,784	3	0	3	1	NaN	Detected in control only	B8NUG2	B8NUG2	1	AFLA_099240	D-arabinol dehydrogenase ArbD, putative
NaN	NaN	NaN	24,9468	24,8329	24,2013		1,04E-20	4,42E+08	3	3	3	27	26,851	24,6603	NaN	24,6603	3	0	3	1	NaN	Detected in control only	B8NUN1	B8NUN1	1	AFLA_100840	Pyridoxamine phosphate oxidase, putative
NaN	NaN	NaN	28,1967	28,514	28,7807		0	6,87E+09	12	12	12	45.2	54,633	28,4971	NaN	28,4971	3	0	3	1	NaN	Detected in control only	B8N7N3	B8N7N3	1	AFLA_104760	Purple acid phosphatase (EC 3.1.3.2)
NaN	NaN	NaN	NaN	23,1509	23,2382		9,47E-07	55611000	2	2	2	10.6	33,212	23,1945	NaN	23,1945	2	0	2	1	NaN	Detected in control only	B8N8F1	B8N8F1	1	AFLA_107450	Pirip, putative
NaN	NaN	NaN	NaN	25,3324	24,9761		9,07E-77	2,12E+08	4	4	4	11.4	75,17	25,1543	NaN	25,1543	2	0	2	1	NaN	Detected in control only	B8N8P3	B8N8P3	1	AFLA_108370	Tyrosinase, putative
NaN	NaN	NaN	25,6679	26,0469	26,1643		5,28E-12	4,69E+08	4	4	4	17.7	37,584	25,9597	NaN	25,9597	3	0	3	1	NaN	Detected in control only	B8N9K7	B8N9K7	1	AFLA_111530	Zinc-containing alcohol dehydrogenase, putative
NaN	NaN	NaN	24,4964	24,4215	NaN		1,41E-24	5,39E+08	8	8	8	11.7	97,024	24,4592	NaN	24,4592	2	0	2	1	NaN	Detected in control only	B8NAA2	B8NAA2	1	AFLA_113980	Cyclin dependent kinase inhibitor Pho81, putative
NaN	NaN	NaN	23,7777	NaN	24,6947		8,11E-07	1,28E+08	3	3	3	18.6	35,485	24,2362	NaN	24,2362	2	0	2	1	NaN	Detected in control only	B8N177	B8N177	1	AFLA_114490	Histidinol-phosphatase
NaN	NaN	NaN	24,508	24,7829	NaN		7,14E-09	3,55E+08	4	4	4	7.7	78,476	24,6454	NaN	24,6454	2	0	2	1	NaN	Detected in control only	B8NW15	B8NW15	1	AFLA_119430	Sect1 family superfamily
NaN	NaN	NaN	27,3167	28,3767	28,4127		3,55E-141	2,03E+09	12	12	12	25.9	85,243	28,0353	NaN	28,0353	3	0	3	1	NaN	Detected in control only	B8NW03	B8NW03	1	AFLA_119700	Alpha-1,2-mannosidase family protein
NaN	NaN	NaN	NaN	26,0267	25,9783		5,20E-32	4,36E+08	5	5	5	31.5	34,269	26,0075	NaN	26,0075	2	0	2	1	NaN	Detected in control only	B8NN48-R	B8NN48	2	AFLA_124820	Uncharacterized protein
NaN	NaN	NaN	NaN	27,5362	27,6342		3,18E-09	8,43E+08	3	3	3	14.1	31,401	27,5852	NaN	27,5852	2	0	2	1	NaN	Detected in control only	B8NNE2	B8NNE2	1	AFLA_127530	BCAS2 family protein
NaN	NaN	NaN	25,3139	26,244	NaN		8,48E-12	4,81E+08	5	5	5	14.1	58,327	25,7789	NaN	25,7789	2	0	2	1	NaN	Detected in control only	B8NGN2	B8NGN2	1	AFLA_136590	Phenylalanyl-tRNA synthetase alpha subunit (PodG), putative
NaN	NaN	NaN	NaN	24,2863	23,8987		5,20E-14	1,91E+08	6	6	6	17.3	58,227	24,0925	NaN	24,0925	2	0	2	1	NaN	Detected in control only	B8NH15	B8NH15	1	AFLA_136790	Thiamine pyrophosphate enzyme, putative
NaN	NaN	NaN	23,7701	NaN	24,0625		1,58E-05	68467000	2	2	2	19.4	12,311	23,9163	NaN	23,9163	2	0	2	1	NaN	Detected in control only	B8NHV1	B8NHV1	1	AFLA_138870	Uncharacterized protein
NaN	NaN	NaN	24,2299	26,2617	25,5851		7,42E-14	2,96E+08	7	7	7	22.7	44,372	25,3589	NaN	25,3589	3	0	3	1	NaN	Detected in control only	B8NI51	B8NI51	1	AFLA_028260	Probable glucan 1,3-beta-glucosidase A (EC 3.2.1.58) [Exo-1,3-beta-glucanase 1] (Exo-1,3-beta-glucanase A)
NaN	NaN	NaN	NaN	24,0153	24,0315		2,75E-08	1,26E+08	3	3	3	7.2	62,91	24,0234	NaN	24,0234	2	0	2	1	NaN	Detected in control only	B8NT14	B8NT14	1	AFLA_098240	Probable D-xylulose kinase A (Xylulokinase A) (EC 2.7.1.17)

V. DISCUSIÓN

V.1. Espectro de actividad antimicrobiana de PgAFP *in vitro*

La proteína PgAFP había mostrado su capacidad para reducir el desarrollo de algunos mohos toxigénicos como *Penicillium expansum*, *P. commune* y *A. niger* (Acosta et al. 2009), aunque no se había establecido el grado de susceptibilidad de otros microorganismos que se encuentran habitualmente en alimentos de humedad intermedia. PgAFP no mostró actividad inhibitoria frente a ninguna bacteria o levadura en los ensayos realizados. La falta de actividad frente a bacterias y levaduras es común en este tipo de proteínas pequeñas y básicas producidas por mohos (Marx 2004) y solo la proteína Anafp, producida por *A. niger*, muestra cierta actividad frente a algunas levaduras como *Candida albicans*, *Saccharomyces cerevisiae* o *Trichosporon beigeli* (Gun Lee et al. 1999). Esta falta de sensibilidad de bacterias y levaduras puede considerarse una ventaja, dado que algunos de estos microorganismos juegan un papel fundamental en el desarrollo del aroma característico durante la maduración de los derivados cárnicos curado-madurados (Andrade et al. 2010; Ruiz-Moyano et al. 2011; Cano-García et al. 2014). Por otra parte, este hecho puede permitir la utilización conjunta de la proteína PgAFP con levaduras y bacterias para combatir el desarrollo de mohos toxigénicos en productos madurados.

En el grupo de mohos estudiados se observaron diferentes niveles de sensibilidad frente a PgAFP. Entre los mohos cuyo crecimiento se ve reducido se encuentran especies frecuentes en alimentos curado-madurados con gran potencial toxigénico. Así se observaron diferentes grados de inhibición de mohos productores de ocratoxina A (*A. carbonarius*, *A. ochraceus*, *P. nordicum* y *P. verrucosum*), de aflatoxinas (*A. flavus* y *A. parasiticus*), esterigmatocistina (*A. versicolor*) y patulina (*P. expansum* y *P. griseofulvum*).

Por lo tanto, dada la problemática que supone la producción de micotoxinas en alimentos madurados de humedad intermedia (Núñez et al. 2007; Rodríguez et al. 2012d), PgAFP podría ser útil dentro de una estrategia de biocontrol de mohos toxigénicos en este tipo de alimentos. Sin embargo, algunas de las cepas estudiadas se mostraron resistentes incluso a la concentración mayor de PgAFP ensayada (312,7 µg/ml), incluyendo a la cepa de *P. chrysogenum* productora de PgAFP, *P. polonicum* y *Rhizopus oryzae*. Aunque ninguna de estas especies ha sido relacionada con micotoxicosis alimentarias (Richard 2007), el hecho de existir cepas resistentes puede suponer una limitación para el uso de esta proteína como agente protector.

V.2. Aplicación de PgAFP en alimentos

Para evaluar de forma más precisa su potencial para el control de mohos toxigénicos en alimentos madurados, la capacidad antifúngica de PgAFP se probó en salchichón y queso. En estos alimentos es posible que se produzcan interacciones con la matriz, más compleja que un medio de cultivo, que puedan limitar el efecto antifúngico de la proteína. En los ensayos realizados se observaron resultados dispares dependiendo del alimento.

Sobre salchichón, PgAFP fue capaz de reducir el crecimiento de *A. flavus* y *P. restrictum* tras una incubación de 5 días (Delgado et al. 2015a), por lo que podría descartarse que las interacciones de la proteína con los componentes del embutido anulen su actividad antifúngica, lo que permitiría su aplicación en este tipo de productos. Sin embargo, considerando que esta proteína no muestra una actividad fungicida, sino fungistática, no es esperable que el efecto protector frente a mohos toxigénicos pueda extenderse durante el procesado completo de los embutidos. En este sentido, a pesar de que durante las primeras 24 h tras el tratamiento con PgAFP se produce una disminución en las proteínas relacionadas con la ruta biosintética de aflatoxinas en *A. flavus* (Delgado et al. 2015b), al no producirse una inhibición total del crecimiento de mohos toxigénicos, a más largo plazo puede provocar un estímulo de la producción de aflatoxinas al inducir un estrés oxidativo en el moho productor (Delgado et al. 2015b). En consecuencia, a pesar de que la aplicación de PgAFP puede ser útil para el control del peligro que supone el desarrollo de mohos toxigénicos en este tipo de alimentos, es preciso plantearse su utilización como una medida complementaria junto a otras estrategias de biocontrol, como puede ser la utilización de cultivos iniciadores.

Por otra parte, en un ensayo similar realizado sobre queso, PgAFP fue incapaz de inhibir el crecimiento de *A. flavus* utilizando concentraciones que habían sido eficaces en medios de cultivo y en el salchichón. Dado que la concentración de PgAFP, las condiciones de temperatura, actividad de agua, humedad relativa, fueron similares en ambos experimentos, y que la concentración de NaCl y el pH entre 1 y 12 no afectan a la actividad antifúngica (Delgado et al. 2015a), la diferencia en cuanto a eficacia del tratamiento antifúngico debe residir en compuestos que estén presentes en queso y no en salchichón. Entre los compuestos presentes en queso susceptibles de disminuir la eficiencia de PgAFP se encuentran diferentes cationes, especialmente el calcio (Chekri et al. 2012). Los cationes pueden jugar un papel fundamental en la reducción de la eficacia de proteínas antifúngicas (Galgóczy et al. 2013; Kaiserer et al. 2003; Theis et al. 2003; Thevissen et al. 1999, 1996) y al encontrarse en concentraciones relativamente altas en queso, podrían ser los responsables de la pérdida de actividad de PgAFP en este alimento. Para evaluar su efecto sobre la actividad antifúngica, *A. flavus* se trató con PgAFP en

medios enriquecidos con CaCl_2 , MgCl_2 y KCl . Las sales que aportaron iones divalentes redujeron drásticamente la eficiencia de PgAFP siendo el más notable el caso de Ca^{2+} , mientras que el K^+ no tuvo un efecto reseñable sobre la actividad antifúngica de PgAFP (Delgado et al. 2015d). El papel del calcio en los mecanismos de resistencia de *A. flavus* frente a PgAFP se discutirá más adelante.

La falta de actividad de PgAFP en queso y probablemente en otros alimentos ricos en calcio, junto con la limitación de que puede no ser suficiente para evitar el crecimiento de mohos toxigénicos durante un período prolongado y el hecho de que algunos mohos toxigénicos de interés en alimentos, como *A. parasiticus*, sean poco susceptibles a PgAFP (Delgado et al. 2015a) obligan a diseñar estrategias que permitan aumentar la eficacia de PgAFP asegurando el control de la producción de micotoxinas. Como se ha indicado anteriormente, el uso de bacterias y levaduras que no se vean inhibidas por PgAFP abriría una nueva vía para su uso combinado con PgAFP, incrementado su efecto antifúngico. Como un paso previo para la utilización de esta estrategia se probaron en medio de cultivo con y sin adición de calcio diferentes combinaciones de PgAFP, *D. hansenii* y *P. acidilactici*, microorganismos habitualmente presentes en alimentos madurados. Las cepas de *D. hansenii* Dh253 (Andrade et al. 2014; Núñez et al. 2015) y *P. acidilactici* fargo 35 fueron seleccionadas por su capacidad antifúngica.

Dependiendo del sustrato se obtuvieron resultados distintos. *P. acidilactici* fue el agente que mostró mayor efecto inibidor en medio de cultivo, de modo que provocaba la mayor reducción de micotoxinas tanto cuando se inoculaba de forma aislada como en diferentes combinaciones con PgAFP o *D. hansenii* Dh253. Se asume que *P. acidilactici* produce una bacteriocina que es eficaz en el control de *Listeria monocytogenes* (Montiel et al. 2013), sin embargo se desconocen qué condiciones se produce esta bacteriocina, así como su efecto frente a mohos. Por otra parte, se ha descrito la liberación de sustancias de carácter peptídico y bajo peso molecular al medio por bacterias lácticas, que sin inhibir el crecimiento de mohos son capaces de reducir la producción de toxinas (Chang and Kim 2007; Gourama and Bullerman 1995). En cuanto al efecto de PgAFP, en medio de cultivo al que no se le añadió CaCl_2 , provocó un aumento de producción de micotoxinas por parte de *A. parasiticus*. Este hecho podría estar relacionado con la capacidad de PgAFP de inducir ROS, que contribuyen al inicio de la síntesis de micotoxinas (Jayashree and Subramanyan 2000; Reverberi et al. 2012). Sin embargo, el incremento de la biosíntesis de micotoxinas debido al estrés oxidativo puede descartarse observando los valores de expresión del gen *foxA*, íntimamente ligado a la biosíntesis de aflatoxinas (Reverberi et al. 2012). Por tanto, el estrés oxidativo por sí solo no parece explicar el aumento en la producción de micotoxinas. Además, el papel de las ROS en la producción de

aflatoxinas es controvertido. Recientemente se ha demostrado que durante la producción de aflatoxinas se producen ROS, que a su vez aumentan la tolerancia de las nuevas esporas al estrés oxidativo (Roze et al. 2015). Por otra parte, el aumento en la producción de micotoxinas no se observó en el mismo medio de cultivo cuando contenía calcio, donde tampoco se produjo efecto fungistático. La no estimulación de producción de micotoxinas por parte de PgAFP en presencia de calcio parece ser debida al efecto de la calcineurina y la gamma glutamiltranspeptidasa aumentadas, que limitarían los estímulos estresantes como se discutirá después.

Teniendo en cuenta los resultados obtenidos en medios de cultivo, en alimentos se probaron las combinaciones PgAFP + Dh253 y PgAFP + Dh253 + Pa fargo 35. En salchichón y queso el efecto conjunto de PgAFP y *D. hansenii* disminuyó drásticamente tanto los recuentos como la producción de aflatoxinas por *A. parasiticus*, durante al menos 15 días en un rango amplio de valores de a_w , sin que *P. acidilactici* aportase ningún efecto antifúngico adicional. El efecto conjunto de PgAFP y *D. hansenii* permite maximizar el efecto antifúngico de ambos, ya que la acción aislada de PgAFP se ve limitada en el tiempo (Delgado et al. 2015a) y no es eficaz en alimentos ricos en calcio (Delgado et al. 2015d), y *D. hansenii* no muestra actividad antifúngica a valores de a_w de alrededor de 0.84 (Andrade et al. 2014). De modo que esta combinación muestra un efecto antifúngico duradero y extrapolable a las condiciones físico-químicas de maduración de productos cárnicos crudo-curados y queso. Y por tanto podría incluirse en el sistema de Análisis de Peligros y Puntos de Control Crítico, utilizándose estos agentes bioprotectores tanto como una medida preventiva para evitar el desarrollo de mohos toxigénicos, así como medida correctora, tras eliminar la población fúngica de riesgo. Sorprendentemente, el efecto conjunto de estos dos agentes que carecen de acción por separado en las condiciones probadas ofrece una inhibición de mohos satisfactoria. Este hecho podría explicarse por la acción conjunta de los diferentes mecanismos de acción propuestos para cada uno de estos agentes. De modo que esta cepa de *D. hansenii* compite por el sustrato y el espacio además de producir compuestos volátiles que inhiben el desarrollo de mohos (Núñez et al. 2015), mientras que PgAFP permeabiliza las membranas e induce ROS y apoptosis (Delgado et al. 2015b). Por tanto, este efecto conjunto permitiría desestabilizar la fisiología del moho toxigénico, dando lugar a un efecto inhibitor potenciado.

V.3. Mecanismo de acción de PgAFP

Se analizó la respuesta de una cepa aflatoxigénica sensible de *A. flavus* con y sin la adición de calcio en el medio de cultivo, ya que existen evidencias de que la presencia de estos iones reduce la actividad de proteínas antifúngicas (Galgóczy et al., 2013; Kaiserer et al., 2003; Theis et al., 2003; Thevissen et al., 1999, 1996). Por otra parte, se estudió la respuesta que

permite no ser inhibidos por PgAFP a dos mohos resistentes: la propia cepa de *P. chrysogenum* productora de PgAFP y *P. polonicum*.

En primer lugar se observaron diferencias claras en cuanto al lugar de unión de PgAFP marcada con FITC. En *A. flavus* PgAFP apareció tanto unida en la superficie externa como en el interior celular (Delgado et al. 2015b). Por tanto, el patrón seguido por esta proteína en cuanto a su localización en el moho sensible se asemeja a AFP (Oberparleiter et al. 2003). En este caso las pruebas realizadas no permiten discernir si la localización intracelular es necesaria para que la proteína complete su actividad antifúngica o se produce como consecuencia de esta actividad, y debido al aumento de la permeabilidad celular que se discutirá más adelante. En cuanto a los mohos resistentes se observó una unión de PgAFP en la cubierta externa de *P. polonicum* y de *A. flavus* cultivado en presencia de calcio, mientras que no se unió a la cepa productora *P. chrysogenum* CECT 20922.

Por otra parte, PgAFP no provocó cambios morfológicos en ninguno de los ensayos, tanto en la cepa sensible como en las resistentes, por lo que PgAFP puede catalogarse como proteína no morfogénica, de forma análoga a lo propuesto por (Terras et al. 1992; Osborn et al. 1995) para defensinas de plantas.

Para el estudio de los mecanismos de acción de PgAFP tanto en cepas sensibles como resistentes se evaluaron los cambios en el proteoma utilizando dos técnicas de proteómica comparativa: 2D-PAGE y Label-Free Comparative Proteomics (LFP), ya que cada una de ellas ofrecía ventajas e inconvenientes.

A partir de las alteraciones observadas en la abundancia relativa de proteínas tras el tratamiento con PgAFP, se realizaron diferentes pruebas para comprobar el efecto y el alcance de dichos cambios sobre el metabolismo y la viabilidad de los mohos tratados.

Cada uno de los tres ensayos realizados mostró un número considerable de proteínas cuya concentración relativa se vio alterada por efecto de PgAFP. Fue común en todos los mohos tratados un incremento en el grupo de proteínas ribosomales y del espliceosoma, que además constituyen los grupos más numerosos en los que se observaron diferencias por el tratamiento (Delgado et al. 2015b; Delgado et al. 2015c; Delgado et al. 2015d). Por tanto, esta parece ser una respuesta común de mohos sensibles y resistentes frente a PgAFP, y que no sirve por sí sola para explicar los fenómenos de sensibilidad y resistencia.

Los principales cambios en el proteoma de *A. flavus* tratado con PgAFP radicarón en proteínas relacionadas con el metabolismo energético, la respuesta al estrés y el metabolismo del glutatión, la integridad de la pared celular y la síntesis de aflatoxinas (Delgado et al. 2015b).

De entre esos grupos, las proteínas que se consideran clave para el efecto de PgAFP son la subunidad beta de la proteína G CpcB y la Rho GTPasa Rho1 (Tabla V1), ambas detectadas en menor cantidad en los cultivos tratados. La proteína G se ha relacionado con la señalización de apoptosis en *Aspergillus nidulans* (Binder et al. 2010) por la acción de la proteína antifúngica PAF. En *A. flavus*, una menor cantidad de la subunidad beta provocada por la acción de PgAFP podría desencadenar fenómenos de apoptosis y necrosis (Fig V1). Este extremo se confirmó tras las tinciones realizadas con AO/EB y Anexina-FITC/yoduro de propidio (Delgado et al. 2015b). Rho1 es una proteína clave para la integridad de la pared celular y está relacionada con la biosíntesis de quitina (Levin 2005). Su disminución en *A. flavus* tratado podría relacionarse con la cantidad de quitina depuesta en la pared celular (Fig V1) de *A. flavus* tratado observada tras la tinción realizada con clacoflúor y un incremento de la permeabilidad del moho al SYTOX Green (Delgado et al. 2015b). El aumento de la permeabilidad podría ser la causa de la localización de PgAFP en el interior celular, como se ha comentado anteriormente y también se ha descrito dentro de los mecanismos de acción de otras proteínas antifúngicas como AFP y varias defensinas (Thevissen et al. 1999; Moreno et al. 2006). Los cambios observados en proteínas implicadas en el metabolismo del glutatión pueden ser indicios de una respuesta a un presunto estrés oxidativo desencadenado como consecuencia de la actividad de PgAFP, tal como se ha señalado para PAF y NFAP (Leiter et al. 2005; Galgóczy et al. 2013). Sin embargo, este incremento parece ser insuficiente para contrarrestar los mayores niveles de ROS provocados por PgAFP (Delgado et al. 2015b), que también podrían influir en la puesta en marcha de los fenómenos de apoptosis observados. Además, la inhibición observada también debe estar relacionada con una menor disponibilidad de energía, a raíz de los datos ofrecidos por los análisis de proteómica comparativa. PgAFP produjo un descenso en varias proteínas pertenecientes a las rutas metabólicas de glucólisis/gluconeogénesis, que se tradujo en una menor actividad metabólica en *A. flavus* observada mediante la tinción con FUN-1 (Delgado et al. 2015b). Por último, cabe destacar la menor cantidad de proteínas relacionadas con la biosíntesis de aflatoxinas. Este efecto es prometedor para el control de estos metabolitos en alimentos. Sin embargo, hay que tener en cuenta que PgAFP desencadena estrés oxidativo, y que este hecho podría estimular la síntesis de micotoxinas (Jayashree and Subramanyan 2000; Reverberi et al. 2012). Por lo tanto, es necesario estudiar la cantidad de estas proteínas en incubaciones más prolongadas y que permitan evaluar de una forma más precisa el efecto de PgAFP sobre la síntesis de aflatoxinas.

proteína, de mohos resistentes de forma natural, como *P. polonicum* o de la resistencia inducida en *A. flavus* por la presencia de calcio.

La resistencia del moho productor de PgAFP, *P. chrysogenum* CETC 20922, parece estar relacionada con la ausencia de receptores para esta proteína en la capa externa celular, dado que no se observa la presencia de PgAFP marcada con FITC en ninguna estructura ni extra ni intracelular (Delgado et al. 2015b). Por lo tanto PgAFP no interacciona con *P. chrysogenum* CETC 20922 y consecuentemente no produce ningún efecto inhibitor. Este hecho se vio corroborado por la ausencia de cambios en los ensayos metabólicos o de viabilidad realizados.

Tampoco los ensayos metabólicos y de viabilidad mostraron cambios en *P. polonicum* tratado con PgAFP. Sin embargo, en este caso sí se observó una unión de PgAFP en la cubierta externa del moho (Delgado et al. 2015c). Como consecuencia de esta unión el proteoma de *P. polonicum* se vio afectado, lo que permite descartar que la carencia de interacción entre PgAFP y el moho sea la causa de la resistencia, sino más bien diferentes mecanismos que *P. polonicum* pone en marcha para contrarrestar el efecto de PgAFP. La mayor cantidad de la proteína Rho GTPasa Rho1 detectada en las muestras tratadas con PgAFP parece ser fundamental para la mayor deposición de quitina observada en el moho con respecto al control no tratado (Fig V1). Este hecho explica parcialmente la disminución de permeabilidad al SYTOX Green en las hifas tratadas con PgAFP, contribuyendo todo ello a la protección frente a PgAFP. Dada la localización de PgAFP, exclusivamente en la cubierta externa de este moho, y que la síntesis de quitina está relacionada con la resistencia, podría pensarse que la proteína antifúngica podría unirse específicamente a la quitina, como se ha observado para AFP (Liu et al. 2002). Sin embargo, PgAFP no tiene capacidad de unirse a quitina regenerada (Delgado et al. 2015c). Por otra parte, *P. polonicum* fue relativamente sensible al tratamiento conjunto con quitinasa y PgAFP. Por lo tanto, la cantidad de quitina depuesta, mediada por Rho1, juega un papel clave en la sensibilidad o resistencia de los mohos a PgAFP. La resistencia en *P. polonicum* va acompañada de un aumento de la quitina, mientras que la sensibilidad de *A. flavus* va ligada a una disminución de quitina (Delgado et al. 2015b) (Fig V1). En consecuencia, puede proponerse la utilización conjunta con quitinasa para aumentar el espectro de inhibición de mohos de PgAFP y por lo tanto la eficiencia del tratamiento antifúngico.

V.4.1. Influencia del calcio en la actividad inhibitora de PgAFP

Como se ha indicado anteriormente, *A. flavus* deja de ser sensible al tratamiento con PgAFP en presencia de calcio, observándose un crecimiento normal y una respuesta a los diferentes ensayos metabólicos y de viabilidad idéntica a la del moho sin tratar. La resistencia

de los mohos a proteínas antifúngicas en presencia de cationes, en el caso de AFP se ha atribuido a que éstos impiden la unión de específica de la proteína al moho porque bloquean por saturación los receptores específicos (Marx 2004). Sin embargo, esta hipótesis puede descartarse en el caso de *A. flavus* tratado con PgAFP en medio enriquecido en calcio, dado que por una parte se observó una unión de la proteína en el exterior del moho y por otra, que se detectaron alteraciones en su proteoma. Estos cambios en el proteoma parecen estar relacionados con una respuesta satisfactoria de *A. flavus* para contrarrestar el efecto de PgAFP gracias a la presencia de calcio, como por ejemplo el aumento de la gamma glutamiltranspeptidasa. La presencia de calcio, tanto en *A. flavus* tratado como sin tratar con PgAFP, provoca un aumento de la subunidad reguladora de la calcineurina que se une al Ca^{2+} Calcineurina CnaB (Delgado et al. 2015d). Dado que la ruta de la calcineurina está implicada en la adaptación al estrés (Juvvadi et al. 2003), este aumento en la señalización ayudaría a contrarrestar los efectos de PgAFP. Por otra parte, también se observó una mayor cantidad de CpcB, cuya importancia en el mecanismo de inhibición se ha descrito anteriormente, siendo mayor en *A. flavus* tratado con PgAFP en presencia de calcio que sin adición de este catión (Tabla V1), lo que puede relacionarse con la ausencia de ROS y de señales apoptóticas. Todo parece indicar, que gracias a los mayores niveles de calcineurina que provoca el calcio *per se*, *A. flavus* consigue mantener el balance redox en las primeras horas de exposición a PgAFP. Esto puede explicar que se mantengan los niveles de Rho1 y la cantidad de quitina depuesta. Por tanto, limitaría el acceso de PgAFP al citoplasma, permitiendo al moho poner en marcha mecanismos para contrarrestar las ROS, como mayores niveles de gamma glutamiltranspeptidasa, resultando en un balance antioxidante positivo (Fig V1).

El estudio del proteoma de *A. flavus* cultivado en cuatro diferentes combinaciones de ausencia/presencia de PgAFP y 0/0.1M CaCl_2 , realizando un agrupamiento jerárquico y *heat map*, ha permitido obtener las diferencias que se muestran en la Fig. V2. Los perfiles de los dos cultivos de *A. flavus* en ausencia de calcio, tratado y no tratado con PgAFP, son los que se encuentran más alejados el uno del otro, como puede observarse en el agrupamiento jerárquico realizado a partir de los proteomas obtenidos. Por el contrario, los dos proteomas más parecidos son los pertenecientes a *A. flavus* tratado con PgAFP y sin tratar cultivados con 0.1M de CaCl_2 . Este hecho parece deberse a que el efecto del calcio *per se* induce cambios en *A. flavus* que le permiten contrarrestar el efecto de PgAFP.

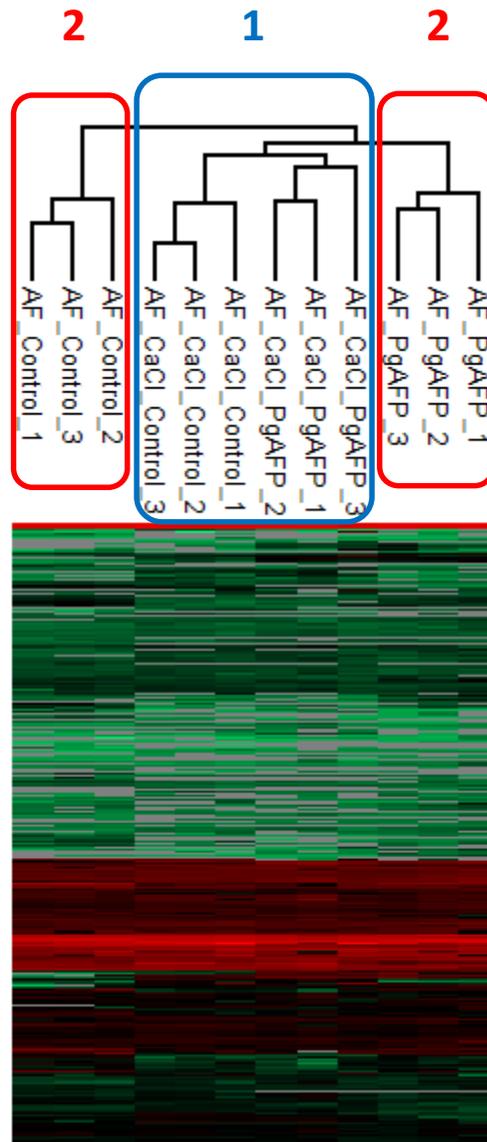


Figura V2. *Heat map* demostrando el agrupamiento jerárquico del análisis comparativo por LFP. Este análisis demuestra que *A. flavus* cultivado en medio rico en CaCl_2 exhibe menos variabilidad cuando es tratado con PgAFP (1), que en ausencia de CaCl_2 (2).

De todo ello se desprende que existen rutas metabólicas comunes para los fenómenos de sensibilidad y resistencia, y que una mayor o menor cantidad de algunas proteínas claves pertenecientes a estas rutas parecen modular la señalización que acaba conduciendo a la supervivencia o muerte de los mohos (Fig V1). Entre estas proteínas cabe destacar la CpcB, la Rho GTPase Rho1 y otras pertenecientes a la ruta del glutatión (Tabla V1). Sin embargo, no siempre están todas implicadas en los mecanismos de sensibilidad/resistencia que se han evaluado en este trabajo, sino que de forma aislada pueden actuar modulando las respuestas que marcan la diferencia entre supervivencia o muerte de los mohos (Fig V1).

Tabla V1. Aumento (↑) o disminución (↓) relativa en la cantidad de proteínas implicadas en los fenómenos de resistencia/sensibilidad frente a PgAFP.

Nombre de la proteína	<i>Aspergillus</i>	<i>Aspergillus flavus</i>	<i>Penicillium</i>
	<i>flavus</i>	0.1 M CaCl ₂	<i>polonicum</i>
G protein complex beta subunit CpcB	↓	↑	-
Rho GTPase Rho1	↓	-	↑
Gamma-glutamyltranspeptidase	↓	↑	-
Glutathione S-transferase	↓	-	-
Cys-Gly metallopeptidase Dug1	↑	-	-
Glutathione synthetase	↑	-	-
Glutathione S-transferase GliG-like	↑	↑	-
Glutathione-S-transferase theta, GST	↑	-	-
Cell wall biogenesis protein glutathione transferase (Gto1)	-	-	↑

Por todo lo anteriormente expuesto, se puede considerar que las proteínas antifúngicas producidas por mohos comparten similitudes en cuanto a sus mecanismos de acción, pero no son exactamente iguales para todas las proteínas. En particular, la resistencia y sensibilidad frente a PgAFP está modulada a través de dos vías, relacionadas con la deposición de quitina y aumento/disminución de ROS mediadas respectivamente por Rho1 y CpcB (Fig. V1), donde las cantidades de estas dos proteínas juegan un papel fundamental en la supervivencia del moho. Además, algunas de las proteínas implicadas en la ruta metabólica del glutatión contribuyen a una respuesta satisfactoria o insatisfactoria frente a las ROS inducidas por PgAFP. En particular, la gamma glutamiltranspeptidasa parece que juega un papel fundamental contrarrestando las ROS, mientras las demás no ofrecen una respuesta de supervivencia satisfactoria (Tabla V1 y Fig. V2). Estos cambios parecen estar relacionados con los altos niveles de calcineurina provocados por una alta concentración de calcio extracelular.

Este trabajo se ha orientado al desarrollo de estrategias para controlar mohos toxigénicos en alimentos. Se ha estudiado el mecanismo de acción y el de resistencia frente a la proteína antifúngica PgAFP, habiéndose diseñado sistemas complementarios para maximizar el efecto de PgAFP. Dado el resultado satisfactorio de la combinación de PgAFP y *D. hansenii* para controlar mohos toxigénicos, se propone su uso como cultivo protector para alimentos madurados de humedad intermedia. De este modo se podría mejorar la seguridad alimentaria para este tipo de alimentos y se reduciría el riesgo para la salud del consumidor.

VI. CONCLUSIONS

PgAFP inhibits a wide range of unwanted moulds in culture media, including the main mycotoxin-producing species. The mechanism of action involves lower relative quantity of Rho1 and G-protein subunit β CpcB and leads to apoptotic and necrotic events triggered by reduced metabolic activity, altered cell wall integrity and increased oxidative stress.

PgAFP increases aflatoxin production by *Aspergillus parasiticus* in culture medium, being not related to changes in peroxisomal β -oxidation.

Intrinsic resistance to PgAFP is due to an activated cell wall integrity pathway through increased Rho1 levels leading to higher chitin deposition in *P. polonicum* or the lack of specific receptors in the outer layer of the PgAFP-producer *P. chrysogenum*.

Calcium abolishes PgAFP inhibition of *A. parasiticus* in culture medium but efficiently decreases aflatoxin production, keeping cell wall integrity and redox balance where increased calcineurin and γ -glutamyltranspeptidase levels play a key role. Similarly, PgAFP displays valuable antifungal ability on dry-fermented sausage but not on ripened cheese, which is also attributed to the high calcium content of the latter.

Pediococcus acidilactici dramatically lowers aflatoxin production by *A. parasiticus* in culture media, even with a high calcium content, but does not enhance the antifungal activity accomplished by the other biopreservative agents on intermediate moisture foods.

The combined treatment of *Debaryomyces hansenii* and PgAFP overcomes the limitations of their individual use, efficiently lowering both aflatoxigenic mould load and aflatoxin production in dry-fermented sausage and ripened cheese.

Appropriate combinations of PgAFP with other biopreservative agents would improve intermediate moisture foods safety by efficiently lowering toxigenic molds counts and mycotoxin production.

VII. BIBLIOGRAFÍA

- Acosta R (2006) Selección de *Penicillium* productores de péptidos antifúngicos para su utilización en productos cárnicos madurados. Tesis doctoral
- Acosta R, Rodríguez-Martín A, Martín A, Núñez F, Asensio MA (2009) Selection of antifungal protein-producing molds from dry-cured meat products. *International Journal of Food Microbiology* 135:39–46. doi: 10.1016/j.ijfoodmicro.2009.07.020
- Andrade MJ, Córdoba JJ, Casado EM, Córdoba MG, Rodríguez M (2010) Effect of selected strains of *Debaryomyces hansenii* on the volatile compound production of dry fermented sausage “salchichón.” *Meat Science* 85:256–264. doi: 10.1016/j.meatsci.2010.01.009
- Andrade MJ, Córdoba JJ, Sánchez B, Casado EM, Rodríguez M (2009) Evaluation and selection of yeasts isolated from dry-cured Iberian ham by their volatile compound production. *Food Chemistry* 113:457–463. doi: 10.1016/j.foodchem.2008.07.080
- Andrade MJ, Thorsen L, Rodríguez A, Córdoba JJ, Jespersen L (2014) Inhibition of ochratoxigenic moulds by *Debaryomyces hansenii* strains for biopreservation of dry-cured meat products. *International Journal of Food Microbiology* 170:70–77. doi: 10.1016/j.ijfoodmicro.2013.11.004
- Armando MR, Dogi CA, Poloni V, Rosa CAR, Dalcero AM, Cavaglieri LR (2013) In vitro study on the effect of *Saccharomyces cerevisiae* strains on growth and mycotoxin production by *Aspergillus carbonarius* and *Fusarium graminearum*. *International Journal of Food Microbiology* 161:182–188. doi: 10.1016/j.ijfoodmicro.2012.11.016
- Asefa DT, Kure CF, Gjerde RO, Langsrud S, Omer MK, Nesbakken T, Skaar I (2011) A HACCP plan for mycotoxigenic hazards associated with dry-cured meat production processes. *Food Control* 22:831–837. doi: 10.1016/j.foodcont.2010.09.014
- Asefa DT, Møretrø T, Gjerde RO, Langsrud S, Kure CF, Sidhu MS, Nesbakken T, Skaar I (2009) Yeast diversity and dynamics in the production processes of Norwegian dry-cured meat products. *International Journal of Food Microbiology* 133:135–40. doi: 10.1016/j.ijfoodmicro.2009.05.011
- Asensio MA; Núñez F, Bermúdez E, Martín A, Alonso M, Acosta R, Sosa MJ, Córdoba JJ (2004) Interés Del Control de los mohos en el jamón curado, Avances en la ciencia y Tecnología y comercialización del jamón, Editorial Conjamón.
- Asensio MA, Núñez F, Delgado J, Bermúdez E (2014) Control of Toxigenic Molds in Food Processing. In: Rai VR, Bai AJ (eds) *Microbial Food Safety and Preservation Techniques*. CRC Press (Taylor and Francis), Boca Raton, (Florida, E.E.U.U.), pp 329–357
- Baskić D, Popović S, Ristić P, Arsenijević NN (2006) Analysis of cycloheximide-induced apoptosis in human leukocytes: fluorescence microscopy using annexin V/propidium iodide versus acridin orange/ethidium bromide. *Cell Biology International* 30:924–932. doi: 10.1016/j.cellbi.2006.06.016
- Bernáldez V, Rodríguez A, Martín A, Lozano D, Córdoba JJ (2014) Development of a multiplex qPCR method for simultaneous quantification in dry-cured ham of an antifungal-peptide *Penicillium chrysogenum* strain used as protective culture and aflatoxin-producing moulds. *Food Control* 36:257–265. doi: 10.1016/j.foodcont.2013.08.020
- Bertuzzi T, Gualla A, Morlacchini M, Pietri A (2013) Direct and indirect contamination with ochratoxin A of ripened pork products. *Food Control* 34:79–83. doi: 10.1016/j.foodcont.2013.04.011
- Bezerra da Rocha ME, Oliveira Freire FDC, Feitosa Maia FE, Florindo Guedes MI, Rondina D (2014) Mycotoxins and their effects on human and animal health. *Food Control* 36:159–165. doi: 10.1016/j.foodcont.2013.08.021
- Binder U, Bencina M, Eigentler A, Meyer V, Marx F (2011) The *Aspergillus giganteus* antifungal protein AFPNN5353 activates the cell wall integrity pathway and perturbs calcium homeostasis. *BMC Microbiology* 11:209. doi: 10.1186/1471-2180-11-209
- Binder U, Oberparleiter C, Meyer V, Marx F (2010) The antifungal protein PAF interferes with PKC/MPK and cAMP/PKA signalling of *Aspergillus nidulans*. *Molecular Microbiology* 75:294–307. doi: 10.1111/j.1365-2958.2009.06936.x
- Boselli E, Rodriguez-Estrada MT, Fedrizzi G, Caboni MF (2009) Cholesterol photosensitized oxidation of beef meat under standard and modified atmosphere at retail conditions. *Meat Science* 81:224–229. doi: 10.1016/j.meatsci.2008.07.023
- Breuer U, Harms H (2006) *Debaryomyces hansenii* - An extremophilic yeast with biotechnological potential. *Yeast* 23:415–437. doi: 10.1002/yea.1374
- Broekaert WF, Terras FRG, Cammue BPA, Vanderleyden J (1990) An automated quantitative assay for fungal growth inhibition. *FEMS Microbiology Letters* 69:55–59. doi: 10.1111/j.1574-6968.1990.tb04174.x

- Bruna JM, Hierro EM, De La Hoz L, Mottram DS, Fernández M, Ordóñez JA. (2001) The contribution of *Penicillium aurantiogriseum* to the volatile composition and sensory quality of dry fermented sausages. *Meat Science* 59:97–107. doi: 10.1016/S0309-1740(01)00058-4
- Bullerman LB (1984) Effects of potassium sorbate on growth and patulin production by *Penicillium patulum* and *Penicillium roqueforti*. *Journal of Food Protection* 47:312–320.
- Bullerman LB, Bianchini A (2007) Stability of mycotoxins during food processing. *International Journal of Food Microbiology* 119:140–146. doi: 10.1016/j.ijfoodmicro.2007.07.035
- Byczkowska A, Kunikowska A, Kaźmierczak A (2012) Determination of ACC-induced cell-programmed death in roots of *Vicia faba* ssp. minor seedlings by acridine orange and ethidium bromide staining. *Protoplasma* 250:121–128. doi: 10.1007/s00709-012-0383-9
- Cagas SE, Jain MR, Li H, Perlin DS (2011) Profiling the *Aspergillus fumigatus* proteome in response to caspofungin. *Antimicrobial Agents and Chemotherapy* 55:146–154. doi: 10.1128/AAC.00884-10
- Cano-García L, Belloch C, Flores M (2014) Impact of *Debaryomyces hansenii* strains inoculation on the quality of slow dry-cured fermented sausages. *Meat Science* 96:1469–1477. doi: 10.1016/j.meatsci.2013.12.011
- Carberry S, Molloy E, Hammel S, O’Keeffe G, Jones GW, Kavanagh K, Doyle S (2012) Gliotoxin effects on fungal growth: mechanisms and exploitation. *Fungal Genetics and Biology: FG & B* 49:302–312. doi: 10.1016/j.fgb.2012.02.003
- Carberry S, Neville CM, Kavanagh KA, Doyle S (2006) Analysis of major intracellular proteins of *Aspergillus fumigatus* by MALDI mass spectrometry: identification and characterisation of an elongation factor 1B protein with glutathione transferase activity. *Biochemical and Biophysical Research Communications* 341:1096–1104. doi: 10.1016/j.bbrc.2006.01.078
- Carpentier SC, Witters E, Laukens K, Deckers P, Swennen R, Panis B (2005) Preparation of protein extracts from recalcitrant plant tissues: an evaluation of different methods for two-dimensional gel electrophoresis analysis. *Proteomics* 5:2497–2507. doi: 10.1002/pmic.200401222
- Casas E, de Ancos B, Valderrama MJ, Cano P, Peinado JM (2004) Pentadiene production from potassium sorbate by osmotolerant yeasts. *International Journal of Food Microbiology* 94:93–6. doi: 10.1016/j.ijfoodmicro.2004.01.001
- Castellanos L, González LJ, Padrón G (2004). *Proteómica. Combinatoria molecular*. Ed: Dania del Rosario Silva Hernández y Ana María Mariña Leyva
- Chalutz E, Wilson CL (1990) Postharvest biocontrol of green and blue mold and sour rot of citrus fruit by *Debaryomyces hansenii*. *Plant Disease* 74:134.
- Chang I, Kim J (2007) Inhibition of aflatoxin production of *Aspergillus flavus* by *Lactobacillus casei*. *Mycobiology* 35:76–81.
- Chekri R, Noël L, Millour S, Vastel C, Kadar A, Sirot V, Leblanc JC, Guérin T (2012) Calcium, magnesium, sodium and potassium levels in foodstuffs from the second French Total Diet Study. *Journal of Food Composition and Analysis* 25:97–107. doi: 10.1016/j.jfca.2011.10.005
- Chen Z, Ao J, Yang W, Jiao L, Zheng T, Chen X (2013) Purification and characterization of a novel antifungal protein secreted by *Penicillium chrysogenum* from an Arctic sediment. *Applied Microbiology and Biotechnology* 97:10381–10390. doi: 10.1007/s00253-013-4800-6
- Chu KT, Liu KH, Ng TB (2003) Cicerarin, a novel antifungal peptide from the green chickpea. *Peptides* 24:659–663. doi: 10.1016/S0196-9781(03)00134-7
- Cigić IK, Prosen H (2009) An overview of conventional and emerging analytical methods for the determination of mycotoxins. *International Journal of Molecular Sciences* 10:62–115. doi: 10.3390/ijms10010062
- Cociancich S, Ghazi A, Hetru A, Hoffman JA, Letellier L (1993) Insect defensin, an inducible antibacterial peptide, forms voltage-dependent channels in *Micrococcus luteus*. *The Journal of Biological Chemistry*. 268:19239-19245
- Coelho AR, Celli MG, Ono EYS, Wosiacki G, Hoffmann FL, Pagnocca FC, Hirooka EY (2007) *Penicillium expansum* versus antagonist yeasts and patulin degradation in vitro. *Brazilian Archives of Biology and Technology* 50:725–733. doi: 10.1590/S1516-89132007000400019
- Collins C, Keane TM, Turner DJ, O’Keeffe G, Fitzpatrick DA, Doyle S (2013) Genomic and proteomic dissection of the ubiquitous plant pathogen, *Armillaria mellea*: Toward a new infection model system. *Journal of Proteome Research* 12:2552–2570. doi: 10.1021/pr301131t
- Comi G, Iacumin L (2013) Ecology of moulds during the pre-ripening and ripening of San Daniele dry cured ham. *Food Research International* 54:1113–1119. doi: 10.1016/j.foodres.2013.01.031

- Comi G, Manzano M, Brichese R, Iacumin L (2014) New cause of spoilage in San Daniele dry cured ham. *Journal of Food Safety* 34:263–269. doi: 10.1111/jfs.12122
- Comisión Europea (2010a) Reglamento (EU) N° 165/2010 de la comisión que modifica, en lo que respecta a las aflatoxinas, el Reglamento (CE) n o 1881/2006 por el que se fija el contenido máximo de determinados contaminantes en los productos alimenticios. *Diario Oficial de la Unión Europea* 8–12.
- Comisión Europea (2010b) Reglamento (UE) 105/2010 de la Comisión de 5 de febrero de 2010 que modifica el Reglamento (CE) 1881/2006, por el que se fija el contenido máximo de determinados contaminantes en los productos alimenticios por lo que se refiere a la ocratoxina A. *Diario Oficial de la Unión Europea* L35:7–8.
- Comisión Europea (2006) Reglamento (CE) 1881/2006 de la Comisión, de 19 de diciembre de 2006 por el que se fija el contenido máximo de determinados contaminantes en los productos alimenticios. *Diario Oficial de la Unión Europea* 2006:5–24.
- Comisión Europea (2007) Reglamento (CE) 1126/2007 de 28 de septiembre de 2007 que modifica el Reglamento (CE) no 1881/2006 por el que se fija el contenido máximo de determinados contaminantes en los productos alimenticios por lo que se refiere a las toxinas de *Fusarium* en el maíz. *Diario Oficial de la Unión Europea* L 255:14–17.
- Comisión Europea (2005) Directiva 2005/38/CE de la Comisión de 6 de junio de 2005 por la que se establecen los métodos de muestreo y de análisis para el control oficial del contenido de toxinas de *Fusarium* en los productos alimenticios. *Diario Oficial de la Unión Europea* L 143:18–26.
- Cox J, Mann M (2008) MaxQuant enables high peptide identification rates, individualized p.p.b.-range mass accuracies and proteome-wide protein quantification. *Nature Biotechnology* 26:1367–1372. doi: 10.1038/nbt.1511
- Crowley S, Mahony J, Van Sinderen D (2013) Current perspectives on antifungal lactic acid bacteria as natural bio-preservatives. *Trends in Food Science and Technology* 33:93–109. doi: 10.1016/j.tifs.2013.07.004
- Dalié DKD, Deschamps AM, Richard-Forget F (2010) Lactic acid bacteria - Potential for control of mould growth and mycotoxins: A review. *Food Control* 21:370–380. doi: 10.1016/j.foodcont.2009.07.011
- Delgado J, Acosta R, Rodríguez-Martín A, Bermúdez E, Núñez F, Asensio MA (2015a) Growth inhibition and stability of PgAFP from *Penicillium chrysogenum* against fungi common on dry-ripened meat products. *International Journal of Food Microbiology* 205:23–29. doi: 10.1016/j.ijfoodmicro.2015.03.029
- Delgado J, Owens RA, Doyle S, Asensio MA, Núñez F (2015b) Impact of the antifungal protein PgAFP from *Penicillium chrysogenum* on the protein profile in *Aspergillus flavus*. *Applied Microbiology and Biotechnology* 99:8701–8715. doi: 10.1007/s00253-015-6731-x
- Delgado J, Owens RA, Doyle S, Asensio MA, Núñez F (2015c) Increased chitin biosynthesis contributes to the resistance of *Penicillium polonicum* against the antifungal protein PgAFP. *Applied Microbiology and Biotechnology*. doi: 10.1007/s00253-015-7020-4
- Delgado J, Owens RA, Doyle S, Asensio MA, Núñez F (2015d) Proteome changes explain calcium-mediated ineffectiveness of the antifungal protein PgAFP against *Aspergillus flavus* in cheese. Unpublished paper
- Druvefors UA, Passoth V, Schnürer J (2005) Nutrient effects on biocontrol of *Penicillium roqueforti* by *Pichia anomala* J121 during airtight storage of wheat. *Applied and environmental microbiology* 71:1865–9. doi: 10.1128/AEM.71.4.1865-1869.2005
- Dolan SK, Owens RA, O’Keeffe G, Hammel S, Fitzpatrick DA, Jones GW, Doyle S (2014) Regulation of nonribosomal peptide synthesis: bis-thiomethylation attenuates gliotoxin biosynthesis in *Aspergillus fumigatus*. *Chemistry & Biology* 21:999–1012. doi: 10.1016/j.chembiol.2014.07.006
- El-Ghaouth A, Wilson CL, Wisniewski M (1998) Ultrastructural and cytochemical aspects of the biological control of *Botrytis cinerea* by *Candida saitoana* in apple fruit -. *Phytopathology* 88:282–291.
- Feroli F, Caboni MF, Dutta PC (2008) Evaluation of cholesterol and lipid oxidation in raw and cooked minced beef stored under oxygen-enriched atmosphere. *Meat Science* 80:681–685. doi: 10.1016/j.meatsci.2008.03.005
- Friedrich C, Scott MG, Karunaratne N, Yan H, Hancock RE (1999) Salt-resistant alpha-helical cationic antimicrobial peptides. *Antimicrobial Agents and Chemotherapy* 43:1542–1548.
- Galgóczy L, Kovács L, Karácsony Z, Virágh M, Hamari Z, Vágvölgyi C (2013) Investigation of the antimicrobial effect of *Neosartorya fischeri* antifungal protein (NFAP) after heterologous expression in *Aspergillus nidulans*. *Microbiology (Reading, England)* 159:411–419. doi: 10.1099/mic.0.061119-0
- Gautam P, Shankar J, Madan T, Sirdeshmukh R, Sundaram CS, Gade WN, Basir SF, Sarma PU (2008) Proteomic and transcriptomic analysis of *Aspergillus fumigatus* on exposure to amphotericin B. *Antimicrobial Agents and Chemotherapy* 52:4220–4227. doi: 10.1128/AAC.01431-07

- Geisen R (2000) *P. nalgiovense* carries a gene which is homologous to the *paf* gene of *P. chrysogenum* which codes for an antifungal peptide. *International Journal of Food Microbiology* 62:95–101. doi: 10.1016/S0168-1605(00)00367-6
- Gil-Serna J, Patiño B, Cortés L, González-Jaén MT, Vázquez C (2011) Mechanisms involved in reduction of ochratoxin A produced by *Aspergillus westerdijkiae* using *Debaryomyces hansenii* CYC 1244. *International Journal of Food Microbiology* 151:113–118. doi: 10.1016/j.ijfoodmicro.2011.08.012
- Görg A, Drews O, Lück C, Weiland F, Weiss W (2009) 2-DE with IPGs. *Electrophoresis* 30 Suppl 1:S122–32. doi: 10.1002/elps.200900051
- Gourama H, Bullerman LB (1995) Inhibition of growth and aflatoxin production of *Aspergillus flavus* by *Lactobacillus* species. *Journal of Food Protection*. 58- 1249-1256
- Groll AH, De Lucca AJ, Walsh TJ (1998) Emerging targets for the development of novel antifungal therapeutics. *Trends in Microbiology* 6:117–24.
- Gun Lee D, Shin SY, Maeng CY, Jin ZZ, Kim KL, Hahm KS (1999) Isolation and characterization of a novel antifungal peptide from *Aspergillus niger*. *Biochemical and Biophysical Research Communications* 263:646–651. doi: 10.1006/bbrc.1999.1428
- Hajji M, Jellouli K, Hmidet N, Balti R, Sellami-Kamoun A, Nasri M (2010) A highly thermostable antimicrobial peptide from *Aspergillus clavatus* ES1: Biochemical and molecular characterization. *Journal of Industrial Microbiology and Biotechnology* 37:805–813. doi: 10.1007/s10295-010-0725-6
- Harris SD, Morrell JL, Hamer J (1994) Identification and characterization of *Aspergillus nidulans* mutants defective in cytokinesis. *Genetics* 532:517–532.
- Harwig J, Scott PM (1971) Brine shrimp (*Artemia salina*) larvae as a screening system for fungal toxins. *Applied Microbiology* 21:1011–1016.
- Hegedus N, Leiter E, Kovács B, Tomori V, Kwon N-J, Emri T, Marx F, Batta G, Csernoch L, Haas H, Yu J-H, Pócsi I (2011) The small molecular mass antifungal protein of *Penicillium chrysogenum*-a mechanism of action oriented review. *Journal of Basic Microbiology* 51:561–571. doi: 10.1002/jobm.201100041
- Heid CA, Stevens J, Livak KJ, Williams PM (1996) Real time quantitative PCR. *Genome Research* 6:986–994. doi: 10.1101/gr.6.10.986
- Hernández E, Huerta T (1993) Evolution of the microbiological parameters of cured ham. *Microbiologia SEM* 9:10-19
- Hernández A, Martín A, Córdoba MG, Benito MJ, Aranda E, Pérez-Nevado F (2008) Determination of killer activity in yeasts isolated from the elaboration of seasoned green table olives. *International Journal of Food Microbiology* 121:178–188. doi: 10.1016/j.ijfoodmicro.2007.11.044
- Hernández-Montiel LG, Ochoa JL, Troyo-Diéguez E, Larralde-Corona CP (2010) Biocontrol of postharvest blue mold (*Penicillium italicum* Wehmer) on Mexican lime by marine and citrus *Debaryomyces hansenii* isolates. *Postharvest Biology and Technology* 56:181–187. doi: 10.1016/j.postharvbio.2009.12.010
- Hicks JK, Yu JH, Keller NP, Adams TH (1997) *Aspergillus* sporulation and mycotoxin production both require inactivation of the FadA Gα protein-dependent signaling pathway. *EMBO Journal* 16:4916–4923. doi: 10.1093/emboj/16.16.4916
- Hilpert K, McLeod B, Yu J, Elliott MR, Rautenbach M, Ruden S, Bürck J, Muhle-Goll C, Ulrich AS, Keller S, Hancock REW (2010) Short cationic antimicrobial peptides interact with ATP. *Antimicrobial Agents and Chemotherapy* 54:4480–4483. doi: 10.1128/AAC.01664-09
- Holzappel WH, Geisen R, Schillinger U (1995) Biological preservation of foods with reference to protective cultures, bacteriocins and food-grade enzymes. *International Journal of Food Microbiology* 24:343–362. doi: 10.1016/0168-1605(94)00036-6
- Hong SY, Park TG, Lee KH (2001) The effect of charge increase on the specificity and activity of a short antimicrobial peptide. *Peptides* 22:1669–74.
- Hoover DM, Wu Z, Tucker K, Lu W, Lubkowski J (2003) Antimicrobial Characterization of Human α -Defensin 3 Derivatives. *Antimicrobial Agents and Chemotherapy* 47:2804–2809. doi: 10.1128/AAC.47.9.2804
- Jayashree T, Subramanyan C (2000) Oxidative stress as a prerequisite for aflatoxin production by *Aspergillus parasiticus*. *Free Radical Biology & Medicine* 29:981–985.

- Juvvadi PR, Kuroki Y, Arioka M, Nakajima H, Kitamoto K (2003) Functional analysis of the calcineurin-encoding gene *cnaA* from *Aspergillus oryzae*: evidence for its putative role in stress adaptation. *Archives of Microbiology* 179:416–422. doi: 10.1007/s00203-003-0546-3
- Kaiserer L, Oberparleiter C, Weiler-Görz R, Burgstaller W, Leiter E, Marx F (2003) Characterization of the *Penicillium chrysogenum* antifungal protein PAF. *Archives of Microbiology* 180:204–210. doi: 10.1007/s00203-003-0578-8
- Kim JH, Yu J, Mahoney N, Chan KL, Molyneux RJ, Varga J, Bhatnagar D, Cleveland TE, Nierman WC, Campbell BC (2008) Elucidation of the functional genomics of antioxidant-based inhibition of aflatoxin biosynthesis. *International Journal of Food Microbiology* 122:49–60. doi: 10.1016/j.ijfoodmicro.2007.11.058
- Kniemeyer O, Schmidt AD, Vödisch M, Wartenberg D, Brakhage AA (2011) Identification of virulence determinants of the human pathogenic fungi *Aspergillus fumigatus* and *Candida albicans* by proteomics. *International Journal of Medical Microbiology* 301:368–377. doi: 10.1016/j.ijmm.2011.04.001
- Köppen R, Koch M, Siegel D, Merkel S, Maul R, Nehls I (2010) Determination of mycotoxins in foods: Current state of analytical methods and limitations. *Applied Microbiology and Biotechnology* 86:1595–1612. doi: 10.1007/s00253-010-2535-1
- Kovács L, Virágh M, Takó M, Papp T, Vágvölgyi C, Galgóczy L (2011) Isolation and characterization of *Neosartorya fischeri* antifungal protein (NFAP). *Peptides* 32:1724–1731. doi: 10.1016/j.peptides.2011.06.022
- Lacadena J, Martínez Del Pozo A, Gasset M, Patiño B, Campos-Olivas R, Vázquez C, Martínez-Ruiz A, Mancheño J, Oñaderra M, JGG (1995) Characterization of the antifungal protein secreted by the mould *Aspergillus giganteus*. *Archives of Biochemistry and Biophysics* 324:273–281.
- Leiter É, Szappanos H, Oberparleiter C, Kaiserer L, Csernoch L, Pusztahelyi T, Emri T, Pócsi I, Salvenmoser W, Marx F (2005) Antifungal protein PAF severely affects the integrity of the plasma membrane of *Aspergillus nidulans* and induces an apoptosis-like phenotype. *Antimicrobial Agents and Chemotherapy* 49:2445–2453. doi: 10.1128/AAC.49.6.2445
- Lennox JE, McElroy LJ (1984) Inhibition of growth and patulin synthesis in *Penicillium expansum* by potassium sorbate and sodium propionate in culture. *Applied and Environmental Microbiology* 48:1031–1033.
- Lessing F, Kniemeyer O, Wozniok I, Loeffler J, Kurzai O, Haertl A, Brakhage AA (2007) The *Aspergillus fumigatus* transcriptional regulator AfYap1 represents the major regulator for defense against reactive oxygen intermediates but is dispensable for pathogenicity in an intranasal mouse infection model. *Eukaryotic Cell* 6:2290–2302. doi: 10.1128/EC.00267-07
- Levin DE (2005) Cell wall integrity signaling in *Saccharomyces cerevisiae*. *Microbiology and Molecular Biology Reviews* 69:262–291. doi: 10.1128/MMBR.69.2.262
- Li H, Zhang S, Lu J, Liu L, Uluko H, Pang X, Sun Y, Xue H, Zhao L, Kong F, Lv J (2014) Antifungal activities and effect of *Lactobacillus casei* AST18 on the mycelia morphology and ultrastructure of *Penicillium chrysogenum*. *Food Control* 43:57–64. doi: 10.1016/j.foodcont.2014.02.045
- Li Z, Adams RM, Chourey K, Hurst GB, Hettich RL, Pan C (2012) Systematic comparison of label-free, metabolic labeling, and isobaric chemical labeling for quantitative proteomics on LTQ Orbitrap Velos. *Journal of Proteome Research* 11:1582–1590. doi: 10.1021/pr200748h
- Liang Y, Baker ME, Yeager BT, Denton MB (1996) Quantitative analysis of aflatoxins by high-performance thin-layer chromatography utilizing a scientifically operated charge-coupled device detector. *Analytical Chemistry* 68:3885–3891. doi: 10.1021/ac960670g
- Lie JL, Marth EH (1967) Formation of aflatoxin in cheddar cheese by *Aspergillus flavus* and *Aspergillus parasiticus*. *Journal of Dairy Science* 50:1708–1710. doi: S0022-0302(67)87698-7 [pii]r10.3168/jds.S0022-0302(67)87698-7 [doi]
- Liu R, Huang H, Yang Q, Liu W-Y (2002) Purification of alpha-sarcin and an antifungal protein from mold (*Aspergillus giganteus*) by chitin affinity chromatography. *Protein Expression and Purification* 25:50–58. doi: 10.1006/prep.2001.1608
- Liu S-Q, Tsao M (2009) Biocontrol of dairy moulds by antagonistic dairy yeast *Debaryomyces hansenii* in yoghurt and cheese at elevated temperatures. *Food Control* 20:852–855. doi: 10.1016/j.foodcont.2008.10.006
- Livak KJ, Schmittgen TD (2001) Analysis of relative gene expression data using real-time quantitative PCR and the 2⁻(Delta Delta C(T)) Method. *Methods (San Diego, Calif)* 25:402–408. doi: 10.1006/meth.2001.1262
- López-Díaz TM, Santos JA, García-López ML, Otero A (2001) Surface mycoflora of a Spanish fermented meat sausage and toxigenicity of *Penicillium* isolates. *International Journal of Food Microbiology* 68:69–74.

- Lowry OH, Rosebrough NJ, Farr L, Randall RJ (1951) Protein measurement with the folin phenol reagent. *The Journal of Biological Chemistry* 193:265–275.
- Lozano-Ojalvo D, Rodríguez A, Cordero M, Bernáldez V, Reyes-Prieto M, Córdoba JJ (2014) Characterisation and detection of spoilage mould responsible for black spot in dry-cured fermented sausages. *Meat Science* 100C:283–290. doi: 10.1016/j.meatsci.2014.10.003
- Luber CA, Cox J, Lauterbach H, Fancke B, Selbach M, Tschopp J, Akira S, Wiegand M, Hochrein H, O’Keeffe M, Mann M (2010) Quantitative proteomics reveals subset-specific viral recognition in dendritic cells. *Immunity* 32:279–289. doi: 10.1016/j.immuni.2010.01.013
- Luque MI, Córdoba JJ, Rodríguez A, Núñez F, Andrade MJ (2013) Development of a PCR protocol to detect ochratoxin A producing moulds in food products. *Food Control* 29:270–278. doi: 10.1016/j.foodcont.2012.06.023
- Mann DA, Beuchat LR (2008) Combinations of antimicrobials to inhibit the growth of molds capable of producing 1,3-pentadiene. *Food Microbiology* 25:144–153. doi: 10.1016/j.fm.2007.06.005
- Marquina D, Barroso J, Santos A, Peinado JM (2001) Production and characteristics of *Debaryomyces hansenii* killer toxin. *Microbiological Research* 156:387–391.
- Martín A, Asensio MA, Bermúdez ME, Córdoba MG, Aranda E, Córdoba JJ (2002) Proteolytic activity of *Penicillium chrysogenum* and *Debaryomyces hansenii* during controlled ripening of pork loins. *Meat Science* 62:129–137.
- Martín A, Córdoba JJ, Aranda E, Córdoba MG, Asensio MA (2006) Contribution of a selected fungal population to the volatile compounds on dry-cured ham. *International Journal of Food Microbiology* 110:8–18. doi: 10.1016/j.ijfoodmicro.2006.01.031
- Martín A, Córdoba JJ, Benito MJ, Aranda E, Asensio MA (2003) Effect of *Penicillium chrysogenum* and *Debaryomyces hansenii* on the volatile compounds during controlled ripening of pork loins. *International Journal of Food Microbiology* 84:327–338. doi: 10.1016/S0168-1605(02)00474-9
- Martín A, Jurado M, Rodríguez M, Núñez F, Córdoba JJ (2004) Characterization of molds from dry-cured meat products and their metabolites by micellar electrokinetic capillary electrophoresis and random amplified polymorphic DNA PCR. *Journal of Food Protection* 67:2234–2239.
- Marx F (2004) Small, basic antifungal proteins secreted from filamentous ascomycetes: a comparative study regarding expression, structure, function and potential application. *Applied Microbiology and Biotechnology* 65:133–142. doi: 10.1007/s00253-004-1600-z
- Marx F, Binder U, Leiter E, Pócsi I (2008) The *Penicillium chrysogenum* antifungal protein PAF, a promising tool for the development of new antifungal therapies and fungal cell biology studies. *Cellular and Molecular Life Sciences* 65:445–454. doi: 10.1007/s00018-007-7364-8
- Marx F, Haas H, Reindl M, Stöffler G, Lottspeich F, Redl B (1995) Cloning, structural organization and regulation of expression of the *Penicillium chrysogenum paf* gene encoding an abundantly secreted protein with antifungal activity. *Gene* 167:167–171.
- Marx F, Salvenmoser W, Kaiserer L, Graessle S, Weiler-Görz R, Zadra I, Oberparleiter C (2005) Proper folding of the antifungal protein PAF is required for optimal activity. *Research in Microbiology* 156:35–46. doi: 10.1016/j.resmic.2004.07.007
- Masih EI, Paul B (2002) Secretion of β -1,3-glucanases by the yeast *Pichia membranifaciens* and its possible role in the biocontrol of *Botrytis cinerea* causing grey mold disease of the grapevine. *Current Microbiology* 44:391–395. doi: 10.1007/s00284-001-0011-y
- Masoud W, Poll L, Jakobsen M (2005) Influence of volatile compounds produced by yeasts predominant during processing of *Coffea arabica* in East Africa on growth and ochratoxin A (OTA) production by *Aspergillus ochraceus*. *Yeast* 22:1133–1142. doi: 10.1002/yea.1304
- McMeekin TA, Brown J, Krist K, Miles D, Neumeyer K, Nichols DS, Olley J, Presser K, Ratkowsky DA, Ross T, Salter M, Soontranon S (1997) Quantitative microbiology: a basis for food safety. *Emerging Infectious Diseases* 3:541–549.
- Ministerio de Sanidad y Consumo (2001) Real Decreto 90/2001, de 2 de febrero, por el que se establecen los métodos de toma de muestras y de análisis para el control oficial del contenido máximo de aflatoxinas en cacahuets, frutos de cáscara, frutos desecados, cereales, leche y los productos de. BOE 47:6996–7000.
- Ministerio de Sanidad y Consumo (2003) Real Decreto 294/2003, de 7 de marzo, por el que se establecen los métodos de toma de muestras y de análisis para el control oficial del contenido de ocratoxina A en cereales y uvas pasas. BOE 60:9482–9485.

Ministerio de Sanidad y Consumo (2004) Real Decreto 481/2004, de 26 de marzo, por el que se fijan los métodos de toma de muestras y de análisis para el control oficial del contenido de patulina en determinados productos alimenticios. BOE 88:14897–14900.

Ministerio della Sanità (1999) Direttive in materia di controllo ufficiale sui prodotti alimentari: valori massimi ammissibili di micotossine nelle derrate alimentari di origine nazionale, comunitaria e Paesi terzi. Gazzetta Ufficiale della Repubblica Italiana 135:52–57.

Montiel R, Bravo D, Medina M (2013) Commercial biopreservatives combined with salt and sugar to control *Listeria monocytogenes* during smoked salmon processing. Journal of Food Protection 76:1463–1465. doi: 10.4315/0362-028X.JFP-12-560

Moreno AB, Martínez Del Pozo Á, San Segundo B (2006) Biotechnologically relevant enzymes and proteins: Antifungal mechanism of the *Aspergillus giganteus* AFP against the rice blast fungus *Magnaporthe grisea*. Applied Microbiology and Biotechnology 72:883–895. doi: 10.1007/s00253-006-0362-1

Nakaya K, Omata K, Okahashi I, Nakamura Y, Kolkenbrock H, Ulbrich N (1990) Amino acid sequence and disulfide bridges of an antifungal protein isolated from *Aspergillus giganteus*. Europe Journal Biochemistry 38:32–38.

Núñez F, Díaz MC, Rodríguez M, Aranda E, Martín A, Asensio MA (2000) Effects of substrate, water activity, and temperature on growth and verrucosidin production by *Penicillium polonicum* isolated from dry-cured ham. Journal of Food Protection 63:231–236.

Núñez F, Lara MS, Peromingo B, Delgado J, Sanchez-Montero L, Andrade MJ (2015) Selection and evaluation of *Debaryomyces hansenii* isolates as potential bioprotective agents against toxigenic penicillia in dry-fermented sausages. Food Microbiology 46:114–120. doi: 10.1016/j.fm.2014.07.019

Núñez F, Rodríguez M, Aranda E, Martín A, Díaz MC, Bermúdez ME (1998) Influencia de la población fúngica en la maduración del jamón. Eurocarne 70, 39-48

Núñez F, Rodríguez MM, Bermúdez ME, Córdoba JJ, Asensio MA (1996a) Composition and toxigenic potential of the mould population on dry-cured Iberian ham. International Journal of Food Microbiology 32:185–197.

Núñez F, Rodríguez MM, Córdoba JJ, Bermúdez ME, Asensio MA (1996b) Yeast population during ripening of dry-cured Iberian ham. International Journal of Food Microbiology 29:271–280. doi: 10.1016/0168-1605(95)00037-2

Núñez F, Westphal CD, Bermúdez E, Asensio MA (2007) Production of secondary metabolites by some terverticillate penicillia on carbohydrate-rich and meat substrates. Journal of Food Protection 70:2829–2836.

Oberparleiter C, Kaiserer L, Haas H, Ladurner P, Andratsch M, Marx F (2003) Active internalization of the *Penicillium chrysogenum* antifungal protein PAF in sensitive *Aspergilli*. Antimicrobial Agents and Chemotherapy 47:3598–3601. doi: 10.1128/AAC.47.11.3598

O’Keeffe G, Hammel S, Owens RA, Keane TM, Fitzpatrick DA, Jones GW, Doyle S (2014) RNA-seq reveals the pan-transcriptomic impact of attenuating the gliotoxin self-protection mechanism in *Aspergillus fumigatus*. BMC Genomics 25:1–26. doi: 10.1186/1471-2164-15-894

O’Keeffe G, Jöchl C, Kavanagh K, Doyle S (2013) Extensive proteomic remodeling is induced by eukaryotic translation elongation factor 1 β deletion in *Aspergillus fumigatus*. Protein Science 22:1612–1622. doi: 10.1002/pro.2367

Osborn RW, De Samblanx GW, Thevissen K, Goderis I, Torrekens S, Van Leuven F, Attenborough S, Rees SB, Broekaert WF (1995) Isolation and characterisation of plant defensins from seeds of Asteraceae, Fabaceae, Hippocastanaceae and Saxifragaceae. FEBS Letters 368:257–262. doi: 10.1016/0014-5793(95)00666-W

Ouedraogo JP, Hagen S, Spielvogel A, Engelhardt S, Meyer V (2011) Survival strategies of yeast and filamentous fungi against the antifungal protein AFP. The Journal of Biological Chemistry 286:13859–13868. doi: 10.1074/jbc.M110.203588

Owens RA, Hammel S, Sheridan KJ, Jones GW, Doyle S (2014) A proteomic approach to investigating gene cluster expression and secondary metabolite functionality in *Aspergillus fumigatus*. PloS one 9:e106942. doi: 10.1371/journal.pone.0106942.g001

Patharajan S, Reddy KRN, Karthikeyan V, Spadaro D, Lore A, Gullino ML, Garibaldi A. (2011) Potential of yeast antagonists on invitro biodegradation of ochratoxin A. Food Control 22:290–296. doi: 10.1016/j.foodcont.2010.07.024

Petersson S, Hansen MW, Axberg K, Hult K, Schnürer J (1998) Ochratoxin A accumulation in cultures of *Penicillium verrucosum* with the antagonistic yeast *Pichia anomala* and *Saccharomyces cerevisiae*. Mycological Research 102:1003–1008. doi: 10.1017/S0953756297006047

Pitt JI, Hocking AD (1997) Fungi and food spoilage. Blackie Academic and Professional. London, Great Britain

- Poma JP (1998) Le jambon sec et les petites salaisons. Es. Erti. París.
- Ponsone ML, Chiotta ML, Palazzini JM, Combina M, Chulze S (2012) Control of ochratoxin A production in grapes. *Toxins* 4:364–372. doi: 10.3390/toxins4050364
- Qin G, Tian S, Xu Y (2004) Biocontrol of postharvest diseases on sweet cherries by four antagonistic yeasts in different storage conditions. *Postharvest Biology and Technology* 31:51–58. doi: 10.1016/S0925-5214(03)00130-3
- Rabilloud T, Vaezzadeh AR, Potier N (2009) Power and limitations of electrophoretic. *Mass Spectrometry Reviews* 28:816–843. doi: 10.1002/mas
- Razavi-Rohani SM, Griffiths MW (1999) Antifungal effects of sorbic acid and propionic acid at different pH and NaCl conditions. *Journal of Food Safety* 19:109–120. doi: 10.1111/j.1745-4565.1999.tb00238.x
- Reverberi M, Fabbri AA, Zjalic S, Ricelli A, Punelli F, Fanelli C (2005) Antioxidant enzymes stimulation in *Aspergillus parasiticus* by *Lentinula edodes* inhibits aflatoxin production. *Applied Microbiology and Biotechnology* 69:207–215. doi: 10.1007/s00253-005-1979-1
- Reverberi M, Punelli M, Smith CA, Zjalic S, Scarpari M, Scala V, Cardinali G, Aspate N, Pinzari F, Payne GA, Fabbri AA, Fanelli C (2012) How peroxisomes affect aflatoxin biosynthesis in *Aspergillus flavus*. *PloS one* 7:e48097. doi: 10.1371/journal.pone.0048097
- Richard JL (2007) Some major mycotoxins and their mycotoxicoses—an overview. *International Journal of Food Microbiology*. 119:3–10. Doi: 10.1016/j.ijfoodmicro.2007.07.019
- Rivas L, Andreu D (2003) Péptidos antibióticos eucarióticos : ¿una nueva alternativa en clínica? *Enfermedades Infecciosas Microbiología Clínica* 21:358–365.
- Rodríguez A, Córdoba JJ, Werning ML, Andrade MJ, Rodríguez M (2012a) Duplex real-time PCR method with internal amplification control for quantification of verrucosidin producing molds in dry-ripened foods. *International Journal of Food Microbiology* 153:85–91. doi: 10.1016/j.ijfoodmicro.2011.10.020
- Rodríguez A, Luque MI, Andrade MJ, Rodríguez M, Asensio MA, Córdoba JJ (2011) Development of real-time PCR methods to quantify patulin-producing molds in food products. *Food Microbiology* 28:1190–1199. doi: 10.1016/j.fm.2011.04.004
- Rodríguez A, Rodríguez M, Luque MI, Justesen AF, Córdoba JJ (2012b) A comparative study of DNA extraction methods to be used in real-time PCR based quantification of ochratoxin A-producing molds in food products. *Food Control* 25:666–672. doi: 10.1016/j.foodcont.2011.12.010
- Rodríguez A, Rodríguez M, Luque MI, Martín A, Córdoba JJ (2012c) Real-time PCR assays for detection and quantification of aflatoxin-producing molds in foods. *Food Microbiology* 31:89–99. doi: 10.1016/j.fm.2012.02.009
- Rodríguez A, Rodríguez M, Martín A, Delgado J, Córdoba JJ (2012d) Presence of ochratoxin A on the surface of dry-cured Iberian ham after initial fungal growth in the drying stage. *Meat Science* 92:728–734. doi: 10.1016/j.meatsci.2012.06.029
- Rodríguez A, Rodríguez M, Martín A, Nuñez F, Córdoba JJ (2012e) Evaluation of hazard of aflatoxin B1, ochratoxin A and patulin production in dry-cured ham and early detection of producing moulds by qPCR. *Food Control* 27:118–126. doi: 10.1016/j.foodcont.2012.03.009
- Rodríguez M, Martín A, Nuñez F (2001) Población microbiana del jamón Ibérico y su contribución en la maduración. Jesús Ventanas. Ed. Mundi prensa. Madrid
- Rodríguez M, Nuñez F, Córdoba JJ, Bermúdez ME, Asensio MA (1998) Evaluation of proteolytic activity of microorganisms isolated from dry cured ham. *Journal of Applied Microbiology* 85:905–912.
- Rodríguez M, Nuñez F, Sanabria C, Bermúdez E, Asensio MA (1994) Short Communication Characterization of *Staphylococcus* spp. and *Micrococcus* spp. isolated from Iberian ham throughout the ripening process. *International Journal of Food Microbiology* 24:329–335.
- Rodríguez-Martín A (2009) Tesis doctoral. Caracterización de proteínas con actividad antifúngica producidas por *Penicillium chrysogenum*.
- Rodríguez-Martín A, Acosta R, Liddell S, Nuñez F, Benito MJ, Asensio MA (2010) Characterization of the novel antifungal protein PgAFP and the encoding gene of *Penicillium chrysogenum*. *Peptides* 31:541–547. doi: 10.1016/j.peptides.2009.11.002
- Roze L, Laivenieks M, Hong S-Y, Wee J, Wong S-S, Vanos B, Awad D, Ehrlich K, Linz J (2015) Aflatoxin biosynthesis is a novel source of reactive oxygen species—A potential redox signal to initiate resistance to oxidative stress? *Toxins* 7:1411–1430. doi: 10.3390/toxins7051411

- Ruiz J, García C, Carmen Díaz M Del, Cava R, Florencio Tejeda J, Ventanas J (1999) Dry cured iberian ham non-volatile components as affected by the length of the curing process. *Food Research International* 32:643–651. doi: 10.1016/S0963-9969(99)00142-8
- Ruiz-Moyano S, Martín A, Benito MJ, Hernández A, Casquete R, de Guia Córdoba M (2011) Application of *Lactobacillus fermentum* HL57 and *Pediococcus acidilactici* SP979 as potential probiotics in the manufacture of traditional Iberian dry-fermented sausages. *Food Microbiology* 28:839–847. doi: 10.1016/j.fm.2011.01.006
- Ryu EH, Yang EJ, Woo ER, Chang HC (2014) Purification and characterization of antifungal compounds from *Lactobacillus plantarum* HD1 isolated from kimchi. *Food Microbiology* 41:19–26. doi: 10.1016/j.fm.2014.01.011
- Saxena M, Mukerji KG, Raj HG (1988) Positive correlation exists between glutathione S-transferase activity and aflatoxin formation in *Aspergillus flavus*. *The Biochemical journal* 254:567–570.
- Schmittgen TD, Livak KJ (2008) Analyzing real-time PCR data by the comparative CT method. *Nat Protocols* 3:1101–1108.
- Sergeeva YE, Galanina LA, Kochkina GA, Feofilova EP (2009) The effect of the preservative sorbic acid on the lipid composition of the ascomycete fungus *Penicillium roqueforti* Thom. *Microbiology* 78:630–635. doi: 10.1134/S0026261709050166
- Shevchenko A, Tomas H, Havlis J, Olsen J V, Mann M (2006) In-gel digestion for mass spectrometric characterization of proteins and proteomes. *Nature Protocols* 1:2856–2860. doi: 10.1038/nprot.2006.468
- Simoncini N, Rotelli D, Virgili R, Quintavalla S (2007) Dynamics and characterization of yeasts during ripening of typical Italian dry-cured ham. *Food Microbiology* 24:577–84. doi: 10.1016/j.fm.2007.01.003
- Simoncini N, Virgili R, Spadola G, Battilani P (2014) Autochthonous yeasts as potential biocontrol agents in dry-cured meat products. *Food Control* 46:160–167. doi: 10.1016/j.foodcont.2014.04.030
- Skouri-Gargouri H, Gargouri A (2008) First isolation of a novel thermostable antifungal peptide secreted by *Aspergillus clavatus*. *Peptides* 29:1871–1877. doi: 10.1016/j.peptides.2008.07.005
- Sonjak S, Ličen M, Frisvad JC, Gunde-Cimerman N (2011) Salting of dry-cured meat - A potential cause of contamination with the ochratoxin A-producing species *Penicillium nordicum*. *Food Microbiology* 28:1111–1116. doi: 10.1016/j.fm.2011.02.007
- Soriano del Castillo JM (2007) Micotoxinas en alimentos. Área de nutrición y bromatología. Departamento de Medicina Preventiva y Salud Pública, Ciencias de los Alimentos. Valencia, España
- Sosa MJ, Córdoba JJ, Díaz C, Rodríguez M, Bermúdez E, Asensio MA, Núñez F (2002) Production of cyclopiazonic acid by *Penicillium commune* isolated from dry-cured ham on a meat extract-based substrate. *Journal of Food Protection* 65:988–992.
- Souza CP, Burbano-Rosero EM, Almeida BC, Martins GG, Albertini LS, Rivera ING (2009) Culture medium for isolating chitinolytic bacteria from seawater and plankton. *World Journal of Microbiology and Biotechnology* 25:2079–2082. doi: 10.1007/s11274-009-0098-z
- Spadaro D, Lorè A, Garibaldi A, Gullino ML (2013) A new strain of *Metschnikowia fructicola* for postharvest control of *Penicillium expansum* and patulin accumulation on four cultivars of apple. *Postharvest Biology and Technology* 75:1–8. doi: 10.1016/j.postharvbio.2012.08.001
- Speers AE, Wu CC (2007) Proteomics of integral membrane proteins--theory and application. *Chemical Reviews* 107:3687–3714. doi: 10.1021/cr068286z
- Suanthie Y, Cousin MA, Woloshuk CP (2009) Multiplex real-time PCR for detection and quantification of mycotoxigenic *Aspergillus*, *Penicillium* and *Fusarium*. *Journal of Stored Products Research* 45:139–145. doi: 10.1016/j.jspr.2008.12.001
- Taniwaki MH, Hocking AD, Pitt JI, Fleet GH (2001) Growth of fungi and mycotoxin production on cheese under modified atmospheres. *International Journal of Food Microbiology* 68:125–133.
- Terras FRG, Schoofs HME, De Bolle MFC, Van Leuven F, Rees SB, Vanderleyden J, Cammue BPA, Broekaert WF (1992) Analysis of two novel classes of plant antifungal proteins from radish (*Raphanus sativus* L.) seeds. *Journal of Biological Chemistry* 267:15301–15309.
- Theis T, Stahl U (2004) Antifungal proteins: targets, mechanisms and prospective applications. *Cellular and Molecular Life Sciences* 61:437–455. doi: 10.1007/s00018-003-3231-4
- Theis T, Wedde M, Meyer V, Stahl U (2003) The antifungal protein from *Aspergillus giganteus* causes membrane permeabilization. *Antimicrobial Agents and Chemotherapy* 47:588–593. doi: 10.1128/AAC.47.2.588

Thevissen K, Ghazi A, De Samblanx GW, Brownlee C, Osborn RW, Broekaert WF (1996) Fungal membrane responses induced by plant defensins and thionins. *The Journal of Biological Chemistry* 271:15018–15025.

Thevissen K, Terras FR, Broekaert WF (1999) Permeabilization of fungal membranes by plant defensins inhibits fungal growth. *Applied and Environmental Microbiology* 65:5451–5458.

Var I, Erginkaya Z, Kabak B (2009) Reduction of ochratoxin A levels in white wine by yeast treatments. *Journal of the Institute of Brewing* 115:30–34. doi: 10.1002/j.2050-0416.2009.tb00341.x

Varga J, Frisvad JC, Samson RA (2009) A reappraisal of fungi producing aflatoxins. *World Mycotoxin Journal* 2:263–277.

Virgili R, Simoncini N, Toscani T, Camardo Leggieri M, Formenti S, Battilani P (2012) Biocontrol of *Penicillium nordicum* growth and ochratoxin A production by native yeasts of dry cured ham. *Toxins* 4:68–82. doi: 10.3390/toxins4020068

Wang H, Ng TB (2002) Isolation of cicadin, a novel and potent antifungal peptide from dried juvenile cicadas. *Peptides* 23:7–11.

Wisniewski M, Biles C, Droby S, McLaughlin R, Wilson C, Chalutz E (1991) Mode of action of the postharvest biocontrol yeast, *Pichia guilliermondii*. I. Characterization of attachment to *Botrytis cinerea*. *Physiological and Molecular Plant Pathology* 39:245–258. doi: 10.1016/0885-5765(91)90033-E

Yang L, Tan R, Wang Q, Huang W, Yin Y (2002) Antifungal cyclopeptides from *Halobacillus litoralis* YS3106 of marine origin. *Tetrahedron Letters* 43:6545–6548. doi: 10.1016/S0040-4039(02)01458-2

Zheng MZ, Richard JL, Binder J (2006) A review of rapid methods for the analysis of mycotoxins. *Mycopathologia* 161:261–273. doi: 10.1007/s11046-006-0215-6

VIII. ABSTRACT

VIII. ABSTRACT

Moulds growing on foods with intermediate moisture, such as cheeses or dry-cured meats, can contribute to the final sensory characteristics in these products. However, these moulds can produce mycotoxins that are potentially hazardous for consumers. To control the mycotoxin occurrence through food processing, the prevention of toxigenic mould growth is a key issue. One of the best strategies is those based on the use of antifungal proteins and their combination with bioprotective microorganisms to enhance their potential inhibition. To maximize the antifungal effect of these proteins is necessary to know the mechanism of action as well as the survival response of resistant moulds. The main objective of this work was to study the antifungal effect and the mechanism of action of PgAFP protein produced by *Penicillium chrysogenum* against common toxigenic moulds. The combined action of PgAFP with *Debaryomyces hansenii* and *Pediococcus acidilactici* has been also evaluated. For that, comparative proteomics, metabolic, and viability tests and gene expression methods have been used.

The antifungal protein PgAFP exhibited an efficient fungistatic effect against toxigenic moulds usually present in dry-cured foods both in culture medium and on dry-fermented sausage, but not on cheese. On the other hand, PgAFP increased aflatoxin production in culture media, but this fact seems not to be consequence of oxidative stress, given that the unaltered expression of *foxA*, a marker for fatty acid oxidation linked to aflatoxin production. In culture media, *Pediococcus acidilactici* alone or combined with PgAFP and/or *D. hansenii* dramatically reduced aflatoxin production. Nevertheless, on dry-fermented sausage as well as on cheese PgAFP and *D. hansenii* reduced significantly mould counts and aflatoxin production, whilst *P. acidilactici* did not enhance the inhibitory activity of this efficient combination. Therefore, the combined use of PgAFP and *D. hansenii* can be proposed as a preventive action or corrective measure to control unwanted moulds in critical stages of dry-cured products to enhance the food safety.

PgAFP is located both inside and bound to the outer layer on treated sensitive *A. flavus*. Comparative proteomic analyses revealed that the mechanism of action of PgAFP on the sensitive *Aspergillus flavus* seems to be multifactorial. Lower relative amounts of Rho1 and G-protein subunit β CpcB play a key role triggering apoptosis or necrosis through increasing cell permeability, reducing chitin content in cell wall, and increasing reactive oxygen species (ROS). A decrease of proteins involved in aflatoxin biosynthesis was also noticed.

PgAFP neither bound nor penetrated in the resistant PgAFP-producer *P. chrysogenum*. Then, the resistance of this mould should be due to the absence of receptors in its outer layer. However, PgAFP bound to the outer layer of resistant *P. polonicum*, provoking an increase of G-protein subunit β CpcB and Rho1. Thus, the absence or block of receptors in this mould can be ruled out, and the successful response of the resistant mould seems to be based on the higher abundance of protein Rho1 that would lead to the increased chitin deposition via cell wall integrity (CWI) signaling pathway. Indeed, a combined treatment with PgAFP and chitinase provoked *P. polonicum* inhibition, showing synergistic effect. Thus, this can be a strategy to exploit to enhance the PgAFP range of inhibition.

The addition of calcium to substrate provokes a loss of inhibitory activity of PgAFP against the sensitive *A. flavus*. In medium with 0.1 M CaCl₂, PgAFP bound to the outer layer of *A. flavus*, but it was not able to penetrate into the cytoplasm. Moreover, PgAFP did not alter metabolic capability, chitin deposition, intracellular ROS levels, and hyphae viability. *A. flavus* resistance to PgAFP in 0.1 M CaCl₂ seems to be mediated by calcineurin, G-protein, and γ -glutamyltranspeptidase that combat oxidative stress and impede apoptosis.

The results obtained in this work could serve to design new strategies to improve the bicontrol of toxigenic moulds in dry-cured foods using PgAFP combined with *D. hansenii* and *P. acidilactici*.